ORNL-NSIC-21

Contract No. W-7405-eng-26

Nuclear Safety Information Center

TECHNOLOGY OF STEEL PRESSURE VESSELS FOR WATER-COOLED NUCLEAR REACTORS

A Review of Current Practice in Design, Analysis, Materials, Fabrication, Inspection, and Test

G. D. Whitman G. C. Robinson, Jr.
A. W. Savolainen

R. G. Berggren
D. A. Canonico
J. L. English
G. R. Irwin
J. M. Krafft
R. W. McClung
J. G. Merkle
E. C. Miller
S. E. Moore
P. C. Paris
P. Patriarca
H. D. Raleigh
A. A. Wells
F. J. Witt

LEGAL NOTICE

This report was prepared as an account of Government sponsored work. Neither the United States, nor the Commission, nor any person acting on behalf of the Commission:

A. Makes any warranty or representation, expressed or implied, with respect to the accuracy, completeness, or usefulness of the information contained in this report, or that the use of any information, apparatus, method, or process disclosed in this report may not infringe privately owned rights; or

B. Assumes any liabilities with respect to the use of, or for damages resulting from the use of any information, apparatus, method, or process disclosed in this report.

As used in the above, "person acting on behalf of the Commission" includes any employee or contractor of the Commission, or employee of such contractor, to the extent that such employee or contractor of the Commission, or employee of such contractor prepares, disseminates, or provides access to, any information pursuant to his employment or contract with the Commission, or his employment with such contractor.

DECEMBER 1967

OAK RIDGE NATIONAL LABORATORY
Oak Ridge, Tennessee
operated by
UNION CARBIDE CORPORATION
for the
U.S. ATOMIC ENERGY COMMISSION

DISTRIBUTION OF THIS DOCUMENT IS UNLIMITED

BLANK PAGE

Printed in the United States of America. Available from Clearinghouse for Federal Scientific and Technical Information, National Bureau of Standards, U.S. Department of Commerce, Springfield, Virginia 22151
Price: Printed Copy $3.00; Microfiche $0.65

LEGAL NOTICE

This report was prepared as an account of Government sponsored work. Neither the United States, nor the Commission, nor any person acting on behalf of the Commission:

A. Makes any warranty or representation, expressed or implied, with respect to the accuracy, completeness, or usefulness of the information contained in this report, or that the use of any information, apparatus, method, or process disclosed in this report may not infringe privately owned rights; or

B. Assumes any liabilities with respect to the use of, or for damages resulting from the use of any information, apparatus, method, or process disclosed in this report.

As used in the above, "person acting on behalf of the Commission" includes any employee or contractor of the Commission, or employee of such contractor, to the extent that such employee or contractor of the Commission, or employee of such contractor prepares, disseminates, or provides access to, any information pursuant to his employment or contract with the Commission, or his employment with such contractor.

FOREWORD

This report, which was authorized by the USAEC Division of Reactor Development and Technology, summarizes the current state of pressure vessel technology as applied to water-cooled nuclear reactors. It was prepared as a task in the ORNL Nuclear Safety Program and is being distributed as an NSIC report to take its place with the other state-of-the-art studies that the Center periodically issues on topics of significance to safety. It is by far the most comprehensive treatment of the subject yet prepared and should receive considerable attention in light of the questions on pressure vessel integrity raised by the Advisory Committee on Reactor Safeguards (November 24, 1965).

While the authors emphasize that it is not possible to arrive at an absolute position on all important points relative to pressure vessel integrity, they do conclude that under the present conditions of quality control during fabrication "there is no apparent reason for poor performance within the design limits specified." The important subjects of design, materials, codes and standards, fabrication, inspection, operation, and maintenance are discussed in detail. The report identifies areas in which additional research is needed and provides information for evaluating the worth of upgrading codes and standards. The authors made extensive use of the nation's authorities on various facets of pressure vessel technology. They contacted system designers, material suppliers, and experts in the various disciplines involved; visits were made to the various industrial organizations that design and fabricate vessels; and consultants were retained to review the report and to prepare certain sections where such expertise appeared to be warranted.

Wm. B. Cottrell, Director
Nuclear Safety Information Center

PREFACE

The Nuclear Safety Information Center was established in March 1963 at the Oak Ridge National Laboratory under the sponsorship of the U.S. Atomic Energy Commission to serve as a focal point for the collection, storage, evaluation, and dissemination of nuclear safety information. A system of keywords is used to index the information cataloged by the Center. The title, author, installation, abstract, and keywords for each document reviewed is recorded on magnetic tape at the central computer facility in Oak Ridge. The references are cataloged according to the following categories:

1. General Safety Criteria
2. Siting of Nuclear Facilities
3. Transportation and Handling of Radioactive Materials
4. Aerospace Safety
5. Accident Analysis
6. Reactor Transients, Kinetics, and Stability
7. Fission Product Release, Transport, and Removal
8. Sources of Energy Release Under Accident Conditions
9. Nuclear Instrumentation, Control, and Safety Systems
10. Electrical Power Systems
11. Containment of Nuclear Facilities
12. Plant Safety Features
13. Radiochemical Plant Safety
14. Radionuclide Release and Movement in the Environment
15. Environmental Surveys, Monitoring and Radiation Exposure of Man
16. Meteorological Considerations
17. Operational Safety and Experience
18. Safety Analysis and Design Reports
19. Bibliographies

Computer programs have been developed which enable NSIC to (1) produce a quarterly indexed bibliography of its accessions (issued with ORNL-NSIC report numbers), (2) operate a routine program of Selective Dissemination of Information (SDI) to individuals according to their particular profile of interest, and (3) make retrospective searches of the references on the tapes.

Other services of the Center include principally (1) preparation of state-of-the-art reports (issued with ORNL-NSIC report numbers), (2) preparation of the quarterly technical progress review, Nuclear Safety,

BLANK PAGE

(3) answering technical inquiries as time is available, and (4) counsel and guidance on nuclear safety problems.

Services of the NSIC are available without charge to government agencies, research and educational institutions, and the nuclear industry. Under no circumstances do these services include furnishing copies of any documents (except NSIC reports), although all documents may be examined at the Center by qualified personnel. Inquiries concerning the capabilities and operation of the Center may be addressed to

J. R. Buchanan, Assistant Director
(Phone 615-483-8611, Ext. 3-7253)
Nuclear Safety Information Center
Oak Ridge National Laboratory
Post Office Box Y
Oak Ridge, Tennessee 37830

ACKNOWLEDGMENT

This documentation of current practice employed in the design, fabrication, inspection, and testing of steel pressure vessels for water-cooled nuclear reactors was made possible to a considerable degree by the cooperation of those actively engaged in the industry. The information obtained through personal contacts, inspection of shop facilities, and the review of draft material by the nuclear systems designers, vessel designer-fabricators, and materials fabricators provided the sources of information and the requisite understanding of the technology that could not have otherwise been obtained.

CONTENTS

Page

ABSTRACT xix
1. INTRODUCTION 1
REFERENCES 7
2. CONCLUSIONS AND RECOMMENDATIONS 8
2.1 VESSEL FEATURES 9
2.2 ENVIRONMENTAL AND SERVICE CONDITIONS 10
2.3 MATERIALS 13
2.4 EFFECT OF ENVIRONMENT ON MATERIALS 16
2.4.1 Temperature 16
2.4.2 Corrosion 17
2.4.3 Hydrogen Embrittlement 20
2.4.4 Radiation Effects 22
2.4.4.1 Effects on Mechanical Properties 23
2.4.4.2 Fracture Mechanics 27
2.4.4.3 Critical Factors 28
2.5 DESIGN 32
2.5.1 Definition of Loading Conditions 34
2.5.2 Analytical Analyses 35
2.5.3 Experimental Analyses 36
2.5.4 Stress Reviews 37
2.6 BASIC ASPECTS OF CRACK GROWTH AND FRACTURE 37
2.6.1 Linear Elastic Modeling of Cracks 39
2.6.2 Plasticity Analysis 40
2.6.3 Slow, Stable Crack Growth 41
2.6.4 Leak Before Break 41
2.6.5 Fracture Analysis Diagram 42
2.6.6 Recommendations for Fracture Mechanics Research 43
2.7 FABRICATION 44
2.8 QUALITY ASSURANCE 46
2.8.1 Chemical and Mechanical Properties 47

BLANK PAGE

2.8.2 Flaw Detection 48
2.8.3 Fabrication 50
2.8.4 Design 51
2.8.5 Inspection Methods — Capabilities and Limitations 51
2.9 TESTING AND SERVICE PERFORMANCE SURVEILLANCE 52
2.9.1 Hydrostatic Testing and Postoperational Hydrostatic Testing 52
2.9.2 Postoperational and In-Service Nondestructive Examination 53
2.9.3 Postoperational Material Surveillance 58
3. ENVIRONMENTAL AND SERVICE CONDITIONS 60
3.1 TEMPERATURE 60
3.2 PRESSURE OR SERVICE LOADING 60
3.3 PROCESS FLUIDS 62
3.4 RADIATION 66
3.5 DOSIMETRY 66
3.5.1 Damage Models 69
3.5.2 Dosimetry Methods 70
3.5.3 Problems with Specific Activants 72
3.5.4 Cross-Section Data 74
3.5.5 Neutron Flux Calculations 76
3.5.6 ASTM Recommended Practice 78
3.5.7 Conclusions and Recommendations 79
3.6 SERVICE LIFE 79
3.7 TRANSIENTS 80
3.8 MECHANICAL LOADING 82
REFERENCES 82
4. MATERIALS 85
4.1 MATERIALS PROPERTIES 87
4.2 METALLURGICAL CONSIDERATIONS 90
4.2.1 Element Effects 93
4.2.2 Melting Practice 103
4.2.3 Vacuum Treatment 104
4.2.4 Working Processes 105
4.2.4.1 Rolling 106

4.2.4.2 Forging 106
4.2.4.3 Forming 107
4.2.5 Microstructure 109
4.2.6 Mechanical Properties 111
4.2.7 Size Effects 113
4.2.8 Welding 114
4.2.8.1 Weldability 114
4.2.8.2 Welding Processes 117
4.2.8.3 Overlaying 122
4.3 MATERIALS FABRICATION 123
4.3.1 Plate 124
4.3.1.1 Procurement Standards 124
4.3.1.2 Melting Practice 126
4.3.1.3 Pouring 128
4.3.1.4 Breakdown 129
4.3.1.5 Rolling 130
4.3.1.6 Finishing 131
4.3.1.7 Inspection and Testing 131
4.3.1.8 General Remarks 132
4.3.2 Forgings 132
4.3.2.1 Procurement 133
4.3.2.2 Melting Practice 134
4.3.2.3 Shell- and Head-Flange Forgings 134
4.3.2.4 Nozzle Forgings 138
4.3.2.5 Shell-Course Forgings 139
4.3.2.6 General Remarks 139
4.3.3 Bolting Material 140
4.3.4 Weld Metal 142
4.3.4.1 Welding Processes 144
4.3.4.2 Weld Filler Metals 144
REFERENCES 147
5. EFFECT OF ENVIRONMENT ON MATERIALS 150
5.1 TEMPERATURE 150
5.2 CORROSION 152
5.2.1 Carbon and Low-Alloy Steels 152

5.2.1.1 General Corrosion 152
5.2.1.2 Crevice Corrosion 171
5.2.1.3 Galvanic Corrosion 174
5.2.1.4 Stress-Corrosion Cracking 175
5.2.2 Austenitic Stainless Steel 178
5.2.2.1 General Corrosion 178
5.2.2.2 Crevice Corrosion 187
5.2.2.3 Galvanic Corrosion 190
5.2.2.4 Stress-Corrosion Cracking 192
5.2.3 Results of Pressure Vessel Examinations 196
5.2.3.1 Yankee Reactor 196
5.2.3.2 Experimental Boiling Water Reactor 198
5.2.3.3 Heavy-Water Components Test Reactor ... 203
5.2.3.4 Elk River Reactor 206
5.2.4 Conclusions 207
5.3 HYDROGEN EMBRITTLEMENT 209
5.3.1 Carbon Steel 212
5.3.1.1 Blistering 213
5.3.1.2 Decarburization 214
5.3.1.3 Delayed Failure 214
5.3.1.4 Reduction in Postyield Ductility 215
5.3.2 Austenitic Stainless Steel 217
5.3.3 Conclusions 219
5.4 RADIATION EFFECTS 221
5.4.1 Effects on Mechanical Properties 222
5.4.1.1 Tensile Properties and Stress-Strain Curves 223
5.4.1.2 Notch-Impact Strength 225
5.4.1.3 Fracture Mechanics 230
5.4.1.4 Fatigue Strength 232
5.4.1.5 Creep Properties 235
5.4.2 Critical Factors 238
5.4.2.1 Integrated Fast-Neutron Flux (Dose) ... 238
5.4.2.2 Neutron Flux 240
5.4.2.3 Neutron Spectrum 242

5.4.2.4 Exposure Temperature 249
5.4.2.5 Materials 251
5.4.3 Surveillance Program Results 254
5.4.4 Components Removed from Service 259
5.4.5 Postirradiation Heat Treatment 259
5.4.6 Pressure Vessel Cladding 266
REFERENCES 267
6. DESIGN OF NUCLEAR PRESSURE VESSELS 282
6.1 Stress Analysis of Pressure Vessels 285
6.1.1 Mathematical Theory of Elasticity 287
6.1.1.1 Displacements and Strains 289
6.1.1.2 Forces and Stresses 294
6.1.1.3 The Stress-Strain Relations 297
6.1.1.4 Principal Stresses and Stress Intensity 298
6.1.1.5 Thermal Stresses 299
6.1.2 Theory of Shells 300
6.1.3 Strength of Materials 307
6.1.4 Experimental Stress Analysis 309
6.1.5 Applications of Stress Analysis 312
6.1.5.1 Stress Analysis for Steady State 313
6.1.5.2 Cyclic or Fatigue Analysis 321
6.2 STRESS EVALUATION FOR NUCLEAR PRESSURE VESSELS 323
6.2.1 Background 324
6.2.2 Design Aspects of Strength and Fracture 331
6.2.2.1 Fatigue 331
6.2.2.2 Plasticity 337
6.2.2.3 Derivation of the Stress Limits for Primary Stresses Based on Plastic Collapse 338
6.2.2.4 Fracture Mechanics and Plasticity 339
6.2.2.5 Fracture Mechanics and Fatigue 347
6.2.2.6 The Fracture Analysis Diagram 347
6.2.3 Stress Evaluation 350
6.2.4 Other Design Considerations 364
6.2.4.1 Division of Responsibility 364

6.2.4.2 Material Selection and Geometric Design 365
6.2.4.3 Fabrication 366
6.2.4.4 Hydrotesting and Operations 366
6.2.4.5 Surveillance, In-Service Inspection, and Maintenance 367
6.3 CURRENT RESEARCH ON THE DESIGN OF PRESSURE VESSELS 367
6.3.1 Theoretical and Experimental Research 368
6.3.2 Large-Model and Full-Scale Strength Tests 372
6.3.2.1 The PVRC Series 372
6.3.2.2 The British Series 390
6.3.2.3 The PM-2A Tests 399
6.3.3 Brittle Fracture of a Pressure Vessel 401
6.4 CURRENT DESIGN PRACTICE AND THE STRESS REPORT 406
6.4.1 Current Design Practice 406
6.4.2 Stress Report 410
6.5 SUMMARY AND RECOMMENDATIONS 412
REFERENCES 419
7. BASIC ASPECTS OF CRACK GROWTH AND FRACTURE 430
7.1 DEFECTS AND FRACTURE CONTROL 430
7.2 LINEAR ELASTIC MODELING OF CRACKS 443
7.2.1 Progressive Crack Extension 443
7.2.2 Linear-Crack Stress-Field Analysis 446
7.2.3 Experimental Fracture Mechanics Analysis 452
7.3 PLASTICITY ANALYSIS CONCEPTS FOR CRACKS 455
7.3.1 The r_Y Plasticity Adjustment Factor 456
7.3.2 The Strip-Yield Zone Concept 457
7.3.3 The Mode III Elastic-Plastic Treatment 459
7.3.4 Fracture Characterization Problems in Relation to Plastic Analysis 462
7.4 SLOW, STABLE CRACK GROWTH 465
7.4.1 Crack Growth Rates as Affected by Fatigue 465
7.4.2 Crack Growth Rates as Affected by Environment .. 474
7.5 CRACK PROPAGATION AND FRACTURE TOUGHNESS 476
7.5.1 Measurements of K_c and K_{Ic} for Very-High-Strength Metals 476

7.5.2 The Brittle-Ductile Fracture Transition 480
7.5.3 Double-Cantilever and Face-Grooved Specimens ... 483
7.5.4 General Aspects of Dynamic-Crack Stress-Field Analysis 487
7.5.5 Fracture-Process Zone, Time-Rate Effects, and Minimum Fracture Toughness 489
7.5.6 Fracture Toughness in Relation to Plastic Flow Properties 494
7.5.7 Dynamic Fracture-Toughness Measurements and Fracture Transition Temperature Tests 498
7.5.8 Comments on Crack-Opening Dislocation Measurements 506
7.5.9 Comments on Load Toughening and Strain Aging ... 508
7.6 FRACTURE CONTROL PLANS 510
7.6.1 Elimination and Slow Growth of Defects 510
7.6.2 Fracture Safety in Relation to Crack Arrest 512
7.6.3 Relationship of Fracture Toughness to Pressure Vessel Design Load in Terms of a Leak-Before-Break Criterion 517
7.6.4 NRL Fracture Analysis Diagram 522
7.6.5 Proof Test Estimates of Critical Crack Size in Relation to Fracture-Safe Life 524
7.6.6 Radiation Effects Relative to Fracture Properties and σ_{LB} 528
7.7 RECOMMENDATIONS 531
REFERENCES 534
8. FABRICATION 539
8.1 FACILITIES 541
8.2 OPERATIONS AND MATERIALS 544
8.3 SHELL FORMING 545
8.4 HEAT TREATMENT OF FORMED SHELL PLATES 551
8.5 ASSEMBLY OF FORMED SHELL PLATES INTO COURSES 553
8.6 ASSEMBLY AND HEAT TREATMENT OF ELECTROSLAG-WELDED SHELL COURSES BY ELECTROSLAG WELDING 555
8.7 JOINING SHELL COURSES INTO SHELL SUBASSEMBLIES 560
8.8 FABRICATION OF VESSEL SUPPORTS 561
8.9 NOZZLES AND DISSIMILAR METAL WELDS 561
8.10 WELD-OVERLAY CLADDING 564

8.11 HEAD SUBASSEMBLY 566
8.12 FLANGE AND NOZZLE FORGINGS 567
8.13 MACHINING 570
8.14 TESTING 572
8.15 CLEANING 574
REFERENCES 575
9. QUALITY ASSURANCE 577
9.1 CHEMICAL AND MECHANICAL PROPERTIES 579
9.1.1 Chemical Analyses 579
9.1.2 Mechanical Properties 580
9.1.2.1 Plate 581
9.1.2.2 Forgings 583
9.1.2.3 Bolting Materials 585
9.1.2.4 Filler Metal 586
9.1.2.5 Welding Procedures and Weld Tests 586
9.2 FLAW DETECTION 588
9.2.1 Examination Procedures 589
9.2.2 Plates 590
9.2.3 Forgings and Bars 593
9.2.4 Castings 594
9.2.5 Tubular Products 596
9.2.6 Bolts and Bolting Material 598
9.2.7 Examination After Accelerated Cooling 598
9.2.8 Procedures and Personnel 599
9.3 FABRICATION 600
9.4 DESIGN 604
9.4.1 Stress Analysis and the Stress Report 604
9.4.2 Effects of Acceptable Deviations from Specifications 605
9.5 INSPECTION METHODS – CAPABILITIES AND LIMITATIONS 609
9.5.1 Macroscopic or Visual Examination 610
9.5.2 Radiography 612
9.5.3 Ultrasonic Testing 621
9.5.4 Magnetic-Particle Examination 624
9.5.5 Liquid-Penetrant Examination 625

9.5.6 Electromagnetic Methods 626
REFERENCES 627
10. TESTING AND SERVICE PERFORMANCE SURVEILLANCE 629
10.1 HYDROSTATIC TEST 629
10.2 POSTOPERATION TESTING 637
10.2.1 Material Surveillance 637
10.2.2 Hydrostatic Retest 643
10.2.3 Nondestructive Examination 645
10.2.3.1 Present Practice 647
10.2.3.2 Possible Postoperation Examination Methods 649
10.2.3.3 Nondestructive Detection of Radiation Damage 660
10.3 IN-SERVICE EXAMINATION 661
10.3.1 Ultrasonic Scanning Systems 662
10.3.2 Fixed-Probe Systems 662
10.3.3 Other Monitoring Systems 664
REFERENCES 664
INDEX 669

ABSTRACT

The current practices in the design and fabrication of steel pressure vessels for light-water-cooled nuclear reactors in present and immediate-future commercial use are reviewed. The specified service and predicted environmental conditions are identified, along with an evaluation of the effects of these parameters on materials behavior. Materials fabrication and materials properties of interest in pressure-vessel fabrication are reviewed, and the metallurgy of these materials is discussed. The basic aspects of fracture mechanics and crack growth are examined, with emphasis on the low-alloy steels of current interest. The codes and standards applied in the technology are discussed, and areas where augmentation and/or revision to these standards appears warranted are identified. The techniques for postoperational and in-service inspection are summarized and evaluated.

TECHNOLOGY OF STEEL PRESSURE VESSELS FOR WATER-COOLED NUCLEAR REACTORS

G. D. Whitman G. C. Robinson, Jr.
A. W. Savolainen

1. INTRODUCTION*

This summary review of present-day pressure vessel technology was prepared as a task under the U.S. Atomic Energy Commission's augmented nuclear safety program. The material, presented as a state-of-the-art review, includes the major areas of materials, design, fabrication, and inspection to provide a body of information that may be used in the assessment of the risk of catastrophic failure of a reactor vessel. The requirements set forth in codes and standards are compared with current practice, and the identification of potential problem areas where additional research or augmented standards would be useful are discussed. Current technology and the immediate-future needs of the technology were of primary interest in the preparation of this report.

The discussion is limited to primary reactor vessels for light-water-cooled nuclear reactors, that is, the boiling-water reactor (BWR) and the pressurized-water reactor (PWR) for civilian power application. These vessels are identified as Class A vessels in the ASME Code, Section III, Nuclear Vessels. This comprehensive review involved the assessment of a wide range of activities, skills, and disciplines, including the interrelationship between nuclear designer, fabricator, and operator. Every effort was made to provide an accurate reflection of the current attitudes of this segment of the nuclear industry, and recognized authorities were retained to prepare certain sections and review the entire report. The principal designers and builders furnished considerable information. Some information was obtained during the course of the evaluation that was of a proprietary nature, and since a detailed accounting of all phases of the technology was not essential to the objectives of the report, such information was not included.

---

*This chapter was prepared by G. D. Whitman of Oak Ridge National Laboratory.

The reactor vessel is one of the major components in a nuclear facility in that it performs the very critical functions of housing the radioactive core and provides a pressure-tight membrane to retain the coolant. Pressure vessel technology per se is not new, and vessels have been designed and fabricated that have good performance records of many years duration. This was not always the case. In the early 1900's, as a result of catastrophic failures of boilers, the ASME undertook the task of providing a minimum set of standards for the design, materials, and construction of a class of these devices. The first Boiler Code was published in 1914. Through the intervening years, additional codes have been written and published, with today's accepted standard for nuclear reactor vessels being the aforementioned Section III of the ASME Code. The primary intent of these codes is to establish levels of safety, and when applied within the bounds of good engineering judgment and the limitations set forth, a new product of adequate quality should be produced.

The nuclear industry, as any viable segment of the economy, undergoes constant change. Considering the phenomenal growth of nuclear power stations in both numbers and unit size, the potential for catastrophic failure needs to be under constant surveillance. The first water-cooled reactor vessels were designed and fabricated in accordance with Section I of the ASME Code, and these vessels have performed well. As the technology progressed and more advanced methods of design and fabrication came into general acceptance, standards and codes were published to incorporate a more sophisticated level of control on quality, and the product is more closely tailored to an intended service. The Section III rules are primarily applicable to vessels operating below 800°F, the creep limit for the materials of interest. Provisions for limiting primary, secondary, and other stresses and stress concentrations, as well as the control of stress-cycle fatigue, are incorporated. Rules for the control of external influences and environmental factors, such as corrosion and radiation effects, are not specified, but the designer or owner is made responsible for taking such into consideration.

A major emphasis in the technology today is on the fabrication of larger vessels. In terms of electric power production, 1000-Mw(e) stations are under contract, and units with up to 1500-Mw(e) capacity are

being seriously considered, in contrast to the 200- to 300-Mw(e) stations built a few years ago. It should be noted that the smaller units built by today's standards are the only ones with any operating history. As of this writing, 47 reactors with a total capacity of 27,574 Mw(e) have been built, are being built, or are committed under the U.S. commercial nuclear power program.[1]

As of today there are only two companies in the United States, Babcock & Wilcox and Combustion Engineering, actively engaged in the design and fabrication of shop-fabricated vessels of interest in this report. Their unique capabilities, facilities, and experience place them in a preeminent position in this regard.

Another factor that just recently came into prominence is field fabrication of vessels for water-cooled reactors. At sites where there is no navigable waterway or overland transportation of a completed vessel is not possible, field fabrication is being considered. In fact, a 545-Mw(e) BWR vessel of some 600 tons was subcontracted to Chicago Bridge and Iron by General Electric for a plant at Monticello, Minnesota.[1]

The vessels for the two systems of interest have immediately discernible differences in that the BWR vessels are thinner walled, larger in diameter, and taller. Table 1.1 gives relative sizes of vessels for comparable plants.

The differences in proportions of the vessels are due primarily to the higher pressure of the PWR system and the space needed above the core in the BWR for mechanical steam separators. Dimensions of interest for

Table 1.1. Comparison of Sizes of Pressure Vessels for Comparable Plants

Reactor type	BWR	PWR
Identification	Dresden-2	Palisades
Net electrical output, Mw	715	710
Design pressure, psi	1250	2500
Cylinder wall thickness, in.	6 1/8	8 1/2
Inside diameter, in.	251	172
Height, in.	816	480 3/4

a number of vessels are listed in Chapter 3 of this report, and Figs. 1.1 and 1.2 show typical vessel proportions for the BWR and PWR systems, respectively. These figures also show the size evolution and the applicable ASME Code used in the design and fabrication.

The plate and forging material from which these vessels are fabricated today is low-alloy manganese-molybdenum carbon steel, with a nickel addition for improved fracture toughness. A quenching and tempering operation is used to improve the fracture toughness and, as applied to heavy sections, it helps attain the same strength levels as those specified for the normalized and tempered grades in lesser thicknesses. The continuing development of increasingly larger vessels will eventually involve the use of higher strength materials. The particular requirements for nuclear reactor service demand that considerable information be developed on any potential material; this information may include the effects of neutron irradiation and the effect of flaws or defects in the behavior of the material under the conditions of service.

It is important to emphasize at this point that it is not possible to arrive at an absolute position on many key items, and furthermore, in order to evaluate the incredibility of failure of a pressure vessel when incorporated into a system such as a power reactor complex, limits must be specified for the environmental conditions. The nuclear systems designer specifies a set of service conditions, including abnormal events, that form the basis for design input. The vessel designer provides analyses that demonstrate the adequacy of the structure for these specified service conditions, and fabrication is performed with considerable quality control so that there is no apparent reason for poor performance within the design limits specified. A system of checks and balances is invoked throughout the course of a project that establishes multiple review of the design, material, fabrication, and quality control. Checks are made on the completed vessel that insure its capability to withstand overpressure loading, and measurements are made to check deflections and displacements of the loaded vessel to back check the design predictions.

Information gathered in this review indicates that the industry is producing high-quality vessels in terms of the standards set forth and required by the Code, since these requirements are generally exceeded in

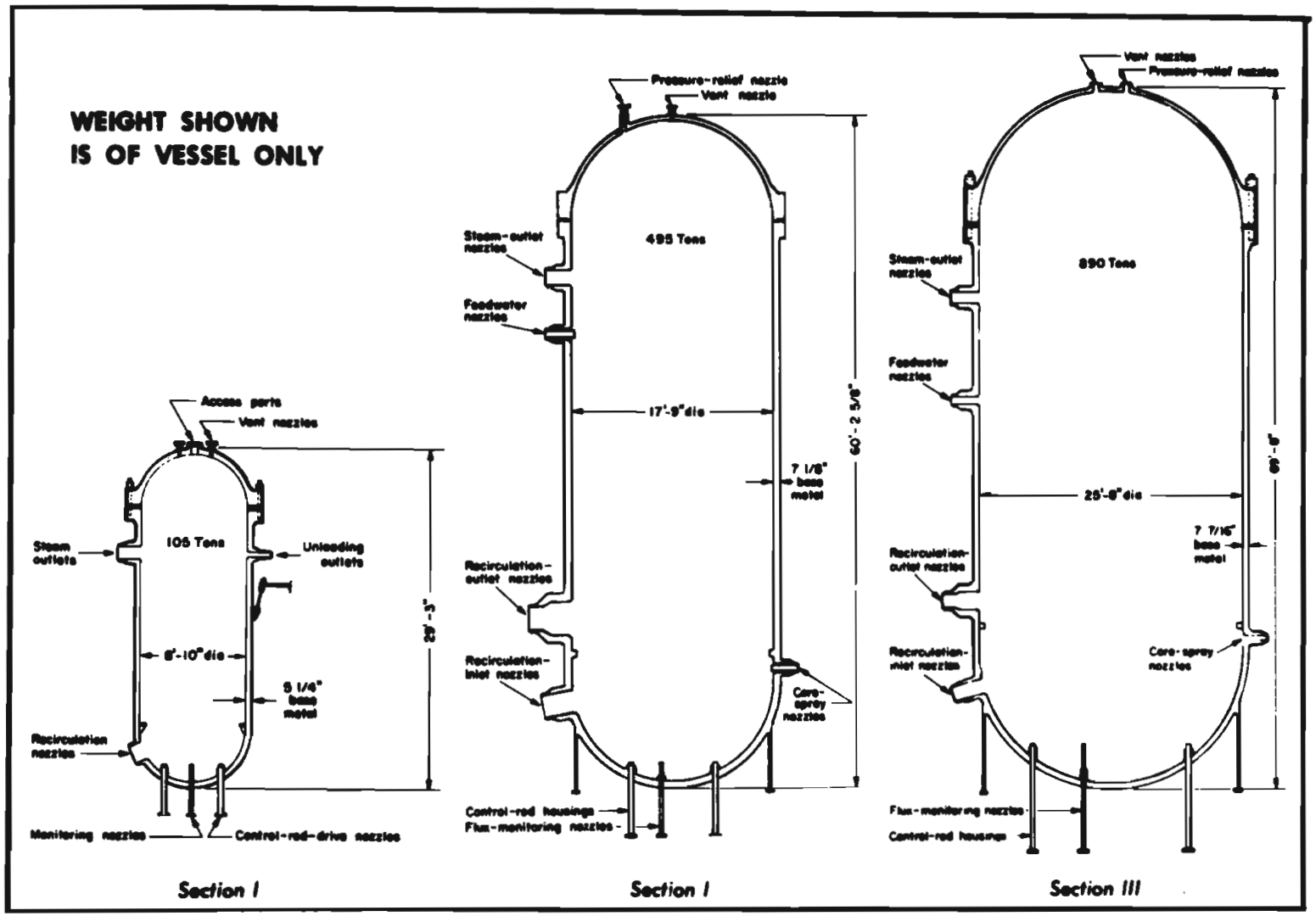

Fig. 1.1. BWR Pressure Vessels. Section numbers refer to ASME Code. (Courtesy of Combustion Engineering, Inc.)

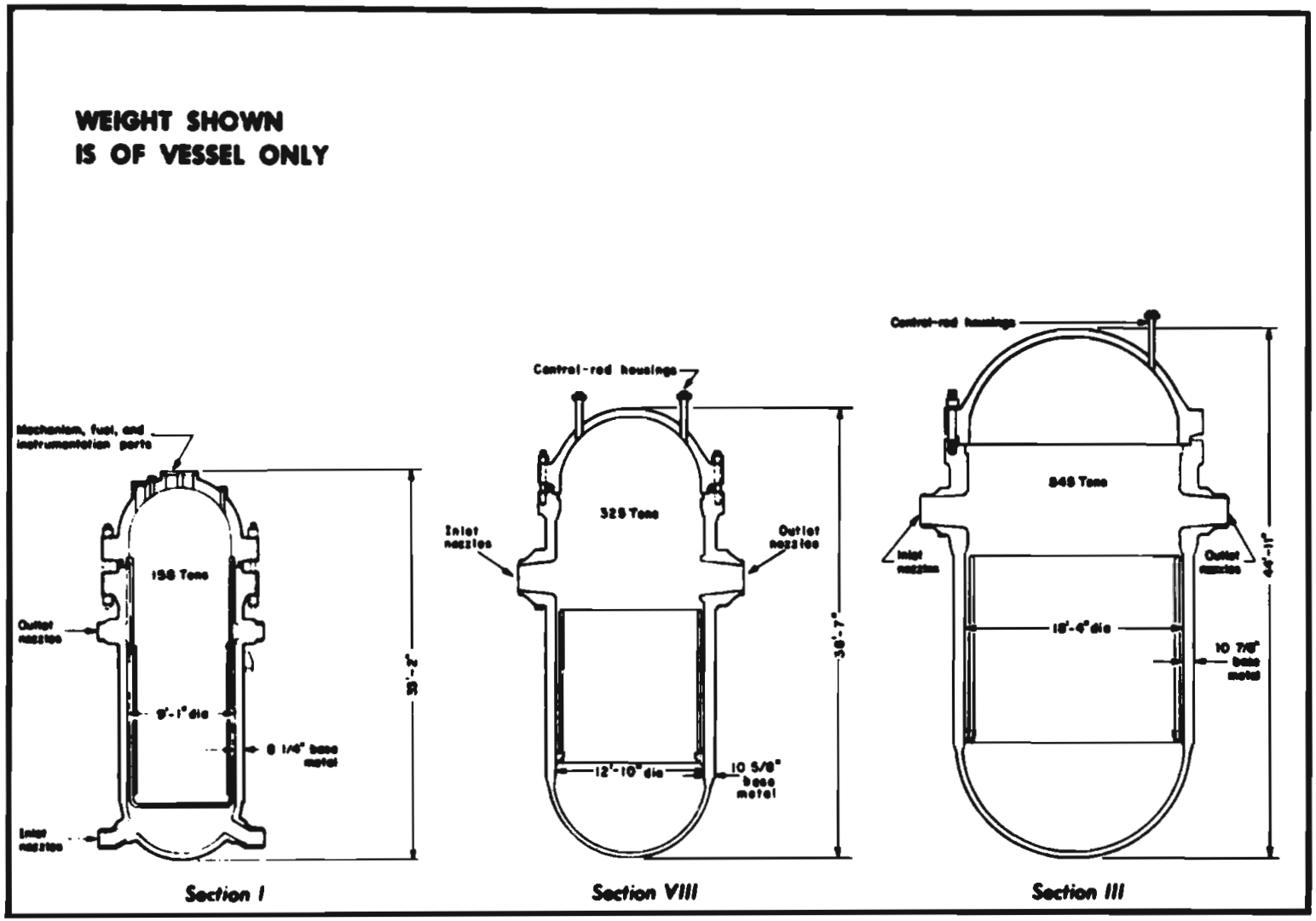

Fig. 1.2. PWR Pressure Vessels. Section numbers refer to ASME Code. (Courtesy of Combustion Engineering, Inc.)

all phases of the manufacturing process. This practice has evolved because of the recognized importance of vessel integrity to safety and plant availability. The vessel is one of the major components controlling construction scheduling and involves considerable financial investment, which further emphasizes the importance of control on quality to the parties concerned. Finally, the difficulties involved in inspection after plant startup are an overriding incentive to place quality control in a commanding position.

The major subjects discussed in this report identify areas where increased knowledge or further augmentation of standards would better establish limits of certainty on behavior with time and further remove factors of ignorance in design, analysis, and fabrication. It is also important to emphasize that new materials and methods will continue to be devised and discovered. A change in material properties to achieve more economical construction or increased performance might sacrifice a margin of safety previously enjoyed, and therefore more exact predictions of behavior will be required.

The subjects covered in this report represent a variety of disciplines and skills. Many individuals with different specialities, interests, and experience contributed material, and there is some repetition between certain chapters. Although such redundancy was minimized to a degree deemed practical, some remains because a more complete presentation of a particular subject required emphasis on or assessment of background material from a somewhat different viewpoint.

REFERENCE

1. Field Fabrication: A New Dimension, Nucleonics, 24(9): 19-20 (September 1966).

2. CONCLUSIONS AND RECOMMENDATIONS*

The information developed in this report represents the current nuclear pressure vessel technology as obtained from the literature and from the experience of those engaged in designing and fabricating steel pressure vessels for commercial light-water-moderated and -cooled reactors. The detail developed on particular subjects varies, and some of the discussion has been included to present a more complete treatment for those not familiar with the fundamentals or particular disciplines involved. It is the purpose of this chapter to briefly summarize the major observations, conclusions, and recommendations. In most cases this information has been used verbatim from the authors' material. Additional detail on a particular subject can be obtained from the remaining text and the references cited at the end of each chapter.

The pressure vessels of interest meet the Class A requirements of the ASME Code, Section III, Nuclear Vessels. These structures have the primary function of containing the reactor core and coolant and are complicated by penetrations, flanges, and appurtenances needed to permit coolant circulation, refueling, reactor control, vessel support, etc., consistent with a practical power-producing complex.

Babcock & Wilcox and Combustion Engineering are the only suppliers of the shop-fabricated reactor vessels of interest. Their experience, facilities, and demonstrated capabilities make them unique in this regard. Chicago Bridge and Iron has contracted to fabricate a boiling-water reactor vessel on site, and they have had considerable experience in the construction of vessels for the petrochemical industry that have required the solution to metallurgical and fabrication problems similar to those encountered in the fabrication of large light-water reactor pressure vessels. General Electric and Westinghouse are the major nuclear systems designers who, along with Babcock & Wilcox and Combustion Engineering, make up the remaining capability in the United States.

---

*The chapter was prepared by G. C. Robinson, Jr., and G. D. Whitman of Oak Ridge National Laboratory.

It may be concluded that the principal organizations involved in the design and fabrication of commercial water-reactor vessels are few. Their experience, capabilities, interest, and facilities are directed toward the production of a reliable product, and there is no evidence that recognized quality standards are being compromised. In fact, the requirements set forth in the accepted codes and standards are generally exceeded.

It should be noted that a degree of standardization is being achieved with regard to design and size to the end that previous experience is brought heavily to bear on new installations. Even though this elimination of "new models" for the immediate period establishes a more mature industry, and the extension of the technology to the current generation is very rational, operating experience for the larger systems now being designed is still nonexistent.

2.1 VESSEL FEATURES

The concept of the load-bearing structure is a vertical cylinder having hemispherical heads with the upper head being flanged and bolted for core access. The material thicknesses for large-size vessels range from 7 to 11 in., and the weights approach 1000 tons. Heights vary from 45 to 70 ft, and vessels with diameters in excess of 20 ft are being fabricated. The pressurized-water reactor vessels are the heavier wall, shorter structures in comparison with the boiling-water reactor vessels.

The wetted surfaces are clad with a corrosion-resistant material for coolant protection. The mid-section of the vessel opposite the reactor core is free of penetrations and discontinuities; this eliminates complications in analysis, fabrication, and inspection in the region where radiation damage to the material is most likely to occur.

Penetrations are located in the heads and end regions of the cylindrical sections for control, venting, injection, coolant circulation, etc., as required primarily for heat removal, control, and safety. The largest number of a single type of penetration is associated with control-rod-drive requirements, and these penetrations are located in the vessel head.

Generally speaking, pressurized-water reactor vessels are supported from pads or nozzles located at the upper cylindrical section. Boiling-water reactor vessels are supported by continuous skirts attached to the bottom head.

The materials of construction are low-alloy steel and manganese-molybdenum steel with a nickel addition. Stainless steel or Inconel cladding added on the interior surface of the low-alloy structural steel by metallurgical bonding forms the wetted surface.

The primary evolutionary features have been increases in size and attendant weight. The reactor core required to produce sufficient thermal energy for current 1000-Mw(e) plants can be housed in a single vessel. Studies are being made to extend the technology to vessels for cores in 1500-Mw(e) and larger plants. However, it appears that a current commercial plateau has been achieved at or near the 1000-Mw(e) plant level.

2.2 ENVIRONMENTAL AND SERVICE CONDITIONS

Current designs of boiling-water reactor vessels are based on a temperature of 575°F and a pressure of 1250 psig. The pressurized-water reactor vessels are based on design conditions of 650°F and 2500 psig. These specified levels provide margin for operational maneuvering, transients, and set-point ranges for relief and safety valves.

Methods for effecting water-chemistry control for pressurized-water reactors are very similar to those used in modern high-pressure and supercritical fossil-fueled steam plants. The total solids content level is maintained by means of bypass stream flows through demineralizers to less than 1 ppm in order to remove radioactive crud and limit the chloride content to less than 0.15 ppm. A bypass stream may also be utilized to pass flow through a gas stripper-deaerator to remove xenon, krypton, and other gases before returning the stream to the primary loop. Hydrogen and a pH control chemical, usually hydrazine, are introduced to control the dissolved oxygen level and to maintain a pH between 9.5 and 10. Since only stainless steel, Inconel, and Zircaloy are used in the wetted

surface regions throughout the primary loop, a major effort has been made to effect water conditions that are ideal for these materials.

Because of the gas stripping action of the condenser in the boiling-water reactor, it is not feasible to utilize hydrogen as in the pressurized-water reactor for suppression of the oxygen produced by radiolytic decomposition of water in the reactor. In the presence of an excess of oxygen, hydrazine will break down in the reactor environment to form nitric acid, and as a consequence boiling-water reactors have not used an oxygen and pH control scheme comparable to that for pressurized-water reactors. Developmental programs were undertaken to examine the corrosiveness of an environment that depended on low total dissolved and suspended solids, low oxygen and chlorides, variable pH, and a stoichiometric ratio of hydrogen and oxygen both in the water and steam phases. Out-of-pile test loop operation of such an environment for stainless steels, carbon steels, Zircaloys, Inconel, copper alloys, and copper-nickel alloys typical of the entire system have to date demonstrated very low corrosion rates and rates of release of corrosion products to systems.

Radiation effects on the behavior of materials from which reactor pressure vessels are fabricated are among the unique factors to be considered in reactor pressure vessel performance. The accumulated neutron flux for energies greater than 1 Mev is the accepted measure of radiation dose. The threshold level for incipient damage is generally accepted to be 10^{18} neutrons/cm^2, and designers avoid high stresses and discontinuities in regions where the accumulated neutron dose will exceed this value. Boiling-water reactor vessels receive a lower dose than pressurized-water reactor vessels by virtue of a greater clearance between the core and the vessel wall, with the resultant attenuation of the radiation by the coolant and hardware in the clearance region. The peak design life dose levels for boiling-water reactor vessels are less than 10^{19} neutrons/cm^2, with best estimates being less than 5×10^{17} neutrons/cm^2. The peak design life dose levels for newer pressurized-water reactor units are predicted to be approximately 3×10^{19} neutrons/cm^2.

A precise understanding of the extent and type of radiation damage suffered as a function of radiation dose, dose rate, and temperature has not yet been attained. Also, methods for predicting accumulated radiation

dosage are subject to considerable uncertainty. Consequently current reactor vessels are monitored for possible radiation damage by means of surveillance programs patterned after ASTM Standards E 170 and E 199. Dosimetry accompanying the surveillance specimens depends upon activation analysis, which is subject to considerable uncertainty due to lack of an adequate knowledge of the cross-section data of the useful activants. Also a serious gap in the neutron energy spectrum, approximately 1 kev to 1 Mev, is measurable only with fissionable materials, and a difficult technique and considerable expense are involved. Further basic work on cross-section data is needed so that the accumulated data from surveillance programs may be beneficial in understanding the basic mechanisms of radiation damage.

Economic considerations usually result in design lives for power reactors that vary from 20 to 40 years. All current designs are aimed at a life expectancy of 40 years.

Fatigue analyses of vessels involve loadings from three major categories of cycles. These are (1) startup and shutdown cycles, (2) normal operation involving load changes, and (3) transients associated with safety action and integrity tests. The permissible temperature and pressure rates of change for startup and shutdown are primarily controlled by restrictions imposed to insure against the possibility of brittle fracture.

In general, the pressure and temperature transients associated with minor load adjustments do not produce severe service and result in negligible or low calculated cumulative damage factors. The most severe transients are associated with safety actions. In order to achieve low cumulative damage factors, thermal barriers are required on certain areas, such as nozzles. In order to properly interpret the design data as time functions of temperature, pressure, and combinations of temperature and pressure, specifications must be prepared carefully, and even with good specifications very close coordination is required between system and vessel designers so that no misunderstanding exists as to the character of these loadings.

The mechanical loadings considered are piping reactions, loading from mechanical devices that are appurtenances to the vessel, hydraulic

loading, bolting loads at flanges, and seismic loading. Although loadings from overpressure tests equivalent in magnitude to the loadings of the initial hydrotest are being considered for routine inspections, no generally accepted recommendation in this regard is evident.

2.3 MATERIALS

Relatively few materials have been used or considered for use in light-water reactor vessels. This has resulted from a cautious approach to material selection because qualification requires a thorough knowledge of the physical and mechanical properties and fabricability of the material, as well as a backlog of relevant experience and proven economics. Some of the early reactor vessels were fabricated from carbon-silicon ASTM A 212 grade B steel plate. Although there has been extensive successful use of this steel in steam boiler drums in all thicknesses up to the 6- to 7-in. range, ts fracture toughness was not as high as desired for nuclear vessel service. Later vessels were fabricated from a nickel-modified version of ASTM A 302 grade B plate, a manganese-molybdenum steel. The current designation for this material is ASTM A 533; the corresponding forging material is ASTM A 508 class 2. Vessels currently in fabrication or planned will use these materials.

Since prospective 1500-Mw(e) or larger reactors would involve a tenuous extrapolation of the properties of ASTM A 533 grade B class 1 steel, two additional high-strength alloys are currently being investigated. One is a chromium-molybdenum alloy (2 1/4% Cr–1% Mo) that is defined in ASTM specifications A 542 (plate) and A 541 class 7 (forgings). The other is a nickel-chromium-molybdenum alloy (3% Ni–1.75% Cr–0.5% Mo) that is defined in ASTM specifications A 543 (plate) and A 508 class 4 or A 541 class 8 (forgings).

The heavy plate sections, greater than approximately 6 in. in thickness, required for light-water reactor vessels are obtainable from a single source of supply. The prospective demand for heavy plate has not as yet appeared attractive enough to warrant the large capital investment required for competition in the field. In addition, the present trend

is to attempt to develop high-strength alloys that can be used in thinner sections. A successful development of this type would favor a broader base of competition, since no additional capital outlay would be required. In spite of this unique supply feature, the industry has not appeared to suffer from extended supply schedules, excessive costs, or reduced quality, and no immediate change in this healthy situation appears imminent.

For vessel fabrication methods involving the use of electroslag welding, there is a single source of supply of braided wire with the tailored chemistry required. Here again, the single source of supply has apparently created no serious difficulties.

The accent on good low-temperature notch toughness in nuclear plate and forgings and the desirability of uniformity of properties has given impetus to the use of manufacturing procedures that are generally acknowledged to enhance the desired mechanical properties. Examples are the preference for basic electric-furnace rather than basic open-hearth methods to obtain better homogeneity in the final structure and to reduce phosphorus and sulfur contents. Vacuum degassing of the charge is also generally used to substantially lower the content of gases, particularly hydrogen, to obtain more thorough homogenization of the molten metal and to reduce the amount of aluminum required to tie up the residual oxygen and consequently reduce the nonmetallic inclusions and possible aluminum intermetallic compounds. The improvements in mechanical properties resulting from these manufacturing techniques, though not dramatic, are significant enough so that consideration should be given to making their use mandatory for both plate and forgings. It furthermore appears that a very worthwhile endeavor would be a basic investigation of the effects on mechanical properties of tramp trace elements, refined control of basic constituents, and microstructure variations in both unirradiated and irradiated materials.

The current fabricators are well versed in the techniques for devising, developing, and implementing adequate weld processes. In spite of the fact that the weld processes used — submerged-arc, electroslag, stick-electrode, shielded-metal-arc, and inert-gas-shielded — are common to the welding industry in general, the problems peculiar to the nuclear pressure vessel industry have required greater effort because of the

massive sections involved and the quality desired. In early vessel work, a significant number of welding problems arose that required careful selection of filler metal and flux and careful qualification of the procedure and therefore entailed a considerable proprietary effort. It is anticipated that newcomers to the nuclear pressure vessel field will be forced through such a development stage unless appropriate petrochemical experience has been accrued.

Of the current processes used, electroslag welding is perhaps attended with the greatest uncertainty in quality due to limited experience. Since the weld formed may consist of as much as 60% base metal, there is cause for concern for reproducibility of the properties because of the high degree of filler metal dilution and because of the grossly segregated microstructure. It therefore appears prudent to require that each weldment include a runoff tab and that the tab be tested for its response to the quenching and tempering heat treatments.

A review of the mechanical property data indicates that the reference material, ASTM A 533, is generally satisfactory for the presently imposed requirements up to sections approximately 12 in. thick. Some uncertainty exists in the ability of A 533 steel to meet the required notch impact properties in the heavier sections; however, there is some evidence that the presently imposed requirement for the Charpy V-notch "fix" may be too conservative. Further effort should be invested to clarify this point.

Since the notch impact properties of A 533 steel are marginal in the heavier sections, as has been previously mentioned, consideration has been given by industry to the use of ASTM A 542 and A 543 steels for the next generation of light-water reactor pressure vessels. These materials respond to quenching and tempering heat treatment and have mechanical properties in the high-strength category. As is subsequently discussed, the use of high-strength materials will, in general, impose a need for a more stringent review of crack-propagation resistance, including a greater involvement of fracture mechanics techniques.

There is some evidence that A 542 steel has a very sensitive relationship between the tempering temperature and the notch toughness that leads to a very disconcerting scatter in the measured values. ASTM A 543 steel is a more highly alloyed steel than A 533 or A 542, and the

alloying materials may contribute to greater difficulties in welding. Its high nickel content may contribute to an embrittling effect that can result in a loss of notch toughness. Further effort should be invested in the development and qualification of these steels to remove these potentially troublesome aspects.

2.4 EFFECT OF ENVIRONMENT ON MATERIALS

The effects of environmental factors, such as temperature, radiation, corrosion, and hydrogen embrittlement, are of considerable concern with respect to safe operation of nuclear reactor vessels. Perhaps concern for the possible problems is emphasized because, in general, they are not currently amenable to solution by codification. For this reason, Section III of the ASME Code does not give an extensive body of rules, but rather an admonition to the designer to make proper provisions for environmental factors.

2.4.1 Temperature

The consideration of temperature in Chapter 5 is restricted to critical metallurgical effects, since it is apparent that in the broad context temperature is a significant parameter in almost every phase of metallurgy. Therefore, many other important temperature-related effects are considered in Chapter 4 and are summarized in previous Section 2.3.

Since the maximum temperature at which light-water reactor pressure vessels are designed to operate is 650°F, there are no problems solely attributable to loss of tensile properties due to temperature. Also creep and stress-rupture effects need not be considered. Therefore the primary concern for temperature is its relationship to critical metallurgical effects involving embrittlement. Embrittlement effects are quite complex, and the behavior mechanisms of the materials of interest are very divergent for comparable temperature treatments. This wide divergence ensues as a consequence of the great sensitivity to temperature-related

metallurgical changes created by seemingly slight variations in alloying and tramp element content.

It is possible that the current reference materials, ASTM A 533, A 508, and A 540 steels, may embrittle as a consequence of an aging phenomenon involving nickel and aluminum. Fortunately, the current radiation-surveillance programs will permit detection of any significant changes, and some will permit differentiation between radiation and temperature-related metallurgical effects resulting from placement in regions of low fast-neutron flux. It is also possible that similar embrittling problems may be involved with the usage of the candidate materials, ASTM A 542 and, in particular, A 543 steels, because of their higher nickel content, as previously mentioned. The understanding of embrittling processes is of paramount importance and should be an area for an extensive research effort not only to elucidate the significant factors for the reference materials but also for any canidate materials.

2.4.2 Corrosion

A tremendous backlog of information, both experimental and operational, has been accumulated during the past 10 to 15 years on the corrosion of carbon, low-alloy, and stainless steels in water systems related to nuclear reactor applications. The effects of numerous variables on corrosion behavior of these materials have been investigated in a thorough manner. Among the variables that have been examined are water pH, temperature, time, water velocity, material composition, stress, heat treatment, water resistivity, and the presence of oxygen, hydrogen, and other gases in the water. In addition, a fair amount of information is available on the crevice and galvanic corrosion of the materials in question. In order to minimize the problems of corrosion and of corrosion products passing into the recirculating water system, it has been general practice to utilize austenitic stainless steel as the major construction material on the wetted primary boundary in most designs for water-cooled nuclear power reactors.

Carbon or low-alloy steels have not as yet been used because of the question of whether such materials would exhibit acceptable corrosion-

resistance under the contemplated operating conditions. However, with appropriate thickness allowances, general (uniform) corrosion of carbon and low-alloy steels for pressure vessels would not present a problem, other than perhaps that of iron-to-system release, in the operation of water-cooled nuclear reactor systems. The difference in corrosion behavior of the plain carbon and the low-alloy steels with up to 5% chromium is insignificant.

No noticeable effect has been found on the corrosion of plain carbon and low-alloy steels as a function of temperature in the range 500 to 600°F. However, at temperatures around 140°F, when the reactor is shut down and when oxygen is readily available to the system, the corrosion rate may be as high as 10 to 15 mpy. The water velocity at which carbon and the low-alloy steels are susceptible to erosion-corrosion effects has not been established, but it is known that velocities up to 35 fps are below the range where effects occur.

There does appear to be an effect of oxygen on the corrosion behavior of carbon and low-alloy steels, particularly in low-temperature water where the rate is appreciably high. Some differences in behavior, however, have been observed by various investigators in high-temperature water that depend on the level of oxygen content. At high-oxygen concentration levels, better behavior has been observed than at lower oxygen levels. In neither case is the rate excessive. The role of dissolved hydrogen has not been definitely established, but there is evidence that in neutral water, the addition of hydrogen suppresses corrosion attack noticeably.

Water pH, as mentioned above, has been found to exert a rather marked effect on the corrosion of carbon and low-alloy steels. Corrosion rates decrease as the pH is raised from the range 7.0 to 9.5 to the range of 10.5 to 11.5. Tests have shown that at the higher pH, generally obtained by the addition of lithium hydroxide, the steady-state rate after 10,000 hr is about 0.1 mpy.

Pitting of pressure-vessel materials, such as the carbon and low-alloy steels, does not appear to be a problem at operating temperatures of a nuclear reactor system, but it is highly likely that some pitting will occur during reactor startup and shutdown periods despite the high

resistivity of the water. It has been determined experimentally that pits formed in room-temperature water are not intensified or accelerated during subsequent operation in high-temperature water. Once the high-temperature film is formed on pressure-vessel materials, appreciable protection is afforded against the formation of pits during later exposure to room-temperature conditions. As best as can be determined from observations of experimental data, pitting does not present any serious problems so far as depth of penetration is concerned.

The severity of both crevice and galvanic corrosion (the latter when carbon or low-alloy steel is coupled to a more noble material, such as austenitic stainless steel) is greatly diminished as the dissolved oxygen content of the water is decreased. Galvanic corrosion, as might be expected to occur in a specific case where a defect in a stainless steel cladding over a carbon steel or low-alloy base metal would expose the latter to the aqueous environment, would be greatly lessened by the high resistivity of the water.

Stress-corrosion cracking of the carbon or low-alloy steels in water-cooled reactor systems does not appear to be a problem simply because no mechanism exists whereby concentration effects in water environments could produce sufficiently high alkalinity ranges to induce cracking. Experimental data for specimens stressed in water systems at pH 10.2 to 11.2 show no cracking after periods as long as nearly three years during reactor preoperational and operational times.

Austenitic stainless steels used as a cladding material for nuclear pressure vessels present no problems so far as general pitting, crevice, or galvanic corrosion are concerned. Corrosion rates under a wide variety of conditions are about 0.1 mpy. Stress-corrosion cracking susceptibility remains a constant threat in the case of inadvertent admission of chloride ion to the aqueous system. However, except for a few specialty items, such as materials of spring temper, stress-corrosion cracking is not known to be a problem in primary water systems.

2.4.3 Hydrogen Embrittlement

Some metals, when stressed, crack on exposure to corrosive environments, but corrosion is not a necessary part of either crack initiation or crack growth. Examples of this kind are therefore not properly called stress-corrosion cracking, despite certain similarities. For example, a stressed martensitic 12% Cr-Fe stainless steel in dilute sodium chloride solution may crack after several months of exposure or, if immersed in dilute sulfuric acid, may crack within less than 5 min. The failures have the outward appearance of stress-corrosion cracking, but, if the alloy is cathodically polarized, cracking still occurs.

The evidence in numerous cases is that the cracking is caused by hydrogen entering the metal either through a corrosion reaction that liberates hydrogen at the surface or by cathodic polarization. Steels containing interstitial hydrogen are not always damaged. They almost always lose ductility (hydrogen embrittlement), but only under conditions of sufficiently high applied or residual stress does cracking take place. Failures of this kind are called hydrogen stress cracking or hydrogen cracking.

An analysis of the available data shows that it is highly unlikely that pressure vessels fabricated from low-alloy steels will undergo hydrogen damage such as embrittlement, blistering, or fissuring from service conditions encountered during operation of water-cooled nuclear reactor systems. This does not appear to be the case, however, for pressure vessels fabricated from plain carbon steel. In the case of plain carbon steel the corrosion rate would have to be on the order of less than 0.1 mpy to insure protection from the damaging effects of hydrogen produced from the corrosion reaction.

The major source of hydrogen in a water-cooled nuclear reactor system operating at temperatures between 500 and 600°F has been established as that produced by the corrosion reaction between the water and the carbon steel or low-alloy steel pressure vessel. In the case of the Yankee Reactor, for example, it was shown that at operating temperatures and coolant conditions, the corrosion rate and the diffusion rate of

hydrogen through the vessel wall are such that the maximum hydrogen concentration in the steel of the lower head is approximately 0.3 ppm. This amount is at least an order of magnitude below the concentration that could cause reduction in ductility even at low temperatures. The partial pressure of hydrogen equivalent to this concentration was determined to be only 21 psi, which is not enough to cause any concern about decarburization reactions. Furthermore, it has been shown from experience that no permanent damage to steels of low-alloy types, such as A 302 grade B, has been caused by even high pressures of hydrogen at temperatures below 600°F. During reactor shutdown, the hydrogen concentration will not change appreciably in the steel, so a hydrogen damage problem is most unlikely.

The literature states that hydrogen damage is most likely to occur in high-strength steels. In steels, such as A 302 grade B and other low-alloy compositions, where the tensile strength is on the order of 80,000 psi, hydrogen embrittlement is rarely encountered. In addition, these low-yield-strength steels are stressed to values around two-thirds of the yield strength at operating conditions. In contrast, the delayed-failure mechanism of hydrogen embrittlement requires very high stresses to become operative, even in the high-strength steels.

Finally, in instances where a defect exists in a low-alloy steel pressure vessel clad with austenitic stainless steel and where the defect extends into the base metal, the stainless steel cladding would serve as a cathode, and any corrosion-generated hydrogen would be discharged on the stainless steel surface. The latter is immune to hydrogen forms of damage under conditions encountered during nuclear-reactor operation. As has been clearly shown in the literature, it is quite difficult to create indications of hydrogen damage in the fully austenitic stainless steels. Only by extremely severe treatment, such as cathodic charging in poisoned acid solutions, can some signs of hydrogen damage be observed. Such treatments are indeed quite removed from conditions encountered in the operation of water-cooled nuclear reactor systems.

2.4.4 Radiation Effects

Nuclear reactor pressure vessels are exposed to an environmental condition that is almost exclusive to the nuclear energy field, bombardment by high-energy particles. Prior to the advent of nuclear energy, the materials engineer was concerned with environmental conditions such as temperature, stress, strain, and various gaseous and liquid media. The nuclear engineer has the same environmental problems and must consider, as well, the effects on materials properties of bombardment with high-energy nuclear particles.

The major irradiation-induced changes in the mechanical properties of pressure vessel steels are brought about by the displacement of atoms within the metal structure by fast neutrons. The primary collision of a fast neutron with an atom has a high probability of transferring enough energy to the atom to displace the atom from its lattice site. This leaves a vacancy in the lattice. The neutron continues to displace atoms either until its energy is dissipated or it escapes from the material. A secondary effect results from the energy imparted to the "knock-on" atom. This atom collides with other atoms in the lattice, transfers energy to them, and removes them from their lattice sites. Finally, these "knock-on" atoms come to rest either in vacant lattice sites or interstitial positions. These lattice defects, vacancies, and interstitials can be randomly distributed in the material or concentrated in small regions termed "clusters" or "spikes." In addition, the capture of a thermal (or epithermal) neutron by a lattice atom can result in the emission of a gamma photon or particle of sufficient momentum that the atom will be displaced from its lattice site by recoil. This effect is, however, not considered significant in power reactor pressure vessels.

Another effect of neutron irradiation may be the transmutation of one element to another element. Such effects are regarded as of minor significance in pressure vessel steels.

At the operating temperatures of nuclear power reactor pressure vessels, many of the defects will be mobile, and annealing of the radiation effects may occur. However, in certain temperature ranges, an excess concentration of lattice vacancies in a radiation flux can accelerate

diffusion-controlled metallurgical reactions. Effects of such reactions in pressure vessel steels have either not been observed or not recognized as such.

The defects introduced in metals by nuclear radiation can alter mechanical properties, such as flow stress and fracture toughness, to a considerable extent. Even with this brief review of the mechanisms of radiation effects, it is obvious that the critical factors determining radiation effects in steels include composition, metallurgical structure, neutron energy distribution (spectrum), total neutron exposure (dose), and exposure temperature and may include rate of bombardment (neutron flux) and stress.

2.4.4.1 Effects on Mechanical Properties

Radiation effects on the physical properties of metals, for example, electrical and thermal resistivity, density, and elastic moduli, have been observed and studied in detail. The primary objective of these physical property studies has been to understand the mechanism of interaction of radiation with atoms of a solid and the effect of various lattice defects on metal properties. Physical property changes resulting from irradiation are rarely of engineering significance above room temperature.

The mechanical properties of metals, however, may be modified by nuclear radiation to a degree that is of considerable engineering significance. The basic cause of most radiation-induced mechanical property changes is generally considered to be the interaction of dislocations with the lattice defects, vacancies, clusters, spikes, dislocation loops, etc. introduced by radiation. Dislocation motion in the metal lattice is either prevented or impeded by these defects and the observed result is an increase in the flow stress or yield strength of the metal. Other mechanical property changes may be various manifestations of this primary effect.

Accompanying the increase in yield strength is a concurrent but generally lesser increase in ultimate tensile strength. As a result, the ratio of yield strength to tensile strength tends to approach unity. Yield-to-ultimate strength ratios above 0.95 have been observed in steels

irradiated to 7×10^{18} neutrons/cm^2 ($E > 1$ Mev) at less than 400°F. Irradiation to greater than 1×10^{20} neutrons/cm^2 was required to reach a ratio of 0.95 when the exposure temperature was 550°F. Ductility parameters generally are decreased by irradiation. The uniform elongation (strain prior to onset of "necking") is decreased most rapidly with lesser decreases in total elongation and reduction of area. Significant decreases in reduction of area generally occur only at very high neutron doses. Irradiation decreases the rate of work hardening at a given strain and the value of the work-hardening exponent.

The brittle failure of large steel structures is a problem that has attracted the attention of engineers and scientists to an ever-increasing extent in the past two decades. The dramatic failures of a number of merchants ships, bridges, pressure vessels, pipelines, and storage tanks by brittle fracture have been widely discussed. The investigations and analyses that followed these incidents showed that the origin of the failures lay in the tendency of a broad class of metals and alloys to exhibit low-temperature brittleness. This tendency is increased as a result of exposure to radiation, and hence the possible embrittlement of reactor pressure vessels in service has been a matter of concern.

This radiation embrittlement phenomenon is manifested, among other ways, by a shift in the brittle-to-ductile transition, or nil-ductility transition (NDT), temperature. Data with which to factor the NDT temperature shift into design considerations with a high degree of confidence have not been established. What have been commonly used in predicting this shift as a function of integrated neutron exposure are compilations of experimental results obtained for a wide variety of conditions.

The temperature at which the ductile-to-brittle transition takes place is not an inherent constant of the material. Instead, the ductile-to-brittle transition temperature depends upon the type of test used to measure it and upon the specimen geometry. The transition temperature usually increases with the loading rate and the triaxiality of the stress state to which the sample is subjected. Many tests have been devised to evaluate the ductile-to-brittle characteristics of metals. The Charpy V-notch impact test has been used for most of the studies of radiation effects on transition temperature. Most of the other test methods

require specimens of substantial size that are too large to be practical for exposure in a nuclear reactor. The transition temperature measured by the Charpy V-notch impact test has been correlated with service performance in a number of cases. The increases of transition temperature with increasing neutron exposure are apparent as are the variations of radiation sensitivity of different steels and even of steels of the same grade.

Several methods are used to apply available data on the radiation-induced transition temperature shift to nuclear pressure vessel operation. The simplest method is to use the upper bound of all the experimental results to establish operating limits for the pressure vessel. Some advantage may be gained by using the upper bound of experimental results for the particular grade of steel used for the pressure vessel and for the operating temperature of the pressure vessel. If irradiation data are available for the heats of steel, heat treatments, and temperature of irradiation that correspond exactly to the particular pressure vessel, these data may be used to establish operating limits for the reactor. Lastly, samples corresponding exactly to the pressure vessel are irradiated near the pressure vessel wall of the particular reactor. This last method, termed "surveillance testing," eliminates most of the uncertainties inherent in the other methods. One drawback of surveillance tests is that the data are available only after a considerable period of operation of the reactor.

The safety analyses of many nuclear pressure vessels are based on the Naval Research Laboratory's fracture analysis diagram. A major parameter in this analysis is the NDT temperature of the steel as experimentally determined by the drop-weight test. Although most radiation effects data on notch ductility have been obtained from Charpy V-notch impact tests, the Charpy V-notch transition temperature has been correlated with drop-weight NDT temperature over a range of temperatures and neutron exposures up to 5×10^{19} neutrons/cm^2 for a variety of steels.

The phenomena of fatigue cracking and failure of metals must also be considered in many structures and components, including nuclear reactor pressure vessels. The ASME Boiler and Pressure Vessel Code, Section III, incorporates specific methods of fatigue analysis based on test

data for unirradiated steels. The specified methods are based on strain-controlled fatigue data. While a considerable body of strain-controlled fatigue data is available for unirradiated pressure vessel steels, only a small body of fatigue data is available for irradiated pressure vessel steels.

In unirradiated steels the high-cycle fatigue strength is related to tensile strength (higher tensile strength materials have higher fatigue strength), and low-cycle fatigue strength is governed by ductility (high-ductility materials have higher fatigue strengths in this range where plastic flow occurs during each fatigue cycle). Since neutron irradiation of steels increases yield and tensile strengths and decreases ductilities, it would follow that fatigue strengths would be increased in the high-cycle range and decreased in the low-cycle range. However, irradiation tests conducted to date have not yielded results consistent with this hypothesis.

On the basis of the small body of data available on fatigue properties of irradiated pressure vessel steels, the radiation-induced changes in fatigue strength or life tend to be rather small, and in no case has the observed fatigue life been less than three times the allowable design life permitted by the Code. However, the data are not conclusive and additional study appears warranted. One particular area of ignorance is the effect of irradiation on fatigue-crack growth rates. Such information is necessary for predicting the growth of fatigue cracks from preoperational defects, as well as the initiation and growth of fatigue cracks.

There are no reported data on the creep or stress-relaxation properties of pressure vessel steels for the temperature range in which water-cooled nuclear reactor pressure vessels operate (400 to 600°F). This situation is readily understandable for several reasons:

1. Creep, creep rupture, and stress relaxation are observable in unirradiated steels only at temperatures several hundreds of degrees above the operating range or at stresses considerably higher than those that exist in these pressure vessels.

2. In this low-temperature range, creep and stress relaxation are governed by yield or flow stress. Since yield and flow stresses are

increased by irradiation at these temperatures, it follows that creep and stress-relaxation rates should be lower in irradiated steels than in unirradiated steels.

3. Creep ductility could, in view of decreased tensile ductility, decrease as a result of irradiation. However, the magnitude of tensile ductility changes does not indicate any problem of creep rupture of reactor pressure vessels at operating conditions.

In the current state of the art, the internal surfaces of light-water reactor vessels are clad with stainless steel weld overlay. Although there are no radiation data for overlays per se, the data available on welded stainless steel indicate that irradiation will not adversely affect the serviceability of commercial water-cooled reactors for present or contemplated operating conditions.

2.4.4.2 Fracture Mechanics

In the design of nuclear reactor pressure vessels, one of the modes of failure that must be considered is brittle fracture. One method of insuring against brittle fracture is the imposition of regulations based on a ductile-to-brittle transition temperature. However, there are limitations to the application of transition temperature concepts to large, heavy-section structures such as nuclear reactor pressure vessels, and there is a real need for more quantitative methods that can be incorporated into design procedures. The approach known as fracture mechanics has received the most attention by theoreticians, experimentalists, and designers. Considerable success has been achieved with this approach for structures built of materials with low ductility.

Several types of specimens are being used by various researchers to determine the effects of neutron irradiation on fracture mechanics properties of pressure vessel steels. Some of these are the single-edge-notch (SEN) specimens being used by the U.S. Naval Research Laboratory, the double cantilever beam (DCB) being used by the Pacific-Northwest Laboratories of Battelle Memorial Institute, and the wedge-opening-loaded (WOL) specimens being used by the Westinghouse Atomic Power Division and Bettis Atomic Power Laboratory. Data reported on the irradiation of fracture mechanics specimens indicate that the temperature shift at a

low value of plane-strain toughness (K_{Ic}) and a low level of observed Charpy V-notch energy correspond closely.

The increasing activity in the measurement of plane-strain fracture toughness of irradiated steels, coupled with anticipated improvements and extensions of fracture mechanics methods to more ductile steels, may provide more quantitative design and analysis procedures for insuring against brittle failure of nuclear reactor pressure vessels.

2.4.4.3 Critical Factors

A number of factors influence the mechanical property changes resulting from irradiation of metals. Attempts to isolate these factors and obtain general relationships have been largely unsuccessful. Material parameters such as composition and metallurgical structure and exposure parameters such as time-integrated fast-neutron flux and temperature are all interrelated. In addition, the relationships between flow and fracture properties are not thoroughly understood for unirradiated steels. For these reasons, the study of radiation effects is a very complex endeavor. The information on the influence of the various factors in radiation effects is largely empirical, even though there are theoretical bases for interpretation of many of the effects.

It was realized at an early stage of radiation effects studies that radiation-induced changes in mechanical properties were not linear functions of the time-integrated neutron flux (also called dose or fluence). The precise relationships of the increases in tensile yield strength and ductile-to-brittle transition temperature with neutron dose have been and still are the subject of some discussion. However, for the range of neutron doses of interest with respect to commercial power reactor pressure vessels, the various proposed relationships predict nearly the same property changes.

Research groups studying the effects of neutron irradiation on mechanical properties of pressure vessel steels have conducted most of these studies in neutron fluxes several orders of magnitude greater than those to which reactor pressure vessels are exposed. While the accelerated accumulation of neutron exposure is necessary in order to complete research programs in reasonable time periods, there exist questions

regarding the application of the results to prediction of the properties of pressure vessel steels exposed to long-time low neutron fluxes. Theoretical studies have indicated that the neutron-flux (dose-rate) and neutron-energy spectrum differences between test reactor facilities and power reactor pressure vessel locations may be of sufficient magnitude to affect the applicability of test reactor program results to power reactor operation. An interim method of avoiding these problems is the surveillance program discussed in Chapter 10.

Study of flux (dose-rate) effects has been difficult because reactor facilities that provide widely different neutron fluxes usually have quite different neutron spectra. Thus, flux and spectrum effects are usually encountered in combination, and separating them is most difficult.

At the present time the radiation damage suffered by a particular steel in a given neutron spectrum in a given exposure time can probably be predicted within a factor of about 3 by comparisons with data obtained on specimens of an identical steel irradiated in a very different spectrum. Much progress has been made toward defining the neutron spectra in various reactor facilities, but more information about the nature of the damage produced must be obtained. Computer studies of radiation damage show much promise, but more basic information about interatomic potentials and interactions of defects in metals is required for input to these programs.

Radiation-induced mechanical property changes are temperature dependent. At moderately elevated temperatures many of the defects caused by radiation are mobile, and annealing of the radiation effects may occur. Vacancies are mobile at the operating temperatures of nuclear power reactor pressure vessels and will diffuse to dislocations, grain boundaries, and inclusions or will coalesce to form larger lattice defects. In addition, the larger defects will grow by vacancy diffusion at the expense of the smaller defects, and the total effect can be strikingly similar to aging and overaging in a precipitation-hardenable alloy. The temperatures at which the major portion of radiation-induced mechanical property changes are annealed or recovered are generally lower than for recovery of cold work. In fact, the temperature range for the recovery

of the major portion of radiation effects is also the temperature range in which most commercial water-cooled nuclear pressure vessels operate. Thus there are radiation damage and at least partial recovery of the effects occurring simultaneously in the nuclear pressure vessel. This combination of effects has been observed and studied both in accelerated irradiations in test reactors and in surveillance programs.

The effects of irradiation of a specific alloy at a given exposure temperature can, at present, be determined only by irradiation test. There is some evidence that radiation-induced changes of tensile properties are related to changes of transition temperature and, further, that temperatures for "simultaneous recovery" of tensile properties and transition temperature are also related. However, some studies have shown that tensile properties and transition temperature do not always recover at the same temperatures. Yield- and tensile-strength recovery may require exposure temperatures 100°F higher than required for transition-temperature recovery.

A number of studies have been conducted in which attempts were made to determine the roles of composition, metallurgical structure, and heat treatment in radiation effects. A study of medium- and high-strength steels led to the following conclusions: (1) the higher strength steels exhibit a general trend toward lower initial NDT; (2) along with higher strength and lower initial NDT, there is also a tendency for smaller radiation-induced increases in transition temperature; (3) a marked and progressive advantage in terms of lower radiation embrittlement is observed with the higher strength steels irradiated at 550°F; and (4) there appears to be a general tendency for earlier saturation of radiation embrittlement with increasing strengths; this is particularly marked for an irradiation temperature of 550°F.

Other studies indicate that the finer metallurgical structures lead to lower radiation sensitivities. The predominant factor appears to be the cooling rate from austenitization temperature. Composition variables appear to have an indirect influence on radiation sensitivity, primarily by altering the metallurgical structure attainable with a given cooling rate from the austenitization temperature.

Because the extent of steel embrittlement due to radiation can be quite large, several studies have been conducted to assess the possibilities of embrittlement relief by means of thermal annealing cycles. The majority of these studies have been for single annealing cycles following irradiation. A few studies have included reirradiation after annealing and multiple irradiation-annealing cycles. A number of factors are operative in determining the effectiveness of postirradiation heat treatment. These factors include neutron exposure, the material, exposure temperature, and annealing temperature and duration.

Although striking recovery of mechanical properties has been achieved through postirradiation annealing, some studies have shown a serious reembrittlement phenomenon. Therefore, the measures required to accomplish full restoration of properties remain in doubt to a great degree.

The effects of temperature on radiation-induced property changes in pressure vessel steels are complex. It is hoped that study of postirradiation annealing kinetics and irradiation at elevated temperatures will lead to an understanding of radiation effects and recovery. Such an understanding should permit the prediction of properties for the more complex cases of intermediate annealing and changing operating temperature.

There exist fewer data on radiation effects in weld metal and weld heat-affected zones than on plate materials. The major portion of this information indicates radiation-induced transition temperature shifts of the same magnitude in welds and heat-affected zones as has been described for plate materials.

While the results of irradiation studies conducted to date do not permit prediction (in a satisfactorily precise manner) of the property changes of a given alloy heat treated in a specific manner and exposed to a particular nuclear environment, the probable direction of further research is evident, and there is considerable promise that materials can be produced that are insensitive to radiation effects at the operating temperatures of nuclear power reactor pressure vessels. Until such materials can be consistently produced, the irradiated properties of a pressure vessel material (plate, forging, weld, or heat-affected zone)

must be determined either in a test reactor study or surveillance program, or the most pessimistic results must be considered in design and operating procedures.

2.5 DESIGN

The publication of Section III, Nuclear Vessels, of the ASME Boiler and Pressure Code brought about an emphatic change in philosophy in the role and tools of design of nuclear pressure vessels. Previously design was largely accomplished by the adherence to semiempirical code rules and by evolutionary solution to problems by a combination of rigorous and nonrigorous analytical solutions, experimental techniques, or related experience in actual fabrication of vessels. In its new role, design is intended to give an appraisal in depth of the stress and/or strain state with time for the projected loading history in order to evaluate all the failure modes and to select materials to accommodate the expected behavior. However, Section III of the Code was not devised nor intended to serve as a comprehensive handbook of analysis for all conceivable loadings and environmental conditions but rather to establish the minimum requirements that must be met to assure a safe and reliable design. Analytical treatments are provided, which although not always the most rigorous available, were intended to provide adequate conservatism coupled with the desirable element of increased simplicity of solution. In its present form, Section III guides the designer toward sophisticated solution of stress problems but allows for pragmatic approaches, since rigorous theoretical solutions are not always available.

In the broad context, pressure vessels are subject to the following failure modes: (1) excessive plastic deformation, including plastic instability and buckling, (2) cracking-leakage or brittle fracture due to initial flaws or flaw growth by fatigue or corrosion, (3) elastic deformation, including buckling, and (4) excessive creep deformation or creep rupture. In the specific context of light-water reactor vessels, Section III provides partial analytical treatments for the solution of only the first two categories of problems. Analytical treatment is provided only

for crack propagation by fatigue; nothing is provided to assist the designer in coping with brittle fracture. The geometries presently used and envisioned are not believed subject to elastic instability, and the present and immediately forecasted temperature operating conditions do not present a creep problem. Nonetheless, development trends toward the use of higher strength steels, thinner sections, larger sizes, and higher operating temperatures could require the consideration of these failure modes also. The design analyses required by Section III to cover conditions for the first two failure modes are based on the following premises:

1. The materials of construction are ductile and retain significant ductility throughout the operating history.

2. The maximum shear stress theory (Tresca theory) describes the limiting or ultimate loading possible.

3. The general theory of elasticity, special cases thereof, and approximate strength of materials solutions describe the state of stress.

4. The states of stress may be categorized as primary, secondary, and local or peak so that elastically calculated stresses exceeding the yield for the latter two categories may be accommodated by material ductility, and a consequent "shakedown" to a stable elastic condition occurs.

5. The adequacy of protection against fatigue failure may be analyzed by the determination of peak stresses, application of the peak stresses to a modified Goodman diagram using Miner's hypothesis, and comparison with strain-controlled fatigue data.

6. The approximations of thin-shell theory, discontinuity analysis, and linear superposition of stresses are valid and conservative.

7. Experimental analyses are to be performed to verify that otherwise unverified approximate analytical solutions are conservative.

8. Provision shall be made for deterioration of materials due to radiation, material instability, and loading effects such that the preceding assumptions are always valid.

Our review of the efforts by the current systems designers and pressure vessel designers to implement the design rules of Section III have led us to conclude that, in general, an honest and systematic effort is made to comply with Code intent. Also it appears that the vast majority

of problems encountered with current pressure vessel concepts may be adequately handled with current rules. Notwithstanding this generally favorable conclusion, we believe that a number of potential problem areas exist with respect to the definition of loading conditions, implementation of Code analytical and experimental analyses, and in the review of the design effort. We also recognize that vigorous efforts are under way by Code committees, by industry groups, and by AEC sponsored organizations to deal with many of these problems. The subsequent descriptions of the problem areas therefore primarily serve to identify the weaknesses and not to indict the present state of technology nor those who employ it.

2.5.1 Definition of Loading Conditions

Obviously, the most rigorous and careful analytical stress analyses would be to no avail if the basic character of the loading conditions were wrongly assessed or interpreted. In general the loading conditions described by the system designers appear to be quite conservative for the temperature and pressure cycles associated with base-load and load-following plants.

Definitions of transient conditions that give rise to thermal and pressure loading present one of the greatest problems of communication between the systems designers and the vessel designer. Some clearly unambiguous format needs to be developed to assure accurate statement of the problems.

There has been considerable recent interest in the probability and consequences of impact or pressure-pulse loadings resulting from accident conditions. Analyses of such loads are not included in the present technology. Neither the probability, character, nor structural response to such loadings is presently known. Whether methods should be developed by the Code for analyzing such loading depends upon study of the presently unsubstantiated relevancy of the problem.

2.5.2 Analytical Analyses

In order to comply with the rules of Section III, the designer must perform a complete stress analysis. However, rigorous elastic solutions are not available for many areas; for example, they are not available for nonradial and cluster nozzles and nozzles in cylinders, and therefore approximate solutions must be used. The consequent designer's dilemma is that although a vast body of technical literature may be available and may pertain to the solution, there usually is little evidence as to the correlation of such analytical approaches with experimental analysis, and therefore there is no basis for judging the conservatism of the approach. The current vigorous effort by the professional societies to identify the most useful and important contributions should be emphasized. The strong and vigorous program for theoretical analyses of pressure vessels should be continued. Areas such as nozzle-to-cylinder attachments and nozzles attached in clusters to vessels are currently of prime importance. However, other asymmetric configurations, such as a nozzle closely attached to a spherical head-to-cylinder junction, occur in almost every design. Such problems should also be covered in the general outline of analytical work to be done. Unfortunately, these more complex problems must often await the successful analysis of the simpler problems currently being studied. In addition, the validity of linear superposition of stresses and discontinuity analyses for the massive sections now employed should be reexamined, and this approach should be reviewed for conservatism.

Studies of welds, heat-affected zones, out-of-roundness, biaxiality of stresses as related to fatigue, load-cycling rates, and slow growth of cracks by fatigue should be continued and implemented. A vigorous effort should be applied to the analysis of brittle failure. Although the Griffith-Irwin theory appears to be adequate for brittle materials and near brittle materials (highly irradiated), no adequate treatment exists for high-strength steels with significant ductility. Some existing evidence indicates that the presently used semiempirical fracture analysis diagram approach to fast fracture prevention may be nonconservative for fixed-load energy-release-rate conditions.

The study of strength of pressure vessels below the transition temperature where brittle failure could perhaps occur should be continued. In the case of ductile fracture, an extension of the fracture mechanics approach probably has the best chance of providing a reliable estimate of strength. Section size and stored energy should be considered in the transition temperature evaluation of pressure vessels.

The behavior of flaws in the presence of different geometries, residual stresses, stress gradients, yielding, and irradiation should be studied as a function of size. In particular, fracture mechanics should be extended to include these variables.

The hydrotest and "warm prestressing" should be more carefully evaluated as means of preventing failure. In particular, the superposition of loadings on nozzles as a part of the hydrotest should be considered.

2.5.3 Experimental Analyses

In the present state of the technology, experimental analyses are primarily limited to techniques employing strain gage, three-dimensional photoelasticity, and photostress techniques. Unfortunately, much of the current experimental information is inapplicable due to the lack of recognition that the foregoing techniques should be complementary and particularly that the placement of strain gages must be determined by the part geometry and stress-field prediction of the related techniques. Also, little recognition has been given to the gross deviations that normal vessel tolerances may cause compared with those in models having closely controlled tolerances. Such lack of refined techniques causes much information to be doubted.

The current experimental stress analysis efforts should be continued and expanded. Such efforts not only give data to support the theoretical analyses but also present interim information for design purposes. The experimental effort should be expanded to include the more common configurations for which theoretical analyses are not currently available. These configurations include closely spaced and grossly asymmetric configurations (e.g., a large nozzle near a major junction), brackets, and general support arrangements other than skirts.

2.5.4 Stress Reviews

Section III of the Code should specify precisely what is acceptable as a stress report and what is not. Specifically, it is recommended that the stress report contain such details as would be necessary for a third-party review. Also, the fabricator should give evidence as to the accuracy of his analyses. For example, most boiling- and pressurized-water reactor pressure vessels have nozzles that penetrate the cylindrical portion of the vessel. Only recently has a method existed for the analysis of such a design feature, and the procedure is not in common use. Short of an experimental analysis, it is difficult to say what would be acceptable for the stress report in this case.

To maintain a high quality of design and structural performance, it is recommended that a review of the stress report by a qualified engineer representing the system designer or owner be mandatory. Such a review should be timely so that recommendations by the reviewers could be incorporated into the design.

2.6 BASIC ASPECTS OF CRACK GROWTH AND FRACTURE

Strength failures of structures can be either of the yielding-dominant or the fracture-dominant type, and defects are of importance in both types of failure. The significant defects of concern in fracture-dominant failures are crack like in character. In fracture-dominant failures the size scale of the defects of major significance depends on the toughness of the material. For common structural steels, surface scratches, regardless of acuity, do not lower the strength of a tensile specimen unless the temperature at loading is far below the NDT temperature. The artificially introduced flaws used in fracture testing, for example, the Charpy V-notch, are indications of the significant flaw size for steels in the NDT temperature range when tensile stress equal to the dynamic yield stress is applied. Rapid crack propagation at smaller stresses or lower loading speeds would require cracks of larger size. At temperatures near or above the NDT temperature in the vessels of interest in

this report, a crack-like flaw of substantial size would have to be present in order for fracture to occur prior to general yielding. The size necessary for crack propagation is a function of toughness and average tensile stress.

Depending on the size and shape of a structural element and on its stress-environment history during service, a critical condition for crack propagation may develop gradually in the following ways:

1. crack growth by fatigue,
2. crack growth by stress corrosion (or hydrogen embrittlement), and
3. reductions of crack toughness, for example, by radiation damage.

It is unlikely that a crack large enough for propagation by a normal service load would be introduced during fabrication. In any case, the pressure vessels of interest are pressure tested at pressure levels larger than the largest expected during service. Thus, attention for fracture control should focus on achievement of a satisfactory time duration of fracture-safe operation relative to the three aforementioned conditions of crack growth or loss of crack toughness.

The most reliable indication of defects likely to cause serious fracturing of the pressure vessels of interest would be obtained through extensive testing of vessels of similar thickness, geometry, materials, and fabrication. Such a program would not, however, settle all doubts, since differences in design, size, location, and fabrication would result in conditions unique to a particular vessel. Unquestionably continued accumulations of experience will be quite helpful, but a requirement for nearly absolute fracture safety should be based on a very conservative fracture control plan. For such a plan it must be assumed that any crack-like defect which is plausible and which has not been proved absent by inspection may actually exist in the vessel. The plan must then establish methods of estimating fracture-safe life based on stable crack growth data, service environment, and service stress cycles. An additional degree of confidence can be predicted if the toughness and stress level at the end of the safe life correspond to a leak-before-break condition. A complete specification of such a fracture control plan requires a more detailed understanding of progressive fracturing than currently exists. However, present fracture mechanics technology

provides general features of the control plan and a number of answers that are of interest.

2.6.1 Linear Elastic Modeling of Cracks

The fracture behavior for which a suitable analysis is needed is termed progressive crack extension. The combination of local plastic strains, advance separations, elastic constraint, and tension near the leading edge of a crack may be sufficient, or less than sufficient, to cause sudden rapid spreading of a crack. If less than sufficient, that is, subcritical in character, plastic strain reversals near the leading edge may occur and cause stable growth of the crack. Onset of rapid crack extension provides a relatively abrupt end point for stable crack growth and initiation of sudden rapid expansion of the flaw. The environment, with or without fatigue assistance, may cause stable spreading of the crack.

Studies of running cracks have been conducted with a variety of techniques to measure crack speed and stresses near the crack. Progressive crack-extension behavior ranges from slow, stable extension through the fast, stable regime. At very high crack speeds a limiting velocity is observed, and then there are crack division tendencies when the tensile driving force is further increased. A single service fracture failure may exhibit all these crack-extension behaviors. In order to understand and prevent such fractures, appropriate use of experimental data from laboratory testing is essential. The characterization of these fractures should permit application of laboratory data to service components in the simplest adequate way. Linear-elastic fracture mechanics provides an appropriate and simple characterization method applicable to any component in which there is a reasonable knowledge of the stress distribution. With care the linear analysis method retains usefulness as the stress level approaches a general yielding condition. The method is not suitable for use at higher stresses.

For purposes of linear stress analysis, a crack is regarded as a flat separation bounded within the material by a leading edge that is approximated as a simple curve. At a relatively small tensile stress

across the cracked region, plastic strains are confined to a small zone at the leading edge of the crack. A stress-intensity parameter, K, is normally used to provide a simple characterization of the stress required to cause crack extension. The addition of subscripts I, II, or III indicates the mode of loading corresponding to opening (tensile), forward shear, and parallel shear, respectively. The value K_{Ic} indicates a critical value for onset of fast crack extension under an opening mode of loading. The use of a strain-energy release rate $\mathcal{G}$ corresponding to a K value is optional and equivalent.

The tensile crack stress field near the leading edge of a crack is regarded as either of the plane-strain or of the plane-stress type. The plane-strain model is three-dimensional, since the stress conditions are uniform in the z direction, parallel to the crack leading edge. The crack has a nominally elastically stressed zone, which is large compared with the size of the zone containing plastic strains. The plastic zone is then held within a plane-strain stress system. If a crack is presumed to be a through-crack with the leading edges right through the plate thickness, even if the plastic zone is small a plane-strain condition near the free surfaces is not possible and plane-stress exists.

2.6.2 Plasticity Analysis

Studies of fracture suggest that a close relationship exists between plastic flow properties and fracture. It is impossible to explore interests of this kind in a quantitative manner without the use of analytical models to define properties which can be computed as well as observed. Exact elastic-plastic solutions are not available for the tensile cracks of interest. Furthermore, structural metals contain fine-scale inhomogeneities, and this limits the realistic accuracy of any continuum mechanics representation. Despite these difficulties, significant progress has been made with the aid of several relatively simple analytical methods. These are the plasticity adjustment factor, the strip-yield zone concept, and the mode III elastic-plastic treatment.

2.6.3 Slow, Stable Crack Growth

In assessing the severity of flaws, the possibility of their growth to a dangerous size must be considered in assessing the safety of the structure. The effects of repeated loading, including cyclic thermal stresses, and/or environment must be considered.

The increment of crack growth experienced in a cycle of loading depends primarily on the stress-intensity factor range, ΔK, and secondarily on the relative mean value of the stress-intensity factor or relative mean load. The frequency of loading, plate-thickness effects, and processing of material are of secondary importance; however, they must be included in a refined analysis. Data, although meager, indicate that crack growth rates for A 302 grade B pressure vessel steels under zero-tension loading show similar behavior to those for low-alloy medium-strength rotor steels and high-alloy very-high-strength rocket-engine pressure vessels. Available data on A 302 grade B material indicate, however, that a simulated boiler-water environment increases the rate of fatigue-crack growth by a factor of 2.5.

2.6.4 Leak Before Break

The leak-before-break criterion was originally proposed in connection with fracture problems of steel solid-propellant rocket chambers. In this instance, leakage prior to catastrophic bursting was not of importance in the rocket applications. The criterion was simply a reasonable guess that adequate toughness would permit a crack twice as long as the plate thickness to be stable at a tensile stress equal to the yield strength of the material.

With reference to thick-walled reactor pressure vessels, the leak-before-break criterion can provide additional safety, since crack arrest is presumed to occur as the energy is expended in the pressurizing medium. In the case of thick-walled reactor pressure vessels, the influence of temperature elevation in terms of plane-stress toughening is gradual and not very large. No support can be found on this basis for a step-function diagram of the limiting allowable load based on a critical temperature.

The allowable load based on a leak-before-break approach would be one of gradual increase with temperature to the point where decrease of yield strength with temperature is a limiting consideration. It appears that the application of the leak-before-break criterion is possible; however, restrictions must be placed on allowable stresses, since the assumed defects are relatively large and no assumption is made with regard to the actual defects that would be established by inspection or testing.

2.6.5 Fracture Analysis Diagram

A number of tests of the transition temperature have received considerable use to provide fracture-toughness information. In view of the complexities of a transition-temperature toughness rating and with the aid of a collection of fracture-failure data, Pellini and his associates assembled guide lines for fracture-safe design in terms of their NDT type of fracture testing. The resulting Naval Research Laboratory's fracture analysis diagram was intended to provide guidance for fracture-safe design as nearly as possible without reference to loading speed, elastic constraint, and crack location, with only gross estimates of stress level. Cautions were provided for increases of plate thickness, low shear tear, strength, quality level of inspection, and opportunities for growth of large flaws under operating conditions.

Approximate methods applicable to low- and medium-strength steels can be followed to translate conditions such as the NDT temperature plus 60°F and the NDT temperature plus 120°F into the design stress level that would satisfy a leak-before-break criterion under dynamic conditions of loading. The practice appears conservative in reference to low-strength steels about 1 in. in thickness. The practice tends to become marginal for steels of that thickness with yield strengths above 100,000 psi and for low-strength steels with section thickness greater than 2 in. Large welded structures are generally designed for stresses below the yield strength and, often, service loads are essentially static. Hence, a large degree of success from use of the fracture analysis diagram would be expected and has been experienced.

Relative to the thick-walled pressure vessels of interest here, there is a major handicap to the use of the method because the NDT measurement points for tough steels of principal interest are too far below the range for service operation. A similar handicap would pertain to all the presently customary methods of toughness evaluations in terms of a transition temperature.

There is also a scarcity of K_{Ic} data for high-toughness steels except at low temperatures. Although higher temperature large-specimen data of the K_{Ic} type should be available soon, fracture-toughness information from direct measurement for high-toughness steels at temperatures above 200°F will probably require completion of testing plans based on one of the plasticity analysis methods previously discussed.

2.6.6 Recommendations for Fracture Mechanics Research

Sharp-notch tests of full section thicknesses should be performed over the design temperature range on the materials that are developed for service. The notches should be fatigued so as to obtain more exact conditions for fracture mechanics analysis. The tests should be both static and dynamic and instrumented for load and displacement and either crack-opening displacement or transverse contraction at the notch root. Since a limited number of tests of full-thickness specimens can be performed, tests of intermediate thicknesses, such as one-half or one-fourth, should be performed to determine a reasonable full-thickness correlation.

If full-scale vessel testing of representative thick material is to be conducted, a nozzle-to-sphere junction should be included, since the intersection region is considered to be the most critical in terms of the presence of defects. Further investigations of these regions should be conducted with models constructed of a brittle transparent material in which stable crack extension is assisted by moisture or a model constructed of a low-toughness metal in which stable crack extension is produced by fatigue. The residual compressive type of protection that might be provided in such complex regions from the overpressure testing method should be investigated.

The possibility of having microstructures at welded joints that give rise to low toughness cannot be discounted. Tests of welded joints or small-scale tests of the various sections of welded regions should be performed.

For corrosion considerations, a fracture-toughness stress-corrosion-cracking threshold level should be established for the materials considered for vessel fabrication. Determinations should be made for crack growth rates for fatigue under plane-strain and plane-stress conditions as a function of thermal and environmental conditions of interest. Hopefully, the fracture-toughness indices for corrosive environments will be very close to those determined with no provision for the additional environmental effect. However, if these effects prove to be limiting on fracture toughness, they must be considered in any design-life analysis.

At the present time, correlation studies between plastic flow properties and crack toughness need additional support from plasticity analyses. Plasticity investigations intended to assist extension of fracture mechanics toward basic factors on a finer scale should provide help in terms of better plasticity models. Computer calculations of plastic strain fields near a tensile crack should be undertaken to assist in the characterization work either in terms of a crack-opening displacement concept or along the lines of plastic instability.

The influence of irradiation hardening and embrittlement above a dosage of 10^{19} neutrons/cm^2 should be investigated for the influence of loading speed on fracture toughness and on isothermal strain hardening.

2.7 FABRICATION

The techniques employed in fabricating nuclear pressure vessels are not unlike those for heavy-walled vessels for the petrochemical industry. A superficial examination reveals that the same types of materials are used and that the same types of procedures are used for cutting, forming, welding, and machining. Also, the final general geometries may be quite similar. Such a cursory review, however, does not reveal that nuclear pressure vessels belong to a quality class primarily by virtue of the

refining steps taken throughout design, fabrication, testing, and inspection to assure that the final product is free from any deleterious fault. Such special care is reflected in Article 5, Fabrication, of Section III, Nuclear Vessels, of the ASME Boiler and Pressure Vessel Code and in the continuing review and revisions being made thereto by the Code committees.

Another subtle and yet significant fact is often overlooked in assessing the fabrication problems peculiar to nuclear reactor vessels; that is, the two current suppliers of shop-fabricated vessels have extensive backgrounds in the production of many similar vessels for the naval reactors program. This association with the naval reactors program has provided these companies valuable training for their personnel and has developed a demonstrated competence that few competitors newly arrived on the scene can match. In fact, a lack of similar experience to provide awareness of acute problems and a previous developmental solution thereto has no doubt been a major contributing factor in the unpleasant results experienced by vessel-fabricating firms no longer competing on the nuclear scene.

In addition, this previous and continuing association with the naval reactors program has developed an attitude toward quality control that is almost unique in the industry. There is a considerable effort expended by these fabricators beyond the requirements of the Code and also beyond the requirements of the customer. An example of this attitude is the continued complementary use of the vessel test plates formerly required by the 1965 Code Edition and subsequently amended by the winter 1966 addenda in favor of a welding materials test program. In many other areas, fabrication procedures are used that exceed the minimum Code and customer requirements not only to protect the fabricators investment but also simply to assure that the highest achievable quality is obtained.

The very fact that this vigilant attitude is manifested and doubtless required presents a potential danger in that the burgeoning industry may lead some, perhaps new, competitors in the field to conclude that all problems are solved and such care is passé. However, it is evident that one of the prices of quality and reliability in the nuclear pressure vessel field is eternal vigilance and that a constant reappraisal must be made of the fabrication procedures used and in the minimum standards

required by the Code. To this end Code strengthening in the following areas is recommended.

One of the present practices of the current fabricators is the comprehensive development of written procedures of all operations required for fabrication. In order to assure adequate quality control, we believe this should be a Code requirement.

Consideration should also be given to making mandatory the current practice of preheating prior to cutting or weld repair to avoid susceptibility to cracking. Also a review should be made of requirements to eliminate deleterious heat-affected zones resulting from severe cutting, and more thorough outlining of inspection requirements following the operation should be required.

Reexamination should be made of the possible deleterious effects of severe cold forming; for example, embrittling may follow such operations in subsequent heat treatments. As a consequence, further stipulations may be required in Code procedure-qualification requirements.

It is our opinion that some of the currently permitted nozzle joint designs are inadequate. A reexamination should be made to assure that every reasonable effort is made to provide a design that is amenable to revealing the flaws likely to exist by nondestructive testing.

Currently fabricators are running full-range Charpy curves on test sections from each plate to develop both the upper and lower shelf values. We believe that this practice, or at least the establishment of the upper shelf value, should be made mandatory in order to assure that the heat treatment has been satisfactory. There is evidence that plates may occasionally meet the impact test values presently required and yet have a low upper shelf value that indicates inadequate toughness.

2.8 QUALITY ASSURANCE

As has been previously discussed, perhaps the single most acutely significant facet of importance to nuclear reactor vessels is the initial establishment and continued enforcement of the goal of quality throughout the rank and file of a fabricator's organization. It has been repeatedly

demonstrated that adherence to minimal inspection and testing requirements as a final acceptance procedure will not assure quality. Rather this goal must be infused in the manager, designer, craftsman, and inspector alike.

A large portion of the total effort and cost of nuclear reactor vessels, much greater than for conventional vessels, is associated with quality assurance. This additional burden is generally acknowledged to be required to assure reliability in the interest of public safety. Our review of the current state of the industry convinces us that the present fabricators are well aware of this need. However, it is exceedingly important that this same principle be developed by others who may enter the field. The continued strengthening and updating of Code rules with advancing technology is necessary but not sufficient to implement this goal. Continued cooperation between the systems designer, fabricator, utility customer, and governmental regulatory and safety organizations will obviously be required.

2.8.1 Chemical and Mechanical Properties

We have been impressed that the current fabricators have developed a very significant body of information on quality control procedures required for materials and fabrication inspections and tests and their relation to design, but to a large degree this information may be uncorrelated. It is therefore not always clear that the present Code rules are the most meaningful method of assuring quality. In our subsequent criticisms, we recognize that the solutions may be found either in the development of information from the AEC-ORNL heavy-sections steel technology program and the PVRC industrial cooperative program and/or from the existing body of information. Our criticisms therefore underscore those areas where information must be available in the public domain to permit analyses and correlations required for development and revision of Code rules.

Information should be developed to determine macroscopically the distribution of chemical elements that are prone to segregate, for example, carbon, manganese, and silicon, from top to bottom and through the

thickness of heavy section plates for the materials of interest. Complementary with this study should be a correlation of the impact properties, with impact specimens being taken at locations adjacent to the drillings obtained for the chemical analyses. If an impact test does not correlate with the corresponding macroscopic chemical segregation analysis, microscopic study of the impact specimen should be made.

Similarly data should be developed or existing data used to analyze statistically the relevancy of the existing Code rules on the location and number of specimens for testing of mechanical properties, Charpy V-notch "fix" values, and tensile specimen size for both plates and forgings. An examination should also be made of what values of the upper shelf region of the Charpy curve are significant to assure adequate toughness.

There should be a reevaluation of the validity of using test plates of similar rather than actual heats for material test certification to resolve the question of segregation and variant chemistry. As has been previously discussed, since base metal is the predominant portion of an electroslag weld verification is needed that the normal variations in chemistry to be expected between heats are not harmful.

An unambiguous method of obtaining impact specimens of heat-affected zones needs to be devised. Ideally the specimen notch should be placed in the region possessing the poorest impact properties; however, Code rules presently permit the actual location to be determined at the discretion and integrity of the tester.

2.8.2 Flaw Detection

The techniques required by the Code in nondestructively examining the materials forms, welds, and fabricated components of nuclear pressure vessels are the same as those employed for conventional vessels, that is, ultrasonics, radiography, liquid penetrants, magnetic particles, and eddy current or other electrical means. Nuclear vessel inspection requirements are, however, more stringent than those for conventional vessels. It is also the general practice in many instances for the fabricator to exceed the Code requirements. This additional expenditure in

quality control often provides substantial monetary and time savings in that significant flaws are discovered early and eliminated before large investments in parts are made and possibly lost.

Although the inspection techniques employed are quite conventional and have sufficient inherent capability to reveal the significant flaws, there is occasionally a lack of appreciation that these techniques must be used in a complementary fashion and also that their use should follow any forming or heat-treating operation likely to initiate or propagate flaws. It also should be recognized that some fabrication procedures may require restrictions in order to make subsequent inspections meaningful. For instance, surface undulations or roughness must be controlled in order to prevent difficulties in radiography and ultrasonic testing. Also sandblasting for surface preparation and cleaning may be harmful in that the mechanical peening action may close flaws and thereby prevent detection by liquid-penetrant techniques. An additional difficulty is the lack of a calibration standard for magnetic particle and liquid-penetrant testing in the codes or standards or otherwise; unfortunately none appears to be readily available.

We recommend that the following specific points be considered in future Code revisions:

1. With regard to tubular products, the Code permits examination by either radiographic, ultrasonic, magnetic-particle, liquid-penetrant, or eddy-current methods. Since there are times in which a test may be applicable but inadequate or inappropriate, it appears that additional clarification or supplementary requirements by the Code would be beneficial.

2. Additional clarification is needed on the limits of acceptability of radiographic examination of tubular products with wall thicknesses greater than 1/2 in.

3. Consideration should be given to the additional requirement of ultrasonic testing of stud bolts.

4. Complementary inspection rather than a choice of either magnetic-particle, liquid-penetrant, or ultrasonic methods would appear to be desirable to assure that all significant flaws are revealed.

5. Uniform methods of testing or demonstrating the competence of nondestructive testing operators need to be devised.

2.8.3 Fabrication

The implementation of all Code process requirements, such as those for forming, heat treating, testing, examining, etc., is the province of quality assurance in fabrication. Although the Code stipulates many requirements with regard to materials, fabrication processes, testing, and inspection, many other very crucial details supporting these Code requirements are matters of the individual fabricator's choice. For example, detailed Code postweld heat-treatment requirements obviously imply a properly designed and instrumented furnace having adequate control of the desired temperature and assurance that undesirable temperature gradients do not exist. Also detailed requirements are provided as to acceptable deviations from true part geometry; however, the actual means employed for mensuration and the attendant accuracy thereof are left to the discretion of the fabricator. These Code omissions are intentional and are simply a recognition that undue encroachment has undesirable economic and legal implications without a commensurate increase in quality. By philosophy the Code generally is comprised only of those rules absolutely essential for adequate quality and therefore requiring uniform industry compliance.

Nevertheless, the attendant host of implied, unspecified, but required details for nuclear vessels presents a very demanding necessity. The demonstrated competence to deal with these problems is limited to only a few companies. Assurance of manufacturing competency is at present accomplished by limiting bid invitations to a select group of firms. Some study is under way to determine the possibility of establishing standards for manufacturers so that in the future a perhaps more rational basis will be available for judging competency.

One of the marks of manufacturing competency is the careful detailed preparation of all fabrication procedures. Such foresightedness and attention to detail has been a principal factor in eliminating major

blunders. As previously stated, we believe that such procedures should be mandatory provisions of the Code.

Another area of concern is the relevancy of present requirements of "authorized inspectors" as established by the National Board of Boiler and Pressure Vessel Inspectors with regard to nuclear pressure vessels. The existing requirements are heavily weighted toward the needs of Sections I and VIII rather than III. Consequently presently qualified inspectors may not have sufficient understanding of the design requirements and nondestructive test methods required for nuclear vessels. We therefore recommend the upgrading of qualifications of Code inspectors of nuclear pressure vessels to a level of competency achieved by professionally educated and experienced personnel. An effort in this direction is now under way.

2.8.4 Design

The role of design in quality assurance has been to a large degree discussed previously in Section 2.5. In addition to our previous discussions of analytical and experimental analyses and design review thereof, we would like to point out that the current provisions of Section III of the Code for rigorous analysis, with its attendant considerable effort and cost, also to a degree alleviate this cost burden because of the higher stress values permitted. In comparing the previous rules with those of Section III, it is clear that the new rules consider failure to be associated rarely with a nominal primary stress but rather with discontinuities, flaws, and/or associated secondary stresses, so the new higher allowable primary stress values should not necessarily result in a reduced margin of safety. Nonetheless, a considerable burden is placed on the designer with the increased sophistication of Section III to assure that quality is not sacrificed.

2.8.5 Inspection Methods — Capabilities and Limitations

An evaluation of the present methods of inspection leads us to conclude that they are generally capable of revealing significant flaws.

In addition, these methods also provide for the early rejection of defective materials and, as a curbing influence, enhance the production of relatively flaw-free welds and thereby minimize the amount of weld repair required. We would neither categorize, as some do, that the techniques approach infallibility nor, as others do, that they are grossly limited as to the type, size, and orientation of flaws that can be established. Rather it is clear that each method does have very definite limitations and consequently that complementary use of the methods is necessary for maximum effectiveness. We do emphasize that those who expect exact numbers and positive assurance of detectability will be disappointed, for the effectiveness of nondestructive testing in reactor vessel technology is a matter of probability and approximation, not certainty.

2.9 TESTING AND SERVICE PERFORMANCE SURVEILLANCE

Traditionally pressure vessels have been subjected to various tests and inspections throughout the course of their operating history to demonstrate that continued operation will not result in catastrophic failure. Most of the techniques currently employed for similar inspections and tests for nuclear pressure vessels are patterned after those employed in general pressure vessel use. The comparatively more critical function of nuclear pressure vessels and the greater attendant difficulty of inspection due to radioactivity following operation places even greater emphasis on the meaningfulness of these inspections and tests.

2.9.1 Hydrostatic Testing and Postoperational Hydrostatic Testing

Hydrostatic testing has had a long history of Code usage as a technique for inspecting pressure vessels. It usually is recognized as a useful leak and strength verification test and it may often serve to detect improper design, gross flaws, and faulty materials and to evaluate brittle fracture susceptibility. Its role has sometimes been described as beneficial in preventing brittle fracture by the mechanisms described as plastic reshaping, mechanical stress relief, stress redistribution,

notch nullification, or crack blunting and localized strain hardening, among others. On the other hand, it has been ascribed a detrimental role because of excessive deformations and metallurgical damage from overstressing, for example, embrittlement, as a result of the test. A review some years ago by the Pressure Vessel Research Committee educed that its beneficial effects warranted its continued use. More recently a considerable controversy has arisen over the possible merits of conducting "warm" or "hot" prestressing via hydrotesting at temperatures approaching operating temperatures. This type of test also is credited with possible metallurgical benefits or contrariwise with detriments that either prevent or lead to catastrophic failure.

We believe the excellent record of hydrostatic testing substantiates its use for preoperational testing. The potential promise of postoperational hot overpressure tests is sufficient to warrant a thorough study of the problems. Consideration for adoption as a Code or regulatory requirement should hinge upon a metallurgical and fracture analysis evaluation for each material of interest.

2.9.2 Postoperational and In-Service Nondestructive Examination

It is common practice to subject nonnuclear vessels to nondestructive examination at periodic intervals. The usual techniques employed are unaided or optically augmented visual and liquid-penetrant examinations. These same practices are to a large measure used or projected for use with nuclear vessels. Currently, heavy dependence is placed on visual examination.

Periodic examination of nuclear vessels is presently impeded to a great degree by (1) the requirement that inspection must coincide with scheduled reactor shutdown, (2) the fact that design of internal and external reactor core and/or vessel components impede or prevent access for inspection, and (3) the fact that the intense background radiation limits human access and restricts the application of visual techniques. These restrictions and the wide recognition of the inherent limitations of unaided visual examination have spurred a considerable interest in

developing techniques for performing more meaningful periodic examinations and/or continuous in-service examinations.

The most promising candidates for such examinations appear to involve some form of acoustic phenomena (either sonic or ultrasonic), although radiography and other methods have been considered. Conceptually, either fixed-probe or mechanical-scanning-probe acoustic systems appear feasible. Considerable development effort would be required before an operating mechanical-scanning-probe acoustic system could be applied as a standard test for postoperation examination. Some of the questions that must be answered or problems which must be overcome are listed below:

1. A quantitative determination is needed of the effect on ultrasonic penetration and propagation of the austenitic stainless steel weld-overlay cladding. This includes the effects of the attenuation of the cladding, the acoustic mismatch at the carbon—cladding interface, and the irregular surface of the weld-deposited cladding.

2. A method is needed for assuring consistent angles of incidence of the introduced sound beams.

3. Complex scanning requirements around nozzles due to joint configurations should be studied. This is especially important because of higher stress levels in these areas.

4. Consideration should be given to the probable requirement for removal of some of the internal components to allow scanning of the areas of most concern. This statement presupposes that the optimum scanning method would be from the interior of the vessel. The possibility should not be overlooked that the optimum scanning method could be from the outside of the vessel. This would require the capability of temporarily removing external insulation and shielding.

5. A method is needed for establishing bench marks for orientation and reproducing scans at successive inspections.

6. A method is needed for producing continuous records that can be maintained and compared with records from previous inspections. This requirement would coordinate closely with the previous one and both would be accomplished better with an automated system and thus less dependence on operator interpretation and recording.

7. Assurance is needed that ultrasonic techniques are adequate and sufficiently sensitive to detect and properly interpret flaws of concern at all suspected orientations in the thick pressure vessel sections being used or planned.

An alternate fixed-probe acoustic scheme can be developed as an active system in which the probe generates and receives energy or as a passive system in which the probe only receives the energy generated by other conditions. For both of these fixed-probe systems, further development would be required before an operating system could be applied as a standard test. Many of the questions that must be resolved are common to the scanning systems discussed previously. For convenience, the problems that seem to be pertinent are listed here, along with those peculiar to the fixed-probe systems.

1. A determination is needed of the effects on ultrasonic propagation of the weld-overlay cladding and the interface between cladding and carbon steel. Probably the probes would be affixed to the outer surface of the vessel.

2. Methods are needed for establishing bench marks for orientation and reproducing scans at successive inspections. This would be particularly important in the Dickinson system in which sound beam angles can be adjusted.

3. A method for producing continuous records that can be maintained and compared with records from previous inspections is needed. As mentioned earlier, this would coordinate closely with the previous requirement (No. 2) and both would be accomplished better with an automated system and thus less dependence on operator interpretation and recording.

4. Assurance is needed that the ultrasonic techniques are adequate and sufficiently sensitive to detect and properly interpret flaws of concern at all suspected orientations in the thick pressure vessel sections being used or planned.

5. Assurance is needed that the number, spacing, or position of the fixed probes is adequate to detect flaws of concern. This is particularly important around changes of section thickness and various penetrations such as nozzles.

6. A determination should be made of the effect of radiation and other environmental effects on the electrical or mechanical functioning of all components and constituents of the probes. If service life of the probes is significantly affected, means must be devised for removing the probes during reactor operation and reestablishing the probe position, orientation, coupling, calibration, etc., or the system will not be usable.

7. A determination is needed of the effect of radiation damage on the ultrasonic properties of the vessel materials, since it may influence the propagation of ultrasonic energy.

A considerable effort is also being expended on passive systems based on the phenomenon of acoustic emission. Detectors would be placed at strategic locations to monitor acoustic stress waves released as a consequence of metal deformation or crack propagation.

As with previously discussed systems, further development effort would be required before an acoustic emission system could be considered as standard for postoperation examination. Some of the problem areas are common to the other approaches and will be repeated here. The various considerations include the following:

1. There is need for introduction of stress to generate deformation or defect propagation which, in turn, may be detected by the passive probe system. For postoperation examination this could be accomplished during hydrostatic testing.

2. A determination is needed of the effect of nozzle and other penetrations on the propagation of the acoustic wave.

3. A determination is needed of proper number, position, and spacing of probes to assure detection of any stress wave originating within the vessel.

4. A method is needed for producing continuous records that can be maintained and compared with records from previous inspections.

5. A determination is needed of the effect of radiation and other environmental effects on the functioning of all components and constituents of the probes.

6. If service life of the probes is significantly affected, means must be devised for removing the probes during reactor operation and

reestablishing the probe position, orientation, coupling, calibration, etc., or the system will not be usable.

7. A determination is needed of the effect of radiation damage on the sonic propagation properties of the vessel material at the frequencies of interest.

8. A determination should be made of whether all anticipated failure mechanisms in the pressure vessel materials will produce a detectable stress wave; for example, how will stress-corrosion cracking differ from the failure modes and what will be the effect of hydrogen or radiation embrittlement on the generated stress wave?

9. Data processing systems should be developed that can provide prompt display and interpretation of data.

10. Improved resolution is needed for locating the origins of signals. This will include both improved instrumentation and probes, as well as better knowledge of propagation velocities.

11. It should be determined with assurance that the system can be applied to large thicknesses without difficulty.

12. It should be demonstrated that adequate discrimination can be made between signals due to defects and those due to noises in or around the vessel.

13. Means should be provided for quantitatively relating the signal to the increment of crack growth so that record summation can be used to determine total crack size. If this latter requirement cannot be satisfied, a supplementary means of examination would be needed to investigate areas of significant acoustic emission to determine the total crack size.

Although it is more difficult at the present state of technology to hypothesize on the merits of other nondestructive examinations, it would appear to be prudent to continue to examine new approaches for feasibility. Such studies should continue not only for those systems that primarily monitor fault initiation and growth but also those which deal with the change of physical and mechanical properties. A considerable effort has already been expended on the search for an easily measured physical property that can be correlated with mechanical property deterioration associated with radiation damage. Such studies have not succeeded as yet

in revealing any significant relations; nevertheless we believe a vigorous effort should be continued.

All the previous discussion of acoustic systems has been primarily premised on the assumption that monitoring would be accomplished at shutdown periods determined by normal power scheduling. It may be hypothesized as a possible future development that under some conditions an approach to a critical failure condition could be attained over a rather short time. In this event it would be necessary to perform examinations more frequently than would be afforded by periodic postoperational inspections. Such examinations could be similar to those previously discussed, with the exceptions of greater frequency of inspection and subjection to operating rather than shutdown environments. Operation under such conditions places paramount interest in the following problems: maintainability, safety, and reliability, with assurance of noninterference with reactor system instrumentation and controls and resistance to the radiation, temperature, etc. associated with the environment. In addition, all the previously listed development problems for scanning and fixed-probe acoustic systems and acoustic-emission systems would be applicable to in-service systems.

2.9.3 Postoperational Material Surveillance

Even with the most careful attention to materials specifications, design details, fabrication procedures, and inspection procedures, it is currently not possible to assure the continuance of the initial materials properties nor to predict unfailingly any change, deterioration or otherwise, of materials properties with time. The overlapping and possibly opposing influences of environmental parameters, such as radiation, temperature, stress state, possible corrosive action, etc., regiment against a thorough and precise knowledge of the effect of a single environmental parameter. Section III of the Code recognizes the current state of the technology in that the designer is warned that such effects shall be considered to assure that the design life may be attained.

The designers currently fulfill a portion of this obligation by conducting a materials radiation surveillance program generally in accordance

with ASTM E 185, "Recommended Practice for Surveillance Tests on Structural Materials in Nuclear Reactors." These programs are implemented by subjecting tensile and impact materials specimens, taken from beltline courses of the shell, to temperature and radiation conditions representative of that seen by the vessel. The continuous monitoring of the radiation-induced changes thereby permits evaluation of the safety and reliability of continued operation of the vessel for the prescribed approved operating conditions. Evaluation is currently premised on the applicability of the transition-temperature approach, previously discussed in Section 2.5. In addition, as a secondary purpose, these surveillance tests hopefully will contribute to a basic understanding of radiation effects, lead to the ability to forecast radiation effects for each of the materials of interest and, as a consequence, eliminate the need of a surveillance program.

Continued vigorous usage of these radiation surveillance programs appears to be necessary for monitoring and evaluation and for basic radiation-effects studies. In addition, the recommendations previously made with regard to specimen preparation and dosimetry should be considered.

3. ENVIRONMENTAL AND SERVICE CONDITIONS*

There have been relatively minor changes in the design and operating conditions during the course of development of light-water reactors. Table 3.1 presents a summary of the conditions and design data for the pressure vessels of commercial power reactors up to the present time. These and other environmental and service conditions are discussed in the following sections.

3.1 TEMPERATURE

Current designs of pressurized-water reactor vessels are based on a temperature of 650°F and boiling-water reactor vessels on a temperature of 575°F. A margin of approximately 40 to 50°F is provided above the maximum fluid operating temperature of approximately 600°F for pressurized-water reactor vessels and a margin of approximately 25 to 30°F above the maximum fluid operating temperature of approximately 545°F for boiling-water reactor vessels.

3.2 PRESSURE OR SERVICE LOADING

Current designs of pressurized-water reactor vessels are based on a pressure of 2485 to 2500 psig and boiling-water reactor vessels on a pressure of 1250 psig. The corresponding operating pressures are 2050 to 2235 psig for pressurized-water reactor vessels and approximately 1000 psig for boiling-water reactor vessels. The margin between operating and design pressure provides allowances for operation maneuvering, system transients, and a set-point range for relief and safety valves.

---

*This chapter was prepared by G. C. Robinson, Jr., and G. D. Whitman, Oak Ridge National Laboratory.

Table 3.1. Summary of Design and Operating Conditions for Light-Water Reactor Vessels

Reactor Name	Type of Reactor	Power Capacity (Mw)		Operating Pressure (psig)	Operating Temperature (°F)	Design Pressure (psig)	Design Temperature (°F)	Vessel Design Code	Inside Diameter	Overall Length[a]	Wall Thickness (in.)					
											Top Head		Bottom Head		Cylinder	
		Thermal	Net Electrical								Base	Cladding	Base	Cladding	Base	Cladding
Shippingport	PWR	525	150	1985	512.1–599.9	2500	600	ASME, Sect. I	109 in.	31 ft 6 in.	10	1/4	6.2	0.2	8 3/8	1/4
Dresden-1	BWR	700	200	1000	546–621[b]	1250	650	ASME, Sect. I	12 ft 2 in.	40 ft 10 1/8 in.	5 1/4	3/8	9 and 5 1/4	3/8	5 1/4 6 1/2	3/8 3/8
Yankee	PWR	540	155	2000	499–609[b]	2500	650	ASME, Sect. VIII	109 in.	31 ft 6 in.	7	0.109[c]	3 7/8	0.109[c]	7 7/8	0.109[c]
Saxton	PWR	23.5	5	2000	550[b]	2485	650	ASME, Sect. VIII	58 in.	18 ft	5 1/4		4 1/2		5[d]	
Indian Point-1	PWR	585	151	1500	486.5–519	1800	650	ASME, Sect. I and Navy	117 ft	36 ft 9 3/16 in.			6 15/16	0.109	6.94	0.109[c]
Big Rock Point	BWR	240	70	1035–1485[b]	593	1700	650	ASME, Sect. I and Navy	106 in.	28 ft 8 1/2 in.	5 1/4	5/32,[c] 7/32[e]	5 1/4	5/32,[c] 7/32[e]	5.5	5/32[c]
Elk River	BWR	58.2	15	936	425–536	1250	650	ASME, Sect. VIII and Code Case 1234	7 ft	25 ft					3.0	0.109[c]
Humboldt Bay	BWR	240	69	1000–1150	561	1250	650	ASME, Sects. I and VIII and Code Cases; Navy	10 ft	40 ft 5 in.	3 1/2	1/4[c]	3 5/8	1/4[c]	Cone, 4 3/4 4 5/16	1/4[c] 1/4[c]
BONUS	BWR	50	17	975	540	1150	600	ASME, Sect. VIII and Navy	7 ft	26 ft 7 in.	5	1/4	2 3/16	1/4	3 1/8	1/4
Pathfinder	BWR	188.9	59	600	489	700	500	ASME, Sect. VIII and Code Cases; Navy	11 ft	31 ft 6 in.	2 3/8	1/8	3	1/4	3	1/4
LaCrosse	BWR	165	50	1285	578	1400	650	ASME, Sect. VIII and Code Cases; Navy	8.25 ft	37 ft					4	0.188
San Onofre	PWR	1210	450	2050	549–595	2485	650	ASME, Sect. VIII and Code Cases 1270N, 1273N	142 in.	44 ft 4 3/8 in.	7 1/4	7/32	5	7/32	9 3/4	7/32[c]
Connecticut Yankee	PWR	1473	646	2050	569	2485	650	ASME, Sect. VIII and Code Cases 1270N, 1273N	154 in.	41 ft 6 1/8 in.	7 3/4	7/32	5 3/16	7/32	10 5/8	7/32[c]
Oyster Creek	BWR	1600	515	1000	546	1250	575	ASME, Sects. I and VIII and Code Cases 1270N, 1273N	17 ft 9 in.	61 ft 2 in.	4 5/16	7/32	8 3/4	7/32	7 1/8	7/32
Nine-Mile Point	BWR	1538	500	1000	530–546	1235	575	ASME, Sects. I and VIII and Code Cases 1270N, 1273N	17 ft 9 in.	61 ft 2 in.	4 5/16	7/32	8 3/4	7/32	6 1/8	3/16
Dresden-2	BWR	2300	715	1000	547	1250	575	ASME, Sect. III	20 ft 11 in.	68 ft	4	3/16	8	3/16	6 1/8	1/8
Malibu	PWR	1473	550	2050	546–592	2485	650	ASME, Sect. III	154 in.	46 ft 6 1/8 in.	7 3/4	7/32	5 3/16	7/32	9 5/16	7/32
Millstone Point	BWR	1727	549	1000	546	1250	575		18 ft 8 in.	64 ft 8 in.					5 11/16	1/8
Brookwood	BWR	1300	420	2235	581	2485	650	ASME, Sect. III	132 in.	39 ft	5 3/8	5/32	4 1/8	5/32	6 1/2	5/32[c]
Indian Point-2	PWR	2758	873	2235	570	2485	650	ASME, Sect. III	173 in.	42 ft 4 in.	7	7/32	5 5/16	7/32	8 5/8	5/32[c]
Palisades	PWR	2200	710	2085	545–591.1	2500	650	ASME, Sect. III	172 in.	40 ft 3/4 in.	7 3/8	1/4	4 3/8	1/4	8 1/2	3/16
Turkey Point-3	PWR	2097	652	2235	574	2485	650	ASME, Sect. III	155.5 in.	41 ft	6 3/16	5/32	4 3/4	5/32	7 3/4	5/32[c]
TVA Browns Ferry	BWR	3293	1075	1005	547	1250	575	ASME, Sect. III	251 in.	72 ft 6 1/2 in.	4	0	8	3/16	6 1/8	3/16

[a]Inside radius at tangent to heads. [b]Maximum. [c]Minimum. [d]Multilayer. [e]Nominal.

3.3 PROCESS FLUIDS

In the current designs of both boiling-water and pressurized-water reactors, it is a common practice to employ corrosion-resistant materials on the wetted primary boundary and to use treatment measures that produce high-purity water. The primary motivations for this practice are two-fold: (1) to prevent a corrosion rate that results in the transport and deposition of radioactive crud into components where accumulation might impede mechanical action or prevent contact maintenance and (2) to prevent deleterious accumulation of corrosion products or other solids on critical heat transfer surfaces, such as the fuel elements and tubes of heat exchangers. Test loop operation and reactor operating experience to date have given no evidence of severe corrosion. Although various mechanisms, such as hydrogen embrittlement of the base material at breaks in the stainless steel cladding, are considered as potential problems, no evidence of such mechanisms exists to date.

Methods for effecting water chemistry control for pressurized-water reactors are similar to those used in modern high-pressure and supercritical fossil-fired steam plants. Figure 3.1 shows a simplified flow diagram of a typical pressurized-water reactor and illustrates the principal equipment used to effect water chemistry control. A bypass stream flows through demineralizers to reduce the total solids to a very low level (<1 ppm) and thereby remove radioactive crud and limit the chloride content to an acceptable level. A bypass stream may also flow through a gas-stripping deaerator to remove xenon, krypton, and other gases before returning to the primary loop. Hydrogen and a pH control chemical, usually hydrazine, are introduced into the bypass stream to effect control of dissolved oxygen and to maintain a high pH level. Boron, usually in the form of boric acid, is used for chemical shim reactivity control. The boric acid is introduced into the primary loop batch-wise via the metering pump and removed as required via a bypass stream by means of demineralizers. Since only stainless steel, Inconel, and Zircaloy are used as the wetted surfaces throughout the primary loop and the various

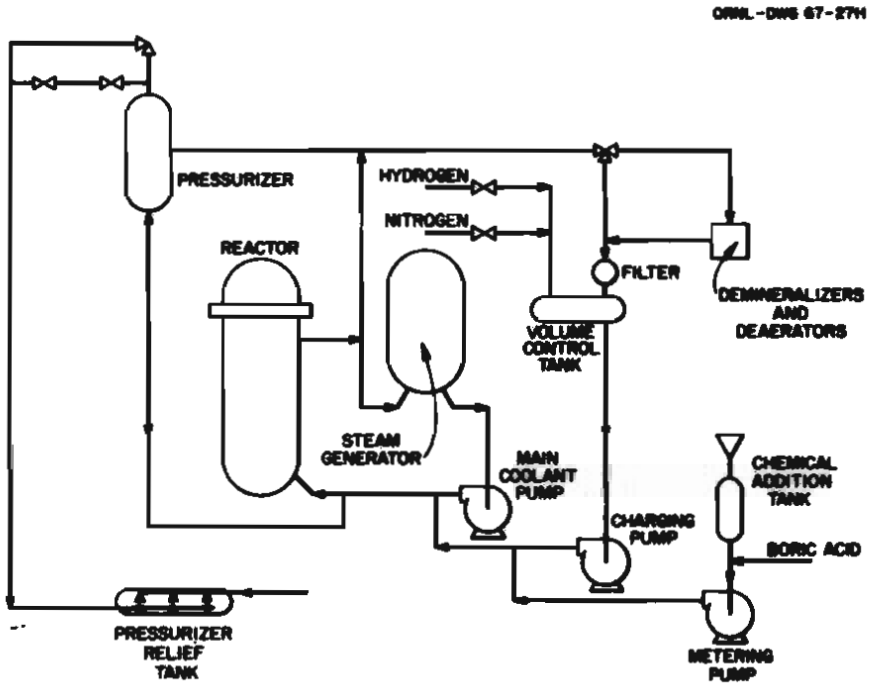

Fig. 3.1. Simplified Flow Diagram of Pressurized-Water Reactor Illustrating Water Chemistry Control.

auxiliary loops, the primary effort has been to effect water conditions considered ideal for these very corrosion-resistant alloys.

Because of the gas-stripping action of the condenser in the boiling-water primary loop, it is not feasible to utilize hydrogen as in the pressurized-water reactors for suppression of the oxygen produced by radiolytic decomposition of the water in the reactor. In the presence of an excess of oxygen, hydrazine will break down in the reactor environment to form nitric acid. Consequently boiling-water reactors have not used oxygen and pH control schemes comparable to those of pressurized-water reactor systems. Figure 3.2 shows a simplified flow diagram of a typical boiling-water reactor to illustrate the scheme used for water chemistry control. Since the measures employed for pressurized-water reactors to control oxygen and pH would be ineffective, a development program was instituted to examine the corrosiveness of an environment that depended on low total dissolved and suspended solids, low oxygen and chlorides, variable pH, and a stoichiometric ratio of hydrogen and oxygen both in the water and steam phases. Out-of-pile test loop operation of

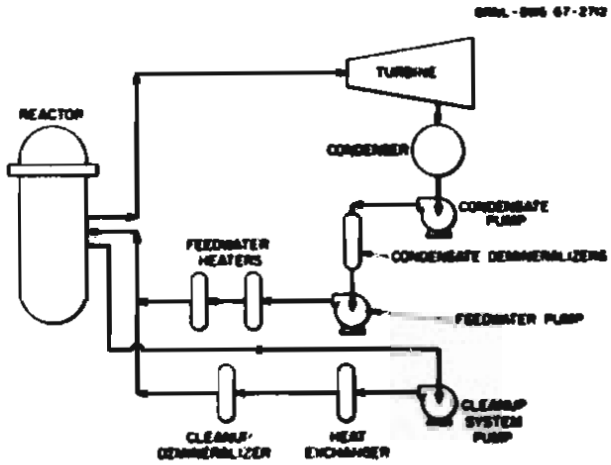

Fig. 3.2. Simplified Flow Diagram of Boiling-Water Reactor Illustrating Water Chemistry Control.

such an environment for not only stainless steel but also carbon steels, Zircaloys, Inconel, copper alloys, and copper-nickel alloys typical of conventional condensate and feedwater systems have demonstrated to date very low corrosion rates and rates of release of corrosion products to systems.

Table 3.2 lists the coolant conditions specified for both early and recent designs of boiling-water and pressurized-water reactors. Typical pressurized-water reactor coolant conditions are:

Dissolved oxygen	≤0.1 ppm
Chloride	≤0.15 ppm
Total dissolved solids (excluding boron)	≤0.50 ppm
Total suspended solids	≤1.0 ppm
Hydrogen	25–35 cc (STP)/kg
pH	9.5–10
Conductivity	1–2 μmho/cm
Boron	0–23,000 ppm

Typical boiling-water reactor coolant conditions (liquid phase) are:

Dissolved oxygen	≤0.1 ppm
Chloride	≤0.1 ppm
Total suspended solids	≤0.2 ppm
pH	4–10
Conductivity	0.1 μmho/cm

Table 3.2. Summary of Coolant Conditions of Light-Water Reactors

Reactor Name	Type of Reactor	Dissolved Oxygen[a] (ppm)	Chloride[a] (ppm)	Fluoride[a] (ppm)	Total Halogens[a] (ppm)	Total Dissolved Solids[a] (ppm)	Total Suspended Solids[a] (ppm)	Other Elements[a] (ppm)	Hydrogen[b] [cc (STP)/kg]	Conductivity[a] (mho/cm)	pH[b]	Composition of Major Components	Radiolitic Gas Production [cfm/Mr(t)]	Oxygen in Feed (ppb)	Radioactivity[a] (counts/ml) Iodine	Radioactivity[a] (counts/ml) Total	pH Control	Reactivity Control
Shippingport	PWR	0.14	0.5				0.004-0.1		15-60	7-75	9.5-10.5	Zirconium fuel, stainless steel system					LiOH, 0.6 ppm	None
Dresden-1	BWR	(c)	0.1, 0.5[d]							1	6.5-7.5	Zirconium and stainless steel fuel, stainless steel system, Monel and copper-nickel feedwater heater tubes, carbon steel feedwater piping	0.04	10			None	None
Yankee	PWR	0.1	0.1			2.0		Boron, 5	24-45	2		Stainless steel fuel, stainless steel system					Hydrogen and hydrazine injection, ion exchange	Core 4, chemical shim, 1000 ppm boron
Saxton	PWR	0.14	0.1			0.5		Potassium, 3.8; boron, 2500	25-35									
Indian Point-1	PWR	0.01	0.1			1.0		Boron, 40 as boric acid	20-40		7.0	Stainless steel fuel				30	None	3000 ppm boron for shutdown
Big Rock Point	BWR	(c)	0.1, 0.5[d]				0.1			1	5.5-8.5	Stainless steel fuel, stainless steel system, Admiralty and 70% Cu-30% Ni feedwater heater tubes, carbon steel feedwater piping	0.07	10			None	None
Elk River	BWR	0.04	0.1						0	0.1	6.7	Zirconium fuel, stainless steel system	4×10^{-4}	9×10^{6}[e] 5×10^{6}			None	None
Humboldt Bay	BWR	0.5	0.1, 0.5[d]					Boron, 100		1	5.5-8.5	Stainless steel fuel, stainless steel system, Admiralty feedwater heater tubes (being changed to stainless steel), carbon steel feedwater piping	0.04	5		50	None	None
BONUS	BWR	0.5	<1.0			<10.0				1	6.5-7.5	Zirconium and Inconel fuel; stainless steel system; Admiralty, copper-nickel, and carbon steel feedwater system	0.05	35	<35		None	None
Pathfinder	BWR		0.1					Boron, 100		5, 10[e]	4-10					20		
LaCrosse	BWR									0.1	7						5×10^{-5} to 5×10^{-4} molar NaOH (tentative)	
San Onofre	PWR	0.1	0.15	0.15		0.5			25-35								5×10^{-5} to 5×10^{-4} molar NaOH	
Connecticut Yankee	PWR	0.1	0.15	0.15		0.5[f]			25-35									
Oyster Creek	BWR	(c)	0.1, 0.5[d]							1	5.5-8.5	Stainless steel feedwater heater tubing, carbon steel feedwater piping, zirconium fuel, stainless steel system					None	None
Brookwood	BWR	0.1	0.15	0.1		0.5[f]		Lithium, 0.2-2.2	25-35								Injection of ^{7}Li as LiOH	
Indian Point-2	PWR	0.1	0.15	0.1			1.0	Boron, 0-23,000 as boric acid	25-35								0.3×10^{-4} to 3.2×10^{-4} molal strong base, or up to 20 ppm NH_3	Boric acid
Palisades	PWR	0.1			0.15	0.5		Lithium, 0.25-2.0; boron, 0-1720	25-35		5.2-9.5	Zirconium fuel, stainless steel system					^{7}Li level controlled by mixed-bed resins	Boric acid
Turkey Point-3	PWR	0.1	0.15	0.1			1.0	Boron, 0-23,000 as boric acid	25-35								0.3×10^{-4} to 3.2×10^{-4} molal strong base, or up to 20 ppm NH_3	Boric acid

[a]Specified maximum.
[b]Specified range.
[c]Not specified; normally 0.2 to 0.3 ppm due to $2H_2O \rightarrow 2H_2 + O_2$ reaction and air inleakage into feedwater.
[d]Two weeks per year.
[e]Transient.
[f]Exclusive of additives.
[g]In condensate.

3.4 RADIATION

The primary concern with respect to radiation is the well-known embrittling effect of neutron irradiation on carbon and low-alloy steels. Although in other types of reactor, for example, the aqueous homogeneous, the effect of radiation is also important in its effect on coolant conditions that are detrimental to the wetted boundary of the pressure vessel, there are no known or suspected similar detrimental reactions catalyzed by radiation in the pressurized- and boiling-water reactors. Such effects are considered highly unlikely. It is anticipated that the considerable good out-of-pile test experience will be verified as reactor operating experience is rapidly accumulated.

The current stated aim of water-reactor designers is to avoid high stresses and discontinuities in regions of the vessel where it is estimated that the accumulated fast-neutron (>1 Mev) flux over the reactor life will exceed 10^{18} neutrons/cm^2. Consequently, the only region for which any embrittlement or shift in the design transition temperature is anticipated is the cylindrical belt region at the core center line. Although the methods of estimation of flux, energy spectrum, rate effects, monitor cross section, and axial and radial profiles have significance in the estimation of radiation damage, the current data generally presented for safety evaluation are the nominal and maximum time-integrated fast-neutron (>1 Mev) flux values for the belt-line location and the anticipated design transition temperature shifts for each. Table 3.3 presents the data currently available for safety evaluation of radiation damage.

3.5 DOSIMETRY

In the context of this report, neutron dosimetry is linked inseparably to the effects of neutron irradiation on pressure vessel steels. The following discussion of the development of neutron dosimetry, the present state of dosimetry art, and the course of future development accents the experimental techniques in use and the various schemes proposed for reporting data. Radiation damage is fully discussed in Section 5.4, and

Table 3.3. Data for Estimation of Radiation Damage

Reactor Name	Type of Reactor	Method of Establishing Flux Spectrum	Name of Code Used	Type of Code	Number of Energy Groups	Axial Peaking Factor Used in Calculation	Radial Material Arrangement, Kind, and Thickness	Reactor Life (years)	Assumed Thermal Power (Mw)	Assumed Plant Factor	Calculated Integrated Flux Over Reactor Life at Vessel Inner Surface at Belt Line (neutrons/cm²)			Belt Line Initial NDT Temperature (°F)	Estimated NDT Shift at Belt Line at End of Reactor Life (°F)		Reference Da (Curves) Used Correlate NI Shift with Neutron Expos
											Thermal	0.1 to 1.0 Mev	>1.0 Mev		Minimum	Maximum	
Shippingport	PWR	Calculation and measurement						20	225			2.23×10^{19}	6.0×10^{19}	36	320	400	
Dresden-1	BWR	Calculation and measurement						40	626	0.8			2.5×10^{19}	60	150	160	See footnote
Yankee	PWR	Calculation	P1MG	Diffusion	55	1.5		30	600	0.85	6.4×10^{19}	4.1×10^{19}	2.5×10^{19}	<10		305	
Saxton	PWR	Calculation	P1MG	Diffusion	55	1.5		5	23	0.60	4.0×10^{19}	3.3×10^{19}	2.0×10^{19}	25		225	
Indian Point-1	PWR	Calculation	P1MG	Diffusion				40	615	0.80		3.6×10^{19}	7.5×10^{18}	-30	205	320	
Big Rock Point	BWR	Calculation						40	157	1.0			3.63×10^{18}	≤10		50	See footnote
Elk River	BWR	Calculation						20	51	0.60			1.9×10^{19}	30	215	310	
Humboldt Bay	BWR	Calculation						20	163	1.0			3.4×10^{18}	≤10		60	See footnote
BONUS	BWR	Calculation	C17		10	1.43	Mean core diameter, 58 in.; 3/8-in.-thick stainless steel core barrel; 1-in.-thick stainless steel thermal shield	20	50	1.0	8.2×10^{19}	Not available	1.65×10^{18}[f]	<10	135	260	See footnote
Pathfinder	BWR	Calculation						20	200				1.14×10^{18}	10	25	80	
LaCrosse	BWR					1.8		20		0.60			9.5×10^{18}				
San Onofre	PWR	Calculation	P1MG	Diffusion	55	1.5		30	1347	0.9	4.7×10^{20}	9.0×10^{19}	6.1×10^{19}			320	
Connecticut Yankee	PWR	Calculation	P1MG	Diffusion	55	1.5		30	1473	0.9	2.5×10^{20}	4.1×10^{19}	2.5×10^{19}			245	
Oyster Creek	BWR							40	1860	1.0			9.2×10^{17}[h]	≤10	10	70	See footnote
Nine-Mile Point	BWR								1846	1.0			7.26×10^{17}[h]	≤10	10	60	See footnote
Dresden-2	BWR							40	2467	1.0			2.4×10^{17}[h]	≤40	0	20	See footnote
Millstone Point	BWR								1727[a] 2011[b]	1.0 1.0			4.1×10^{17}[h] 4.9×10^{17}[h]	 ≤40	0 0	40 40	See footnote
Brookwood	BWR	Calculation	P1MG	Diffusion	55	1.5		40	1300	0.8	2.2×10^{20}	3.2×10^{19}	2.2×10^{19}	100[j]		233	
Indian Point-2	PWR	Calculation	P1MG	Diffusion	55	1.5		40	2758	0.8	5.6×10^{19}	1.2×10^{19}	0.9×10^{19}			166	
Palisades	PWR	Calculation	C-17 (fast), WAFLB (thermal)		10	1.5	0.5 in. stainless steel, 6.5 in. H_2O, 1.5 in. stainless steel, 2.75 in. H_2O, 3 in. stainless steel, 4 in. H_2O, 0.25 in. stainless steel	40	2450	0.80	9.7×10^{19}		9.4×10^{18}[f]	40		175	
Turkey Point-3	PWR	Calculation	P1MG	Diffusion	55	1.5		40	2300	0.8	1.6×10^{20}	3.8×10^{19}	2.6×10^{19}			250	
TVA Browns Ferry	BWR							40	3293	1.0			3.5×10^{17}[h]	≤40	0	40	See footnote
Dresden-3	BWR							40	2467	1.0			$<1.0 \times 10^{18}$[f]	≤40		20	See footnote
Quad Cities-1	BWR							40	2527	1.0			2.4×10^{17}[h]	≤40	0	20	See footnote
Monticello	BWR							40	1674	1.0			5.4×10^{17}[h]	≤40	0	50	See footnote
Vermont Yankee	BWR							40	1593	1.0			1.0×10^{17}[h]	≤40	0	0	See footnote

[a] Initial.

[b] Guaranteed.

[c] M. S. Hersh, F. A. Brandt, and B. C. Beaudreau, Dresden (I) Nuclear Power Station Reactor Vessel Steel Surveillance Program, USAEC Report GECR-5165, General Electric Company, May 1966.

[d] J. P. Higgins, Modified Surveillance Program for General Electric BWR Pressure Vessel Steels, USAEC Report APED-5490, General Electric Company, May 1967.

[e] F. A. Brandt, Humboldt Bay Power Plant Unit No. 3 Reactor Vessel Steel Surveillance Program, USAEC Report GECR-5492, General Electric Company, May 1967.

[f] Maximum.

[g] Oak Ridge National Laboratory, Solid State Division Annual Progress Report for Period Ending August 31, 1959, USAEC Report ORNL-2629.

[h] Estimated.

[i] G. F. Carpenter, N. R. Knopf, and E. S. Byron, Anomalous Embrittl Effects Observed During Irradiation Studies on Pressure Vessel Steels, Nucl. Sci. Eng., 19(1): 16–36 (May 1964).

[j] Assumed.

therefore only brief mention of radiation damage theories is provided in this section where such references will provide clarity.

Throughout the course of development of light-water reactor technology, there has been recognition of the potential deleterious effect of neutron irradiation on pressure vessel steels. Experimental studies were initiated early in the 1950's at a number of laboratories to assess the quantitative changes that could be expected. Since there was a great urgency for data, all the early irradiations took place in experimental reactors at accelerated conditions, that is, at instantaneous dose rates many orders of magnitude greater than anticipated for the affected pressure vessel structure.

A number of methods were available at that time for measurement of neutron flux; for example, there was proton recoil spectroscopy, crystal spectroscopy, photographic plates and emulsions, and activation analysis. Except for activation analysis, however, none of these was suitable for monitoring steel irradiation, either because of excessive space requirements or because of sensitivity to the high gamma intensities or temperature conditions that existed at the irradiation position. Activation analysis therefore became, by default, the standard technique for flux measurement.

Many major difficulties, some of which are discussed below, plagued the experimenter in the use of activation analysis. As a consequence some reliance was initially placed on corroboration of activation analysis data with data furnished by the experimental reactor operating staff. Also in many instances radiation damage data were based solely on the data furnished by the reactor staff. Such "staff" data were generally obtained from calculations, estimations, or surveys at low power levels and usually did not take into account changes in fuel loading or control rod programming and structural changes at the irradiation position. The resulting data correlations were often marginal or poor.

Some of the requisite properties of activation monitors for ideal dosimetry are the following:

1. The threshold energy should be sensitive to the complete energy spectrum.

2. The daughter product of the detector material should decay by a single radiation process and should have a relatively long half-life.

3. The detector material and product should be chemically and physically stable and compatible with the environment and operating conditions of the irradiation space.

4. The detector material should be available in a form for which there are insignificant competing nuclear reactions.

5. The daughter product should be insensitive to ionizing radiation.

6. The daughter product radiation should be easily isolated and measured accurately.

In practice most of the candidate materials for activation monitoring fail to fulfill one or more of the preceding requirements. A further factor is cost. Although technically the fission threshold monitors are feasible and satisfactory and they are the only ones available that cover the portion of the neutron spectrum from thermal to fast, the high cost of an analysis has severely limited their use. Most of the early experimenters used ^{59}Co or cadmium-shielded ^{59}Co, ^{32}S, and ^{58}Ni to monitor the thermal, resonance, and fast fluxes, respectively. Since these activants are virtually insensitive in the range from 1 kev to 1 Mev, this portion of the spectrum was neglected. Because of this limitation, the reporting of fluxes greater than 1 Mev became the vogue, and some experimenters gave these measurements a quasi-physical-property status. However, with subsequent improvements in dosimetry and with the development of damage theories that reflect experimental evidence, there has been increased attention to the need for monitoring and reporting fluxes less than 1 Mev.

3.5.1 Damage Models

Many theoreticians have advanced models of radiation damage. Among them are Kinchin and Pease,[1] Snyder and Neufeld,[2] Brinkman,[3] Churchman, Mogford and Cottrell,[4] Rossin,[5] Dahl and Yoshikawa,[6] and Beeler.[7] Some of the parameters considered in these studies are (1) energy and temperature dependence of radiation damage, (2) energy dependence of neutrons and primary knock-on atoms for production of vacancies, interstitials, and displacement spikes, (3) precipitation of impurity atoms, (4) effect of channeling and quasi-channeling along preferential lattice directions, (5) space dependence of production of vacancies, interstitials, and

displacement spikes, and (6) annihilation of damage by overlapping of damage areas. Although no well-ordered consensus may yet be written, these studies have revealed many of the factors that provide logical explanations for the radiation damage effects observed experimentally. There is general agreement by theoreticians and experimenters that increased attention should be given to the assessment of fluxes less than 1 Mev, with the precise method of reporting the flux and energy threshold for damage dependent upon the particular damage model employed. Even more important, it has become increasingly clear that a basic understanding of the damage process will require more precise knowledge of the flux spectrum and the flux spatial profile. The need for better characterization of the incident flux has given impetus recently to the determination of better activation-monitor cross sections.

3.5.2 Dosimetry Methods

In activation analysis, three different types of nuclear reaction are used to monitor the flux spectrum. A large group of activants has an exceedingly high probability for an (n,γ) reaction for thermal energies; in fact, this probability of reaction is only exceeded by sharply peaked resonance energy (n,γ) reactions for epithermal energies. To separate these two competing reactions, some monitors are clad with cadmium to virtually prevent any incident thermal-neutron flux and provide a means for assessing the activation due only to thermal energies. Decay activity of the activated monitor is counted by a Geiger-Mueller counter or by gamma-ray spectroscopy. The count rate observed is compared with that of control monitors exposed to a standard flux in order to determine the flux level.

Fissionable materials constitute the second grouping of activation monitors. Following irradiation the fission products are chemically separated and the radioactivity counted. The observed activity can then be related to the flux by the known yield percentage of the fission product. Uranium-235 and ^{239}Pu have been used to determine the thermal flux; and ^{237}Np, ^{238}U, ^{236}U, and ^{232}Th, because of their close approximation to threshold-energy step functions, have been used to measure flux over

the range from 0.5 to 3 Mev. However, the high cost and complexity of the analysis have drastically curtailed the use of this group of monitors.

The third group of monitors consists of those having an (n,p) or (n,α) nuclear reaction. Although these reactions occur to some extent throughout the complex flux spectrum, the primary activants have reactions approximating a step function at energy levels of 2 Mev and greater. Figure 3.3 shows the probability of the (n,p) reaction for ^{32}S as a function of neutron energy.[8] The irregularities of cross section versus energy depicted by this activant are typical of the behavior of most of the activants of this group. In spite of the irregularities of the shape of the cross section versus energy curve exhibited by these monitors, the assumption is made that the behavior can be approximated by the conversion of the actual curve shape to one of a step function. Figure 3.4 illustrates a typical activant cross-section versus energy curve with such a superimposed, idealized threshold-energy step function.

Most of the irradiation experiments conducted to date have been based primarily on the use of this last group of monitors. The experimenter is usually faced with the dilemma that insufficient space exists to permit

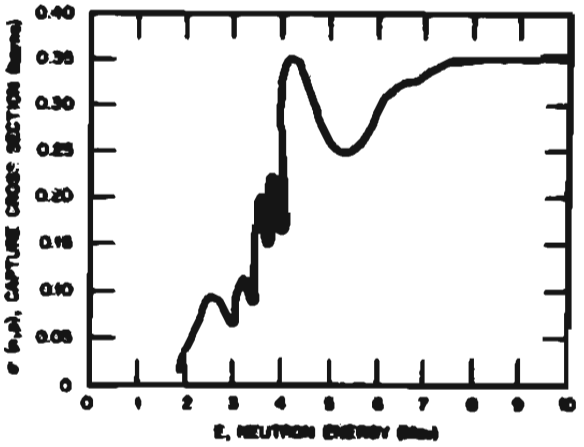

Fig. 3.3. A Cross Section or Probability for $^{32}S(n,p)^{32}P$ Reaction. It increases rapidly with neutron energy and reaches an irregular plateau at about 3 Mev. (From Ref. 8)

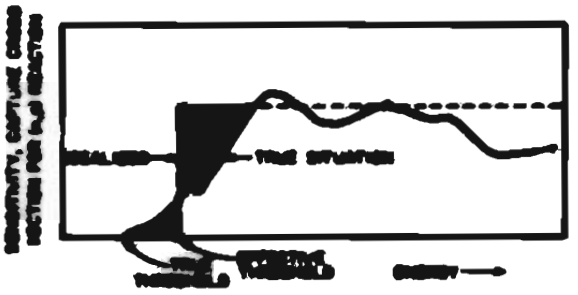

Fig. 3.4. Illustration of Method for Conversion of a Typical Cross-Section Curve to an Idealized Threshold-Energy Step Function. (From Ref. 8)

the use of monitors that provide for synthesizing the incident flux spectrum. From the earliest experiments until recently, the usual practice has been to employ threshold-type monitors, such as $^{32}S(n,p)^{32}P$ or $^{58}Ni(n,p)^{58}Co$, to determine the flux level and to assume that the incident flux has the form of the fission spectrum determined by Watt[9] or by Cranberg and his co-workers.[10] More recently experimenters have used one or more of the now available computer codes to determine the spatial and energy profile of the incident neutron flux, but there has been a continued dependence on threshold-energy-type monitors to fix the absolute flux level.

3.5.3 Problems with Specific Activants

Although the feasibility of activation analysis has been demonstrated, its use is attended by many difficulties. Those of determining the basic cross sections and neutron flux are discussed in following sections.

In a number of instances, use of the (n,p) threshold-type monitors has been seriously impaired by the lack of adequate experimental information on the differential cross section (i.e., cross section as a function of energy). Some experimenters have used the approximate method suggested by Hughes[11] to estimate fission spectrum cross sections. More recently methods developed by Roy and Howton[12] and by Lubitz, Dunford, and Francis[13] have given better agreement with existing data. Some of the other difficulties experienced with the most useful activants are briefly enumerated below.

$^{32}S(n,p)^{32}P$:

1. Its physical form often requires encapsulation.

2. It cannot be irradiated at high temperatures as elemental sulfur because it sublimes.

3. Unless ^{32}P is separated from the sulfur, ^{35}S activity must be attenuated.

4. Beta decay of ^{32}P requires careful sample preparation.

5. The short half-life of 14.3 days limits the useful irradiation time.

6. Differences of a factor of 2 in cross-section data are reported, but the latest values are in better agreement.

$^{58}Ni(n,p)^{58}Co$:

1. The ^{58}Co isomers have large thermal cross sections; therefore corrections must be made for burnup.[14,15]

2. Cobalt impurities must be kept low to prevent competing activity.

3. A few days waiting time must be allowed for the decay of ^{57}Ni and ^{65}Ni to prevent interference in the counting of ^{58}Co.

4. Impurity pickup of ^{187}W was observed when the monitor was fabricated from nickel carbonyl in a tungsten crucible. Allowance for decay time of the ^{187}W is required.

5. While later cross-section values are in better agreement, discrepancies of almost a factor of 2 still exist.

$^{54}Fe(n,p)^{54}Mn$:

1. Corrosion susceptibility requires encapsulation in some environments.

2. When exposed to a significant thermal flux, ^{59}Fe provides interfering activity.

3. Although there is considerable disagreement among the published cross-section values, later values, particularly differential cross-section values, are in much better agreement.

4. The potential ^{54}Mn burnout has not been firmly established. Existing data tend to show no problem.

$^{46}Ti(n,p)^{46}Sc$:

1. Titanium is difficult to purify. Pickup of impurities has been experienced. Cobalt-60 has been a source of interfering activity.

2. Cross-section data are still not well known.

$^{63}Cu(n,\gamma)^{60}Co$:

1. Impurities such as iron, cobalt, and silver are not uncommon and cause interfering activity.

2. Differential cross-section data are not well known.

3. Elevated-temperature irradiations require precautions to prevent oxidation.

4. The long half-life of ^{60}Co of 5.3 y and small cross section make this an ideal activant for long-term irradiations. Contrariwise, there may be insufficient sensitivity for short irradiations.

3.5.4 Cross-Section Data

Perhaps the greatest problem that the experimenter has is the lack of basic cross-section data or uncertainty of the experimental values reported. Most of the data have been derived from irradiation in a presumed fission spectrum. The available differential cross-section data are meager. In some instances the fast spectrum used may have deviated significantly from a true fission spectrum and thereby biased the data. In a number of instances, cross sections have been determined in comparison with a presumed known standard cross section. For example, the reaction $^{32}S(n,p)^{32}P$ has been used as a reference standard with assumed cross-section values in a fission spectrum of both 30 and 60 mb.

The large variations of cross-section data may also be explained in part by other difficulties, such as self-shielding of the activant, flux depression at irradiation position, activant impurities having a daughter product with a similar competing decay reaction, loss of activant by chemical reaction, or physical attrition. Collations of the cross sections for the common activants by Rochlin,[16] Mellish,[17] Moteff,[18] and Passell and Heath[19] point out some gross diagreements and illustrate the basic difficulty that the experimenter has had through the years in acquiring precise data. Since data developed in recent years are materially better, significant improvements in the collations have resulted. Table 3.4 presents a collation of the differential cross section of the $^{58}Ni(n,p)^{58}Co$

Table 3.4. Differential $^{58}Ni(n,p)^{58}Co$ Cross Section

E, Neutron Energy (Mev)	σ, Cross Section (mb)
1.04	1.2 ± 0.1
1.15	3.8 ± 0.2
1.25	5.6 ± 0.4
1.46	10.5 ± 0.7
1.625 ± 0.01	18.5 ± 2.5
1.67	18.4 ± 1.3
1.87	31.1 ± 2.2
2.22 ± 0.16	142 ± 10
2.23 ± 0.13	138 ± 17
2.37	97 ± 7
2.53 ± 0.14	178 ± 21
2.58 ± 0.19	175 ± 13
2.6 ± 0.2	
2.67	139 ± 10
2.75 ± 0.13	193 ± 21
2.88 ± 0.14	200 ± 24
3.04 ± 0.20	214 ± 24
3.15 ± 0.12	188 ± 23
3.23 ± 0.14	235 ± 26
3.27 ± 0.09	172 ± 21
3.3 ± 0.01	
$3.52^{+0.2}_{-0.35}$	305 ± 34
3.55 ± 0.10	195 ± 12
3.6 ± 0.1	
$4.20^{+0.2}_{-0.3}$	475 ± 52
4.7 ± 0.05	
$4.98^{+0.13}_{-0.32}$	509 ± 56
$5.49^{+0.13}_{-0.35}$	604 ± 60
$6.20^{+0.2}_{-0.4}$	582 ± 58
$7.30^{+0.25}_{-0.31}$	646 ± 71
8.33 ± 0.3	670 ± 74
13.5	
14.0	310 ± 62
14.1	560 ± 110
$14.8^{+0.5}_{-0.2}$	292 ± 32
14.8	237 ± 20

reaction by Passell,[20] and Table 3.5 is a collation of the differential cross section of the $^{54}Fe(n,p)^{54}Mn$ reaction by Shure.[21]

Table 3.5. Differential $^{54}Fe(n,p)^{54}Mn$ Cross Section

E, Neutron Energy (Mev)	σ, Cross Section (mb)
2.32	26
2.6 ± 0.2	143 ± 14
3.3 ± 0.1	181 ± 18
3.55 ± 0.13	226 ± 22
3.6 ± 0.1	200 ± 20
3.82	208
3.94 ± 0.13	303 ± 30
4.32 ± 0.14	254 ± 25
4.63 ± 0.15	379 ± 38
4.7 ± 0.05	220 ± 70
4.93 ± 0.16	387 ± 37
5.21 ± 0.16	440 ± 42
5.49 ± 0.17	462 ± 44
5.76 ± 0.17	478 ± 46
6.02 ± 0.18	465 ± 45
14.1	307 ± 34
15.7 ± 0.7	286 ± 29
17.4 ± 0.7	257 ± 26

3.5.5 Neutron Flux Calculations

Although there has been relatively little use of synthesis of the incident flux spectrum from activation analysis for steel irradiations, the need for such techniques in experimental reactor physics has spurred considerable activity. Trice[22] and Hartmann[23] independently developed a method for expressing the flux as a series of orthonormal functions that consist of linear relations of the monitor cross section. Donnert[24] provided an additional arbitrary term in the Trice-Hartmann expansion to permit a better fit with experimental data. Uthe[25] developed a number of methods that use polygonal and polynominal expressions to fit the experimental data. Lanning and Brown[26] have further developed the orthonormal

technique of Trice and Hartmann to reduce the oscillation tendency. Dietrich and Thomas[27] in a study of a number of approaches indicated a preference for a semiempirical method they developed. The fits of curves derived by these techniques with theoretically derived curves are generally very sensitive to the number of activants used. Although the activant-number sensitivity prevents widely accepted use of these techniques for incident flux-spectrum synthesis, they are quite applicable to presurvey assessments of irradiation facilities.

In recent years there has been considerable theoretical study of the deviations that might be expected in the assessment of damage based on incident fission-spectrum flux versus a calculation of the actual incident flux spectrum and on the effect of instantaneous dose rate. Steele and Hawthorne[28] recently made an experimental investigation of spectrum versus dose rate effects in an irradiation of specimens in the BGR, MTR, and LITR. For the conventional mode of correlation and the assumed fission spectrum, and with consideration only of flux greater than 1 Mev, there appeared to be a marginal effect on NDT shift from dose rate differences of one order of magnitude. In a review of these data, Yoshikawa[29] considered spectral differences of the three test facilities in correlating the NDT shift with the damage models of both Rossin[5] and Kinchin and Pease.[1] Based on arbitrary threshold-energy levels of damage of 0.5 and 0.18 Mev, he obtained correlations that indicated no statistically significant effect of dose rate. Other investigators, for example, Rossin,[5] Claiborne,[30] Pawlicki,[31] Shure,[21] and Harries, Barton, and Wright,[32] obtained considerable variations in spectral effect on damage that vary from marginal to dramatic. Nevertheless, there seems to be general agreement that a significant improvement will be made in radiation-damage studies by the employment of computer codes to determine the actual incident flux spectrum. Yoshikawa[29] and Shure[21] discuss the results of employing various codes that utilize diffusion, transport, and Monte Carlo theory. Steep gradients in the spatial distributions of flux in accelerated test positions and surveillance test positions cited by Yoshikawa,[29] Shure,[21] and Serpan and his co-workers,[33] reinforce the argument for use of computer calculations to determine the spectral and spatial behavior of the flux.

3.5.6 ASTM Recommended Practice

In any rapidly developing field of study, there is an initial widely divergent probing for the dominant parameters and a consequent considerable degree of conflict and confusion in reported results. Neutron dosimetry studies of the structural materials of reactor vessels has suffered through such a preparatory stage. As realization of the significant parameters has become better resolved, it has become very desirable to standardize on nomenclature, parameters observed and reported, and method of reporting. ASTM Committee E-10 on Radioisotopes and Radiation Effects has been instrumental in resolving these problems through the preparation of ten standards:

ASTM E 170	Standard Definitions of Terms Relating to Dosimetry
ASTM E 184	Recommended Practice for Effects of High-Energy Radiation on the Mechanical Properties of Metallic Materials
ASTM E 185	Recommended Practice for Surveillance Tests on Structural Materials in Nuclear Reactors
ASTM E 199	Recommended Practice for Measuring Neutron Flux Environment for Reactor Irradiated Specimens
ASTM E 261	Measuring Neutron Flux by Radioactivation Techniques
ASTM E 262	Measuring Thermal-Neutron Flux by Radioactivation Techniques
ASTM E 263	Measuring Fast-Neutron Flux by Radioactivation of Iron
ASTM E 264	Measuring Fast-Neutron Flux by Radioactivation of Nickel
ASTM E 265	Measuring Fast-Neutron Flux by Radioactivation of Sulfur
ASTM E 267	Determination of Uranium and Plutonium Concentrations and Isotopic Abundances

These standards present terminology definitions; recommended methods and conditions of various irradiation tests; recommendations for obtaining and reporting the neutron flux, neutron-energy spectrum, and temperature of specimens; recommendation for incorporation of correlation monitors in

irradiation programs; and techniques for measuring neutron flux and presenting radioactivation data on iron, nickel, sulfur, uranium, and plutonium for measuring neutron flux.

Although there has been a general subscription of industry to the recommendations of these standards, very little information is available to date on this basis. Brandt and Alexander,[34] Landerman,[35] and Steele and Hawthorne[28] have reported on surveillance programs for Dresden I and Yankee that were, in general, patterned after the recommendations of ASTM E 185.

3.5.7 Conclusions and Recommendations

The rational approach taken by the ASTM standards should be encouraged. Many of the aspects of radiation damage will continue to be poorly understood unless a rigorous and rational attitude is taken toward neutron dosimetry. This is particularly true in regard to the power reactor surveillance programs, since much of the uncertainty of spectral and rate effects can only be cleared up through these efforts.

In addition, an ad hoc group, such as the ASTM E-10 Committee, should continue the review of techniques and cross-section data for the most useful activants in accelerated and surveillance irradiation programs. Where gaps and uncertainties are found to occur in existing data, a special program should be instituted to obtain the necessary data.

Furthermore, it would also appear desirable for the ASTM E-10 Committee to select certain damage models as representative or covering the possible range of interest as a standard method of reporting. The proliferation of damage models currently considered and the terminology attendant thereto tend toward confusion and certainly present an information barrier to designers not intimately acquainted with the subject.

3.6 SERVICE LIFE

Economic conditions dictate that the design life of power reactors be from 20 to 40 years. All current designs are based on a life expectancy of 40 years.

3.7 TRANSIENTS

In the fatigue analysis of vessels, consideration is given to essentially three major categories of cycles: (1) startup and shutdown cycles, (2) normal operation or power cycles, and (3) cycles associated with safety actions, accidents, or integrity tests.

The permissible temperature and pressure rates of change for the startup and shutdown cycles are primarily controlled by the restrictions imposed to insure against the probability of brittle fracture. Since economics dictate that power reactors must operate reliably for long periods of time, it is generally assumed that approximately two to three such cycles per year will occur. In some cases up to 12 cycles per year have been considered where additional conservatism or other judgment factors have been involved. Reactor experience to date has tended to verify the low assumptions made thus far.

Rate of temperature and pressure change considered for power cycles reflect the system condition changes required for minor load adjustments. In general, the pressure and temperature transients associated with this class of cycles are not very severe and result in a negligible or low calculated cumulative damage factor.

The most severe transients of pressure and temperature are associated with the third class of cycles, those resulting from safety actions or accidents. In order to have a design with a low cumulative damage factor, it is often necessary to provide features such as thermal sleeves in, for example, emergency coolant nozzles.

Currently the analysis of the transients leading up to a code fatigue analysis of a component is divided between the systems designer and the vessel designer. Bulk stream pressure and temperature changes associated with the various transients are developed for each component by the systems designer. At this point an interplay of heat transfer and fluid flow data and calculations is required between the systems designer and vessel designer to establish local temperature and pressure transient conditions on the component boundary. The pressure vessel designer then determines the temperature versus time structure of the component and subsequently performs the fatigue analysis.

Although relatively few pressure vessels have thus far been designed according to Section III of the ASME Code, and thus no trends are available, the vessel design transients listed in Table 3.6 appear to be representative, at least in part, for the current designs. Past experience of fossil-fueled plants has demonstrated that because of the increased efficiency and lower power costs of the newer plants, the older plants

Table 3.6. Vessel Design Transients

Type of Transient	Number of Cycles
Startup and shutdown cycles	
Plant heatup from room temperature to design condition at 100°F per hour	100-500
Plant cooldown from design conditions to room temperature at 100°F per hour	100-500
Power cycles	
Power loading in load range of 0 to 100% at 5% per minute	0-15,000
Power unloading in load range of 0 to 100% at 5% per minute	0-15,000
Power loading in load range of 50 to 100% at 15% per minute	2,000-15,000
Power unloading in load range of 50 to 100% at 15% per minute	2,000-15,000
Step load power increase at 10% of full power in load range 0 to 100%	0-2,000
Step load power decrease at 10% of full power in load range 0 to 100%	0-2,000
Step load power decrease at 50% of full power in load range 50 to 100%	0-200
Steady-state fluctuations, ±50 to 100 psi, ±5°F	300,000-∞
Safety, accident, or integrity testing transients	
Reactor trip	200-400
Turbine trip	0-40
Hydrostatic test	5-40
Leak test	5-300
Safety and relief valve actuation	0-200
Actuation of emergency core cooling	10

are transferred from base-load to peak-load status. An obvious speculation is that such a situation will also develop for the nuclear power industry. In such an event, the transient loadings will become much more significant and will require a reevaluation of the vessel to assure that adequate fatigue resistance will exist for the projected life under peak-load conditions.

3.8 MECHANICAL LOADING

Mechanical loadings to be considered by the pressure vessel designer include the following:

1. reactions from piping systems in which the reactor pressure vessel serves as an anchor,
2. reactions from mechanical devices, such as mechanical or jet pumps, valves, or control rod drives,
3. vibrational or static hydraulic loading resulting from core or component flow characteristics and consideration of credible accidents, such as severed external loop piping,
4. bolting and gasket seal loads at main vessel and nozzle flanges and bolting loads at demountable component support locations,
5. seismic loads.

REFERENCES

1. G. H. Kinchin and R. S. Pease, The Displacement of Atoms in Solids by Radiation, Rept. Progr. Phys., 18: 1–15 (1955).
2. W. S. Snyder and J. Neufeld, Disordering of Solids by Neutron Radiation, Phys. Rev., 97(6): 1636–1646 (Mar. 15, 1955).
3. J. A. Brinkman, On the Nature of Radiation Damage in Metals, J. Appl. Phys., 25(8): 961–970 (August 1955).
4. A. T. Churchman, I. Mogford, and A. H. Cottrell, The Hardening and Embrittlement of Steel by Irradiation with Neutrons, Phil. Mag., 2(8)(22): 1271–1275 (October 1957).
5. A. D. Rossin, Dosimetry for Radiation Damage Studies, USAEC Report ANL-6826, Argonne National Laboratory, March 1964.

6. R. E. Dahl and H. H. Yoshikawa, Neutron-Spectra Calculations for Radiation-Damage Studies, Nucl. Sci. Eng., 17: 398–403 (1963).

7. J. R. Beeler, Jr., Primary Damage State in Neutron-Irradiated Iron, J. Appl. Phys., 35(7): 2226–2236 (July 1964).

8. USAEC Conference on the Status of Radiation Effects Research on Structural Materials and the Implications to Reactor Design, Chicago, Illinois, October 15–16, 1959, USAEC Report TID-7588, October 1960.

9. B. E. Watt, Energy Spectrum of Neutrons from Thermal Fission of ^{235}U, Phys. Rev., 87(6): 1037–1041 (Sept. 15, 1952).

10. L. Cranberg, G. Frye, N. Nereson, and L. Rosen, Fission Neutron Spectrum of ^{235}U, Phys. Rev., 103(3): 662–670 (Aug. 1, 1956).

11. D. J. Hughes, Pile Neutron Research, Chapter 4, Fast Neutron Research, pp. 93–128, Addison-Wesley, Cambridge, Massachusetts, 1953.

12. J. C. Roy and J. J. Howton, Table of Estimated Cross Sections for (n,p), (n,γ) and (n,2n) Reactions in a Fission Neutron Spectrum, Canadian Report 1181, December 1960.

13. C. R. Lubitz, C. L. Dunford, and N. C. Francis, Calculation of (n,p) Cross Sections, Trans. Amer. Nucl. Soc., 8(1): 215–216 (June 1965).

14. C. H. Hogg, L. D. Weber, and E. C. Yates, Thermal Neutron Cross Sections of the ^{58}Co Isomers and the Effect on Fast Flux Measurements Using Nickel, USAEC Report IDO-16744, Phillips Petroleum Company, June 18, 1962.

15. W. C. Morgan, Foils: A Program for Computing Neutron Exposures from Foil Activation Data, USAEC Report HW-81367, Hanford Atomic Products Operation, April 1964.

16. R. S. Rochlin, Fission-Neutron Cross Sections for Threshold Reactions, Nucleonics, 17(1): 54–55 (January 1959).

17. C. E. Mellish, Neutron Threshold Reactions – An Intercomparison, Nucleonics, 19(3): 114–115 (March 1961).

18. J. Moteff, Neutron Flux and Spectrum Measurement with Radioactivants, Nucleonics, 20(12): 56–60 (December 1962).

19. T. O. Passell and R. L. Heath, Cross Sections of Threshold Reactions for Fission Neutrons: Nickel as a Fast Flux Monitor, Nucl. Sci. Eng., 10: 308–315 (1961).

20. T. O. Passell, The Use of Nickel-58 and Iron-54 as Integrators of Fast Neutron Flux, in Neutron Dosimetry, Vol. I, pp. 501–513, Proceedings of the Symposium on Neutron Detection, Dosimetry and Standardization, Harwell, England, Dec. 10–14, 1962, IAEA, Vienna, 1963.

21. K. Shure, Radiation Damage Exposure and Embrittlement of Reactor Pressure Vessels, USAEC Report WAPD-TM-471, Westinghouse Electric Corporation, Bettis Atomic Power Laboratory, November 1964.

22. J. B. Trice, Preliminary Report of an Analytical Method for Measuring Neutron Spectra, USAEC Report APEX-408, General Electric Company, Apr. 2, 1957.

23. S. R. Hartmann, A Method for Determining Neutron Flux Spectra from Activation Measurements, ASTIA-AD-142029, Report WADC-TR-57-375, Wright Air Development Center Materials Laboratory, June 14, 1957.

24. H. J. Donnert, A Method for the Analysis of Activation Foil Data, paper 1 in Proceedings of Fourth Radiation Effects Symposium Sponsored by Air Research and Development Command September 15–16, 1959, USAEC Report NP-9333, Vol. II, General Electric Company, 1959.

25. P. M. Uthe, Attainment of Neutron Flux Spectra from Foil Activation, Thesis, Report WADC-TR-57-3, GNE-9, Institute of Technology, Wright-Patterson AFB, March 1957.

26. W. D. Lanning and K. W. Brown, Calculated and Measured Neutron Energy Spectra Distributions Using the Threshold Detector Technique, Trans. Amer. Nucl. Soc., 4(2): 267 (November 1961).

27. O. W. Dietrich and J. Thomas, Fast-Neutron Spectra by Threshold-Detector Activation, in Physics of Fast and Intermediate Reactors, Proceedings of the Seminar in Vienna, Aug. 3–11, 1961, Vol. 1, pp. 377–386, IAEA, Vienna, 1962.

28. L. E. Steele and J. R. Hawthorne, Neutron Embrittlement of Reactor Pressure-Vessel Steels, in Materials and Fuels for High-Temperature Nuclear Energy Applications, Proceedings of the National Topical Meeting of the American Nuclear Society, San Diego, April 11–13, 1962, Chapt. 16, pp. 366–401, M.I.T. Press, Cambridge, Massachusetts, 1964.

29. H. H. Yoshikawa, In Pile Dosimetry for Radiation Damage Studies, USAEC Report HW-SA-3541, General Electric Company, Hanford Atomic Products Operation, June 2, 1964.

30. H. C. Claiborne, An Estimate of the Effect of Neutron Energy Spectrum on Radiation Damage of Steel, Trans. Amer. Nucl. Soc., 5(1): 250–252 (June 1962).

31. S. S. Pawlicki, Neutron Exposure Criteria for Reactor Vessels, Trans. Amer. Nucl. Soc., 6(1): 149–150 (June 1963).

32. D. R. Harries, P. J. Barton, and S. B. Wright, The Effects of Neutron Spectra and Dose Rate on Radiation Hardening and Embrittlement in Steels, British Report AERE-R-4222, December 1962.

33. C. Z. Serpan, Jr., H. E. Watson, J. R. Hawthorne, and L. E. Steele, Yankee Reactor Pressure Vessel Surveillance: Evaluation of Specimens Exposed During the Second Core, Report NRL-6179, Naval Research Laboratory, Nov. 24, 1964.

34. F. A. Brandt and A. J. Alexander, Effect of Neutron Irradiation at 550 F on Charpy Impact Properties of ASTM A 302 Grade B Steel, in Symposium on Radiation Effects on Metals and Neutron Dosimetry, Los Angeles, California, Oct. 2–3, 1962, pp. 212–232, ASTM-STP-341, Philadelphia, Pa., 1963.

35. E. Landerman, Surveillance Tests on Structural Materials in Nuclear Reactors, in Symposium on Radiation Effects on Metals and Neutron Dosimetry, Los Angeles, California, Oct. 2–3, 1962, pp. 233–252, ASTM-STP-341, Philadelphia, Pa., 1963.

4. MATERIALS*

There is potentially a relatively large number of materials that could be used in the construction of nuclear pressure vessels (see Table N-421 in Section III of ASME Code), but there are relatively few in use or contemplated for use. Materials selection is influenced by many factors, among which are suitability of mechanical and physical properties, fabricability, weldability, adequacy of production capacity in the forms required, material and fabrication costs, and a backlog of relevant experience by the fabricator in the use of the material. Accommodation of these various factors, that is, qualification of a material, requires a substantial expenditure of time and funds by the fabricator. Consequently, any new or unconventional material from the fabricators' viewpoint must either show potentially a substantial economic benefit or must possess significantly improved mechanical and physical properties such that its use is virtually demanded by technological advances. This conservative and cautious trend in material selection is illustrated by Table 4.1.

As indicated, a few reactor vessels have been fabricated from ASTM A 212 grade B, a carbon-silicon steel. This material has found wide usage in the power and petrochemical industries, and therefore its economics, fabricability, production problems, etc., are generally well known. Its selection for the early nuclear reactor vessels was therefore natural and reasonable. Unfortunately this material suffers marked deterioration in toughness in heavy sections and is not materially improved by fine-grain practice nor by heat treatment. In addition, it has comparatively low strength. Consequently, most of the later vessels have been made from a modified version of ASTM A 302 grade B steel. With the addition of nickel, as permitted by ASME Code Case 1339, this material has enhanced response to heat treatment and thereby exhibits improved impact strength in heavy sections. This modified version of ASTM A 302 grade B is now identified as ASTM A 533. It is at present the

---

*This chapter was prepared by D. A. Canonico, P. Patriarca, and G. C. Robinson, Jr.

Table 4.1. Summary of Materials Specified for Light-Water Reactor Vessels

Reactor Name	Plate	Course and Flange Forgings	Nozzle Forgings	Bolting	Nuts	Supports	Pipe	Weld Rod	Cladding
Shippingport	A 302 grade B								Stainless
Dresden-1	A 302 grade B	SA 336 grade F-1	SA 336 grade F-1	SA 193 grade B14	SA 193 grade 3	SA 212 grade B		Clad E 308 L	Stainless
Yankee	A 302 grade B modified	A 105 II modified	A 182 modified to A 302 grade B	SA 193 grade B16	AISI 4340	A 212 grade B	A 106 C	Clad 308 L	SA 240 grade S (s[illegible] welded sheet)
Saxton	A 212 grade B	A 350-58T	A 350-58T	AISI 4340	AISI 4340	A 212 grade B	A 376 TP 316	Clad 308 L	Stainless
Indian Point-1	A 212 grade B								Stainless
Big Rock Point	A 302 grade B	SA 336 modified		SA 193 meeting AISI 4340	SA 194 meeting AISI 4340	Type 304 (internal)		Clad 308, 309, Inconel	A 264-44T grade 3 type 304
Elk River	A 302 grade B	A 105 II	A 105 II, A 182 F 304	SA 193 grade 7			B 167	E 7016 clad A 371, type 308 L, 309	SA 264-3
Humboldt Bay	A 302 grade B	SA 336 modified	SA 336 modified	SA 193 grade B16	SA 193 grade B16	SA 302 grade B	A 213, B 167		Type 304
BONUS	A 212 grade B	A 105 II	A 182 F22	SA 193 grade 7	SA 194-2H	A 212 grade B	A 240-304, A 312-304, A 106 B, A 376 TP 304	E 7016 clad A 371, type 308 L, 309	Type 304
Pathfinder	A 212 grade B		A 105 grade 2, A 335 grade P22	A 437	A 437		A 155 grade KC70		Type 304 L
LaCrosse	A 302 grade B	A 336 modified, A 182 TP F 304	A 336 modified	A 437 grade B4	A 194 grade 4	A 302 grade B, B 166, A 276 TP 304	B 166, B 167, A 312 TP 304	Clad 308 L	Type 304 L
San Onofre	A 302 grade B	SA 336	SA 336	SA 193 meeting AISI 4340	SA 194 meeting AISI 4340	A 302 grade B	A 376 TP 316	Clad 308, 309	Stainless
Connecticut Yankee	A 302 grade B	SA 336 modified	SA 336 modified	SA 320 L43	SA 320 L43	SA 336 modified	A 376 TP 316	Clad 308, 309	
Oyster Creek	A 302 grade B	SA 336 modified, Code Case 1236-1	SA 336 modified, Code Case 1236-1	A 193 grade AISI 4340	A 193 grade AISI 4340	SA 312 grade B, SA 336 modified, Code Case 1236-1	A 213, A 249, A 312, A 376 TP 304, 316	Clad E 308	Type 304
Nine-Mile Point	A 302 grade B	SA 336 modified, Code Case 1236-1	SA 336 modified, Code Case 1236-1	A 193 grade AISI 4340	A 193 grade AISI 4340	SA 212 grade B, SA 336 modified, Code Case 1236-1	A 213, A 249, A 312, A 376 TP 304, 316	Clad E 308	Type 304
Dresden-2	A 302 grade B modified	A 336 modified	A 182-F304, A 336 F8, F8m, A 105 grade II	A 193 grade B16, A 320 grade L43 modified	A 193 grade 2H	A 276 TP 304, A 240 TP 304	A 213, A 249, A 312, A 376 TP 304, 316	A 233, A 298, A 316 clad A 371, ER 308 L, ER 309	Type 304
Carolina	A 302 grade A	SA 336 modified	SA 336 modified	SA 320 L43	SA 320 L43	SA 336 modified	A 376 TP 316	Clad 308, 309	Type 304
Millstone Point	A 302 grade B	A 508 class 2	A 508 class 2	A 540 grade B24	A 540 grade B24	A 508 class 2, A 516 grade 70	A 240 TP 304, A 312 TP 304 A 212 grade B, A 106 grade B	Clad E 308	Type 304
Brookwood	A 302 grade B	A 508 class 2, SA 336 modified	SA 336 modified	SA 320 L43 class 3	SA 320 L43 class 3	SA 212 grade B, SA 336 modified	A 376 TP 316	Clad 308 L	Type 304
Indian Point-2	A 302 grade B	SA 336 modified	SA 336 modified	SA 320 L43	SA 320 L43	SA 336 modified	A 376 TP 316	Clad 308, 309	Type 304
Palisades	A 302 grade B	A 508 class 2	A 508	Alloy steel A 540, B24	Alloy steel A 540, B24	A 336	SA 212 grade B	ER 308, ER 309, E8018-C3, A 316, A 298, A 371, Inco 182, A 233	Type 304
Turkey Point-3	A 302 grade B	A 508 class 2	A 508 class 2	SA 320 L43 class 3	SA 320 L43 class 3	SA 336 modified	A 376 TP 316	Clad 308 L	Type 304
TVA Browns Ferry	SA 302 grade B	SA 336 modified	SA 336 modified	A 193 grade B7	A 194 grade 2H	A 276 TP 304, A 240 TP 304	A 213, A 249, A 312, A 376 TP 304, 316 or A 240 TP 304	A 233, A 298, A 316, A 371, ER 308 L, ER 309	Type 304

sels

Pipe	Weld Rod	Cladding
		Stainless
	Clad E 308 L	Stainless
A 106 C	Clad 308 L	SA 240 grade S (spot-welded sheet)
A 376 TP 316	Clad 308 L	Stainless
		Stainless
	Clad 308, 309, Inconel	A 264-447 grade 3, type 304
B 167	E 7016 clad A 371, type 308 L, 309	SA 264-3
A 213, B 167		Type 304
A 240-304, A 312-304, A 106 B, A 376 TP 304	E 7016 clad A 371, type 308 L, 309	Type 304
A 155 grade KC70		Type 304 L
B 166, B 167, A 312 TP 304	Clad 308 L	Type 304 L
A 376 TP 316	Clad 308, 309	Stainless
A 376 TP 316	Clad 308, 309	
A 213, A 249, A 312, A 376 TP 304, 316	Clad E 308	Type 304
A 213, A 249, A 312, A 376 TP 304, 316	Clad E 308	Type 304
A 213, A 249, A 312, A 376 TP 304, 316	A 233, A 298, A 316 clad A 371, ER 308 L, ER 309	Type 304
A 376 TP 316	Clad 308, 309	Type 304
A 240 TP 304, A 312 TP 304 A 212 grade B, A 106 grade B	Clad E 308	Type 304
A 376 TP 316	Clad 308 L	Type 304
A 376 TP 316	Clad 308, 309	Type 304
SA 212 grade B	ER 308, ER 309, E8018-C3, A 316, A 298, A 371, Inco 182, A 233	Type 304
A 376 TP 316	Clad 308 L	Type 304
A 213, A 249, A 312, A 376 TP 304, 316 or A 240 TP 304	A 233, A 298, A 316, A 371, ER 308 L, ER 309	Type 304

reference plate material where plate is used for primary nuclear pressure vessels for light-water reactors. Forgings meeting ASTM A 508 class 2 requirements are equivalent to A 533 in response to heat treatment and fabrication and are similarly used for primary nuclear pressure vessels for light-water reactors as nozzles and shell courses.

There are two additional alloys presently being investigated for future use. One is a chromium-molybdenum alloy (2 1/4% Cr–1% Mo) and is defined in ASTM A 542 (plate) and ASTM A 541 class 7 (forgings). The other is a nickel-chromium-molybdenum alloy (3% Ni–1.75% Cr–0.5% Mo) that is defined in ASTM A 543 (plate) and ASTM A 508 class 4 or ASTM A 541 class 8 (forgings). The latter materials are covered by ASME Code Case 1358.

Most of the bolting materials currently selected are covered in ASTM A 540 and are of the chromium-nickel-molybdenum 4340 type. The electrode most often selected at present for base-material pressure vessels is E 8018 C3, which contains 1% nickel and meets the requirements of ASME SA 316. The electrode and flux used for submerged-arc welding are in many instances proprietary and therefore will not be covered in any detail in this report. For electroslag welding, a 2% Mn–1/2% Mo filler material is used. Various types of stainless steel electrodes are used for the cladding and attachment of internal support. Inconel filler wire is also used for dissimilar-metal welding and overlay as bearing surfaces of the shell flanges.

4.1 MATERIALS PROPERTIES

Table 4.2 presents the chemical composition of materials which have been used, are being used, and are proposed for use in the near future in light-water reactor pressure vessels. In some instances materials are listed under two specifications as a consequence of recent specification revisions. Table 4.3 provides a cross index between the current ASTM designation and previously used ASTM and commercial designations. Table 4.4 presents the mechanical properties of these same materials of interest.

Table 4.2. Chemical Compositions of Reactor Vessel Materials[a]

Material Designation	Chemical Composition (wt %)									
	C	Cr	Ni	Fe	Mo	Mn	P	S	Si	Other Elements
Carbon steel plate										
A 212 grade B firebox to A 300	0.31			Balance		0.85–1.20	0.035	0.040	0.15–0.30	
A 515 grade 70 firebox	0.35			Balance		0.90	0.035	0.040	0.15–0.30	
Low-alloy steel plate										
A 302 grade B firebox	0.25			Balance	0.45–0.60	1.15–1.50	0.035	0.040	0.15–0.30	
A 302 grade B firebox modified[b]	0.25		0.4–1.0	Balance	0.45–0.60	1.15–1.50	0.035	0.040	0.15–0.30	
A 533 grade B	0.25		0.40–0.70	Balance	0.45–0.60	1.15–1.50	0.035	0.040	0.15–0.30	
A 533 grade C	0.25		0.70–1.00	Balance	0.45–0.60	1.15–1.50	0.035	0.040	0.15–0.30	
A 542	0.15	2.00–2.50		Balance	0.90–1.10	0.30–0.60	0.035	0.035	0.15–0.30	
A 543[c]	0.23	1.50–2.00	3.00–4.00	Balance	0.45–0.60	0.40	0.02	0.02	0.20–0.35	0.03 V
High-alloy steel plate										
A 240 type 304[d]	0.08	18.00–20.00	8.00–12.00	Balance		2.00	0.045	0.030	1.00	
A 240 type 304 L	0.03	18.00–20.00	8.00–12.00	Balance		2.00	0.045	0.030	1.00	
A 240 type 316[e]	0.08	16.00–18.00	10.00–14.00	Balance	2.00–3.00	2.00	0.045	0.030	1.00	
Welded or seamless carbon steel pipe										
A 106 grade B	0.30			Balance		0.29–1.06	0.048	0.058	0.10 min	
A 106 grade C	0.35			Balance		0.29–1.06	0.048	0.058	0.10 min	
A 155 grade KC70	0.31			Balance		0.85–1.20	0.035	0.40	0.15–0.30	
Seamless low-alloy pipe										
A 335 grade P22	0.15	1.90–2.60		Balance	0.87–1.13	0.30–0.60	0.030	0.030	0.50	
Welded or seamless high-alloy pipe and tubing[e]										
A 213 grade TP 304	0.08	18.00–20.00	8.00–11.00	Balance		2.00	0.040	0.030	0.75	
A 213 grade TP 316	0.08	16.00–18.00	11.00–14.00	Balance	2.00–3.00	2.00	0.030	0.030	0.75	
A 249 grade TP 304	0.08	18.00–20.00	8.00–11.00	Balance		2.00	0.040	0.030	0.75	
A 249 grade TP 316	0.08	16.00–18.00	11.00–14.00	Balance	2.00–3.00	2.00	0.040	0.030	0.75	
A 312 grade TP 304	0.08	18.00–20.00	8.00–11.00	Balance		2.00	0.040	0.030	0.75	
A 312 grade TP 316	0.08	16.00–18.00	11.00–14.00	Balance	2.00–3.00	2.00	0.040	0.030	0.75	
A 376 grade TP 304	0.08	18.00–20.00	8.00–11.00	Balance		2.00	0.030	0.030	0.75	
A 376 grade TP 316	0.08	16.00–18.00	11.00–14.00	Balance	2.00–3.00	2.00	0.030	0.030	0.75	
Nickel-chromium-iron seamless pipe or tubing										
B 167[f]	0.15	14.0–17.0	72.0 min	6.0–10.0		1.0		0.015	0.5	0.5 Cu
Carbon steel forgings										
A 105 grade II	0.35			Balance		0.90	0.05	0.05	0.35	
A 105 grade II, modified chemistry	0.30			Balance		0.90	0.035	0.040	0.35	
A 350 grade LF-1 modified[g]	0.30		2.0	Balance		1.35	0.040	0.050		
Low-alloy steel forgings										
A 182 grade F1	0.30			Balance	0.44–0.65	0.50–0.85	0.045	0.045	0.15–0.35	
A 182 grade F1 modified to meet A 302 grade B firebox	0.25			Balance	0.45–0.60	1.15–1.50	0.035	0.040	0.15–0.30	

[a]All single value entries are a maximum unless otherwise noted; only ladle values are given; all plate values are for 4-in. or greater thickness.

[b]Modified by ASME Code Case 1339, paragraph 1.

[c]Supplemental requirements added to A 541 and A 543 to restrict phosphorus and sulfur contents per Code Case 1358.

[d]Used for structural supports and as cladding conforming to ASTM A 264.

[e]Solution heat treated.

[f]Modified by ASME Code Case 1336.

[g]Modified by ASME Code Case 1332.

Table 4.2 (continued)

Material Designation	Chemical Composition (wt %)									
	C	Cr	Ni	Fe	Mo	Mn	P	S	Si	Other Elements
Low-alloy steel forgings (continued)										
A 182 grade F22	0.15	2.00–2.50		Balance	0.87–1.13	0.30–0.60	0.040	0.040	0.050	
A 336 modified[g]	0.27	0.25–0.45	0.50–0.90	Balance	0.55–0.70	0.50–0.80	0.040	0.050	0.15–0.35	
A 508 class 2, A 541[c] class 2	0.27	0.25–0.45	0.50–0.90	Balance	0.55–0.70	0.50–0.80	0.025	0.025	0.15–0.35	0.06 V
A 541[c] class 7	0.15	2.00–2.50		Balance	0.90–1.10	0.30–0.6	0.02	0.02	0.50	
A 541[c] class 8, A 508 class 4	0.23	1.25–2.00	2.75–3.90	Balance	0.40–0.60	0.20–0.40	0.02	0.02	0.30	0.03 V
High-alloy steel forgings										
A 182 F 304	0.08	18.00–20.00	8.00–11.00	Balance		2.00	0.040	0.030	1.00	
A 182 F 304 L	0.035	18.00–20.00	8.00–13.00	Balance		2.00	0.040	0.030	1.00	
A 336 class F8	0.08	18.00–20.00	8.00–11.00	Balance		2.00	0.040	0.030	1.00	
A 336 class F8m	0.08	16.00–18.00	10.00–14.00	Balance	2.00–3.00	2.00	0.040	0.030	1.00	
Low-alloy steel castings										
A 356 grade 10[h]	0.20	2.00–2.75		Balance	0.90–1.20	0.50–0.80	0.05	0.05	0.60	
Alloy steel bolting										
A 193 grade B16	0.36–0.44	0.80–1.15		Balance	0.50–0.65	0.45–0.70	0.04	0.04	0.20–0.35	0.25–0.35 V
A 193 meeting A 151 4340	0.38–0.43	0.70–0.90	1.65–2.00	Balance	0.20–0.30	0.60–0.80	0.040	0.040	0.20–0.35	
A 320 grade L43[i]	0.38–0.43	0.70–0.90	1.65–2.00	Balance	0.20–0.30	0.60–0.85	0.040	0.040	0.20–0.35	
A 437 grades B4B, B4C	0.20–0.25	11.00–12.50	0.40–0.80	Balance	0.90–1.25	0.40–0.80	0.025	0.025	0.20–0.50	0.20–0.30 V, 0.90–1.25 W, 0.05 Al, 0.05 Ti, 0.04 Sn
A 540 grade B24	0.37–0.44	0.70–0.95	1.65–2.00	Balance	0.30–0.40	0.70–0.90	0.025	0.025	0.20–0.35	0.40 V
Ferritic and alloy steel nuts										
A 194 grade 4	0.40–0.50			Balance	0.20 min	0.50–0.95	0.04	0.05	0.15 min	
A 194 meeting AISI 4340	0.38–0.43	0.70–0.90	1.65–2.00	Balance	0.20–0.30	0.60–0.80	0.040	0.040	0.20–0.35	
A 194 grade 8	0.08	18.00–20.00	8.00–12.00	Balance		2.00	0.045	0.030	1.00	
Nonferrous and high-alloy steel bar										
A 276, type 304[j]	0.08	18.00–20.00	8.00–12.00	Balance	2.00		0.045	0.030	1.00	
B 166[f]	0.15	14.00–17.00	72.00 min	6.00–10.00		1.00		0.015	0.5	0.5 Cu
Welding electrodes and filler materials										
A 316 class E8018-C3	0.12		0.80–1.10	Balance		1.00		0.04	0.80	
Electroslag filler				Balance	0.5	2.00				
A 316 class E9018-B3	0.12	2.00–2.50		Balance	0.9–1.20	0.90		0.04	0.80	
A 298 class E 308[k]	0.08	18.00–21.00	9.00–11.00	Balance		2.50	0.04	0.03	0.90	
A 298 class E 309[k]	0.15	22.0–25.0	12.00–14.00	Balance		2.50	0.04	0.03	0.90	
A 371 class ER 308[k]	0.08	19.5–22.0	9.0–11.0	Balance		1.0–2.5	0.03	0.03	0.25–0.60	
A 371 class ER 309[k]	0.12	23.0–25.0	12.0–14.0	Balance		1.0–2.5	0.03	0.03	0.25–0.60	
Inconel 82	0.10	18.0–22.0	67 min	3.0		2.5–3.5		0.015	0.50	0.50 Cu, 2.00–3.00 Cb, 0.30 Ta, 0.75 Ti
Inconel 182	0.10	15.0	Balance	8.0		7.5		0.015	1.00	
Inconel 92	0.10	14.0–17.0	67 min	10.0		2.00–2.75		0.015	0.35	2.5–3.5 Ti

[h] Modified by ASME Code Case 1333.

[i] Modified by ASME Code Case 1335, paragraph 4.

[j] Modified by ASME Code Case 1334.

[k] Also 308 L and electrodes of 308 and 309 selected for low carbon content.

Table 4.3. Cross Index of Designations of Pressure Vessel Steels

Current ASTM Designation	Grade	ASTM and Commercial Designations Previously Used	Composition Type	Condition	Minimum Yield Strength or Point (ksi)
A 515	55	A 201 or A 212	C-Si	Hot rolled or normalized	30
	60		C-Si	Hot rolled or normalized	32
	65		C-Si	Hot rolled or normalized	35
	70		C-Si	Hot rolled or normalized	38
A 516	55	A 201 or A 212	C-Mn-Si	Hot rolled or normalized	30
	60		C-Mn-Si	Hot rolled or normalized	32
	65		C-Mn-Si	Hot rolled or normalized	35
	70		C-Mn-Si	Hot rolled or normalized	38
A 517	A	N-A-XTRA 100	Mn-Si-Cr Mo-Zr-B	Quenched and tempered	100
	B	"T-1" type A	Mn-Cr-Mo V-Ti-B	Quenched and tempered	100
	C	Jalloy-S-100	Mn-Mo-B	Quenched and tempered	100
	D	SSS-100A	Cr-Mo-Ti Cu-B	Quenched and tempered	100
	E	SSS-100	Cr-Mo-Ti Cu-B	Quenched and tempered	100
	F	"T-1"	Mn-Ni-Cr-Mo V-Cu-B	Quenched and tempered	100
	G	Phoenix N-A-XTRA 100	Mn-Si-Cr Mo-Zr-B	Quenched and tempered	100
	H	"T-1" type B	Mn-Ni-Cr-Mo V-B	Quenched and tempered	100
	J	HQ-100A	Mn-Mo-B	Quenched and tempered	100
A 533	A	A-302	Mn-Mo	Quenched and tempered	50, class 1 70, class 2
	B	A 302 (Ni-Mod)	Mn-Mo-Ni (0.40-0.70 Ni)	Quenched and tempered	50, class 1 70, class 2
	C	A 302 (Ni-Mod)	Mn-Mo-Ni (0.70-1.00 Ni)	Quenched and tempered	50, class 1 70, class 2
A 537	A	A 212 normalized	Mn-Si	Normalized	50
	B	A 212 quenched and tempered	Mn-Si	Quenched and tempered	60
A 542		A 387D quenched and tempered 2 1/4 Cr-1 Mo	Cr-Mo	Quenched and tempered	85, class 1 100, class 2
A 543		HY-80; HY-100	Ni-Cr-Mo	Quenched and tempered	85, class 1 100, class 2

4.2 METALLURGICAL CONSIDERATIONS

The chemical constituents, choice of melting practice, pouring techniques, rolling and forging parameters, and welding methods and material must be selected to provide a product that will meet the specified requirements. A review of the relative importance of these variables on the metallurgy of the materials in the forms required for the vessel fabricators involves an assessment of considerable commercial practice and metallurgical experience. In order to better understand and appreciate

Table 4.4. Required Mechanical Properties of Reactor Vessel Materials[a]

Material Designation	Tensile Strength (psi)	Yield[b] Strength (psi)	Elongation in 8 in. (%)	Elongation in 2 in. (%)	Reduction of Area (%)	Charpy V-Notch Impact Value[c] (ft-lb)		Maximum Hardness Number	
						Average for Three Specimens	One Specimen	Brinell	Rockwell B
Carbon steel plate									
A 212 grade B firebox	70,000–85,000	38,000	19	22		20	15		
A 515 grade 70 firebox	70,000–85,000	38,000	19	23		20	15		
Low-alloy steel plate									
A 302 grade B firebox	80,000–100,000	50,000	17	20		30	25		
A 302 grade B firebox modified[d]	80,000–100,000	50,000	17	20		30	25		
A 533 grades B and C, class 2	90,000–115,000	70,000		18.0		30	25		
A 542, class 2	115,000	100,000		15		35	30		
A 543, class 2	105,000	85,000		16		35	30		
A 543, class 2	135,000	115,000		16		35	30		
High-alloy steel plate									
A 240 type 304	75,000	30,000		40.0				202	88
A 240 type 304 L	70,000	25,000		40.0				202	88
A 240 type 316	75,000	30,000		40.0				217	95
Welded or seamless carbon steel pipe									
A 106 grade B	60,000	35,000		22 longitudinal 12 transverse[e]		15	10		
A 106 grade C	70,000	40,000		20 longitudinal 12 transverse[e]		20	15		
A 155 grade KC70	70,000–85,000	38,000	19	22		20	15		
Seamless low-alloy pipe									
A 335 grade P22	60,000	30,000		22 longitudinal 14 transverse[e]		15	10		
Welded or seamless high-alloy pipe									
A 213 grade TP 304, 316	75,000	30,000		35					
A 249 grade TP 304, 316	75,000	30,000		35					
A 312 grade TP 304, 316	75,000	30,000		35					
A 376 grade TP 304, 316	75,000	30,000		35					
Nickel-chromium-iron seamless pipe									
B 167[f]	80,000	30,000 min–35,000 min		30–35					
Carbon steel forgings									
A 105 grade II	70,000	36,000		22	30	20	15		
A 350 grade LF-1 modified[g]	60,000	30,000							
Low-alloy steel forgings									
A 182 grade F1	70,000	40,000		25.0	35.0	20	15	201	
A 182 grade F22	70,000	40,000		20.0	30.0	20	15	201	

[a]All single entries are minimum values unless otherwise noted.

[b]Yield defined as 0.2% offset value.

[c]Charpy impact values are those required by paragraph N-330 of Section III of the ASME Code.

[d]Modified by ASME Code Case 1339, paragraph 1.

[e]Tabulated values are for standard round 2-in. gage length test specimen.

[f]Modified by ASME Code Case 1336.

[g]Modified by ASME Code Case 1332.

Table 4.4 (continued)

Material Designation	Tensile Strength (psi)	Yield[b] Strength (psi)	Elongation in 8 in. (%)	Elongation in 2 in. (%)	Reduction of Area (%)	Charpy V-Notch Impact Value[c] (ft-lb)		Maximum Hardness Number	
						Average for Three Specimens	One Specimen	Brinell	Rockwell B
Low-alloy steel forgings (continued)									
A 336 modified[g]	80,000	50,000		20		30	25		
A 508 class 2	80,000	50,000		18	38	30	25		
A 508 class 4	105,000	85,000		16		35	30		
A 541 class 6	80,000	60,000		20	50	35	30		
A 541 class 7	105,000	85,000		18	48	35	30		
High-alloy steel forgings									
A 182 F 304	75,000	30,000		45	50				
A 182 F 304 L	65,000	25,000		30	50				
A 336 class F8, F8m	[illegible],000	30,000		30	35				
Low-alloy steel castings									
A 356 grade 10[h]	84,000	55,000		20.0	35.0	30	25		
Alloy steel bolting									
A 193 grade B16, 2 1/2 to 4 in. in diameter	125,000	105,000		18	50	35	30		
A 193 grade B, over 4 to 7 in. in diameter	110,000	95,000		17	45	35	30		
A 320 grade L43	125,000	105,000		16	50	35	30		
A 437 grade B4B	145,000	100,000		13	30	35	30		
A 437 grade B4C	115,000	80,000		18	50	35	30		
A 540 grade B24[i]	115,000-165,000	100,000-150,000		10-15	35-50	30-35	25-30	248-311 to 331-429	
Ferritic and alloy steel nuts									
A 194 grade 4								200 min	94 min[j]
A 194 grade 8								149 min	81 min
Nonferrous and high-alloy steel bar									
A 276 type 304[k]	75,000 min-90,000 min	30,000 min-45,000 min		35 min-40 min	45 min-50 min				
B 166[f]	80,000	35,000		30					
Welding electrodes and filler materials									
A 316 class E8018-C3	80,000	67,000		19					
A 316 class E9018-B3	90,000	77,000		17					
A 298 class E 308	80,000			35					
A 298 class E 309	80,000			35					
A 371 class ER 308	80,000			35					
A 371 class ER 309	80,000			35					
Inconel 82[m]	80,000	40,000		30					
Inconel 92[m]	80,000	40,000		30					80
Inconel 182[m]	80,000	40,000		30					90

[h]Modified by ASME Code Case 1333.

[i]Properties required vary with diameter.

[j]Proof load stress of 175,000 psi.

[k]Modified by ASME Code Case 1334.

[m]Properties are given as welded.

the significance of the processes involved, a brief review of some of the fundamental aspects follows.

4.2.1 Element Effects

The mechanical properties of steel are greatly influenced by the presence of elements that are especially added as alloying materials, as well as those unwanted residuals that are always present. However, to understand the effects of these elements and the role they play in the production and fabrication of steel components, a basic understanding of the metallurgy of steel is needed.[1-5]

Steel is essentially iron and carbon. Iron is an element that, in the solid state, can on cooling (at 1670°F) undergo an allotropic transformation in which its crystal structure changes from an atomic arrangement that is face-centered cubic (fcc) to one that is body-centered cubic (bcc). Although this atomic transformation is not observable except by x-ray diffraction techniques, its resultant effect on the microstructure of the steel is readily observable and is the basis for much of the correlation between properties and atomic crystal structure. The face-centered cubic structure is present at the elevated temperature and is a solid solution that has been designated as austenite. As the temperature of the austenite is lowered, it may transform through a diffusion process to ferrite (the body-centered cubic structure) or some other body-centered cubic structure (pearlite or bainite). If the austenite is rapidly cooled, a diffusionless transformation to martensite may occur. Martensite is a metastable body-centered tetragonal (bct) structure in which the carbon is present at interstitial sites that extend the normally body-centered cubic lattice.

There are a number of common elements that are specifically added to iron to enhance its mechanical properties. These are carbon, manganese, nickel, chromium, molybdenum, silicon, and aluminum. In addition, there are other elements, such as nitrogen, sulfur, and phosphorus, that although unwanted are always present. Of the specifically added elements listed above, carbon has by far the most influence on the mechanical properties of steel. It is the element that is responsible for the strength[6] obtainable

in the low-alloy (<5%) class of steels. The plot of Fig. 4.1 shows the influence of carbon (and manganese) on tensile strength of plain carbon steels. It is evident that small additions of carbon have a great effect on tensile strength.

The easiest way to discuss the influence of the specifically added elements on the microstructure of steel is to consider their effects on isothermal transformation (TTT) diagrams. These TTT diagrams are for isothermal conditions and do not truly represent what will occur under practicable conditions; however, continuous cooling diagrams are not necessary for this discussion, and it is sufficient to say that the results obtained under conditions of continuous cooling will exaggerate the effects illustrated by the TTT diagram. Normally, the transformations are transposed to longer times and lower temperatures.

Figure 4.2 shows TTT diagrams[7] for plain carbon steels (the manganese that is present is a residual from the iron ore that was originally charged into the blast furnace). The higher carbon content (see lower portion of Fig. 4.2) transposes the transformation lines to the right (to longer times). Nickel, manganese (below 1%), and silicon have similar effects. To appreciate what is being exemplified in an isothermal transformation diagram, it is necessary to be familiar with an equilibrium diagram for

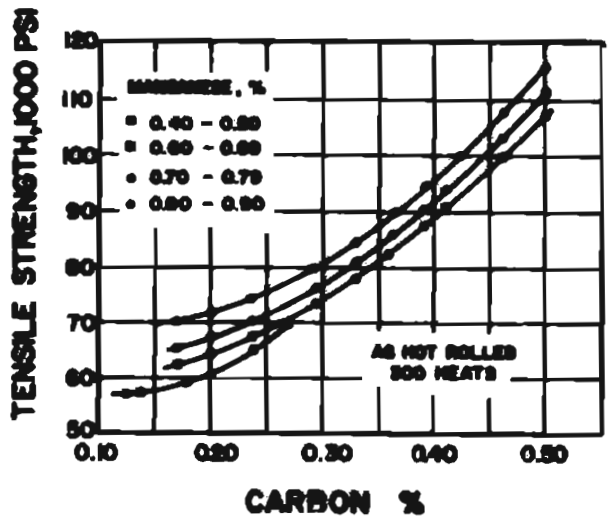

Fig. 4.1. Effect of Manganese and Carbon on the Tensile Strength of Carbon Steel in the Hot-Rolled Condition. (Taken from Ref. 6)

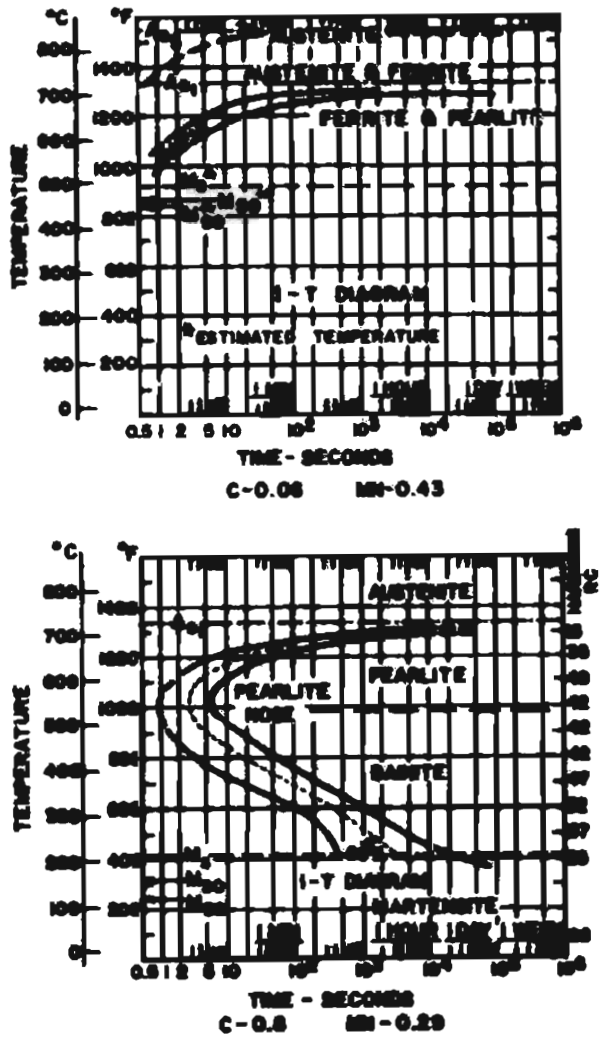

Fig. 4.2. Isothermal Transformation Diagrams Showing the Effects of Carbon on the Pearlite Nose and Martensite Starting Temperature. (Taken from Ref. 7)

the steel. Normally only iron and carbon are considered because of the number of elements involved, and the iron-carbon binary phase diagram is used.

The section of the iron-carbon binary equilibrium phase diagram[8] that includes carbon contents up to 5% is shown in Fig. 4.3. The steels that are normally used for reactor pressure vessels seldom go above 0.4% carbon; consequently, this diagram is more than adequate. In this equilibrium diagram, only three regions are of importance for this iiscussion. The region above the line marked A_3 is the face-centered cubic austenite.

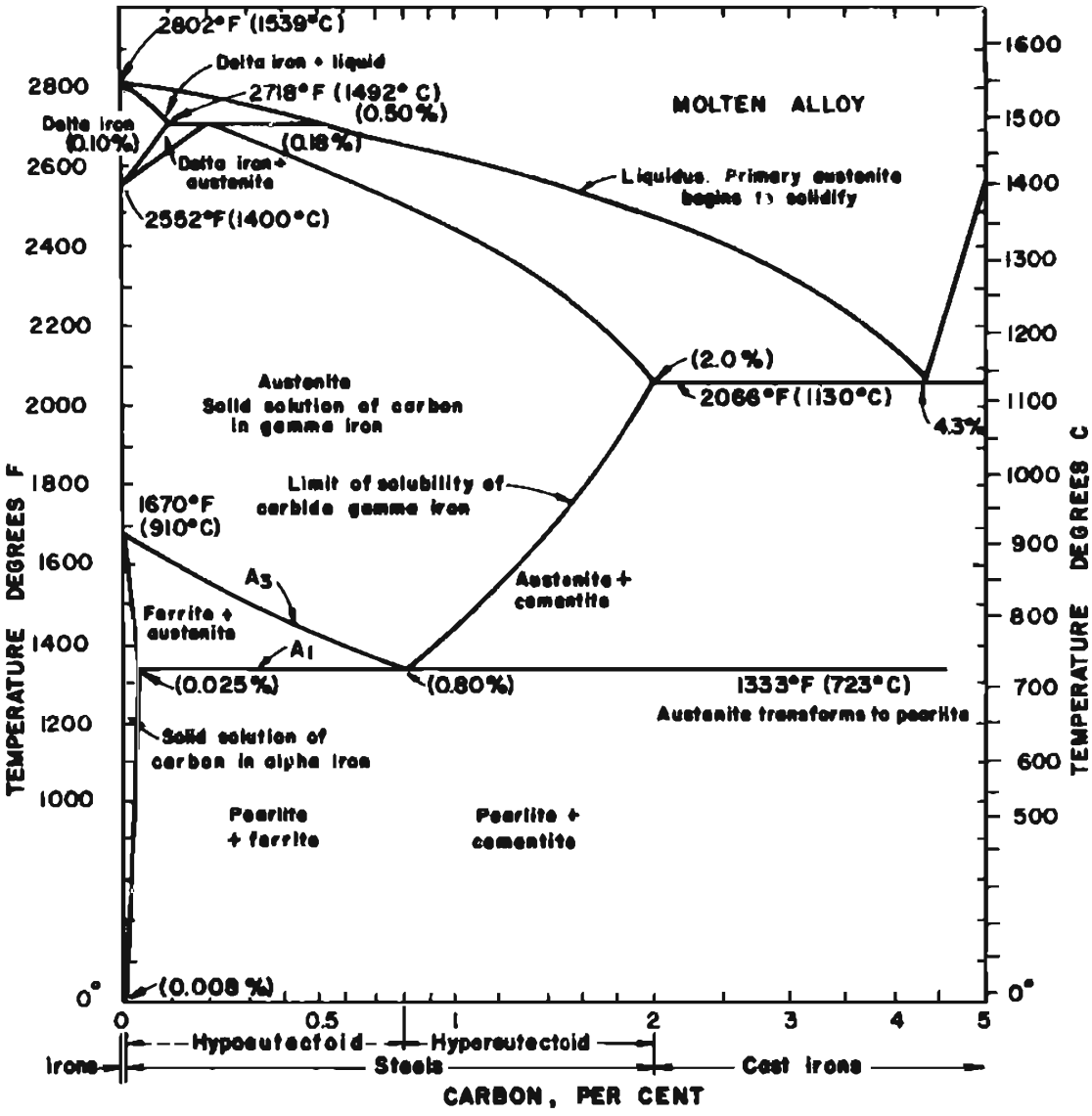

Fig. 4.3. The Iron-Carbon Binary Equilibrium Phase Diagram. The right-hand ordinate of the complete diagram is usually placed at 6.67% carbon. (Taken from Ref. 8)

Carbon is soluble (in the solid state) in austenite from a maximum of 2% at 2066°F to a minimum of 0.8% at 1333°F. Consequently, because the carbon levels of the reactor-grade steels are below 0.8%, there is no need to be concerned with carbon precipitation in the austenite.

The second region of interest lies in the area between A_3 and A_1. This is a two-phase region within which both austenite (fcc) and ferrite

(bcc) structures may coexist. The presence of ferrite is due to the allotropic transformation (fcc to bcc) that was previously mentioned. To fully understand what has occurred here, it would be best to follow the cooling of 0.20%-carbon steel from some elevated temperature (for example, 1650°F) through a temperature drop. When the 0.2%-carbon alloy cools to approximately 1570°F, the solid solution of austenite begins to decompose into primary crystals of ferrite, which has a much lower tolerance for carbon (<0.025% vs 1.2%). Carbon is rejected by the decomposing austenite. Consequently, the remaining austenite is enriched in carbon, and its composition is no longer 0.2% but, rather, a higher carbon level. This transformation of austenite to ferrite continues down to 1333°F, where the last of the austenite decomposes into ferrite and iron carbide (a compound of iron and carbon that occurs at 6.67% carbon and has the stoichiometric composition Fe_3C).

The two-phase ferrite plus Fe_3C region below 1333°F is the third area of interest. The product of this decomposition at 1333°F is called eutectoid. Under the equilibrium conditions discussed it has a characteristic ferrite-carbide lamellar morphology. Coarse pearlite and ferrite would be the equilibrium microstructure for this 0.2%-carbon alloy. Unfortunately, this equilibrium structure leaves much to be desired from a mechanical properties point of view. Fortunately, the morphology of the ferrite plus carbide structure can be varied. The isothermal transformation diagram shown in Fig. 4.2 helps to illustrate the structures that can be obtained under other than equilibrium conditions. The Ae_3 and Ae_1 lines represent the A_3 and A_1 intersection in the binary equilibrium diagram (Fig. 4.3). If there is a deviation from absolute equilibrium, the isothermal transformation diagrams show the products of the austenite decomposition as a function of the transformation temperature. As the temperature at which the austenite is allowed to decompose is decreased, the product to which it transforms will vary. At the higher temperature, it will be coarse lamellar pearlite. As the temperature is decreased, the pearlite becomes finer (the interlamellar distance decreases) until it no longer transforms to a lamellar product but, rather, to a more featherlike product that is less diffusion dependent. This lower temperature transformation product is called bainite. Within the

bainitic range, there is also a gradation in fineness of structure. The lowest temperature transformation product occurs by an instantaneous shear mechanism (nondiffusion) and is called martensite, as has already been stated. The martensite transformation results in a metastable body-centered tetragonal crystal structure. Associated with this martensite transformation is a volumetric growth (~4%) that gives rise to high stresses.

Three factors influence the transformation behavior of these steels. These are composition, homogeneity, and austenite grain size. As has been pointed out, certain elements, such as carbon and nickel, move the isothermal transformation diagram to the right without appreciably altering its shape. These elements promote the transformation to martensite (by increasing the minimum time necessary to cool the steel below the "nose" of the isothermal transformation diagram). Other elements, such as molybdenum and chromium, also move the diagram to the right; in addition, they alter its shape. These elements tend to promote the transformation to bainite by transposing the pearlite region to the right without noticeably affecting the lower temperature transformations.

Austenitic grain size affects the transformation to pearlite. Coarse grains tend to retard the transformation to pearlite and make the steel behave as if molybdenum or chromium were added. However, a fine austenitic grain size yields better mechanical properties. Nonhomogeneous distribution of chemical elements will result in segregated microstructures, which will cause certain areas to transform before other regions. This results in a microstructure that may have severely impaired mechanical properties.

Normally, the strength of the alloy will be inversely related to the transformation temperature. Coarse pearlite is weaker than fine pearlite. The same is true for bainite. Martensite, the lowest temperature transformation product, is the strongest. However, strength is not particularly a problem in reactor-grade steels. The yield strengths currently required for ASTM A 533 grade B steel are attainable in heavy-section sizes both at the 1/4 T (thickness) position and at the 1/2 T position. There is evidence[9] that bainitic microstructures are possible at the midthickness of 12-in.-thick A 533 steel plates. Moreover, there is evidence[10] that ASTM A 542 steel also can meet the required tensile properties at its midthickness. The problem does not lie in strength, but

rather in notch toughness. It is when this property is considered that meeting specification requirements can become troublesome.

Notch toughness is defined as the ability to resist brittle crack initiation and propagation and is essentially a material property. The notch toughness of a material can be measured by the energy required to cause its rupture. It has been found that body-centered cubic materials undergo a transition wherein the energy required for their fracture precipitously drops and the fracture characteristics change from a shear mode to one of cleavage. This transition is temperature dependent and for relatively pure iron occurs over a very small temperature range. Figure 4.4 illustrates the effect of carbon on the shape of the steel transition curve. This figure was taken from the work of Rinebolt and Harris[11] in which they discuss the effects of various elements on the Charpy V-notch 15 ft-lb transition temperature. Their data showed that the results obtained were structure dependent; however, general trends held true. Briefly, their results can be summarized as follows: elements that increase the transition temperature in pearlitic steels are boron, carbon, chromium, copper, molybdenum, phosphorus, and silicon; elements that decrease (enhance) the transition temperature are manganese and nickel. Aluminum, when present in small amounts, tends to decrease the

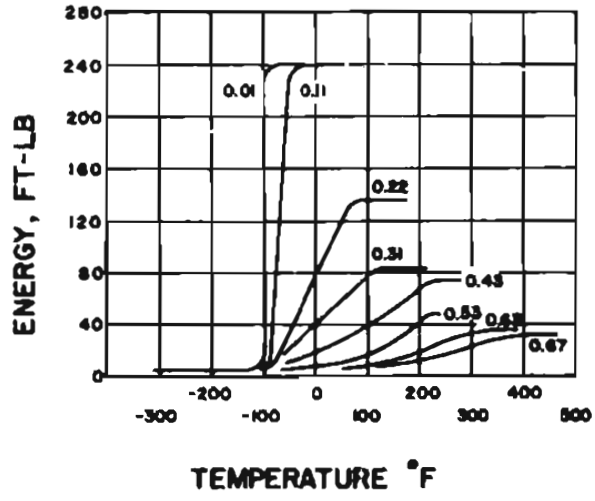

Fig. 4.4. Effect of Carbon Content on the Shape of the Charpy V-Notch Transition Temperature Curve for Steel. Values on curves are carbon content in wt %. (Taken from Ref. 11)

transition temperature because of its combination with oxygen and nitrogen. Another study[12] has shown arsenic to have a detrimental effect on the impact properties of pearlitic steels.

Figure 4.5 shows the effect of the various alloying elements on the corrected 15 ft-lb Charpy V-notch transition temperature. It is evident

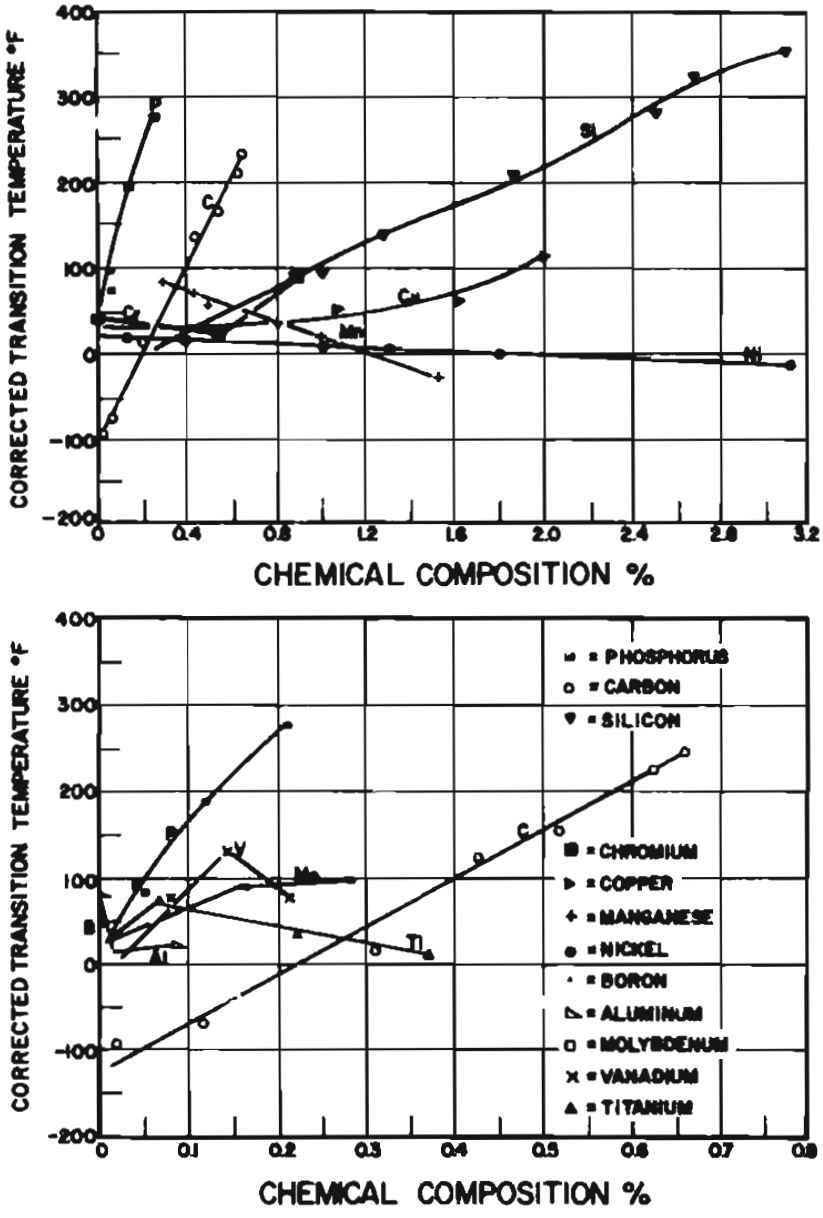

Fig. 4.5. Effect of Chemical Composition on Corrected 15 ft-lb Charpy V-Notch Transition Temperature. (Taken from Ref. 11)

from this figure that the elements are not equal in their effects on the notch toughness. Of the elements indicated, carbon and phosphorus are by far the most detrimental. For the microstructures studied by Rinebolt and Harris,[11] an increase of 0.01% raised the 15 ft-lb Charpy V-notch transition temperature 5.7°F and 14°F for carbon and phosphorus, respectively. Arsenic had an effect similar to that of carbon. Some of the other elements have, in their own right, only a minor effect; however, often there is twofold benefit. Such is the case for manganese. Manganese is a strengthening agent and, hence, in addition to decreasing the transition temperature, permits the use of a lower carbon content. This second factor is even more effective in improving notch toughness than the manganese itself. Nickel is the other major element that enhances notch toughness, and its beneficial effects have been recognized by including it in ASTM specification A 533, which is essentially ASTM A 302 grade B with a nickel modification (as permitted by ASME Code Case 1339).

Thus far this discussion has been concerned primarily with the effects of certain elements on the notch toughness of steel and has touched on their effects on strength. However, in addition to the elements mentioned above, other elements are present in steels. These include the gases H_2, O_2, and N_2 and sulfur. It is desirable to maintain sulfur at as low a level as possible because it is responsible for hot shortness in steels. Hot shortness is attributed to the presence of a small amount of a lower melting constituent. This constituent usually is found in the grain boundaries and results in a weakness in the hot-working range. The tendency toward hot shortness with sulfur is exaggerated[13] if nickel is present. This hot shortness is reflected in both the hot workability of a steel ingot and in weldability. Hot cracking (microfissuring) is prevalent in the weld-metal and heat-affected zones of sulfur-bearing steels.

Of the gases mentioned, hydrogen has the greatest detrimental effect on the properties of steels. Hydrogen is dangerous because it is readily soluble as monatomic hydrogen in face-centered cubic austenite; however, its solubility is considerably less in body-centered cubic ferrite and pearlite. In addition, even if the quantity present is small, its solubility in ferrite is negligible at room temperature. Hence, as the steel is cooled and undergoes transformation, the ferrite becomes supersaturated

with hydrogen. This hydrogen diffuses out of the metal lattice and recombines as molecular H_2 or can form methane at discontinuities and voids within the steel. When this occurs, the pressure buildup is of fracture-strength magnitude. This pressure buildup is responsible for the flakes and shatter cracks[14] seen in massive forgings and is also responsible for the cold cracking often noted in the heat-affected zones of weldments made in low-alloy high-strength steels.

Nitrogen, probably the second most important gas, has been blamed[15] for the strain-aging phenomenon observed in low-carbon steels. Strain aging is the loss of ductility and notch toughness after a steel has been cold worked and heated into the range 400 to 700°F. It is attributed to the movement of atomic nitrogen to the high-energy (cold-worked) sites where it tends to prohibit the movement of dislocations.

Oxygen, the last of the previously mentioned gases, has an adverse effect[16] on notch toughness. In addition, its presence usually results in greater quantities of nonmetallics being distributed throughout the steel. These nonmetallics, which include not only oxides but also sulfides, such as manganese sulfide, are potential stress raisers and may result in premature failure.

In summary, most of the elements discussed in this section serve a functional purpose in that they provide the possibility of greater strength or an improved notch toughness. Often, when an element is added for one purpose, such as strength, its side effects may prove deleterious to another property. Usually, the composition selected is based on a balance in which ductility and toughness are often sacrificed to achieve strength or vice versa. Other elements such as aluminum and manganese (that quantity added over the alloying requirement) are added to chemically combine with and tie up another element. Aluminum is a good deoxidizer; it removes oxygen and also has been found to reduce strain aging by combining with the nitrogen.[17] Oxygen can also be removed through the use of other deoxidizing agents, such as silicon and vanadium, and through the recently developed technique of vacuum deoxidation. The manganese combines with sulfur and ties up that undesirable element as manganese sulfide, a higher melting compound. However, their presence results in nonmetallics, and these are undesirable. Nickel has been added to steels for improved

notch toughness; however, there is evidence[18] that it may be responsible for the embrittlement that was noted after these steels were aged at 700°F for long periods of time.

4.2.2 Melting Practice

Essentially only two types of melting process are currently employed for the production of large (multiton) ingots for nuclear reactor pressure vessel components. These are the basic open hearth and the basic electric furnace processes. The choice of the basic furnace lining over the acid furnace allows the use of a basic slag and thereby implements the removal of phosphorus. Today, in the United States, regardless of the melting technique, the processes used are basic.

The ASTM specifications for quenched and tempered alloy steel plates (such as A 514, A 515, A 516, A 517, A 533, A 542, and A 543) currently permit the use of either melting process for producing plate. However, the Lukens Steel Company, which is the major producer of heavy-section plate, normally melts the steel in an electric furnace[19] and, indeed, the advantages warrant the selection of this process over that of the basic open hearth. The major advantages[20] of the electric furnace lie in its use of charge materials that are initially lower in phosphorus content and the fact that the phosphorus-bearing oxidizing slags may be removed prior to furnace deoxidation; this avoids the reversion of phosphorus to the molten steel. It is evident from Section 4.2.1 that the removal of phosphorus is important.

In addition to the phosphorus removal, the electric furnace inherently has other benefits. These are that the furnace can be operated with minimum slag volumes (the furnaces are tiltable and hence slags can be removed) which can be controlled quickly and thereby permit a relatively high recovery efficiency for oxidizable elements, such as chromium, manganese, etc. Also, because of slag control, the ladle deoxidation is minimized and the resultant steel is cleaner (fewer sulfide and oxide inclusions).

The modern ASTM specifications most often referenced for nuclear-grade forgings (ASTM A 508) dictate that only the basic electric furnace

process be used. The use of this specification recognizes the inherent advantages of the more controllable electric furnace melting practice.

It is evident that the use of the electric furnace will increase in the future. The manufacturers of forgings have recognized that their extremely large forgings (many of which require multifurnace heats to pour an ingot) receive, by comparison, a small amount of work and, because of their massive sizes, are not readily heat treatable to the maximum mechanical properties attainable for their compositions. The trend toward heavy sections is more recent in the plate-producing industry and is only now being recognized. Indeed, the maximum work that can be done on an ingot that is to result in a plate thickness of 8 to 12 in. is quite nominal and, in many instances, less than that done on heavy ring forgings. In addition these heavier sections limit the response of the material to heat treatment and thereby necessitate that the original starting material be at its optimum from a cleanliness point of view.

4.2.3 Vacuum Treatment

As has been pointed out, hydrogen has an adverse effect on the weldability and soundness of low-alloy high-strength steels. In order to reduce the hydrogen level in steel ingots, particularly those that were to result in massive forgings, vacuum degassing was introduced a little over ten years ago. The total benefits that have been derived from vacuum degassing have been clouded by the fact that during this period melting practices and compositional limitations have been improved also. Figure 4.6 shows the improvement in the surface sonic indications of rotor forgings since 1950. It is evident from this figure that the trend in improved sonic indications was already well under way prior to the introduction of vacuum degassing in 1956. An excellent discussion of vacuum treatments can be found in the Battelle Memorial Institute report on "Vacuum-Degassed Steels from the Consumer's Viewpoint."[21] (Figure 4.6 was taken from that document.)

The fact that vacuum degassing lowers the hydrogen level and improves the cleanliness of very large forgings has been substantiated.[22] The decrease in hydrogen has resulted in the production of massive forgings

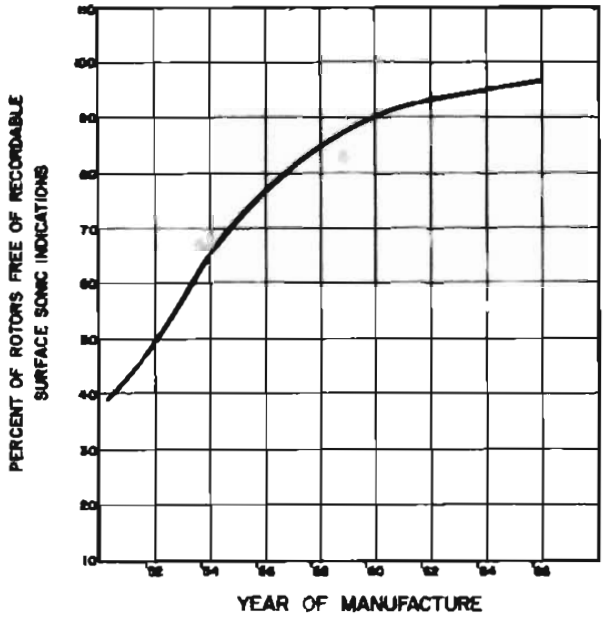

Fig. 4.6. Improvements in the Soundness of Rotor Forgings. (Taken from Ref. 21)

free from flake and shatter cracks. The reduction of the hydrogen level will also be reflected in improved weldability.

A more recent innovation in vacuum treatments has been the vacuum deoxidation[23,24] of the molten steels. The vacuum degassing process, in addition to lowering the hydrogen levels, reduces the oxygen and nitrogen levels. This reduction of oxygen decreases the amount of deoxidizer required and yields a steel even cleaner than that obtained from only vacuum degassing. This reduction in the nonmetallic inclusion content is reflected in improved fatigue properties.

4.2.4 Working Processes

The working processes are rolling, forging, and forming. Rolling and forging are both performed on a steel slab that has previously been soaked and broken down from its original ingot form. The soaking operation, which is done at a very high temperature (>2150°F), combined with the breaking down of the ingot to slab, does much toward homogenizing the originally heterogeneous ingot.

The forming operation is performed on a rolled plate that is usually supplied to the fabricator in the hot-rolled condition.* Forgings are always supplied in the heat-treated condition.

4.2.4.1 Rolling

The current requirements for plates are such that the nominal section size being used is greater than 6 in. in thickness. Moreover, thicknesses of 12 to 15 in. are being considered for the larger, greater than 1000-Mw(e), reactors. The amount of work (reduction in thickness) that can be performed on a slab (or ingot) that is to result in a plate thickness of the magnitude discussed here is marginal. Usually, the reduction is about 4 to 1; however, 3 to 1 is the minimum being currently allowed.

The rolling operation is carried out in the temperature range where the steel is austenitic. The process serves two main purposes: (1) the heating operations tend to develop a uniform chemical composition by breaking up and eliminating the segregated dendritic structure, and (2) because the rolling temperature is above the recrystallization temperature, the rolling serves to refine the austenitic grain size. The final austenitic grain size is controlled both through the deoxidation practice employed during pouring and the temperature at which the last passes are made. A fine austenitic grain size is preferred. Finally, and what may also be an additional advantage, the ductility is usually superior in the primary rolling direction.

As is evident the reduction possible in rolling these plates is considerably less than what would be done on thinner gage materials. Consequently the benefits in homogeneity and cleanliness that can be obtained from the electric furnace and vacuum treatments become quite important and should be so recognized.

4.2.4.2 Forging

The flange and shell-course ring forgings that are used in nuclear pressure vessels are produced by essentially two techniques, mandrel

*Current information indicates that this will not be true for the field-erected pressure vessels. They are to be supplied in the heat-treated condition and cold formed.

forging and ring rolling. The mandrel forging operation is a process whereby the flange is elongated or enlarged in a steplike manner. The forging blank is incrementally upset between the tophead and the mandrel. There is an appreciable time lapse between increments of upset for adjacent positions around the forging blank. In contrast, the ring rolling operation is a continuous process quite like rolling. The time during one revolution of the forging blank is negligible.

It appears that the ring rolling process should inherently yield a product that is more uniformly worked and consequently has more uniform properties than the product of the mandrel process and, indeed, this is the position taken by advocates of the ring rolling operation. However, the size of the forging and the fact that the operations are carried out at quite high temperatures will probably minimize these advantages. It is possible that slightly different properties may exist due to the difference in finishing temperature between the various locations; however, the massive size of these forgings and their associated slow cooling rates probably negate this possibility.

Nozzles may be produced by either the open or tight mandrel processes, depending on their size.

The forgings, regardless of how they were manufactured, are contour machined essentially to finished dimensions, quenched and tempered, and then finish machined prior to shipment to the fabricator. Therefore, it is the forger's responsibility to assure that the required mechanical properties are met.

4.2.4.3 Forming

Forming can be classified as either hot or cold. Hot forming is carried out at temperatures at which the steels are austenitic, and the comments on rolling are applicable here. The plates are the only components that are hot formed, and this is done to provide the required shapes for fabricating a shell course, a torus section, or a head. As was previously mentioned, the plates are supplied in the hot-rolled condition. The fact that they are to be hot formed justifies this requirement. The plates are reaustenitized and soaked prior to the forming operation. Often this operation is terminated before the plates begin to

transform; however, one fabricator does allow working to be performed at temperatures as low as 1000°F. In this temperature range, it is possible to get some cold work, but because the formed parts are always reaustenitized and quenched this work need not be considered. After the quenching and tempering operation, some realignment may be required, and this is done cold. The amount of strain induced by this dimensioning process is in the order of less than 0.1% and is ignored. If cold forming becomes one of the prominent fabricating processes, however, its effect on mechanical properties must be considered. There is evidence[25] that the plates for the field-erected pressure vessels are to be purchased in the heat-treated condition and subsequently cold formed. In view of this possibility, the effects of cold working are discussed here.

Cold forming is usually done near room temperature and definitely below the recrystallization temperature. It results in the steel remaining in a strain-hardened condition in which the microstructure is visibly distorted. The results of this strain hardening are reflected in higher strength and reduced ductility and notch toughness.

There is evidence[26] that cold forming can have a significant effect on the properties, particularly notch toughness, of plain carbon steel. Stress relieving produces virtually no improvement in the strained material.

Stout and his colleagues[27,28] have studied the effect of cold straining a number of pressure vessel steels. They showed that all the steels were affected by straining and, perhaps even more important, by a subsequent strain aging. For example, an ASTM A 302 grade B steel studied at Lehigh University had an increase of approximately 60°F in its 15-mil lateral expansion temperature correlation due to the combined effects of 5% straining and aging in the temperature range (500 to 700°F) currently being employed for nuclear reactors. This strain-aging phenomenon has been tied in with the presence of carbon, nitrogen, and oxygen. Nitrogen is considered by far the most dangerous. The use of the vacuum treatment helps to eliminate much of these gases and, in so doing, reduces the tendency toward strain aging. Stress relieving will normally relieve this strain-aging embrittlement; however, excessive exposure to elevated temperatures can be dangerous.

4.2.5 Microstructure

It has been pointed out that certain elements were added to the basic iron-carbon steel composition because they enhanced mechanical properties. The mere presence of these elements is not important; it is their effect on the resultant transformation product that is the measure of their influence. There are five microstructures that are important when discussing pressure-vessel steels. These are austenite, ferrite, pearlite, bainite, and martensite. The properties of a steel are dependent on which microstructure is present and its quantity. Ideally, the final microstructure should be a tempered medium carbon (~0.2%) martensite in order to have the best balance of properties, that is, good strength and good notch toughness. However, to obtain a martensitic structure, it is necessary to cool the steel at a rate equal to or faster than some critical value. If the material is foil, the cooling rate is no problem. The foil, regardless of the cooling medium, will lose heat at an extremely fast rate. As the foil thickness increases, its ability to lose heat decreases and, consequently, a medium (such as water) capable of removing heat at a faster rate must be selected in order to assure that the cooling rate is subcritical. Eventually, as the thickness progresses to that of sheet and, subsequently, plate, it may become impossible, regardless of the cooling medium, to achieve the critical cooling rate. At this point, other compromises must be made. These compromises and their effect on mechanical properties are discussed here.

The cooling rate is a function of the size of the section being cooled and the cooling medium. It is, for all practical purposes (as long as the discussion is confined to plain carbon and low-alloy steels), independent of the chemical composition. Therefore, for a section of given size being cooled in a given medium, the cooling rate for a plain carbon steel (such as ASTM A 212) is the same as for a more highly alloyed steel (such as ASTM A 302, A 533, or A 542). However, the resultant microstructure will not necessarily be the same. This is due primarily to the influence of chemical composition. As was pointed out earlier, the individual elements affect the isothermal transformation diagrams by shifting the start of the austenitic transformation to longer times.

This, in effect, permits a slower critical cooling rate. Actually, certain elements do no more than allow a given thickness of steel to transform to a microstructure that would otherwise be possible only with a thinner section.

Because of the plate thicknesses currently being used, it is extremely difficult to obtain a martensitic microstructure in low-alloy steels, even after accelerated cooling. In most instances, because of the presence of a certain element, such as molybdenum, or other elements, a bainitic structure can be obtained. The presence of these elements retards the pearlitic transformation and enhances the austenite-to-bainite transformation. In plain carbon steels, the pearlitic transformation acts like a roof and minimizes the possibility of lower temperature transformation products (see Fig. 4.2). Insofar as it is nearly impossible to produce martensite (the critical cooling rate is not attainable in these section sizes), the fabricators prefer to have the transformation occur at as low a temperature as possible. Usually, for the steels being discussed, the resultant microstructure is 100% bainite or a bainite-ferrite aggregate, with the fineness of each being dependent on the section size being cooled (cooling rate). Other factors such as the condition of the austenite and its grain size also influence the transformation product; however, their effect is relatively minor. (Although these effects are considered to be independent, they are related to the chemical composition of the steel. For instance, aluminum is added as an austenite grain refiner.)

This discussion and the one previously given in Section 4.2.1, "Element Effects," are both directed at what is known in steels as hardenability. Hardenability is defined as the ease with which martensite can be produced. Thus the position of the pearlite nose is an index of hardenability. The most commonly used method for measuring hardenability is the Jominy End Quench Test (JEQT). Investigators have attempted[29] to predict the mechanical properties of pressure vessel steels based on this test. Their correlation is quite good for tensile properties; however, the notch toughness cannot be correlated. The use of the JEQT test for predicting tensile properties is applicable for thin-section materials, and its use is appropriate for differentiating the hardenability between

various steels. However, its slowest cooling rate is faster than the rates being obtained in 10- to 15-in.-thick water-quenched steel plate. Hence, the coarsest microstructure possible in the JEQT is finer than that obtained in the steels being discussed. Perhaps an effort should be expended to devise a test more directly applicable to the heavier section sizes and thus provide a more rapid means of predicting their final properties.

The cooling rate is essentially thickness dependent; however, the surface condition of the plate and the temperature and agitation of the coolant are extremely important. If steam is allowed to blanket the surface due to a tenacious surface scale, the water is stagnant, or the water temperature is too high, the cooling rate will be retarded and the resultant microstructure much coarser than expected. These problems are overcome by assuring that the water temperature does not exceed some maximum value (about 150°F) and by agitation during quenching. The scale problem can be avoided through conditioning the surface of the plate with a composition that will assure that the scale will expunge during quenching.

4.2.6 Mechanical Properties

The mechanical properties being discussed here are essentially the tensile properties, including ductility, and notch toughness. Other properties, such as fatigue resistance, are also important, but their limitations are often reflections of the previously mentioned properties.

Achieving the required tensile properties has been no problem. The minimum ASTM values for A 533 (A 302 grade B modified) steel can be met at both the required 1/4 T position and at the midthickness for section sizes up to 12 in. The microstructures obtained are ferrite and coarse bainite. Both Lehigh University[9] and Lukens Steel[30] report that the microstructures obtained in 6- and 12-in. sections are quite similar. Lukens, in fact, presented data for 15-in.-thick plate with center and surface properties essentially identical and both in excess of the minimum 50,000-psi yield strength, which is a requirement of the ASTM specification for A 533 grade B class 1 steel. The Lehigh data were for

microstructures that were obtained by simulating the cooling rates usually obtained in 6- and 12-in. plate thicknesses. Their data were based on cooling rates that were the most conservative of a number available to them.

There are data for A 533 steel in section sizes up to 12 in. which show that a maximum nil-ductility transition (NDT) temperature of +10°F can be maintained. If a 30 ft-lb Charpy V-notch "fix" (see Section III of ASME Code) with the drop-weight nil-ductility temperature is correct for this grade of steel, the NDT temperatures were about 0 and +25°F, respectively for the 6- and 12-in.-thick A 533 steel reported by Lehigh University. The +25°F NDT temperature is in excess of the desired +10°F; however, there is evidence that the fix energy decreases with increasing plate thickness. This point should be investigated to ascertain its authenticity and, if proven to be correct, should offer solace in that the 30 ft-lb fix will be conservative.

There are also mechanical property data available for ASTM A 542 (A 387 grade D) steel. This chromium-molybdenum steel is being suggested as a possible choice for the next generation of pressure vessels. There does not appear to be any difficulty in achieving the required tensile properties, at least up to 8-in.-thick sections. However, there are contradictory[9,31] data available for 12-in.-thick sections. These differences may be due to slight differences in the chemical compositions of the material or perhaps heat treatment.

Notch toughness does present a problem. The chromium-molybdenum steel is quite temperature sensitive, and an incorrect tempering temperature can result in very poor impact properties. Sterne[30] has presented data that show a drop in the +10°F Charpy V-notch energy from approximately 50 ft-lb for an 1150°F temper to 11 ft-lb for an 1100°F temper. The results of the Charpy V-notch tests at Lehigh University for A 542 steel contained a considerable amount of scatter. The Charpy V-notch 30 ft-lb energy value was achieved at 0°F for the simulated cooling rate for the 6-in. section; however, it was about +75°F for the simulated cooling of the 12-in. section. Similar scatter is present in drop-weight data presented earlier[31] for 2-in.-thick A 387 grade D steel. Further, the earlier work suggested a 35 ft-lb "fix" between Charpy V-notch and NDT

temperature for the 2 1/4% Cr–1% Mo steel. These data relative to ASTM A 542 are rather disconcerting and should be investigated further. The sensitivity of the steel to heat treatment may be responsible in great measure for these results.

In addition to the data for ASTM A 533 and A 542 steels, there are data available for ASTM A 543, a nickel-chromium-molybdenum steel. This is a more highly alloyed steel than either A 533 or A 542. Its tensile properties approximate those of A 542; however, it exhibits considerably better notch toughness properties. The 30 ft-lb Charpy V-notch energy value for the simulated 12-in.-thick section was obtained at almost –100°F.

This steel appears to possess the best combination of strength and toughness; however, it is more highly alloyed, which will cause it to be more expensive and, depending upon experience, more difficult to weld. The presence of the high nickel content may contribute to an embrittlement effect that can result in a loss of notch toughness.

4.2.7 Size Effects

Earlier in this section it was pointed out that because of the heavy section sizes being employed, the amount of work performed on an ingot is minimal. For this reason, the distribution of properties throughout the length, width, and thickness of a plate becomes of interest. It is known that the elemental distribution can vary within an ingot; however, the steel producers do attempt to overcome this problem by adjusting each individual heat that contributes to the quantity of molten metal necessary for a large ingot. However, these steels are highly alloyed and segregation may become more prominent as the alloying content increases. Certain elements tend to segregate when in the presence of other elements. Carbon and manganese can cause banding (areas depleted in carbon or manganese).

The data brought forth thus far do not indicate that through-thickness deviations in properties are a problem. In fact, except for some data on ASTM A 542 (A 387 grade D) steel, the opposite has been the case. Both tensile and notch-toughness properties have been confined to narrow

limits for a given heat of steel. Some data presented for ASTM A 542 steel have contained excessive scatter, and this may be due to segregation. This point can easily be investigated.

The distribution of properties from the top to the bottom of the plate are not so well documented. No doubt cutouts from a number of plates have either been tested or are avilable for testing but, depending upon the availability of these data or the material, this question may or may not be easily answered.

It has been established that the center line of a large ingot usually contains most of the unwanted residuals. This being the case, it is encouraging to see the uniformity of properties from surface to surface. This speaks well for the electric furnace and vacuum treatment techniques. However, it cannot be denied that the center line may possess the poorest chemical composition. If this is true, perhaps forged shell courses should be encouraged. The trepanning or plugging operation done prior to ring rolling or mandrel forging will remove most of the unwanted core.

4.2.8 Welding

Welding problems can be divided essentially into two parts: weldability, which is metallurgical in nature, and the metal-joining processes. It is difficult to separate these two areas because of their interrelationship. For example, the chemical composition of the filler metal selected is dictated by the joining process that is to be used. An effort will be made to discuss them separately; however, an exact line of demarcation is impossible.

4.2.8.1 Weldability

The selection of the composition of the filler metal is dependent on whether the weld is expected to respond to an austenitizing heat treatment. Usually welds are deposited by a multipass technique, and a complete reheat treatment is not necessary. When this is the case, the carbon level is usually held to a much lower value (~0.12% vs 0.22%) than is normally found in the base steel. In addition, the compositional levels of some of the other elements are varied, depending upon whether they

are easily transferred across the arc. Usually as-deposited weld metals have no difficulty in meeting strength requirements; however, because of their highly segregated as-cast structure, they possess poor notch-impact properties unless microstructurally modified by both compositional control and multipass welding procedures. As has already been pointed out, carbon is minimized and, as a further measure toward improving the impact properties, nickel is added (as in A 533 grade B steel). Usually, the nickel content of the weld metal is higher than that of the base metal.

Deoxidizers, such as silicon, are also found in the filler metals, and usually their levels are much higher than are found in the base metals.

When welding steel, assuming that the mechanical property requirements are reasonable, hydrogen is by far the most important element to be considered. Its effect on weldability has been recognized for a number of years and care is taken to eliminate (or at least minimize) its presence when welding carbon steels. However, hydrogen may not be a problem if the steel does not transform to martensite.[32] It is the synergistic effect of the hydrogen and martensite that produces underbead cracking (hydrogen-induced, heat-affected-zone cracking that occurs near room temperature). The propensity for a steel to be subject to underbead cracking is dependent on its tendency to form martensite, and a number of researchers have studied this problem. The result has been the prediction of weldability based on a carbon equivalent. Winterton[33] has laboriously reviewed many of the formulas proposed for predicting the tendency toward an austenite-to-martensite transformation (this has been called a carbon equivalence). The relationship between underbead cracking and the carbon equivalent is given in Fig. 4.7.

As pointed out above, underbead cracking is a problem only if martensite is present. If hydrogen is eliminated or if martensite is not allowed to form, the problem will not exist. Vacuum treatment of the weld-rod alloy and the base metal will assure that these are not sources for hydrogen. The next source (and probably the most important) lies in the slag covering that protects a weld deposit during solidification. (This source does not exist when welding with the inert-gas processes.)

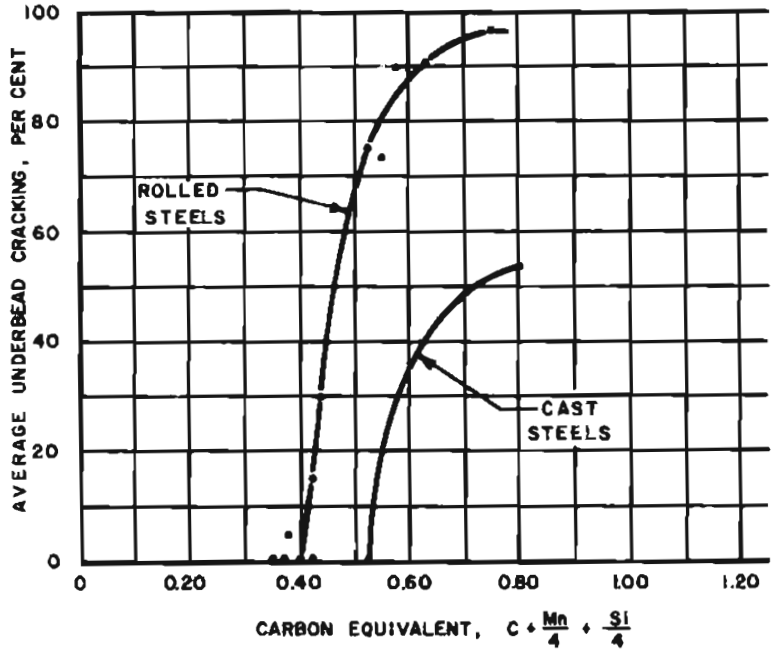

Fig. 4.7. Relation Between Underbead Cracking and Chemical Composition of 1-in.-Thick Carbon-Manganese Steels. (Taken from Ref. 30)

The coating on a stick electrode may be composed of hydrogen-containing compounds. The use of low-hydrogen electrodes eliminates this problem, and the only hydrogen source remaining is moisture. If the welder is careful and uses only thoroughly dried coated electrodes and submerged-arc fluxes, this source is eliminated also. As a further assurance that underbead cracking will not occur, a preheat of usually greater than 250°F (for low-alloy high-strength steels) is used. Proper preheat assures that the transformation product in the heat-affected zone of the weldment is not martensite but, rather, lower bainite. The upper limit for the preheat is usually about 500 to 600°F because, if the steel should transform above this temperature, the required properties may not be met.

The above discussion has been concerned with cold cracking (cracks that occur near room temperature). This type of cracking is most prevalent in steel welding; however, hot cracking, that is, microfissuring of the weld metal and heat-affected zone near the melting point of the steel, cannot be ignored. This hot cracking is attributed to the segregation of residual elements (primarily sulfur) to the grain boundaries

of the heat-affected zone and the interdendritic regions of the weld metal. The melting point of the segregated region is below that of the bulk alloy, and any strain placed across it can result in a fracture. Both the hot cracks and underbead cracks are microscopic, and because of their size they often go undetected.

The selection of the filler metal composition is left to the discretion of the fabricator. However, properties, weld qualification, and development test results are subject to the approval of the customer. The fabricator's actual analysis and the technique whereby he obtains that analysis are quite often proprietary information.

Much welding experience has accumulated on the steels currently being used in the reactor pressure vessels. The need for low hydrogen content and preheat is recognized, and underbead cracking need not be a problem in fabrication. Although problems will not initiate from welds made under correct conditions, a haphazard arc strike on a steel surface can cause a problem. The massive sections used in these reactors present heat sinks that impose infinitely fast cooling rates on the molten crater. These arc strikes may go undetected and could trigger a failure.

4.2.8.2 Welding Processes

Currently, three processes are being used to join the large components that make up a nuclear pressure vessel. These are the submerged-arc process, the manual stick-electrode process, and the electroslag process. The field-fabricated Monticello reactor in Minnesota will be manual stick-electrode welded. The discussion below on the submerged-arc process can be extended to be applicable to multipass stick-electrode welds.

The submerged-arc welding process was, until the introduction of the electroslag process, the highest deposition-rate technique available. The process is capable of being operated with high currents and, due to the large heat input, often melts a considerable amount of base metal, particularly when used with the thinner sections. Consequently, the composition of the base metal has a great influence on the composition of the weld metal. In the very thick sections currently being utilized in the reactor pressure vessel industry, it is necessary to use a multipass

technique to make the welds. The fact that each pass is subsequently reaustenitized contributes greatly to the mechanical properties of the submerged-arc welds. This reheat treatment refines the weld metal to the point where its properties after postweld heat treatment are normally superior to those of the base metal. No doubt the selection of the chemical composition of the filler metal contributes to this superiority. A multipass submerged-arc weld is shown in Fig. 4.8. The relationship between the individual passes can be seen easily. The microstructure of the weld metal can be controlled through heat input. Consequently, there is considerable latitude possible in the level of the mechanical properties obtainable in the weld metal for a given chemical composition.

The electroslag process is a very high deposition-rate process (see Chapter 8 for details of this welding process). For the purpose of this discussion, picture a large electric furnace that is capable of producing a continuous casting. The difference is that in the electroslag process the furnace moves and not the casting. An electroslag weld joining 3-in.-thick steel plates is shown in Fig. 4.9. The weld has the appearance of an ingot; that is, it has coarse columnar-type grains at the mold wall (the plate in this case) and finer equiaxed grains in the center. This photograph indicates that inhomogeneities exist in the weld toward the base-metal interface and that the center is homogeneous. Figure 4.10 shows that this is not true but, rather, that the center is also made up of columnar grains; however, the method of sectioning falsely leaves the impression that they are equiaxed. Figure 4.10 also illustrates one other very important feature; that is, the weld metal is composed of about 60% base metal. Therefore, the base-metal composition will have a strong influence on the resultant weld-metal composition.

The as-cast structure is unacceptable and electroslag welds must be reaustenitized and cooled (accelerated cooling is required for the section sizes of interest). Further, the extremely high heat input necessary to produce the welds results in a heat-affected zone that extends for some distance into the base metal. This fact also is evident in Fig. 4.9.

The filler metals used for electroslag welds are selected with this requirement in mind. It is necessary that the weld metal, as well as the base metal, respond to an austenitizing and quenching heat treatment.

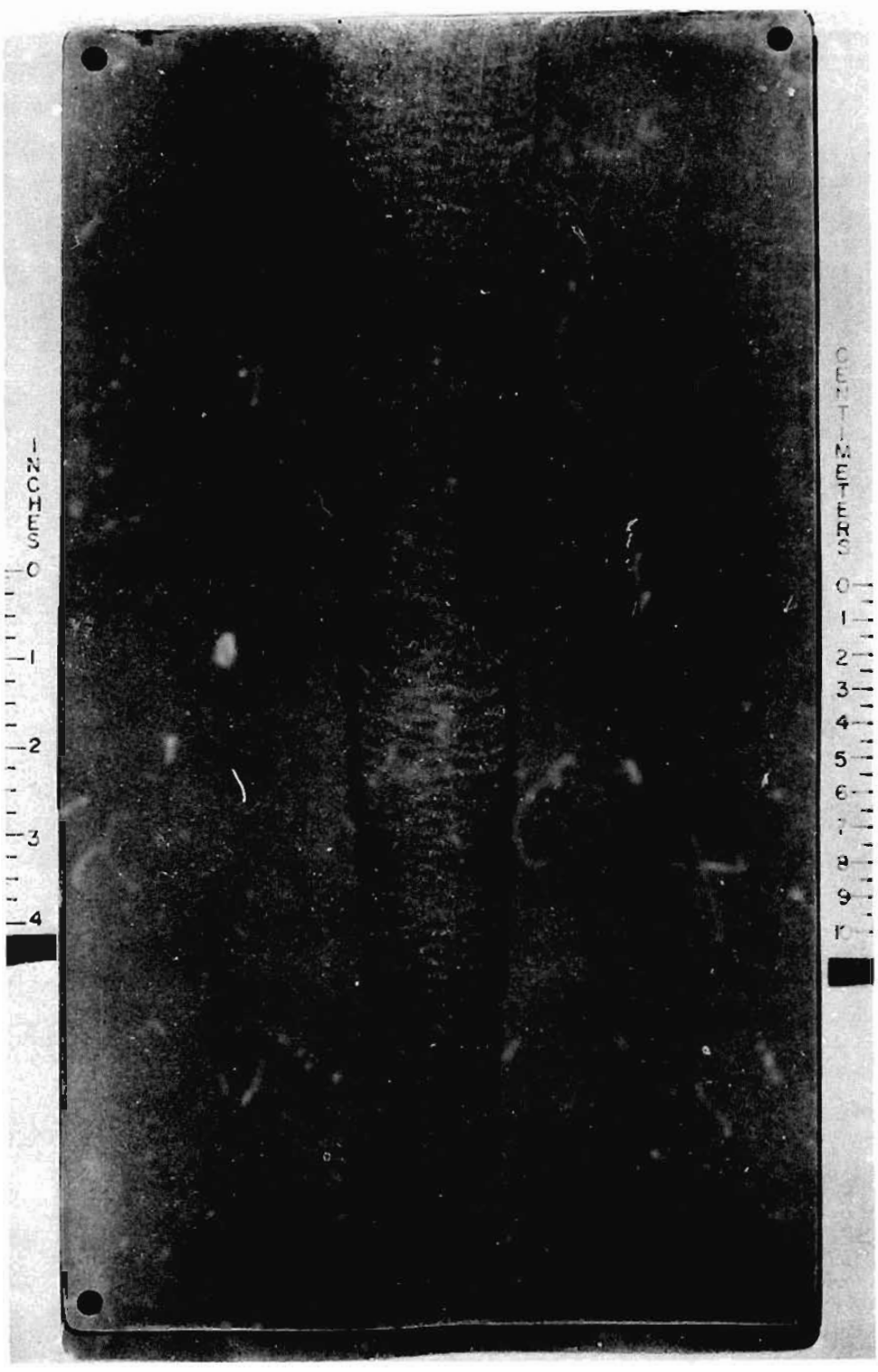

Fig. 4.8. Photomacrograph of a Transversely Sectioned Multipass Submerged-Arc Weld in a Heavy Section Carbon Steel Plate. (Photograph from Combustion Engineering, Inc.)

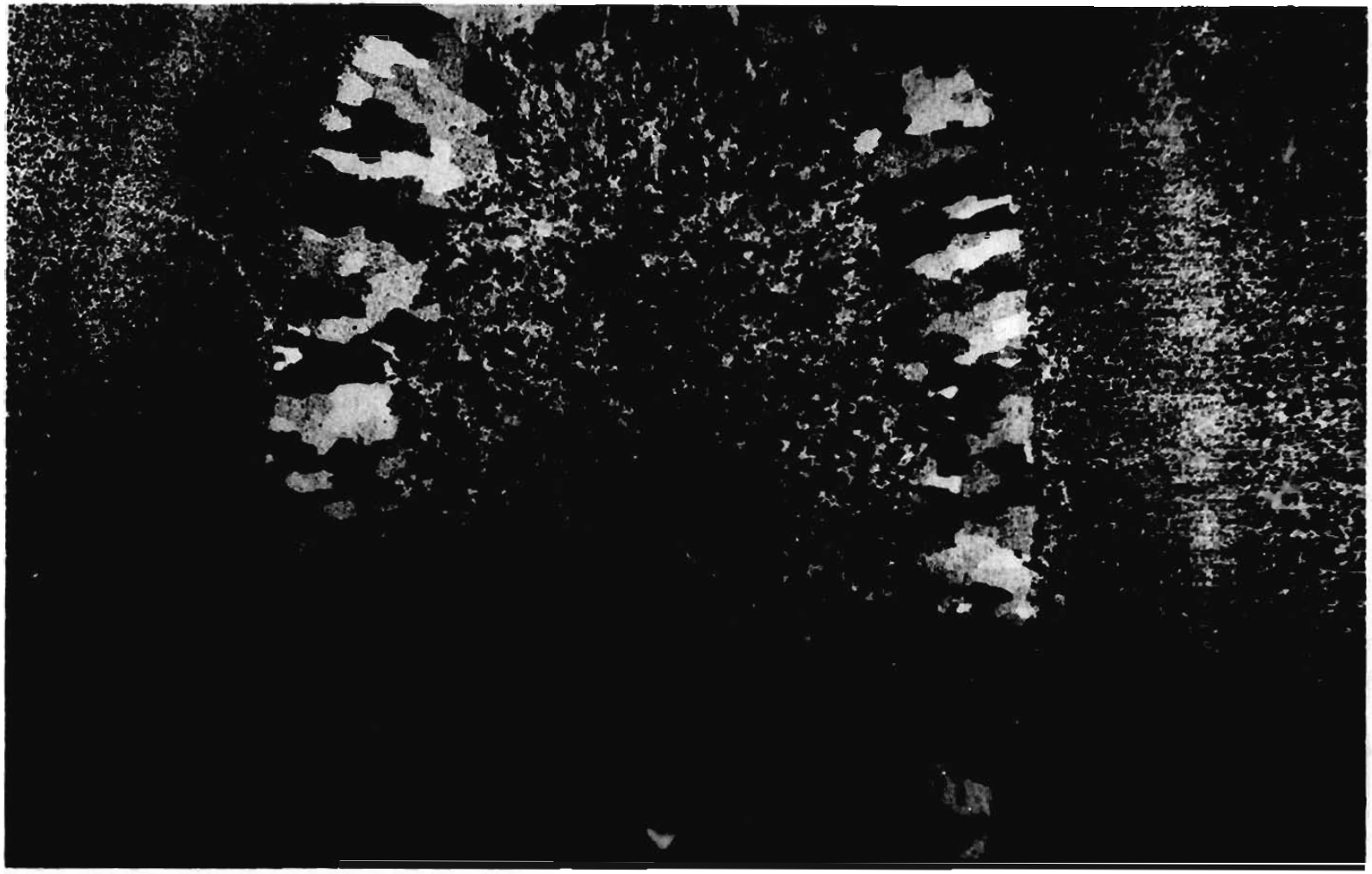

Fig. 4.9. Photomacrograph of a Transversely Sectioned Electroslag Weld in a 3-in.-Thick Carbon Steel Plate. 2× (Photograph from Arcos Corporation)

The use of the electroslag process for welding reactor pressure vessel components is new. Its major advantage appears[34] to lie in the fact that the welds produced possess a degree of cleanliness and soundness not found in other processes. Data pertaining to the notch toughness of the heat-treated welds are sketchy and contradictory.[35,36]

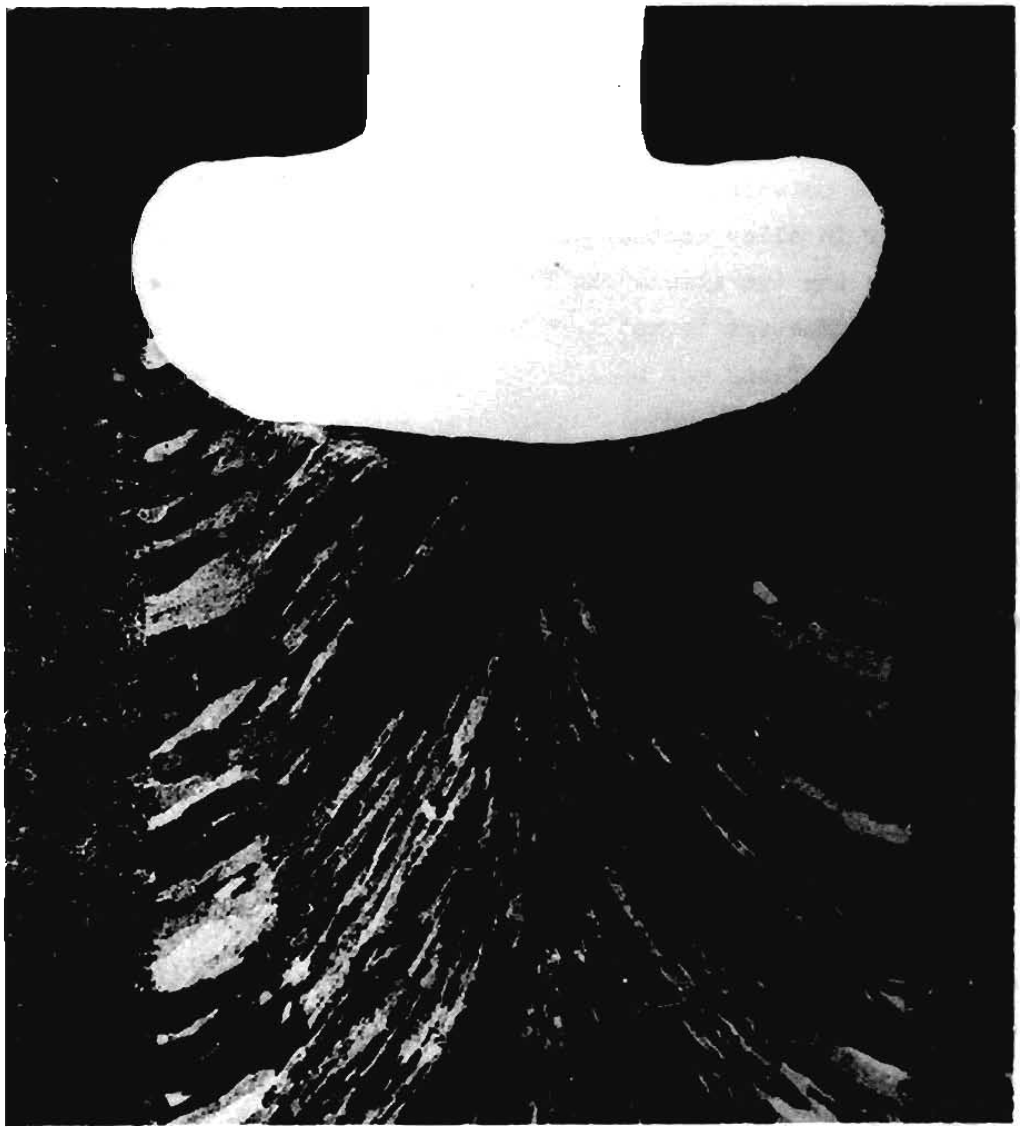

Fig. 4.10. Photomacrograph of a Longitudinally Sectioned Electroslag Weld in a 3-in.-Thick Carbon Steel Plate. 1.5× (Photograph from Arcos Corporation)

4.2.8.3 Overlaying

The internal surfaces of the reactor pressure vessels are overlaid with the equivalent of an 18-8 stainless steel. The techniques currently used for overlaying consist of single- or multiple-electrode processes in which the resultant chemical composition is essentially type 304 stainless steel. Except for those inaccessible areas where an inert-gas process (metal-arc, manual stick-electrode, or tungsten-arc) is utilized, the submerged-arc process is employed.

The metallurgy involved in weld overlaying is quite complicated. The overlay is an austenitic (fcc) steel, highly alloyed and low in carbon. The substrate on which it is deposited is a ferritic (bcc) steel considerably lower in alloy content and quite high in carbon. The transition zone between the two steels can be quite complicated and, if the choice of welding parameters is not carefully made, this area will contain defects. These defects may be microfissures, brittle phases, or an actual separation at the base metal and overlay interface.

The microfissures (hot cracks) are prevalent in nickel-bearing materials and are attributed to the segregation of residuals. They are most often found in the area of the weld bead that has been reheated, due to an adjacent bead, to a temperature closely proximating its melting point. This is actually a heat-affected-zone failure; however, the heat-affected zone in this case is not base metal but, rather, previously deposited weld metal.

The brittle phase may exist because of any one of three metallurgical conditions that tend to promote its occurrence. The first condition and potentially the most dangerous is the formation of martensite due to excessive dilution of the overlay by the base metal. If the composition of the overlay becomes diluted to the point that either the nickel or chromium falls below certain minimum values, the austenite will transform to martensite.

Sigma phase, an iron-chromium intermetallic compound that may form at elevated temperatures due to chromium enrichment, is the second most prevalent metallurgical condition that can result in brittle structure. This is usually most prevalent in ferritic stainless steels; however,

chromium-enriched regions in austenite can also promote its formation. The possibility of sigma-phase formation is increased by prolonged austenitizing and stress-relieving treatments.

The third cause for the formation of a brittle phase is attributed to carbon diffusion, which results in decarburization (and accompanying loss of strength) of the ferritic steel and an increase in the carbon level in the austenitic steel. This higher carbon level decreases the ductility and toughness of the stainless steel weld metal.

The third complication that can arise in the transition zone is separation between the overlay and the substrate. This could be caused by a lack of fusion resulting from the choice of incorrect welding parameters, or it could occur after stress relieving due to the differences in the thermal coefficient of expansion between the cladding and base metal. These stresses can very easily be of fracture-strength magnitude.

Defects of the types mentioned above have been studied[37] at the Southwest Research Institute. They have shown that the microfissure type of defect is much more tolerable than the type attributable to the presence of a hard brittle phase such as martensite.

The Schaeffler diagram is extremely useful in deducing the microstructures that may prevail when overlaying ferritic steels. Its use, coupled with the proper welding procedures and techniques, can eliminate these problems.

4.3 MATERIALS FABRICATION[19]

With the exception of weld filler metals, which are tailored by the fabricators to suit an individual welding process and/or material, there are essentially three grades of steel that must be considered in current practice. These are nominally the ASTM A 533 grade B (a manganese-molybdenum-nickel plate steel), ASTM A 508 class 2 (a nickel-chromium-molybdenum forging steel), and ASTM A 540 (a bolting steel).

ASTM A 533 is a plate steel whose major application is in the shell courses, the heads, and the tori of the nuclear pressure vessels. ASTM A 508 steel is predominantly used for flanges and nozzles, however, it

is also being used as shell course material, particularly in the pressurized-water reactor vessels. Bolts, nuts, and washers are made from ASTM A 540 steel.

4.3.1 Plate

The shell courses, head domes, and tori of the current and projected pressure vessels for light-water reactors are primarily constructed from a low-alloy high-strength steel commonly referred to as A 302 grade B nickel modified. This steel is currently described in the ASTM specification A 533-65, "Manganese-Molybdenum and Manganese-Molybdenum-Nickel Alloy Steel Plates, Quenched and Tempered for Pressure Vessels." The reference steel conforms to grade B in this specification.

The two primary fabricators of vessels for pressurized-water reactors and boiling-water reactors are the Babcock & Wilcox Company and Combustion Engineering, Inc. A third fabricator, the Chicago Bridge and Iron Company, has recently been contracted to field erect a vessel for a BWR.

Plates for the shells and heads of the PWR and BWR vessels are supplied only by the Lukens Steel Company. In general the PWR vessels require steel approximately 10 in. in thickness, whereas the BWR vessels require steel approximately 6 in. in thickness. Each of the fabricators orders plates to his individual specification, which complements the ASTM specification.

4.3.1.1 Procurement Standards

Combustion Engineering, Inc. (CE). The plates ordered by CE are of firebox quality and are melted to fine-grain practice and delivered in the as-rolled condition. To assure the response of these plates to subsequent fabrication heat treatments, CE requires that the supplier provide the results of tests conducted on samples that have received simulated heat treatments. CE supplies the heat-treating schedules to which these samples will be exposed. The parameters include the austenitizing temperature range, the holding time at temperature, and the maximum cooling rate, depending on plate thickness. Also, CE specifies the

tempering temperature range, the holding time, and the cooling rate. Simulated postweld heat treatments are also performed. Again, the stress-relief temperature range, holding time, and cooling rate are specified.

These requirements have led to the development (by Lukens) of a continuous cooling apparatus that can prepare simulated specimens that have been thermally treated in a manner identical to the plate. The authenticity of the simulated data has been substantiated through tests conducted on large plates by both Lukens Steel and CE. Both CE and Lukens checked the cooling rate at the 1/4 T and 1/2 T of a 14-in.-thick plate and obtained matching cooling rates. Lukens feels that the cooling curves set by CE are conservative and that the properties of the plate are superior to those of the simulated specimens. Lukens heat treats oversize 0.505-in.-diam tensile blanks and 1/2 × 1/2-in. impact blanks. These are subsequently machined to 0.505-in. tensile specimens or Charpy V-notch specimens. Lukens has checked the results of these simulated specimens against data from full-size 4-, 8-, and 10 1/2-in.-thick plates of several steels, including A 302 grade B, and found the results to be conservative.

The representative specimens are tested to assure that the required mechanical properties will be met in the fabricated vessel. As an additional requirement, the supplier provides CE with a check chemical analysis of each specimen.

Babcock & Wilcox Company (B&W). B&W orders plate to its own specifications, which are modifications of A 302 grade B and ASME Code Case 1339, which permits nickel additions. (This combination of specifications is currently described by ASTM as A 533-65.) The plates are ordered as of firebox quality, melted to fine-grain practice, and delivered in the as-rolled condition. Further restrictions include a requirement for vacuum degassing and limiting the nickel content to the lower end of the allowable range. Generally no mechanical testing of heat-treated test specimens is required* of the supplier. Response to fabrication heat treatment is assured through the control of the chemical composition. Babcock & Wilcox assumes the responsibility for the response of the steel to subsequent heat treatments.

*However, B&W heat treats and tests a representative sample of each heat of steel after receipt and prior to processing.

Chicago Bridge and Iron Company (CB&I). As indicated previously, CB&I is a recent entry into the field of fabrication of primary nuclear pressure vessels. In all probability the ASTM specification A 533 will be used for plate procurement, complemented by additional requirements comparable to those of CE and B&W.

4.3.1.2 Melting Practice

Furnace Types. Nuclear grades of steel plate have been manufactured in both the basic electric furnace and the basic open hearth. In the future it is expected that melting will be done exclusively in the electric furnace. Lukens' experience has demonstrated that the quality level is higher in the electric-furnace product. There is better control over bath temperature, the oxygen level of the steel, and the final chemical analysis. The use of the electric furnace permits excellent control of the charging of scrap, the fluxing of impurities, and the adjustment of the carbon level. It is possible to work to lower sulfur and phosphorus levels and to obtain better homogeneity in the final structure, particularly in the larger ingots (75 tons and up). Variations in composition from heat to heat are minimized through the use of the electric furnace, particularly when coupled with vacuum degassing.

Quite a large amount of A 302 grade B plate was made with the basic open-hearth practice, at least up to three years ago. This was particularly true for the larger ingots, because the melting capacity for producing large ingots was not available in the Lukens electric shop. Lukens does not feel that there is any serious disadvantage to using the basic open hearth; however, there are advantages to using the electric furnace, as previously discussed.

Makeup of Charge. Lukens shop is not integrated and thus has no hot metal available. The bulk of their charge is scrap. An elaborate computer-controlled program is currently in use. Much of the scrap is internally generated. For every 100 tons of steel poured, approximately 50 tons is returned to the furnace. Internally generated scrap is color coded at the cut yard. There are 24 categories in which this material may be classified. It is stocked on the basis of alloy content, that is,

nickel-chromium, molybdenum, nickel, etc. These classifications, along with the available quantities, are fed into a computer. The computer determines the best charge to get the utmost benefit from the principal alloying elements present. Lukens also purchases scrap, which is spectrographically analyzed, classified, and either stored or charged directly from its delivery car. The plant has been computerized for about three years. Previously the same basic plan was used but with manual calculation.

Virgin material is added to the charge as ferrosilicon, ferromanganese, nickel, and molybdenum to achieve the required composition. Some nickel and molybdenum are recovered from the scrap; however, it is always necessary to supplement these quantities with virgin stock. Carbon is obtained from broken molds, cast iron, coke, and graphite.

Charging Sequence. Lukens charges the electric furnace by the following sequence. First, coke or broken carbon electrode and the first bucket of scrap are charged. After the initial meltdown the lime and the second and third buckets of scrap are charged. The lime is added to remove the sulfur. After meltdown a chemical analysis for sulfur and other elements is performed and adjustments are made. A lance is then immersed into the melt, and oxygen is blown through the molten metal. This oxygen serves two purposes: it removes phosphorus and it agitates the molten steel and thereby promotes the lime-sulfur reaction. Following the oxygen flow the furnace is flushed and a chemical analysis is performed. Flushing consists of tilting the furnace forward and allowing the high-sulfur-phosphorus slag to run off. The bath is then oxidizing and it is above the equilibrium oxygen level. The furnace is returned to its normal position, adjusted to the desired temperature range of 2940 to 2980°F, and ferromanganese and ferrosilicon are added to "block" the heat. These additions stop the oxidizing action and begin to deoxidize the bath. Approximately 25% of the manganese and 90% of the silicon that is added is oxidized and goes into the slag. During blocking the arc is put on the bath to get a stirring action and also to compensate for the temperature drop due to the cold charge.

Tapping. The furnace is then tilted and the steel tapped into a ladle. If the heat of steel is to be vacuum degassed, silicon is added

to get a semikilled condition. If degassing is not to be done, silicon and aluminum are added to kill the steel. Other minor adjustments, such as to the molybdenum, nickel, and manganese contents, may also be made in the ladle at this time.

Vacuum Degassing. Lukens has had a vacuum degassing apparatus since December 1964. The steel plate will be degassed if it is ordered degassed. Lukens intends to degas all nuclear grades of steel. However, Lukens does not feel obliged to degas steel that is not ordered degassed and may not degas it if circumstances arise that prohibit it (scheduling, breakdowns, etc.).

The importance of degassing has been previously discussed. The principal advantage is the lowering of the hydrogen level to 1 to 2 ppm. If the steels are not degassed, the hydrogen level is from 2 to 5 ppm, and flaking and hydrogen embrittlement or both may occur.

Lukens' degassing process operates in a manner similar to siphoning. The vacuum chamber is placed over the ladle with its intake spout immersed into the molten steel and pumped down to 100 torr. Then the steel is allowed to rush into the refractory-lined vacuum chamber. About 10% of the total steel in the ladle will be drawn into the chamber with each surge. These surges occur at the rate of four per minute for a total of about 40 cycles. During this degassing process, the vacuum level falls to 1 torr. Composition adjustments are made within the chamber to bring the composition to the prescribed level; manganese, silicon, carbon, and aluminum are added. Approximately 0.8 lb of aluminum is used per ton in a degassed heat. An added advantage to the degassing process is that it equalizes the temperature and thoroughly homogenizes the molten metal throughout the bath.

If the ladle of steel were not degassed, aluminum and silicon would be added to kill the steel. For killing nondegassed A 533 steel, 1.2 to 1.6 lb of aluminum is required per ton of steel.

4.3.1.3 Pouring

Lukens normally bottom pours all nuclear plate ingots. The advantages gained by bottom pouring are (1) improved surface quality, that is, a more dense, less crack-susceptible surface, and (2) floating of dislodged

refractory particles to the surface so that they are not entrapped. On rare occasions, as when an extremely tall ingot is needed, Lukens may top pour. Tall ingots tend to generate a back pressure (due to the head of steel) that retards the upward flow, and a combination of top and bottom pouring is necessary.

The size and configuration of the ingot depend on the final plate dimension requirements. Lukens avoids casting an ingot any larger in cross section than is necessary. Ingots with large cross sections tend to be more segregated than thinner ingots. Lukens selects the ingot size to get a minimum reduction ratio of 3 during rolling. The ingot is always corrugated on four sides to break up the dendritic structure that is formed during freezing. For better surface finish, it is always cast in a warm mold at 100 to 300°F. Hold time after casting depends on the ingot size and will vary from 6 to 8 hr to assure complete solidification.

The ingots are stripped and placed in the soaking pits as hot as possible. The ingot is placed in a pit with the heat off and allowed to equalize in temperature. If an ingot is hotter than 800°F, it is placed in a hot pit and heated directly to the breakdown temperature (2300 ± 25°F). If it is less than 800°F, it is placed in a chilled pit (about 1500°F), allowed to set for 3 hr, and then heated directly to the breakdown temperature.

4.3.1.4 Breakdown

Breakdown (slabbing) is accomplished by cross rolling. This operation reduces the ingot cross section by about 25%. After breakdown, the slab is removed to the conditioning yard and placed in a cooling bin. The slab is slowly cooled to a temperature range of 300 to 500°F. It is then removed and scarfed with an oxygas torch at a minimum temperature of 300°F to remove about 1/2 in. of metal from the surfaces. This operation removes surface decarburization and defects that may be present after the slabbing operation and assures surface integrity. When necessary, more extensive defects are also removed. Slabs are often acid etched during scarfing to reveal any visually undetected flaws. The top and bottom are cropped at this time.

4.3.1.5 Rolling

Prior to rolling the slab is placed on end in a chilled (1500°F max) soaking pit, held for a minimum of 2 hr, and then heated directly to 2300°F. The soaking time depends on the number of slabs charged into the pit. The first slab is not removed for rolling until the temperatures of the slabs are uniform. Two techniques are used to ascertain this uniformity: (1) visual observations and (2) reducing the flow of heating gas as the control temperature is approached. The total time in the soaking pit ranges from 15 to 20 hr. The slabs are then grasped on their edges and transferred to the rolling table. The surface temperature drops 100 to 150°F during transfer. Most of the nuclear plate that has been produced has a minimum longitudinal-to-transverse cross rolling ratio of 3.

The initial reduction per pass depends on the condition of the slab surface. The adherence of the scale dictates the permissible draft (reduction per pass). When possible, 1-in. drafts are used; however, 1/2-in. drafts are more common. Scaling problems are controlled by the use of wet burlap, salt, or both. The wet burlap is used initially to remove tenacious sections of scale. Later, salt is shoveled onto the surface, and high-pressure water is sprayed onto the slab. As the final dimension is approached, the drafts are reduced. If during rolling a defect appears (these may be cracks that had not been previously observed), the operation is halted, the slab is removed to the conditioning yard, and the conditioning operation is repeated. This is an extremely rare occurrence.

The finishing temperature is about 1600 to 1700°F for thick plate. For plates approximately 6 in. in thickness, the finishing temperature is in the range 1500 to 1600°F. Finishing temperatures below 1500°F are extremely rare in plate rolling. The slab is rolled to the final plate thickness with no intermediate soaks. After rolling, the surfaces of thick plates increase in temperature by 50 to 100°F as heat flows from their hotter centers.

The descaling practices used during rolling produce a good surface. Normally, only a thin (acceptable) uniform secondary scale exists on the plate surfaces.

Vacuum-degassed steels are stack annealed in a tight pile; the pile itself tends to retard the cooling rate. If the plates have not been vacuum degassed (hydrogen treatment), they are buried in sand and cooled slowly to room temperature to permit sufficient time at temperature for the hydrogen to diffuse out of the steel. Hydrogen is not a sensitive problem for vacuum-degassed steels.

4.3.1.6 Finishing

When there is no customer requirement for ultrasonic testing the plate surfaces are left in the as-rolled condition, if the secondary scale is uniformly thin. However, Lukens does use ultrasonic testing to achieve the optimum plate layout. Prior to trimming by the oxygas process, the plate is preheated to within the range 300 to 500°F to assure that a low-temperature transformation temperature will not result. After cutting, the plate is maintained at a minimum of 300°F and is transferred to a stress-relieving furnace; stress-relieving is done at 1100 to 1250°F for 24 hr.

If the customer requires ultrasonic testing by the plate supplier, the surfaces of the as-rolled plate are sand blasted to assure maximum sensitivity. Following testing the plate is trimmed and stress-relieved as previously described.

4.3.1.7 Inspection and Testing

Nondestructive Testing. Following the stress-relieving operation, edges and surfaces are visually inspected for defects and, if warranted, further tested by magnetic-particle or dye-penetrant techniques. If a defect larger than acceptable by customer standards is detected in the finished plate, Lukens will ask the customer to remove the flaw and repair by welding rather than have an automatic rejection of the plate.

Mechanical Testing. For Combustion Engineering, samples representative of the top and bottom of the finished plate are removed in accordance with ASTM A 20, "General Requirements for Delivery of Rolled Steel Plates of Flange and Firebox Qualities." Specimen blanks are prepared, heat treated as described in Section 4.3.1.1, finish machined, and tested.

As indicated previously, the results of these tests must demonstrate the plate's ability to meet the mechanical-property requirements of the fabricated vessel.

As was noted in Section 4.3.1.1, B&W assumes the responsibility for the plate's response to fabrication heat treatments; consequently, no mechanical testing of heat-treated plates is conducted at the mill.

The field fabricator, CB&I, plans to require the plate manufacturer to supply quenched and tempered plates. In this event Lukens will prepare and test specimens in accordance with ASTM A 533 and supplementary customer requirements and thereby will assure conformance to the ASME Code.

Chemical Analysis. As previously discussed in Section 4.3.1.2, Lukens does the normal preliminary chemical analysis during melting to ascertain that the required composition is being obtained and to permit making any additions that may be required. Ladle analyses are made during teeming, usually early in the pouring operation and again during the hot topping. The sampling conforms with ASTM A 20. Lukens uses spectrographic analysis for all elements except carbon and sulfur, which are analyzed for by the combustion technique. A direct-reading spectrograph, which is standardized before each analysis, is used.

4.3.1.8 General Remarks

In the melting practice currently employed, the most significant contributor to quality appears to be the vacuum degassing operation. It results in better homogeneity, lower gas contents (in particular hydrogen), and lower aluminum content, and it thereby enhances cleanliness. Making this operation mandatory for all plates for nuclear service should be considered.

4.3.2 Forgings

The process used for manufacturing nuclear-grade forgings is dictated by the size required. Four processes are applied: ring rolling (for the largest head-flange forgings), open mandrel (for the smaller

head-flange forgings), tight mandrel (for the larger nozzles), and machining of forged bar stock (for the small nozzles).

4.3.2.1 Procurement

Combustion Engineering, Incorporated. Combustion Engineering orders shell and plate forgings to company specifications that satisfy the requirements of ASTM A 508, "Quenched and Tempered Vacuum Treated Carbon and Alloy Steel Forgings for Pressure Vessels." The steel is melted in basic electric furnaces and vacuum treated. This specification incorporates the requirements of ASTM A 336, "Alloy Steel Seamless Drum Forgings," and ASME Code Case 1332, paragraph 5. The CE purchase specification requires that the forging also meet the supplementary requirements S1 and S2 of ASTM A 508. Of these, S1 requires that the mechanical properties be determined on material that has been subjected to a simulated postweld heat treatment in addition to the quench and temper requirements, and S2 requires that the forging supplier establish a Charpy V-notch impact transition curve that includes the shelf energies. Another limitation imposed by CE is that the Charpy impact requirements be met at +10°F (rather than +40°F) for class 2 material.

As required by ASTM A 508 magnetic-particle and ultrasonic tests are conducted by the supplier.

Babcock & Wilcox Company. Babcock & Wilcox orders their forgings in a similar manner. The basic B&W specification requires conformance to ASTM A 336 and Code Case 1332. As mentioned previously, this combination satisfies the requirement of ASTM A 508. Limitations to the reference specifications are imposed by B&W. These include an ASTM grain size of 5 or finer and mechanical tests on material that has received the simulated postweld heat treatment in addition to the required quench and temper. The minimum notch ductility requirements are established at +10°F or +40°F, depending on B&W's customer requirements.

As required by Section III of the ASME Code, the forging must receive ultrasonic and magnetic-particle inspection.

Chicago Bridge and Iron. Chicago Bridge and Iron will be limited by the applicable codes and standards in their procurement and will probably also impose supplementary requirements.

4.3.2.2 Melting Practice

Steel forging stock is melted in the electric furnace and vacuum degassed, usually during pouring. This is a requirement of the ASTM A 508 specification, which experience has shown will eliminate most of the objectionable gases, particularly hydrogen, as well as yield a cleaner steel. The specification does not require the use of aluminum as a grain-refining agent; however, the minimum grain size requirement is easily met in these alloy steels without its addition, and the lack of alumina formation contributes to the cleanliness of the product. Individual melting shops have their own preferences regarding the use of vanadium; the specification only sets the maximum value and does not require its use. Vacuum degassing reduces the hydrogen level to about 1 ppm and thus prevents hydrogen embrittlement.

Because of the size of the ingots required for producing the extremely large forgings, multiple furnace heats are often required. Close control is necessary over composition, particularly carbon content. Also close control is needed over the temperature from heat to heat and over the sequence of pouring the heats. Normally top pouring is used to obtain the required compositional homogeneity. The holding time of the ingot within its mold is critical (within limits), and an ingot is never moved while any part of it is still molten. Assurance that the forging billet is of the highest quality is enhanced by the fact that the weight of the croppings from the top and bottom of the original ingot often equals the final billet weight. Furthermore, the center core that is removed in the forging process is the most highly segregated area and contains the unwanted residual elements.

4.3.2.3 Shell- and Head-Flange Forgings

The primary supplier of large forgings (213 in. in diameter and up) is the Ladish Company. These forgings are produced by ring rolling. Smaller diameter shell and head forgings are predominantly produced by U.S. Steel, Inc., Bethlehem Steel Company, and Midvale-Hippenstall Company. These are produced by a mandrel-forging process.

Ring Rolling. As previously indicated, Ladish is currently the sole supplier of large (greater than 213-in.-diam) ring-rolled forgings. They

do not have hot-metal facilities and therefore procure their starting billets from a major steel supplier who melts them in a manner similar to that already described. Steel is ordered to a Ladish specification that supplements ASTM A 508. In addition to the required vacuum degassing, Ladish orders to a composition standard that is more restrictive in that it limits the carbon range and increases the minimum manganese, silicon, and nickel contents. The billet supplier does not guarantee the properties of the final product; however, he usually will assure Ladish that the material will have the capability of meeting minimum ultrasonic and magnaflux requirements. Normally the mill will supply the top and bottom crops from which the heat-treating parameters can be approximated. These pieces weigh several tons and are worked in a manner that simulates the actual forging. Moreover, these croppings are used to assure conformance with the composition, grain size, and cleanliness requirements. Ladish receives a cold billet that has been conditioned by 100% scarfing.

The starting weight of a billet for a large ring-rolled forging is approximately 175,000 lb. The billet is charged into a warm (600 to 800°F) furnace, progressively heated and equalized through several intermediate temperatures to 2400°F, and then held for 6 hr at 2400°F. This heating cycle was established experimentally to assure a uniform temperature throughout the billet.

The first hot-working operation consists of upending the billet and reducing its height by approximately 50%. Immediately following this operation a center plug weighing approximately 1000 lb is removed. The billet is reheated to 2200°F in preparation for a ring-rolling operation. The plugged billet is then placed in a ring-rolling apparatus and the rolling operation is initiated. When the temperature of the ring has dropped to about 1800°F the faces are squared by a step-pressing operation known as paddling.

The ring-rolling process results in continuous and uniform working. In addition the paddling operation provides work through the height of the ring. Several reheat, rolling, and paddling cycles are required before the ring is of the required size. The forged ring is finished at approximately 1600°F.

The ring is air cooled to 1050 to 1150°F and recharged into a 1200°F furnace and held for 12 hr to assure complete transformation from austenite to ferrite and pearlite. This heat-treating cycle promotes the elimination of hydrogen and thereby further minimizes flaking problems.

An annealing cycle is then performed. This consists of reaustenitizing at 1650°F and then furnace cooling to 1200°F and holding to allow complete transformation. The forging is then removed from the furnace and air cooled.

Following the annealing treatment, the ring forging is blasted and then spot checked by ultrasonic testing. Although the surfaces are not ideal for such testing, they are adequate for the intended purpose.

Prior to the final heat treatment the highly stressed surface is contour machined. This machining is mandatory to assure that the material in the highly stressed area in the final product has received the optimum heat treatment.

The ring is then loaded into a furnace at 600 to 800°F, heated to 1600 to 1800°F, and held for 20 min per inch of thickness (8 to 10 hr total time). Ladish uses multiple thermocouples during this heat treatment to assure that the temperature is within the permissible range.

The ring is quenched in the horizontal position in agitated water at 45 to 70°F. The body is removed after the surfaces reach 80 to 90°F. After the ring is removed from the quench tank, it is tempered at a temperature of at least 1200°F for 1 hr per inch of cross section. It is then removed from the tempering furnace and again quenched. Selection and control of the tempering temperature are considered vital for the achievement of optimum impact properties.

To verify that the properties of the forging fulfill the specified requirements, specimens are removed from the top face of the ring, given a simulated postweld heat treatment, and tested. The properties are determined from tensile, Charpy V-notch, and drop-weight specimens.

The ring forging is then finish machined to specified tolerances. Prior to shipment the forging is given a magnetic particle test, on a 6-in. grid, and a 100% ultrasonic test.

Any defects that are detected are later repaired where necessary by the pressure vessel fabricator with qualified welding procedures and operators.

Mandrel Forgings. The smaller flange forgings are normally produced by the open mandrel technique. Usually the suppliers of these forgings have their own melting shops, and they melt and cast their ingots and then prepare their billets in a manner similar to that already discussed under Section 4.3.2.2, "Melting Practice." These suppliers have an advantage over a cold shop in that they can utilize the heat in the original billet by charging it directly into their soaking furnaces after blocking and thereby eliminate the need to heat a cold billet.

A typical mandrel forging operation consists of approximately five major steps: (1) blocking and trimming the ingot, (2) upsetting and removing the center core, (3) aligning the center hole, (4) lengthening the billet to the correct dimensions, and (5) enlarging the circumferential dimensions to meet the rough forging requirements. The degree of working during forging can be illustrated by reduction ratios. These are approximately 4 during upsetting, 1.8 during blocking, and 1.6 during finishing. The maximum furnace temperature employed is 2300°F; no working is done at a temperature below 1550°F. At the completion of the last enlargement operation the forging is moved directly to a heat-treating furnace and normalized. It is then air cooled to approximately 600°F and returned to the furnace, and the temperature is allowed to equalize by holding the forging at this low temperature for an extended period of time and then reheating it for tempering.

After tempering the rough forging is preheated to 600°F, flame cut to the correct dimensions, stress relieved, and machined to provide parallel internal and external surfaces and flat ends. The machined forging is 100% ultrasonic tested at this point with a 10% overlap technique. This testing is done at this stage in the operation because it is the last time the shape of the forging is ideally suited for a 100% test. Later, the contours involved complicate a complete test.

After ultrasonic testing the forging is contour machined and heat treated. It is charged into a 1550°F furnace and held at temperature for from 3/4 to 1 hr per inch of thickness. It is quenched in agitated

water and is held there until it is cooled to the water temperature. It is removed, its temperature is equalized, and it is then heated to 1150°F for tempering. The forging is air cooled from the tempering temperature.

The mechanical-property (tensile and Charpy) certification specimens are removed and given a simulated postweld heat treatment in accordance with the purchaser's instructions. Following the certification of the properties the forging is machined to its final dimensions and its surface is magnetic-particle inspected. It is again given an ultrasonic test to detect any effect from the quenching and tempering operation.

4.3.2.4 Nozzle Forgings

Nozzle forgings are procured to the ASTM A 508 (or its equivalent) specification that has already been discussed. These smaller forgings are usually supplied by a producer who has hot-metal facilities and uses a melting practice similar to that discussed for mandrel-forged flanges. The intermediate sizes are usually produced with a tight mandrel technique in which the cored billet is only lengthened and not enlarged. Often a "tube" technique is applied and several nozzles are produced from one billet. The number of nozzles available from a given tube is dependent on the nozzle size. The tube is normalized and tempered in a manner similar to that used for flanges. It is machined to provide parallel sides and 100% ultrasonically tested. Then the individual nozzles are cut out and contour machined.

Heat treatment requirements are stringent for this type of product. All the nozzles from a given billet must be austenitized at the same time. Although they may be individually quenched, tempering is also done simultaneously. Test specimens for certifying the mechanical properties are removed from the top and bottom nozzles of the original tube.

Small nozzles are usually machined from forged bar stock. They are handled in a manner similar to that used for the multiple nozzle forgings, that is, simultaneous heat treatment and certification testing of top and bottom specimens. These nozzles are contour machined after heat treating and testing. They are then ultrasonically tested and magnetic-particle inspected prior to shipment.

4.3.2.5 Shell-Course Forgings

Forgings that meet the ASTM A 508 Class 2 specification are being produced for use as shell courses in pressurized-water reactors. They are fabricated in a manner similar to that employed for open-mandrel flange forgings. The melting practice (Sect. 4.3.2.2 above) is identical with that previously described. The forging practice, except for degree of work in the upsetting and lengthening operations, is similar to that used for producing flanges. The lengths of these forgings are considerably greater than those of the flanges (over 100 vs 40 in.), and consequently the working during upsetting is reduced to a ratio of about 1.7 from 4.

After the forging operations the shell is normalized and machined for the final heat treatment. Because of its contour the shell need not be ultrasonically tested prior to heat treating.

The final heat treatment imposed on the shell-course forgings is exactly the same as that given to the flanges. After tempering, the certification test specimens are removed and tested. These specimens are taken from a location 2 in. below the surface (this is approximately the 1/4-T position for these section sizes) and 1 T in from an end. This location for removing specimens more nearly corresponds to the plate requirements than the forging requirements. The specimens are removed as sets 180° apart in accordance with forging requirements. The 30-ft-lb average at +10°F and usual tensile property requirements are also mandatory for the shell-course forgings.

After certification approval has been obtained, the shell course is finish machined and ultrasonically and magnetic-particle tested.

4.3.2.6 General Remarks

Differences do exist between the manufacturing processes employed to produce a ring-rolled flange forging and those used for an open-mandrel flange forging. However, the end products are quite similar and, indeed, have undergone comparable degrees of working. Both forgings are subjected to similar amounts (~1.8 reduction ratio) of working during the blocking of the ingot. However, the mandrel forging is upset to a

greater degree (ratio of 4 rather than 2), and the mandrel technique requires that a larger volume of the core be removed.

The ring-rolling operation consists of uniform continuous forging quite similar to the plate rolling process. Mandrel forming on the other hand is an intermittent process. The uniform ring-rolling process does appear to be advantageous because the working around the circumference is essentially all done at one temperature. However, the exponents of mandrel forging claim that the temperature loss in one revolution is negligible in these section sizes.

All the forging suppliers treat their forgings to remove hydrogen, although they do not necessarily say they do. This treatment, coupled with the vacuum degassing during pouring, assures an extremely low hydrogen level and also provides an added degree of homogeneity to the composition of the forging.

Other differences in processing result from the practices of different manufacturers. These lie mostly in the area of heat treatment. Austenitizing and tempering temperatures, cooling rates, and holding times can differ greatly. However, the fabricator considers the final mechanical testing as a guaranty that satisfactory fabrication procedures have been followed.

4.3.3 Bolting Material

The most commonly used bolting material nominally corresponds to AISI 4340 steel, which is a deep hardening steel. Specifically the bolting materials are procured to satisfy the requirements of ASTM A 540, "Alloy Steel Bolting Materials for Special Applications." It may also be purchased to an essentially equivalent combination of standards, namely ASTM A 320, "Alloy-Steel Bolting Materials for Low-Temperature Service," ASTM A 193, "Alloy-Steel Bolting Materials for High-Temperature Service," and ASME Code Case 1335.

Although the ASTM specifications permit open-hearth melting, electric furnace melting is commonly used. Furthermore, the most recent specification, A 540, permits vacuum melting, and its use will probably become common.

The steel is hot formed into bar stock or tubing depending upon whether the material is to be used for manufacturing studs, nuts, or washers. The material is austenitized, quenched, and tempered to achieve the required mechanical properties. Mechanical-property tests include tensile, hardness, and Charpy impact. The specimens are taken from a location approximately 1 in. below the surface of the finished product in the case of heavy sections or at the midradius of thinner sections. For all grades, classes, and sizes, a 35 ft-lb test is mandatory. This energy level must be met at either +10°F or +40°F, depending upon the requirement of the customer's procurement specification.

The strength properties required by current practice are nominal. Future designs may require higher strength bolting materials.

Although ultrahigh strength may be obtained through proper control of the quenching and tempering operation on AISI 4340, the increase in strength is also attended by a marked reduction in ductility and toughness and a marked increase in susceptibility to hydrogen embrittlement. Figure 4.11 illustrates the effect of tempering temperature on the ultimate strength, yield strength, reduction of area, and elongation. Figure 4.12 shows typical stress-strain curves for various strength levels, and Fig. 4.13 shows the effect of tempering and test temperature on impact strength of AISI 4340 bar. These three figures dramatically illustrate the improvement in ductility and toughness obtained by adhering to a minimum tempering temperature of 1200°F.

Sachs and Beck,[38] in a survey of the susceptibility of high-strength steels to hydrogen embrittlement, concluded that if the ultimate strength is held below 200,000 psi, only in extremely rare instances would hydrogen embrittlement appear to be a problem.

All these attendant problems of quenching and tempering AISI 4340 to hard tempers, that is, poor ductility, toughness, and susceptibility to hydrogen embrittlement, are prevented by the ASME Code stipulation in Table N-422 that the minimum tempering temperature shall be 1200°F.

Ultrasonic testing is conducted on the heat-treated forging prior to machining to assure the soundness of the product. Final acceptance of the bolting material is contingent upon the results of a wet magnetic-particle test. The ASME Code (Section III) does not permit axial linear

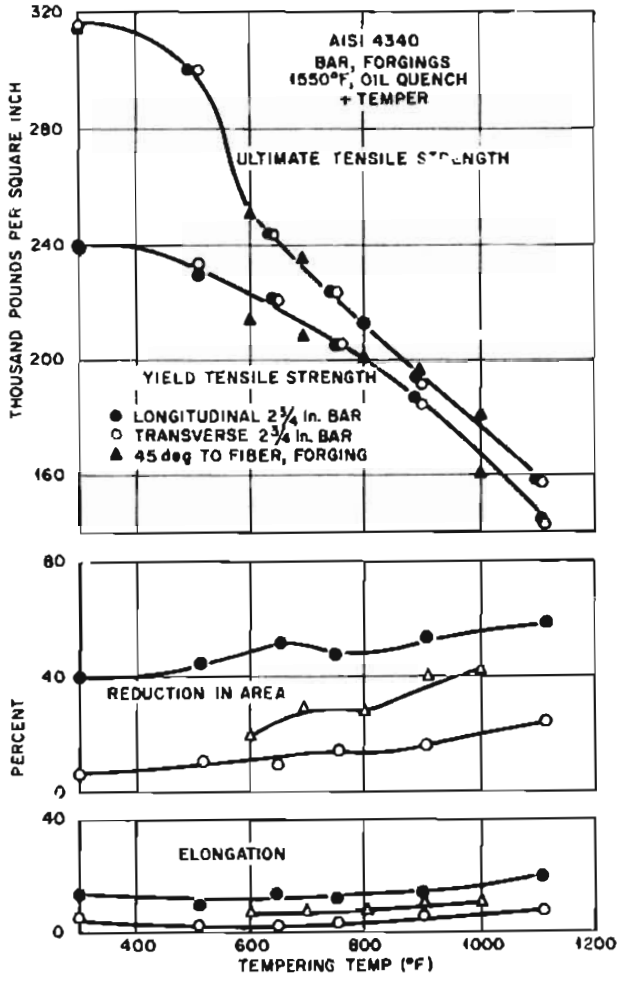

Fig. 4.11. Effects of Tempering Temperature and Test Direction on Tensile Properties of Bar and Forgings. (Taken from Ref. 38)

defects in excess of the thread depth nor does it permit any nonaxial defects.

4.3.4 Weld Metal

The joining and cladding of the various components that make up the reactor pressure vessel are done by fusion welding. The choice of filler metals is normally dictated by the applicable process being used and the material being welded.

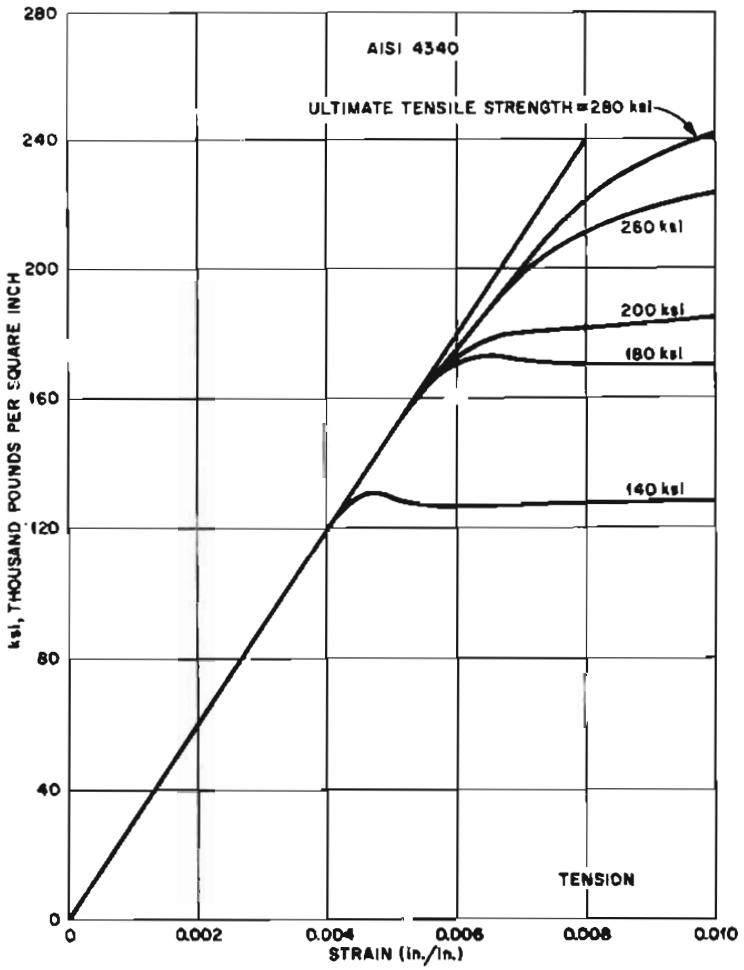

Fig. 4.12. Typical Stress-Strain Curves for Various Strength Levels. (Taken from Ref. 38)

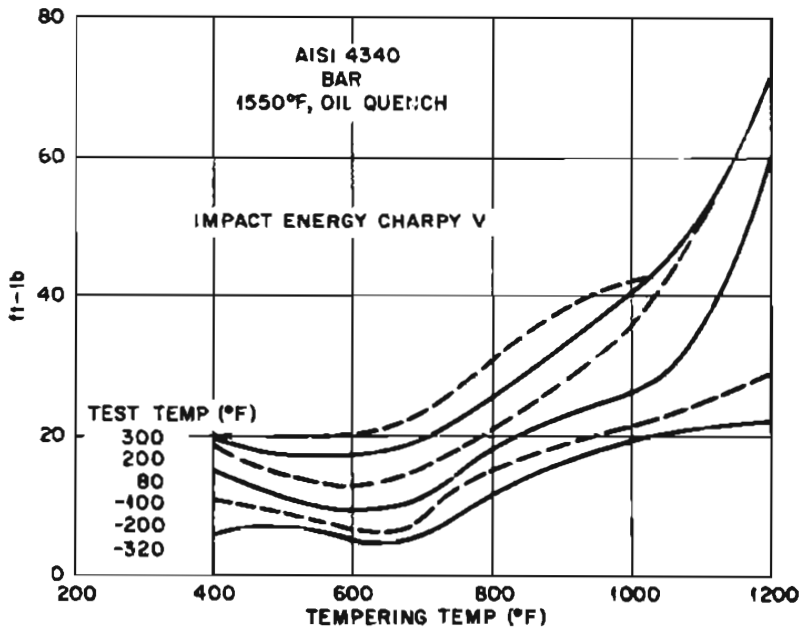

Fig. 4.13. Effect of Tempering and Test Temperatures on Impact Strength of Bar. (Taken from Ref. 38)

4.3.4.1 Welding Processes

The welding processes that are currently being used for joining the various components are the submerged-arc process, the electroslag process, the shielded-metal-arc (coated-electrode) process, the manual metal-arc process, and the inert-gas-shielded process. Overlays are predominantly accomplished through the use of the submerged-arc process; however, it is necessary in some areas to use the coated-electrode and inert-gas-shielded processes.

Historically, except for the electroslag process, these joining techniques have been used in the construction of nearly all the reactor pressure vessels built to date. The use of the electroslag process, although not new to the metal-joining industry, is novel insofar as its application for the construction of nuclear pressure vessels is concerned. For the construction of the longitudinal seams in the Dresden-2 vessel, B&W is using this process and plans to continue to use it in fabricating other vessels that contain longitudinal shell-course welds.

4.3.4.2 Weld Filler Metals

Normally, the compositions of the weld filler metals (where applicable) are selected to provide a resultant weld-metal composition conforming to the nominal composition of the base metal. In the submerged-arc and electroslag processes the filler metals are tailored to provide the strength and toughness required by the code or customer or both. The individual fabricators, by calling upon their experience, obtain the desired alloy through their selection of a flux, a solid wire, or a stranded cable, with each tailored to provide the required weld-metal composition.

Coated electrodes, on the other hand, are usually purchased or manufactured to the ASTM specification A 316, "Low-Alloy Steel Covered Arc-Welding Electrodes." The AWS-ASTM electrode classification is used in E8018-C3 for the A 533 Class B steel or its equivalent.

In addition to the filler metals described above for joining, others are used to overlay the internal surfaces of the reactor vessel with a corrosion-resistant alloy. Stainless steel filler metals are predominantly used. These are usually either type 308L or 309L stainless steel

(or combinations thereof) and are described in the ASTM specification A 371, "Corrosion-Resisting Chromium and Chromium-Nickel Steel Welding Rods and Bare Electrodes." The O-ring mating surfaces of flanges are usually overlaid with a nickel-base alloy of the nominal Inconel composition. A similar filler metal is used for buttering nozzle ends in preparation for joining these nozzles to stainless steel piping.

The shielded-metal-arc and submerged-arc processes are characterized by the use of multipass welding techniques. In multipass welding of carbon and low-alloy steels, weld metal is built up from a succession of beads. The original structure of the underbeads will be partly or completely altered by the heating effect of the subsequent passes. If the metal underneath is heated to above the transformation range, the as-cast weld metal will be refined in grain size and the columnar structure will tend to become equiaxed. Further, each bead is tempered by the subsequent passes so that the resultant microstructure is optimized. To promote notch toughness, the carbon content of the weld metal is kept at a lower level than that of the base metal. The tensile and impact properties of such multipass welds are usually superior to those of the base metal and invariably surpass the minimum code requirements. Moreover, the energy inputs are such that the base-metal heat-affected zone cooling rates are sufficiently high to eliminate the need for reheat treating of the weldment.

In the case of the electroslag process the structure of the weld deposit is as cast throughout and must be heat treated to achieve the required properties. Austenitizing, quenching, and tempering of the entire shell course are necessary to develop acceptable properties. In contrast to the chemical composition of the submerged-arc and coated-electrode weld metals, which are not required to respond to a heat treatment, the electroslag filler metal more nearly matches the composition of the base metal to permit its response to the quenching and tempering heat.

In the case of overlays, achievement of the nominal chemical composition of type 304 stainless steel requires the use of weld filler metals that will compensate for dilution by the base metal and for arc losses.

Proper control of composition eliminates fissuring of the stainless steel while satisfying the corrosion resistance of the overlay.

As has been mentioned previously, an Inconel composition is used for buttering ferritic steel nozzle ends that will be joined to stainless steel piping. The selection of this procedure is based on experimentation that has shown the superior resistance of this combination under conditions of thermal fatigue. Experience in this area has proved that the limited dilution of weld metal that does occur will not affect the nominal properties of the weldment. Therefore there is assurance that the use of the qualified welding procedure for the fabrication of the reactor vessel will result in weldments whose properties are acceptable; that is, the individual weldments need not be verified.

The electroslag welding process closely resembles a continuous casting operation. The base metal may contribute as much as 60% of the resultant weld metal. Under the current code requirements the welding procedure is qualified by examining all single-thickness test weldments. The test weldment consists of using the reference filler metal to join two base plates whose composition conforms to ASTM A 533 grade B. Available data on the mechanical properties of the plates, particularly the notch-toughness properties, have shown that variations can be expected within the nominal ranges permitted by the ASTM specification. These variations sometimes require that the heat treatment of the plates be modified to fulfill the mechanical property requirements. In addition, the as-deposited microstructure of an electroslag weld is grossly segregated. This structure is considerably refined in the subsequent double quenching and tempering heat treatment imposed on the welded course.

However, in view of the high degree of dilution of the filler metal by the base metal and the grossly segregated as-welded microstructure, there may be cause for concern regarding the reproducibility of the properties of the weld metal. It would appear prudent to require that each weldment include a runoff tab and that it be tested for its response to the quenching and tempering heat treatments.

REFERENCES

1. G. E. Dieter, Jr., Mechanical Metallurgy, McGraw-Hill, New York, 1961.
2. J. Wulff, H. F. Taylor, and A. J. Shaler, Metallurgy for Engineers, Wiley, New York, 1952.
3. R. M. Brick and A. Phillips, Structure and Properties of Alloys, McGraw-Hill, New York, 1949.
4. D. A. Canonico, The Effect of Accelerated Cooling on the Mechanical Properties of Plain Carbon Steels, Dissertation for Doctor of Philosophy Degree, Lehigh University, 1963.
5. R. D. Stout and W. D. Doty, Weldability of Steels, Welding Research Council, 1953.
6. Metals Handbook, Vol. I, Properties and Selection of Metals, 8th edition, American Society for Metals, 1961.
7. Atlas of Isothermal Transformation Diagrams, United States Steel Company, 1951.
8. Metals Handbook, 1948 edition, American Society for Metals.
9. S. S. Strunck, A. W. Pense, and R. D. Stout, The Properties and Microstructure of Spray-Quenched Thick Section Steels, Institute of Research, Lehigh University, January 1967.
10. O. R. Carpenter, Reactor Vessel Metallurgy, paper presented at Reactor Vessel Design and Construction Seminar, Babcock & Wilcox Company, June 14–15, 1966.
11. J. A. Rinebolt and W. J. Harris, Jr., Effect of Alloying Elements on Notch Toughness of Pearlitic Steels, Trans. Amer. Soc. Metals, Vol. XLIII, pp. 1175–1214, 1951.
12. D. A. Canonico and H. Schwartzbart, Arsenics Effect on Mechanical Properties of Welds in Mild Steel, Welding Eng., 43(11): 32–35 (November 1958).
13. Op. cit., Ref. 5, p. 148.
14. A. R. Troiano, The Influence of Hydrogen on the Mechanical Behavior of Steel, Iron and Steel Institute, Special Report No. 73.
15. Op. cit., Ref. 1, p. 136.
16. The Making, Shaping and Treating of Steels, pp. 822–823, United States Steel Corporation, 1957.
17. E. H. Kottcamp, Jr. and R. D. Stout, Effect of Microstructure on Notch Toughness, Part IV, Welding J., 38(11): 435S–440S (November 1959).
18. A. W. Pense, A Study of Subcritical Embrittlement in Pressure Vessel Steels, a Dissertation for Doctor of Philosophy Degree, Lehigh University, 1962.

19. Private communications in visits and discussion of ORNL representatives with personnel of Combustion Engineering Company (Chattanooga), Babcock & Wilcox Company (Mount Vernon and Barberton), Chicago Bridge and Iron Company (Birmingham), Lukens Steel Company (Coatesville, Pennsylvania), Bethlehem Steel Company (Bethlehem, Pennsylvania), and Ladish Company (Cudahy, Wisconsin), during summer of 1966.

20. Op. cit., Ref. 16, p. 339.

21. Vacuum-Degassed Steels from the Consumer's Viewpoint, DMIC Memorandum 219, Battelle Memorial Institute, Sept. 15, 1966.

22. M. V. Herasimchyk, Products of Vacuum Degassed Forging Ingots, pp. 174–181 in Transactions of the Vacuum Metallurgy Conference, American Vacuum Society, Boston, Mass., 1963.

23. G. E. Danner and G. Taylor, Vacuum Deoxidation of Steel for Large Ingots, pp. 225 to 233 in Transactions of the Vacuum Metallurgy Conference, American Vacuum Society, Boston, Mass., 1961.

24. K. Brotzmann, Experiences with the DORTMUND-HORDER Process, pp. 201–213 in Transactions of the Vacuum Metallurgy Conference, American Vacuum Socity, Boston, Mass., 1962.

25. Private communication to P. Patriarca of Oak Ridge National Laboratory from A. Meyer of Chicago Bridge and Iron Company.

26. R. D. Wylie, The Important Materials Parameters Affecting the Performance of Nuclear Reactor Pressure Vessels, pp. 438–450 in Flaw and Fracture of Metals and Alloys in Nuclear Environments, Special Technical Publication No. 380, American Society for Testing Materials, 1965.

27. A. I. Rubin, J. H. Gross, and R. D. Stout, Effect of Heat Treatment and Fabrication on Heavy-Section Pressure Vessel Steels, Welding J., 38(4): 182S–187S (April 1959).

28. A. W. Pense, R. D. Stout, and E. H. Kottcamp, Jr., A Study of Subcritical Embrittlement in Pressure Vessel Steels, Welding J., 42(12): 541S–546S (December 1963).

29. E. H. Kottcamp, Jr., D. A. Canonico, and R. D. Stout, Prediction of the Properties of Heavy Section Pressure Vessel Steels from End-Quench Tests, Welding J., 41(8): 350S–354S (August 1962).

30. R. H. Sterne, Jr., Heavy Gage Plate Steels for Nuclear Service, Lukens Steel Company Report, June 1966.

31. W. C. Griffin and G. N. Emmanuel, Properties and Fabrication of High Strength 2 1/4% Chromium–1% Molybdenum Materials, Welding J., 40 (9): 353S–399S (September 1961).

32. Op. cit., Ref. 5, pp. 164–165.

33. K. Winterton, Weldability Prediction from Steel Composition to Avoid Heat-Affected Zone Cracking, Welding J., 40(6): 253S–258S (June 1961).

34. J. E. Norcross, Properties of Electroslag and Electrogas Welds, Welding J., 44(3): 135S–140S (March 1965).

35. J. E. Norcross, Electroslag/Electrogas Welding in the Free World, Welding J., 44(4): 177–186 (March 1965).

36. C. C. Woodley, M. A. Burdekin, and A. A. Wells, Electroslag Welded Wide Plate Tests on 3 in. Thick Mild Steel, Brit. Welding J., 13(3): 165–173 (March 1966).

37. R. D. Wylie, J. McDonald, Jr., and A. L. Lowenberg, Weld Deposited Cladding of Pressure Vessels, Brit. Welding J., 12: 378–393 (August 1965).

38. G. Sachs and W. Beck, Survey of Low-Alloy Aircraft Steels Heat Treated to High Strength Levels, Part 1. Hydrogen Embrittlement, Report WADC TR 53-254, Syracuse University for Wright Air Development Center, December 1963.

5. EFFECT OF ENVIRONMENT ON MATERIALS*

In discussing the scope of the minimum safety requirements for new construction of reactor pressure vessels, Section III of the ASME Code specifically delineates that the Code does not cover deterioration that may occur in service as a consequence of radiation effects, material instability, or material sensitivity to vibratory or shock loadings. However, specific instructions are given to consider these effects and their interrelationships in evaluating the adequacy of the vessel.

The abundant related experience with conventional fossil-fueled steam power plants provides much understanding of the environmental effects of temperature, corrosion, hydrogen embrittlement, and loading. However, the introduction of radiation effects has reduced the clarity with which these problems are understood. In addition, the margin of safety demanded for nuclear reactor vessels demands that a more rigorous and thorough understanding of these problems be sought. Therefore, this chapter summarizes what is known about these effects, attempts to underscore those areas in which potential problems are thought to exist, and recommends areas of research and development that should be pursued.

5.1 TEMPERATURE

The maximum temperature at which light-water reactor pressure vessels are designed to operate is 650°F. No problems attributable solely to the loss of tensile properties due to temperature are anticipated for the materials being used in the construction of nuclear pressure vessels provided the steels possess at least the minimum tensile properties stated in Table N-424 of Section III of the ASME Code. Adherence to these properties can be assured by imposing supplementary requirements on the material supplier, such as those given in S7, High Temperature Tension Tests, of ASTM Specification A 533. At least one pressure vessel customer currently requires that tensile data be obtained at 550 and 650°F for the shell plate material as part of the fabrication test program. Furthermore,

---

*This chapter was prepared by R. G. Berggren, D. A. Canonico, J. L. English, and P. Patriarca of Oak Ridge National Laboratory.

the operating temperatures are within the upper temperature limits for the design stress values given in Table N-421 of Section III of the Code. Thus creep rate and stress rupture effects need not be considered.

The loss of tensile properties due to the annealing effect (softening) of the operating temperature is negligible. The fact that in all instances the pressure vessels have undergone lengthy (30 to 50 hr) high-temperature (greater than 1100°F) treatments considerably decreases the probability of a strictly thermal effect on tensile properties. The impact properties normally increase with temperature and would have their highest energy-absorbing ability (shelf-energy values) during operation. Indeed, there are data which show that the increase in transition temperature (radiation effects) is less at the higher temperatures than at lower temperatures.

The above discussion takes into account only the softening effects that normally occur when a material has been subjected to an elevated temperature. It does not consider metallurgical effects that should be evaluated. There is evidence which suggests that nickel-containing steels (and all the principal materials in the pressure vessel contain nickel) may embrittle when exposed, for excessively long times, to elevated temperatures if the steels also contain aluminum.[1] Higher nickel-content steels have shown embrittlement, as measured by Charpy V-notch impact tests, when exposed to temperatures in the pressure vessel operating range for time periods approaching two years. It is possible that the steels, ASTM A 533, A 508, and A 540, currently being used in the fabrication of pressure vessels, may also embrittle. This phenomenon, if it does take place in the steels for the service of interest, will be detected in the course of the surveillance program, since any increase in transition temperature will be observed. However, the surveillance program will not differentiate between radiation effects and other effects.

The embrittlement in the nickel-bearing steels has been attributed to an aging phenomenon, which accompanies the precipitation of Ni_3Al. It should be pointed out that

1. There is no aluminum in A 508 steel.
2. The nickel content is low (0.40 to 0.70%) in A 533 steel.
3. Vacuum degassing decreases the amount of aluminum required (by about 50%) to deoxidize a heat of steel.

These facts indicate that the embrittling may be negligible. However, whether or not it does occur will not be positively established under current testing programs. The fact that the reactors currently being built are expected to last upward of 30 years may be impetus enough to investigate this embrittlement possibility.

5.2 CORROSION

A tremendous backlog of information, both experimental and operational, has been accumulated during the past 10 to 15 years on the corrosion of carbon, low-alloy, and stainless steels in water systems related to nuclear reactor applications. The effects of numerous variables on corrosion behavior of these materials have been investigated in a thorough manner. Among the variables that have been examined are pH, temperature, time, water velocity, material composition, stress, heat treatment, and the presence of oxygen, hydrogen, and other gases in the water. In addition, a fair amount of information is available on the crevice and galvanic corrosion of the materials in question.

It is the express purpose in the following sections to summarize briefly the current status of corrosion knowledge of these materials pertaining to their use in the primary coolant systems of two types of nuclear reactors, boiling-water (BWR) and pressurized-water (PWR). Among the topics to be considered are general and pitting corrosion, crevice corrosion, galvanic corrosion, and stress-corrosion cracking.

5.2.1 Carbon and Low-Alloy Steels

5.2.1.1 General Corrosion

In order to minimize the problems of corrosion and of corrosion products passing into the recirculating water system, it has been general practice to utilize austenitic stainless steel as the major construction material in most designs for water-cooled high-temperature nuclear power reactors. If corrosion behavior would permit carbon or low-alloy steels to be substituted for stainless steel in primary coolant system components in nuclear reactors, capital costs would be decreased markedly.

An additional potential gain would be the elimination of the omnipresent problem of stress-corrosion cracking of the more costly stainless steels when chlorides are a contaminant in the cooling water. However, one of the main deterrents to the use of either carbon or low-alloy steels for nuclear applications involving water coolants has been the question of whether such materials would exhibit acceptable corrosion resistance under the contemplated operating conditions.

Prior to the advent of the nuclear industry, a broad background of experience with carbon and low-alloy steels was available, but it was not directly applicable to the conditions and problems peculiar to nuclear reactor applications. Within recent years, many investigations were undertaken with these materials to determine their usefulness as a material of construction for water-cooled BWR- and PWR-type nuclear power reactors. These investigations were conducted, for the most part, under conditions that simulated as closely as possible those encountered during reactor operation. Numerous and varied corrosion tests were performed at the Bettis Plant of the Westinghouse Electric Corporation, the Knolls Atomic Power Laboratory, and the Babcock & Wilcox Company. It would be nearly impossible to reference all work that has been carried out during the past ten years or so on the corrosion of carbon and low-alloy steels in connection with nuclear reactor research and development. However, where possible, appropriate references are cited in the following discussion.

Corrosion Theory. Although appreciable information[2-13] has been reported in the literature on the theory of carbon steel corrosion in water, no attempt will be made here to present a detailed analysis of the mechanisms involved. Rather, by way of a brief review, it may be stated that in some systems, for example corrosion of iron by seawater, the reactions at the solid-liquid interface are rate-determining. These half-reactions are classed as two types, anodic and cathodic, and they must balance. The driving force so distributes itself that both half-reactions proceed at the same rate. The reaction requiring the greater driving force for a given rate is said to be rate-controlling.

In anodic processes, the metal passes into the ionic state. This can take place by metal dissolution or by the direct formation of a film.

For the iron-water system, the possible anodic reactions are

$$Fe \rightarrow Fe^{++} + 2e^{-} , \tag{1}$$

$$Fe + 2OH^{-} \rightarrow FeO + H_2O + 2e^{-} , \tag{2}$$

$$Fe + 2OH^{-} \rightarrow Fe(OH)_2 + 2e^{-} . \tag{3}$$

Magnetite (Fe_3O_4) formation in degassed high-temperature water can occur through any of the following three reactions:

$$3Fe(OH)_2 \rightarrow Fe_3O_4 + 2H_2O + H_2 , \tag{4}$$

$$3FeO + H_2O \rightarrow Fe_3O_4 + H_2 , \tag{5}$$

$$3Fe + 4OH^{-} \rightarrow Fe_3O_4 + 2H_2 + 4e^{-} . \tag{6}$$

In neutral or slightly basic high-purity water such as that of primary interest for reactor coolants, the metal dissolution by the passage of ferrous ions into solution in reaction (1) can be neglected. Ferrous oxide in reaction (2) is likely to be hydrated when first formed.[14] Reaction (3) is not believed to be the rate-controlling step above 250°F.[15] Furthermore, magnetite formation in reactions (4), (5), and (6) is markedly catalyzed by the presence of traces of impurities, even at room temperatures.[4,16] Above 122°F only magnetite is found as a corrosion product of pure iron in oxygen-free water.[17] In air-saturated water, saturation of the solution with ferrous hydroxide is not obtained due to rapid oxidation of ferrous ions and the generation of insoluble γ-FeOOH.[18,19]

The electrons left behind in the metal by the anodic reaction must be balanced by a corresponding cathodic reaction. If this cathodic process can be restrained or prevented, the anodic process is likewise affected. This is an extremely important point, since cathodic polarization so often determines the overall steady-state corrosion rate. In degassed pure water the only possible cathodic reaction is the discharge of hydrogen ions:

$$2H^{+} + 2e^{-} \rightarrow H_2 \tag{7}$$

or

$$2H_2O + 2e^- \rightarrow H_2 + 2OH^- \ . \tag{8}$$

If air is present, the cathodic reaction may be reduction of oxygen:

$$O_2 + 2H_2O + 2e^- \rightarrow 2OH^- + H_2O_2 \tag{9}$$

or

$$4H^+ + O_2 + 4e^- \rightarrow 2H_2O \ . \tag{10}$$

Hydrogen-ion discharge will take place if the potential of any point on the water—solid phase interface is below the thermodynamic electrical potential of this reaction. Hydrogen evolution is dependent upon (1) the pH of the solution, (2) the potential of the particular film or metallic surface exposed to the solution, and (3) the overvoltage characteristics of that surface or of the inclusion contained therein.[20]

Material Composition. A number of investigators have reported that there is no significant difference in the corrosion behavior of carbon and low-alloy steels in high-temperature water. Tackett and his co-workers[21] tested carbon, low-alloy, and low-manganese steels under a variety of conditions which included: (1) demineralized, distilled, or degassed water; (2) dissolved hydrogen in the range 20 to 30 cc/liter; (3) ammonia in the range 0.2 to 2 ppm; (4) pH between 8.0 and 9.5, (5) temperatures from 500 to 600°F; and (6) water velocities from 12 to 30 fps. Generally, in these tests a portion of the circulating water was purified continuously by passing through a mixed-bed hydrogen-hydroxyl demineralizer. Results showed clearly that all steels tested had approximately the same degree of corrosion resistance. LaQue and Copson[22] report that extensive corrosion studies on carbon and low-alloy steels (up to 5% alloy) under conditions simulating those in a nuclear boiling-water system show practically no difference in the steels tested.[21]

Vreeland and his co-workers[23,24] exposed 13 steels with up to 5% chromium in a boiling-water loop with near-neutral water at temperatures from 456 to 535°F in subcooled water and in saturated water. Oxygen contents were 1 ppm in subcooled water, 0.1 ppm in saturated water, and 15 ppm in the steam phase. The hydrogen content of the steam and steam-water

phases was 2 ppm. Chloride concentration was less than 0.1 ppm. Results showed no clear differences among any of the steels tested. Corrosion rates were around several tenths of a mil per year (mpy) after periods up to nearly 6000 hr.

It is obvious, as reported by Uhlig,[13] that so long as oxygen diffusion is controlling, which is the case between pH 4 and 10 in aerated neutral water at room temperature, any variation in chemical composition of a steel or its heat treatment, or whether it is cold worked or annealed, has no bearing on corrosion properties. Oxygen concentration, temperature, and velocity of the water alone determine the reaction rate. This means that whether a high- or low-carbon steel, or a low-alloy steel, or wrought or cast iron, or cold-rolled mild steel is exposed to fresh water (or to seawater), the observed corrosion rates in a given environment are all essentially the same.

Effect of pH. Hydrogen-ion activity is greater in high-temperature water than in room-temperature water. However, methods for an accurate determination of pH in water at elevated temperatures have not been developed, and therefore all the following comments are based on pH measurements made at room temperature.

Iron has relatively poor resistance in the neutral range of aerated aqueous solutions.[22] Yet, if undisturbed, a film continues to develop for years that slows the corrosion rate. Hydrogen evolution is suppressed by the lowered hydrogen-ion concentration and by solid films of corrosion product. Corrosion rates within this range are controlled by the diffusion of oxygen through these films and are largely independent of hydrogen-ion concentration. Alkaline solutions produce a protective corrosion-product film. Film development within the alkaline range is more effective than in the neutral range. Resistance increases with alkalinity and hydroxyl-ion concentration. In contrast with neutral solutions, aeration has a much smaller effect on the rate of corrosion of iron, with the effect decreasing rapidly above pH 9 to 10. The attack of iron by acid and alkaline solutions is normally uniform, whereas pitting is usual in neutral solutions.

Uhlig[13] states that within the pH range of about 4 to 10, the corrosion rate of iron and steel is independent of pH in aerated room-temperature water and depends only on how rapidly oxygen diffuses to the metal surface. The major diffusion barrier of hydrous ferrous oxide is continuously renewed by the corrosion process. Regardless of the observed pH of water within this range, the iron surface is always in contact with an alkaline-saturated solution of hydrous ferrous oxide, the pH of which is about 9.5. Above pH 10, an increase in alkalinity of the environment raises the pH at the iron surface. The corrosion rate decreases correspondingly because iron becomes increasingly passive in the presence of alkalies and dissolved oxygen. In confirmation of the occurrence of passivity, the potential of iron in water of pH greater than 10 changes from an active value of around −0.5 v (with respect to a saturated calomel electrode) to a noble value of 0.1 v in 1 N NaOH, with an accompanying decrease in the corrosion rate. If the alkalinity is markedly increased to, say, 16 N NaOH, passivity is disrupted, and the potential achieves the very active value of nearly −0.9 v. The corrosion rate increases slightly up to 4 mpy. In this region, iron corrodes with the formation of soluble sodium ferrite ($NaFeO_2$). In the absence of dissolved oxygen, the reaction proceeds with hydrogen evolution to form sodium hypoferrite (Na_2FeO_2). The fact that ferrous ion is complexed by hydroxyl ion in strong alkalies to form FeO_2^-, with accompanying reduction in activity of ferrous ion, accounts for the observed active potential of iron. Although the rate of formation of FeO_2^- in concentrated alkalies at room temperature is low, the rate becomes excessively high at boiler temperatures.

For carbon steel to be used successfully in either conventional power plants or primary systems of nuclear reactors, it has been believed necessary (1) to raise the pH of the water to the range 10.5 to 11.5 and (2) to keep the oxygen content of the water at very low levels.[11] The necessity for maintaining high pH in conventional boiler systems has been questioned, however. For example, Voyles[25] cites industrial experience with 19 high-pressure boilers in which the only water treatment used, other than initial demineralizing, was the feeding of hydrazine, which is used for oxygen

scavenging. The use of hydrazine also produces a moderate increase in water pH. Laboratory tests[4,26] have indicated that raising the pH of water from neutral to as high as 12 at temperatures in the range 484 to 680°F has no effect on the corrosion of carbon steel. A pH between 10 and 12, however, may have some advantage over a neutral pH in high-velocity water streams.[19]

Tackett and his co-workers[21] reported that the corrosion of carbon steel in high-purity water at 500 to 600°F under dynamic conditions appears to decrease with increasing alkalinity from the pH range 7 to 9.5 to the pH range 10.5 to 11.5. Furthermore, the corrosion rate decreases much more rapidly in high-alkalinity water (pH 10.5 to 11.5) than it does at lower alkalinity (pH 7 to 9.5). At about 1000 hr, the instantaneous descaled corrosion rate ranged from about 30 to 50 $mg/dm^2/mo$* (~0.2 to 0.3 mpy). The extrapolated steady-state rate at 10,000 hr is about 10 mdm (0.07 mpy). On the other hand, the rate in low-alkalinity water seems to reach a steady state beyond 500 hr and ranges from about 150 to 200 mdm (0.9 to 1.2 mpy). In addition, Lobsinger[27] has reported a lower corrosion of carbon steel in pH 10 lithiated water than in pH 9 ammoniated water.

Tackett and his co-workers[21] summarize the results of many studies by various investigators by stating that of all the variables considered in the range of water conditions investigated, only the alkalinity of the water appears to have a really significant and consistent effect on the corrosion of carbon steel in high-purity high-temperature water in dynamic systems. The corrosion rate after 1000 hr in degassed water is on the average three to six times more severe than it is after the same exposure in high-alkalinity water (pH 10.5 to 11.5 with LiOH or NH_4OH).

Effect of Temperature. When corrosion is controlled by diffusion of oxygen, the corrosion rate at a given oxygen concentration approximately doubles for every 86°F rise in temperature.[28] In an open vessel that allows oxygen to escape, the rate increases up to about 176°F and then falls to a very low value at the boiling point. The falling off of the

---

*The unit milligrams per square decimeter per month is abbreviated mdm in the following text.

rate above 176°F is related to a marked decrease of oxygen solubility in water as the temperature is raised; this effect eventually overshadows the accelerating effect of temperature alone. In a closed system, oxygen cannot escape, naturally, and the corrosion rate continues to increase with temperature until all the oxygen is consumed. When corrosion is attended by hydrogen evolution, the rate increase is more than double for every 86°F temperature rise.

Tipton[29] reports that plain carbon and low-alloy steels have acceptable corrosion rates up to 600°F under normal water-cooled reactor conditions. They are, however, susceptible to local attack and pitting. Mild steel corrodes at a rate of about 2000 mdm (13 mpy) in 140°F water containing an oxygen concentration of about 4 cc/liter. At 600°F the steady-state metal-loss rate is less than 50 mdm (~0.3 mpy) in alkaline solutions containing hydrogen.

No significant effect of temperature in the range between 500 and 600°F in flowing high-temperature high-purity water, with wide variations in water composition, was observed by Tackett and his co-workers[21] on the corrosion of carbon and low-alloy steels. Further, thermal cycling between 200 and 600°F at the rate of one cycle per day (8 hr at 200°F and 16 hr at 600°F) had no noticeable effect on the corrosion behavior of these materials.

Effect of Time. The total corrosion of carbon steel in high-purity high-temperature high-alkalinity water, as plotted from data by numerous investigators, is shown in Fig. 5.1 (from Ref. 21). The calculated instantaneous corrosion rate is shown in Fig. 5.2 (from Ref. 21). The corrosion rate decreases rapidly with exposure time and reaches a value of 30 to 50 mdm (0.2 to 0.3 mpy) at about 1000 hr. The total descaled corrosion of carbon steel in neutral and moderately alkaline water is shown in Fig. 5.3 (from Ref. 21); note the significant difference between the correlation for these data and the Babcock & Wilcox mean line that correlates the high-alkalinity data. Also the corrosion rate for these conditions decreases much more slowly with exposure time than does the corrosion rate calculated from the Babcock & Wilcox mean line. The corrosion rate seems to reach a steady-state value at about 500 hr. The corrosion rate at 1000 hr is about 150 to 200 mdm (0.9 to 1.2 mpy).

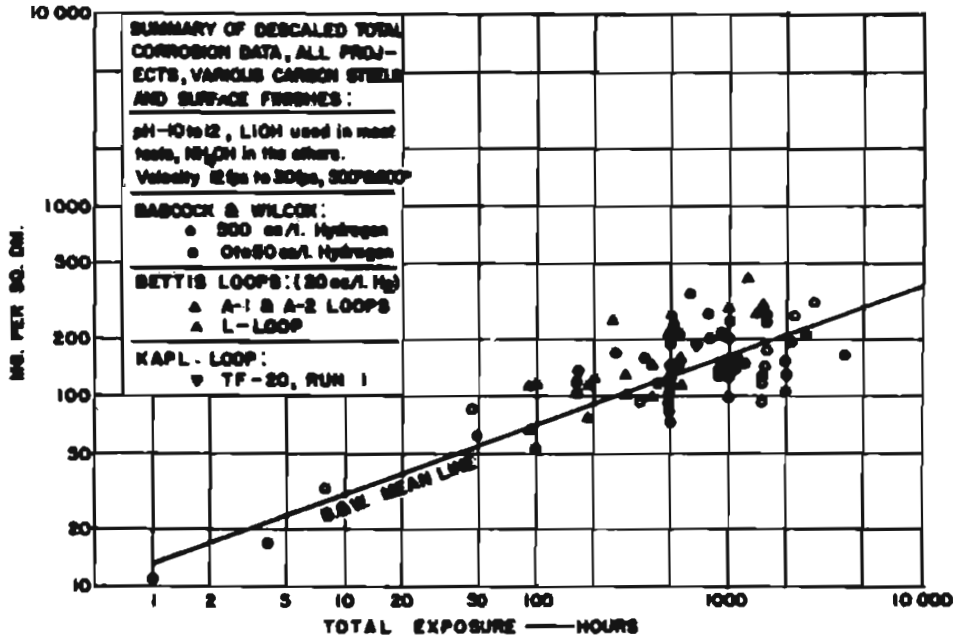

Fig. 5.1. Summary of Carbon Steel Descaled Corrosion in High-Temperature Water at a pH of 10 to 12. (From Ref. 21)

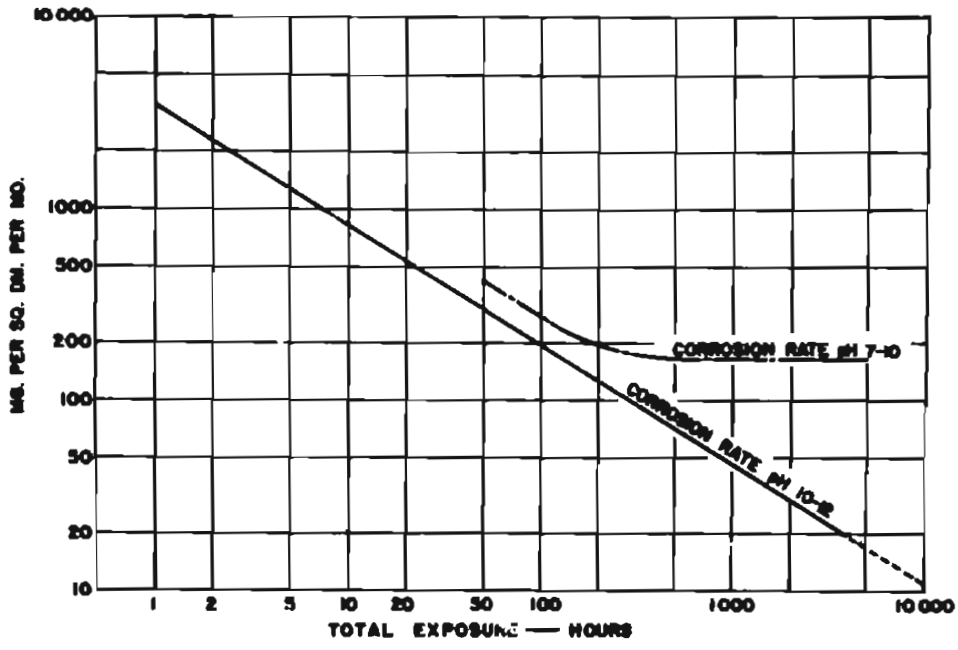

Fig. 5.2. Instantaneous Descaled Corrosion Rate of Carbon Steel in High-Temperature Water. (From Ref. 21)

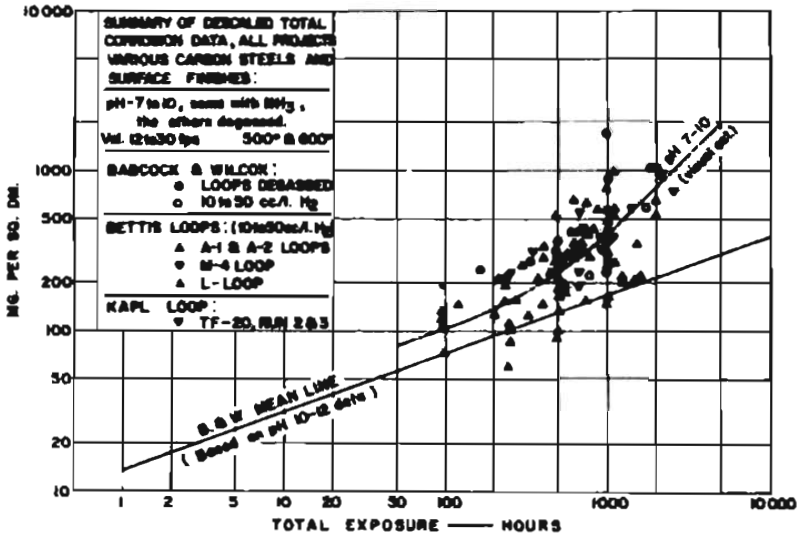

Fig. 5.3. Summary of Carbon Steel Descaled Corrosion in High-Temperature Water at a pH of 7 to 10. (From Ref. 21)

Effect of Velocity. It has been stated by Copson[30] that an increase in the velocity of aerated water generally leads to an increase in corrosion rates for carbon steels, both by supplying oxygen at a greater rate and by thinning the diffusion film at the metal-water interface. Higher velocity, however, promotes greater protectiveness of the ferric hydroxide film. As a result, corrosion rates occasionally decrease with increasing velocity.[31]

Erosion in high-velocity or highly turbulent water leads to accelerated corrosion due to breakdown of the protective oxide film.[14] Erosion-corrosion tests were conducted by Wagner and his co-workers[32] in deaerated steam condensate at 250°F flowing at 125 to 450 fps. They found that cast carbon steel was severely attacked as compared with more corrosion-resistant materials that formed good protective films, such as martensitic and austenitic stainless steels, bronze, and Monel.

The velocity below which carbon steel is not susceptible to erosion-corrosion effects is relatively unknown.[14] However, it is known that velocities of 35 fps maximum used in carbon steel test loops are below the range where erosion-corrosion should be a problem.[33] Similarly, there are available data taken at velocities up to 30 fps which indicate that the corrosion rates for type 304 stainless steel and Inconel are not

significantly affected by varying the flow rates.[34,35] The critical velocity below which there is no corrosion effect is expected to be considerably higher for austenitic stainless steel and Inconel than for carbon steel. Zelenski's[36] erosion-corrosion data also show that carbon steel started eroding at a much lower velocity than austenitic stainless steel.

The effect of velocity, among other variables, was examined with AISI C1008 carbon steel under simulated BWR and PWR conditions with pH 7 water.[23] Specimens were exposed in the PWR test at 500°F to water containing 6 ppm hydrogen and about 0.1 ppm oxygen. The BWR test was operated at 546°F in saturated water containing 0.02 to 2 ppm oxygen and about 0.01 ppm hydrogen. Water velocities were different, however, being 18 fps in the PWR test and 6 fps in the BWR test. However, it has been reported that in studies with materials for PWR applications, corrosion rates were not appreciably affected by water velocities ranging between 1/60 and 30 fps.[12] After 1000 hr in the PWR test, the corrosion rate was 1.3 mpy compared with a rate of 0.2 mpy after 1945 hr in the BWR test. This behavior was attributed to hydrogen and oxygen effects rather than to velocity difference.

A velocity effect was reported with A 212 carbon steel in deaerated 600°F borated water with a pH between 5.2 and 6.3 and 100 cc of hydrogen per kilogram of water.[37] After 640 hr, the following rates were obtained: 0.2 mpy at 2 fps, 0.4 mpy at 20 fps, and 3 mpy at 36 fps.

For systems operating at 500 to 600°F with demineralized, distilled, or deoxygenated water with dissolved hydrogen between 20 and 30 cc/liter, ammonia in the range 0.2 to 2.0 ppm, and pH between 8.0 and 9.5, Tackett and his co-workers[21] reported that as long as the velocity past the specimen surface was in the range of about 10 to 35 fps, there did not appear to be any significant effect on corrosion. However, some tests at around 12 fps showed a heavier scale buildup than tests at higher velocities.

Effect of Oxygen. At ordinary temperatures in neutral or near-neutral water, dissolved oxygen is necessary for appreciable corrosion of iron.[13] In air-saturated water, the initial corrosion rate may reach 3000 mdm (about 18 mpy). This rate diminishes over a period of days as the iron oxide is formed and acts as a barrier to oxygen diffusion. The

steady-state corrosion rate may be 300 to 750 mdm (approximately 2 to 5 mpy) and will tend to be higher the greater the relative motion of water with respect to iron. Since the diffusion rate at steady state is proportional to oxygen concentration, it follows that the corrosion of iron is also proportional to oxygen concentration. In the absence of dissolved oxygen, the room-temperature corrosion rates for both pure iron and steel are negligible.

Although an increase in oxygen concentration accelerates corrosion of iron at first, it is found that beyond a critical concentration the corrosion rate again drops to a low value.[38] In distilled water at ambient temperature the critical concentration of oxygen above which corrosion decreases again is about 12 ml/liter. This value increases with dissolved salts and with temperature, and it decreases with increases in velocity and pH. At a pH of about 10, the critical oxygen concentration reaches the value for air-saturated water, 6 ml/liter, and is still less for more alkaline solutions.

In 1952, 30% of U.S. Navy boiler-tube condenser failures were attributed to corrosion from dissolved oxygen.[39] Modern boilers operating with dissolved oxygen contents less than 0.05 ppm (through mechanical deaeration and oxygen scavenging with sulfite or hydrazine) have largely eliminated the oxygen pitting problem.[40] Seebold[41] concluded from his studies that the presence of a sufficient concentration of oxygen in 600°F dynamic water also inhibited the corrosion of carbon steel. This finding agrees with the observation made by Breeden and his co-workers[42] whereby a "good" result was obtained with carbon steel in high-temperature water containing about 240 ppm oxygen as compared with a "poor" result in water containing about 45 ppm oxygen. Similarly Cataldi and his co-workers[43] noted in autoclave tests at 545°F that carbon steel appears to get deeper pits with 50 ppm oxygen than with 100 ppm. Apparently, there are intermediate oxygen levels (>0.1 ppm) that promote pitting.

Ruther and Hart[44] showed that the corrosion of electrolytic iron in low-oxygen water (<0.1 ppm) at 500°F resulted in formation of a uniform brown-black coating of magnetite (Fe_3O_4). Severe pitting developed in water containing about 35 ppm oxygen over the entire temperature range from 125 to 600°F. The average metal-loss rates were also much higher

than obtained in a low-oxygen environment (<0.1 ppm). With adequate oxygen present, the pure iron does not pit, and a thin temper film of hematite ($\alpha \cdot Fe_2O_3$) is formed. This film formation is a function of temperature and oxygen content. In the case of mild and low-alloy chromium steels, an improvement in corrosion resistance over that of pure iron in high-temperature water containing approximately 35 ppm oxygen was noted, particularly with regard to pitting. This is attributed to the carbon and chromium contents, which promote film-forming ability. The benefits from operating in the temper-film region are twofold for reactor applications. First, the total corrosion is lower than for typical low-oxygen (<0.1 ppm) conditions. Second, and more important, the nature of the corrosion product is such that much less of it would be released to the water stream. This may decrease the "crud" problem of carbon steel reactors to tolerable levels.

Vreeland[11] has discussed the oxygen effect. In water-cooled nuclear reactors, water is decomposed radiolytically, and the possible problem of oxygen in the coolant water arising from such decomposition is resolved for pressurized-water reactors by introducing an excess of hydrogen into the coolant water.[45] The radiolytic recombination of hydrogen and oxygen is accelerated so that little or no residual free oxygen remains in the water. In a boiling-water reactor power plant, steam generated in the reactor passes directly to the turbine, whereas in a pressurized-water power plant, water heated in the reactor generates steam in a secondary steam generator. Maintaining an excess of externally added hydrogen to force the recombination of radiolytic oxygen and hydrogen in a boiling-water system where the noncondensable gases exit through a stack would be impractical. Oxygen from the radiolytic decomposition of the water is therefore expected to be present in the steam and in the recirculating water of a boiling-water reactor. As determined by the specific characteristics of the particular boiling-water reactor under consideration, the oxygen content of the steam will be 10 to 30 ppm[46] with a dynamic equilibrium quantity in the recirculating water. As a result of water decomposition, the total oxygen present will be in the stoichiometric ratio of 8:1 with the hydrogen. The use of chemical additives to adjust pH in a boiling-water reactor is undesirable because the distilling action

in the reactor could result in the formation of deposits on reactor parts. From the foregoing, it is apparent that the construction materials for the primary system of a BWR are exposed to neutral pH water, steam, and/or mixtures thereof, all containing both hydrogen and oxygen.

References in the literature indicate that some concentrations of dissolved oxygen in water do not accelerate corrosion of carbon or low-alloy steel and may actually inhibit corrosion of the steel by the formation of a protective oxide film.[11] This inhibition can occur either at room or higher temperature, but there appears to be no agreement as to the amount of dissolved oxygen in the water to cause inhibition. One factor responsible for the lack of agreement may be the velocity of the test water. Copson[30] has pointed out that there is an interrelation between the effects of water velocity and oxygen concentration on the corrosion of carbon steel. Uhlig[47] states that at 86°F and a velocity of 0.25 fps, the corrosion rate of mild steel in distilled water is 60 mpy at about 22 ppm dissolved oxygen and 5 mpy at about 34 ppm dissolved oxygen. Frese[48] found that at 72 to 77°F, mild steel showed a maximum corrosion rate in distilled water at an oxygen concentration below 40 ppm; at higher oxygen content, the corrosion rate decreased. At low oxygen concentrations, the corrosion products were loose and fluffy; at higher oxygen contents, they were hard and adherent, an indication of a more protective film. Vernon[49] suggested increased aeration rather than deaeration to reduce corrosion of steel in water or dilute salt solutions.

In high-temperature water, Breeden and his co-workers[42] indicate good results for A 212 grade B carbon steel in water containing a large concentration of oxygen and poor results in water containing much less oxygen. Moore[50] tested carbon steel in 482°F water at 26 fps with 6-, 30-, 90-, and 400-psi oxygen pressures. Tests at the lower oxygen pressures produced heavy scales of corrosion products that were easily removed and were identified as predominantly magnetite (Fe_3O_4). Corrosion rates in these tests ranged from 5 to 16 mpy. In tests at higher oxygen pressures, the oxide films produced on specimens were thin and very adherent, and they showed more hematite ($\alpha \cdot Fe_2O_3$) than those in the lower oxygen pressure systems. Corrosion rates in the higher oxygen pressure systems varied between 5 and 6 mpy. Seebold[41] concludes from his tests that the presence

of a proper concentration of oxygen in water inhibits the corrosion of carbon steel in loop systems at temperatures up to 600°F.

When oxygen is present in water, corrosion products that may be formed are $\alpha \cdot FeOOH$, $\beta \cdot FeOOH$, $\gamma \cdot FeOOH$, $\gamma \cdot Fe_2O_3$, and $\alpha \cdot Fe_2O_3$ (Ref. 11). If steel is exposed continuously to air-saturated room-temperature water, $\gamma \cdot FeOOH$ forms, sloughs off the surface, and appears as loose particulate matter either suspended in or settled from solution. If the temperature is elevated to about 600°F, the $\gamma \cdot FeOOH$ is converted to $\alpha \cdot Fe_2O_3$ as a nonadherent corrosion product, which may then be reduced to nonadherent Fe_3O_4 by corrosion-generated hydrogen at the high temperature. Bloom's[19] experiments led him to believe that the presence of oxygen in aqueous systems in contact with steel at elevated temperatures may in some circumstances produce more protective films than are formed in its absence. He states that this phenomenon is probably associated with the occurrence of $\gamma \cdot Fe_2O_3$ as an insulating film over Fe_3O_4 in contact with the steel.

Pearl and Wozadlo[51] investigated the effect of oxygen in a dynamic test loop under conditions that simulated the various environments found in a nuclear BWR system. Water and steam conditions were based on 20 ppm oxygen and 2.5 ppm hydrogen in the 546°F saturated steam, a condition representative of the oxygen and hydrogen formed in a BWR from radiolytic water decomposition. The corresponding oxygen content in the recirculating water was 0.2 ppm. The pH of the high-purity water used was neutral; no chemicals were added. The corrosion rate of carbon steel averaged less than 10 mdm (<0.1 mpy) in approximately 5300 hr. There was little, if any, difference in corrosion or metal lost to the system that could be attributed to testing in the four available environments: steam, steam-water, saturated water, or subcooled water. The low corrosion rates that were obtained on the carbon steels were the result of the action of oxygen, or oxygen and hydrogen, which apparently helped form a protective oxide on the steel. This oxide appeared to protect the steel against corrosion when it was exposed subsequently to water that was low in oxygen and hydrogen content. Startups with oxygen and hydrogen contents of the water quickly raised to levels similar to those in a BWR resulted in less corrosion than when oxygen and hydrogen were added a few hours after startup.

It was pointed out[21] that in the high-purity high-temperature water containing representative BWR conditions of hydrogen and oxygen, most of the initial corrosion formed a protective oxide film on the steels instead of being carried off in the water. It was further indicated that the form of the existing oxide changed upon the initial addition of the oxygen and hydrogen to the system; any nonadherent oxides were at least partially removed by the loop water. Another item of importance was the finding that the corrosion-release rate in the presence of oxygen and hydrogen was appreciably lower than in a neutral pH system with hydrogen but no oxygen in the water.

It is hypothesized by Tackett and his co-workers[21] that the addition of hydrogen but no oxygen in the water during startup will give the typical PWR corrosion and metal-to-system losses until the time when the oxygen and hydrogen are added stoichiometrically. At that time, the entire corrosion process will change essentially to the more typical BWR type, and a certain portion of the corrosion product that has accumulated up to that time will be released to the system and be reflected as an iron-to-system loss.

An analysis[51] leads to the important conclusion that there is essentially no iron-to-system loss, regardless of time, once the system has been properly brought to operating conditions with hydrogen and oxygen addition. If this effect can be proved to be true, one of the major limitations in using carbon steel in boiling-water reactors will have been eliminated.

This understanding has been an empirical development based on engineering application data. It is of interest to determine whether the interpretation and results are consistent with the mechanism studies carried out by others. Bloom[19] observed that those oxides with a spinel structure, Fe_3O_4 (magnetite) and $\gamma \cdot Fe_2O_3$ (maghemite), form adherent protective films, whereas the oxide $\alpha \cdot Fe_2O_3$ (hematite), of a corundum structure, is a less adhering insulated powder. He further noted that Fe_3O_4 oxidizes to $\gamma \cdot Fe_2O_3$ when exposed to oxidizing environments. This transformation results in a change that might be more favorable to developing more protective and pit-resistant films. He visualized an insulating film of $\gamma \cdot Fe_2O_3$ over the Fe_3O_4 in contact with the steel. Ruther and

Hart[44] found $\alpha \cdot Fe_2O_3$ formed initially as a thin film on pure iron in oxygenated water in contrast with the Fe_3O_4 coatings produced in deoxygenated water. Potter and Mann[52] observed a double oxide layer of Fe_3O_4 in studies of magnetite growth on carbon steel in essentially oxygen-free steam. Under certain conditions the outer layer was nonadherent.

If it is assumed in the work of Pearl and Wozadlo[51] that the oxide formed during startups before adding oxygen is in the form of a double layer of Fe_3O_4, as observed by Potter and Mann,[52] the following might be expected upon the addition of oxygen. The outer layer would be oxidized to $\alpha \cdot Fe_2O_3$, with the resultant loss of some iron to the system. The outer surface of the inner layer would be gradually oxidized to $\gamma \cdot Fe_2O_3$ to form an insulating layer over the Fe_3O_4 adjacent to the metal. During the time of developing the $\gamma \cdot Fe_2O_3$ layer, the corrosion rate would not necessarily increase from that existing just before adding oxygen. As the insulating layer became more complete, the rate would decrease until a low linear rate was established based on the rate-controlling process of diffusion of anions inward through an insulating layer of constant thickness.

Effect of Hydrogen. Limited information is available on the corrosion of carbon steel as influenced by the presence of dissolved hydrogen in high-purity high-temperature water. It has been shown that a nominal partial pressure of hydrogen will not affect the iron-water equilibrium appreciably.[14] Therefore, this would not be expected to reduce noticeably corrosion rates of iron and carbon steel. However, the introduction of hydrogen into a nuclear reactor or an in-pile test loop has a marked effect on the quantity of corrosion products released to the system. The benefits afforded by hydrogen additions are reported by Welinsky and his co-workers.[53]

Tackett and his co-workers[21] have reported that the hydrogen concentration seems to have little effect on carbon steel corrosion in high-alkalinity water (pH 10.5 to 11.5), at least when oxygen concentrations are low. However, in neutral water, the removal by continuous degassing of hydrogen released by corrosion seems to accelerate attack, while addition of hydrogen to increase the concentration to about 50 cc/liter appears to greatly reduce corrosion.

Effect of Dissolved Salts. The presence of dissolved salts in water modifies the usual corrosion mechanism for iron or carbon steel.[22] The salts take part in reactions at the cathode and the anode even though the end products continue to be ferrous hydroxide and hydrous ferric oxide. These salts influence corrosion rates by their effect on adherence, location, and physical nature of the rust layer, as does the presence of certain alloying elements in the metal. Many salts yield a precipitate that adds to the obstructive effect of the rust and the diffusion layer of solutions.

Certain anions, such as chromates, phosphates, silicates, borates, etc., are more or less effective as corrosion inhibitors.[14] According to Huddle[5] it seems possible that these anodic inhibitors function by catalyzing the formation of true oxide, as opposed to a hydrated oxide or hydroxide film. The exact mechanism by which these complex ions impart a true oxide rather than a hydroxide has not been firmly established. However, they compete with hydroxyl ions and other anions present in the solution for participation in the reaction at the anode surface. If their adsorption is such as to exclude the hydroxyl ion from the reaction, it is suggested that the complex ion donates its own oxygen to the film and regains this oxygen from the solution. Certain of the complex ions are only effective in oxygen-containing solutions; this indicates that the time function of the complex ion may well be to act only as a catalyst in the anodic transfer of dissolved oxygen from the solution to the film. Thus, it appears that an anion inhibitor more likely affects the corrosion of iron (and stainless steel and Inconel) in oxygen-containing water than in oxygen-free reactor water.

Pitting Corrosion. Despite the high-resistivity of reactor-grade water, it is expected that carbon and low-alloy steel components in a water-cooled nuclear reactor would be subject to rusting, pitting, and local attack by the water during reactor startup and shutdown periods when the water might be at or near room temperature and the reactor might be open to air.[11] Several tests of carbon and low-alloy steels in reactor-grade water (air-saturated deionized water at room temperature) confirmed the above expectations. After less than 5 min of exposure to the water, rust patches could be observed on AISI 1008 carbon steel with the aid of

a low-power microscope. In about 6 min the rust patches could be observed with the unaided eye.

Bloom and Strauss[54] indicated that the occurrence of pitting may depend on the type of exposure at room temperature. For example, they found that (1) filling a thermal-convection loop constructed of previously unexposed SAE 1010 steel with distilled air-saturated water at room temperature and operating it for several weeks or more at 600°F, produced a uniform film of magnetite on the steel with no evidence of pitting; (2) when the loop was filled with oxygenated water and pressurized with 300-psi oxygen at room temperature, and the loop was then heated to 600°F and operated at this temperature for 21 days, previously unexposed SAE 1010 piping contained a liberal distribution of circular red patches of α-Fe_2O_3, each of which overlaid a pit; and (3) when previously unexposed SAE 1010 loop piping was filled with degassed distilled water and heated as rapidly as feasible to 600°F, and the loop after operation at this temperature for 10 to 15 min was pressurized with oxygen at about 300 psi and run for 21 days, no signs of pitting were evident.

Specimens of carbon and low-alloy steels were exposed to simulated BWR conditions in a test loop at 546°F to determine[11] (1) whether pitting and local attack in room-temperature water would be intensified during subsequent exposure at loop-operating conditions, (2) whether low-alloy steels might be expected to be more resistant to pitting and local attack than carbon steel exposed to reactor-quality water at room-temperature, and (3) whether carbon and low-alloy steels, which are first exposed to high-temperature water, will form a protective film of oxide that will prevent pitting and local attack during subsequent exposure of the steel to water at room temperature. Room-temperature exposures were for about 300 hr, while high-temperature runs lasted around 1030 hr. Results indicate the following:

1. Pitting, local, and general attack on steels tested in room-temperature water are not intensified or accelerated during subsequent exposure to high-temperature water. The effects of exposure to room-temperature water followed by exposure to high-temperature water appear to be additive rather than accelerative.

2. When the steels were first exposed to high-temperature water, the oxide formed afforded considerable protection to the steels when they were then exposed to room-temperature water. However, the protection was not complete. The few pits that did form were generally as deep or deeper than those formed on specimens exposed to room-temperature water without the benefit of the protective oxide. In any case, pits did not exceed 4 mils in depth.

3. Steels exposed to room-temperature water and then to high-temperature water and then descaled were not subject to intensified corrosion when given an additional exposure to high-temperature water. This indicates that reactor components fabricated of steels containing up to 5% chromium could be descaled or decontaminated without suffering accelerated corrosion upon exposure at operating conditions.

Specimens of several steels were exposed to water at 535°F in the subcooled test section of a boiling-water loop during several runs and shutdowns to determine whether pitting and local attack would occur during this type of exposure, which simulates high-temperature operation and periodic shutdowns of a BWR.[11] The specimens were exposed first for 155 hr in high-temperature water, then for 118 hr in room-temperature water with access to air, next for 309 hr in high-temperature water, and finally for 146 hr in room-temperature water with access to air. Corrosion rates for the total exposure period were 0.2 mpy for types ASTM A 212 grade B and ASTM A 302 grade B steels, about 0.2 mpy for AISI type 502 steel containing 5% chromium, and 0.1 mpy for AISI type 304 stainless steel. All steels showed pitting to 5 mils in depth, except the type 304 steel, which was free from pitting.

5.2.1.2 Crevice Corrosion

In the corrosion field, the term "crevice corrosion" has acquired a very general meaning that normally includes all observations of accelerated attack at the junction between two metals exposed to a corrosive environment. Operational experiences of the PWR and Naval reactor programs show that the oxygen content of the water is almost unmeasurable with the addition of hydrogen.[12] Further, information shows that crevice corrosion is not normally a problem that requires special attention in systems with

low-oxygen contents on the order of 0.1 cc per kilogram of water. Much of the reported work, however, is based on systems containing 1 to 10 cc oxygen per kilogram of water.

Metal-Ion Concentration Cell. The form of crevice corrosion that is defined as a metal-ion concentration cell results from corroding currents that arise in those regions where there exists a difference in metal-ion concentration.[12] The extent of accelerated corrosion at these points depends primarily upon the magnitude of the corroding current which, in turn, is related directly to the metal-ion concentration difference at the points in question. The direction of the corroding current determines the location of the corrosion from the accelerated attack. Corrosion occurs at those points where the current leaves the metal. In this case, the current travels from the metal outside the crevice to the metal inside the crevice. Therefore the corrosion products form at the mouth of a crevice or at the perimeter of the contact area. It is also apparent that this type of corrosion could be considerably minimized by continuously replacing the water in the crevice with fresh water from the outside to minimize or eliminate a difference in metal-ion concentrations. It is expected also that this form of corrosion could be minimized or even eliminated by increasing the crevice gap so that sufficient flow and displacement of water could occur at the mouth of the crevice to prevent the formation of differential metal-ion concentrations.

Oxygen-Concentration Cell. The form of crevice corrosion that is defined as an oxygen-concentration cell results from corroding currents that arise at those points where a differential oxygen concentration occurs.[12] As in the case of the metal-ion concentration cell, the magnitude of the corroding current is related directly to the difference in the oxygen concentration at the point in question. The corroding current flows from the low-oxygen-bearing medium to the metal. Therefore, in contrast to the metal-ion concentration cell, accelerated attack could be expected to occur at the entire interface surfaces of both materials rather than at the mouth of the crevice. This form of corrosion may be controlled in the same manner as mentioned earlier for the metal-ion concentration cell.

Stagnant-Area Corrosion. Strictly speaking, stagnant-area corrosion is not normally considered a form of crevice corrosion.[12] However, since

it has been found to play an important part in the analysis of crevice-corrosion problems, it is considered desirable to discuss this form of corrosion to indicate its importance in relation to other forms of crevice attack and to actual design problems. Stagnant-area corrosion, as related to crevices, may be defined as general accelerated attack that may occur within a crevice or any stagnant area. It results directly from the increased corrosivity of the environment which, in turn, is a direct result of the accumulation of both soluble and insoluble corrosion products within the crevice. In contrast, the accelerated attack that occurs in both the metal-ion and oxygen-concentration cells results from differential effects. Since essentially no circulation of water normally takes place within crevices, it would be expected that the concentration of corrosion products would increase almost indefinitely and thereby produce more corrosion than would be normally expected for the same material exposed to the environment outside the crevice. For example, if a crevice is exposed to high-purity water having a total solids content of 1 ppm, it is very possible that the water within the crevice may eventually have a total solids content 100 or 1000 times greater than that of the surrounding environment. The corrosion resistance of the particular metal involved may be entirely inadequate in the relatively impure water as compared with the pure water. Although this form of corrosion does not depend on differential effects, the methods of controlling the problems are essentially the same as for metal-ion and oxygen-concentration effects. The mechanism of corrosion involved in stagnant areas of all kinds is the same as that described for stagnant-area corrosion in crevices.

Only limited information is available on the effect of hydrogen on crevice corrosion.[11] However, there are sufficient data to indicate that hydrogen plays an important role in the control of crevice corrosion by minimizing the adverse effects of oxygen. On the basis of the corrosion inhibition generally afforded by hydrogen, a concentration of hydrogen on the order of 25 to 50 cc per kilogram of water would be expected to provide adequate protection against crevice corrosion. However, additional work will be required for subtantiation of this statement.

A few observations have been made on the crevice-corrosion behavior of carbon and low-alloy steels under simulated BWR conditions consisting

of 546°F water at pH 6.4 with 0.1 ppm oxygen in the water and 2 ppm hydrogen in the steam.[11] After the tests, specimens were examined for crevice corrosion in the areas where stainless steel spacers used in mounting the specimens in the holders contacted the specimens. Visually, no attack was noted, but at up to 40x magnification it was revealed that the test materials were subject to very slight crevice corrosion. It is believed possible that the crevice corrosion might occur during the part of the test when the loop is being brought to temperature before test conditions are reached. This hypothesis was strengthened by the fact that the crevice corrosion did not appear to increase as the test time increased. Ruther and Hart[44] found no evidence of increased corrosion in crevices when they tested 5% chromium steel and type 304 stainless steel for 85 days in water containing 35 ppm oxygen or 98 days in water containing 530 ppm oxygen at 500°F. The subject of crevice corrosion for carbon and low-alloy steels in water-cooled nuclear reactors requires further attention under both operating and shutdown reactor conditions.

5.2.1.3 Galvanic Corrosion

Galvanic corrosion may arise when two dissimilar metals are in contact in an aqueous environment. The potential difference between them will initiate attack at a corrosion rate that is largely dependent upon the surface reactions of the two metals.[55] Surface films affect the efficiency of an electrode. A bare metal is a much better cathode than one covered with an oxide which, apart from its possible interference with hydrogen evolution, puts an additional resistance into the electrochemical circuit. The stability of the oxide in the solution is therefore of some importance. Since the diffusion of oxygen is frequently the rate-determining factor in aqueous corrosion, large cathode-to-anode ratios will frequently result in intense galvanic attack. Such effects are most likely to occur at points where structures are joined by a different metal.

Because of the possibility that galvanic attack might occur in high-purity primary water systems for nuclear reactors at dissimilar-metal junctions, such as welds, and especially at welds between carbon or low-alloy steel and stainless steel in a reactor system that included carbon or low-alloy steel as a construction material, tests were conducted under

simulated boiling-water reactor conditions with welded dissimilar-metal welded specimens.[11] The specimens included welded carbon steel and low-alloy steel and carbon steel and alloy steel welded to stainless steel. The exposure, of 1000 hr duration, was carried out in near-neutral high-purity water at about 546°F in steam, steam-water, saturated water, and subcooled water (535°F) environments containing from 0.1 ppm oxygen in the saturated water to 15 ppm oxygen in the steam and 2 ppm hydrogen in the steam and steam-water mixture. The chloride content of the water was less than 0.1 ppm. Visual, low-power microscopic, and metallographic examinations revealed no traces of galvanic, selective, or accelerated corrosion in or near weld zones of any of the welded specimens. The absence of accelerated attack on the carbon steel or low-alloy steel portions of the dual-metal welded specimens indicates that galvanic corrosion is not an important factor in these systems, a situation which is probably related to the poor conductivity of the water.

Ruther and Hart[44] also found no evidence of increased corrosion in galvanic couples when they tested 5% chromium steel and type 304 stainless steel at 500°F for 85 days in water containing 35 ppm oxygen or 98 days in water containing 530 ppm oxygen.

5.2.1.4 Stress-Corrosion Cracking

When mild steel is stressed in tension to stresses near or beyond the elastic limit and exposed specifically to hot concentrated alkaline or hot concentrated nitrate solutions, it suffers stress-corrosion cracking along intergranular paths. The required stress may be applied or it may be residual in the metal.[13] Time to failure is a matter of minutes under severe conditions of stress and environment or of years when conditions are less severe.

Stress-corrosion cracking was first encountered in a practical way in riveted steam boilers.[13] Stresses at rivets always exceed the elastic limits, and boiler water is normally treated with alkalies to minimize corrosion. Crevices between rivets and boiler plate allow boiler water to concentrate until the concentration of alkali suffices to induce stress-corrosion cracking, which is sometimes accompanied by explosion of the boiler. Because alkalies were recognized as one of the causes, failures

of this kind were first called caustic embrittlement. With the advent of welded boilers and with improved boiler-water treatment, stress-corrosion cracking has become less common. Its occurrence has not been eliminated entirely, however, because stresses, for example, may be set up at welded sections of boilers or in tanks used for storing concentrated alkalies.

It has been claimed by some that stress-corrosion cracking of steels in alkalies is a form of hydrogen embrittlement or hydrogen cracking, but this has never been proved. On the contrary, cathodic polarization of stressed steel in hot caustic soda solution protects against cracking and indicates that hydrogen does not take part in the mechanism.[56]

Even though well supported, there is presently some doubt that the electrochemical mechanism alone is adequate to explain all features of the stress-corrosion cracking phenomenon.[13] Steel, for example, is peculiarly susceptible to hydroxyl and nitrate ions but not to nitrite, sulfate, chloride, and many other ions. This has led to the hypothesis[57,58] that cracking occurs in part through adsorption, which reduces the surface energy of the metal at the apex of the crack and encourages the metal to part under tensile forces. Langmuir[59] demonstrated that only a monolayer of adsorbate is needed to cut off major surface affinities of underlying atoms. Furthermore, ions primarily effective in this respect are those that specifically chemisorb on a given metal surface. Crack propagation aided by adsorption has been suggested as explaining the fracture of steels containing hydrogen.[60]

The preferred path of chemisorption may occur selectively along specific paths in the metal where there are dislocations, perhaps locked in position by impurities, or at vacancies where certain alloying components are concentrated.[13] Hence, cracking may follow the same routes, that is, it may proceed along the grain boundaries or through the grains that favor galvanic action. In fact, the natural emf of galvanic cells may well favor chemisorption of specific ions on one or both electrode surfaces. Applied anodic or cathodic polarization of the metal may alter adsorption behavior of ions and may even serve to displace some ions with others less damaging. In this respect, cathodic polarization can be beneficial, independent of a corrosion mechanism.

Mild steel undergoes cracking under high-temperature high-concentration alkaline conditions.[55] This phenomenon is usually referred to as caustic cracking. Caustic cracking represents a serious hazard in boilers and steam equipment, where crevices or porous scale in highly stressed regions, for example, a rivet or seam, can become regions of high pH and initiate explosive failure. The cracks are intergranular, although there is attack on pearlitic cementite, and the iron dissolves as oxyanions. Magnetite is precipitated, but usually not at the crack tip, so there is no stifling. Hydrogen is produced during the attack, and it may help crack propagation by forming internal blisters. Stress relieving mild-steel structures helps to reduce the probability of cracking, but this is usually combined with inhibitive methods aimed at eliminating the possibility of alkaline-concentration buildup. Phosphate, which precipitates at high pH but below dangerous levels, is widely used and added so that the ratio $Na_2O:P_2O_5$ is just less than 3:1. Sodium nitrate is another additive that has been successfully employed to eliminate cracking on locomotive boilers. Under some circumstances, nitrate may accelerate cracking.

It is believed that carbon and low-alloy steels are not susceptible to stress-corrosion cracking under BWR or PWR conditions.[11] Stress-corrosion cracking of steels containing up to 5% chromium is most frequently observed in caustic and nitrate solutions and in media containing hydrogen sulfide.[47,61] At temperatures above about 1058°F in steam, mild steel may be decarburized and embrittled, because of attack on cementite by corrosion-generated hydrogen,[19] with the formation of methane in accordance with the following equation:

$$Fe_3C + 4H \rightarrow 3Fe + CH_4 \ .$$

Prevention of this type of attack requires the addition to the steel of elements that form stable carbides, such as niobium, titanium, vanadium, tungsten, chromium, molybdenum, and manganese.

Duplicate U-bend specimens of carbon and low-alloy steels were exposed to simulated BWR conditions in a test loop for periods up to 300 hr.[11] Conditions included a temperature of 546°F, 0.1 ppm oxygen in saturated water, 15 ppm oxygen in steam, and 2 ppm hydrogen in steam. The chloride

content of the pH-6.4 high-purity water was less than 0.1 ppm. No cracking was detected with steels containing up to 5% chromium. Because of the limited number of stress specimens exposed, the results should be regarded only as an indication of the resistance of carbon and low-alloy steels to stress-corrosion cracking.

Stressed specimens of types ASTM A 106 and A 212 carbon steel were exposed for periods up to approximately 24,000 hr (33 months) during the preoperational and operational phases of the Heavy-Water Components Test Reactor (HWCTR).[62,63] The environment was heavy water (light water during the preoperational period) at nearly 600°F and 2000 psi, which was maintained at a pD of 10.7 ± 0.5 by lithium hydroxide addition. Deuterium was added to the helium pressurizing gas and controlled to give a dissolved deuterium concentration of 10 to 20 cc per kilogram of heavy water in the high-pressure system. The dissolved deuterium combined radiolytically with dissolved oxygen to give a dissolved oxygen concentration of less than 0.004 cc/kg or approximately 5 ppb. No cracking was observed on any of the stressed specimens.

5.2.2 Austenitic Stainless Steel

5.2.2.1 General Corrosion

From the beginning of the reactor program, chromium-nickel austenitic stainless steel has been the basic material for contact with the primary fluid (high-purity water) for cooling purposes. These alloys have exhibited a definite susceptibility to stress-corrosion cracking under certain conditions that may be encountered by the heat-exchanger tubes on the secondary side but, nevertheless, stainless steel components generally have exhibited excellent corrosion behavior in reactor service. The possibility of reducing material costs has prompted several studies of the feasibility of substituting carbon and low-alloy steels for stainless alloys. So far, results of such explorations have not provided a sufficiently well-established basis for use of these materials in primary systems of water-cooled reactors.[22] The most important deterrents have been evidences of susceptibility to localized attack, possibilities of hydrogen embrittlement by dissociated hydrogen, impairment in ductility

by radiation, and the fact that possible savings in cost might well be offset by added expense in dealing with the greater amount of corrosion products generated.[43,64,65]

The alloys of iron, chromium, and nickel are the most versatile non-precious corrosion-resistant materials. Most investigators believe that the corrosion resistance of these alloys results from the presence on the surface of the alloy of a thin oxide or hydrate film that is stabilized by chromium.[29] It is generally agreed that passivation is not a continuous state and that it exists only in certain environments or under certain conditions. Under many conditions, the range of passivity is broad, while in others the range is relatively narrow and may be destroyed by slight environmental changes. Stainless steels are normally passive in natural fresh water, mine water, boiler condensate, and steam at elevated temperatures. Under the usual conditions of exposure, these alloys remain substantially free of pits and rust. However, improper heat treatment or strong cell concentrations may bring about superficial rusting or incipient pitting.

The corrosion resistance of the 300 series stainless steels in high-temperature water is generally excellent and these alloys have been used extensively in various nuclear reactors. Sensitized 300 series steels are not susceptible to intergranular attack in water at high temperatures.[29] However, case hardening of stainless steels, either by nitriding or malcomizing, decreases the initial corrosion resistance to such an extent that the usefulness is limited in water at elevated temperatures.[66]

The structural integrity and reliability of pressure-circuit components and consequently the operational status of a nuclear reactor plant are closely dependent on the corrosion behavior of the system materials. The dominant properties of the primary coolant are its pH and oxygen content, although other agents added to the water for special purposes may also influence its aggressiveness. For example, boron in the form of boric acid may be added to the primary fluid as a means of supplementing the control rods to override additional reactivity produced by the fuel in excess of the critical mass at startup.

Considerable corrosion testing of the austenitic stainless steels has been conducted in autoclaves and test loops in which the oxygen, hydrogen,

pH, temperature, and water velocity could be controlled. The effects of these variables are discussed in the following sections.

Effect of Oxygen. The corrosion rates of stainless steels in high-temperature distilled water are relatively insensitive to the amount of dissolved oxygen present.[29] Low rates are observed in the range <0.5 to 7 cc oxygen per kilogram of water. Above this range, corrosion increases slowly and has a tendency to level off until oxygen concentrations in the neighborhood of 1000 cc per kilogram of water are reached. At these higher concentrations, corrosion decreases slightly.

In pH-8 to -10 high-purity water at 500°F with up to 5 ppm NH_3 and 20 to 30 cc H_2 per kilogram and in pH-10 to -11 (by lithium hydroxide addition) water at 600°F with 25 cc oxygen per kilogram of water, stainless steel corrodes uniformly at exceedingly low rates, less than 10 mdm (~0.06 mpy), at velocities between 7 and 15 fps.[67] Carbon steel also corrodes relatively uniformly under similar conditions but at rates about ten times greater than for stainless steel. A stainless steel rate of 0.06 mpy is considered negligible with respect to design life for equipment. However, for a typical pressurized-water reactor plant, even this low rate would lead to some 0.25 to 0.5 lb of corrosion product per month, which could represent a significant amount. In neutral water, the crud from stainless steel occurs both as loose magnetite (Fe_3O_4) containing also chromium and nickel oxides and as an adherent thin film on the metal. At high pH, the quantity of loose solid corrosion products is considerably reduced and the adherent corrosion films are thicker. In tests similar to those described above, the effect of small amounts of dissolved oxygen on the corrosion of type 304 stainless steel was examined. At low oxygen concentrations (10 ppb or less) the observed rate was 1.2 mdm (~0.01 mpy) after 2100 hr. At an oxygen concentration of 10 ppb with three or more surges up to and exceeding 100 ppb, the rate was 9.4 mdm (~0.04 mpy) after nearly 2000 hr.

Wanklyn and Jones[68] report that additions of dissolved oxygen have little effect on the corrosion of austenitic stainless steels in high-purity high-temperature water nor do small amounts of nitrogen, argon, helium, and ammonia.

Effect of Hydrogen. The addition of hydrogen (50 cc per kilogram of water or more) is effective in reducing the corrosion of the austenitic stainless steels in high-temperature high-purity water.[29] Many stainless steels show no visible corrosion when tested at 500°F in water containing dissolved hydrogen. In operating systems containing hydrogen, the most beneficial effects are obtained by introducing the desired amount of hydrogen at room temperature before bringing the system to operating temperature and pressure. Wanklyn and Jones[68] also report that the addition of dissolved hydrogen has little effect on the corrosion of the austenitic stainless steels. Vreeland[69] summarizes the results of numerous investigations on the hydrogen effect by stating that little or no effect on the corrosion of austenitic stainless steels in high-temperature high-purity water results from the presence of 0 to 45 ppm dissolved hydrogen.

Effect of pH. Some information on the effect of water pH on the corrosion of austenitic stainless steels has been included in the preceding section on the "Effect of Oxygen." Vreeland[69] reports that in high-purity high-temperature water, variations in the pH between 7 and 11 apparently have little effect on the general corrosion of austenitic stainless steels, although the variations may influence the behavior of suspended corrosion products. Maintenance of a high pH at the reactor operating temperature may tend to reduce both the formation and deposition of corrosion products.[67] Under reactor operating conditions, lithium hydroxide is more stable and therefore more effective than ammonium hydroxide in maintaining a higher pH for any level of initial crud formation.

Effect of Temperature. There is no significant difference in the rate of corrosion of the austenitic stainless steels with water temperatures from 200 to 500°F.[69] However, it has been indicated that between 500 and 600°F, corrosion may increase by a factor of 5, although Wanklyn and Jones[68] feel that little effect is to be expected. Apparently any increase in general corrosion of the chromium-nickel stainless steels caused by increasing the temperature up to 600°F is not of practical importance in water-cooled nuclear-power plants.

Effect of Velocity. Corrosion rates of the austenitic stainless steels are not appreciably affected in high-temperature water at velocities between 1/60 and 30 fps.[70] There is a marked difference, however, in

corrosion rates between static and dynamic conditions. The indications are that general corrosion is about 20 times less under static conditions than under dynamic conditions up to 30 fps. Tipton[29] states also that there is no appreciable effect of velocity noted on the stainless alloys in high-temperature water. Tests have been made at water velocities up to 30 fps at 500, 600, and 640°F without appreciable erosion. Higher velocities have not been investigated. High-velocity water at 30 fps, understandably, has more of a tendency to remove corrosion products than low-velocity water at 1 fps.

Effect of Time. Bloom and his co-workers[26] found that a comparatively high initial corrosion rate with type 347 stainless steel in high-purity water at 600°F resulted with values of about 200 mdm (1.2 mpy) after a 1-hr test. This high initial rate dropped off rapidly as the time of testing increased. After about 2000 hr, a rate of 10 mdm (<0.1 mpy) was normal. In other te.ts conducted with types 302, 304, 316, and 347 stainless steels under simulated PWR conditions, corrosion rates ranged between 5 and 15 mdm (0.03 to 0.09 mpy).[12,23,24,71] McKibben[63] reported corrosion rates not in excess of 0.01 mpy for annealed and sensitized type 304 stainless steel specimens, type 304 stainless steel with 1% boron added, and annealed type 316 stainless steel after periods of up to 992 days in-core and out-of-core at the HWCTR. The environment for all specimens, except during 65 days for preoperational testing in light water, was heavy water at a pD of approximately 10.5 and a temperature of 315°C.

Effect of Heat Treatment. Intergranular or grain-boundary corrosion resulting from carbide precipitation in the 300 series stainless steels is not experienced in high-temperature water service,[29] nor do stresses in the range up to 10,000 psi or greater impair their resistance in water. In austenitic stainless steels, the most important metallurgical change caused by heat treatment is sensitization — the precipitation of chromium as chromium carbide ($Cr_{23}C_6$) along the grain boundaries of the unstabilized grades — which may result from heating during welding, stress-relieving, etc. The susceptibility to intergranular corrosion attack of sensitized austenitic stainless steels in certain environments is well known, such as in the use of acidic solutions for decontamination of nuclear systems. However, intergranular corrosion of sensitized steels does not occur in

reactor coolant water, with or without oxygen, with pH variations between 7 and 11 and at temperatures up to about 640°F.[12] It is therefore unnecessary to use the more expensive stabilized or extra-low-carbon grades of stainless steel in preference to the unstabilized regular-carbon grades in primary-circuit applications of water-cooled nuclear reactors, and in this respect such reactors as Dresden, EBWR, Yankee, and the N.S. Savannah are successfully using type 304 stainless steel in their primary systems.

Some evidence has been revealed[72] of intergranular attack on sensitized specimens of type 304 stainless steel exposed for 22 months to the wet steam-water environment within the evaporator boxes of the Elk River Reactor. The depth of the penetration was about 7 mils. The temperature in the water box was 539°F. The amount of moisture present in the incoming steam to the evaporators was about 0.5%, and the water solids carryover in the steam did not exceed 1 ppb. Oxygen and hydrogen contents in the steam leaving the reactor were on the order of 1100 and 130 ppm, respectively. The chloride content of the pH-6 to -8 reactor water was less than the sensitivity of the analytical procedure employed, that is, 35 ppb.

A doubt is raised immediately regarding the validity of the incidence of intergranular penetration of sensitized type 304 stainless steel described above as to whether the selective attack occurred as a direct result of the extended exposure. Information describing the occurrence did not include whether the specimens were chemically pickled after sensitization. It has been well documented that acid cleaning of sensitized steels should be avoided.[12,73] The use of some acid-cleaning solutions, notably nitric-hydrofluoric acid solutions, may result in intergranular corrosion during cleaning, although damage in addition to that occurring during pickling will probably not take place when sensitized and pickled components are subsequently exposed to primary water at about 580°F.[73]

Effect of Additives. Inorganic inhibitors, such as hydroxides, chromates, molybdates, tungstates, etc., are effective in changing the corrosion characteristics of stainless steels.[29] Hydroxides and ammonia or basic amine inhibitors are widely used in the boiler industry for corrosion control. Organic inhibitors are probably unsatisfactory for use in high-temperature water reactors because of thermal and radiation instability. No experimental data are reported on specific beneficial

effects of inhibitors in high-temperature-water stainless steel reactor systems other than hydrogen. In general, the use of inhibitors offers a possibility of improving corrosion resistance.

Boron additions sometimes are made to the coolant-moderator in order to supplement the mechanical control of pressurized-water reactors at startup. The quantity of boron required for this purpose will vary with the system design and operation but usually is in the range 600 to 1600 ppm.[67] Apparently, such additions do not have an appreciable effect on the aggressiveness of the primary coolant, even though several cases have been reported where cracking of stainless steels occurred during exposure in an aqueous borated environment.[74] These tests were carried out in static 500°F water containing 600 ppm boron as boric acid. The materials exhibiting cracking were fully hardened AISI type 440-C and Armco 17-4 PH stainless steels. In the same tests, Armco 17-7 PH aged at 1050°F and AISI type 304 stainless steel, among others, were not subject to cracking.

The good corrosion behavior of chromium-nickel austenitic steels was corroborated in another investigation designed to evaluate structural materials for the Yankee Atomic Electric nuclear plant.[75] The tests were run at 600°F in flowing water containing 1600 ppm boron as boric acid, 0.3 ppm lithium hydroxide, and 25 to 30 cc hydrogen per kilogram of water.

White and Krieg[70] showed that corrosion of austenitic stainless steel was not seriously affected by the addition of 1500 ppm H_3BO_3 to the water as a neutron absorber for control purposes, although this resulted in lowering the water pH to about 5.

Effect of Wet Oxygenated Steam. In a boiling-water reactor, the net products of the radiolytic decomposition of water pass through the turbine. In the Dresden nuclear station, the oxygen content of the steam is anticipated to be 10 to 30 ppm, consistent with a dynamic-equilibrium quantity in the recirculating water.[46] Therefore the environmental conditions produced by the steam-oxygen mixture can lead not only to general corrosive and erosive action but may give rise also to oxygen-concentration cell effects conducive to pitting and crevice corrosion.

These possibilities have been the subject of a thorough investigation of turbine materials.[43] The first phase of the study was conducted with

industrial steam at 430°F and pH 6, with 0.05, 80, and 110 ppm oxygen. Erosion and corrosion effects were explored in the second phase with wet steam at 272°F, 70 to 110 ppm oxygen, and a pH of 8.8 to 9.5. The third phase was designed to produce information on the possible extents of pitting, crevice, and galvanic corrosion in water and steam in autoclaves at 545°F with 50 to 110 ppm oxygen, initially, and a pH of 7. It was found that at pH 7, with high and low oxygen contents, the logarithms of the corrosion rates varied approximately linearly with the reciprocal of the absolute temperature. With low oxygen content, minor pitting occurred only in carbon steel, whereas with high oxygen content, all materials pitted, with carbon steel suffering the most severe attack. There was no correlation between hardness of the materials and erosion, which generally followed the order of expected corrosion behavior; that is, stainless steels were most resistant, with low-alloy steels next, and carbon steel and cast iron least resistant.

Some of these observations were substantiated in another study of carbon, low-alloy, and stainless steels tested in a boiling-water loop.[64] Experimental conditions were 546°F in the steam, steam-water, and saturated-water sections and 537°F in the subcooled water section of the stainless steel loop. The water and steam conditions were based on 10 to 20 ppm oxygen in the steam, with a 1:8 stoichiometric ratio of hydrogen to oxygen. No significant differences were noted in the corrosion rates of the carbon and low-alloy steels tested, although all showed higher rates than the austenitic stainless steels tested. Also, the steels containing up to 5% chromium were subject to slight pitting and crevice attack. The amount of corrosion and iron-to-system release rates for carbon and low-alloy steels were considerably lower than those obtained by other investigators for similar materials in test loops simulating pressurized-water systems operated at neutral and high pH with deoxygenated water. It should be noted, however, that the corrosion of these materials might be aggravated by the rapid local fluctuations occuring in the temperature of the oxide on the metal during boiling-water reactor operation. These fluctuations might crack the oxide by thermal shock, reduce its protective properties, and lead either to increased general corrosion or to pitting.

Crud Sources and Effects. Most waterborne impurities originate from the steady-state corrosion and wear of core and out-of-flux structural components.[67] Therefore the extent and nature of the depositable crud species formed is governed largely by the water chemistry and the compositions of the system materials. The partly or completely transportable suspended and soluble corrosion products found in the primary coolant are of great significance for two reasons. First, the radioactivity induced by exposure to neutrons during transport through, or sojourn in, the core and the subsequent deposition of the activated corrosion products throughout the system might create a biological hazard that would result in restricted accessibility for plant maintenance. Secondly, crud deposition and buildup might foul heat-transfer surfaces, increase the hydraulic friction factor and core pressure drop, and interfere with the proper functioning of valves, control rod mechanisms, and other sensitive devices. In a stainless steel system, the effect of radiation and dissolved oxygen generally is to enhance crud formation, whereas maintenance of a high pH at the operating temperature tends to reduce both the formation and deposition of corrosion products. Under reactor operating conditions, lithium hydroxide is more stable and therefore more effective than ammonium hydroxide in maintaining a higher pH for any level of initial concentration. For instance, while the normal crud level is 0.05 to 0.25 ppm in a system operating with neutral water, and 0.01 to 0.2 ppm with ammonium hydroxide, it is only 3 ppb when lithium hydroxide is used as the pH-controlling agent.

Effect of Irradiation. The corrosion behavior of austenitic and martensitic stainless steels, carbon steel, and other materials both in the presence and absence of nuclear radiation was examined at 500 and 600°F.[76] The test media were flowing neutral water, pH-8.9 to -9.5 ammoniated water, and pH-4.5 water containing 1 ppm oxygen. The data revealed that irradiation up to an integrated flux of 1.1×10^{21} neutrons/cm^2 had a tendency to decrease the corrosion rates of alloys that characteristically develop adherent oxide films and, conversely, to increase the rates for materials that do not form such protective films. A plausible explanation may be that by decreasing the activation energy of the corrosion process, radiation enhances the initial rate of corrosion reactions of metals. This, in turn, leads to rapid film formation of the

first corrosion-product layers, which, if of favorable character, inhibit further corrosion. Such a hypothesis explains why carbon steel and martensitic stainless steel, whose initial corrosion-product films are less protective, were the least corrosion resistant of the alloys investigated under irradiation. For all materials tested, the quantity of deposits formed in a carbon-steel test loop was appreciably greater than that in an austenitic stainless steel loop. As would be expected, an increase in water pH by the addition of ammonium hydroxide effectively decreased general corrosion and minimized loose deposit formation. Some typical rates in the 600°F tests were 10 mdm (0.06 mpy) out of pile for type 304 stainless steel and 5 mdm (0.03 mpy) for the same material in-pile. Carbon steel corroded at a rate of 120 mdm (0.7 mpy) out of pile and 180 mdm (1.1 mpy) in-pile.

5.2.2.2 Crevice Corrosion

Crevice or contact corrosion occurs when surfaces of stainless steels are used in contact with each other and the surfaces are wetted by the corrosion medium or when a crack or crevice is permitted to exist in a stainless steel component exposed to such media.[47] This type of corrosion has been noticed particularly in stainless steel joints made with gaskets to obtain a tight fit. So long as the joint is tight and does not become wetted, crevice corrosion will not occur. Otherwise, failure may take place. Rapidly moving well-aerated solutions have less tendency to cause contact corrosion at crevices, such as in threaded joints or blind pockets. Contact or crevice corrosion is corrosion produced at the region of contact of, usually, nonmetallic materials with passive metals. It may occur at washers, under barnacles or applied protective films, and at pockets formed by threaded joints. Whether or not stainless steels are free of pit nuclei, they are always susceptible to this kind of corrosion because a nucleus is not necessary. Contact corrosion may begin through action of a concentration cell. The accumulation of passivity-destroying corrosion products at stagnant areas soon converts the cell to a more rapidly acting passive-active cell. Corrosion then proceeds by a mechanism identical to that of pit growth.

Ellis and LaQue[77] state that in environments capable of breaking down the passivity of metals, it is common for accelerated corrosion to occur within any crevices into which the corrosive medium may seep. As with other forms of electrochemical attack, a distinction must be made between the chance or incidence of crevice corrosion and the intensity of the attack when it does take place. There is good foundation for the belief that the mechanism of crevice corrosion involves electrochemical action between the surfaces of the crevice and those exposed freely to the environment outside it. In the simplest case, this would be a differential aeration or oxygen-concentration cell effect, with the metal within the crevice (which is shielded from free access to dissolved oxygen) becoming anodic to the outside surfaces freely exposed to the oxygen-bearing solution. When stainless steels or other metals and alloys that resist corrosion as a result of the favorable influence of oxygen or other oxidizing media and which likewise exhibit a more noble potential when in this passive state, the matter becomes complicated and aggravated by the active-passive galvanic cells that may become established. The metal within the crevice that is shielded from oxygen may become active, while that outside in free contact with oxygen will maintain its passivity. The difference in potential between the active and passive states will become a driving force in the galvanic corrosion of the anode within the crevice. It can be assumed therefore that the crevice corrosion of a passive metal is simply a particular kind of galvanic cell, with the anode being the active metal within the crevice and the cathode the passive metal outside it. This being the case, the action of this cell should obey the rules of other galvanic cells. In particular, in environments where the galvanic cell reaction is under cathodic control (e.g., where the supply of oxygen to depolarize the cathodes has a controlling effect) the extent of corrosion of the anodes within the crevice should be determined principally by the area of the freely exposed surfaces (cathodes) outside the crevices, in accordance with the "Catchment Area Principle" based on experiments by Whitman and Russell.[78] It would follow then that corrosion in crevices should be most serious where the area of freely exposed metal outside is relatively large, and least serious under circumstances where the metal outside the crevice is relatively small, and

perhaps even nonexistent as in the case of a continuous crevice such as would exist where only metal within the crevice would be exposed to the corrosive liquid. These principles, advanced by Ellis and LaQue,[77] were substantiated in subsequent experiments with crevice-type stainless steel specimens exposed in seawater.

Vreeland[69] comments that corrosion in crevices can occur because of (1) an increase in metal-ion concentration within the crevice as compared with the concentration outside the crevice, which may then result in concentration-cell corrosion; (2) a decrease in oxygen concentration inside the crevice, which may then result in oxygen-concentration-cell corrosion; or (3) increased corrosivity resulting from the accumulation of soluble and insoluble corrosion products formed within the crevice. All three of these mechanisms are the result of little or no fluid circulation through the crevice. The following variables are important in the consideration of crevice corrosion:[12] composition of the material, oxygen content of the water, hydrogen content of the water, water pH, and temperature. Also important in applications involving moving components are the amount of clearance between surfaces and the relative movement between surfaces.

In many crevice tests conducted at elevated temperatures with different materials,[12] it was found that the extent of crevice corrosion generally decreased with the increasing corrosion resistance of the material tested. Straight chromium stainless steels and high-nickel-bearing alloys were subject to slight pitting in crevice areas, whereas austenitic stainless steels were not. The choice of materials for applications in which crevices occur should probably be limited to those that do not show pitting and which show the least amount of corrosion-product buildup.

To determine the oxygen effect on crevice corrosion, tests were run at 500°F in high-purity water containing either 0.014 ppm or less than 0.001 ppm dissolved oxygen.[12] In the degassed water, the amount of crevice corrosion observed was insignificant, but high operational torque or seizure occurred in the water with the higher oxygen content. It has been shown also in water at elevated temperatures containing about 45 ppm hydrogen and 0.007 to 0.014 ppm oxygen that hydrogen can control crevice corrosion by minimizing the adverse effects of oxygen.[12] These tests showed that crevice corrosion is virtually eliminated in water containing

sufficient hydrogen. No great problems have been encountered with crevice corrosion in boiling-water reactors that have both oxygen and hydrogen in the cooling water. Also, limited tests in high-temperature water indicated that a high pH (10 to 11) has an inhibiting effect similar to that observed for hydrogen additions.[12]

5.2.2.3 Galvanic Corrosion

Galvanic corrosion may arise when two dissimilar metals are in contact in an aqueous environment. The potential difference between them will initiate attack at a corrosion rate that is largely dependent upon the surface reactions of the two metals.[55] As mentioned earlier, surface films affect the efficiency of an electrode. A bare metal is a much better cathode than one covered with an oxide, which, apart from its possible interference with hydrogen evolution, puts an additional resistance into the electrochemical circuit. The stability of the oxide in the solution is therefore of some importance. Since the diffusion of oxygen is frequently the rate determining factor in aqueous corrosion, large cathode-to-anode surface area ratios will frequently result in intense galvanic attack. Such effects are most likely to occur at joints of structures joined together by a different metal.

In the passive state the stainless steels have a noble galvanic potential; hence, when connected under corrosive conditions with more active metals, like carbon steel, for example, accelerated corrosion will occur on the latter.[47] This is true particularly if the areas of the two dissimilar metals are equal to each other or if the area of the stainless steel is greater. Stainless steel may be coupled with active metals in some environments if its area is much less than that of the active metal. A good example is the use of an 18-8 stainless steel rivet in a carbon steel plate immersed in sea water; in this instance the 18-8 steel does not appreciably increase the corrosion of the carbon steel plate.

LaQue and Copson[22] state that galvanic corrosion provides an excellent example of the separation of anodic and cathodic reactions. If an electrical contact is made between two metals that have different potentials, current must flow between them. The more active metal becomes the anode. On this member of the couple, the potential shifts in a more noble

direction, with a corresponding increase in the metal oxidation reaction and decrease in the reduction reactions. On the other member of the couple the current produces cathodic protection. It causes the potential to shift in the active direction, with a corresponding decrease in the metal oxidation reaction and increase in reduction reactions. The two metals polarize to about the same potential, with any difference being equal to the IR drop through the solutions. The importance of surface areas should be stressed, because it is the current density and not the total current that determines the corrosion rate. It is unwise to combine a small area of the anodic member of a couple with a large area of the cathodic member. The reverse relationship is usually not troublesome.

In galvanic behavior, iron is usually anodic (less noble) to stainless steels and other metals, such as nickel, brasses, bronzes, etc.[22] In any neutral solution corrosive to iron, the attack will be accelerated when a cathodic metal is coupled with the iron.

The active-passive relationship of stainless steels has an important influence on their galvanic behavior. In the active condition, stainless steels behave galvanically like iron and steel.[79] For example, copper and copper alloys will accelerate the attack of active stainless steel[80] but will not result in galvanic corrosion when the stainless steel is in a passive state.

Stainless steels will not suffer accelerated attack when coupled with other metals in any solution so long as they remain passive.[22] Coupling with other metals can break down passivity in special circumstances. Severe damage to stainless steel can result when a localized area of the surface becomes active for any reason. At this area, galvanic acceleration takes place with the adjacent passive surfaces serving as part of the cathode area. Although stainless steel is not usually attacked galvanically, it may accelerate attack on the other contacting metal because of its strongly cathodic nature.[81,82] Hydrogen deposition at an 18-8 stainless steel cathode does not necessarily destroy its passivity, as has been shown by current and potential measurements.[22]

There appears to be a paucity of information in the literature on the galvanic corrosion behavior of carbon steel and stainless steel couples in high-temperature high-purity water. What little information was

found originated from the Westinghouse Electric Corporation.[37] In the tests reported, carbon steel coupled directly with stainless steel was exposed at low and high temperatures under conditions simulating those encountered during operation of the Yankee nuclear power reactor. At 140 to 160°F in pure water containing 0.5 to 2 ppm oxygen, the principal form of attack on the carbon steel was due to galvanic corrosion.[83] At the lower oxygen content, the total attack produced a corrosion rate of 1.3 mpy, of which 1.1 mpy was attributed to galvanic corrosion. At the higher oxygen level, the attack attributed to galvanic corrosion was 9.0 mpy, which was about the same as the total attack rate. With 7 ppm LiOH and 0.5 ppm oxygen present, the attack due to galvanic corrosion was reduced drastically to 0.03 mpy after 82 days. The total attack rate in this case was 0.05 mpy. In other tests, the room-temperature rate for carbon steel coupled to stainless steel in an air-saturated solution containing 3000 ppm boron as boric acid was 5.3 mpy. Uncoupled carbon steel in the same environment corroded at a rate of 6.4 mpy. Under flow conditions at 600°F, with 0.05 to 0.15 M H_3BO_3, water pH from 5.2 to 6.3, flow from 2 to 36 fps, and 100 cc of hydrogen per kilogram of water, the corrosion rates, including both galvanic and general corrosion, ranged from 0.07 to 3.0 mpy for carbon steel coupled with stainless steel depending on (1) the velocity of the fluid passing the specimens, (2) exposure time in fluid, and (3) boric acid concentration. The tests were run in deaerated water. In semistatic galvanic tests with carbon steel coupled with stainless steel, corrosion rates for the carbon steel ranged from 0.7 to 0.9 mpy under a variety of conditions that included temperatures from 600 to 650°F, boric acid concentrations from 0 to 0.1 M, oxygen content of less than 0.1 ppm, and hydrogen from 0 to 100 cc per kilogram of water.

5.2.2.4 Stress-Corrosion Cracking

Stress corrosion is a type of corrosive attack that occurs through the combined action of tensile stress and a corrosive environment. Considerable information has appeared in the literature, particularly during recent years, with regard to stress-corrosion cracking of the austenitic stainless steels and related materials, but there is no generally accepted

consolidated theory on the mechanism involved in such cracking processes The stress may be either applied or residual within the metal. However, it must be a tensile stress. No cases have been reported where stress-corrosion cracking occurred under compressive stress in a conducive environment. The aggressiveness of the corrosive environment required to cause cracking may vary for different materials. The environment may be quite mild and produce little or no corrosive action in the absence of stress. However, the same environment might cause cracking of the same material in the stressed condition. Stress-corrosion attack takes the form of cracks that grow slowly or rapidly depending on environmental conditions. The cracks may be intergranular, transgranular, or a combination of both.

Stress-corrosion cracking can be caused by two corrosive media in nuclear power plants.[12] One is the high-purity water in the primary coolant system of water-cooled reactors; the other is the boiler water in the secondary steam-generation system. In addition, the action of these waters can vary depending on whether a material is exposed in the liquid phase or in the vapor phase. Except for a few specialty items, such as materials of spring temper, stress-corrosion cracking is not known to be a problem in primary water systems. It appears that the few problems that do exist can be circumvented without much difficulty by the proper selection of materials and their heat treatment. Much can be accomplished toward the reduction or elimination of stress-corrosion cracking in austenitic stainless steels by the use of annealed steels, stabilized steels, and stress-relief treatments and by keeping design and operating stresses as low as possible. However, these measures alone are not always enough, and positive control can be achieved only by employing special precautions to inactivate the corrosiveness of the reactor water.

It appears that cracking of austenitic stainless steels can be inhibited effectively in the liquid phase of ordinary chloride-free boiler water by an alkaline-phosphate water treatment similar to that used in conventional naval boilers.[12] However, this treatment is not effective in the steam phase, and it is here that more extreme methods of control must be

exercised. The most critical areas in the steam phase are those in which the equipment is subjected to intermittent wetting and drying. This can come about above the water level by splashing on heated surfaces, carry-over, etc.

Highly critical areas can also exist below the water level. Zones that are especially vulnerable exist in crevices formed by tube joints and under corrosion deposits, where local hot spots can develop and cause the water to flash to steam. The intermittent wetting and drying leads to the concentration of boiler water constituents (and chloride, if present) and thereby creates a locally agressive medium in an otherwise mild environment.

It has been demonstrated that for stress-corrosion cracking to occur in susceptible materials, such as the austenitic stainless steels, both oxygen and chloride must be present in the environment.[12,84-87] Keeping the chloride content at a low average level is helpful but not foolproof under conditions where local concentration can take place. One of the most effective methods to prevent cracking, particularly in the secondary system, is to keep the oxygen content at the lowest possible level. This may necessitate the use of oxygen scavengers.

The stress-corrosion cracking behavior of austenitic stainless steels in primary-system water has not been explored as extensively as might be desired, but available evidence shows that cracking is not a problem in major constructional components of nuclear systems.[12,69] Such components are generally fabricated from annealed materials or are stress-relieved after fabrication. Operational stresses are not sufficiently high to promote cracking in high-purity primary water systems. On the other hand, heavy cold working of these alloys may induce susceptibility to cracking, particularly in water containing oxygen. The results of a limited number of tests in BWR environments of stressed but not cold worked specimens indicate that stress-cracking of austenitic steels of the chromium-nickel, chromium-manganese-nickel, and chromium-manganese-nitrogen types does not occur during exposure to BWR conditions in which both oxygen and hydrogen are present in the water.[24]

Uhlig[13] states that in environments for austenitic stainless steels, the two most damaging ions are chloride and hydroxyl. In sodium chloride and other neutral solutions, cracking is observed only if dissolved oxygen is present,[87] and the amount of chloride needed to cause damage can be extremely small. Cracking of 18-8 stainless steel heat-exchanger tubes has been observed in practice after contact with cooling water containing 25 ppm chloride or less, and cracking has also been induced by small amounts of chloride in magnesia insulation wrapped around stainless steel tubes.[88] In these instances, there is evidence that small pits form first at which chlorides concentrate by electrolytic transference, and then cracks are initiated by concentrated ferrous chloride and analogous chlorides within the pits. Hence, oxygen is needed for stress-corrosion cracking in sodium chloride solutions because pitting occurs only in its presence or in the presence of other depolarizers. It should not be assumed, however, that pitting is a requisite for cracking to occur. Cracking by alkaline solutions requires relatively high concentrations of hydroxyl ions. Therefore cracking of 18-8 stainless steel usually takes place not in alkaline boiler water but rather within the splash zone above the waterline, where dissolved alkalies concentrate by evaporation. Dissolved oxygen is not required in such solutions for failure to occur.[89] It is expected, however, as in the case of chlorides, that depolarizers accelerate cracking.

Scully[55] states that service failures occur in pressurized water at 392 to 572°F and above with as little as a few ppm of chloride ion and a few ppm of dissolved oxygen present. Often the cracks are associated with a white corrosion product. In service failures, cracks are sometimes found filled with corrosion products, and it has been suggested that these serve to "wedge open" cracks like ice breaking up rocks by forming from water in fissures.[90] Hydrogen is evolved during the cracking of austenitic stainless steels, although most of the cathodic reaction is the reduction of oxygen. It has been suggested that hydrogen causes the cracking by embrittlement or by the formation of a very active hydride that is readily dissolved.[91] Since cathodic polarization stops cracking, although it produces more hydrogen, hydrogen embrittlement seems to be a wrong explanation. The active hydride theory requires more experimental data.

5.2.3 Results of Pressure Vessel Examinations

5.2.3.1 Yankee Reactor

As of January 1965, the total power generation of the Yankee pressurized-water reactor, which first went critical in August 1960, passed four billion kwhr.[92] The reactor with a current heat output of approximately 600 Mw has design conditions of 650°F and 2500 psig. During the 1965 refueling, all fuel was unloaded, and the core barrel and core-support structure were removed to permit a partial inspection of the pressure vessel.[37] It was found that one material irradiation capsule had broken up and released Charpy impact specimens and other debris into the lower head area. In the process, several small areas were worn in the lower head cladding in the northwest quadrant.

The lower-head material is A 302 grade B carbon steel clad by the Babcock & Wilcox intermittent spot welding process with 0.109-in.-thick type 304 stainless steel. The cladding process results in a welded bond over approximately 70% of the area, with the rest of the carbon steel—stainless steel interface unbonded. The unbonded areas are interconnected, so in the event of a cladding defect, 30% of the interface of one 4- by 8-ft sheet could be exposed to the reactor coolant.

Although there were numerous scratches and gouges in the cladding, the carbon steel was apparently exposed only in two small adjacent areas totaling about 2 in.^{2}. The minimum original thickness of the A 302 grade B carbon steel, as measured after forming the hemisphere, was 4.110 in. This compares with a minimum allowable thickness, as required by Section VIII of the ASME Code, of 3.774 in. and, as required by Section III, of something less than 3.0 in. The maximum depth of the defect through the 0.109-in.-thick cladding, measured by impressions, was not more than 0.115 in. If it is assumed that 0.010 in. of general wear took place near the penetrations, the reduction in thickness of the carbon steel was approximately 0.016 in. This leaves a present thickness of 4.094 in. and at least 0.3 in. of material available before the minimum allowable dimension is reached. On the basis of extensive investigations and analyses, this is considered to be more than adequate corrosion allowance for the lifetime of the vessel.

The total penetration by corrosion of the exposed A 302 grade B carbon steel is estimated to be less than 100 mils for the rest of the plant lifetime. This is made up of 25 years of hot operation with a penetration of 1 mpy and 30 cold shutdowns of 2 months, each with a penetration of 1.5 mils per shutdown. As is shown above, there is presently 300 mils over the minimum thickness, so a total corrosion penetration of 100 mils is acceptable.

The penetration rate during normal operation used in the previous analysis is based on a corrosion rate of 150 mdm (1 mpy). This rate in turn is based on available experimental information that was developed at conditions of temperature, flow, and boric acid concentration quite similar to those at Yankee. No allowance is included for galvanic corrosion, since with the high-resistivity water and low oxygen conditions of normal operation, this is not expected to exert an appreciable effect.

The penetration rate during refueling is based on a corrosion rate of approximately 1500 mdm (10 mpy). This corrosion rate is a conservative estimate that includes an allowance for the effect of the galvanic corrosion that may take place in the aerated water present in the vessel during this period. It seems clear that any galvanic corrosion will take place primarily at the area of cladding penetrations and will very rapidly diminish away from this area because of polarization of the stainless steel cathode due to the buildup of hydrogen in the region between the stainless steel and the carbon steel.

During normal operation there will be no oxygen in the coolant, and crevice corrosion does not generally occur in the absence of oxygen. The available data show that during cold shutdown conditions, rates of crevice corrosion will be even less than the general corrosion rate. Although there is more oxygen in the coolant during shutdown, the availability of oxygen behind the tightly fitting stainless steel cladding will be very limited.

No mechanism exists in the area of penetration for the concentration of the alkali without which stress-corrosion cracking will not take place. Furthermore, ammonium hydroxide, the only alkaline additive normally used in the main coolant, is not subject to concentration because of its volatility.

5.2.3.2 Experimental Boiling Water Reactor

The Experimental Boiling Water Reactor (EBWR) was designed to produce 20 Mw of heat in the form of 600-psig saturated steam (489°F), which was fed directly to a turbine-generator producing 5 Mw of electricity.[93] Full-power operation at the design level of 20 Mw(t) was obtained in December 1956. In 1960, modifications were made to permit operation at 100 Mw(t), which was realized in 1962. The plant was then shut down due to termination of the boiling-water program at the EBWR.

With the release of the EBWR from the water-cooled reactor program, Argonne National Laboratory requested participation in the plutonium recycle program on the phase of work that would be appropriate for use of the EBWR facility. Preparations for operating EBWR in this program included examination of the reactor vessel. The pressure vessel was designed and fabricated in 1955-56 in accordance with Section I, Power Boilers, of the ASME Boiler and Pressure Vessel Code (1952 Revision). The vessel was fabricated from SA 212 grade B carbon steel plate and was clad with 0.109-in.-thick AISI type 304 stainless steel. The vessel plates for the shell and lower head were clad by intermittent spot-resistance welding of the stainless steel to the carbon steel plate. The cladding was resistance welded to the base plate while both were submerged in water. Integrity of the cladding on the finished vessel was established by introducing nitrogen at 900 psi between the cladding and the base plate and testing for cracks with liquid soap on the surface of the cladding. A few cracks were detected that were repaired by welding prior to shipping the vessel.

During the postoperation examinations, visual and dye-penetrant inspections of the accessible portions of the interior of the pressure vessel revealed numerous cracks in the resistance-welded cladding of the cylindrical part of the vessel. The removal of the steam-collector duct and the shock shield permitted inspection of approximately half the reactor vessel. All cracking was found to be in the resistance-welded cladding. The upper-ring forging, vessel head, and nozzles, which were clad by weld-overlay techniques, were free of cracks. In many instances the cladding cracks extended through the stainless steel to the carbon steel base plate, as determined by gas tests. The through cracks were ground

out to the pressure vessel base metal, with dye-penetrant inspections interspersed during the process. The grinding and inspection were extended to, and slightly into, the SA 212 grade B base metal. No evidence was found of crack propagation into the base metal nor was there evidence of gross generation of iron oxide or local pitting at the cladding—base metal interface.

When cracking was first discovered in the pressure vessel cladding, it was assumed that the cracking had developed over the past five or six years as a result of service conditions, for example, radiation effects, thermal fatigue, and possibly stress corrosion. The fact that similar failures occurred on practice plates used to develop welding procedures, apparently to an even greater degree, even though they were not exposed to a reactor environment but only to an atmospheric environment, led to an intensive investigation designed to determine the cause of cracking.

The majority of the through cracks in the cladding were ground out to the base metal. Since the cracks appeared to increase in size and number as the cladding was ground out, it appeared that they may have originated at the interface between the cladding and the base metal. This was generally true for cracks that extended through the cladding, but it could not be definitely stated for all such cracks, since it was found that many of the cladding cracks started at a point remote from the interface, such as at the weld nugget. Approximately 40 linear feet of cracks was ground out, and the area was examined. The surface was carefully cleaned, and dye-penetrant inspection was continued approximately 10 to 15 mils into the base metal. No evidence of cracking of the base metal was found nor was there any indication of parting in the resistance welds bonding the cladding to the vessel wall.

Approximately 30 in.^{2} of the SA 212 grade B steel behind the cladding became available for examination when strips of cladding were removed for chemical analyses. In all exposed areas, the carbon steel wall was found to be covered with a thin layer of black oxide, probably magnetite (Fe_3O_4). No pitting attack or red oxide were found. The interface side of the cladding was also covered with a thin, adherent, black oxide film and was free of reddish-brown iron rust.

Chemical, macroscopic, and microscopic examination of the type 304 stainless steel cladding yielded much graphic and qualitative data. Attempts were made to obtain samples of the thin oxide film on the pressure vessel wall for chloride analysis after the cladding had been removed, since during resistance welding of the cladding to the carbon steel plate by the fabricator, softened water containing chlorides was used to remove the heat of welding. It was speculated that some chloride ions may have been trapped at the interface during the welding process. However, the nature of the black oxide film was such that suitable samples could not be obtained for analysis. Instead, drillings from the pressure vessel wall were analyzed for chloride. Chloride contents were found to vary from 6 to 425 μg. Since it is known that some oxides, particularly aluminum oxide, have the ability to concentrate chlorides by factors of 10 to 100,[94] tests were carried out by Argonne National Laboratory to determine whether Fe_2O_3 and Fe_3O_4 would absorb chloride ion preferentially from water containing sodium chloride. Although there was a slight indication of adsorption by the Fe_2O_3, the amount was almost within the range of experimental error, so no definite conclusion could be drawn that selective adsorption had occurred. For various reasons, the results of the chloride analyses from the pressure vessel wall drillings were believed to grossly overestimate the actual chloride contents by virtue of accidental chloride contamination.

Metallographic examination showed the stainless steel to be severely sensitized. This phenomenon in unstabilized or low-carbon grades is brought about by subjecting the stainless steel to temperatures in the range 900 to 1500°F. The most critical range is 1150 to 1200°F. The degree of chromium carbide precipitation under such conditions is also time dependent. During stress relief of the pressure vessel after fabrication, the type 304 stainless steel cladding was held at 1150 to 1200°F for at least 9 hr and was in the temperature range above 900°F for at least an additional 6 hr during heating and cooling.

Although the cracking of the vessel cladding was of prime interest, all samples examined were searched for evidence of concurrent cracking in the SA 212 grade B vessel plate. Several microcracks up to 8 mils in depth were found. A number of deeper microcracks were filled with

intruded type 304 stainless steel from the cladding process. Many intrusions of molten stainless steel into oxide interfaces were found also. Metallographic studies on test plates not exposed to the reactor environment showed conclusively that the unfilled microcracks in the SA 212 grade B plate existed before the cladding was applied and were probably formed during the initial fabrication of the plate. None of the specimens examined showed any evidence of propagation of the surface microcracks as a result of the cladding process, vessel fabrication, or reactor operation. Propagation of these microcracks is not expected in the furture operation of the vessel, which will occur at the same or lower temperature and pressure levels as in the past.

After very extensive investigation, it was concluded by simple and straightforward calculations that the most probable causes of cracking in the stainless steel pressure vessel cladding were, initially, the differences in the behavior of materials during the fabrication stage and, later, to low-cycle fatigue failures. Other failure mechanisms undoubtedly aided in the development of localized fractures of the reactor vessel cladding, inasmuch as all the type 304 stainless steel was sensitized initially by thermal heat treatments at the fabricator's plant.

Although high cladding stresses, oxygen, and abnormal grain boundaries existed simultaneously in the reactor vessel, the use of an ion-exchange system maintained the water essentially free of chloride ions. Thus the exposed surface of the cladding was free of chloride ions. Chlorides may have been present at the interface between the stainless steel cladding and the carbon steel base metal; however, oxygen and water are required to form the active chloride-induced stress-corrosion cracking mechanism. This mechanism, to be effective, would require a prior breaching of the cladding barrier. Therefore, despite the presence of small amounts of chloride at the cladding interface, it is not believed that the chloride stress-corrosion cracking mechanism was a primary cause of the EBWR vessel cladding cracking because of the following:

1. Cracks in the cladding of the 2-in.-thick practice plate, which should be most susceptible to stress-corrosion cracking by virtue of a moderately high chloride content (5 ppm by chemical analysis) at the carbon-stainless steel interface, originated at the surface of the cladding.

2. There was no means of concentrating chlorides in the reactor vessel, such as a water-steam zone, where the water carries chlorides that precipitate out on evaporation, unless the cladding had already been breached. Even then, the reactor primary water was so carefully controlled that the presence of chloride ions was highly unlikely.

3. Many cracks were internal with respect to the stainless steel cladding and extended neither to the surface nor to the interface.

Since the pressure vessel will be operated without recladding the areas of SA 212 grade B steel laid bare as a result of grinding out cracks in the cladding, an evaluation was undertaken on the corrosion behavior of the exposed carbon steel under reactor operating conditions. The general corrosion of SA 212 grade B carbon steel in 500°F oxygenated water is about 2.5 mpy.[12] While the corrosion of carbon steel coupled with austenitic stainless steel might be expected to accelerate due to galvanic effects, particularly in view of the relatively small area of carbon steel exposed, it must be kept in mind that the reactor primary water is a poor conductor. Copson and Berry reported that galvanic coupling of Inconel to carbon steel or to type 347 stainless steel does not accelerate attack on either member of the couple when exposed to reactor water.[95] Since the potential of Inconel is essentially the same as that of the 300 series stainless steels, it would appear that galvanic corrosion would not be of any significance between the stainless steel cladding and the SA 212 grade B base plate.

Some pitting is possible in the crevices formed by the interface of the SA 212 grade B steel with the type 304 stainless steel. The role of dissolved oxygen is believed to be the controlling factor in pitting. If oxygen is present in small amounts and the corroding solution is stagnant, passivity may not be preserved over the entire surface, and pitting may result. If the concentration of oxygen is sufficient to maintain an unbroken passive film over the entire surface, pits will not form. In the absence of oxygen or some other oxidizing agent, the cathodic areas will not be depolarized, and the development of pits will be arrested. The thickness of the SA 212 grade B pressure vessel wall is about 9/16 in. more than the Code requires, and thus prolonged operation can be sustained at the general corrosion rate of 2.5 mpy.

5.2.3.3 Heavy-Water Components Test Reactor

The Heavy-Water Components Test Reactor (HWCTR) was operated for a three year period from 1962 to 1964 to test candidate fuel elements for heavy-water-moderated and -cooled power reactor systems.[65] Operation was terminated on December 1, 1964. Shutdown and layaway of the HWCTR permitted thorough examination of the equipment.

The HWCTR, a pressurized reactor moderated and cooled with heavy water, had a design temperature of 600°F and a design pressure of 1500 psi. The maximum design power was approximately 70 Mw(t). Mild carbon steels were used for all high-pressure pipe, steam generators, main-system purge cooler, gas pipe, main storage tank, and some of the low-pressure pipe. All secondary coolant equipment was mild steel, except the heat exchangers, which were either stainless steel or Inconel. The reactor vessel was fabricated from ASTM A 212 grade B carbon steel and lined with 0.250-in.-thick type 304 stainless steel. Other types of carbon steel used in the above components were ASTM A 106 grade B, ASME SA 210, and ASME SA 285. In the reactor vessel, no mild steel was exposed to the moderator.

To minimize corrosion of the mild steel, the D_2O moderator coolant was maintained alkaline at pD 10.7 ± 0.5 with lithium hydroxide. Careful control of dissolved oxygen was essential because of the susceptibility of the mild steel to general corrosion and pitting. Deuterium gas was added to the pressurizing gas, helium, and controlled at 1.5 to 3.0% by volume. The dissolved deuterium combined radiolytically with dissolved oxygen to give a dissolved oxygen concentration of approximately 5 ppb. Stainless steel was protected against chloride stress-corrosion cracking by careful control of the chloride contents of the moderator and of such auxiliary materials as lubricants, gaskets, O-rings, insulation, cleaning agents, and filters.

The secondary coolant system was a once-through system. Chemically treated well water served as coolant for miscellaneous heat exchangers and as boiler feed makeup for steam generation. The well water was characterized by low solids (15 to 20 ppm), low pH (4.2 to 5.3), high carbon dioxide (23 to 28 ppm), high dissolved oxygen (3 to 6 ppm), and a chloride content around 2 ppm.

Treatment of the secondary cooling water was entirely by chemical addition; that is, no deionization or deaeration was used.

The basic treatment consisted of the following:

1. Catalyzed sodium sulfite was added for cold-water reaction with dissolved oxygen.

2. Sodium phosphates were added in a "coordinated pH phosphate control" plan to provide alkalinity for corrosion control and to prevent deposition of silica scale.

3. A chelating agent, "Versene," was added to complex calcium and magnesium compounds to eliminate deposition of objectionable hardness scale on heat transfer surfaces.

This system operated satisfactorily with no evidence of oxygen-corrosion pitting until July 1964, when a tube failure occurred in one of the steam generators. Inspection of the cooling water (shell) side of the generator showed that severe pitting corrosion had taken place over the short time interval of a few months since a previous inspection.

A review of performance data showed that the sulfite residual in the feedwater had always been maintained greater than 10 ppm, and the bimonthly analysis for dissolved oxygen had always indicated zero. However, the condition of the steel tubing indicated a type of pitting characteristic of oxygen attack. Extensive investigation disclosed that of two brands of sodium sulfite used during the period preceding the tube failure, one brand failed to remove dissolved oxygen from the water with sufficient rapidity to minimize corrosion to the steam generator. It was also shown that the standard method for testing for oxygen is unsatisfactory in the presence of residual sulfite. A modified Winkler method was developed in which the excess sulfite was removed by iodine as a preliminary step. Using the modified method, laboratory tests on samples taken from the HWCTR feedwater system while using the slow-reacting sodium sulfite showed that 2 to 5 ppm oxygen could have been in the treated feedwater going to the steam generators during the period that this particular brand of sulfite was used.

Corrosion of mild steel was monitored by inspecting corrosion coupons from the reactor (in core and out of core) and storage tank, inspecting equipment, and analyzing the moderator for corrosion products. Numerous

inspections were made of mild-steel equipment and pipe, including the purge cooler heads, steam-generator heads, pipe in several locations, and two sections of tube that were removed from the steam generator. Without exception, the condition of each component was excellent, even after extended shutdowns for as long as three months during which considerable dissolved oxygen was in the water. All the surfaces were covered uniformly with adherent black (magnetite) film and showed no rusting, general corrosion, or pitting.

Prior to initial nuclear operation, corrosion coupons were placed in the heavy-water system at the following locations:

1. reactor vessel, in-core,
2. reactor vessel, above core in D_2O,
3. reactor vessel, at D_2O-gas interface,
4. reactor vessel, in gas phase,
5. storage tank, in D_2O.

Coupons were removed periodically and examined for weight loss, pitting, iron release to moderator-coolant, and cracking of stressed specimens. All weight losses were measured on descaled coupons, and a total of 61 coupons was examined. The period of high-corrosion rates and oxide-film growth apparently ended prior to 4400 hr of exposure. After 4400 hr, the corrosion rates were very low. For example, the average weight loss between 4,400 and 15,240 hr of exposure was only 1.8 mdm (0.01 mpy). The highest corrosion rate observed on any of the samples was only slightly in excess of 0.1 mpy for a specimen of ASTM A 106 exposed above the core of the reactor for 995 days, including 380 days during which the reactor was critical.

Although no pitting was found on mild steel pipe, tubes, or other reactor components, minor pitting did occur on the corrosion coupons. Pits ranged up to 8 mils in depth for exposure periods from 4,400 to 23,880 hr. Two corrosion coupons that were examined were exposed during preoperational light-water testing and then left in the water for further exposure. These two coupons showed less corrosion than the others that were not placed in the reactor until after the light-water test period.

One holder containing nine stressed ASTM A 106 coupons was exposed for 535 days at the D_2O-gas interface in the reactor vessel. The primary purpose of this set of coupons was to determine whether caustic cracking would occur on stressed mild-steel surfaces where lithium hydroxide salt deposits might accumulate. No salt deposits could be seen on the coupons when they were removed and no coupons cracked. Descaled corrosion rates ranged from 0.03 mpy in the vapor to 0.05 mpy in the heavy water. The rates were somewhat lower than the rates for unstressed coupons exposed deeper in the heavy water, so no effect of stress on general corrosion behavior was indicated.

Inspections were made periodically of types 304 and 316 stainless steel equipment, including the reactor vessel lining, pipe, pumps, and internal components of the reactor vessel. Without exception, all surfaces were uniformly covered with a gray-black oxide film. No cracks or other defects were found. A number of types 304 and 316 stainless steel stressed coupons in annealed and in sensitized condition were examined after exposures up to 1004 days in core and out of core. No cracks were found, and corrosion rates were extremely low — not in excess of 0.01 mpy. No difference in rates was seen between in-core and out-of-core specimens.

5.2.3.4 Elk River Reactor

An incidence of cracking of stressed specimens of type 304 stainless steel after an exposure of 22 months to the wet steam-water environment within the evaporator water boxes of the Elk River Reactor[72] has been reported. The stressed specimens were exposed to near-saturated steam at 936 psig and 539°F with approximately 0.5% moisture in the incoming steam to the evaporators. The solids carryover in the steam was about 1 ppm. The concentrations of oxygen and hydrogen of the steam in the water boxes were approximately 1100 and 130 ppm, respectively. Chloride concentrations in the pH 6 to 8 reactor water were maintained at nondetectable levels with an analytical technique sensitive to about 35 ppb.

Cracks were found in all three U-bend specimens that ranged up to 12 mils deep. The conclusion was that the Elk River Reactor environment can lead to stress-corrosion cracking, since there are undoubtedly areas

of high residual stress, high applied stress, or high oxygen concentration, but it was agreed by consultants that no evidence was available to indicate that stress-corrosion cracking could result in catastrophic failure.

5.2.4 Conclusions

With appropriate thickness allowances, general (uniform) corrosion of carbon and low-alloy steels for pressure vessels will not present a problem, other than perhaps that of release of iron to the system, in the operation of high-temperature water-cooled nuclear reactor systems. At operating temperatures in high pH water, evidence indicates a steady-state corrosion rate on the order of 0.5 and less up to 2.5 mpy, depending upon environmental conditions. At lower pH values, it appears that this rate may be somewhat higher. The difference in corrosion behavior of the plain carbon and the low-alloy steels with up to 5% chromium is insignificant.

No noticeable effect has been found on the corrosion of plain carbon and low-alloy steels as a function of temperature between the range 500 and 600°F. However, at temperatures around 140°F when the reactor is shut down for various reasons and when oxygen is readily available to the system, the corrosion rate may be as high as 10 to 15 mpy.

The velocity at which carbon and the low-alloy steels are susceptible to erosion-corrosion effects has not been established, but it is known that velocities up to 35 fps are below the range where such effects are operative.

There does appear to be an effect of oxygen on the corrosion behavior of carbon and low-alloy steels, particularly in low-temperature water, where the rate is appreciably high Some differences in behavior, however, have been observed by various investigators in high-temperature water, depending upon the level of oxygen content. At high oxygen concentration levels, better behavior has been observed than at lower oxygen levels. In neither case are the rates excessive, however. The role of dissolved hydrogen has not been definitely established, but there is evidence that in neutral water the addition of hydrogen suppresses corrosion attack noticeably.

Water pH has been found to exert a rather marked effect on the corrosion of carbon and low-alloy steels. Corrosion rates decrease as the pH is raised from the range 7.0 to 9.5 to the range 10.5 to 11.5. Tests have shown that at the higher pH, generally obtained by the addition of lithium hydroxide, the steady-state corrosion rate after 10,000 hr is about 0.1 mpy.

Pitting of pressure vessel materials such as the carbon and low-alloy steels does not appear to be a problem at operating temperatures of a nuclear reactor system, but it is highly likely that some pitting will occur during reactor startup and shutdown periods despite the high resistivity of the water. It has been determined experimentally that pits formed in room-temperature water are not intensified or accelerated during subsequent operation in high-temperature water. Once the high-temperature film is formed on pressure vessel materials, appreciable protection is afforded against the formation of pits during later exposure to room-temperature conditions. As best as can be determined from observations of experimental data, pitting does not present any serious problem so far as depth of penetration is concerned.

The severity of both crevice and galvanic corrosion (the latter when carbon or low-alloy steel is coupled to a more noble material, such as austenitic stainless steel) is greatly diminished as the dissolved oxygen content of the water is decreased. Galvanic corrosion, as might be expected to occur in a specific case where a defect in stainless steel cladding over carbon steel or low-alloy base metal would expose the latter to the aqueous environment, would be greatly lessened by the high resistivity of the water.

Stress-corrosion cracking of the carbon or low-alloy steels in water-cooled reactor systems does not appear to be a problem, simply because no mechanism exists whereby concentration effects in water environments could produce sufficiently high alkalinity ranges to induce cracking. Experimental data for stressed specimens in water systems at pH 10.2 to 11.2 show no cracking after periods as long as nearly three years during reactor preoperational and operational times.

Austenitic stainless steels used as cladding material for nuclear pressure vessels present no problem so far as general pitting and crevice

or galvanic corrosion are concerned. Corrosion rates under a wide variety of conditions are about 0.1 mpy. Stress-corrosion cracking susceptibility remains a constant threat in the case of inadvertent admission of chloride ion to the aqueous system. However, except for a few specialty items, such as materials of spring temper, stress-corrosion cracking is not known to be a problem in primary water systems.

5.3 HYDROGEN EMBRITTLEMENT

Some metals, when stressed, crack on exposure to corrosive environments, but corrosion is not a necessary part of either crack initiation or crack growth.[12] Examples of this kind of cracking are therefore not properly called stress-corrosion cracking, despite certain similarities. For example, a stressed martensitic 12% Cr—Fe stainless steel in dilute sodium chloride solution may crack after several months of exposure or, if immersed in dilute sulfuric acid, may crack within less than 5 min. The failures have the outward appearance of stress-corrosion cracking but, if the alloy is cathodically polarized, cracking still occurs.

The evidence in numerous cases is that cracking is caused by hydrogen entering the metal either through a corrosion reaction that liberates hydrogen at the surface or by cathodic polarization.[96] Steels containing interstitial hydrogen are not always damaged. They most always lose ductility (hydrogen embrittlement), but only under conditions of sufficiently high applied or residual stress does cracking take place. Failures of this kind are called hydrogen stress cracking or hydrogen cracking.

Ferrous metals are especially susceptible to hydrogen cracking when heat treated to form martensite, but they are less susceptible if the microstructure is ferritic (body-centered cubic). A carbon steel heat treated to form a spheroidized carbide structure is reported to be less susceptible than pearlite, bainite, or martensite.[97] Austenitic stainless steels or 14% Mn—Fe steel (face-centered cubic) in which hydrogen is more soluble than in ferrite and the diffusion rate is lower are immune under most conditions of exposure.[98]

The mechanism of cracking has been explained by development of internal pressure on the assumption that interstitial atomic hydrogen is

released as molecular hydrogen at voids or other favored sites under extreme pressure.[99] Such an effect certainly occurs, as shown by formation of visible blisters containing hydrogen when occasional ductile metals are cathodically polarized or exposed to certain corrosive media. Under similar conditions, a less ductile metal could crack instead. Another proposed mechanism is that hydrogen diffuses to and absorbs at the apex of the crack; this reduces the surface energy of metal atoms subject to tensile force (stress-sorption cracking).[60]

An interesting characteristic of hydrogen cracking is the specific delay time for appearance of cracks after stress is applied. The delay time is only slightly dependent on stress and decreases with increasing hydrogen concentration in the steel.[100] For small concentrations of hydrogen, fracture may occur days after stress is applied.

A minimum critical stress exists below which delayed cracking will not take place in any time.[13] This critical stress decreases with increases in hydrogen concentration. Delay in fracture apparently results because of the time required for hydrogen to diffuse to specific areas near a crack nucleus until the concentration reaches a damaging level. These specific areas are presumably arrays of imperfection sites produced by plastic deformation of metal just ahead of the crack. Hydrogen atoms preferably occupy such sites because they are then in a lower energy state compared with their normal interstitial positions. The situation is analogous in this respect to the mechanism of stress-corrosion cracking in the austenitic stainless steels for which diffusion and segregation of nitrogen atoms probably occurs under similar circumstances. In hydrogen cracking, however, supplementary chemisorption of ions from aqueous solutions is not necessary. The crack propagates discontinuously, as explained by the fact that plastic deformation occurs first, and then hydrogen diffuses to imperfection arrays produced by deformation, whereupon the crack propagates one step further. A sharp notch in a steel surface favors plastic deformation at its base and hence lowers the critical minimum stress and shortens the delay time.

Scully[55] states that stress-corrosion cracking which relies upon an anodic dissolution for at least part of the propagation process can be avoided by cathodic protection. Hydrogen cracking, by contrast, is induced

by cathodic polarization, since this promotes the production of hydrogen. This distinction has been used to discriminate between the two mechanisms.

The effect of hydrogen has been investigated by cathodic charging experiments.[55] The hydrogen appears to have no effect on the elastic modulus of the material. Embrittlement is a reversible process, since a specimen charged with hydrogen will gradually lose it. At very low temperatures, embrittlement by hydrogen does not take place. The amount of hydrogen that a lattice can hold is well above the solubility limit, particularly if the material is cold worked. It appears to collect in voids and cracks associated with localized regions of triaxial strain within the lattice.

Severely cold-worked austenitic stainless steels can also suffer hydrogen cracking in addition to stress-corrosion cracking.[55] The application of either anodic or cathodic polarization shortens the time to failure of such material. Very high-strength carbon steels are particularly prone to embrittlement and extreme care must be exercised in welding them. Some even fail if stressed in ordinary humid atmospheres. One outstanding feature of hydrogen embrittlement is that it is detectable only at low strain rates, and standard notched-bar tests will not indicate the effect. Since it is likely that the hydrogen in the lattice diffuses to the deformed region at the tip of the crack, a high strain rate does not allow the necessary time for this movement to occur.

It is not always easy to distinguish between stress-corrosion cracking and hydrogen embrittlement, particularly in ferritic and martensitic materials.[55] Cathodic polarization should make a clear distinction, but results are not always conclusive. Martensitic steels, for example, in high-temperature water may develop pits or stress-rising notches electrochemically, but the actual cracks, which run straight and unbranching across the specimens and perpendicular to the applied stress, may propagate by some form of hydrogen embrittlement. Such cracks propagate very rapidly, and such rapid failures in ferrous materials arising from hydrogen embrittlement or perhaps caustic cracking constitute a serious hazard. Catastrophic failure can occur with no prior warning. With ferrous materials,

particularly the high-strength steels, failure can take place from embrittlement by hydrogen derived from any aqueous environment. It is thus much harder to avoid.

While it is possible that high-pressure molecular hydrogen exists in voids, current opinion and evidence suggest that atomic hydrogen migrates to the straining region, where it exerts an embrittling effect.[55] The mechanism is not clear. Possibly the hydrogen lowers the bonding of the metal lattice at the tip of the crack. It may collect on dislocation sites and prevent plastic deformation so that the fracture stress at the tip of the crack is reached before any yielding occurs. Some discussion on both hydrogen embrittlement and stress-corrosion cracking has centered around the concept that some ionic species or, possibly, a hydrogen atom absorbs on the crack sides and thus lowers the surface energy of the metal. This adsorption makes propagation much easier, since the stress to cause a crack to propagate can be directly related to the surface energy of the crack face area.[101] If plastic deformation takes place at the crack tip, the surface energy is increased considerably, and it is not at all clear that any adsorption process could lower it sufficiently to have any effect.

5.3.1 Carbon Steel

When absorbed in steel, hydrogen can cause several undesirable effects, such as flaking, hydrogen embrittlement, or delayed brittle fracture, and at high temperatures it can cause decarburization.[102,103] Hydrogen embrittlement is probably the most prevalent of the three,[104] and it causes lowered ductility of the steel at certain strain rates and temperatures.[105] The steps involved are hydrogen adsorption on the surface of the steel, diffusion of dissociated hydrogen through the steel, and retention of the hydrogen at discontinuities in the steel. Hydrogen may be introduced into the steel as a result of exposure of the metal to hydrogen at high temperatures and pressures or as a result of corrosion of the metal in aqueous solution.[106-108] For embrittlement to occur in aqueous solutions, there must be a constant source of atomic hydrogen at the metal surface, and the condition of the surface must be such that

diffusion of the atomic hydrogen into the steel occurs. It is also possible that diffusion of hydrogen through steel may propagate stress-corrosion cracks.[107]

LaQue and Cordovi[67] state that the problem of hydrogen embrittlement in carbon steel under simulated high-temperature water conditions for nuclear reactors was discussed with M. C. Bloom of the Naval Research Laboratory. Bloom stated that in observations of carbon steel samples at 600°F in static tests, there was no evidence of embrittlement after 800 days in distilled water, 400 days in water at pH 10.6, or 275 days in water at pH 11.5. The corrosion rate in the case of the latter greatly exceeded 50 mdm (0.3 mpy) for the first 10 days and exceeded 25 mdm (~0.2 mpy) for about 50 days thereafter. In summary, it must be said that although there is no evidence of embrittlement in Bloom's results with carbon steel at 600°F at throughputs of the order of those to be expected under the stated reactor conditions, specific exploration of hydrogen throughputs in the order of 25 $cm^3/dm^2/mo$, corresponding to a corrosion rate of about 50 mdm (0.3 mpy) or more for extended periods, would be required to be absolutely certain that embrittlement and other related effects would not take place under the stated conditions.

A thorough analysis of the potential hydrogen embrittlement problem as related specifically to the Yankee Reactor has been made,[37] since one of the questions often raised with respect to safe operation of unclad carbon steel reactor components is that of possible hydrogen embrittlement of the steel. There are numerous ways in which hydrogen can harm the properties of steel that can be separated conveniently into permanent and temporary effects. Permanent damage remains even after the hydrogen is removed from the steel, while temporary embrittlement completely disappears upon removal of the hydrogen by diffusion.

Several types of permanent damage that are well documented in the technical literature are discussed in the following sections.[37]

5.3.1.1 Blistering

Under conditions where steel is highly charged with hydrogen, either electrically or by corrosion in the presence of "poisons" such as sulfur,

selenium, phosphorus, etc., large quantities of hydrogen can collect as molecular hydrogen in defects in the steel and build up a pressure that will form blisters on the surface. The steel is permanently damaged by this action. This phenomenon only occurs under special conditions in which very large quantities of hydrogen are forced into the steel.

5.3.1.2 Decarburization

At elevated temperatures and high partial pressures of hydrogen, a reaction between the hydrogen and the carbon in the steel to form methane (CH_4) does take place. Damage to the steel is caused both by reduction in the properties due to decarburization and by formation of methane at high pressures within the steel. This phenomenon has been studied by numerous investigators, and the requisite pressures and temperatures have been well established. In a summary of practical experience, the lowest operating temperature of process equipment that failed by this type of hydrogen damage was 555°F at a hydrogen partial pressure of 500 psi.[109] Furthermore, it has been well established that steels alloyed with carbide formers, such as chromium, molybdenum, vanadium, etc., are more resistant to this form of hydrogen attack because their carbides are more stable.[109,110] The presence of hydrogen dissolved in steel in appreciable amounts has been shown to cause reduction in ductility and resistance to fracture without permanent damage; that is, when the hydrogen is removed, the steel reverts to its original mechanical properties. This effect is generally noticed only under static or slow strain-rate loading. At strain rates such as those associated with impact tests or fast brittle fracture, only very slight effects are observed, if any. Therefore the ductile-brittle transition temperature as determined by impact tests is not affected significantly by hydrogen in the steel.

There are two rather different manifestations of temporary hydrogen embrittlement, delayed failure and reduction in postyield ductility.[37] These are sufficiently different that they should be discussed separately.

5.3.1.3 Delayed Failure

One of the best-known types of hydrogen embrittlement is the phenomenon usually called "delayed failure," or sometimes called "static

fatigue."[111-114] This commonly occurs in high-strength steel components charged with hydrogen during electroplating, for example. Notched parts are particularly sensitive. The characteristic of this problem is that the part will fail in a brittle manner when subjected to a continuous static load. The higher the strength of the steel, the more susceptible it will be to this type of hydrogen embrittlement. Low-strength steels, below about 130,000-psi yield strength, are generally considered not to be affected, since stress of yield-strength magnitude or greater must be applied before failure will occur.[115] This effect is dependent on the hydrogen concentration, and the minimum critical stress below which failure will not occur is higher the lower the strength of the steel and the higher the temperature. Steigerwald and his co-workers[116] show that in high-strength 4340 steel a critical minimum concentration of 5 ppm hydrogen is necessary to cause delayed failure at −321°F. It is probable that this minimum concentration is somewhat higher at higher temperatures. The time to failure under a given stress and hydrogen content is also reduced by higher temperatures, which indicates that diffusion of dissolved hydrogen to the notch or crack tip is a controlling factor.

Consistent with the fact that hydrogen embrittlement is a slow strain-rate phenomenon, the failure does not take place instantaneously. There is a delay or incubation period before cracks appear and then a period of slow brittle crack growth until the remaining section cannot support the load, at which time it breaks without the influence of hydrogen.

5.3.1.4 Reduction in Postyield Ductility

Hydrogen in steel also changes its "necking" characteristics during a tensile test by reducing the ductility, as measured by total elongation and reduction in area.[113,117] The yield strength is not significantly affected, although the breaking stress is, as would be expected by the change in plastic properties. The term "embrittlement" is semantically too severe to be applied to this phenomenon, because the ductility is not reduced to zero but, typically, may be reduced to half its original value. This is another temporary effect, since after the hydrogen diffuses out of the steel, the original plastic properties are regained in full.

Again, this type of hydrogen-induced effect on mechanical properties of steel is much more pronounced on high-strength low-toughness steels. Low-strength steels of the A 302 grade B type with high toughness are affected very little by hydrogen in this manner. Comparatively large amounts of hydrogen are required to show the effect.

Copson[118] comments that many instances of hydrogen attack of steel pressure vessels are recorded in the literature. At high temperatures and pressures the attack is fairly well understood.[119] It is a matter of hydrogen diffusing into the steel and reacting with carbides and other constituents to form methane and other products. High gas pressure at localized sites within the steel results in fissuring. Severe attack can usually be prevented by alloying with suitable elements to form stable carbides.[120]

At lower temperatures the hydrogen generated by corrosion in aqueous solutions can also cause damage to steel, although the nature of the attack is different. Atomic hydrogen formed by the corrosion reaction diffuses through the steel quite readily. Dissociated hydrogen can also leave the steel. However, if the rate at which hydrogen enters steel is greater than that at which it leaves, internal pressures build up due to accumulation of molecular hydrogen in rifts or pockets and cause blistering, embrittlement, and fissuring.[121,122] These effects obviously weaken the steel.

The factors that control the rate at which hydrogen enters steel are not well understood.[118] Many corrosion reactions are harmless, even though plenty of hydrogen is generated. It seems certain that the surface of the steel must actively provide the acceptance of atomic hydrogen rather than catalyze the association of atoms to molecules of hydrogen gas. Once hydrogen accumulates in steel it produces embrittlement and loss of ductility, which shows up as cracking upon bending. Blistering and fissuring may depend, in part at least, on the quality of the steel.[122]

Harries and Broomfield,[123] in a very thorough treatise, conclude that the only significant source of hydrogen with respect to carbon or low-alloy steel pressure vessels in pressurized-water nuclear reactor systems is that due to the corrosion reaction at the steel-water interface, although up to 100 cc of hydrogen per kilogram of water may be added as a

corrosion inhibitor or to suppress radiation decomposition of the water. The maximum concentrations of hydrogen at the inner surfaces of unclad ferritic steel pressure vessels varying in thickness from 0.5 to 10 in. at operating temperatures of 482, 536, and 599°F, together with the equivalent hydrogen partial pressures, were calculated for a "pessimistic" corrosion rate of 75 mdm (~0.5 mpy) and the assumption that all the corrosive hydrogen was absorbed in the steel. The available data on hydrogen in iron and steels suggest that the calculated hydrogen concentrations are insufficient to have any deleterious effects on the properties of low-alloy steels of the 0.5% Mo and 1% Cr—0.5% Mo type. However, plain carbon steels in the form of thick pressure vessels might well be embrittled under similar conditions as a result of decarburization and hydrogen attack leading to the formation of methane gas. Therefore, a corrosion rate of 75 mdm (~0.5 mpy) could not be tolerated for thick plain-carbon steel vessels in pressurized-water reactor systems, and immunity from the embrittling effect of hydrogen could only be guaranteed if the corrosion rate were maintained at 10 mdm (0.07 mpy) or less with a preformed magnetite surface film or austenitic stainless steel cladding on the surface.

5.3.2 Austenitic Stainless Steel

Whiteman and Troiano[124] report that it has been demonstrated recently that nickel and several of its face-centered cubic alloys can be embrittled by hydrogen.[125-128] The nature of the embrittlement in most cases essentially parallels that observed in body-centered cubic metals with regard to temperature and strain-rate sensitivity.

In this light there has been considerable speculation on the susceptibility to hydrogen embrittlement of the face-centered-cubic austenitic stainless steels. All early investigations in this area have been inconclusive. Houdremont and Schrader[129] thermally charged 18-8 stainless steel with hydrogen at a pressure of 1 atm. They concluded that hydrogen did not influence the ductility of this stainless steel as it had influenced that of ferritic steels in similar experiments. Zapffe and Haslem[130] demonstrated that 18-9 stainless steels did not show a susceptibility to hydrogen embrittlement when cathodically charged in a 10% NaOH solution.

On the other hand, they clearly demonstrated that high-carbon chromium steels did exhibit embrittlement when charged in the same solution. Cathodic charging in various acid environments at low current densities did not embrittle austenitic stainless steels of the 18-12 variety according to Mill and Edeskuty.[131] Hobson and Hewitt[132] investigated the influence of thermally introduced hydrogen on the ductility of an 18-10 stainless steel as a function of test temperature. A significant change in ductility was observed only at the lowest test temperature, −112°F. The authors attributed this behavior to hydrogen embrittlement of the body-centered-cubic ferrite formed at this temperature. Eisenkolb and Ehrich[133] cathodically charged 18-9 stainless steel at relatively high current densities. Bend tests indicated the presence of slight embrittlement as a result of charging, but no attempt was made to determine the presence of body-centered-cubic martensite. Blanchard and Troiano[125] showed that even relatively severe electrolytic charging conditions had little effect on the ductility of 25-20 stainless steel.

Previous experiments, then, have found little or no influence of hydrogen in fully austenitic stainless steels. Only when the stainless steel could be made to transform in part to body-centered-cubic martensite was hydrogen embrittlement apparent. This inability of austenite in stainless steels to be embrittled by hydrogen has been implied[57] in attempts to discount the possible role of hydrogen in the transgranular stress-corrosion cracking of these alloys.

Recently it has been observed[126,128] that to embrittle face-centered-cubic metals it is necessary to have a hydrogen content one or two orders of magnitude greater than that necessary in body-centered-cubic alloys. In addition, it has also been recognized[128] that to observe hydrogen embrittlement in these face-centered-cubic metals, this high concentration of hydrogen must penetrate the greater part of the sample cross section. Several investigators[133,134] have shown that even with severe cathodic hydrogenation the depth of hydrogen penetration in austenitic steels was only on the order of 10 to 40 μ. This phenomenon was also observed for nickel and several of its alloys.[125,128]

Whiteman and Troiano[124] conducted tests with type 310 stainless steel in a system cathodically charged with hydrogen in a 1 N H_2SO_4 solution poisoned with 250 mg of arsenic (as sodium arsenite) per liter. The current density was 0.1 amp/cm^2 and the charging time was generally 24 hr. From the results of mechanical tests with these specimens, they concluded that it is now evident that austenitic stainless steels are susceptible to slow strain-rate embrittlement and thermal recovery in an almost complete analogy to the well-documented behavior in body-centered-cubic materials. However, the amount of hydrogen necessary to produce this phenomenon is one or two orders of magnitude greater. In addition, there is strong resistance to penetration of the hydrogen to any appreciable depth for reasons not apparent at the present time. This behavior is probably associated with surface phenomena and helps to explain why embrittlement due to hydrogen had not been reported previously.

Over the years considerable attention has been given to the association of stress-corrosion cracking with hydrogen in austenitic stainless steels. The strongest arguments against such a causative relationship have resided in two observations: (1) a completely austenitic stainless steel is not subject to hydrogen embrittlement, and (2) there are beneficial effects of cathodic polarization. It is now apparent that the first of these, "hydrogen embrittlement," is no longer a valid objection.[124]

5.3.3 Conclusions

An analysis of the available data shows that it is highly unlikely that pressure vessels fabricated from low-alloy steels will undergo hydrogen damage such as embrittlement, blistering, or fissuring from service conditions encountered during operation of water-cooled nuclear reactor systems. However, this does not appear to be the case for pressure vessels fabricated from plain carbon steel, as pointed out by Harries and Broomfield.[123] In the latter case the corrosion rate would have to be on the order of less than 0.1 mpy to insure protection from the damaging effects of hydrogen produced from the corrosion reaction.

The major source of hydrogen in a water-cooled nuclear reactor system operating at temperatures between 500 and 600°F has been established as

that produced by the corrosion reaction between the water and the carbon steel or low-alloy steel pressure vessel. In the case of the Yankee Reactor, for example, it was shown that at operating temperatures and coolant conditions, the corrosion rate and the diffusion rate of hydrogen through the vessel wall are such that the maximum hydrogen concentration in the steel of the lower head is approximately 0.3 ppm. This amount is at least an order of magnitude below the concentration that could cause reduction in ductility even at low temperatures. The partial pressure of hydrogen equivalent to this concentration was determined to be only 21 psi, which is not enough to cause any concern about decarburization reactions. Furthermore, it has been shown from experience that no permanent damage to steels of low-alloy types, such as A 302 grade B, has been caused by even high pressures of hydrogen at temperatures below 600°F. During reactor shutdown, the hydrogen concentration will not change appreciably in the steel, so a hydrogen-damage problem is most unlikely.

The literature states that hydrogen damage is most likely to occur in high-strength steels. In steels, such as A 302 grade B and other low-alloy compositions, where the tensile stress is on the order of 80,000 psi, hydrogen embrittlement is rarely encountered. In addition, these low-yield-strength steels are stressed to values around two-thirds of the yield strength at operating conditions. In contrast, the delayed-failure mechanism of hydrogen embrittlement requires very high stresses to become operative, even in the high-strength steels.

Finally, in instances where a defect exists in a low-alloy steel pressure vessel clad with austenitic stainless steel and where the defect extends into the base metal, the stainless steel cladding would serve as a cathode, and any corrosion-generated hydrogen would be discharged on the stainless steel surface. The latter is immune to hydrogen forms of damage under conditions encountered during nuclear reactor operation. As has been clearly shown in the literature, it is quite difficult to create indications of hydrogen damage in the fully austenitic stainless steels. Only by extremely severe treatment, such as cathodic charging in poisoned acid solutions, can some signs of hydrogen damage be observed. Such treatments are indeed quite removed from conditions encountered in the operation of water-cooled nuclear reactor systems.

5.4 RADIATION EFFECTS

Nuclear reactor pressure vessels are exposed to an environmental condition that is almost exclusive to the nuclear energy field, bombardment by high-energy particles. Prior to the advent of nuclear energy, the materials engineer was concerned only with environmental conditions such as temperature, stress, strain, and various gaseous and liquid media. The nuclear engineer now has the same environmental problems but must add to them the effects on materials properties produced by radiation.

The effects of nuclear radiation on metals were not given serious consideration until the first nuclear reactor was operated in 1943. The first open literature publications on such effects appeared in the early 1950's. Since then, several hundreds of reports have been published in this field.

Although these effects can be the result of the passage of any high-energy particle within structural materials,[135] this discussion is primarily concerned with the effects of neutron irradiation on the mechanical properties of steels, particularly pressure vessel steels. Neutrons are classified into three energy categories: (1) thermal or slow neutrons having energies in the thermal range (~0.025 ev), (2) epithermal neutrons having energies intermediate to thermal and fast neutrons, and (3) fast neutrons having energies of about 400 ev and greater. The lines of demarcation between these categories are ill-defined, particularly between the epithermal and fast categories.

The major changes in the mechanical properties of pressure vessel steels are brought about by the displacement of atoms within the metal structure by fast neutrons. The primary collision of a fast neutron with an atom has a high probability of transferring enough energy to the atom to displace the atom from its lattice site. This leaves a vacancy in the lattice. The neutron continues to displace atoms either until its energy is dissipated or it escapes from the material. A secondary effect results from the energy imparted to the "knock-on" atom. This atom collides with other atoms in the lattice, transfers energy to them, and removes them from their lattice sites. Finally, these "knock-on" atoms come to rest either in vacant lattice sites or interstitial positions. These lattice

defects, vacancies and interstitials, can be randomly distributed in the material or concentrated in small regions termed "clusters" or "spikes." In addition, the capture of a thermal (or epithermal) neutron by a lattice atom can result in the emission of a gamma photon or particle of sufficient momentum that the atom will be displaced from its lattice site by recoil. This effect is, however, not considered significant in power reactor pressure vessels.

Another effect of neutron irradiation may be the transmutation of one element to another element. Such effects are regarded as of minor significance in pressure vessel steels.

At the operating temperatures of nuclear power reactor pressure vessels, many of the defects will be mobile, and annealing of the radiation effects may occur. However, the presence of large numbers of radiation-produced vacancies can increase the rate of diffusion so that diffusion-controlled metallurgical reactions may be accelerated. Effects of such reactions in pressure vessel steels have either not been observed or were not recognized as such.

The defects introduced in metals by nuclear radiation can alter mechanical properties such as flow and fracture to a considerable extent. Even with this brief review of the mechanisms of radiation effects, it is obvious that the critical factors determining radiation effects in steels include composition, metallurgical structure, neutron-energy distribution (spectrum), total neutron exposure (dose), and exposure temperature and may include rate of bombardment (neutron flux) and stress.

5.4.1 Effects on Mechanical Properties

Radiation effects on physical properties of metals, for example, electrical and thermal resistivity, density, and elastic moduli, have been observed and studied in detail. The primary objective of these physical-property studies has been to understand the mechanism of interaction of radiation with atoms of a solid and the effect of various lattice defects on metal properties. Physical-property changes resulting from irradiation are rarely of engineering significance above room temperature.

The mechanical properties of metals, however, may be modified by nuclear radiation to a degree that is of considerable engineering significance. The basic cause of most radiation-induced mechanical-property changes is generally considered to be the interaction of dislocations with the lattice defects, vacancies, clusters, spikes, dislocation loops, etc. introduced by radiation. Dislocation motion in the metal lattice is either prevented or impeded by these defects, and the observed result is an increase in the flow stress or yield strength of the metal. Other mechanical property changes may be various manifestations of this primary effect.

5.4.1.1 Tensile Properties and Stress-Strain Curves

Radiation-induced changes in yield strength by a factor of 3 have been observed in engineering alloys. In relatively weak materials, such as high-purity metals, a factor of 10 increase in yield strength is not unusual. The lower the initial yield strength in a given alloy system, the greater will be the potential increase in strength due to irradiation. Accompanying the increase in yield strength is a concurrent but generally lesser increase in ultimate tensile strength. As a result, the ratio of yield strength to tensile strength tends to approach unity. Yield-to-ultimate strength ratios above 0.95 have been observed in steels irradiated to 7×10^{18} neutrons/cm^2 ($E > 1$ Mev) at less than 400°F. Irradiation to greater than 1×10^{20} neutrons/cm^2 was required to reach a ratio of 0.95 when the exposure temperature was 550°F. Ductility parameters generally are decreased by irradiation. The uniform elogation (strain prior to onset of "necking") is decreased most rapidly, with lesser decreases in total elongation and reduction of area. Significant decreases in reduction of area generally occur only at very high neutron doses. Irradiation decreases the rate of work hardening at a given strain[136] and the value of the work-hardening exponent.[137]

These changes due to radiation are illustrated by the stress-strain curves of Figs. 5.4 and 5.5 (from Ref. 138). A case may be noted in Fig. 5.5 where at high neutron doses the material exhibited little or no plastic strain prior to necking (localized deformation). This phenomenon has been observed only for high neutron doses and relatively low exposure temperatures.

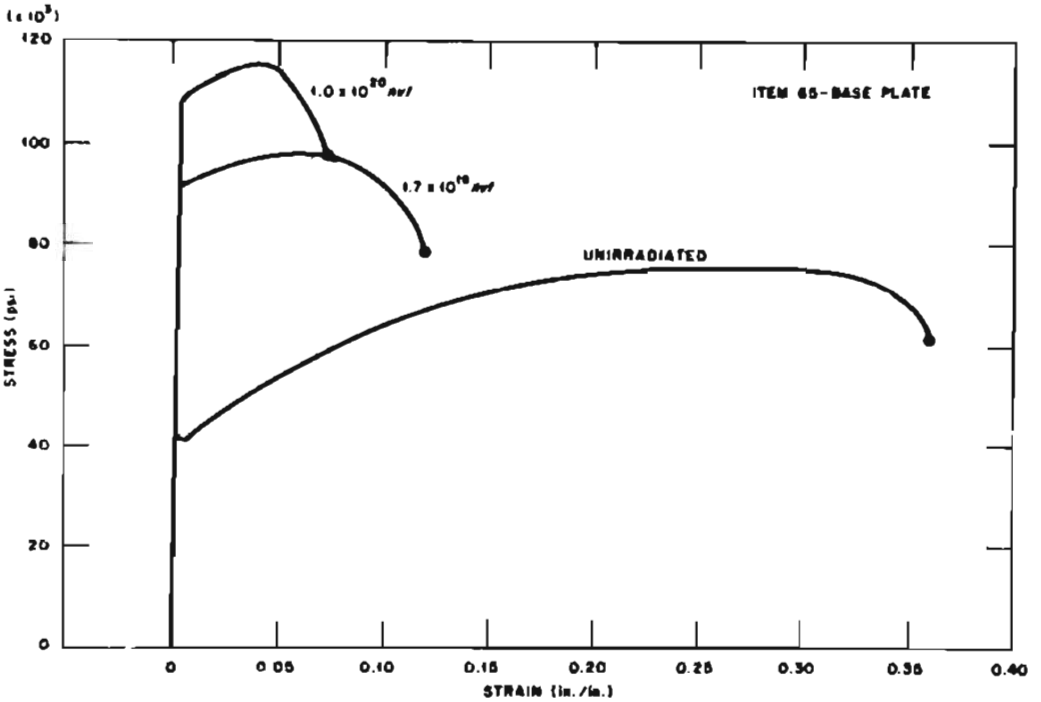

Fig. 5.4. Stress-Strain Behavior of an Irradiated ASTM A 212 Grade B Carbon-Silicon Steel. (From Ref. 138)

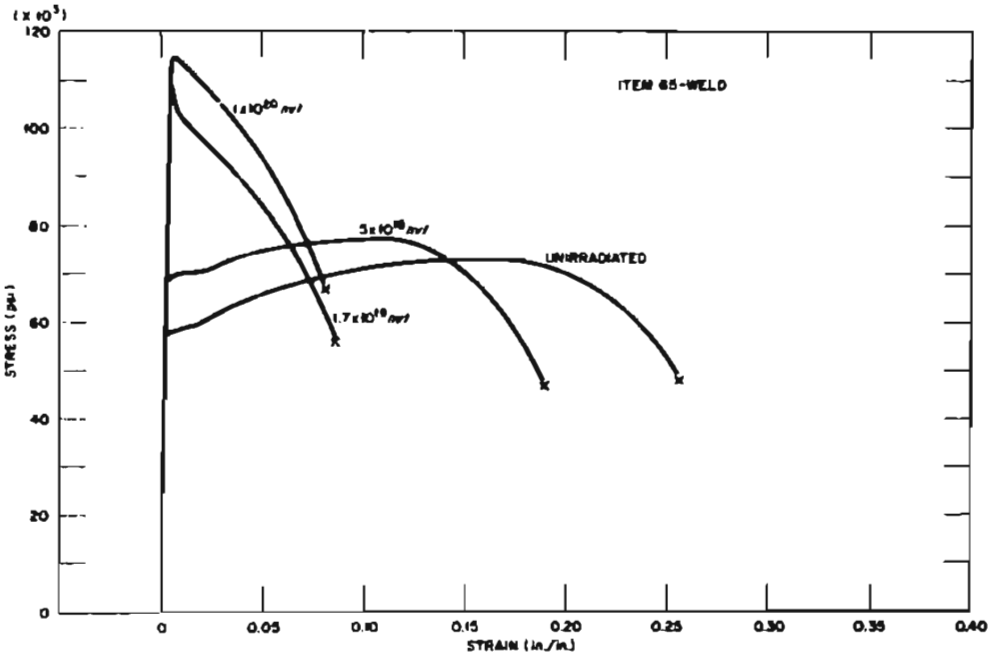

Fig. 5.5. Stress-Strain Behavior of Irradiated E 7016 Weld Metal. (From Ref. 138)

Typical increases of yield strength are shown in Fig. 5.6 for several commerical alloys irradiated at temperatures below 500°F. Factors that influence this and other changes in tensile properties are discussed in Section 5.4.2.

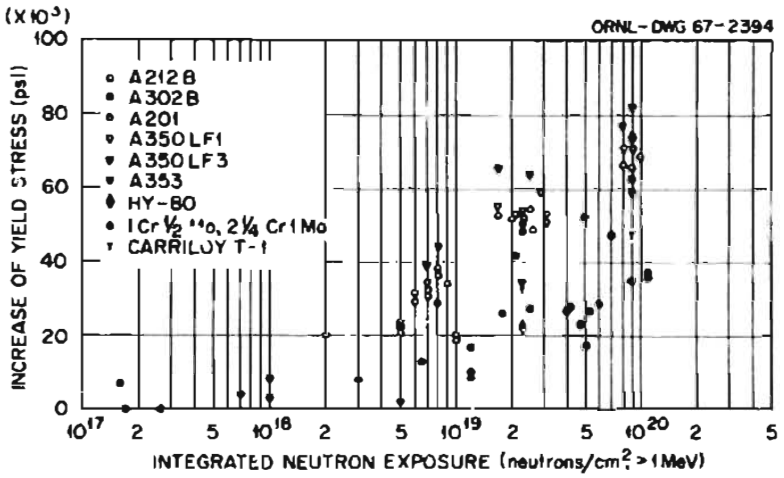

Fig. 5.6. Yield Stress Increases of Steels Irradiated at Less Than 500°F.

5.4.1.2 Notch-Impact Strength

The brittle failure of large steel structures is a problem that has attracted the attention of engineers and scientists to an ever-increasing extent in the past two decades. The dramatic failures of a number of merchant ships, bridges, pressure vessels, pipelines, and storage tanks by brittle fracture have been widely discussed.[139-142] The investigations and analyses that followed these incidents showed that the origins of the failures lay in the tendency of a broad class of metals and alloys to exhibit low-temperature brittleness. This tendency is increased as a result of exposure to radiation, and hence the possible embrittlement of reactor pressure vessels in service has been a matter of concern from the standpoint of nuclear safety.

This radiation-embrittlement phenomenon is manifested, arong other ways, by a shift in the brittle-to-ductile transition, or nil ductility transition (NDT), temperature. Data with which to factor the NDT temperature shift into design considerations with a high degree of confidence

have not been established. What have been commonly used in predicting this shift as a function of integrated neutron exposure are compilations of experimental results obtained for a wide variety of conditions.

The temperature at which the ductile-to-brittle transition takes place is not an inherent constant of the material. Instead, the ductile-to-brittle transition temperature depends upon the type of test used to measure it and the specimen geometry. The transition temperature usually increases with the loading rate of the test and the triaxiality of the stress state to which the sample is subjected. Many tests have been devised to evaluate the ductile-to-brittle characteristics of metals, but the Charpy V-notch impact test has been used in most of the studies of radiation effects. Most of the other test methods require specimens that are too large to be practical for exposure in a nuclear reactor. The transition temperature measured by the Charpy V-notch impact test has been correlated with service performance in a number of cases.[143] The following discussion is therefore based on Charpy V-notch impact tests of irradiated steels.

The changes in Charpy V-notch impact test behavior produced by fast-neutron irradiation are illustrated in Fig. 5.7 (from Ref. 138). If a 20 ft-lb fracture energy is chosen as the transition temperature criterion (a reasonable value for this steel), it is found that neutron irradiation gradually increases the transition temperature from 50°F to about 400°F. There is also a decrease of ductile fracture energy from 70 to 30 ft-lb. The magnitudes of these two radiation effects depend upon integrated fast-neutron dose, neutron energy spectrum, exposure temperature, material composition, heat treatment, and possibly neutron flux. The influence of these factors on observed radiation effects is discussed in Section 5.4.2. Data on Charpy V-notch transition temperature shifts for a variety of steels irradiated at less than 500°F is presented in Fig. 5.8. The increases of transition temperature with increasing neutron exposure are apparent as ar the variations of radiation sensitivity for different steels and even for steels of the same grade.

Several methods are used to apply the available data on radiation-induced transition temperature shifts to nuclear pressure vessel operation.

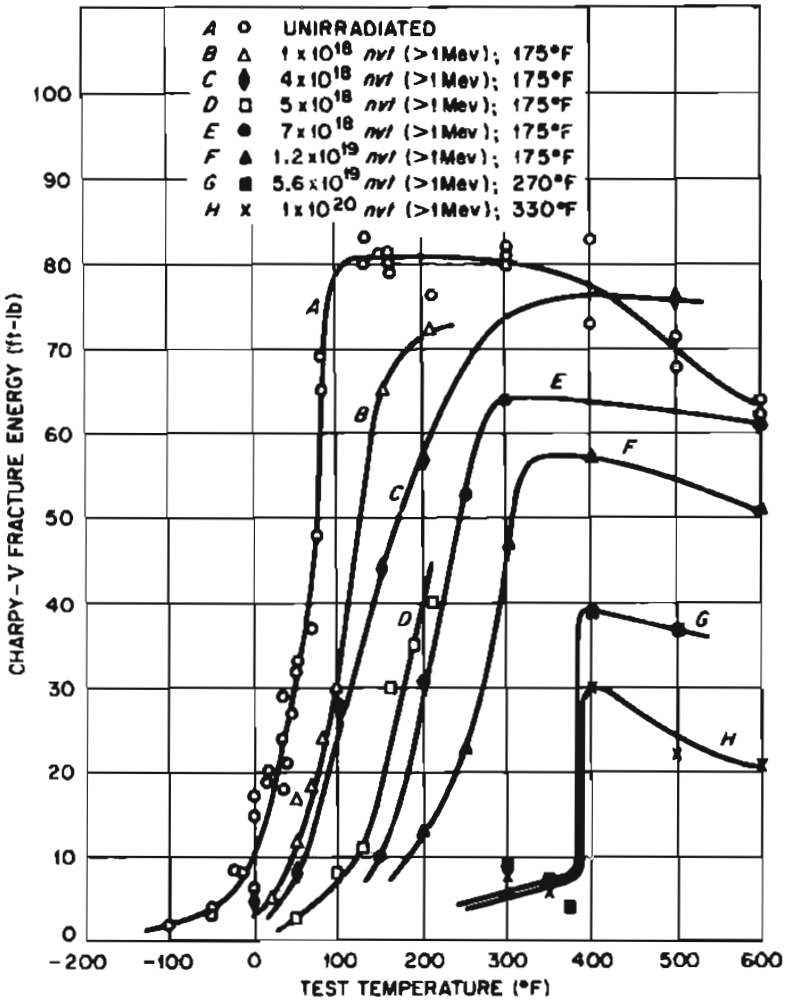

Fig. 5.7. Charpy V-Notch Impact Test Behavior of an Irradiated ASTM A 285 Grade A Carbon Steel (Normalized). (From Ref. 138)

The simplest method is to use the upper bound of all the experimental results to establish operating limits for the pressure vessel. Some advantage may be gained by using the upper bound of experimental results for the particular grade of steel used for the pressure vessel and for the operating temperature of the pressure vessel. If irradiation data are available for the heats of steel, heat treatments, and temperature of irradiation that correspond exactly to the particular pressure vessel, these data may be used to establish operating limits for the reactor. Finally, samples corresponding exactly to the pressure vessel are irradiated near the pressure vessel wall of the particular reactor. This last method is

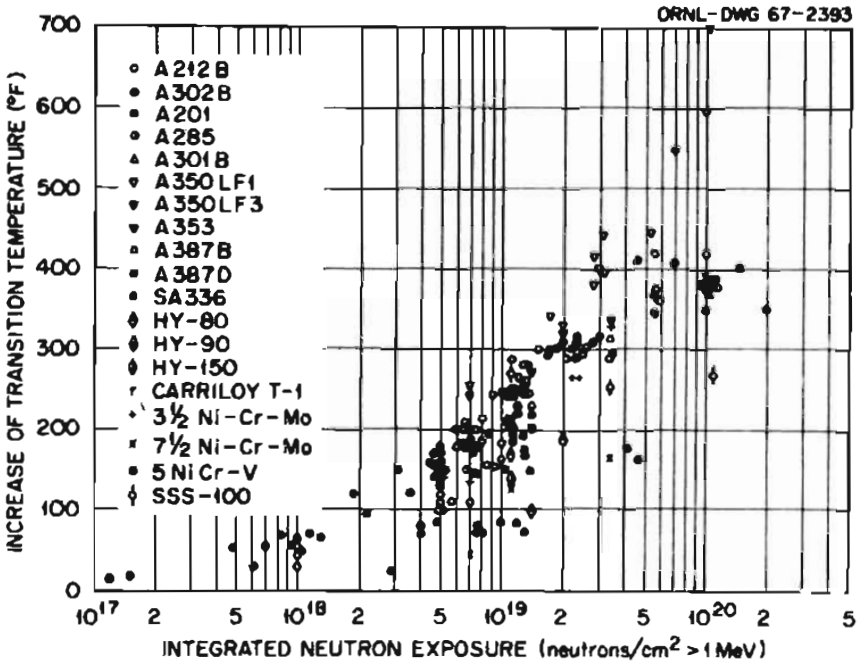

Fig. 5.8. Charpy V-Notch Transition Temperature Increases of Steels Irradiated at Less Than 500°F.

termed "surveillance" testing; it eliminates most of the uncertainties inherent in the other methods. One drawback of surveillance testing is that the data are available only after a considerable period of operation of the reactor.

Accompanying the upward shift in transition temperature is a decrease in the ductile-fracture energy above the transition region (Fig. 5.7). This radiation effect has received some attention in the literature. Pellini and his co-workers[144] have discussed the implications of low-energy ductile tearing, but Charpy energy requirements for prevention of ductile tearing as a mode of pressure vessel failure have not been established. However, the available data on SA 212 grade B and SA 302 grade B steels irradiated at 500°F and above show that fast-neutron (E > 1 Mev) doses approaching 10^{20} neutrons/cm^2 were required to decrease the ductile energy (Charpy V-notch) to about 30 ft-lb. Burghard and Norris[145] have shown a relationship between increase of transition temperature and reduction in Charpy V-notch ductile energy (Fig. 5.9). The application of this information to reactor pressure vessel operation is

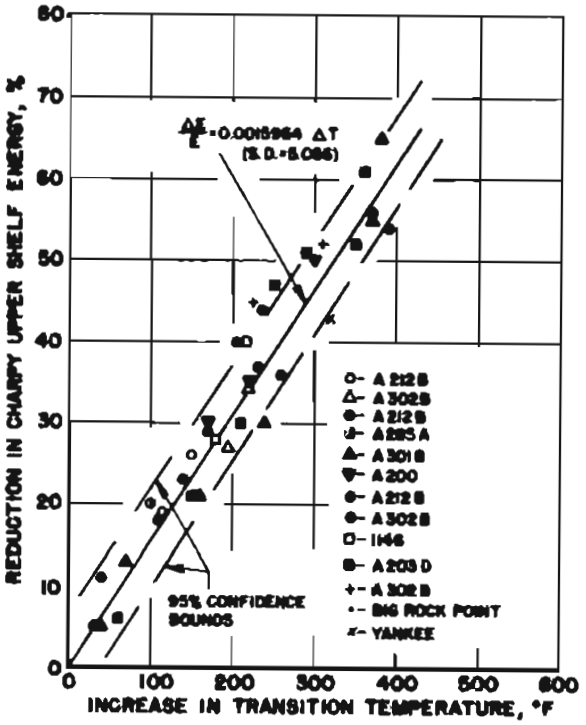

Fig. 5.9. Change in Charpy V-Notch Upper Shelf Fracture Energy as a Function of Shift in Transition Temperature. (From Ref. 145)

presently of dubious merit, primarily because acceptable criteria are not established.

The safety analyses of many nuclear pressure vessels are based on the Fracture Analysis Diagram (see Chap. 7). A major parameter in this analysis is the nil-ductility transition (NDT) temperature of the steel as experimentally determined by the drop-weight test. However, most radiation effects data on notch ductility have been obtained from Charpy V-notch impact tests. The Charpy V-notch transition temperature can be correlated with the drop weight NDT temperature for unirradiated steels.[146] Hawthorne and Steele[147-149] demonstrated a 1:1 correlation of radiation-induced transition temperature increases for Charpy V-notch impact tests and drop-weight tests. The study included eleven materials, irradiation temperatures from 200 to 600°F, and integrated fast-neutron doses from 3×10^{18} to 5×10^{19} neutrons/cm^2. The variance in this correlation was only ±20°F.

5.4.1.3 Fracture Mechanics

In the design of nuclear reactor pressure vessels, one of the modes of failure that must be considered is brittle fracture. One method of insuring against brittle fracture is the imposition of regulations based on a ductile-to-brittle transition temperature. However, there are limitations to the application of transition temperature concepts to large heavy-section structures such as nuclear reactor pressure vessels, and there is a real need for more quantitative methods that can be incorporated into design procedures. The approach known as fracture mechanics has received the most attention by theoreticians, experimentalists, and designers. Considerable success has been achieved with this approach for structures built of materials with low ductility. The present difficulties of applying these methods to the design of structures that will be fabricated of relatively ductile materials are discussed in Chapter 7 of this report.

Studies are presently under way on the determination of the effects of neutron irradiation on fracture mechanics properties of pressure vessel steels. In studies at the U.S. Naval Research Laboratory, single edge-notch (SEN) specimens are used. Studies with double cantilever beam (DCB) specimens with side grooves are in progress at the Pacific Northwest Laboratories of Battelle Memorial Institute. The Westinghouse Atomic Power Division and Bettis Plant are using wedge-opening loaded (WOL) specimens in similar studies. The only results that have been reported in the unclassified literature are data from the Bettis Plant.[150-151]

The results reported from Bettis[150,151] were obtained from WOL specimens of ASTM A 302 grade B steel containing "precompressed notches." Figure 5.10, from Johnson and Pasierb,[150] shows decreases in plane-strain fracture toughness (K_{IC}) resulting from fast-neutron irradiation. Alternatively, the data show increases in test temperature required for a given value of plane-strain fracture toughness as a result of fast-neutron irradiation. These authors also reported Charpy transition temperatures (V-notch, 30 ft-lb) for the same steels at equivalent neutron dosages. These data indicate that "the temperature shift at a low level of K_{IC} and the temperature shift at a low level of absorbed Charpy energy (30 ft-lb) correspond closely."[151] Results from fracture mechanics studies of

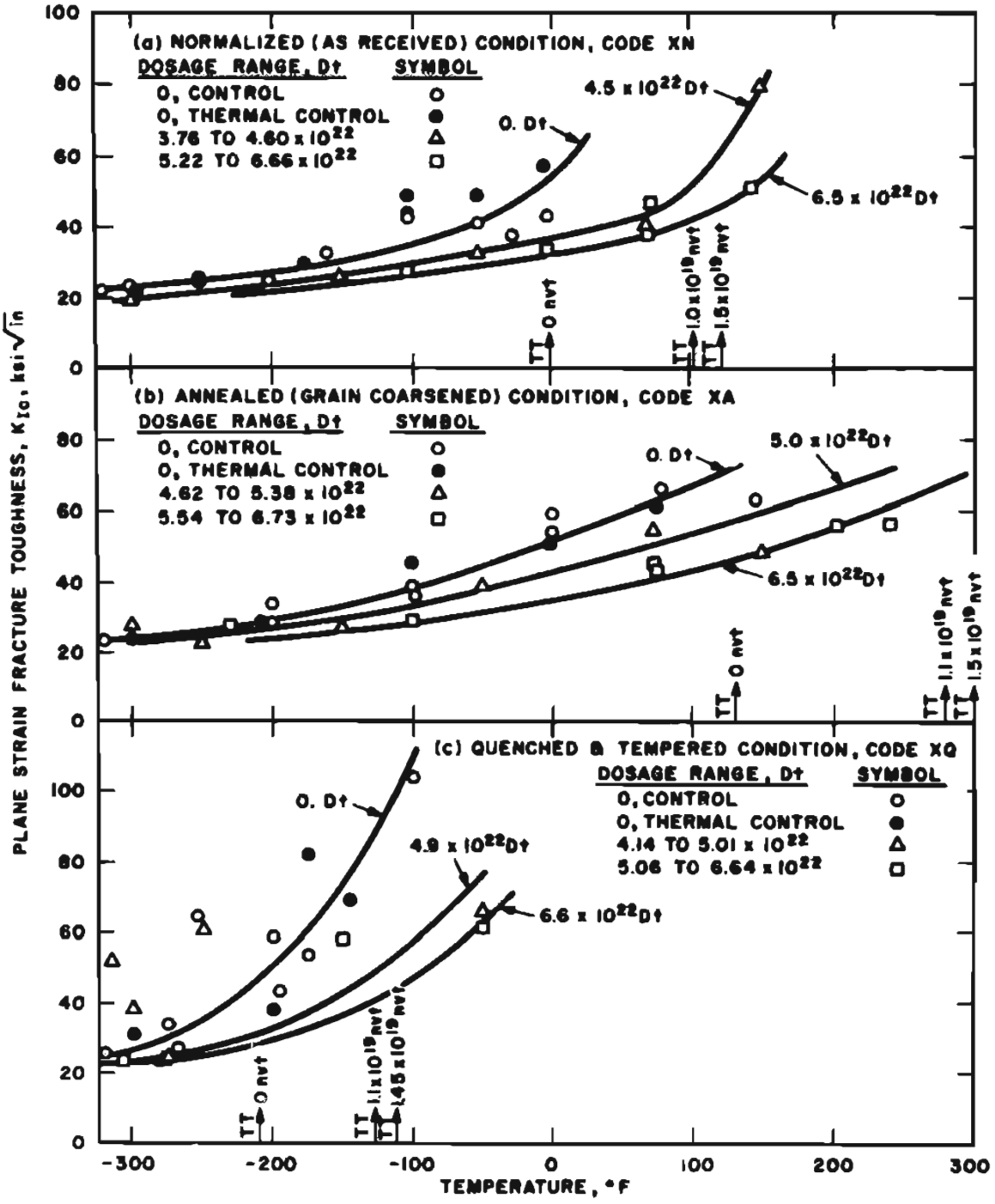

Fig. 5.10. Fracture Toughness as a Function of Test Temperature for Three Conditions of A 302 Grade B Steel Showing Radiation-Induced Changes and Charpy Transition Temperatures at Equivalent Integrated Neutron Exposures. (From Ref. 150)

irradiated steels with fatigue-cracked WOL and SEN specimens should be available in the near future.

The increasing activity in the measurement of plane-strain fracture toughness of irradiated steels coupled with anticipated improvements and extensions of fracture mechanics methods to more ductile steels may provide more quantitative design and analysis procedures for insuring against catastrophic brittle failure of nuclear reactor pressure vessels.

5.4.1.4 Fatigue Strength

The phenomenon of fatigue cracking and failure of metals must be considered in many structures and components, including nuclear reactor pressure vessels. The ASME Boiler and Pressure Vessel Code, Section III,[152] incorporates specific methods of fatigue analysis in which test data for unirradiated steels are used. The specified methods are based on strain-controlled fatigue data. While a considerable body of strain-controlled fatigue data is available for unirradiated pressure vessel steels, only limited data are available on irradiated pressure vessel steels.

In unirradiated steels the high-cycle fatigue strength is related to tensile strength (higher tensile strength materials have higher fatigue strength), and low-cycle fatigue strength is governed by ductility (higher ductility materials have higher fatigue strengths in this range where plastic flow occurs during each fatigue cycle). Since neutron irradiation of steels increases yield and tensile strengths and decreases ductilities, it would be expected that fatigue strengths would be increased in the high-cycle range and decreased in the low-cycle range. In 1956, Leeser[153] reported the results of postirradiation constant-deflection plate-bending fatigue tests on ASTM A 212 steel irradiated to a fast-neutron dose of 1×10^{19} neutrons/cm^2 at 70 to 140°F. He reported a 10% decrease in the unnotched fatigue-endurance limit and a 25% increase in the notched fatigue-endurance limit. The notch-effect factor, K_f (ratio of endurance limits, unnotched to notched), decreased from 1.7 to 1.2 as a result of irradiation.

In 1966, Gibbons, Mikoleit, and O'Donnell[154] reported the results of postirradiation strain-controlled axial fatigue tests on unnotched and

notched specimens of two heats of ASTM A 302 grade B and one heat of ASTM A 212 grade B steels. The specimens were irradiated at 450 to 470°F to fast-neutron (E > 1 Mev) doses of 3.47 to 7.0 × 10^{19} neutrons/cm^2. Their results for unnotched specimens are shown in Figs. 5.11, 5.12, and 5.13. There was no apparent effect of irradiation on the fatigue life of the A 302 grade B heat 21485 material. This was the heat that had been classified as "radiation sensitive" on the basis of Charpy impact tests.[155] There is considerable scatter in the fatigue data for the A 302 grade B heat A-1303 material. However, the fatigue strengths for irradiated specimens generally were lower than those for unirradiated specimens. This heat had been classified as "radiation insensitive" on the basis of Charpy impact tests.[155] The fatigue data for the A 212 grade B steel

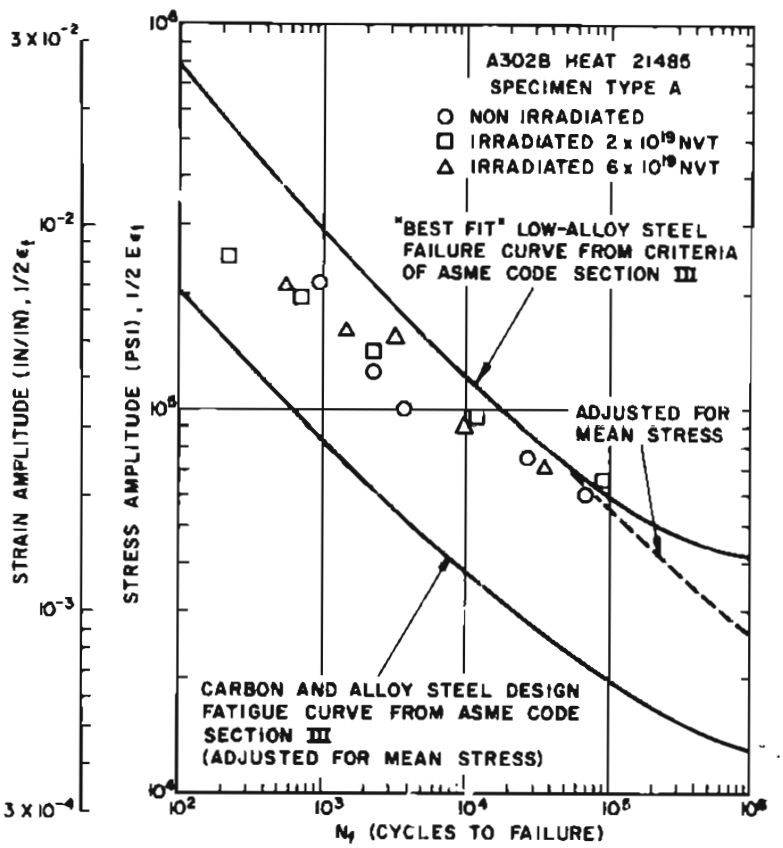

Fig. 5.11. Fatigue-Failure Data for A 302 Grade B Heat 21485 Steel Compared with ASME Best-Fit Curve and ASME Section III Design Curve. (From Ref. 154)

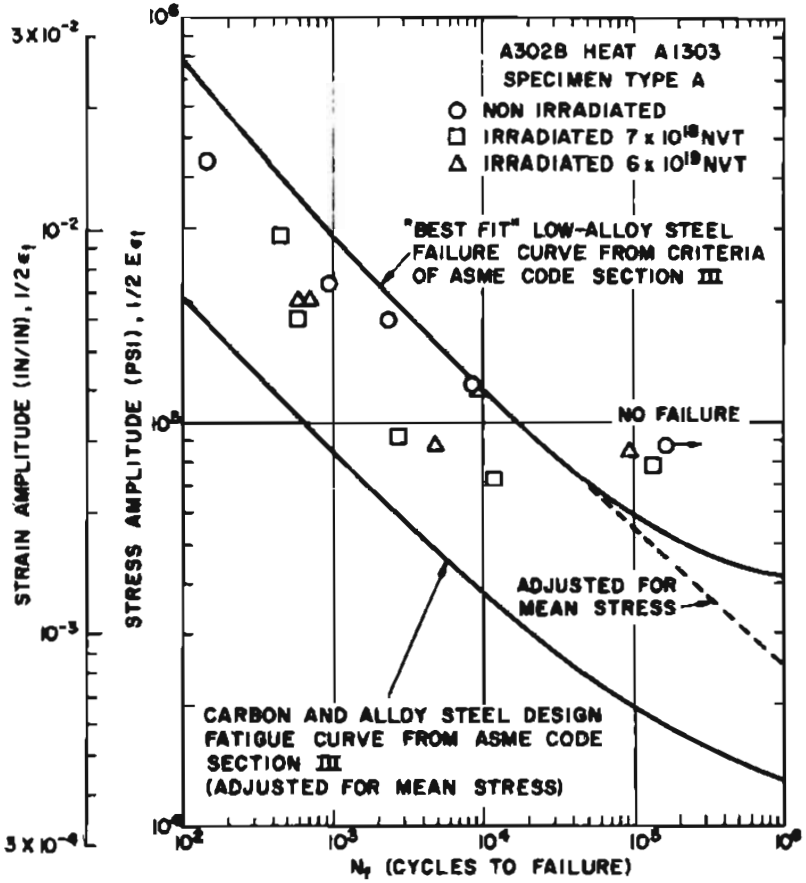

Fig. 5.12. Fatigue-Failure Data for A 302 Grade B Heat A1303 Steel Compared with ASME Best-Fit Curve and ASME Section III Design Curve. (From Ref. 154)

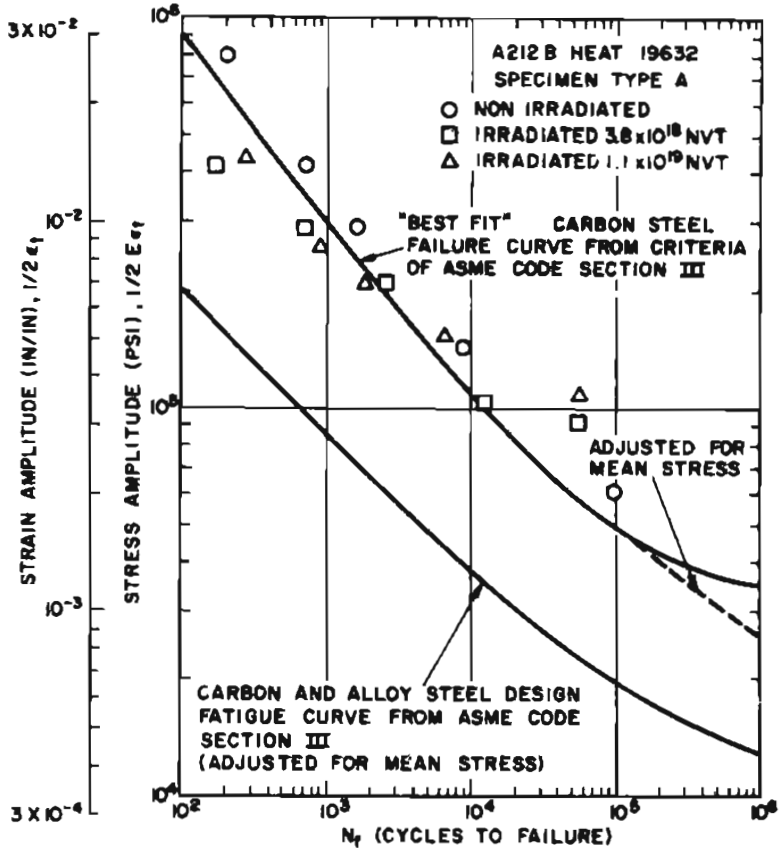

Fig. 5.13. Fatigue-Failure Data for A 212 Grade B Heat 19632 Steel Compared with ASME Best-Fit Curve and ASME Section III Design Curve. (From Ref. 154)

appear to follow the predictions based on strength increase and ductility decrease as a result of irradiation; that is, high-cycle fatigue strength should increase and low-cycle fatigue strength should decrease as a result of irradiation. They did not observe any increase in fatigue notch sensitivity due to irradiation. If there was any change in fatigue notch sensitivity, the data tend to indicate a decrease due to irradiation.

Hawthorne and his co-workers[156-159] have reported the results of controlled-strain beam-bending fatigue tests conducted during irradiation at 500 and 550°F of A 212 grade B and A 302 grade B steels. The results of in-reactor fatigue tests on material from a 6-in. A 302 grade B plate (550°F tests) and a 3-in. A 302 grade B plate (550°F test) show no difference in fatigue strength due to irradiation. However, in-reactor fatigue tests at 500°F (Fig. 5.14) show an increase in high-cycle (>10^4 cycles) fatigue strength of A 212 grade B steel due to irradiation, as predicted. Their data on A 212 grade B steel for fatigue lives of 10^3 to 10^4 cycles (Fig. 5.15) indicate an increased fatigue strength for in-reactor tests. The irradiation history for this latter group of tests was different from that for Fig. 5.14, and this difference may explain the disagreement between the data in the two sets of tests in the region of 10^4 cycles. These data do not extend into the low-cycle region far enough to observe the lowering of fatigue strength predicted on the basis of decreased ductility due to irradiation.

On the basis of the small body of data available on fatigue properties of irradiated pressure vessel steels, the radiation-induced changes in fatigue strength or life tend to be rather small, and in no case has the observed fatigue life been less than three times the allowable design life permitted by the Code.[152] However, the data are not conclusive and additional study appears warranted. One particular area of ignorance is the effect of irradiation on fatigue-crack growth rates. Such information is necessary for predicting the growth of fatigue cracks from preexisting defects, as well as the initiation and growth of fatigue cracks.

5.4.1.5 Creep Properties

There are no reported data on the creep or stress relaxation properties of pressure vessel steels for the temperature range in which

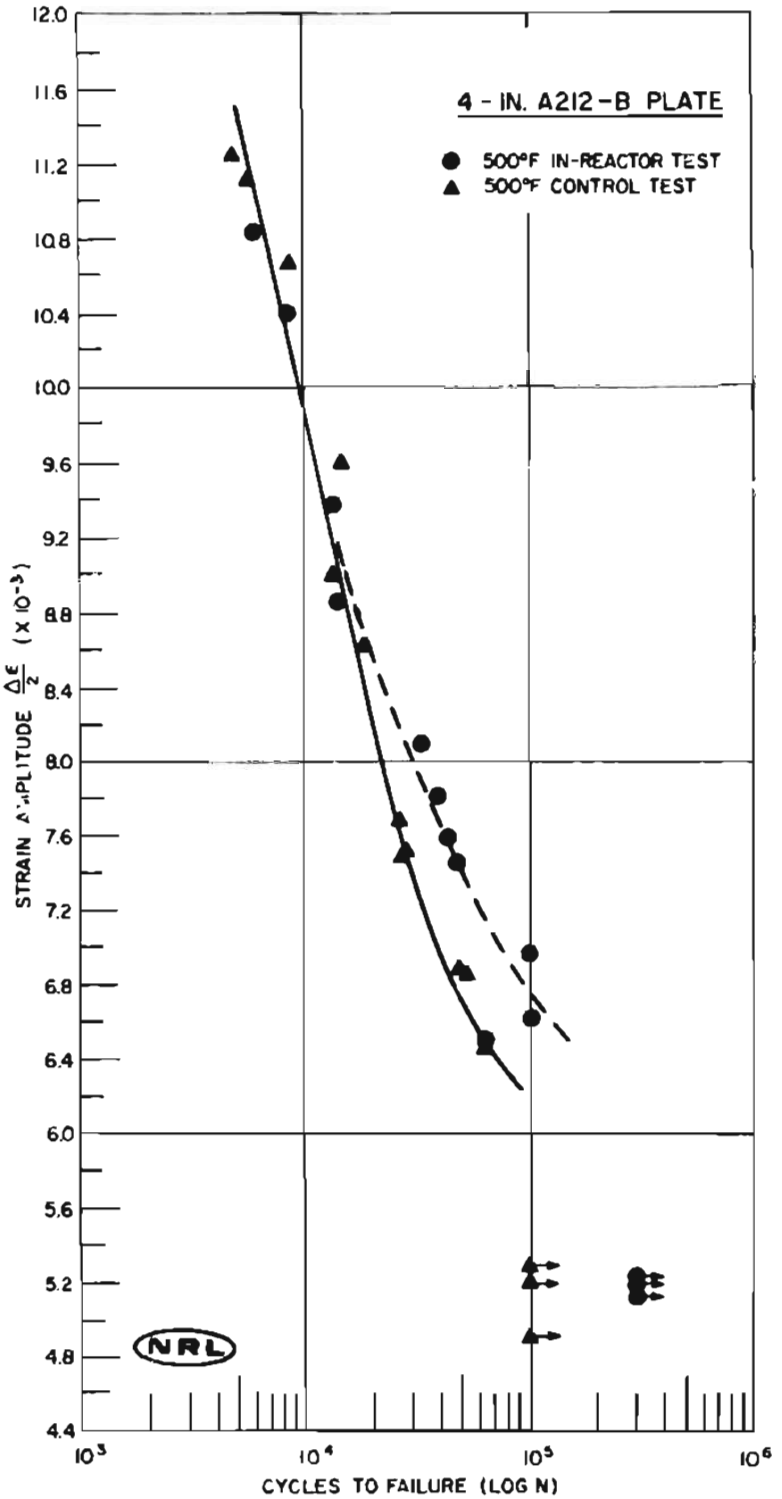

Fig. 5.14. Comparison of 500°F Fatigue Data for A 212 Grade B Steel Developed by In-Reactor Tests with Results of Tests on Unirradiated Material. (From Ref. 159)

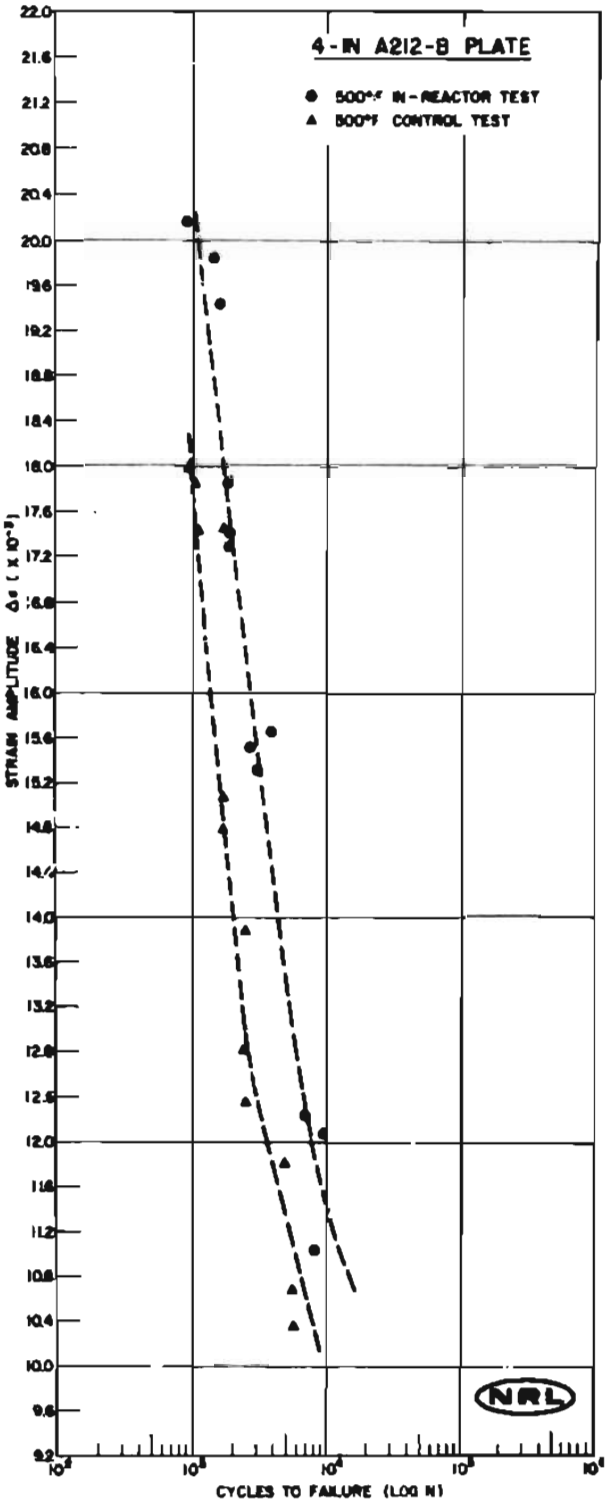

Fig. 5.15. Comparison of 500°F Fatigue Data for A 212 Grade B Steel Developed by In-Reactor Tests with Results of Tests on Unirradiated Material. (From Ref. 159)

water-cooled nuclear reactor pressure vessels operate (400 to 600°F). This situation is readily understandable for several reasons. First, creep, creep rupture, and stress relaxation are observable in unirradiated steels only at temperatures several hundreds of degrees above this range or at stresses considerably higher than exist in these pressure vessels. Further, in this low-temperature range, creep and stress relaxation are governed by yield or flow stress. Since yield and flow stresses are increased by irradiation at these temperatures, it follows that creep and stress relaxation rates should be lower in irradiated steels than in unirradiated steels. Also, creep ductility could, in view of decreased tensile ductility, decrease as a result of irradiation. However, the magnitude of tensile ductility changes does not indicate any problem of creep rupture of reactor pressure vessels at operating conditions.[160]

5.4.2 Critical Factors

A number of factors influence the mechanical-property changes resulting from irradiation of metals. Attempts to isolate these factors and obtain general relationships have been largely unsuccessful. Material parameters, such as composition and metallurgical structure, and exposure parameters, such as time-integrated fast-neutron flux and temperature, are all interrelated. In addition the relationships between flow and fracture properties are not thoroughly understood for unirradiated steels. For these reasons, the study of radiation effects is a very complex endeavor. The information on the influence of the various factors in radiation effects is largely empirical, even though there are theoretical bases for interpretation of many of the effects.

5.4.2.1 Integrated Fast-Neutron Flux (Dose)

It was realized at an early stage of radiation effects studies that radiation-induced changes in mechanical properties were not linear functions of the time-integrated neutron flux (also called dose or fluence). The precise relationships of the increases in tensile yield strength and ductile-to-brittle transition temperature with neutron dose have been and still are the subject of some discussion. However, for the range

of neutron doses of interest with respect to commercial power reactor pressure vessels, the various proposed relationships predict nearly the same property changes.

Cottrell[161] originally predicted, on theoretical and experimental bases, that the change in yield stress ($\Delta\sigma_y$) of a mild steel was proportional to the cube root of the integrated neutron flux (ϕt):

$$\Delta\sigma_y = 8.0(\phi t)^{1/3} ,$$

where $\Delta\sigma_y$ is in units of 1000 psi and ϕt in units of 10^{18} neutrons/cm^2. By using this in combination with his theoretical relationship between $\Delta\sigma_y$ and the increase in transition temperature (ΔTT), Cottrell obtained

$$\Delta TT = 17.5(\phi t)^{1/3} ,$$

where ΔTT is in °C. The coefficients 8.0 and 17.5 represented the best average fit to several data points but could vary considerably with irradiation temperature and material. Cottrell's relationship was also found to lead to considerable error at large doses (>10^{20} neutrons/cm^2).

Makin and his co-workers[162,163] have shown theoretically that the increase of yield stress produced during the early stages of irradiation is proportional to the square root of the integrated neutron flux:

$$\Delta\sigma = A(\phi t)^{1/2} .$$

However, as the integrated neutron flux is increased, they predicted a saturation effect and suggested the expression

$$\Delta\sigma = A\left[1 - e^{-B(\phi t)}\right]^{1/2} .$$

This relationship has been experimentally confirmed for lithium fluoride[162] and for copper.[163] They found that the available data on nickel[163] did not permit an unequivocal choice between these expressions.

Nichols and Harries[164] found that their data on irradiated carbon steel best fit the square-root expression

$$\Delta TT = A(\phi t)^{1/2} .$$

Their data apparently did not extend to high enough integrated neutron fluxes to observe a saturation effect.

In 1960, Steele,[165] Hawthorne,[147] and Berggren[166] proposed a semilogarithmic relationship,

$$\Delta TT = A + B \log (\phi t) ,$$

in the range of 3×10^{18} to 3×10^{19} neutrons/cm^2 ($E > 1$ Mev). This was an empirical relationship based on the available data. Much of the later work has been compared with this expression.

Carpenter, Knopf, and Byron[155] found that their data best fitted a semilogarithmic quadratic expression:

$$\Delta TT = a + b \log (\phi t) + c(\log \phi t)^2 .$$

The additional term in this expression permits a better fit to experimental data than obtained with the linear logarithmic expression. This is particularly true for integrated neutron fluxes below 3×10^{18} neutrons/cm^2. Both logarithmic expressions are empirical and have no known physical basis.

As mentioned earlier, any of these expressions may be used in the dose range of interest to commercial water-cooled power reactor pressure vessels, since the constants in these expressions must presently be experimentally determined for the specific material, material condition, exposure temperature, and neutron spectrum involved.

5.4.2.2 Neutron Flux

Research groups studying the effects of neutron irradiation on mechanical properties of pressure vessel steels have conducted most of their studies in neutron fluxes several orders of magnitude greater than those to which reactor pressure vessels are exposed. While the accelerated accumulation of neutron exposure is necessary in order to complete research programs in reasonable time periods, there exist questions regarding the application of the results to prediction of the properties of pressure vessel steels exposed to low long-time neutron fluxes. Theoretical studies have indicated that the neutron-flux (dose rate) and neutron-energy spectrum differences between test reactor facilities and power reactor pressure vessel locations may be of sufficient magnitude to affect the applicability of test reactor program results to power reactor operation. An

interim method of avoiding these problems is the "surveillance program" discussed in Chapter 10.

At least two neutron-flux effects have been postulated for neutron irradiation at power reactor operating temperatures:

1. Annealing of radiation-induced defects will occur during neutron irradiation at elevated temperature. The properties of a steel during and after elevated-temperature irradiation will be the result of the combined damage rates (a function of neutron flux and spectrum) and annealing rate (a function of temperature). Low-flux long-time irradiation at a given temperature should result in lesser radiation effects for a given dose than high-flux short-time irradiation, since there is a greater time for recovery of the defects.

2. If the increased concentration of defects (vacancies and interstitials) during irradiation accelerates metallurgical reactions and the resulting metallurgical changes affect the mechanical properties, low-flux long-time irradiation may result in greater property changes than high-flux short-time irradiation at the same temperature and the same dose.[167]

The study of flux effects has been difficult because reactor facilities providing widely different neutron fluxes usually have quite different neutron spectra. Thus flux and spectrum effects are usually encountered in combination, and separating them is most difficult.

One study has been conducted on flux effects in which the neutron spectrum was constant. Barton, Harries, and Mogford[168] studied the effects of flux and irradiation temperature on the tensile properties of three mild steels (En2 mild steel, an aluminum-containing grain-size-controlled mild steel, and a silicon-killed mild steel). Irradiation temperatures were 212 to 662°F, and the relative neutron fluxes were in the approximate ratios of 1:4:100. These different fluxes were obtained by operating the PLUTO reactor at different power levels. They concluded that while radiation effects are functions of the irradiation temperature and the type of steel, the effects are not significantly dependent on neutron flux in this temperature range. However, the integrated fast-neutron flux in this study was quite low ($\sim 2.5 \times 10^{17}$ neutrons/cm^2, fission), and a part of the reported data might fit postulate 1 above; that

is, it might fit the equivalent damage expression:[168]

$$\frac{1}{T_1} - \frac{1}{T_2} = \frac{k}{e} \ln \frac{\phi_2}{\phi_1} .$$

Hinkle, Smith, and Wechsler[169] observed no flux effect in studies on high-purity iron irradiated at 200°F to doses of 4.6×10^{18} neutrons/cm^2 (E > 1 Mev). The neutron fluxes were varied by more than a factor of 100. Brandt and Alexander[170] could not identify any flux effects in surveillance tests on SA 302 grade B steel irradiated at 545°F in the Dresden reactor. The neutron flux ratios were slightly greater than 2:1 in this study.

Pellini, Steele, and Hawthorne[171] compared the results of irradiation of A 212 grade B, A 302 grade B, and A 350 grade LF-3 in the highly thermalized spectrum of the Brookhaven Graphite Reactor with results obtained in the higher energy spectra of the MTR and LITR. The neutron flux in the Brookhaven Graphite Reactor is about one-tenth that in the LITR and MTR. The observed differences in radiation effects were attributed to spectrum effects, with flux effects considered insignificant.

5.4.2.3 Neutron Spectrum

This section summarizes current practice for comparing radiation damage effects produced in specimens irradiated in different neutron spectra. The basic effect produced by neutron irradiation of a metal is the displacement of an atom from its normal position in the crystal to an abnormal position called an "interstitial" position. This leaves a vacancy or hole at the normal position. Vacancies and interstitials are always produced in equal numbers by neutron irradiations (except possibly in the immediate vicinity of a surface), and the combination is called a Frenkel defect. In very general terms the change in a mechanical property, ΔM (M may represent yield strength, impact strength, etc.), can be expressed as a function of the number and distribution of these elementary defects. However, most investigators have assumed that the property change is a function only of the number of elementary defects. This assumption is made because otherwise the problem becomes too difficult to handle. The

various methods of calculating defect-production rates and methods of using these calculations to correlate experimental results are discussed first below, and then some of the more sophisticated calculations that attempt to account for defect distributions in interpreting mechanical properties are discussed briefly. According to Seitz and Koehler[172] the displacement production rate is given by

$$Nd = n_0 \int_0^\infty G(E)\, f(E)\, dE ,$$

where

n_0 = number of atoms per unit volume,
$f(E)$ = differential neutron flux,
$G(E)$ = displacement cross section for neutrons of energy E.

The problems associated with the determination of f(E) are discussed in Section 3.5, but it is also necessary to discuss in this section the effects of different methods of approximating f(E). Great progress has been made in recent years toward specifying f(E) for different reactor test positions and reactor pressure vessel walls. However, many experimenters like to report damage exposure in terms of neutron flux greater than a fixed energy (usually 1 Mev).

Various methods are used to approximate G(E). These are described briefly below, starting with the simplest methods and proceeding to the more complicated methods.

1. The displacement cross section is assumed to be a step function:

$$G(E) = 0 , \qquad \text{when } E < E_f$$

and

$$G(E) = \text{constant} , \qquad \text{when } E \geq E_f .$$

This description is equivalent to reporting exposures in terms of flux greater than some fixed neutron energy, since this makes

$$Nd = n_0\, G \int_{E_f}^\infty f(E)\, dE .$$

2. The displacement cross section is a step function as in (1), but E_f is determined for each metal of interest so that for a variety of spectra of interest the displacement production calculated by this method is equal to the displacement production calculated by more elaborate methods.[173]

3. The displacement cross section is given by the product of the neutron elastic-scattering cross section, $\sigma_{el}(E)$, and the displacement cross section for the resulting primary knock-on atom of energy T. This is expressed by the equation

$$G(E) = \sigma_{el}(E) \int_{\alpha}^{T_{max}} g\left(\frac{T}{\alpha}\right) \frac{dT}{T_{max}}$$

$$= \sigma_{el}(E)\ 0.561 \left(1 + \frac{T_{max}}{2\alpha}\right), \qquad \text{for } T_{max} \gg \alpha ,$$

where

$T_{max} = \dfrac{4M}{(M+1)^2} E$ = the maximum energy that can be transferred to an atom of mass, M, by a neutron of energy, E,

α = the minimum energy that an atom must receive before it can be displaced from its lattice position (for iron, about 25 ev),

$g\left(\frac{T}{\alpha}\right)$ = number of secondary displacements produced by an atom of energy T.

According to this model,

$$Nd = C \int_{E_d}^{\infty} \sigma_{el}(E) \left[1 + \frac{2M}{(M+1)^2} \frac{E}{\alpha}\right] f(E)\, dE$$

$$= C \int_{E_d}^{\infty} \sigma_{el}(E)\, f(E)\, dE + C' \int_{E_d}^{\infty} \sigma_{el}(E)\, f(E)\, E\, dE ,$$

where E_d is the minimum neutron energy capable of producing a lattice displacement.

This form is similar to that used by Rossin[174-177] as the basis for a radiation damage unit, RDU. In Rossin's formulation the displacement cross section, which he calls σ_{RDU}, is normalized so that

$$\sigma_{RDU}(E)\ f_f(E)\ dE = 1\ ,$$

where $f_f(E)$ is the fission neutron spectrum. Therefore,

$$\sigma_{RDU}(E) = C\ \sigma_{iso}(E)\ E\ ,$$

where C is a constant of normalization and σ_{iso} is the isotropic elastic scattering cross section.

4. The displacement-production model 3 is modified to account for the fact that some of the energy of the primary knock-on atom is lost through electronic processes.[178,179] This process is important only for high-energy atoms, so many investigators ignore this effect. According to the model of Kinchin and Pease,[178] most of the primary knock-on energy above about 45 kev in the case of iron is lost by electronic processes that produce no displacements. Therefore in this model the displacement-production rate will be given by

$$Nd = C' \left[\int_{E_d}^{E_i} \sigma_{el}(E)\ Ef(E)\ dE + \int_{E_i}^{\infty} \sigma_{el}(E)\ f(E)\ dE \right]\ ,$$

where E_i is the neutron energy that produces primary knock-on energy above ionization threshold. For iron, E_i is 0.8 Mev and E_d is about 36 kev.

5. The Displacement Spike Model. It is known from basic damage studies that the interstitials produced by neutron irradiation move around very rapidly at the temperatures of pressure vessel operation. In iron, for instance, it is thought that the interstitials move around with appreciable rates at about −170°C. Therefore for elevated-temperature irradiations, all the interstitials produced will either annihilate vacancies, form clusters, or go to grain boundaries, dislocations, and free surfaces. In view of these considerations the displacement-production models considered above appear unrealistic, and various other suggestions have been made. One model suggests that each primary knock-on above a

certain energy produces a cluster of vacancies that is immobile and interacts with dislocations to produce hardening effects.[180]

6. Computer Studies. More elaborate studies of radiation damage have been made with high-speed computers to simulate the crystal lattice.[181,182] One of the factors considered in studies of this type is channeling of energetic knock-on atoms in relatively open directions in the crystal. Channeling reduces the calculated damage rate compared with that of other models discussed above. Annealing of the damage is also included in this model so that the final defect configuration is calculated. It is necessary to have rather good knowledge about atomic potentials for studies of this type, and the present information is not good enough. Nevertheless, interesting results are being generated by these studies.

7. Thermal-Neutron Damage. The thermal-neutron energy range is usually neglected in radiation damage calculations because, as stated above, a neutron must have about 36 kev of energy to cause displacement of the atoms by direct collision. However, thermal neutrons can also cause lattice displacements by absorption reactions (n,γ; n,α; n,p), and in some cases these can produce appreciable amounts of damage. In the case of iron the neutron-absorption cross section is small, so the n,γ reaction, which produces a mean recoil energy of 389 ev,[183] does not produce significant damage, except in highly moderated reactors.

In certain cases thermal-neutron absorption by impurities can produce significant damage if the impurity atom has a very high absorption cross section and emits a highly energetic decay product. One such case is boron. Meyers[184] has calculated that the disintegration of one atom of ^{10}B in an iron matrix should produce a total of 765 displacements. Thus, for a steel containing 0.003 wt % boron, the $^{10}B(n,\alpha)$ reaction will produce approximately 4.5% of the total damage if the thermal-neutron flux equals the flux above 1 Mev.[184]

Comparisons of the Models. Table 5.1 lists results of calculations by Grounes[185] comparing three different models and showing how each of the models would assess neutron damage produced by exposure in different spectra. The calculated spectra for each position are shown in Fig. 5.16. Each of the different models is normalized so that the relative damage

Table 5.1. Neutron Spectrum Normalized to That of the R4-10 Reactor

Model	Normalized Spectrum				
	R4-10 Reactor	R4-5 Reactor	G1 Reactor	MTR	Fission
1, with E_T = 3 Mev	1.0	1.3	0.9	1.6	1.9
1, with E_T = 0.5 Mev	1.0	0.9	0.9	0.7	0.7
1, with E_T = 0.2 Mev	1.0	0.9	0.8	0.6	0.5
3	1.0	1.0	0.9	0.8	0.7
5	1.0	0.8	1.1	0.4	0.2

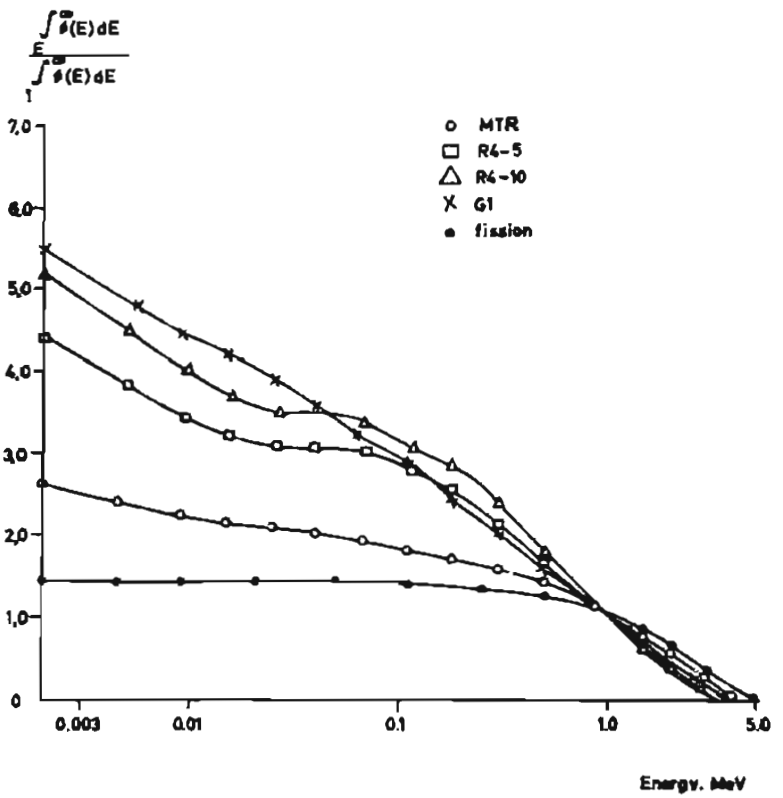

Fig. 5.16. Calculated Neutron Spectra for Table 5.1 Comparison. (From Ref. 185)

for the R4-10 spectrum is one. The spectrum for G1 (French graphite reactor) is the softest. The table shows that if specimens were irradiated in a test reactor, MTR, and an extrapolation was made to determine the expected damage in a highly moderated flux, such as that of the G1, the results could differ by as much as a factor of about 3, depending upon which models were selected. Thus, it is apparent that the model used to describe radiation damage is very important. The differences can be even bigger than a factor of 3 when other factors such as thermal-neutron damage are taken into account.

Attempts to Compare Models with Experiments. A number of investigators have attempted to determine which model is best suited for describing the radiation damage by comparing experimental measurements of mechanical properties on specimens irradiated in different reactor spectra (Refs. 143, 173, 175–177, 182, 185–190). These attempts have not been very successful for the following reasons:

1. The spectra used for the comparison irradiations usually are not different enough to produce effects clearly outside the experimental scatter.

2. The functional dependence of yield stress or ductile-to-brittle transition temperature on radiation damage is not known, so it is difficult to compare different models in a meaningful way.

3. The number of data points having all variables but neutron spectrum constant is quite limited.

Summary. At the present time the radiation damage suffered by a particular steel in a given neutron spectrum in a given exposure time can probably be predicted within a factor of about 3 by comparisons with data obtained on specimens of an identical steel irradiated in a very different spectrum. Much progress has been made toward defining the neutron spectra in various reactor facilities, but more information about the nature of the damage produced must be obtained. Computer studies of radiation damage show much promise, but more basic information about interatomic potentials and interactions of defects in metals is required for input to these programs.

5.4.2.4 Exposure Temperature

Radiation-induced mechanical property changes are temperature dependent. At moderately elevated temperatures many of the defects caused by radiation are mobile, and annealing of the radiation effects may occur. Vacancies are mobile at the operating temperatures of nuclear power reactor pressure vessels and will diffuse to dislocations, grain boundaries, and inclusions or will coalesce to form larger lattice defects. In addition, the larger defects will grow by vacancy diffusion at the expense of the smaller defects, and the total effect can be strikingly similar to aging and overaging in a precipitation-hardenable alloy. The temperatures at which the major portion of radiation-induced mechanical property changes are annealed or recovered are generally lower than for recovery of cold work. In fact, the temperature range for the recovery of the major portion of radiation effects is also the temperature range in which most commercial water-cooled nuclear pressure vessels operate. Thus, radiation damage and at least partial recovery of the effects occur simultaneously in the nuclear pressure vessel. This combination of effects has been observed and studied both in accelerated irradiations in test reactors and in surveillance programs. Figure 5.17 presents the available data on ductile-to-brittle transition temperature shift for several irradiation temperature ranges. The upper bounds of the transition temperature shifts for these exposure temperature ranges decrease markedly between 500 and 600°F. The difference between the upper and lower bounds for the data (at about 3×10^{19} neutrons/cm^2) is about 170°F for irradiation at less than 450°F, 240°F between 450 and 500°F, and 270°F above 500°F. In fact, above a 500°F exposure temperature, one steel showed negligible shift (40°F) at 5×10^{19} neutrons/cm^2. This manner of presentation appears to indicate a very broad temperature range for simultaneous radiation damage and recovery. If the relationship of exposure temperature and transition temperature shift for a given heat of steel is examined, Fig. 5.18 (from Ref. 191), a relatively narrow temperature range is found for "simultaneous recovery" of radiation effects. Other steels or heat treatments will exhibit lower, higher, or wider temperature ranges for "simultaneous recovery."

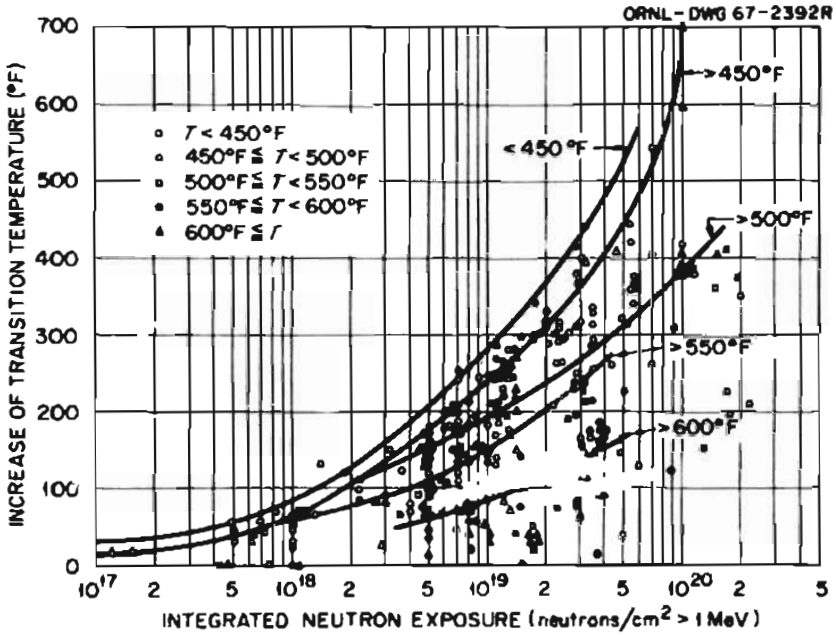

Fig. 5.17. Effect of Irradiation Temperature on Increase of Charpy V-Notch Transition Temperature.

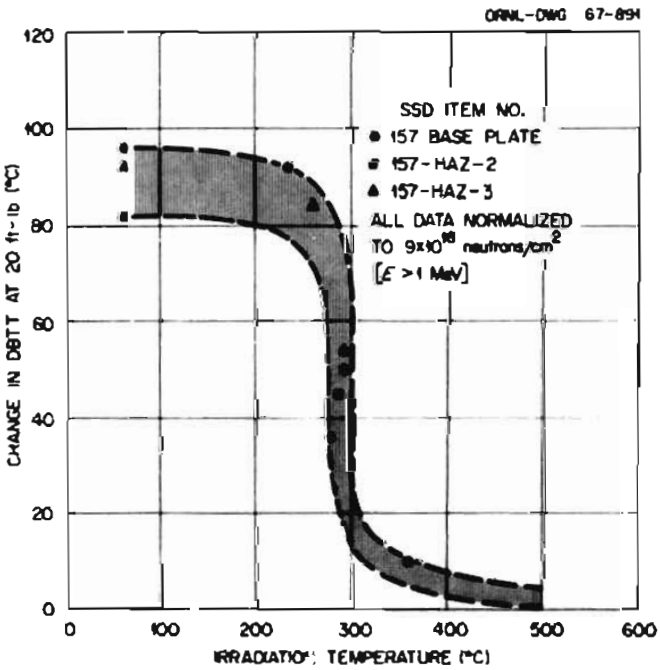

Fig. 5.18. Effect of Irradiation Temperature on Charpy V-Notch Transition Temperature Increase of ASTM A 212 Grade B Steel, Heat A-2056. (From Ref. 191)

The effects of irradiation of a specific alloy at a given exposure temperature can, at present, be determined only by irradiation tests. There is some evidence that radiation-induced changes of tensile properties are related to changes of transition temperature and, further, that temperatures for "simultaneous recovery" of tensile properties and transition temperature are also related. However, some studies[166,192] have shown that tensile properties and transition temperature do not always recover at the same temperatures. Yield and tensile strength recovery may require exposure temperatures 100°F higher than transition temperature recovery.

5.4.2.5 Materials

A number of studies have been conducted that attempted to determine the roles of composition, metallurgical structure, and heat treatment in radiation effects. Carpenter, Knopf, and Byron[155] observed widely different "radiation sensitivities" for various heats of A 302 grade B steel, Fig. 5.19. They could reach no conclusions on the effects of composition variables but did note that the two "sensitive" heats had "large-grained ferrite-bainite structures exhibiting some banding." The insensitive heats had "fine-grained structures principally of ferrite and tempered lower bainite." Further intensive study of these heats[193] was not able to isolate or evaluate the specific influence of composition variables. The influence of gross metallurgical structure differences was corroborated. In the unirradiated condition the sensitive heats exhibited significantly lower yield strength; lower friction stress, σ_i; higher grain-boundary resistance, k_y; and higher transition temperatures than did the insensitive heats. (The classical expression: $\sigma_y = \sigma_i + k_y d^{-1/2}$, was employed in this study.) The irradiation temperatures were 450 to 520°F, and the observed differences of radiation sensitivity may be attributed to differences of "simultaneous recovery" temperature for the different materials.

Steele, Hawthorne, and Gray[194] studied a variety of medium- and high-strength steels. Their results are summarized in Fig. 5.20. They concluded that (1) the higher strength steels exhibit a general trend toward lower initial NDT; (2) along with higher strength and lower initial NDT,

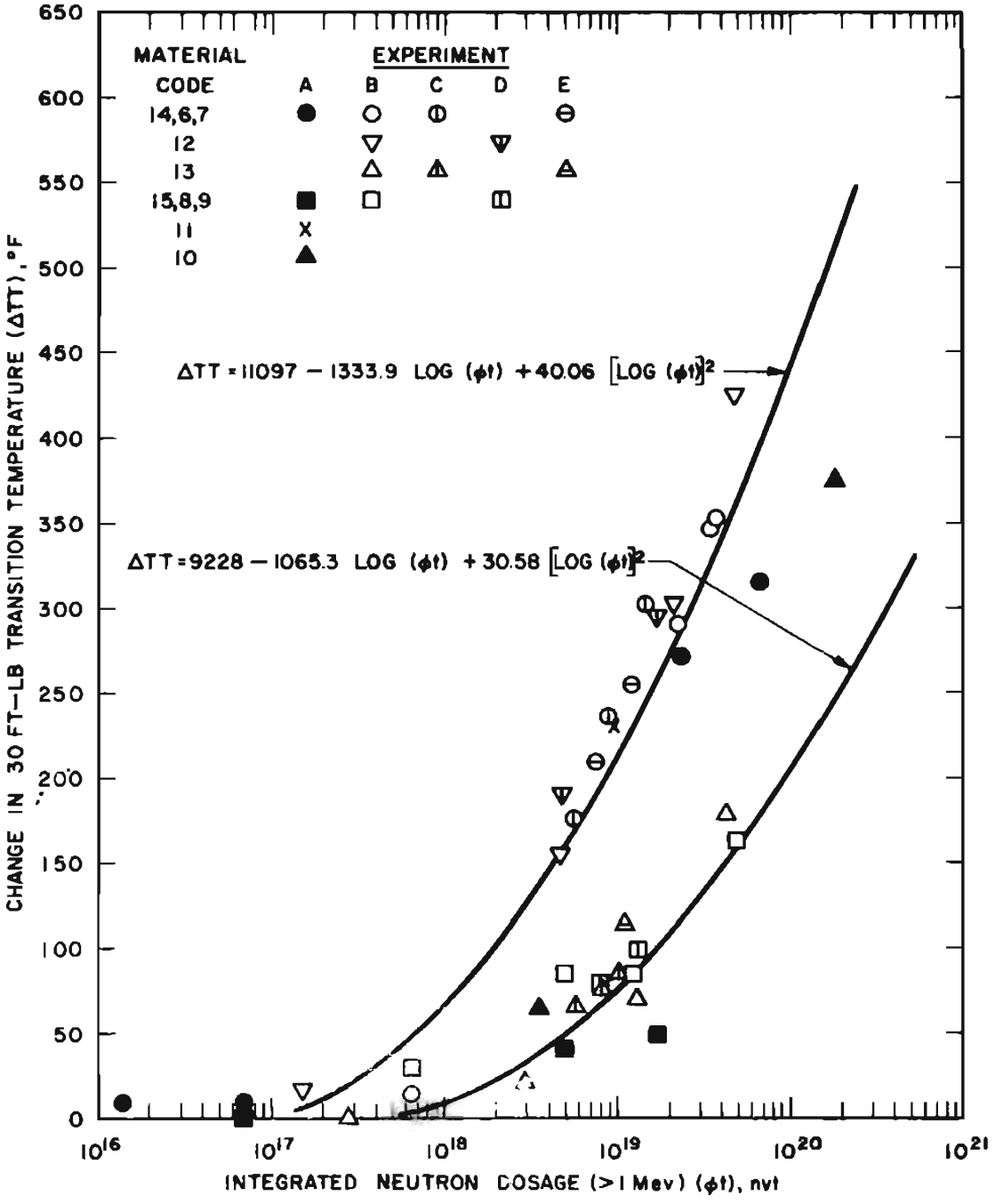

Fig. 5.19. Effect of Irradiation at 450 to 520°F on Various Heats of A 302 Grade B Steel. "Sensitive" and "insensitive" irradiation behavior are demonstrated by the upper and lower curves, respectively. (From Ref. 155)

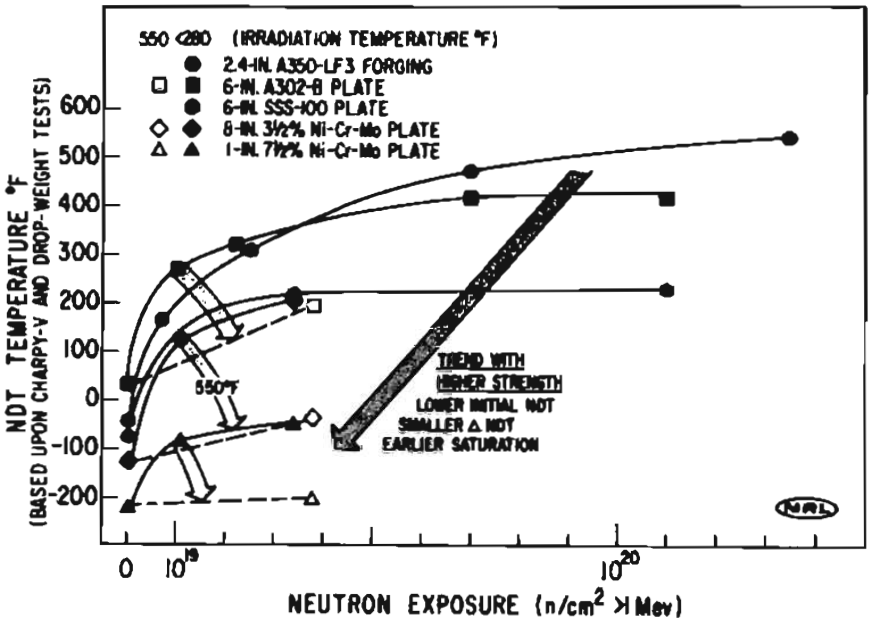

Fig. 5.20. Relative Transition Temperatures (NDT Temperatures) for Five Steels Having Yield Strength Levels from About 60 to 180 ksi Before and After Irradiation at <280 and 550°F (Note Linear Abscissa). (From Ref. 194)

there is a tendency for smaller radiation-induced increases in transition temperature; (3) a marked and progressive advantage in terms of lower radiation embrittlement is observed with the higher strength steels irradiated at 550°F; and (4) there appears to be a general tendency for earlier saturation of radiation embrittlement with increasing strengths that is particularly marked for an irradiation temperature of 550°F.

Most other studies indicate that the finer metallurgical structures lead to lower radiation sensitivities. The predominant factor appears to be the cooling rate from the austenitizing temperature. Composition variables appear to have an indirect influence on radiation sensitivity, primarily by altering the metallurgical structure attainable with a given cooling rate from the austenitizing temperature. One possible exception to this conclusion may be the observations[195] on experimental heats of A 302 grade B steel obtained by the Naval Research Laboratory in collaboration with U.S. Steel Corporation. An air-induction heat with low residual-element content exhibited no shift of transition temperature after

irradiation at 550°F to 3.1×10^{19} neutrons/cm^2 (E > 1 Mev), while a similar heat with nominal residual-element content exhibited a transition temperature shift of 135°F. Approximately equivalent radiation sensitivity was observed for irradiations of the two heats at 240°F.

There exist fewer data on radiation effects in weld metal and weld-heat-affected zones than on plate materials. The major portion of these data indicates radiation-induced transition temperature shifts of the same magnitude in welds and heat-affected zones as has been described for plate materials. The data on two heat-affected zones in A 212 grade B steel, Fig. 5.18, are examples of this behavior. However, one study[196] of radiation embrittlement in a 3 1/2% Ni–Cr–Mo weldment has shown a large difference of radiation sensitivity between weld metal and plate materials. The plate material exhibited a 75°F transition temperature shift after an irradiation at 550°F to 2.9×10^{19} neutrons/cm^2 (E > 1 Mev), while the weld metal exhibited a shift of about 400°F after the same irradiation.

While the results of irradiation studies conducted to date do not permit prediction (in a satisfactorily precise manner) of the property changes of a given alloy heat treated in a specific manner and exposed to a particular nuclear environment, the probable direction of further research is evident, and there is considerable promise that materials can be produced that are insensitive to radiation effects at the operating temperatures of nuclear power reactor pressure vessels. Until such materials can be consistently produced, the properties of irradiated pressure vessel material (plate, forging, weld, or heat-affected zone) must be determined either in a test reactor study or surveillance program, or the most pessimistic results must be considered in design and operating procedures.

5.4.3 Surveillance Program Results

Materials surveillance programs have been established in a number of commercial water-cooled power reactors (see Chap. 10) and also in military power reactors. The results obtained in these programs are of interest not only in determining the condition of the particular reactor pressure vessel but also because comparison with results of "accelerated" irradiations

should provide greater confidence in applying research program results to operating power reactors. The surveillance results available to date have been obtained from the U.S. Army's SM-1 and SM-1A reactors, Dresden, Big Rock Point, Piqua, and Yankee-Rowe reactors.

The original surveillance program in the SM-1 reactor included subsize Izod specimens of A 212 grade B steel. These specimens were mounted in a position that exposed the specimens to a higher neutron flux than the pressure vessel experienced. Standard Charpy specimens were installed at a later date. The results[197-199] of tests of the SM-1 surveillance specimens (Charpy and subsize Izod) agree with predictions based on accelerated irradiation studies. The possible errors in test data and neutron flux are greater than the differences between SM-1 surveillance data and research data. The surveillance test data from the SM-1A reactor, Fig. 5.21 (from Ref. 199), also compare favorably with data from test reactor irradiations.

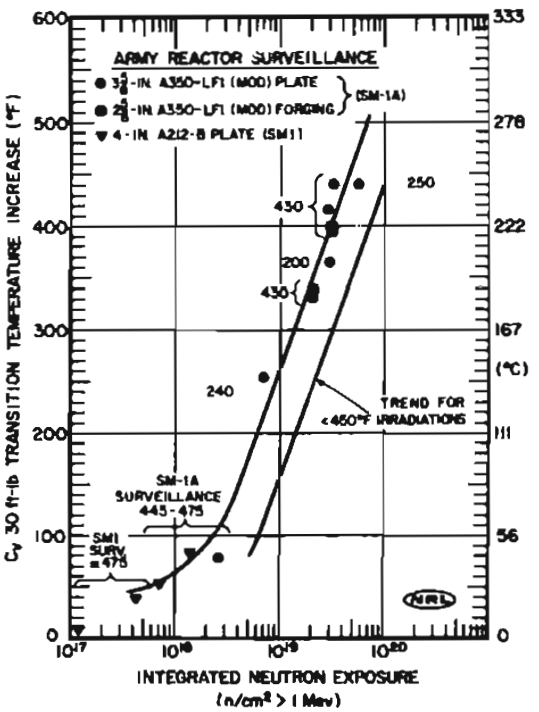

Fig. 5.21. Charpy V-Notch Transition Temperature Increases for SM-1 and SM-1A Pressure Vessel Steels. (From Ref. 199)

The first surveillance specimens from the Yankee-Rowe reactor were from capsules that had been irradiated near the reactor core. Specimens of A 302 grade B steel from ASTM reference plate[200] and from the reactor pressure vessel plate were included in these capsules. The data obtained from the ASTM reference plate agreed with data from accelerated irradiations in test reactors.[199,201-203] The data from the pressure vessel specimens indicated a slightly greater (25%) shift of Charpy V-notch transition temperature than for the reference plate. The difference was within the variations of radiation effects that have been observed for commercial A 302 grade B steel. The surveillance specimens exposed at the pressure vessel wall were recovered after operation of Core IV.[203] The pressure vessel steel specimens again showed a slightly greater radiation sensitivity than did the reference steel. However, both steels showed a greater transition temperature shift than predicted on the basis of the "Yankee near-core" specimens, Fig. 5.22. The shifts were still within the "band" of data for irradiations at less than 450°F. This behavior was probably due to a combination of decreasing operating temperature during specimen exposure and neutron spectrum differences between the vessel wall and "near-core" positions.[203]

On the other hand, surveillance specimens of A 302 grade B steel from the Big Rock Point reactor[204] that were exposed in "near-core" positions showed less radiation sensitivity than the same grade of steel irradiated in test reactors. This may be due to the effect of irradiation temperature, since the temperature was about 600°F for the last one-third of the exposure. The "near-core" Big Rock Point data fall within the observed data scatter for other irradiations. Tests on Big Rock Point surveillance specimens exposed at the pressure vessel wall[199] showed no observable transition temperature shift for base plate or heat-affected zones and 55°F for the weld metal of the pressure vessel steel at 1.5×10^{18} neutrons/cm^2 ($E > 1$ Mev).

ASTM A 212 grade B surveillance specimens from the Piqua reactor showed no significant departure from data obtained from accelerated irradiations.[205]

The largest body of surveillance data presently available is from the Dresden I reactor. Notch-impact (Charpy V) and tensile test specimens

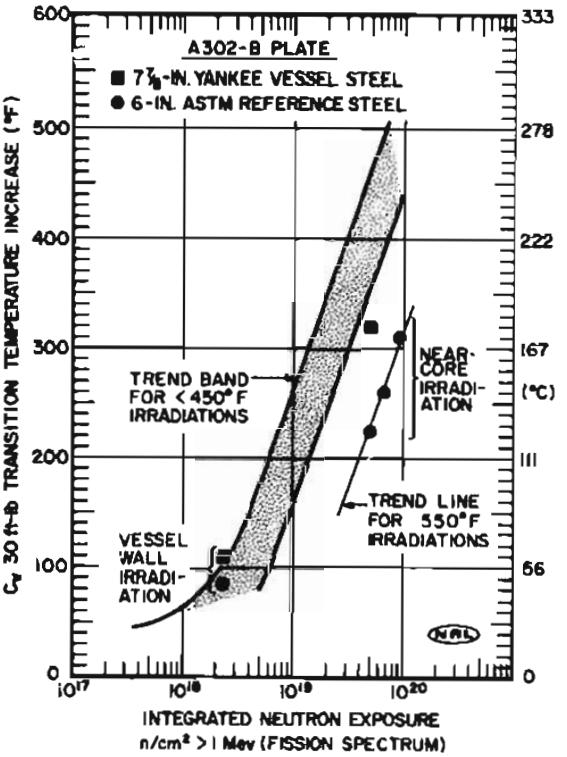

Fig. 5.22. Transition Temperature Increase for Yankee Reactor Test Plate and ASTM A 302 Grade B Reference Steel Specimens Irradiated at a Vessel Wall Surveillance Location in the Yankee Reactor During Operation of Cores II, III, and IV. (From Ref. 203)

of A 302 grade B steel have been tested after irradiation for one-half to four years in the core, near-core, pressure vessel wall, and "turning vane" (negligible neutron flux) positions of Dresden I.[206-8] The materials tested included Dresden I base plate, weld metal, and heat-affected zones and Humboldt reactor base plate. The irradiation temperature was 545°F, and the measured integrated neutron fluxes ranged from 5×10^{17} to 2.3×10^{20} neutrons/cm^2 (E > 1 Mev) for Charpy V-notch data and from 9.8×10^{18} to 2.3×10^{20} neutrons/cm^2 (E > 1 Mev) for the tensile data. All tensile tests were conducted at 550°F, and the Charpy V-notch tests were conducted over a range of temperatures to develop full transition curves. The radiation-induced changes in tensile properties will not affect the serviceability of the Dresden pressure vessel.[208] The radiation-induced increases in notch-impact transition temperature will only

affect the recommended minimum temperature for full-pressure test. This temperature was 220°F for the 1966 refueling outage and will gradually increase to 285°F after 40 years of operation based on the present data.[208]

The tensile test results show irradiation behavior similar to results for the same type of materials irradiated and tested by other investigators. The maximum yield strength increase was approximately 50% for an exposure of 2.3×10^{20} neutrons/cm^2 (equivalent to 250 years of operation), and tensile strength increases were less. The ratio of yield strength to tensile strength at the highest dose reached a value of 0.95 for weld metal. Ratios for other conditions were lower than this value. The results of Charpy V-notch tests, based on the 30 ft-lb criterion, showed transition temperature increases that were slightly greater than for steels termed "insensitive" in other reported studies[155] and much less than for "sensitive" steels.[155] There was no apparent difference in radiation sensitivity for samples cut from the inside or outside of the pressure vessel plate or for samples cut parallel or transverse to the major rolling direction. The weld metal specimens exhibited a considerably lower radiation sensitivity and heat-affected-zone specimens a slightly lower radiation sensitivity than the base plate specimens. The ductile-fracture energy was decreased about 50% for an exposure of 1.7×10^{20} neutrons/cm^2 but would be adequate for exposures equivalent to the anticipated life of the Dresden I pressure vessel (40 years). There were no apparent flux (dose rate) or spectrum effects. There appears to be some correlation between transition temperature increases and yield strength increases. Such a correlation, however, seems to be only approximate and not adequate for prediction of notch-impact behavior based on tensile properties.

The available results from the several surveillance programs that have been summarized here are substantially in agreement with the results of research programs conducted in test reactors. Direct comparison of results from surveillance and research programs is not presently possible due to differences of material composition and heat treatment, irradiation temperature, and integrated neutron flux. The primary purpose of surveillance programs, monitoring the condition of the pressure vessel, is apparently being accomplished, and no unexpected effects have been observed.

5.4.4 Components Removed from Service

A few pressure vessel components have become available for study of radiation effects. None of these are from commerical nuclear power plants.

Test specimens were taken from the SL-1 (U.S. Army) pressure vessel (A 212 grade B steel) after the reactor was dismantled. Charpy V-notch tests on this material gave a transition temperature increase of 65°F for an exposure of about 1.6×10^{18} neutrons/cm^2 (E > 1 Mev) at 420°F.[209] This increase may be slightly greater than obtained in accelerated irradiations of similar steels.

A section of the OMRE grid plate (A 387 grade B steel) has been removed for notch-impact tests.[205] The test results are not inconsistent with accelerated irradiation data. However, no material was available for obtaining preirradiation data, and comparisons with other irradiation data are necessarily only approximate.

An extensive study is in progress on the PM-2A (U.S. Army) pressure vessel.[210] This pressure vessel, which was removed from service, is fabricated from ring forgings of SA 350 grade LF-3 steel and clad with stainless steel. Detailed dimensional measurements and nondestructive inspections of the vessel were performed. The integrated neutron flux to which the various portions of the vessel had been exposed were determined by both analytical and nondestructive methods. The maximum integrated neutron flux was reported to be 1.47×10^{19} neutrons/cm^2 (E > 1 Mev). The study is designed to obtain direct confirmation of pressure vessel brittle-fracture-prevention criteria. The vessel has been ruptured with an artificially introduced flaw under controlled temperature and pressure conditions.[211] Portions of the vessel will be used for laboratory tests of brittle-fracture properties.

5.4.5 Postirradiation Heat Treatment

Because the extent of steel embrittlement due to radiation can be quite large, several studies have been conducted to assess the possibilities of embrittlement relief by means of thermal annealing cycles. Most

of these studies have been for single annealing cycles following irradiation. A few studies have included reirradiation after annealing and multiple irradiation-annealing cycles. A number of factors are operative in determining the effectiveness of postirradiation heat treatment. These factors include neutron exposure, the material, exposure temperature, and annealing temperature and duration.

The recovery of tensile behavior of an SA 212 grade B steel is illustrated in Fig. 5.23 (from Ref. 166). This steel was irradiated at 100°F to an exposure of 1.5×10^{19} neutrons/cm^2 prior to 90-min anneals at the indicated temperatures. Recovery of ductility is seen to be substantial at 400°F. About 25% recovery of yield strength is observed at 550 and 600°F, and almost complete recovery occurs after 90 min at 750°F. That the recovery process may be quite complex is illustrated in Fig. 5.24 (from Ref. 166). Several stages of recovery are evident in this steel.

The effect of postirradiation annealing on the transition temperature, yield strength, and ultimate tensile strength of another heat of SA 212 grade B steel irradiated at temperatures of 450 to 570°F is shown in Fig. 5.25 (from Ref. 192). There was little or no recovery below 570°F. There is some indication of lower recovery temperatures for material irradiated at the lower temperature. The apparent crossover of the recovery curves at 700°F (375°C) may not be real, since the separation of the curves at the 750°F (400°C) recovery temperature may be within the uncertainty of the data. The role of recovery time is illustrated in Fig. 5.26 (from Ref. 209) for an A 350 grade LF-3 forging. In this case increasing recovery times produced greater recovery of the radiation effect. However, a reembrittlement has been observed in several irradiated steels. The results presented in Fig. 5.27 (from Ref. 212) show less recovery of radiation-induced transition temperature shift for 168 hr at 600°F than for 20 hr at 600°F. Other investigators[155] have also observed this reembrittlement phenomenon.

The kinetics of annealing of radiation damage have been studied in an attempt to determine indirectly the mechanism of radiation effects in steels. Isothermal annealing studies[164] on a silicon-killed carbon steel irradiated at 300°F, Fig. 5.28, showed recovery that was exponential with time and a unique activation energy equal to that for self-diffusion

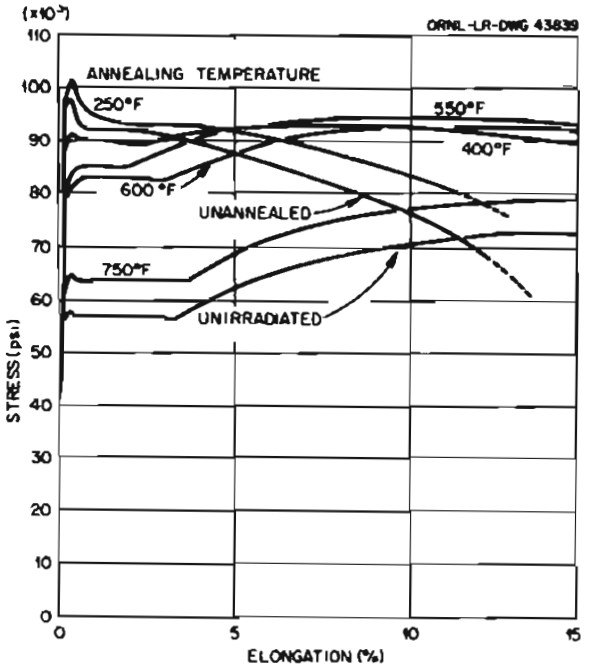

Fig. 5.23. Effect of Postirradiation Annealing on Stress-Strain Curves for an ASTM A 212 Grade B Steel. (From Ref. 166)

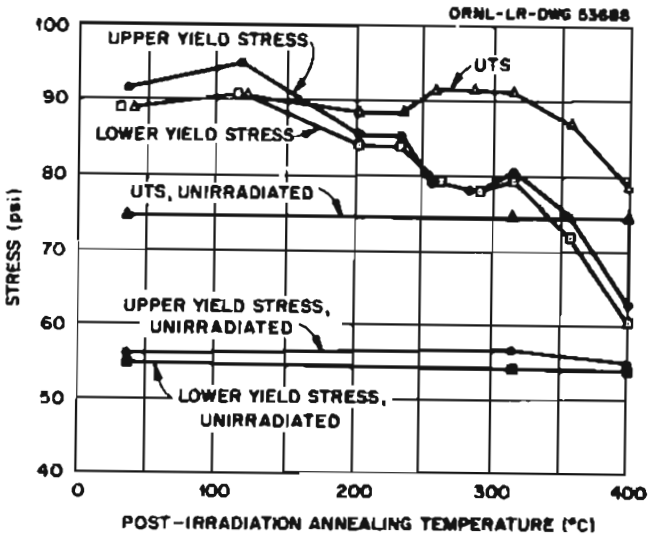

Fig. 5.24. Effect of Postirradiation Annealing on Tensile Properties of an ASTM A 212 Grade B Steel. (From Ref. 166)

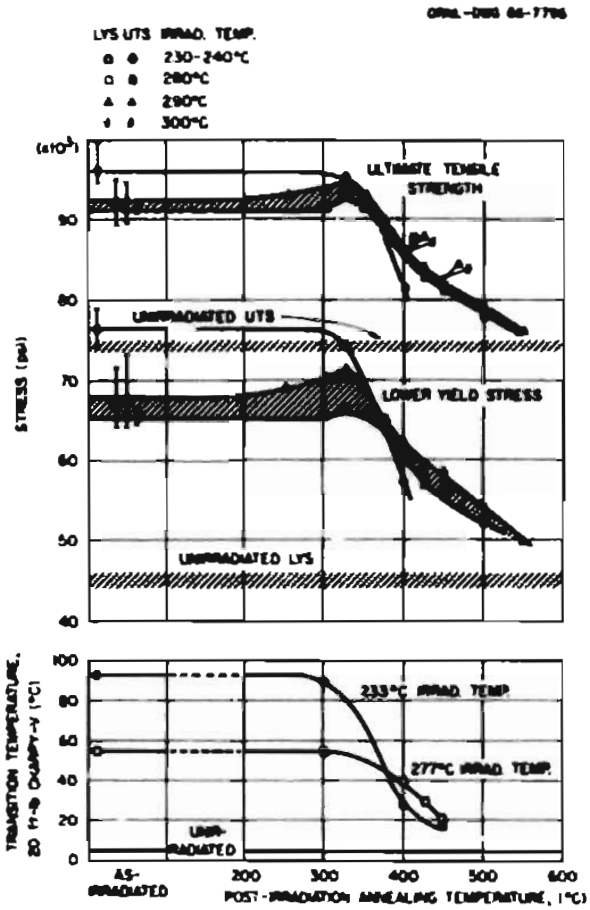

Fig. 5.25. Effect of Postirradiation Annealing on Tensile and Notch-Impact Behavior of an ASTM A 212 Grade B Steel Irradiated at Elevated Temperatures. (From Ref. 192)

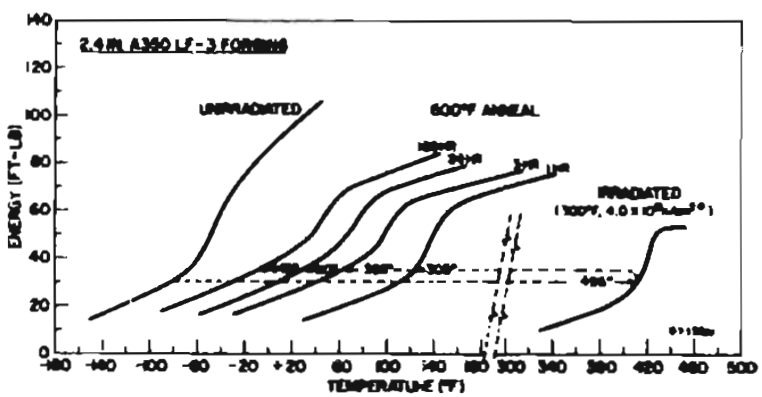

Fig. 5.26. Effect of Postirradiation Annealing Time on Notch-Impact Behavior of an ASTM A 350 Grade LF-3 Forging Steel. (From Ref. 209)

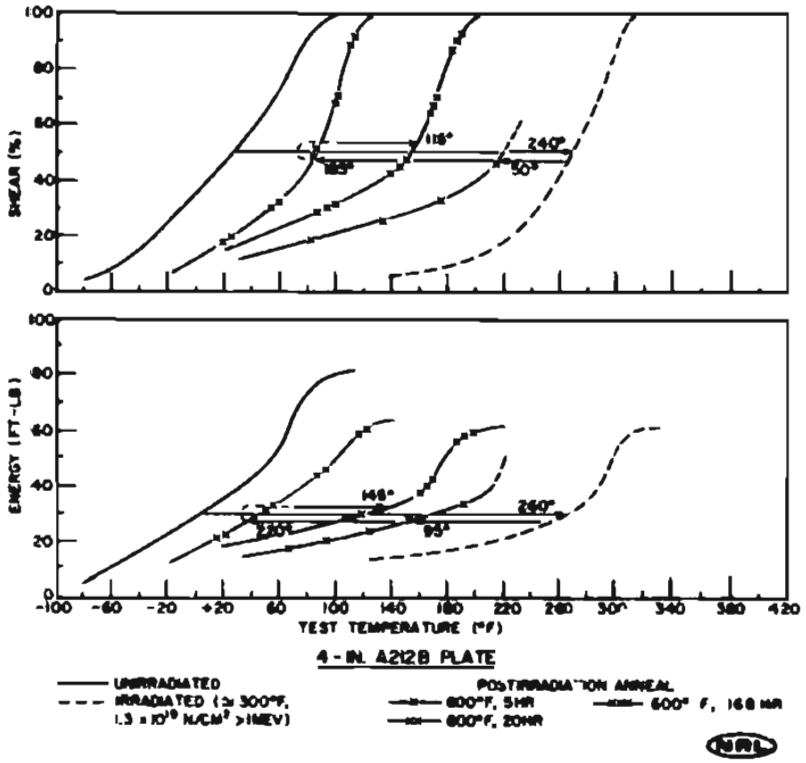

Fig. 5.27. Reembrittlement Phenomenon During Postirradiation Annealing of A 212 Grade B Plate. (From Ref. 212)

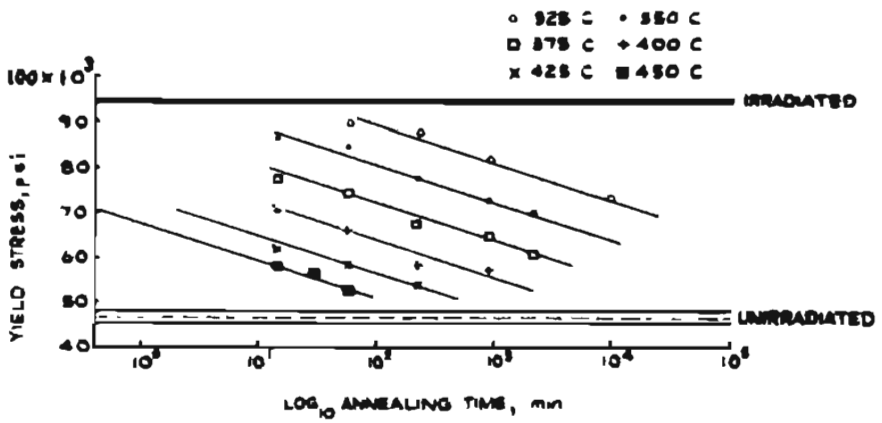

Fig. 5.28. Isothermal Annealing Curves for the Room-Temperature Yield Stress of a Silicon-Killed Carbon Steel Irradiated in the Calder Reactor at 150°C to 9.5 × 10^{18} neutrons/cm^2 (Fission). (From Ref. 164)

in iron. Similar annealing studies have been conducted on material irradiated at 200, 357, and 554°F. The results of these studies,[169] Fig. 5.29, give approximately the same activation energies for three materials and four irradiation temperatures. However, the annealing times for 50% recovery at a given temperature differ by three orders of magnitude.

The application of postirradiation annealing to nuclear pressure vessels poses questions regarding rates of embrittlement during subsequent irradiation. Carpenter, Knopf, and Byron[155] concluded from their studies that "Reirradiation of a sensitive and insensitive heat of A 302 grade B steel that had been irradiated and subsequently annealed at 650°F resulted in transition temperatures that could not be distinguished from those observed after irradiating the same materials to the same total dosages without interim annealing."

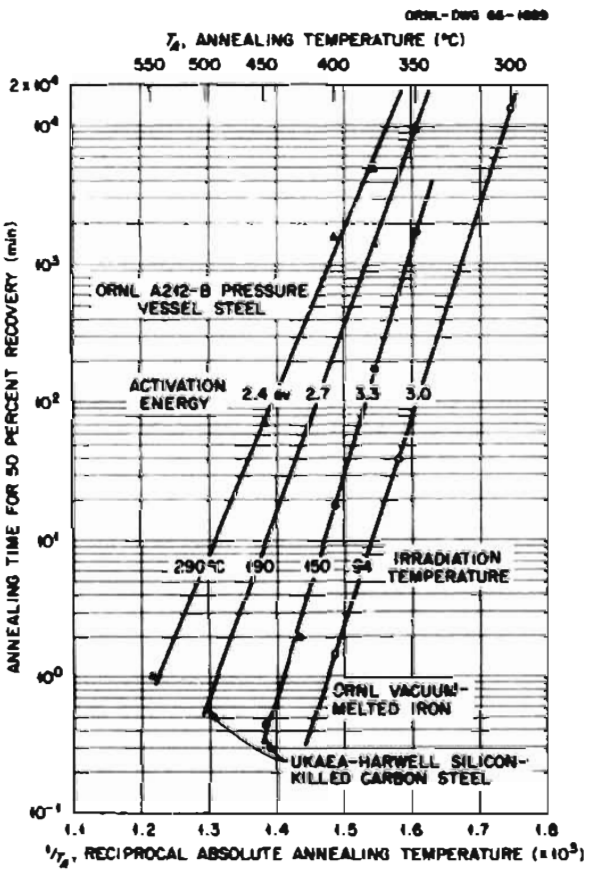

Fig. 5.29. Annealing Time for 50% Recovery of the Yield Stress for Irradiated Iron and Steel. (From Ref. 169)

Steele and Hawthorne[213] have found, in some of their studies, a measurable advantage of intermediate annealing during irradiation, Fig. 5.30.

A number of nuclear power reactors are currently operating at temperatures well below their design temperature. The possibility therefore exists that an increase in operating temperature after a period of initial service would have beneficial effects on the notch-ductility properties of the pressure vessel. That this is true, for at least two cases, is shown in Fig. 5.31 (from Ref. 214). The A 302 grade B steel irradiated at 400°F and then at 540°F exhibited the same transition temperature increase as if it had been irradiated at 540°F during the entire exposure.

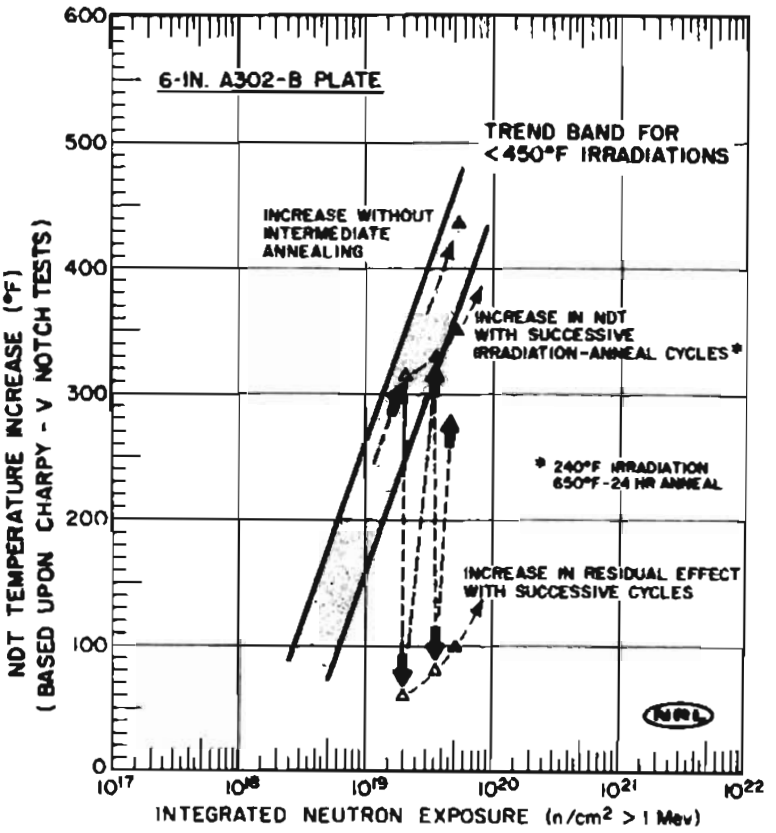

Fig. 5.30. NDT Temperature Behavior of A 302 Grade B Steel at Various Stages of Cyclic Irradiation and Annealing Treatments. (From Ref. 213)

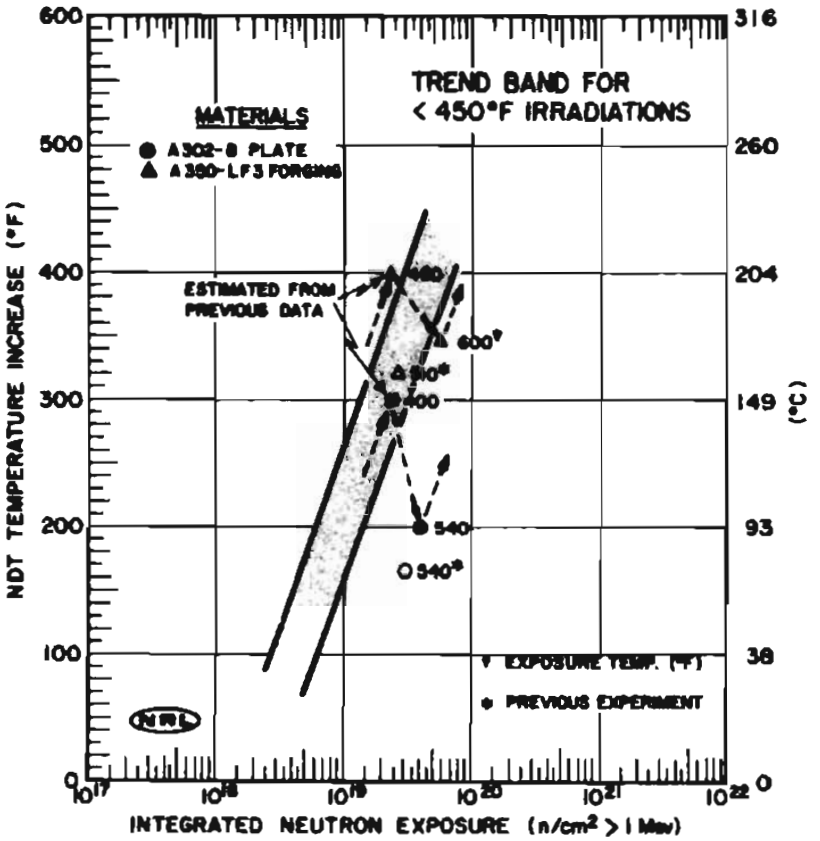

Fig. 5.31. NDT Temperatures of A 302 Grade B and A 350 Grade LF-3 Steels Resulting from Irradiation in a Two-Phase Schedule: First at 400 and 450°F and then at Higher Temperatures of 540 and 640°F. (From Ref. 214)

The effects of temperature on radiation-induced property changes in pressure vessel steels are complex. It is hoped that study of postirradiation annealing kinetics and irradiation at elevated temperatures will lead to an understanding of radiation effects and recovery. Such an understanding should permit the prediction of properties for the more complex cases of intermediate annealing and changing operating temperature.

5.4.6 Pressure Vessel Cladding

The effect of irradiation at various temperatures in the range 120 to 1300°F on the tensile properties of wrought stainless steels has been

studied extensively[215] for neutron doses to 10^{21} neutrons/cm^2. These data show only slight effects on the mechanical properties for doses up to 10^{19} neutrons/cm^2 at temperatures up to 700°F.

Application of data from wrought stainless steel to pressure vessel cladding is not valid, since the cladding is generally performed by a weld overlay process. Thus, it is necessary to use data for welded stainless steel. Leeser[153] reported fatigue data for welds in type 304 stainless steel irradiated to 10^{19} neutrons/cm^2 (fast) at temperatures in the range 70 to 140°F. These data indicate no change in fatigue properties in notched and unnotched specimens. Martin and Slaughter[216] recently published data at temperatures somewhat higher (930°F) than those of interest that indicate a slight rise in yield stress and no change in ductility as a result of irradiation to 10^{20} neutrons/cm^2.

There are no indications that radiation effects in pressure vessel cladding (stainless steels) will adversely affect the serviceability of commerical water-cooled reactors for present or contemplated operating conditions.

REFERENCES

1. A. W. Pense, A Study of Subcritical Embrittlement of Pressure Vessel Steels, Dissertation for Doctor of Philosophy Degree, Lehigh University, 1962.
2. M. C. Bloom and M. Krulfeld, Hydrogen Effusion Method for Determination of Corrosion Rates in Aqueous Systems at Elevated Temperature and Pressure. J. Electrochem. Soc., 104(5): 264–269 (May 1957).
3. M. B. Strauss and M. C. Bloom, Corrosion Mechanisms in the Reaction of Steel with Water and Oxygenated Solutions at Room Temperature and 316°C, J. Electrochem. Soc., 107(2): 73–79 (1960).
4. D. L. Douglas and F. C. Zyzes, The Corrosion of Iron in High-Temperature Water, Parts 1 and 2, Corrosion, 13(6): 361t–374t (June 1957) and 13(7): 433t–436t (July 1957).
5. R. A. U. Huddle, British Report AERE M/R 1313, 1955.
6. R. R. Nash, pp. 1–11 in Fundamental Research in the Aqueous Corrosion of Materials, A Summary of Programs Sponsored by the Division of Research, USAEC, USAEC Report TID-7587, July 1960.
7. G. H. Cartledge, Cathodic Processes in Corrosion, pp. 12–29 in Fundamental Research in the Aqueous Corrosion of Materials, A Summary of Programs Sponsored by the Division of Research, USAEC, USAEC Report TID-7587, July 1960.

8. F. W. Young, Jr., et al., Crystal Imperfections in Reactivity of Metal Surfaces, p. 30 in Fundamental Research in the Aqueous Corrosion of Materials, A Summary of Programs Sponsored by the Division of Research, USAEC, USAEC Report TID-7587, July 1960.

9. M. Pourbaix, Predétermination des circonstances de corrosion et de non corrosion des métaux et alliáges, Corrosion et Anticorrosion, 9(2): 47–62 (1961).

10. J. A. Armentano and V. P. Murphy, Proceedings of International Water Conference, Engineers Society of Western Pennsylvania, p. 111, September 1964.

11. D. C. Vreeland, Corrosion of Carbon Steel and Low Alloy Steels in Primary Systems of Water-Cooled Nuclear Reactors, paper presented at Netherlands–Norweigan Reactor School, Kjeller, Norway, August 1963.

12. D. J. DePaul (Ed.), Corrosion and Wear Handbook for Water Cooled Reactors, USAEC Report TID-7006, 1957.

13. H. H. Uhlig, Corrosion and Corrosion Control, Wiley, New York, 1963.

14. C. F. Cheng, Corrosion Aspects of Iron, Austenitic Stainless Steel and Inconel in High Temperature Water, Corrosion, 20: 341t–349t (November 1964).

15. P. D. Miller et al., Ferrous Hydroxide Solubility, Thermal Decomposition and Role in the Corrosion of Iron, Paper No. 57-A-184 (preprint), ASME Annual Meeting, New York, December 1957.

16. U. R. Evans and J. N. Wanklyn, Evolution of Hydrogen from Ferrous Hydroxide, Nature, 162: 27–28 (1948).

17. V. J. Linnenbom, Reaction Between Iron and Water In Absence of Oxygen, J. Electrochem. Soc., 105(6): 322–324 (June 1958).

18. M. J. Pryor and M. Cohen, The Inhibition of the Corrosion of Iron by Some Anodic Inhibitors, J. Electrochem. Soc., 100(5): 203–215 (1953).

19. M. C. Bloom, A Survey of Steel Corrosion Mechanics Pertinent to Steam Power Generation, preprint, Engineers Society of Western Pennsylvania, 21st Annual Water Conference, Pittsburgh, Pennsylvania, Oct. 24, 1960.

20. J. T. Waber, Corrosion of U and U Alloys, USAEC Report TID-7587, p. 307, July 1960.

21. D. E. Tackett, P. E. Brown, and R. T. Esper, Review of Carbon Steel Corrosion Data in High Temperature, High Purity Water in Dynamic Systems, USAEC Report WAPD-LSR(C)-134, Bettis Plant, Westinghouse Electric Corporation, Oct. 14, 1955.

22. F. L. LaQue and H. R. Copson, Corrosion Resistance of Metals and Alloys, 2nd ed., Reinhold, New York, 1963.

23. D. C. Vreeland et al., Corrosion of Carbon and Low-Alloy Steels in Out-of-Pile Boiling-Water-Reactor Environment, Corrosion, 17(6): 269t–276t (June 1961).

24. D. C. Vreeland et al., Corrosion of Carbon Steel and Other Steels In Simulated Boiling Water Environment: Phase II, Corrosion, 18(10): 368t–377t (October 1962).

25. D. E. Voyles, paper presented at High-Purity Water Symposium, 18th Annual NACE Conference, Kansas City, Mo., March 1962.

26. M. C. Bloom et al., Corrosion Studies in High Temperature Water By a Hydrogen Effusion Method, Corrosion, 13(5): 297t–302t (May 1957).

27. R. E. J. Lobsinger, Corrosion of Zr, Carbon Steel, and Stainless Steel, USAEC Report HW-56995, General Electric Company, Hanford Atomic Products Operation, August 1958.

28. T. W. Farrer et al., Role of Tannates and Phosphates in Preservation of Ancient Buried Iron Objects, J. Appl. Chem., 3(2): 80 (February 1953).

29. C. R. Tipton (Ed.), Reactor Handbook, Vol. I, Materials, Interscience Publishers, New York, 1960.

30. H. R. Copson, Effects of Velocity on Corrosion by Water, Ind. Eng. Chem., 44: 1745 (1952).

31. R. F. Passano and F. R. Nagley, Consistent Data Showing the Influence of Water Velocity and Time on the Corrosion of Iron, Proc. Amer. Soc. Testing Materials, 33(II): 387–404 (1933).

32. H. A. Wagner et al., Corrosion-Erosion of Boiler Feed Pumps and Regulating Valves, Trans. ASME, 69: 389–403 (May 1947).

33. P. E. Brown, Carbon Steel for Water-Cooled Nuclear Reactors, USAEC Report WAPD-257, Bettis Plant, Westinghouse Electric Corporation, September 1961.

34. M. A. Powers and H. L. Tymchyn, Corrosion of Inconel to High-Temperature Water, pp. IV.3–IV.6 in Reactor Technology Report No. 14 – Chemistry, USAEC Report KAPL-2000-11, Knolls Atomic Power Laboratory, September 1960.

35. L. Scheib, Materials for a Water Cooled and Moderated Reactor, USAEC Report ORNL-1915, Oak Ridge National Laboratory, August 1955.

36. V. G. Zelenskii, Stoikost nekotorykh matérialov protiv erozionnogo iznosa pri shchelevom vody, Teploenergetika, 6(2): 63–69 (February 1959).

37. Westinghouse Electric Corporation, Evaluation of Yankee Vessel Cladding Penetration, USAEC Report WCAP-2855, Westinghouse Electric Corporation, Atomic Power Division, October 1965.

38. H. H. Unlig et al., Effect of Oxygen, Chlorides and Calcium Ions on Corrosion Inhibition of Iron by Polyphosphates, J. Electrochem. Soc., 102(2): 59 (February 1955).

39. F. E. Clark, J. Amer. Soc. Naval Engrs., 64: 83–94 (February 1952).

40. W. E. Berry and F. W. Fink, Effect of Heat Transfer on Corrosion of Ferrous Alloys in Boiler Waters, USAEC Report BMI-1626, p. 11, Battelle Memorial Institute, April 1963.

41. R. E. Seebold, Visual Observations on the Water Stream in An Elevated Temperature High Velocity Loop, Corrosion, 15(4): 183t–184t (April 1959).

42. C. R. Breeden et al., Water Corrosion of Structural Materials, USAEC Report ANL-4519, Argonne National Laboratory, July 1957.

43. H. A. Cataldi et al., Investigation of Erosion and Corrosion of Turbine Materials in Wet Oxygenated Steam, Trans. ASME, 80: 1465–1478 (1958).

44. W. E. Ruther and R. K. Hart, Influence of Oxygen on High Temperature Aqueous Corrosion of Iron, Corrosion, 19(4): 127t–133t (April 1963).

45. P. E. Brown, Reactor Chemistry and Plant Materials, p. 110 in Bettis Technical Review, 1(3), USAEC Report WAPD-BT-3, Westinghouse Electric Corporation, Bettis Plant, August 1957.

46. F. J. Brutschy et al., Vallecitos Boiling Water Reactor Coolant Technology, Ind. Eng. Chem., 51(10): 1262–1264 (October 1959).

47. H. H. Uhlig (Ed.), Corrosion Handbook, p. 125, Wiley, New York, 1948.

48. F. G. Frese, Effect of Oxygen on the Corrosion of Steels, Ind. Eng. Chem., 30(1): 83 (January 1938).

49. W. H. J. Vernon, Controlling Factors in Atmospheric and Immersed Corrosion, J. Sci. Instr., 22(12): 226–230 (December 1945).

50. G. E. Moore, Carbon Steel in High Temperature Water, USAEC Report ORNL-CF-57-1-26. Oak Ridge National Laboratory, January 1957.

51. W. L. Pearl and G. P. Wozadlo, Corrosion of Carbon Steel in Simulated Boiling Water and Superheated Reactor Environments, Corrosion, 21(8): 260–267 (August 1965).

52. E. C. Potter and G. M. W. Mann, Mechanism of Magnetite Growth on Low Carbon Steel in Steam and Aqueous Solutions up to 500 C, 2nd International Congress on Metallic Corrosion, New York City, March 11–15, 1963.

53. I. H. Welinsky et al., Chemistry of a Pressurized-Water Nuclear Power Plant, paper presented at American Power Conference, March 1956.

54. M. C. Bloom and M. B. Strauss, Steel Corrosion Mechanisms Under Conditions Pertinent to Steam Power Generation, Report NRL 5427, U.S. Naval Research Laboratory, Dec. 30, 1959.

55. J. C. Scully, The Fundamentals of Corrosion, pp. 90–92, Pergamon Press, New York, 1966.

56. W. Schroeder and A. Berk, Intercrystalline Cracking of Boiler Steel and Its Prevention, U.S. Govt. Printing Office Bulletin 443, 1941.

57. H. H. Uhlig, pp. 1–17 in Physical Metallurgy of Stress-Corrosion Fracture, Interscience, New York, 1959.

58. E. G. Coleman et al., On Surface Energy Mechanism for Stress-Corrosion Cracking, Acta Metallurgica, 9(5): 491 (May 1961).

59. I. Langmuir, The Constitution and Fundamental Properties of Solids and Liquids, J. Amer. Chem. Soc., 38: 2221–2295 (1916), and The Adsorption of Gases on Plane Surfaces of Glass, Mica and Platinum, 40: 1361–1403 (1918).

60. N. Petch and P. Stables, Delayed Fracture of Metals Under Static Load, Nature, 169: 842 (May 1952).

61. G. L. Shvartz and H. M. Kristal, Corrosion of Chemical Apparatus, pp. 53–70, Chapman and Hall, London, 1959.

62. J. M. McKibben, Corrosion Results from the Heavy Water Components Test Reactor, USAEC Report DP-801, Savannah River Laboratory, January 1964.

63. J. M. McKibben, Corrosion and Wear of Equipment in the Heavy Water Components Test Reactor, USAEC Report DP-964, Savannah River Laboratory, 1965.

64. D. C. Vreeland et al., paper presented at 16th Annual Conference of National Association of Corrosion Engineers, Dallas, Texas, March 1960.

65. J. C. Wilson and R. G. Berggren, Effects of Neutron Irradiation in Steel, Proc. ASTM, 55: 689–707 (1955).

66. S. C. Datsko and C. R. Breeden, Corrosion of Metals in High Temperature Water at 500°F and 600°F, USAEC Report ANL-5354, Argonne National Laboratory and Babcock & Wilcox Company, October 1954.

67. F. L. LaQue and M. A. Cordovi, The Corrosion of Pressure Circuit Materials in Boiling and Pressurized Water Reactors, pp. 1–24 in Steels for Reactor Pressure Circuits, Report No. 69, Iron and Steel Institute, London, 1961.

68. J. N. Wanklyn and P. J. Jones, The Aqueous Corrosion of Reactor Metals, J. Nucl. Mater., 6(3): 291–329 (1962).

69. D. C. Vreeland, The Corrosion of Stainless Steel in Primary Systems of Water Cooled Nuclear Reactors, paper presented at Netherlands–Norwegian Reactor School, Kjeller, Norway, Aug. 19, 1963.

70. D. D. White and A. Krieg, Corrosion of Materials of Construction, pp. 55–63 in Quarterly Progress Report for the Period July 1 to September 30, 1940, USAEC Report YAEC-97, Westinghouse Electric Corporation, Atomic Power Department, 1958.

71. A. H. Roebuck, Symposium on High-Temperature Water Corrosion, p. 27 in ASTM Special Technical Publication No. 179, 1956.

72. C. R. Bergen, Elk River Reactor Operations Analysis Program Final Report, Task 615, Corrosion Samples and Tests Evaporator Water Boxes, USAEC Report ACNP-66542, Allis-Chalmers Manufacturing Company, Atomic Energy Division, June 1966.

73. D. C. Vreeland, Corrosion-Erosion of Sensitized AISI Type 304 Stainless Steel in a Thorium Dioxide-Uranium Trioxide Slurry, Corrosion, 17(1): 21t–24t (January 1961).

74. W. K. Boyd and R. S. Peoples, Corrosion in Borated and Deionized Water at Temperatures up to 500°F, USAEC Report BMI-1047, Battelle Memorial Institute, Oct. 14, 1955.

75. A. Krieg, Dynamic Screening Corrosion Tests of Materials of Construction in High Temperature Borated Water, USAEC Report YAEC-116, Westinghouse Electric Corporation, Atomic Power Department, January 1959.

76. G. E. Galonian, paper presented at 15th Annual Conference of National Association of Corrosion Engineers, March 1959.

77. O. B. Ellis and F. L. LaQue, Area Effects in Crevice Corrosion, Corrosion, 7(11): 362–364 (November 1951).

78. W. G. Whitman and R. P. Russell, The Natural Water Corrosion of Steel in Contact with Copper, Ind. Eng. Chem., 16(3): 276–279 (1924).

79. B. Strauss, Electrochemical Behavior of Non-Rusting Steel, Stahl u. Eisen., 45: 1198–1202 (1925).

80. International Nickel Company, Inc., undocumented published and unpublished data.

81. J. N. Friend, Eighth Report on the Communications of Institute of Civil Engineers, 1928; Ninth Report, 1929; Tenth Report, 1930; Eleventh Report, 1930; Thirteenth Report, 1933; and Seventeenth Report, 1938.

82. J. N. Friend, The Relative Corrodibilities of Ferrous and Non-Ferrous Metals and Alloys, Part III – Final Report. The Results of Three Years' Exposure at Southampton Docks, J. Inst. Metals, 48(1): 109–120 (1932).

83. D. G. Sammarone, The Galvanic Behavior of Materials in Reactor Coolants, USAEC Report WCAP-1844, Westinghouse Electric Corporation, Atomic Power Division, 1961.

84. W. Lee Williams, Investigation of Stress Corrosion of Austenitic Stainless Steels and Other Materials in High Temperature Water Environments, Report EES040028K, U.S. Naval Engineering Experiment Station, Mar. 29, 1955.

85. Report on Stress-Corrosion Cracking of Austenitic Stainless Steels, ASTM Special Publication No. 264, March 1960.

86. P. D. Neumann and J. C. Griess, Stress-Corrosion Cracking of Type 347 Stainless Steel and Other Alloys in High Temperature Water, Corrosion, 19(10): 345t–353t (October 1963).

87. W. Lee Williams and J. F. Eckel, Stress Corrosion of Austenitic Stainless Steels in High Temperature Waters, ASME J., 68(1): 93–104 (February 1956).

88. A. Dana, Jr., p. 46 in ASTM Bulletin 225, October 1957.

89. C. Edeleanu and P. P. Snowden, Steel Corrosion of Austenitic Stainless Steels in Steam and Hot Water Systems, J. Iron Steel Inst., 186(4): 406–422 (August 1957).

90. N. A. Neilsen, The Physical Metallurgy of Stress-Corrosion Fracture, p. 247, T. N. Rhodin (Ed.), Interscience, New York, 1959.

91. D. A. Vaughn et al., Relationship Between Hydrogen Pickup and Susceptible Paths in Stress Corrosion Cracking of Type 304 Stainless Steel, Corrosion, 19(9): 315t (1963).

92. G. Reed and E. Tarnuzzer, Examining Yankee Plant Performance in 1965, Nucleonics, 24(3): 42–47 (March 1966).

93. N. Balai et al., Inspection, Evaluation, and Operation of the EBWR Reactor Vessel, USAEC Report ANL-7117, Argonne National Laboratory, November 1965.

94. S. P. Rideout, Stress-Corrosion Cracking of Type 304 Stainless Steel in High-Purity Waters, Second International Conference on Metallic Corrosion, New York, March 1963.

95. H. R. Copson and W. E. Berry, Qualification of Inconel for Nuclear Power Plant Applications, Corrosion, 16(2): 79t–85t (February 1961).

96. A. E. Schuetz and W. D. Robertson, Hydrogen Absorption Embrittlement and Fracture of Steel, Corrosion, 13(7): 437t–458t (1957).

97. P. Bastien, p. 311 in Physical Metallurgy of Stress-Corrosion Fracture, Interscience, New York, 1959.

98. H. H. Uhlig, Influence of Hydrogen on Mechanical Properties of Some Low-Carbon Manganese-Iron Alloys and on Hadfield Manganese Steel, Trans. Amer. Inst. Mining Met. Engrs., 158: 183–206 (1944).

99. C. A. Zapffe and C. E. Sims, Hydrogen Embrittlement, Internal Stress and Defects in Steel, Trans. Amer. Inst. Mining Met. Engrs., 145: 225–271 (1941).

100. A. Troiano, The Role of Hydrogen and Other Interstitials in the Mechanical Behavior of Metals, Trans. Amer. Soc. Metals, 52: 54–80 (1960).

101. A. A. Griffith, The Phenomenon of Rupture and Flow in Solids, Phil. Trans. Roy. Soc. (A), 221: 163–198 (1921).

102. R. W. Buzzard and H. E. Cleaves, Hydrogen Embrittlement of Steel – Review of Literature, U.S. Bureau of Standards, Circ. 511, Sept. 24, 1951.

103. P. P. Smith, Hydrogen in Metals, University of Chicago Press, Chicago, 1948.

104. R. D. Frohmberg et al., Delayed Failure and Hydrogen Embrittlement in Steel, Report WADC-TR-54-32, Case Institute of Technology, June 1954.

105. J. T. Brown and W. M. Baldwin, Hydrogen Embrittlement of Steel, J. Metals, 6(2): 298 (February 1954).

106. G. A. Nelson and R. T. Effinger, Blistering and Embrittlement of Pressure Vessel Steels by Hydrogen, Welding J. Res. Suppl., 20: 12S (January 1955).

107. W. D. Robertson, Stress-Corrosion Cracking and Embrittlement, Wiley, New York, 1956.

108. A. Wachter et al., Hydrogen Blistering of Steel in Hydrogen Sulfide Solutions, Corrosion, 9(5): 163 (1953).

109. G. A. Nelson, Revisions to Published Chart: Metals for High-Pressure Hydrogen Plants, J. Engr. Ind., Trans. ASME, Series B, 81: 92–93 (February 1959).

110. E. P. Partridge, Hydrogen Damage in Power Boilers, J. Engr. Power, Trans. ASME, Series A, 86: 311–324 (July 1964).

111. J. B. Steinman, PVRC Interim Report, Rennselaer Polytechnic Institute, July 1964.

112. D. R. Harries, Hydrogen Embrittlement of a 1 wt % Cr/0.5 wt % Mo Pressure Vessel Steel in High Pressure Water, J. Nucl. Mater., 12(1): 24–27 (May–June 1964).

113. A. R. Elsea and E. E. Fletcher, The Problem of Hydrogen in Steel, DMIC Memorandum No. 180, Battelle Memorial Institute, Oct 1, 1963.

114. A. M. Hall and J. E. Campbell, Report on the Fourth Maraging Steel Project Review, DMIC Report No. 196, Battelle Memorial Institute, Aug. 19, 1964.

115. G. H. Broomfield, Hydrogen Effects in an Irradiated 1% Cr 1/2% Mo PWR Pressure Vessel Steel, J. Nucl. Mater., 16(3): 249–259 (July 1965).

116. E. A. Steigerwald et al., Role of Stress in Hydrogen Induced Delayed Failure, Trans. AIME, 218(5): 832–841 (October 1960).

117. J. D. Fast and D. J. van Ooijen, Phillips Technical Review, Part I, Vol. 24 (1962/63); Part II, Vol. 24 (1962/63).

118. H. R. Copson, Influence of Corrosion on Cracking of Pressure Vessels, Welding J., 32(2): 75S–91S (February 1953).

119. J. Schuyten, Hydrogen Attack on Metals at High Temperatures and Pressures, Corrosion and Materials Protection, 4(5): 13–18 (1947).

120. G. A. Nelson, Metals for High-Pressure Hydrogenation Plants, Trans. ASME, 73(2): 205 (February 1951).

121. M. H. Bartz and C. E. Rawlins, Effects of Hydrogen Generated by Corrosion of Steel. Corrosion, 4: 187–206 (1948).

122. R. T. Effinger et al., Hydrogen Attack of Steel in Refinery Equipment, Oil and Gas J., 50(2): 99 (May 17, 1951).

123. D. R. Harries and G. H. Broomfield, Hydrogen Embrittlement of Steel Pressure Vessels in Pressurized Water Reactor Systems, J. Nucl. Mater., 9(3): 327–338 (1963).

124. M. B. Whiteman and A. R. Troiano, Hydrogen Embrittlement of Austenitic Stainless Steel, Corrosion, 21: 53–56 (1965).

125. P. A. Blanchard and A. R. Troiano, La fragilisation des métaux par l'hydrogène etc., Mémoires Scientifiques de la Revue de Métallurgie, 57(6): 409–422 (June 1960).

126. F. W. Schaller, Ph. D. Thesis, Case Institute of Technology, 1961.

127. T. Boniszewski and G. C. Smith, The Influence of Hydrogen on the Plastic Deformation, Ductility, and Fracture of Nickel in Tension, Acta Met., 11: 165–178 (1963).

128. J. L. Mihelich, Ph. D. Thesis, Case Institute of Technology, 1964.

129. Von E. Houdremont and H. Schrader, Beeintrachtigung von Dehnung und Einschnürung von Stahl bei Glühung in Wasserstoff, Archiv für das Eisenhuttenwesen, 15: 87–97 (1941–42).

130. C. A. Zapffe and M. E. Haslem, A Test for Hydrogen Embrittlement and its Application to Seventeen Per Cent Chromium, One Per Cent Carbon Stainless Steel Wire, Trans. AIME, 167: 281–312 (1946).

131. R. L. Mills and F. J. Edeskuty, Hydrogen Embrittlement of Cold-Worked Metals, Chem. Eng. Progr., 52: 477–480 (1956).

132. J. D. Hobson and J. Hewitt, Effect of Hydrogen on Tensile Properties of Steel, J. Iron Steel Inst., 173(2): 131 (February 1953).

133. F. Eisenkolb and G. Ehrlich, Ueber die Wasserstoffaufnahme austenitischer Staehle bei kathodischer Beladung, Archiv fuer das Eisenhuettenwesen, 25(3–4): 187–194 (March–April 1954).

134. L. Kozlowski, Bull. Acad. Pol. Science, CI, III, 5, p. 519, 1957.

135. D. S. Billington and J. H. Crawford, Jr., Radiation Damage in Solids, Princeton University Press, Princeton, N.J., 1961.

136. D. R. Harries, A. F. Ardy, and A. F. Bartlett, Radiation Hardening in Mild and Low Alloy Steels, British Report AERE-R4407, 1963.

137. E. Cibois, J. Lemaire, and M. Weisz, Irradiation Embrittlement and Hardening of Steels and Zircaloy-2 in Pressurized Components, in proceedings of Symposium on Radiation Effects on Metals and Neutron Dosimetry, ASTM STP No. 341, p. 253, American Society for Testing Materials, Philadelphia, Pa., 1963.

138. R. G. Berggren, Radiation Effects in Ferritic Steels, p. 91 in USAEC Conference on the Status of Radiation Effects Research on Structural Materials and the Implications to Reactor Design, Chicago, 1959, USAEC Report TID-7588.

139. H. G. Acker, Review of Welded Ship Failures, Bulletin No. 19, Welding Research Council, New York, 1954.

140. D. P. Brown, Observations on Experience with Welded Ships, Welding J., 31: 765 (1952).

141. M. L. Williams, Analysis of Brittle Behaviour of Ship Plates, in proceedings of Symposium on Efiect of Temperature on the Brittle Behaviour of Metals, ASTM STP No. 158, p. 11, American Society for Testing Materials, Philadelphia, Pa., 1954.

142. M. E. Shank, A Critical Survey of Brittle Fracture in Carbon Plate Steel Structures Other Than Ships, Bulletin No. 17, Welding Research Council, New York, 1954.

143. W. S. Pellini, L. E. Steele, and J. R. Hawthorne, Analysis of Engineering and Basic Research Aspects of Neutron Embrittlement of Steels, NRL Report 5780, Naval Research Laboratory, 1962.

144. W. S. Pellini et al., Review of Concepts and Status of Procedures for Fracture-Safe Design of Complex Welded Structures Involving Metals of Low to Ultra-High Strength Levels, NRL Report 6300, Naval Research Laboratory, 1965.

145. H. C. Burghard, Jr., and E. B. Norris, The Effect of Neutron Irradiation on the Fracture Characteristics of Pressure Vessel Steels, presented at ASME Metals Engineering Conference, Houston, Texas, April 3–5, 1967 (ASME Paper No. 67-MET-1).

146. P. P. Puzak, A. J. Babecki, and W. S. Pellini, Correlations of Brittle Fracture Service Failures with Laboratory Notch-Ductility Tests, Welding J. Res. Suppl., 37: 391-S (1958).

147. J. R. Hawthorne, Studies of Radiation Effects and Recovery of Notch Ductility of Pressure Vessel Steels, p. 343 in proceedings of Symposium on Steels for Reactor Pressure Circuits, London, 1960, Iron and Steel Institute Special Report No. 69, 1961.

148. J. R. Hawthorne and L. E. Steele, The Effect of Neutron Irradiation on the Charpy-V and Drop-Weight Test Transition Temperatures of Various Steels and Weld Metals, NRL Report 5479, Naval Research Laboratory, 1960.

149. L. E. Steele, J. R. Hawthorne, and H. E. Watson, Irradiation Effects on Reactor Structural Materials, February–April 1965, NRL Memo Report 1611, Naval Research Laboratory, 1965.

150. R. E. Johnson and E. J. Pasierb, Fracture Toughness of Irradiated A-302B Steel as Influenced by Microstructure, Trans. Amer. Nucl. Soc., 9(2): 390 (1966).

151. R. E. Johnson, Fracture Mechanics: A Basis for Brittle Fracture Prevention, USAEC Report WAPD-TM-505, Westinghouse Atomic Power Division, 1965.

152. ASME Boiler and Pressure Vessel Code, Section III, Nuclear Vessels, American Society of Mechanical Engineers, New York, 1965.

153. D. O. Leeser, Radiation Effects on Welds and Notches in Plain Carbon Steels, Stainless Steels, and Non-Ferrous Alloys, p. 154 in proceedings of Symposium on Radiation Effects on Materials, Vol. 1, ASTM STP No. 208, American Society for Testing Materials, Philadelphia, Pa., 1956.

154. W. G. Gibbons, A. E. Mikoleit, and W. J. O'Donnell, Fatigue Properties of Irradiated Pressure Vessel Steels, USAEC Report WAPD-T-1864, Westinghouse Atomic Power Division, 1966.

155. G. F. Carpenter, N. R. Knopf, and E. S. Byron, Anomalous Embrittling Effects Observed During Irradiation Studies on Pressure Vessel Steels, Nucl. Sci. Eng., 19: 18 (1964).

156. J. R. Hawthorne and L. E. Steele, In-Reactor Studies of Low-Cycle Fatigue Properties of a Nuclear Pressure Vessel Steel, p. 350 in Flow and Fracture of Metals and Alloys in Nuclear Environments, ASTM STP No. 380, American Society for Testing Materials, Philadelphia, Pa., 1965.

157. J. R. Hawthorne and L. E. Steele, In-Reactor Studies of Low Cycle Fatigue Properties of a Nuclear Pressure Vessel Steel, NRL Report 6127, Naval Research Laboratory, 1964.

158. J. R. Hawthorne and L. E. Steele, In-Reactor Fatigue Tests of A-302B Steel Representing the Elk River Reactor Pressure Vessel, NRL Memo Report 1596, Naval Research Laboratory, 1965.

159. L. E. Steele et al., Irradiated Materials Evaluation and Reactor Pressure Vessel Surveillance for the Army Nuclear Power Program, NRL Memo Report 1644, Naval Research Laboratory, 1965.

160. R. W. Kelleman, A Survey of the Effects of Neutron Irradiation on the Impact and Other Mechanical Properties of Pressure Vessel Steels for the SM-2 Reactor, USAEC Report APAE 61, Alco Products, Inc., 1960.

161. A. H. Cottrell, Theory of Brittle Fracture in Steel and Its Application to Radiation Embrittlement, p. 3 in proceedings of Brittleness in Metals Conference at Culcheth Lab, November 1957, British I. G. Rep. 145 (RD/C).

162. A. D. Whapham and M. J. Makin, The Hardening of Lithium Fluoride by Electron Irradiation, Phil. Mag., 5: 237 (1960).

163. M. J. Makin and F. J. Minter, Irradiation Hardening in Copper and Nickel, Acta Met., 8: 691 (1960).

164. R. W. Nichols and D. R. Harries, Brittle Fracture and Irradiation Effects in Ferritic Pressure Vessel Steels, p. 162 in proceedings of Symposium on Radiation Effects on Metals and Neutron Dosimetry, ASTM STP No. 341, American Society for Testing Materials, Philadelphia, Pa., 1963.

165. L. E. Steele, Practical Neutron Dosimetry for Steel Irradiation Studies, p. 328 in proceedings of Symposium on Steels for Reactor Pressure Circuits, London, 1960, Iron and Steel Institute Special Report No. 69, 1961.

166. R. G. Berggren, Neutron Irradiation Effects in Steels: Studies at Oak Ridge National Laboratory, p. 370 in proceedings of Symposium on Steels for Reactor Pressure Circuits, London, 1960, Iron and Steel Institute Special Report No. 69, 1961.

167. M. S. Wechsler and R. G. Berggren, Radiation Embrittlement of Reactor Pressure Vessels, Nucl. Safety, 4(1): 42 (1962).

168. P. J. Barton, D. R. Harries, and I. L. Mogford, Effects on Neutron Dose Rate and Irradiation Temperature on Radiation Hardening in Mild Steels, British Report AERE-R 4489, 1963.

169. N. E. Hinkle, N. K. Smith, and M. S. Wechsler, Tensile Tests on Irradiated Iron, p. 8 in Solid State Division Progress Report for Period Ending February 1966, USAEC Report ORNL-3949, Oak Ridge National Laboratory.

170. F. A. Brandt and A. J. Alexander, Dresden Nuclear Power Station Reactor Vessel Steel Surveillance Program, USAEC Report APED-3988, General Electric Company, 1962.

171. W. S. Pellini, L. E. Steele, and J. R. Hawthorne, Analysis of Engineering and Basic Research Aspects of Neutron Embrittlement of Steels, NRL Report 5780, Naval Research Laboratory, 1962.

172. F. Seitz and J. S. Koehler, Displacement of Atoms During Irradiation, Solid State Physics, Vol. 2, p. 309, F. Seitz and D. Turnbull (Eds.), Academic Press, New York, 1956.

173. R. E. Dahl and H. H. Yoshikawa, Neutron-Exposure Correlation for Radiation-Damage Studies, Nucl. Sci. Eng., 21: 312 (1965).

174. A. D. Rossin, Dosimetry for Radiation Damage Studies, USAEC Report ANL-6826, Argonne National Laboratory, 1964.

175. A. D. Rossin, Comparison of Neutron Embrittlement of Steel in Different Reactor Spectra, Nucl. Structural Eng., 1: 76 (1965).

176. A. D. Rossin, Significance of Neutron Spectrum on Radiation Effects Studies, p. 115 in proceedings of Symposium on Radiation Effects on Metals and Neutron Dosimetry, ASTM STP No. 341, American Society for Testing Materials, Philadelphia, Pa., 1963.

177. A. D. Rossin, Radiation Damage in Steel: Considerations Involving the Effect of Neutron Spectra, Nucl. Sci. Eng., 9: 137 (1961).

178. B. H. Kinchin and R. S. Pease, The Mechanism of the Irradiation Disordering of Alloys, J. Nucl. Energy, 1: 200 (1955).

179. G. J. Dienes and G. H. Vineyard, Radiation Effects in Solids, Interscience, New York, 1957.

180. J. A. Brinkman, Production of Atomic Displacements by High-Energy Particles, Amer. J. Phys., 24: 246 (1956).

181. J. R. Beeler, Jr., Computer Studies of Neutron Irradiation and Annealing in Finite BCC Iron Specimens, p. 86 in Flow and Fracture of Metals and Alloys in Nuclear Environments, ASTM STP No. 380, American Society for Testing Materials, Philadelphia, Pa., 1965.

182. J. R. Beeler, Jr., Absolute Number of Defect Clusters Produced in Neutron-Irradiated α-Iron Per Unit Exposure, Report GE-TM 65-12-14, General Electric Company, 1965.

183. M. S. Wechsler, Fundamental Aspects of Radiation Effects on Diffusion-Controlled Reactions in Alloys, p. 86 in proceedings of Symposium on Radiation Effects on Metals and Neutron Dosimetry, ASTM STP No. 341, American Society for Testing Materials, Philadelphia, Pa., 1963.

184. H. P. Myers, Neutron Damage in Steels Containing Small Amounts of Boron, Swedish Report AE-53, 1961.

185. M. Grounes, Review of Swedish Work on Irradiation Effects in Pressure Vessel Steels and on the Significance of the Data Obtained, Swedish Report S-350, 1966; presented at ASTM Symposium at Atlantic City, N. J., June 1966.

186. A. Cowan et al., Irradiation Damage in Mild Steel — A Comparison of Crack Arrest Test and Charpy Criteria and the Influence of Neutron Spectrum, presented at ASTM Annual Meeting, Atlantic City, N. J., June 1966.

187. D. R. Harries, P. J. Barton, and S. B. Wright, Effects of Neutron Spectrum and Dose Rate on Radiation Hardening and Embrittlement in Steels, J. Brit. Nucl. Energy Soc., 2: 398 (1963).

188. D. R. Harries and B. L. Eyre, Effects of Irradiation in Iron and Steels, p. 105 in Flow and Fracture of Metals and Alloys in Nuclear Environments, ASTM STP No. 380, American Society for Testing Materials, Philadelphia, Pa., 1965.

189. C. Z. Serpan, Jr., and L. E. Steele, In-Depth Embrittlement of a Simulated Pressure Vessel Wall of A-302B Steel, NRL Report 6151, Naval Research Laboratory, 1964.

190. C. Z. Serpan, Jr., and L. E. Steele, Damaging Neutron Exposure Criteria for Evaluating the Embrittlement of Reactor Pressure Vessel Steels in Different Neutron Spectra, NRL Report 6415, Naval Research Laboratory, 1966.

191. R. G. Berggren, W. J. Stelzman, and T. N. Jones, Radiation Effects on Pressure Vessel Steels, in Solid State Division Progress Report for Period Ending January 1967, USAEC Report ORNL-4097, Oak Ridge National Laboratory.

192. R. G. Berggren, W. J. Stelzman, and T. N. Jones, Radiation Effects on Pressure-Vessel Steels, p. 1 in Solid State Division Progress Report for Period Ending July 1966, USAEC Report ORNL-4020, Oak Ridge National Laboratory.

193. E. T. Wessel, Variations in the Embrittlement of Irradiated Pressure Vessel Steels, Sendai Conference, Vol. 3, Chapt. E-10.

194. L. E. Steele, J. R. Hawthorne, and R. A. Gray, Jr., Neutron Embrittlement of Several Higher Strength Steels, NRL Report 6419, Naval Research Laboratory, 1966.

195. J. R. Hawthorne, Naval Research Laboratory, private communication.

196. L. E. Steele et al., Irradiation Effects on Reactor Structural Materials Quarterly Progress Report August-October 1966, NRL Memo Report 1731, Naval Research Laboratory, 1966.

197. R. G. Berggren et al., Impact Tests on Irradiated Pressure Vessel Steels, p. 147 in Solid State Division Annual Progress Report for Period Ending August 1962, USAEC Report ORNL-3364, Oak Ridge National Laboratory.

198. D. W. McLaughlin et al., Effect of Radiation Damage on SM-1, SM-1A, and PM-2A Reactor Vessels, USAEC Report APAE-107, General Electric Company, 1961.

199. C. Z. Serpan, Jr., L. E. Steele, and J. R. Hawthorne, Radiation Damage Surveillance of Power Reactor Pressure Vessels, NRL Report 6349, Naval Research Laboratory, 1966.

200. ASTM Standards, Part 31, E 184-62, Paragraph 4.1.2, Recommended Practice for Effects of High-Energy Radiation on the Mechanical Properties of Metallic Materials, American Society for Testing and Materials, Philadelphia, Pa., 1966.

201. C. Z. Serpan, Jr., et al., Yankee Reactor Pressure Vessel Surveillance: Evaluation of Specimens Exposed During the Second Core, NRL Report 6179, Naval Research Laboratory, 1964.

202. L. E. Steele, J. R. Hawthorne, and C. Z. Serpan, Jr., Irradiation Effects on Reactor Structural Materials, May–July 1964, NRL Memo Report 1556, Naval Research Laboratory, 1964.

203. L. E. Steele et al., Irradiation Effects on Reactor Structural Materials, May–July 1966, NRL Memo Report 1719, Naval Research Laboratory, 1966.

204. L. E. Steele et al., Irradiation Effects on Reactor Structural Materials, May–July 1965, NRL Memo Report 1938, Naval Research Laboratory, 1965.

205. L. E. Steele et al., Irradiation Effects on Reactor Structural Materials, November 1965–January 1966, NRL Memo Report 1676, Naval Research Laboratory, 1966.

206. F. A. Brandt and A. J. Alexander, Effect of Neutron Irradiation at 550°F on Charpy Impact Properties of ASTM A-302 Grade B Steel, in proceedings of Symposium on Radiation Effects on Metals and Neutron Dosimetry, ASTM STP No. 341, American Society for Testing Materials, Philadelphia, Pa., 1963.

207. F. A. Brandt, Environmental Exposure of Materials at the Dresden Nuclear Power Station, USAEC Report GECR-4352, General Electric Company, 1963.

208. M. S. Hersh, F. A. Brandt, and B. C. Beaudreau, Dresden Nuclear Power Station Reactor Vessel Steel Surveillance Program, USAEC Report GECR-5165, General Electric Company, 1966.

209. L. E. Steele, J. R. Hawthorne, and H. E. Watson, Irradiation Effects on Structural Materials, November 1962–January 1963, NRL Memo Report 1393, Naval Research Laboratory, 1963.

210. J. M. Monahan and P. A. Halpine, PM-2A Reactor Vessel Test — Phase I, USAEC Report WAPD-TM-604, Westinghouse Atomic Power Division, 1966.

211. J. M. Monahan and T. J. Walker, PM-2A Reactor Vessel Test — Description of Testing and Failure Conditions, USAEC Report WAPD-TM-640, Westinghouse Atomic Power Division, 1967.

212. J. R. Hawthorne, L. E. Steele, and W. S. Pellini, Effects of Nuclear Radiation on the Properties of Reactor Structural Materials, NRL Report 5731, Naval Research Laboratory, 1962.

213. L. E. Steele and J. R. Hawthorne, New Information on Neutron Embrittlement and Embrittlement Relief of Reactor Pressure Vessel Steels, p. 283 in Flow and Fracture of Metals and Alloys in Nuclear Environments, ASTM STP No. 380, American Society for Testing Materials, Philadelphia, Pa., 1965.

214. L. E. Steele, J. R. Hawthorne, and H. E. Watson, Irradiation Effects on Structural Materials, May–July 1963, NRL Memo Report 1448, Naval Research Laboratory, 1963.

215. W. R. Martin and J. R. Weir, The Effect of Irradiation Temperature on the Post-Irradiation Stress-Strain Behaviour of Stainless Steel, p. 251 in Flow and Fracture of Metals and Alloys in Nuclear Environments, ASTM STP No. 380, American Society for Testing Materials, Philadelphia, Pa., 1965.

216. W. R. Martin and G. M. Slaughter, Irradiation Embrittlement of Welds and Brazes at Elevated Temperatures, Welding J. Res. Suppl., 45: 385S (September 1966).

6. DESIGN OF NUCLEAR PRESSURE VESSELS*

Large pressure vessels of the type used in nuclear power plants are rather unique. This uniqueness is emphasized by the necessity of replacing whole reactor cores, by the multitude of vessel penetrations, by the transient operating conditions, by the importance of mechanical and fatigue life, by the size and weight of the vessel, and by the capital outlay. The most significant single item, however, is the importance of reliable operation to the safety of operating personnel and the general public. The discussions of this chapter are devoted to safety as it relates to the design of nuclear vessels.

Design has a variety of connotations. The term design here incorporates not only the sizing of the vessel and the related construction drawings but also the assessment of failure modes, the stress analysis, and the material selection. The stress analysis and failure modes are the main facets covered in this chapter. In this context, an adequate stress analysis includes effects of probable flaws and deviations in geometry.

The ductility of the structural steel is perhaps the most important feature of the pressure vessel. It is this plastic property that enables the vessel to yield under high peak or local stresses and thus accommodate the loading by a more favorable distribution of stresses. This plastic flow affects only local areas where high stresses prevail and, in general, does not affect the elastic behavior of the vessel as a whole. A loss of ductility then is of major concern in pressure vessel design. While the gross stresses, including discontinuity stresses, may be minimized in a vessel by good design, local defects and stress raisers, such as machine marks, flaws, out-of-tolerance dimensions, etc., are factors for concern. Severe economic penalties are often incurred to reduce or eliminate such defects or stress raisers.

Radiation effects on the behavior of nuclear pressure vessel material are also of concern in pressure vessel design. Irradiation

---

*This chapter was prepared by J. G. Merkle, S. E. Moore, and F. J. Witt of the Oak Ridge National Laboratory.

produces damage to the crystal structure of the metal to a degree not yet fully understood. The gross effect, however, is easily detectable. In general, irradiation tends to increase and bring closer together the yield point and ultimate tensile strength. Accompanying this are decreases in the ductility and impact strength. In particular, there is often a large increase in the nil-ductility transition (NDT) temperature and thus an increase in the possibility of brittle failure.

Theoretical methods of stress analysis are currently being developed that cover a wide variety of structural components. Methods based on linear elastic shell analyses have found special application to pressure vessels. Many computer programs based on these methods have been written. It should be realized, however, that all analytical methods are approximate. In general the more approximate the method the more simple it is. Thus, the adequacy and applicability of each analytical method must be judged when applying results from such methods to the design of pressure vessels. As the analytical methods are refined the factors of safety required to cover analytical uncertainties may be decreased, and thereby other factors desirable in a design may be better satisfied.

With the stresses determined the factors that govern the failure of a pressure vessel come into focus. Since even under irradiation some plastic flow may take place before failure occurs, the theories relative to failure of metals for combined loadings are important. Most of these theories are based on assumptions that the material is homogeneous and isotropic and that fracture under combined loadings can be related to invariant constants (usually some uniaxial properties of the material). The more common theories of failure with regard to plastic flow are (1) the maximum shear-stress theory (Tresca theory) and (2) the maximum-distortion strain-energy theory (octahedral shear stress or von Mises theory). The theories of failure with respect to fracture are (1) the maximum normal stress theory, (2) the maximum normal strain theory, (3) the maximum total strain-energy theory, and (4) the Griffith-Irwin theory (fracture mechanics). Only the maximum shear-stress theory and the Griffith-Irwin theory are presently being used in analyses of pressure vessels. These are the only theories discussed in detail here.

The maximum shear-stress theory has gained wide acceptance in the pressure vessel industry and is the basis for the allowable stresses defined in Section III of the ASME Boiler and Pressure Vessel Code. It is also always conservative. The Griffith-Irwin theory is significant in that it attempts to incorporate vessel flaws, such as machine marks, notches, etc., into the prediction of failure. Its application to brittle and near-brittle materials is especially important in examining heavily irradiated metals. Many recent papers are devoted to this subject.

Closely allied with the analytical methods are the necessary experimental programs that must be used in evaluation of the theories. Rather extensive basic experimental programs with both metal and photoelastic models have been conducted and many are currently under way. Supplementing these are the experimental examinations of scale models and actual vessels.

The design engineer is not left to his own innovations, experiences, judgements, and interpretations in designing a pressure vessel. The experience and judgement of engineers and researchers representing most of the areas considered in structural design and analysis are available to him, as documented in the ASME Boiler and Pressure Vessel Code. Originally the first commercial nuclear reactor vessels were designed to the requirements of Sections I and VIII of the ASME Code. More recently, however, Section III was published, and currently this section provides the requirements for primary nuclear containment vessels. It covers the basic areas of design, materials, fabrication, and inspection. Section III goes much further than Sections I and VIII in that it sets allowable stresses for safe limits that cover all types of applied stresses. The primary goal of this code is to provide requirements for new construction and for mechanical and thermal stresses due to cyclic operation. In particular, a stress analysis is required, and the fatigue loads of the vessel are limited.

Since Section III requires a complete stress analysis, the designer must have at his disposal the necessary analytical methods and related computer programs. Thus the basic tools of the theory of elasticity have become a necessary part of the design of pressure vessels built to

nuclear code standards. Since many regions of a pressure vessel are not yet amenable to analytical treatment (nonradial and cluster nozzles, nozzles in cylinders, etc.), methods that are very approximate must be utilized in the stress analysis. Unfortunately, these regions are usually the ones of major concern. Thus, backup experimental examinations continue to play a large role in the design of safe vessels.

A dilemma that confronts the designer is the mass of technical literature, which is often presented from a much too academic viewpoint. The designer is faced with considering all relevant technical information and deciding whether it can be used safely in design. Fortunately, various subcommittees of the Pressure Vessel Research Committee (PVRC) of the Welding Research Council and various professional societies offer assistance in sorting out the important contributions. Such information, if really pertinent, usually finds its way into revisions or interpretations of the ASME Code.

In this chapter the emphasis is on the stress analysis, in its broadest sense, and how such information is obtained and used in current nuclear pressure vessel design. A critique is presented of techniques and assumptions of various stress analysis methods. The significance of stresses and strains and how they are related to fracture are discussed. Also, a summary of current pressure vessel research is given. This is followed by a review of the degree of application of the methods and research in current vessel design. Finally the discussions are summarized, and areas in design that need further research and development are identified.

6.1 STRESS ANALYSIS OF PRESSURE VESSELS

The subject of stress analysis has always been important to the design of pressure vessels. For a number of reasons, however, stress analysis, as a separate subject, has not always played a very prominent role in the design and construction of pressure vessels. The reason for this seeming paradox is a very practical one, and its explanation requires an understanding of what stress analysis is.

It is important to make the distinction at this time between stress analysis and handbook design, since it has only been within the last three years that a comprehensive nuclear vessel code has been in general use which requires that the design of the pressure vessel be based upon an adequate stress analysis. This is not to imply that industry had not performed adequate stress analyses, only that now it is mandatory, whereas previously it was optional. A pertinent item of interest in this connection is that the Office of Technical Services, Department of Commerce, published a document[1] in 1958 that gave a set of design rules based on stress analysis methods. Since that time many nuclear vessel design specifications have included these rules, as well as the ASME Code rules.

Before either Section III of the ASME code or Ref. 1 was available, nuclear vessels were designed according to the rules of Sections I and VIII of the ASME code, and Sections I and VIII are still the basis for designing nonnuclear vessels and class C nuclear vessels. The rules presented provide a number of simplified formulas for computing plate thickness, reinforcements for vessel penetrations, support details, and so forth. These formulas include as a parameter the allowable stress for the different types of steel used in fabrication and were developed by the methods of stress analysis for the appropriate shape. The stress analysis, then, was left largely up to the code committee that wrote the rules. Appropriate safety factors were included in the formulas to account for various unknowns as experience and judgement indicated.

The advent of nuclear power and the importance of reliable vessel operation to public safety reopened the question of stress analysis for every reactor vessel. Studies concerning the failure of structures have continually reemphasized the close relationship between the state of stress at a particular location and the ultimate ability of the structure to perform satisfactorily. This means that in order to evaluate the reliability of a nuclear pressure vessel it is necessary to know the stresses at every point in the vessel. It is for this reason that the new rules of Section III place the responsibility for determining the stresses on the designer.

The exact magnitude of the stresses in an actual pressure vessel, however, can rarely be determined in any but the simplest cases. The

designer is therefore forced to use the best methods available, compute stresses by using idealized models, and check the accuracy and/or the degree of conservatism against carefully controlled experiments. The actual design process requires the knowledge of the locations at which stresses must be calculated, the knowledge of methods of analysis that agree with the best information available as to structural behavior at such locations, and a knowledge of the uncertainty factor of the calculated result.

This section describes what stress analysis is, with particular emphasis on the problems associated with the design of pressure vessels for the pressurized- and boiling-water reactors. A broad overall description of the theories of elasticity, shells, and strength of materials is given. Also, a description of analytical techniques used to determine the state of stress in a pressure vessel is presented. Finally, some of the techniques of experimental stress analysis are discussed that are currently being used either to verify theory or to answer specific questions when the theoretical solution is not available.

Results obtained by the use of procedures based on the theory of elasticity, shell theory, etc., are most useful to the designer if he remembers that failure can only result after inelastic deformation and stress redistribution, even in brittle fracture, and that his concepts of structural action should model real response in order to interpret the results of calculations based on elastic behavior. The designer must also remember that using computer programs as "black boxes" can lead to design errors when the assumptions, simplifications, and limitations of the computer program are not thoroughly understood.

6.1.1 Mathematical Theory of Elasticity

All the theories and applications of stress analysis have their roots in the generalized theory of elasticity as first formalized by Cauchy and Love in the latter part of the 19th century. Many good books have been written on the subject, and it is still being actively worked on. However, the present effort is directed primarily toward extensions and applications. The availability of the electronic computer has made

many problems tractable that, in the past, were of academic interest only. The linear theory for small deformations is for all practical purposes complete in the sense that all the necessary theorems, including uniqueness, are available. For the purposes at hand this is the only theory that needs to be considered.

The objective of the theory is to relate the point-by-point behavior of a solid elastic body in the presence of forces that tend to change the shape of the body. Since the response will change from one position in the body to another, the building block of the theory is a three-dimensional differential-sized element. It is virtually impossible to discuss the theory in a comprehensive manner without using the language of mathematics. In a discussion of this type, a complete discourse on the theory would be out of place. However, in order to lay a groundwork for later discussion, it is necessary to discuss the basic elements and terms used in some detail.

It is convenient to reference each variable to some fixed coordinate system; for example, the Cartesian x,y,z system. The differential element associated with the Cartesian coordinate system is a cube. It is well to remember, however, that real behavior is being discussed, and therefore any equations that are written must be true no matter what coordinate system is used for reference. It will therefore be possible to transform the equations from one coordinate system to another whenever it is of advantage to do so.

There are four sets of primary variables in the theory of elasticity. These are (1) the displacements, u_i, (2) the strains, ϵ_{ij}, (3) the stresses, τ_{ij}, and (4) the body forces, F_j. The sets of primary variables are related to each other by connecting equations. For example, the displacements and strains are related by the strain-displacement relations. The development of the strain-displacement relations and an associated set, the compatibility equations, is the subject of the theory of strain. The strains and stresses are related by a materials law, such as Hooke's law, for elastic materials. In its most general form Hooke's law contains 81 arbitrary constants that must be evaluated from laboratory data. The behavior of most common engineering materials and most mathematical solutions is expressed in terms of only two arbitrary

constants; the others are eliminated by mathematical arguments. The stresses and body forces are related by the equilibrium equations. These equations and various associated equations are the subject of the theory of stress.

One of the best ways of illustrating the theory is to organize the component expressions in diagram form, as follows:[2]

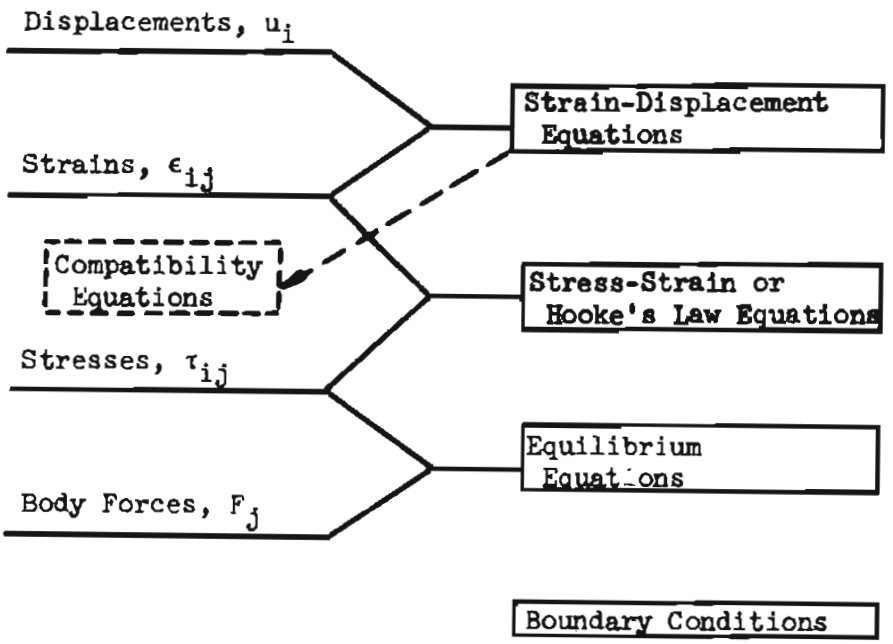

Solutions to problems in the theory of elasticity have received a considerable amount of attention in the past by many of the greatest mathematicians. In view of the complexity of the mathematics (there are 15 coupled partial differential equations in 18 separate primary variables subject to an unspecified number of boundary conditions), it is small wonder that many approximate solutions but few "exact" solutions have been found for many structures of practical interest.

6.1.1.1 Displacements and Strains

The displacements (u,v,w) are a measure of how much the differential element has moved in each of the coordinate directions (x,y,z); see Fig. 6.1. Since each point in the body will, in general, undergo a displacement different from every other point, u, v, and w are functions

ORNL-DWG 67-3787

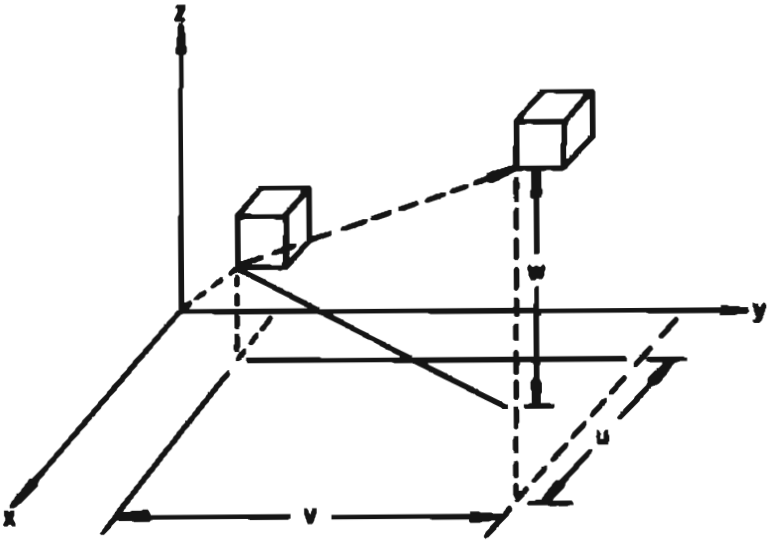

Fig. 6.1. Displacement Components in the Cartesian Coordinate System.

of the coordinates. The displacements may be taken as either functions of their original positions (i.e., in the unstressed state) or of their final position (i.e., in the stressed state). It is more convenient in the study of solid bodies to describe the displacements as functions of the original position.* Thus $u(x,y,z)$ refers to the displacement of the element originally at position (x,y,z) in the x directions, whereas $v(x,y,z)$ refers to the displacement in the y direction. The notation is often condensed for simplicity to the index form u_i, where the subscript i takes on the directions of the coordinate system; thus $u_x = u(x,y,z)$, $u_y = v(x,y,z)$, and $u_z = w(x,y,z)$.

The second set of primary variables, the strains, are a measure of the change in shape of the differential element. Since a differential cube may not only be stretched in each of the three directions but also may become distorted, there are in general nine strain components (see Fig. 6.2). The three strains normal to the faces of the element are called normal strains ϵ_x, ϵ_y, ϵ_z. The other six components measure the

*For a more complete discussion of the reasons, see Chapter 1 of Ref. 3.

ORNL-DWG 67-3788

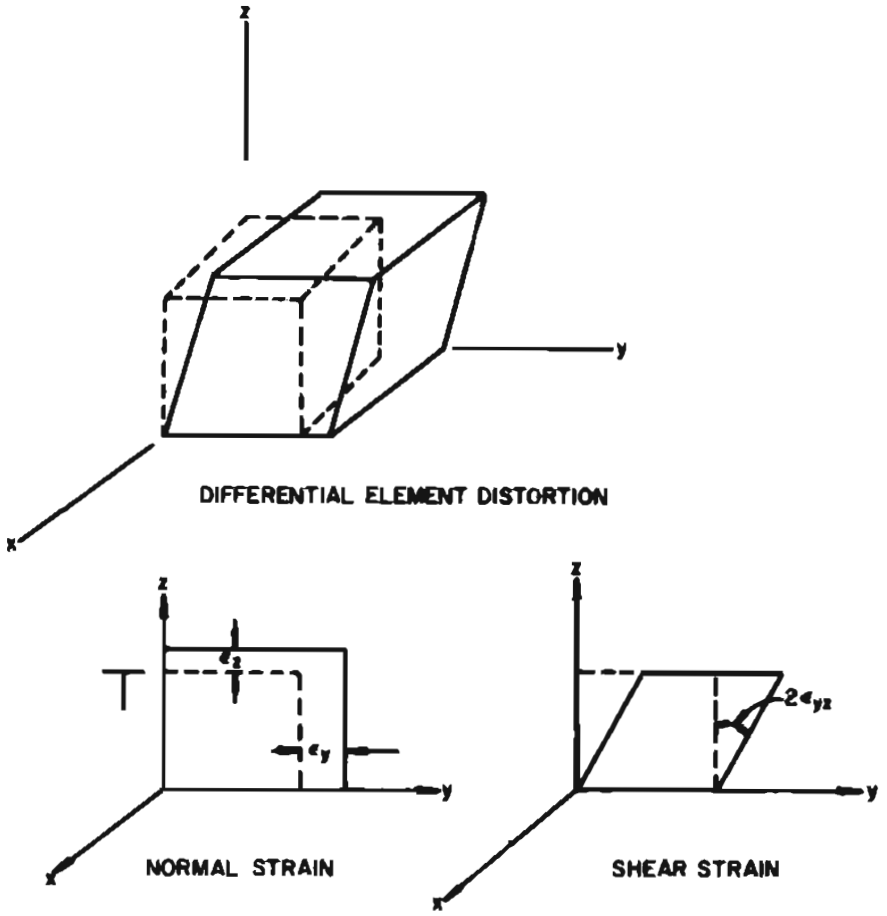

Fig. 6.2. Strain Components in the Cartesian Coordinate System.

changes in the angles between the edges at the corners of the cube. These are called shear strains. For "small" deformations, any other distortions of the cube can be neglected relative to the normal and shear strain components. As in the case of the displacement variables, the strain variables are also functions of the coordinate position of the differential element. Thus, $\epsilon_x(x,y,z)$ is the normal strain in the x direction of the differential element located at position (x,y,z), $\epsilon_{xy}(x,y,z)$ is a shear strain, etc. The index form of the strain variables is ϵ_{ij}, where each of the subscripts takes on the directions of the coordinate system so that $\epsilon_{xx} = \epsilon_x(x,y,z)$, $\epsilon_{xy} = \epsilon_{xy}(x,y,z)$, etc. It can be shown[4] that for small deformations, $\epsilon_{xy} = \epsilon_{yx}$, $\epsilon_{yz} = \epsilon_{zy}$, and $\epsilon_{zx} = \epsilon_{xz}$; that is, the strain tensor is said to be symmetrical. The

nine strain components thus reduce to six independent variables. It should be noted that some authors (e.g., Timoshenko) define the shear strains γ_{ij} as the total change in the angles between the edges rather than 1/2, as was done here. Then, $\gamma_{ij} = 2\epsilon_{ij}$; $i \neq j$.

The displacement variables u_i and the strain variables ϵ_{ij} are related to each other by the strain-displacement equations. Since the displacements are continuous functions of the space coordinates, it should be expected that the strains are related to the rate of change of the displacements with respect to the space coordinates. That this is true can be seen by imagining a line AB of length Δy drawn on the x face of the differential element parallel to the y direction (see Fig. 6.3). If the element is stretched in the y direction an amount δ_y, the strain in the y direction, ϵ_y, is given by $\epsilon_y = \delta_y/\Delta y$, which is also equal to the difference between the displacements of the points A and B divided by the base length Δy; thus,

$$\epsilon_y = \frac{\delta_y}{\Delta y} = \frac{u_y(B) - u_y(A)}{\Delta y} .$$

In the limit this becomes

$$\epsilon_y = \lim_{\Delta y \to 0} \frac{u_y(B) - u_y(A)}{\Delta y} = \frac{\partial u_y}{\partial y} .$$

The relations between the other strain components and the displacements can be developed in a similar manner. Six equations called the strain-displacement relations result and are[5]

$$\epsilon_x = \frac{\partial u_x}{\partial x} , \qquad \epsilon_{xy} = \frac{1}{2}\left(\frac{\partial u_x}{\partial y} + \frac{\partial u_y}{\partial x}\right) ,$$

$$\epsilon_y = \frac{\partial u_y}{\partial y} , \qquad \epsilon_{yz} = \frac{1}{2}\left(\frac{\partial u_y}{\partial z} + \frac{\partial u_z}{\partial y}\right) ,$$

$$\epsilon_z = \frac{\partial u_z}{\partial z} , \qquad \epsilon_{zx} = \frac{1}{2}\left(\frac{\partial u_z}{\partial x} + \frac{\partial u_x}{\partial z}\right) .$$

ORNL-DWG 67-3789

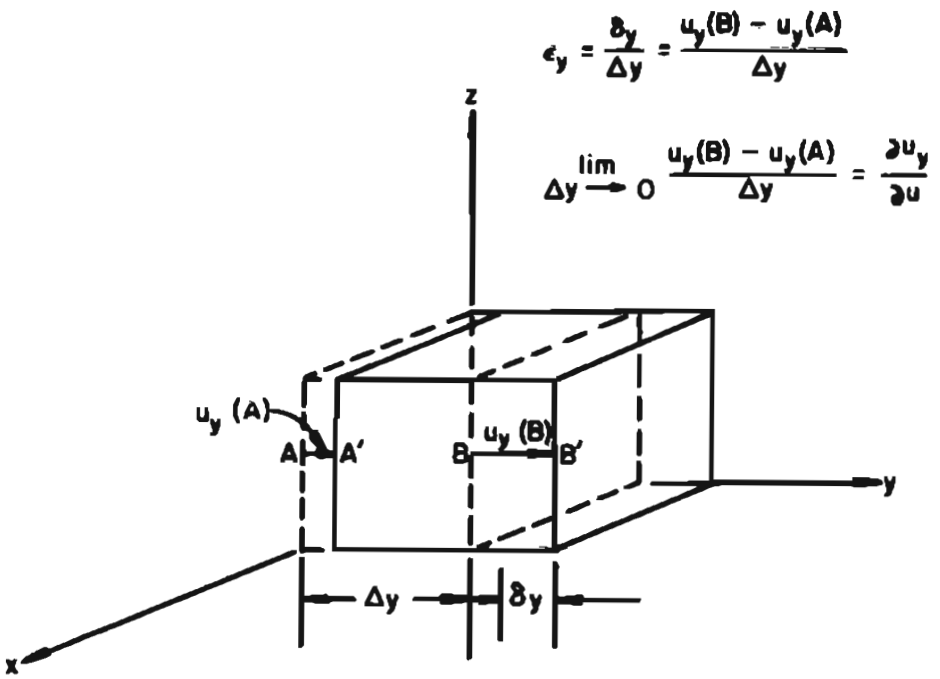

Fig. 6.3. Strain-Displacement Relationships in the Cartesian Coordinate System.

If the coordinate system is relabeled so that the directions x, y, and z are given by the subscript variables x_1, x_2, and x_3, these six relations can be written in compact notation as

$$\epsilon_{ij} = \frac{1}{2}\left(\frac{\partial u_i}{\partial x_j} + \frac{\partial u_j}{\partial x_i}\right), \qquad i,j = 1,2,3 .$$

In this form $\epsilon_{12} = \epsilon_{xy}$ when i and j take on values 1 and 2, respectively.

There is one final set of equations necessary to the discussion of displacements and strains. These are the compatibility equations. It can be appreciated that in a continuous body not every set of displacements or strains is possible. The compatibility equations form the necessary restrictions for eliminating all the inadmissible values and insuring that all the differential elements will still fit together after distortion. In a mathematical sense it can be argued that since the six strain components are completely determined by three displacement

functions, u_x, u_y, and u_z, there must exist additional relations between the strain components. These can be derived by eliminating the displacement variables from the six strain-displacement equations by mathematical manipulation. The resulting relations (compatibility equations) are the set of six second-order partial differential equations given here without proof:[6]

$$\frac{\partial^2 \epsilon_{xx}}{\partial y \partial z} = \frac{\partial}{\partial x}\left(-\frac{\partial \epsilon_{yz}}{\partial x} + \frac{\partial \epsilon_{zx}}{\partial y} + \frac{\partial \epsilon_{xy}}{\partial z}\right), \qquad \frac{2\partial^2 \epsilon_{xy}}{\partial x \partial y} = \frac{\partial^2 \epsilon_{xx}}{\partial y^2} + \frac{\partial^2 \epsilon_{yy}}{\partial x^2},$$

$$\frac{\partial^2 \epsilon_{yy}}{\partial z \partial x} = \frac{\partial}{\partial y}\left(\frac{\partial \epsilon_{yz}}{\partial x} - \frac{\partial \epsilon_{zx}}{\partial y} + \frac{\partial \epsilon_{xy}}{\partial z}\right), \qquad \frac{2\partial^2 \epsilon_{yz}}{\partial y \partial z} = \frac{\partial^2 \epsilon_{yy}}{\partial z^2} + \frac{\partial^2 \epsilon_{zz}}{\partial y^2},$$

$$\frac{\partial^2 \epsilon_{zz}}{\partial x \partial y} = \frac{\partial}{\partial z}\left(\frac{\partial \epsilon_{yz}}{\partial x} + \frac{\partial \epsilon_{zx}}{\partial y} - \frac{\partial \epsilon_{xy}}{\partial z}\right), \qquad \frac{2\partial^2 \epsilon_{zx}}{\partial z \partial x} = \frac{\partial^2 \epsilon_{zz}}{\partial x^2} + \frac{\partial^2 \epsilon_{xx}}{\partial z^2}.$$

One of the more difficult aspects of applied elasticity is the complete satisfaction of the compatibility equations. It is for this reason that special classes of problems, such as axisymmetric and plane-strain problems, are discussed in the literature. There is one point of special interest, however, which is important to the discussion of shells. If it is possible to formulate a problem in terms of displacements u,v,w, the compatibility equations will be automatically satisfied. Whether it is possible to do this conveniently depends largely on how the boundary conditions are written. The only restrictions that have so far been imposed are that all deformations are sufficiently small that higher order terms may be neglected (i.e., the distortion of a cube is restricted to the shape of a parallelopiped).

6.1.1.2 Forces and Stresses

The last two sets of variables, the stresses and the forces, are best discussed in reverse order. For analyzing the forces acting on the differential element, it is necessary to take into account two types of forces: (1) the body (or volume) forces, which are proportional to the

mass in the element, and (2) the surface forces, which act on the faces of the differential cube. Examples of body forces are those that arise from gravitational fields, magnetic fields, and/or accelerated motion. It is apparent that, in general, the total body force is a directed quantity or a vector $\vec{F}$ with components in each of the three coordinate directions F_x, F_y, F_z, or simply F_j, with $j = 1,2,3$.

An example of surface force is the tension acting on any horizontal section of a steel rod suspended vertically. If it is imagined that the rod is cut by a horizontal plane into two parts, the upper and the lower, the action of the weight (body force) of the lower part of the rod is transmitted to the upper part across the surface of the cut. The stress variables are defined as the components of the surface forces acting on the face of the element divided by the area.

A more direct explanation is in terms of the stress vector, which represents the surface force per unit area acting on the elemental face. The stress components are the normal and tangential components of the stress vector acting in the coordinate directions (see Fig. 6.4), where the normal stresses are denoted by σ_x, σ_y, σ_z or τ_{xx}, τ_{yy}, τ_{zz} and the tangential or shear stresses are denoted by τ_{xy}, τ_{yz}, τ_{zx}, τ_{xz}, τ_{zy}, and τ_{yx}. The first subscript indicates the face (the x face is perpendicular to the x coordinate axis, etc.), and the second subscript indicates the positive direction of the stress component. Thus, $\tau_{xx} = \sigma_x$ denotes the normal stress acting on the x face in the x direction, whereas τ_{xy} denotes the tangential or shear stress acting on the x face in the y direction, etc. Taken all together the nine stress components are the components of a tensor τ_{ij}, which is also symmetrical, as is the strain tensor ϵ_{ij}. Thus, $\tau_{xy} = \tau_{yx}$, $\tau_{yz} = \tau_{zy}$, and $\tau_{zx} = \tau_{xz}$, or in index notation, $\tau_{ij} = \tau_{ji}$.

The stress variables, τ_{ij}, and the body forces, F_j, are related by the equilibrium equations necessary to satisfy static equilibrium of the entire body. The physical significance of these equations is, in a sense, similar to the significance of the compatibility equations. In order for each individual differential element, as well as the entire body, to be in static equilibrium, it is necessary that the stresses on companion faces of adjacent differential elements be the same, even though the values of the stress components will vary as a function of position.

ORNL-DWG 67-3790

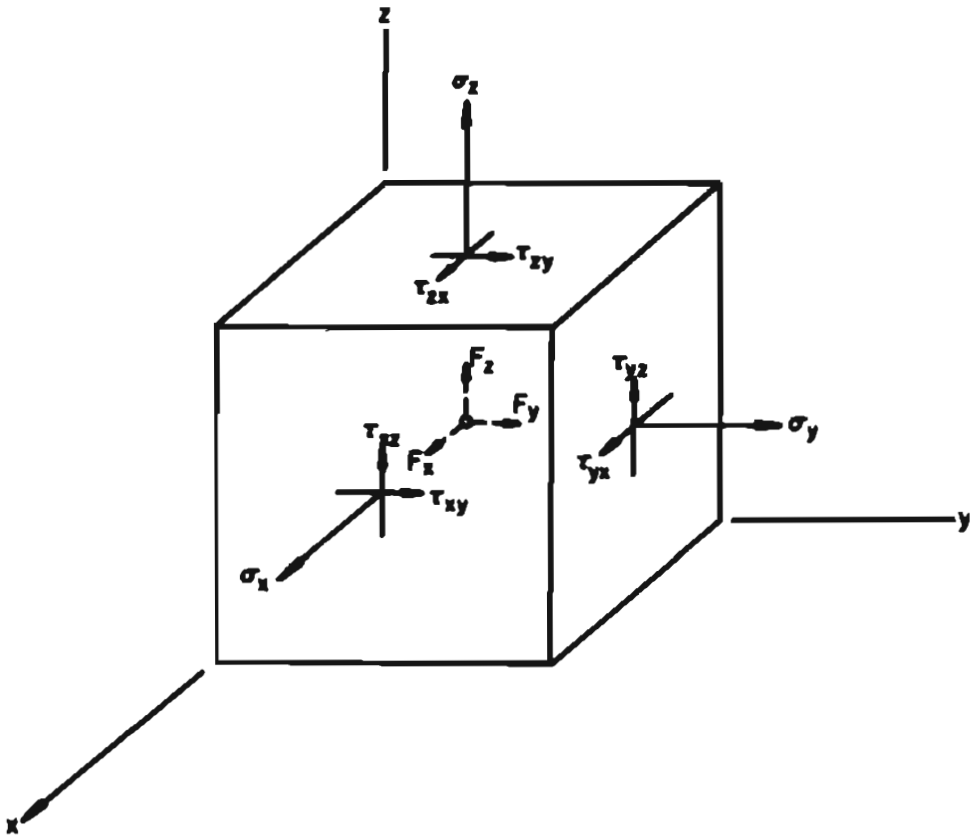

Fig. 6.4. Stress Components in the Cartesian Coordinate System.

The equilibrium equations are expressions of force balance and result in first-order partial differential equations, as follows:[7]

$$\frac{\partial \tau_{xx}}{\partial x} + \frac{\partial \tau_{yx}}{\partial y} + \frac{\partial \tau_{zx}}{\partial z} = -F_x \ ,$$

$$\frac{\partial \tau_{xy}}{\partial x} + \frac{\partial \tau_{yy}}{\partial y} + \frac{\partial \tau_{zy}}{\partial z} = -F_y \ ,$$

$$\frac{\partial \tau_{xz}}{\partial x} + \frac{\partial \tau_{yz}}{\partial y} + \frac{\partial \tau_{zz}}{\partial z} = -F_z \ .$$

Since these are first-order equations, they are, in general, easier to satisfy than the compatibility equations. This fact has led to the development of "stress function" methods for the solution of many specific problems.

6.1.1.3 The Stress-Strain Relations

All the variables and the interrelationships shown on Fig. 6.4 have been discussed except the stress-strain relations. All the equations above were derived on strictly a mathematical basis without the need for experimental data. It is generally true, then, that these equations will hold for a very wide class of materials regardless of whether the material is elastic. However, the theory of elasticity deals with the class of materials that obeys, over a restricted region, a very specific formulation of the stress-strain relations, Hooke's law. In order to validate a set of stress-strain relations it is always necessary to resort to experiment and measure the relations between the stresses and strains for a given material under given environmental conditions.

For an isotropic homogeneous elastic material, Hooke's law is the set of six equations relating the stress variables to the strain variables:[8]

$$\epsilon_x = \frac{1}{E}\left[\sigma_x - \nu(\sigma_y + \sigma_z)\right] , \qquad \epsilon_{xy} = \frac{1+\nu}{E}\,\tau_{xy} ,$$

$$\epsilon_y = \frac{1}{E}\left[\sigma_y - \nu(\sigma_z + \sigma_x)\right] , \qquad \epsilon_{yz} = \frac{1+\nu}{E}\,\tau_{yz} ,$$

$$\epsilon_z = \frac{1}{E}\left[\sigma_z - \nu(\sigma_x + \sigma_y)\right] , \qquad \epsilon_{zx} = \frac{1+\nu}{E}\,\tau_{zx} .$$

where E is the elastic Young's modulus and ν is Poisson's ratio.

It is easy to see how other theories of solid mechanics (and also fluid mechanics to a certain degree), such as the theory of plasticity, come about. Hooke's law is simply replaced by other appropriate stress-strain relations.

6.1.1.4 Principal Stresses and Stress Intensity

Earlier it was remarked that sometimes it is convenient to change the reference coordinate system for one reason or another. Calculation of the "stress intensity" at a point is one of these times. Failure theories are most conveniently expressed in terms of the principal stresses. In particular the maximum shear-stress theory specified by Section III of the ASME Code as the criterion for stress evaluation is expressed as the difference between the algebraically largest and smallest principal stresses at a point. This is, by definition, the stress intensity.

The principal stresses are determined by rotating the coordinate system at the point in question in such a way that the shear stresses in the new coordinate directions vanish. The remaining normal stresses are called principal stresses and the coordinate directions are the principal stress directions. The values of the principal stresses (S) are given by the three roots of the cubic equation[8]

$$S^3 - \theta_1 S^2 + \theta_2 S - \theta_3 = 0 ,$$

where the θ_i are the three stress invariants and are given by

$$\theta_1 = \sigma_x + \sigma_y + \sigma_z ,$$

$$\theta_2 = \sigma_x\sigma_y + \sigma_y\sigma_z + \sigma_z\sigma_x - \tau_{xy}^2 - \tau_{yz}^2 - \tau_{zx}^2 ,$$

$$\theta_3 = \sigma_x\sigma_y\sigma_z + 2\tau_{xy}\tau_{yz}\tau_{zx} - \sigma_x\tau_{yz}^2 - \sigma_y\tau_{zx}^2 - \sigma_z\tau_{xy}^2 .$$

Standard techniques are available for solving cubic algebraic equations.[9] However, a somewhat easier and in many cases more practical method for determining the principal stress magnitudes is by using Mohr's circle of stress[10] when the magnitude and direction of one of the principal stresses are known. For example, at the inner surface of a pressurized part, one of the principal stresses is equal to the negative of the pressure acting normal to the surface. For many pressure vessel calculations the principal stresses are identical to the stresses in the original coordinate direction (i.e., when the shear stresses are all zero).

6.1.1.5 Thermal Stresses

Both Ref. 1 and Section III of the ASME Code require that thermal stresses be computed and accounted for in nuclear pressure vessel design. Thermal stresses arise because of the tendency for materials to expand and/or contract without distortion as a function of a change in temperature. Obviously the parameters that describe this tendency (the coefficients of thermal expansion, α) are material properties, and the only place to incorporate them into the equations of elasticity is in the stress-strain relations.

The theory of thermal stresses results from adding a single term, $\alpha_i T$, to each of the three normal strain equations, where T is the temperature above some arbitrary reference temperature. Since a change in temperature changes only the volume of an unrestrained differential element and not its shape, it is not appropriate to add terms to the shear-stress-strain equations. For an isotropic material that changes volume uniformly in every direction, the stress-strain equations become

$$\epsilon_x = \frac{1}{E}\left[\sigma_x - \nu(\sigma_y + \sigma_z)\right] + \alpha T , \qquad \epsilon_{xy} = \frac{1+\nu}{E}\tau_{xy} ,$$

$$\epsilon_y = \frac{1}{E}\left[\sigma_y - \nu(\sigma_z + \sigma_x)\right] + \alpha T , \qquad \epsilon_{yz} = \frac{1+\nu}{E}\tau_{yz} ,$$

$$\epsilon_z = \frac{1}{E}\left[\sigma_z - \nu(\sigma_x + \sigma_y)\right] + \alpha T , \qquad \epsilon_{zx} = \frac{1+\nu}{E}\tau_{zx} .$$

This is a rather innocent looking addition to the theory of elasticity, and it would not be expected that there would be much difficulty in properly taking it into account. By and large this is true. If it is possible to solve the problem without the thermal expansion terms, a number of standard techniques are also available for solving the thermal-stress problems,[11] provided the temperature distribution in the body can be determined. However, determining the temperature as a function of both position and time can be a major problem, especially if transients in the system cause either large or rapid changes in the temperatures of the body surfaces.

An interesting consequence of the thermal stress theory formulation is that for traction-free bodies (i.e., unconstrained boundaries) zero stresses result everywhere if the temperature distribution is either uniform or varies as a linear function of the Cartesian (x,y,z) coordinate system. Strains and displacements do, of course, exist; normal strains are equal to αT, shear strains are zero, and the displacements are either uniform or linear in the Cartesian coordinate system. Stresses therefore arise only from external constraints that prevent the body from expanding and/or from temperature distributions that differ from a linear function.

Stresses that arise solely as a result of nonlinear temperature distributions (called internal thermal stresses) are self-limiting, since in order to satisfy the equilibrium equations, both tensile and compressive stresses must be distributed in equal quantity. This implies that if any response of the structure causes a reduction in, say, the internal tensile thermal stresses at a point (for example, if yielding occurs), a reduction and redistribution of the internal thermal stresses throughout the structure also occurs. Section III of the ASME Code rules gives credit for this property in allowing higher allowable values of the stress intensity for this type of thermal loading. Thermal stresses arising as a result of preventing displacements, such as those that occur because of different coefficients of thermal expansion or different temperatures in adjacent bodies, must be treated as ordinary discontinuity stresses. These types of stresses are discussed later.

6.1.2 Theory of Shells

In the theory of elasticity, the term shell is applied to structural shapes that are bound by two curved surfaces a small distance apart, that is, small compared with the other dimensions. Thus, if a pressure vessel were segmented into all its various structural shapes, most of these would be classified as shell segments as, for example, the cylindrical body and the spherical heads. A complete discussion of the general theory of shells would be out of place here because of the necessary mathematical development. However, it is important to know that a general theory does

exist and that a number of important problems have been solved in closed form. At the present time the theory of thin shells (and curved plates) is one of the more active branches of the theory of elasticity. To quote Novozhilov from the preface of Thin Shell Theory,[12]

> This is explained by the fact that thin-walled shell constructions combine light weight with high strength, as a result of which they have found wide application in naval, aeronautical and boiler engineering as well as in reinforced concrete roof designs. It must be emphasized that the practical possibilities of the utilization of shells have by no means been exhausted and we are all the time witnesses to the perfection of different types of construction; on the one hand this takes the form of an extension of the range of employment of shells, on the other hand, of a more thorough analysis of their properties (i.e., by improvement of the methods of stress analysis).

One of the ways in which the technologist is improving the methods of stress analysis is to automate much of the computational effort by writing computer programs. It is therefore possible and is fast becoming necessary to stress analyze pressure vessels more thoroughly. Fortunately, the shells most important to the pressure vessel industry are axisymmetric shells; that is, shells that can be generated by revolving a curved line segment about a central axis. The general theory can be significantly simplified for this class of shells.

There are eight simplifying assumptions in the theory of elasticity that result in the theory of shells. These assumptions follow:[13]

1. Shells are "thin," $h/R \ll 1$. This is to say that the ratio of the thickness to the radius of curvature is much less than 1. If $h/R \leq 1/20$, the relative error is less than 5%.

2. Displacements are small in comparison with the thickness.

3. Edge cuts or boundaries of the shell segment are perpendicular to the middle surface. Middle surface, thickness, and edges completely define the geometry, where the middle surface is defined as the locus of points that lie midway between the two structural surfaces. This is an extremely important assumption in that it defines the minimum size of the differential element as being as thick as the shell. As a result the primary variables of stress and strain in the theory of elasticity are replaced by stress resultants and strain parameters that describe the curvature change, bending, and twisting of the structure at the level

of the differential element in terms of what happens to the middle surface.

4. Lines that were perpendicular to the middle surface before deformation remain so after deformation and remain of constant length. This is to say that a shell will not get thinner by being stretched.

5. The normal stresses on planes parallel to the middle surface may be neglected in comparison with the other stresses (i.e., stresses through the thickness of the shell are neglected).

6. The shell is of constant thickness. There are exceptions to this assumption in which the shell may change thickness in some prescribed manner. However, the thickness change must be small and gradual in order for the solution to be valid in light of the other assumptions.

7. The material is isotropic and obeys Hooke's law, including thermal strain terms, where appropriate. This assumption is common to most stress analysis problems and is important in that the material is presumed to have the same physical properties in all directions. Since forming operations are known to introduce some anisotropy, it is important for a valid stress analysis that the degree of anisotropy be checked. There is an anisotropic theory of shells[14] that can be used to evaluate the effects of directional properties; however, it is not in general use.

8. The reference coordinate system is curvilinear; that is, it is described by the lines of principal curvature of the middle surface and the perpendicular distance from the middle surface of the shell. Adoption of the general curvilinear coordinate system considerably simplifies writing the basic theory.

It is also generally assumed, but never explicitly stated, that the shell surface has no sharp discontinuities. This assumption is actually a direct consequence of assumption 3 above. For if a sharp discontinuity did exist, the surface normal would be undefined at that position and the boundaries of the shell segment would be arbitrary. This is often the case when shell segments of different geometry are joined in a structure. Good design practice is to provide smooth transitions in these areas whenever possible. It should be recognized, however, that even in the absence of smooth transition, a consequence of describing the shell

as a mathematical surface is that the fine structure of the stresses and strains in a discontinuity region is ignored. The stresses in regions of discontinuity are most often the highest stresses in a vessel, and a considerable amount of research is currently being done in this area. It is encouraging, however, that analytical predictions based on shell theory are quite often conservative. At present there is no entirely satisfactory analytical means for determining the stresses in the local region of discontinuities, for example, at penetrations in the main vessel. One of the reasons is that the basic assumptions of shell theory are not entirely valid at these regions. A rational approach for design is to analyze the structure by using shell theory and then modify the results by experimental means. Recent developments in numerical solutions to theory-of-elasticity problems should also help in investigating these regions. More discussion of this subject will be found in Section 6.3.

Ten stress resultants are introduced to replace the six primary stress variables τ_{ij}, with the normal stress through the thickness set equal to zero, $\tau_{33} = \sigma_t = 0$ (assumption 5). These are called traction forces and bending and twisting moments.* By denoting the orthogonal curvilinear shell coordinates as x and y in the shell midsurface and z perpendicular to the shell surface (see Fig. 6.5), the stress resultants are defined in terms of the integrals of the stress variables through the shell thickness and the two principal curvature radii r_1 and r_2, as follows:

$$N_x = \int \sigma_x \left(1 - \frac{z}{r_2}\right) dz \ , \qquad N_y = \int \sigma_y \left(1 - \frac{z}{r_1}\right) dz \ ,$$

$$N_{xy} = \int \tau_{xy} \left(1 - \frac{z}{r_2}\right) dz \ , \qquad N_{yx} = \int \tau_{yx} \left(1 - \frac{z}{r_1}\right) dz \ ,$$

$$Q_x = \int \tau_{xz} \left(1 - \frac{z}{r_2}\right) dz \ , \qquad Q_y = \int \tau_{yz} \left(1 - \frac{z}{r_1}\right) dz \ ,$$

*An excellent description of shell theory is given by Langhaar.[15]

ORNL-DWG 67-3791

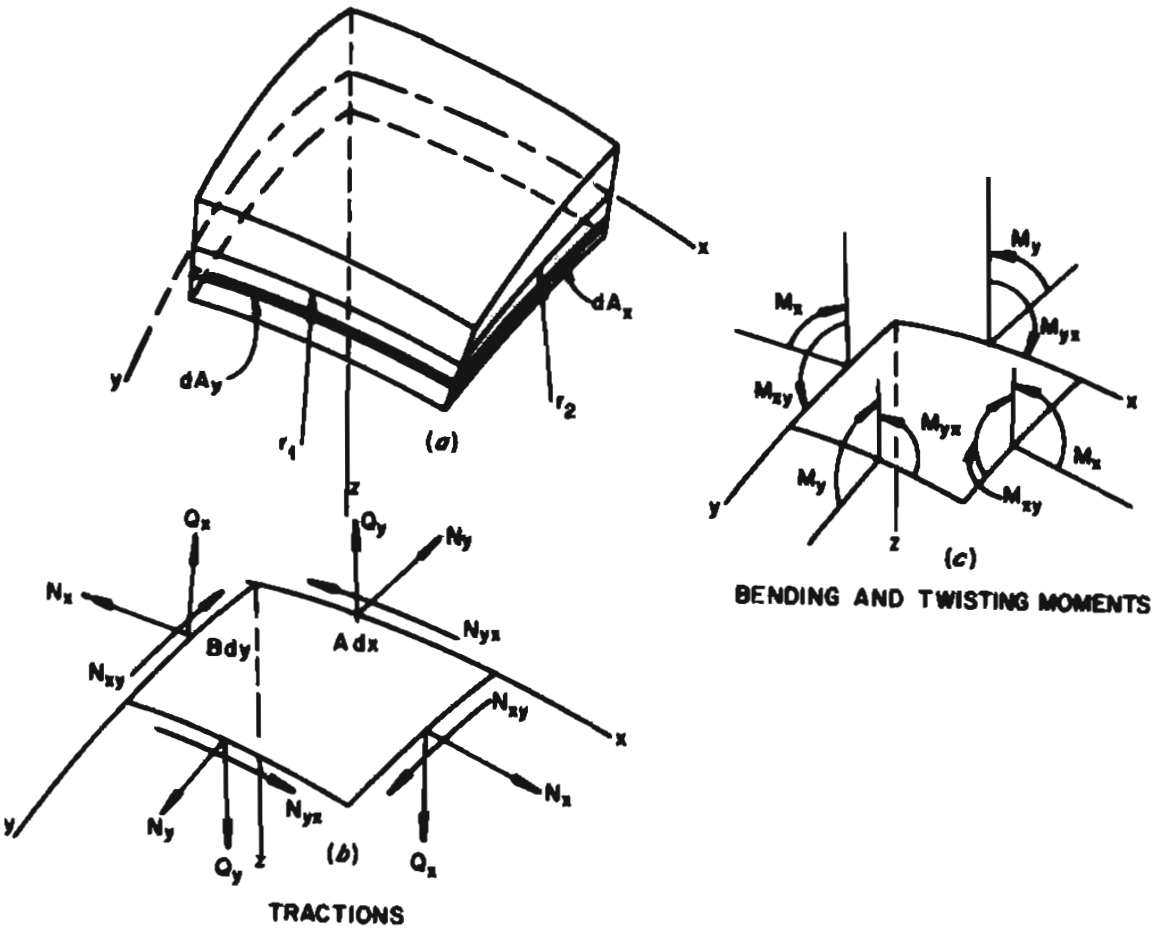

Fig. 6.5. Differential Shell Element and Stress Resultants.

and

$$M_x = \int z \left(1 - \frac{z}{r_2}\right) \sigma_x \, dz \ , \qquad M_y = \int z \left(1 - \frac{z}{r_1}\right) \sigma_y \, dz \ ,$$

$$M_{xy} = \int z \left(1 - \frac{z}{r_2}\right) \tau_{xy} \, dz \ , \qquad M_{yx} = \int z \left(1 - \frac{z}{r_1}\right) \tau_{xy} \, dz \ .$$

The strain parameters are similar to the stress resultants in that the primary variables of the theory of elasticity are replaced by variables that define the behavior of the shell differential element in terms of the middle-surface behavior. The mathematical descriptions[15,16] of

these variables appear more complicated than those for the stress resultants because they involve terms from the differential geometry of curved surfaces; they will therefore not be given here.

Since the primary variables of stress and strain are replaced by stress resultants and strain parameters, Hooke's law can also be converted. This is not entirely a straightforward process, and at least three different formulations appear in the literature. At any rate, enough equations can be written to complete the set, and the result is finally precisely as many equations as unknown variables.

A ladder diagram for the general shell theory may now be constructed, as follows:

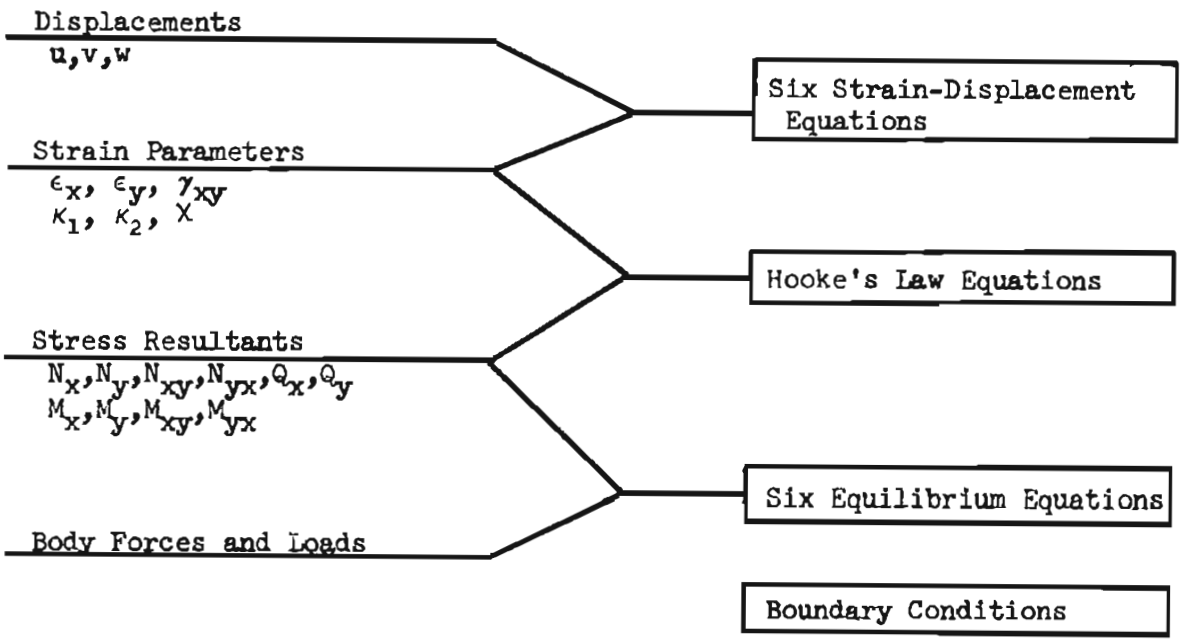

The mathematical process of solving shell problems is quite similar to that for solving problems in the theory of elasticity; that is, a solution must be found that will satisfy all three sets of equations subject to the boundary conditions. There are various ways of doing this that depend on the particular problem being investigated. The most obvious first step is to reduce the number of equations by eliminating variables, and there are at least two ways in which this can be done. One way is to set certain terms equal to zero by physical arguments for

the particular problem. The so-called "membrane" or "momentless" theory results from setting moments M_x, M_y, M_{xy}, and M_{yx} equal to zero. Some shells have very little resistance to bending forces, such as very thin shells or rubber balloons. The bending moments can therefore be neglected relative to the other stress resultants. In other cases, the known boundary conditions do not involve bending moments at the edges, and the shell shape is such that internal bending will not result from direct forces, like a hemisphere under internal pressure. The theory for axisymmetric shells is another result of setting terms equal to zero, provided the boundaries of the shell segment are also axisymmetric; that is, the boundary cuts are perpendicular to the axis of revolution. In this case it can be argued on the basis of symmetry that the twisting terms γ_{xy}, M_{xy}, M_{yx}, N_{xy}, N_{yx}, and Q_y are zero, as well as the unsymmetrical loading terms. The theory of shallow shells results from setting the curvature terms, κ_1 and κ_2, equal to zero. The result of setting certain variables to zero is that frequently a number of the fundamental equations are identically satisfied. This, of course, means that the difficulties associated with finding a solution that satisfies the remaining equations are considerably reduced. A second way of eliminating variables is by the process of substitution.

By using both these methods it is possible in certain cases to reduce the problem of satisfying all the fundamental equations subject to the boundary conditions to a problem of satisfying one equation subject to the same boundary conditions. A simple example is the problem of a cylindrical shell loaded axisymmetrically with an internal pressure.[17] In this case the partial differential equations can be reduced to the single ordinary differential equation

$$\frac{d^4w}{dx^4} + Aw = B ,$$

where A and B are constants evaluated from known geometry and loading terms. This differential equation is easily solved for w in terms of elementary trigonometric functions and four arbitrary constants. Thus, an algebraic equation for the deflection w is available that can be back

substituted into all the equations that were eliminated by mathematical manipulation. The resulting algebraic equations thus completely define the behavior of a cylindrical shell in terms of dimensions and prescribed loads. The arbitrary constants resulting from the solution to the differential equation are evaluated by using the boundary conditions expressed in terms of the deflection w.

Other shell problems have been solved in a manner somewhat similar to the cylindrical shell problem. Some of these problems, which are particularly important to pressure vessel design and have closed-form solutions, are the axisymmetrically loaded spherical shell,[18] conical shell,[19] and ellipsoidal shell.[20] The solution for certain nonsymmetric loadings on the spherical shell is also available. Numerical methods and computer programs that generate solutions for axisymmetric shells of arbitrary shape have also been developed.[21] However, the number of solutions presently available is not impressive. The reasons are varied but the major difficulty is in finding a solution that not only satisfies the partial differential equations but will also satisfy arbitrary conditions or a particular set of boundary conditions.

There are two problems without solutions at present that are of special interest in the design of nuclear pressure vessels. These are noncircular boundaries and boundaries that are nonaxisymmetric in the sphere, cylinder, cone, and ellipsoid such as would result from intersecting these shells with a cylinder (or pipe) at an oblique angle.

6.1.3 Strength of Materials

It was stated above that a pressure vessel could be divided into a number of segments, some of which are shell segments. The other segments, such as the closure flanges, support rings, and brackets, fall within the class of problems covered by the theory of strength of materials. For formal study this is often the only subject in solid mechanics taught at the undergraduate level.

The objective of the theory of strength of materials is to provide the working designer with approximate solutions to structures problems in the theory of elasticity. The emphasis of the strength approach is

to simplify a problem by making certain assumptions about the gross behavior of the structure. One approach quite often used is to assume that the size of the differential element is large. A good example is the strength of materials solution for a beam. In this case, the element is assumed to extend the full depth and width of the beam, so the mathematic problem is reduced from a three-dimensional formulation to a one-dimensional formulation. The distance along the length is the only independent variable remaining. The final differential equation is an ordinary linear one and is quite easily solved. In this sense (giving the differential element finite dimensions) the theory of shells is a strength of materials formulation. In most strength formulations the concepts of both stress resultants and strain parameters are quite useful, so attention is given to bending moments and angular rotations.

Strength of materials solutions are very seldom "exact," but in order to be useful they must provide either a good approximation of the maximum values or an upper bound. It is therefore most important that the accuracy of the solution be checked experimentally. Many times the strength solution can also be discussed theoretically by testing the solution against the theory of elasticity. As a matter of interest, one standard method, called the "semiinverse method,"[22] for finding exact theory of elasticity solutions is to start with the strength of materials solution and modify the solution by adding appropriate terms until the complete theory is satisfied. The strength solution for the beam is used with confidence because both checks give satisfactory results, as follows: (1) experimental measurements confirm that a beam behaves very nearly as the strength of materials solution predicts, and (2) the more exact theory of elasticity solution confirms that the errors are small for the deflections and normal stresses, which dominate, and the shear stresses across the beam can often be neglected.

In view of the rather long history of structural problems (the general theory of elasticity is nearly 100 years old), the number of problems that have been solved approximately is large. However, as the demand for more efficient use of materials and higher allowable stresses increases, many solutions that were adequate in the past are becoming obsolete. It is therefore somewhat disturbing to the design analyst that

adequate solutions to specific problems are not readily available. This fact presents a problem not only to the designer who must provide an adequate structure but also to the entire nuclear power industry. The customer must verify that the design is adequate for his own purposes; the licensing and regulatory authorities must be satisfied that the design meets established requirements; and the code bodies must establish basic design criteria without being so restrictive as to stifle advancements in the study and practice of structural behavior.

Developments in the theories of failure and the adoption of the Tresca theory as the criterion for design against failure by excessive plastic flow (see Sect. 6.2) have special impact on strength-of-materials solutions for pressure vessels. Most of these solutions were designed to give values of maximum stress or deflection and not maximum stress intensity, which requires more detailed knowledge of the stresses. Aside from the problems of penetrations and openings, which are discussed later, most of the problems that currently require a strength-of-materials approach for their solution need to be reexamined. Particularly important are the ones involving external or mechanical loads, such as the support points of a vessel or support points provided by the vessel for internal structures. Fortunately, it is now possible to determine stresses in better detail by experimental methods developed largely within the last 15 years and by numerical methods that are currently becoming available.

6.1.4 Experimental Stress Analysis

It should be fairly obvious from the preceding sections that analytical methods alone are presently incapable of supplying a complete and accurate picture of the state of stress in the entire pressure vessel. Such knowledge is necessary not only because of the potentially serious nature of a nuclear vessel failure but also because the rules of Section III give monetary credit for the information in the form of higher allowable working stresses.

The relative importance of experimental stress analysis can be inferred from the following opening paragraph of the "Criteria" of Section III of the ASME Code:

> The development of analytical and experimental techniques have made it possible to determine stresses in considerable detail. When the stress picture is brought into focus, it is not reasonable to retain the same values of allowable stress for the clear detailed picture as had previously been used for the less detailed one.

In principle, experimental methods for determining stresses in elastic bodies are well understood. Current developments — for example, the use of lasers with scattered-light photoelasticity for three-dimensional work, the better use of computer techniques for data reduction, and the Moire fringe methods for measuring strains and deflections — are continually adding versatility and accuracy to the field. The problems involved in conducting an accurate experimental stress analysis, however, should not be underestimated, particularly in accurately defining and simulating service condition loads such as thermal transients and temperature gradients or extraordinary loadings that may arise during accident conditions.

The commonly accepted methods of experimental stress analysis are (1) strain gaging, preferable in conjunction with a stresscoat or other brittle coating as an aid in proper location of the gages, (2) two- and three-dimensional photoelasticity, and (3) photostress. A comparative analysis[23] conducted under the auspices of the PVRC showed that under favorable circumstances equivalent results could be obtained by all three methods. However, each method has its own particular advantages and disadvantages. In the case of photostress, the surface in question must be available for viewing while the test unit is under pressure; this in general restricts its use to the external surface. For practical purposes, this limitation eliminates photostress as a primary method of measurement on equipment subjected to internal pressure or having limited internal accessibility. However, it is sometimes possible to use a combination of theoretical and photostress methods to determine stresses such as those on the inner surface.[24]

In the event that a theoretical stress analysis is inadequate or design values are unavailable, the Code requires that the critical or governing stresses shall be substantiated by experimental stress analysis (paragraph I-1011) and furthermore that the extent of the experimental stress analysis shall be sufficient to determine the governing

stresses (paragraph I-1062). A detailed report of the test procedures and the results obtained is to be included with the design report. The Code does not, however, provide a clear picture of what constitutes an adequate theoretical stress analysis, particularly when available formulas do not precisely fit the case under consideration. The decision as to when an experimental analysis should be done is left up to the designer or to the customer.

An excellent summary of experimental stress analysis as related to pressure vessel research is given in Welding Research Council Bulletin No. 95 (Ref. 25), as follows:

> The new Section III of the ASME Code, covering nuclear vessels, permits either strain gage or photoelastic methods to be used for experimental stress analysis. From the strain gage characteristics specified, one can infer that it is desired to measure the maximum stresses to an accuracy approaching 10%, which seems fairly reasonable. However, examples of nozzle connections can be shown where measurement of stresses by strain gage within 25% would be unlikely except by the most experienced experimental stress analysts. This is particularly true in "thin-shell" models, where highly localized bending may be involved, ... In such a case it is self-evident that accurate measurement of stresses by strain gage will require gages of short length and very accurate placement of the gages. Unfortunately, such limitations may not be apparent except through prior knowledge of the nature of the stress pattern to be obtained. Much of the data available from the literature is questionable or unusable because of inadequate instrumentation, or failure to report the type of strain gages used and the exact location of measurement.
>
> In addition to the foregoing limitations, ... there are certain other general limitations, as follows:
>
> 1. For photoelastic tests, difficulties in casting and the size of commonly available curing ovens limits the practical size of model which can be tested to perhaps 12 in. OD for cylinders and 16 in. OD for spheres. Also, the minimum wall thickness which can be tested in a meaningful manner is perhaps in the order of 0.05 in. This circumstance limits the feasibility of testing small size nozzles in "thin-shell" vessels. In the PVRC program, the major portion of the testing has been done in relatively "thick-shell" vessels with d/D ratios of 0.05 or greater. A limited amount of testing has been done at D/T = 72.0, with a minimum d/D ratio of 0.129 for an unreinforced nozzle and a d/D ratio of 0.05 for a reinforced nozzle.

> 2. For strain gage tests of metal models, the models are often made using standard production techniques, with certain deviations from the specified contour (such as out-of-roundness) or with certain undefined details (such as external fillets at the nozzle-shell juncture). Whereas, test results from such models can perhaps be considered typical of a production vessel, they are potentially difficult to interpret in terms of establishing a theoretical or empirical means of calculating such stresses. That is, such uncontrolled variables constitute a source of experimental scatter which is almost impossible to assess and thereby increases the difficulty in making a proper evaluation of the data. ... these deficiencies existed (or potentially existed) in the PVRC data, as well as in much of the data reported in the literature. On the basis of such experience, it is concluded that for the purpose of checking a theory, it is highly desirable that machined models be used.

In view of the Section III requirements for an accurate stress analysis and the PVRC assessment of the experimental evidence in the literature, it is apparent that a strong and vigorous program of experimental stress analysis is needed. For those problems common to the industry, a coordinated effort in the form of monetary and technical support would produce the most useful results. In any event, vessel manufacturers and reactor designers should be strongly reminded that adequate experimental data are a prerequisite to good analytical evaluation and design.

6.1.5 Applications of Stress Analysis

The new rules of Section III concerning a complete stress analysis constitute a major change in policy in that the manufacturer or a design agent responsible to him is required to (1) make a complete set of stress analysis calculations, (2) prepare a stress report that not only contains the results of the stress analysis but also includes stress calculations and pressure-part drawings, (3) have the stress report certified by a registered Professional Engineer experienced in pressure vessel design, and (4) file copies of the stress report with the inspector and the enforcement authority at the point of installation. Stress analysis includes both the determination of the stresses for steady-state operation and cyclic operation and the evaluation of the stresses according

to a design criterion. The stress analysis has two purposes, first to obtain a number and second to understand what that number means.

For the first time a pressure vessel code has specified the use of a combined stress theory (the maximum shear stress or Tresca theory and the stress intensity value) as the design criterion. Determination of the stresses is discussed below in two parts: first the determination of stresses for steady-state conditions and second the stress analysis for cyclic operation. Stress evaluation in terms of design criteria is discussed in Section 6.2.

6.1.5.1 Stress Analysis for Steady State

The stress analysis of a pressure vessel starts with the sizing calculations for the overall dimensions that determine the structural shape of the vessel. The methods are relatively simple, since the criterion is that the membrane stress, computed by neglecting bending, must satisfy the limitations on primary stresses. Basic sizing formulas are included in Section III for most situations, although perhaps not for every conceivable situation. These early calculations are quite important, for once they are complete the plate can be ordered and fabrication started. The pressure vessel is a long-lead-time component (up to 36 months), and thus the detailed stress analysis can proceed concurrently with the fabrication because it will not normally result in major structural design changes.

The most common method for calculating the stresses in pressure vessels under static loading is called a discontinuity analysis. This method has been used for many years, and in their simplest form the calculations can be done by hand. However, the computer has made it possible and practical to perform much more complex discontinuity analyses. The major purpose of the discontinuity analysis is to determine the bending component of the stresses and to establish the majority of the design details. There will, however, be some design details that will be governed by peak stresses and by fatigue considerations.

In a discontinuity analysis the pressure vessel is usually divided into a number of basic parts (for example, nozzle, spherical head, support

skirt, etc). Associated with each of these parts is a set of equations that describes the behavior in terms of deformations, strains, and stresses when the part is subjected to a system of loads including pressure, weight, temperature gradients, and prescribed boundary conditions. In order to determine the state of stress in the pressure vessel under static or steady-state conditions, the solution for the parts must be combined to form an analytical description of the original structure. The resulting equations form the basis for a "discontinuity" analysis.

The term discontinuity analysis is perhaps a misnomer, since a structure must remain continuous both during and after application of the load. By common usage it has come to mean the solution of the set of equations that results from putting the parts back together. A good point to remember and one that is often overlooked in analysis is that in the process of deriving the solutions to the basic parts, certain assumptions are made regarding the behavior of the boundaries. Many times in a real structure made up of different shaped components, these assumptions are violated to some degree. Therefore, the answers obtained from a discontinuity analysis are most likely to be in error in the locality of the discontinuity. Since these regions are precisely where the maximum stresses are likely to occur, very careful experimental investigation is required to complete the analysis. In many cases, but not always, the error is in favor of the analysis resulting in higher maximum calculated stress values than actually occur.

In order to perform a discontinuity analysis, three types of equations are needed: (1) equations for each basic part in terms of deformations, including displacements due to thermal expansion, and applied forces, including unknown edge forces and pressure, (2) geometry equations (sometimes called compatibility equations) that express the requirement that two adjacent parts must deform in the same way at their common boundaries and thus preserve continuity, and (3) equilibrium equations that express the requirement that forces acting on one part at a boundary are balanced by forces acting on the adjacent part. The geometry equations and the equilibrium equations can be thought of as boundary

conditions. The edge forces and moments are called discontinuity forces. Edge deformations caused by unit values of these forces are called influence coefficients, and the stresses arising at the edges as a result of discontinuity forces are called discontinuity stresses. Most often the largest single stress occurs at the discontinuity; however, in order to locate the highest stress intensity it may be necessary to calculate the stress distributions away from the edge, especially when thermal gradients exist.

The total number of equations in a discontinuity analysis depends on how many parts are connected together and on the form of the solution to each part. Generally, however, there are four equations for each part, since the solution to axisymmetric shell problems and many of the strength-of-materials bending problems contain four arbitrary constants that must be evaluated from boundary conditions. Two of the four equations are usually geometry equations, and the other two are equilibrium equations. Obviously, the total number of equations can get rather large, and since the entire set must be solved simultaneously, much effort can be expended.

There are a number of ways in which the amount of labor can be reduced. These methods may be classified into two broad categories: (1) computational methods and (2) mathematical uncoupling. Computational methods may include the use of matrix algebra and digital computers, whereas mathematical uncoupling involves separating the complete discontinuity analysis into a number of smaller problems.

An important characteristic of shell problem solutions is that the effect of edge forces and moments tends to die away as a function of the distance from the edge. Therefore if two edges of a shell segment are sufficiently far from each other (the distance is measured according to the characteristic length parameter of the shell), the discontinuity forces at one edge will not significantly influence the displacements or rotations of the other edge. In such cases it is possible to solve two or more smaller sets of equations, since the interaction terms of the large original system are negligible. Caution should be exercised, however, in neglecting interaction terms, since there is seldom a sharp

dividing line between when these terms will or will not affect the solution.

Another important characteristic of shell problems arises from the development of a linear theory for which the property of linear superposition holds. If the problem can be formulated as a linear ordinary differential equation (e.g., the differential equation for a cylindrical shell), it follows that the solution which satisfies the differential equation and all the boundary conditions is equivalent to the linear sum of partial solutions, each of which satisfies the differential equation.[26] The boundary conditions for each partial solution must, however, be formulated so that when the solutions are added, all the original boundary conditions are satisfied. The principal of linear superposition goes much deeper than the application to ordinary differential equations and is the basis for at least one standard method for the solution to linear theory of elasticity problems where it is necessary to work with partial differential equations.[27] This fact is extremely important in research work aimed at developing better methods of stress analysis for pressure vessels and also for validating the practice of applying the principle of linear superposition to nonshell segments.

If linear superposition is valid (i.e., if the linear theory of elasticity is applicable), it is permissible to analyze pressure vessel segments for different types of loading, such as pressure alone with zero edge force constraints, temperature gradients alone, or discontinuity forces alone, and add the results directly to obtain the total stresses. Dividing the problem with regard to types of loads, as well as neglecting small interaction terms, can simplify the analysis. Both these methods are as old as the industry and are the methods most generally treated in text books. There is a danger, however, which is often overlooked. The danger is that even though the methods are correct it is not proper to simply add the highest stresses determined for each loading without regard to the location. Every loading produces a stress distribution that will, in general, differ from the other distributions. Therefore, in order to be sure that the design will meet the stress criteria, it is necessary to add the entire stress distributions rather than just the maximum values for each. This fact may lead to considerably more work

than originally anticipated. It is permissible to add the absolute value of the maximums to obtain a conservative upper bound on the stress. This procedure is, however, often too restrictive for practical design.

A specific example worked in the Code (Article I-7 of Section III, intended to be nonmandatory) gives a detailed computational procedure for performing a discontinuity analysis. In this example the only step left to the discretion of the designer is how to solve the resulting system of equations (see paragraph I-721). Since the resulting equations form a system of linear simultaneous equations in terms of the unknown forces and moments and constant coefficients that can be evaluated from the specific geometry and loads, the methods of linear matrix algebra can be used for their solution.

One of the nice features of matrix algebra is that it provides an extremely convenient bookkeeping arrangement for the computation. Another more important feature, however, is the compatibility between matrix algebra and the electronic digital computer. The algebra has been available for a long time; however, its general use is a direct result of the ease with which it can be programmed onto a digital computer. Standard techniques, numerical algorithms, and computer subroutine programs are currently available to all interested parties. It is an economic necessity among engineering design firms to have, as minimum computing capability, the ability to solve linear systems of equations automatically. It is now standard practice to set up discontinuity analysis problems in terms of matrix algebra for solution on digital computers. As recently as 10 years ago, however, the simultaneous solution of ten linear equations presented a major problem to the design engineer. During these years simplified discontinuity analysis was about the extent of their capability.

Solving a system of linear equations is a small but important step in the overall stress analysis. It is essentially a very small portion of a discontinuity analysis when a computer is available. The rest of the problem, setting up the matrix equation for a particular geometry and computing the stresses after the matrix equation has been solved, still involves much algebraic and arithmetic manipulation. On the other

hand, developing a computer code to do the entire problem usually involves more time and effort than can be justified for a single analysis. Several general computer programs capable of setting up a variety of discontinuity problems and calculating the resultant stresses and stress distributions are available (see Sect. 6.3.1). In addition, otb r techniques that use numerical procedures entirely, such as the finite-element method[28] and the direct solution of the differential equations, are being used for the stress analysis of pressure vessels. As an example, SØR-II solves the differential equations for shells of revolution numerically.[29]

Of these two techniques, the finite element method has perhaps the greatest potential for answering questions about detailed stress distributions in the regions of discontinuity. As mentioned earlier, these are the regions that suffer most from the mathematical idealizations inherent in the shell theory and the standard strength of materials solutions.

The finite element method is a generalization of standard structural analysis procedures that permits the calculation of stresses and displacements in two- and three-dimensional structures by the techniques that are commonly used in the analysis of ordinary frame structures. The basic concept is that a structure may be considered to be an assemblage of individual structural components or elements interconnected at a finite number of joints or nodal points. For example, a pin-jointed truss is analyzed as an assemblage of tension and compression members interconnected at the pin joints. The problem is formulated in terms of the displacements of the pin joints, and the strain energy of the entire truss is obtained as the sum of the strain energy of the individual tension and compression members. Finally the unknown displacements are obtained by applying the principle of stationary potential energy, which states that the partial derivative of the total potential energy (strain energy plus potential energy of the applied forces) with respect to the displacement components at each pin must be zero. Obviously this procedure results in a set of simultaneous equations equal in number to the sum of the displacement components for all the pin joints, and therefore for large complex trusses use of digital computers becomes mandatory.

The important extension of normal structural analysis procedures to two- and three-dimensional elastic structures came with the advent of large computers and the use of two- and three-dimensional structural elements interconnected at a limited number of nodal points to represent an elastic continuum. The actual steps in the analysis remain much the same as described above for trusses. The most difficult problems are those associated with establishing a relationship between forces applied at the nodal points and the deflections of each element and in solving the final system of equations.

In practice this relationship is derived from the basic theory of elasticity by treating each finite element as the basic building block rather than a differential-sized element. The normal assumptions of the theory of elasticity discussed earlier regarding higher order terms in the displacement functions are retained. The stress and strain variables are replaced with stress resultants and strain parameters or displacement components, as was done in the development of the thin-shell theory. One immediate advantage over other strength-of-materials approach formulations is that the size of the basic element is not restricted a priori to conform to any minimum dimension of the structure. The analysis of the basic finite element results in an algebraic relationship between the forces or stress resultants and the displacement components for specific points on the elements. These points are called the node points. Mathematically then the entire structure is described by a system of algebraic equations of the form $\{F\} = [K]\{\delta\}$, where $[K]$ is the stiffness matrix relating the force matrix $\{F\}$ to the displacement matrix $\{\delta\}$. The derivations of the stiffness matrix for various specific shapes of finite elements are contained in the literature.[28,30,31]

When the finite-element procedure is applied to arbitrary shells of double curvature, the continuously curved surface of the shell is frequently approximated by an assemblage of flat-plate elements, usually triangular in shape, joined together at their edges and loaded at the nodal points. Each such element is subject to flexure and to stresses within its plane. To establish continuity between the elements, six displacement components have to be considered at each node (three linear displacements and three rotations) together with six corresponding

generalized force components. Once the relations between forces and displacements have been established, the analysis again proceeds much as in the case of the truss.

The finite-element method is presently being expanded and improved, and although the accomplishments already achieved are substantial, much work remains to be done. Computer programs for general shells are being developed and the method shows much promise in shell analysis. It is possible to include the effects of shear deformation for thick shells; thermal effects can be included directly in the calculations; and there are methods of including nonlinear effects that could possibly be extended to shell analysis.

The cost of developing computer programs is high and, in the past, private companies have had a tendency to regard them as proprietary. More than likely there will always be a small number of privately owned computer programs that will not be generally available. Many of the newer programs, however, are the result of government-sponsored research and therefore are available to the general public. One major side effect is that some computer programs developed with private money can now be more easily obtained either on a swap basis or by purchase at moderate cost. It is also less easy for fabricators to use proprietary computer codes for the design calculations because of the Section III requirement for documenting the stress calculations in a stress report. Exactly how computer code calculations are to be documented in the stress report has not yet been fully resolved.

At present there seems to be very little excuse of a fundamental nature for not taking full advantage of automatic computations in design. Where difficulties exist in using the computer, the problems are transitional and can most often be traced to one of two causes. The first is lack of experience in using computer codes for analysis. This would most often be reflected in not fully understanding the limitations of the computer codes, including the particular theories and techniques on which the code is based. The second is that there are operational problems in converting computer codes from one machine to another. There is always a certain amount of detailed programming work involved in making a computer program operational at one facility when it was developed at a

different facility. The work is greatly increased either when the original programmer is not available to help with the conversion or when the program is not sufficiently well documented. Most of these problems will be resolved as the industry gains more experience with the newer and larger computers. In addition, computer codes are being written that are both more accurate and more versatile. In the near future, computer-oriented stress analysis will become standard practice in the pressure vessel industry.

The fact that the situation is changing rapidly is indicated in a PVRC study published in 1965. At that time, Kraus[32] was able to obtain only five computer programs for study and comparison. His general success in operating the programs was only moderate, primarily because of differences in the computer facilities and incomplete documentation of the programs.

6.1.5.2 Cyclic or Fatigue Analysis

By adopting a theory of failure as the stress criterion, Section III gives special recognition to the fact that pressure vessel steels will continue to deform without failure past the elastic limit of the material. When the stress intensity exceeds the yield stress, the material becomes plastic and, strictly speaking, Hooke's law is no longer valid. Stresses and strains beyond this point are expressed by the theories of plasticity. When a portion of the structure is in the plastic range (for example, the highly stressed inner and outer surface material of a shell segment in bending at a discontinuity), solution of the elasto-plastic equations is exceedingly complex and, for the most part, beyond the present state of the art. For one thing, the principle of linear superposition is not valid because the equations are no longer linear. A recent book on limit analysis[33] deals with this problem in an elementary fashion.

The present Code rules allow the stresses in many portions of the vessel to exceed the yield stress (paragraph N-417.5), since stress intensity values greater than 1.5 S_m may be in the plastic range. (For a more complete discussion, see Sect. 6.2.3.) These stresses include secondary membrane plus bending and peak stresses. Discontinuity stresses

discussed in the preceding section are classed as secondary stresses. The requirements for cyclic or fatigue analysis are primarily intended to evaluate the effect of peak stresses and insure shakedown during early operation to elastic behavior.

In order to insure that the stresses which exceed the elastic range of the material do not lead to failure, the Code gives very specific rules and procedures for their evaluation. Paragraph N-415.1 of Section III details a set of requirements which, if met, relieve the designer from the necessity of performing a complete cyclic analysis. The computational procedures are based on linear elastic methods of analysis in order to reduce their complexity. The stress analysis methods are therefore essentially the same as those discussed in the preceding section, with extra emphasis on temperature distributions and transients. Much more work is involved because of the many different loading conditions that must be considered. It is important, therefore, to recognize that the rules for cyclic analysis (subsection N-415) are not intended to yield mathematically correct values for the stresses. Indeed if the stresses everywhere in the vessel are as high as the Code allows, there are very few places where the stress values arrived at from an elastic analysis (analytically, numerically, or experimentally) are correct. In fact, primary stresses are the only classification required to be below yield.

The rationale for using elastic methods of analysis above the yield point is based on what Manson[34] calls the assumption of elastic-strain invariance, which states that in the range of small deformation, strains computed elastically will have approximately the same numerical value as if they had been computed plastically. This principle has obvious drawbacks, particularly in establishing the upper limit of application. However, if fatigue failure is governed by the effective strain parameters (the counterpart of the stress intensity) and design curves are established experimentally by controlled strain-range tests, the uncertainties in the calculations can be accommodated by the safety factor.

Since the elastically computed stress values are to be used as the basis for establishing the design adequacy, it is extremely important

that the computations be correct or at least conservative. This is especially true for the fatigue evaluation, since the regions where high stresses are likely to occur are precisely the regions where the analytical methods are likely to be in error. Thermal stress determinations are particularly sensitive in this regard, primarily because of the problems associated with determining the temperature distributions in the metal body, including a definition of the surface boundary condition temperatures. Other reasons include the fact that in the past (under Sect. VIII rules) thermal stresses were considered relatively unimportant (because of their self-limiting nature), and well-developed methods for their determination were not widely used. In addition, even the best-written design specifications normally do not supply sufficient information regarding thermal transients for an accurate thermal stress analysis. It is understood that new guidelines for specification writing will partially alleviate this latter problem.

The procedures for cyclic or fatigue evaluation are described in detail in Section III. However, it must be emphasized that the procedures are an analytical device invented by the Code committee for the specific purpose of limiting cumulative damage in nuclear pressure vessels. As such, they must be followed to the letter, of course. However, the designer is still responsible and should understand the bases and criteria upon which the Code is based, as well as the Code itself. Analysis for cyclic operation and fatigue evaluation is an area in which the industry feels less than satisfied about the present state of the art. The Pressure Vessel Research Committee is currently attempting to improve the state of knowledge in this area through research.

6.2 STRESS EVALUATION FOR NUCLEAR PRESSURE VESSELS

This section discusses what is presently known about the significance of stresses in nuclear pressure vessels, and in this context, considers the adequacy of the present methods of stress evaluation. Not all the aspects of stress evaluation that may be required for a given case are specifically covered by the present ASME Code. The Code prescribes minimum

requirements for new construction. Therefore a considerable portion of the stress evaluation function is still a matter of judgement on the part of the vessel and system design engineers. This assertion is true despite the statement that the ASME Code, Section III, was written in such a way that "... the judgement of the writers of the Code rather than the judgement of individual designers" should prevail. Much of this judgement is based on the results of recent research. Therefore, much of this discussion pertains to the results of recent research concerning the strength of steel pressure vessels. The important matter of exactly who is or should be responsible for each aspect of stress evaluation is also discussed.

The question of the credibility of the failure of a nuclear pressure vessel has been raised.[35] One of the prime reasons for the concern is the anticipated difficulty and cost of designing a secondary containment system* to cope with the effects of a pressure vessel failure, especially that of fragmentation.[36] This problem is being discussed in a separate report.[37] Also, it should be remembered that all physically possible modes of failure must be explicitly considered in design.[38] Relevant to this issue are the comparative degrees of safety of steel and concrete containment structures. This topic, however relevant, will not be discussed here.

Considerable importance has been attached to the data on high-strength steel, both because there is an economic incentive to use high-strength steels in nuclear pressure vessels and because high-strength steels have stress-strain diagrams similar to those of irradiated mild steel. However, it should be noted that some of the data on high-strength steel, notably the data on T-1 steel, may no longer be typical of the high-strength steels now considered suitable for nuclear service.

6.2.1 Background

Failure is defined[38] as any mode of behavior that renders a structure incapable of performing the function for which it was intended. It does

*The secondary containment system is defined here as the structure surrounding the reactor pressure vessel.

not necessarily mean total separation or collapse, but it may mean excessive deformation, spalling, cracking, or some sort of unacceptable material behavior, such as corrosion, erosion, embrittlement, permeability to fluids, or change of phase. In structural engineering the word failure is often used in a slightly less general sense to mean structural failure only. A structural failure is any form of failure caused by stress or strain that engineers seek to predict and prevent by applying the principles of mechanics. This definition puts material failures in a separate but no less important category, especially since material failures can cause structural failures.

Design against structural failure is accomplished by anticipating each possible mode of structural failure and then taking specific steps to prevent its occurrence. These steps begin by designing according to a set of rules based on past experience, experimentation, and generalized analysis. Such a set of rules is known as a design code. As mentioned before, in the case of nuclear pressure vessels, the applicable code is the ASME Boiler and Pressure Vessel Code, Section III, Nuclear Vessels, 1963. Once the geometry and the material characteristics of a nuclear pressure vessel have been tentatively established, the next step in the design against failure is a detailed stress analysis for all specified load combinations. The procedures and expected accuracy of this stress analysis are discussed in Section 6.1.5. It should be noted that Section III does not specify the loading conditions for which an analysis must be made. According to Section III, these loading conditions are to be listed in the design specifications.

The next step in the design against failure is a stress evaluation. In stress evaluation, each possible mode of failure is identified, and the states of stress that could produce it are found. These states of stress are obtained by applying failure criteria. Failure criteria lie somewhere between hypotheses and proven conclusions and are selected with the intention of underestimating rather than overestimating true strength. Each failure criterion is compared with the state of stress throughout the vessel to determine the most likely locations for each mode of failure and the margins between the actual load and the load required to cause failure. If this margin is not sufficient, the design is changed until

the margin is sufficient. Much of this procedure is assumed to be accomplished automatically by complying with the Code design rules regarding stress limits. However, since not all strength problems are completely covered by the Code, supplementary analyses are often required. This is particularly true with respect to the long-time effects of irradiation on pressure vessel steel, effects of shock or vibratory loading, material property variations, and protection against brittle fracture during startup and shutdown. It has been pointed out by both Kooistra[39] and Langer[40] that vessel designers must anticipate the properties of a vessel in its final condition, as well as in its initial condition, in order to prevent failure late in the life of the vessel.

All structures can be made to fail under a sufficiently high load. Therefore protection against failure is obtained by insuring that there will always be a sufficient margin between the highest expected load and the load that could cause failure. Pressure vessels can be made to fail in the following modes:[41] (1) excessive plastic deformation, including plastic instability and buckling, (2) cracking, including leakage or brittle fracture due to initial flaws or flaw growth by fatigue or corrosion, (3) elastic distortion, including buckling, and (4) excessive creep deformation or creep rupture.

Brittle fracture is the name given to a type of metal failure in which crack propagation occurs rapidly, without warning, from a preexisting crack, usually in a nominally low stress field.[42] When discussing brittle fracture, the accepted definition of a nominal stress is a stress computed without considering the presence of a crack.[42] Brittle fractures may originate from initial defects or from cracks that have grown by fatigue or corrosion.[43]

The basic factors that affect fracture strength have been determined,[44] although quantitative relationships are not available in many cases. These factors can be grouped under four main headings: (1) environment, (2) loading conditions, (3) design and construction features, and (4) metallurgy. Environment includes temperature, irradiation, and corrosion. Loading conditions include rate of strain, transverse restraint, prior strain history, residual stresses, and method of loading. Design and construction features include flaws, stress concentrations,

and shape. Metallurgy includes chemical composition, material structure, and the effects of welding on the material. These factors usually act in combination with each other. Therefore, most of them will be mentioned in the following discussion.

Section III contains explicit provisions to guard against failure by excessive yielding. Elastic distortion is not structural failure, per se, although it may lead to operating difficulties Buckling can usually occur only if net external loads can act on the pressure vessel. However, certain configurations, such as the knuckle region of a torispherical head, may be subject to local buckling due to bending under internal pressure.[45] Section III avoids the creep problem by prohibiting operation in the creep range. New design rules will be required for operation at higher temperatures. Tentative guidelines for high-temperature design can now be found in Code Case 1331.

Cracking, manifested either by leaking or brittle fracture, is a possible mode of failure for steel pressure vessels. Section III contains explicit rules for stress evaluation to guard against crack growth by fatigue; however, it does not list brittle fracture as a mode of failure per se. Nevertheless, certain precautions against brittle fracture are taken; namely, (1) material selection is based on Charpy V-notch tests, (2) the vessel is hydrotested* at temperatures above the NDT temperature plus 60°F, and (3) consideration is given to the NDT temperature shift caused by irradiation in material selection and operation. The stress intensity limits designed to prevent bursting and fatigue failures may have been intended to guard against brittle fracture also. However, since maximum allowable stress intensity increases with decreasing temperature, while fracture resistance decreases, such a criterion is not completely logical or sufficient by itself. Therefore, the initial hydrotest* must be considered the most direct means for guarding against brittle fracture. If the vessel does not fail in a hydrotest that includes all combinations of service loadings, some assurance is provided that it will not fail in service if cracks do not grow during the hydrotest or in service and its

---

*The British call the hydrotest a proof test; in the USA, a proof test is used to determine the strength of a vessel component that cannot be analyzed. The hydrotest is a hydrostatic overpressure test.

properties do not deteriorate with time. It is, of course, difficult enough to simulate the mechanical loads, but the loads caused by thermal transients, fluid flow, etc., during service cannot be simulated. Normally, a conventional hydrotest does not include thermal loads or external reactions.

Semiempirical rules for material selection are in general use.[1,46,47] These rules consider the effect of irradiation on material properties and are generally assumed to be sufficient for preventing brittle fracture in mild steel. However, the adequacy of these rules for all loading conditions and all materials, notably the high-strength steels* that have not yet been used in nuclear pressure vessels, has not yet been proved conclusively. Therefore it is this phase of pressure vessel safety that requires the most judgement at the present time and which is receiving much attention from researchers.

Mainly as a result of welded ship failures during World War II,[42,44,48] an empirical approach to the prevention of brittle fracture was developed. This approach was based on the observed fact that the fracture energy for a notched specimen of mild steel is an increasing function of temperature, as shown in Fig. 6.6, and that brittle fractures seem to occur only below a temperature corresponding to a certain energy level. For a given shape and strain rate, the highest temperature at which brittle fractures are observed to occur is called the nil ductility transition (NDT) temperature. This temperature is commonly defined by the results of the Naval Research Laboratory small-flaw drop-weight test. In this test, for standardization purposes, specimen thicknesses range from 3/4 to 1 in. Since fracture energy rises over some range of temperature, the change from brittle-to-ductile behavior is not absolutely abrupt but involves a transition. Hence, the name transition temperature.

Since the original transition-temperature approach correlated only fracture energy, temperature, and mode of failure, it did not provide a means of stress evaluation to prevent brittle fracture, but it did provide a means of material selection for the same purpose. When the transition-temperature approach was first introduced, it was believed impossible

*As used in this report, the term high-strength steel means any steel with a yield strength equal to or greater than 100,000 psi.

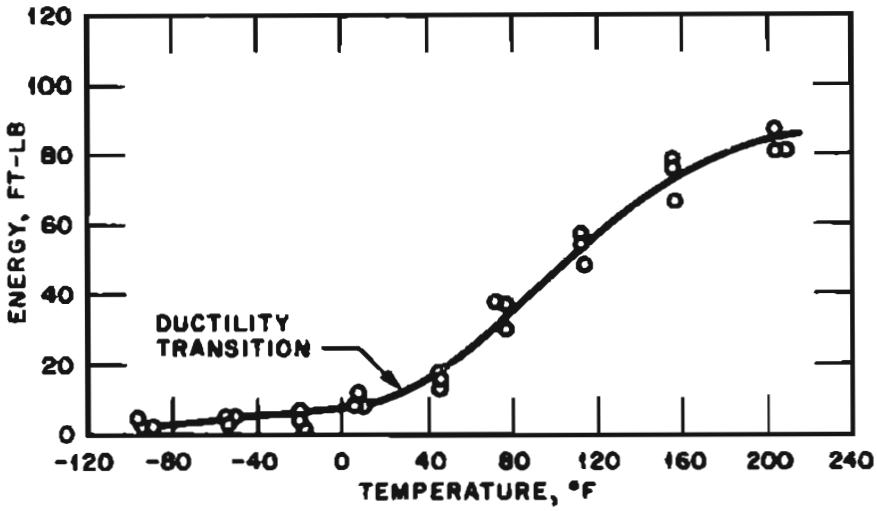

Fig. 6.6. Charpy V-Notch Impact Energy Data for a Hot-Rolled 0.20% Carbon Steel Showing the Transition from Ductile-to-Brittle Behavior as Temperature is Lowered. (From Ref. 44)

to obtain a quantitative measurement of the sensitivity of a steel to brittle behavior in terms of the principal stresses.[44] Such a situation was not satisfactory to design engineers, who believed that the design function is more quantitative than the material selection function.[42] Therefore, efforts were begun to seek more quantitative methods of preventing brittle fracture. As these methods were developed, they were used to refine the transition-temperature approach. These refinements are discussed below after their bases have been explained.

The problem of designing to prevent brittle fracture in the case of nuclear pressure vessels is aggravated by the fact that neutron irradiation decreases the ductility of pressure vessel steels. This problem is discussed in detail in Chapter 5 of this report.

At present, Section III contains no specific rules for stress evaluation based on irradiation damage. However, Ref. 4 specifies that the maximum applied load shall not exceed 20% of the design load for any vessel temperature less than the NDT temperature plus 60°F.[49] Since this type of limitation is empirical, it cannot automatically be assumed to be adequate for all designs.[50]

Trends in structural design are motivated by economy, as well as safety. The unit power costs of a nuclear reactor station improve with

size, and therefore there is an incentive to build larger reactors and larger pressure vessels. However, total weight and gross dimensions of pressure vessels are limited by the capacity of transportation systems, and maximum wall thickness is limited by metallurgical reliability. Therefore, there is an incentive to build larger vessels without exceeding the weight or wall thickness limitations. This provides an incentive for both on-site fabrication and the use of high-strength steels. Many high-strength steels have been developed in the last 15 years.

There are three grades of steel considered for use in nuclear pressure vessels: mild steel (e.g., A 212 grade B), intermediate-grade steel (e.g., A 533 grade B, which is A 302 grade B modified by adding nickel and quenching and tempering), and high-strength steel (e.g., A 542 and A 543). As stated in Chapter 4, A 533 grade B is now the reference material for all primary nuclear pressure vessels for light-water reactors. The steels A 542 and A 543 are presently being investigated for future use. Some high-strength steels have a yield strength-to-cost ratio higher than that for mild steel.[51] However, high-strength steels generally have higher ratios of yield strength to ultimate strength, and therefore less strain-hardening capacity and less strain at necking than mild steel.

High-strength steels have a conventional stress-strain curve* somewhat similar to that for irradiated mild steel, as shown in Fig. 6.7. The curves of fracture energy in an impact test versus temperature for high-strength steel are also similar to those for irradiated mild steel. Both have flatter transitions than unirradiated mild steel. Therefore, there is less certainty that fracture will not occur above the transition temperature for high-strength steel than for mild steel. Consequently, a reliable quantitative understanding of the fracture problem is a prerequisite to the use of high-strength steel in nuclear pressure vessels. It follows that a reliable quantitative understanding of the fracture problem is the key to the use of high-strength steel for larger power reactor vessels.

---

*The conventional stress-strain curve gives load divided by initial area versus elongation divided by initial length.

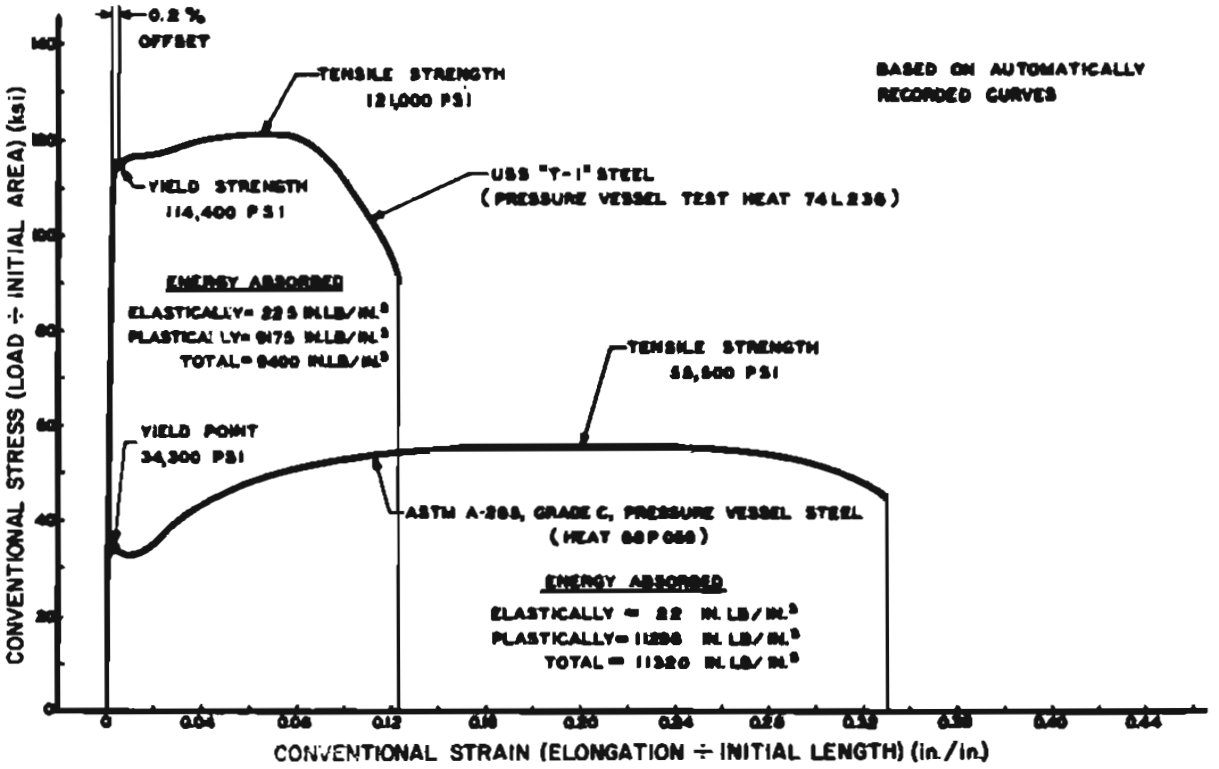

Fig. 6.7. Typical Conventional Tensile Stress-Strain Curves for USS T-1 Steel and A 285 Steel.

6.2.2 Design Aspects of Strength and Fracture

Aside from stress analysis, which is discussed in Section 6.1, three main areas affecting the integrity of pressure vessels have been widely investigated in the last 15 years. These are fatigue, plasticity, and brittle fracture. The first two are considered separately and as related to brittle fracture. Brittle fracture is discussed both from the fracture mechanics and transition temperature approaches.

6.2.2.1 Fatigue

In 1945, the Welding Research Council of the Engineering Foundation organized the Pressure Vessel Research Committee (PVRC).[41] Its principal function is to administer research in pressure vessel safety and technology and to provide the data required by code-writing bodies for achieving safety and economy in pressure vessel design. By 1948, high-strength

steel had been developed to the point where its use in pressure vessels was economically attractive. Therefore, in 1948, the PVRC undertook a study of the possibility of "increasing design stresses in pressure vessels."[39]

The concern over the reliability of high-strength steel vessels arose originally because of the lower crack toughness of such steels. At the time, this lower crack toughness had been observed in terms of lower notched tensile strength, although the test results had not been expressed in terms of the current concepts of fracture mechanics.[52] A plot of such test results is shown in Fig. 6.8, which was taken from Ref. 40. The dashed curve in Fig. 6.8 represents the product of the ordinate and the abscissa and has been added to show that, as the yield strength increases, a maximum occurs in the notched strength. In Fig. 6.8, this maximum occurs at a yield strength of about 85 ksi. Randall and Felgar[53] have shown that the location of this maximum depends upon flaw size: the larger the flaw size, the lower the maximum notched strength and the lower the yield strength at which it occurs. Therefore, the feasibility of using high-strength steel for nuclear pressure vessels is directly related to the sensitivity of nondestructive inspection and to the accuracy of crack growth-rate predictions.

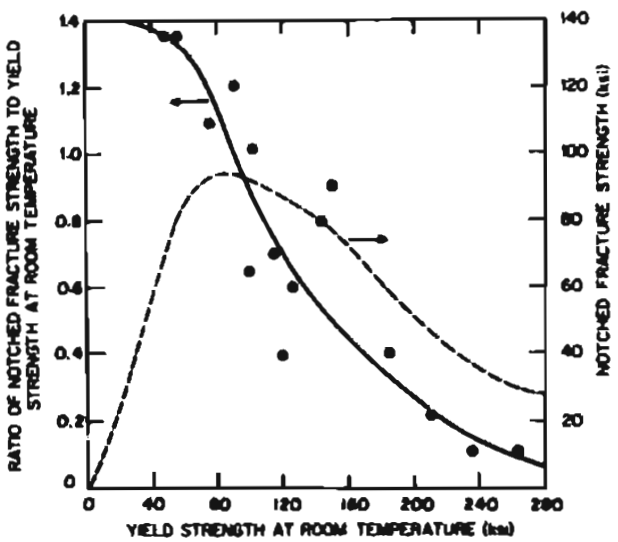

Fig. 6.8. Crack Toughness as Indicated by the Ratio of Notched Fracture Strength to Yield Strength. (From Ref. 40)

In a similar manner, concern could also be expressed with respect to the reliability of high-strength steel vessels because of lower notch fatigue strength with increasing yield strength, particularly when reversible yielding occurs at the notch root. Such decreased notch fatigue strength has been observed even in steels that exhibit an increase in unnotched fatigue strength with an increase in yield strength.[52] Thus, the feasibility of increasing nominal stress levels in pressure vessels (by using high-strength steels) depends on preventing fatigue from governing the design, unless fatigue resistance in the cycle range of interest can be made to increase with increasing yield strength.

It was recognized that, in the past, fatigue had been of relatively minor importance in pressure vessel failures.[39] However, with stress analysis methods known to be imperfect, it was possible that cyclic reversible yielding could occur at points of stress concentration. This type of cyclic loading, in which the material is subjected to reversible plastic strain, has variously been called "low cycle fatigue" or "high strain fatigue." Although it was estimated that most pressure vessels are subjected to only a relatively low number of major pressure cycles in their lifetimes, plastic fatigue could conceivably occur. Furthermore, some high-strength steels have yield strength-to-ultimate strength ratios as high as 0.9, and this was cause for concern with regard to fatigue. Therefore, plastic fatigue tests were conducted on laboratory specimens and small-scale pressure vessel models of mild steel (A 201), intermediate-strength steel (A 302), and high-strength steel (T-1, among others).

It was recognized (and later demonstrated in large-scale tests) that regions of local yielding are cycled mainly by the strain variations of the elastic material surrounding them. It fact, it was found that the strain range leveled off to a constant value in approximately 10 cycles. Therefore, the most reliable type of test would be a strain-cycling test rather than a stress-cycling test.[39]

Since most nuclear pressure vessels will be subjected to between 100 and 15,000 major operating cycles* during their lifetimes,[36] the test

---

*This estimate is taken from Table 3.6, which contains a detailed breakdown of the number of cycles associated with various loading conditions. The data in the table represent current design practice.

results for that range of cycles are especially interesting. A shown in Fig. 6.9, the cyclic total strain range required to cause failure in a specified number of cycles in the low-cycle fatigue range decreases as yield strength increases. For this class of design, there is actually a disadvantage to specifying high-strength steels if vessel strength is governed by low-cycle fatigue. Therefore, in order to utilize high-strength steel in pressure vessels, fatigue must be prevented from governing the design by accurately analyzing and minimizing stress concentrations. Although plastic fatigue in 15,000 cycles or less is very unlikely for pressure loading alone, thermal loading may increase the cyclic strains and therefore increase the severity of the fatigue problem.[39] Such can be the case for nuclear pressure vessels.

An additional result of the large-scale PVRC tests (to be discussed later) was that the most severe and unavoidable discontinuity in a pressure vessel is likely to be a nozzle attachment, which can have an effective strain-raising factor of 4 or more.[36,39] Therefore the development of accurate methods of analysis for nozzle attachments is desirable as a means for minimizing fatigue and making possible the use of high-strength steel in pressure vessels.

Some test results show that temperatures between 0 and 650°F have no significant effect on fatigue strength, but that for a given strain range, cyclic life does decrease as the rate of cycling decreases.[39] Some more recent results indicate that temperature does affect the rate of fatigue crack growth, at least in some steels.[54] As shown in Fig. 6.10, temperature has a strong influence on fatigue-crack growth rates in carbon steel but a negligible influence on fatigue-crack growth rates in 2 1/4% Cr–1% Mo steel.[54]

In 1962, the problem of fatigue failure was considered in connection with the Elk River reactor vessel.[55] Investigations showed that there were "crack-like" defects (including lack of weld penetration and fusion) in the strength welds of the vessel. The structural significance of these defects depends on whether they will grow during the life of the vessel so as to cause fracture or serious leakage. The best safeguard against fracture was considered to be the standard operating limitation based on the NDT temperature. That is, the vessel should not be pressurized at a

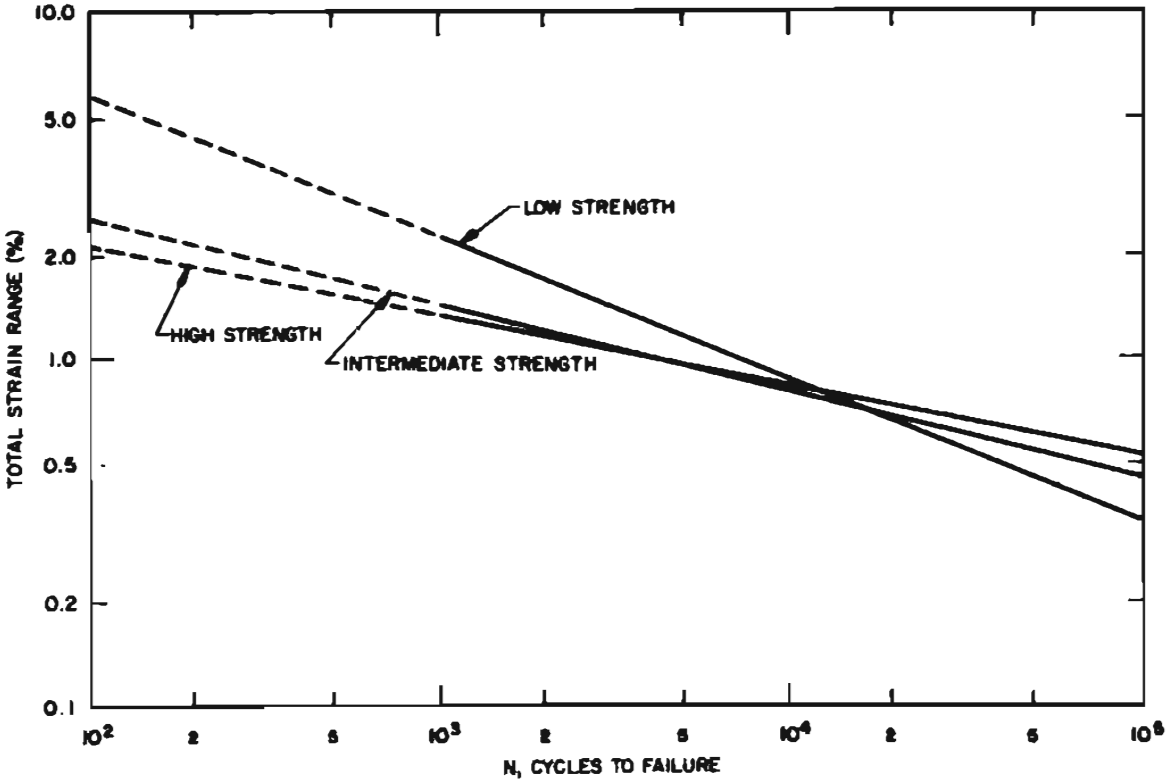

Fig. 6.9. Strain Range Versus Cycles-to-Failure for Three Classes of Steel. (From Ref. 40)

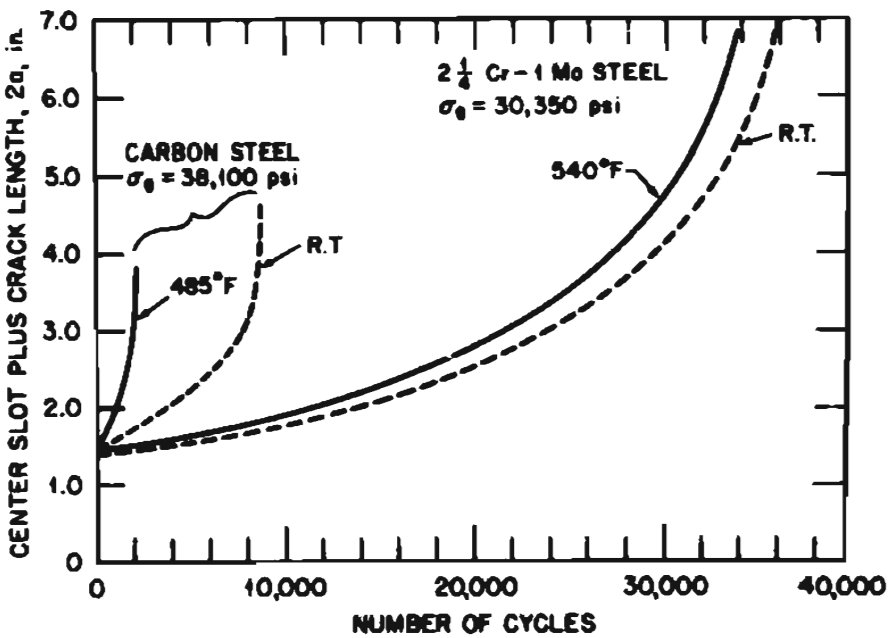

Fig. 6.10. Comparison of Fatigue-Crack Growth in Carbon and 2 1/4% Chromium-1% Molybdenum Steel at Various Temperatures. (From Ref. 54)

temperature less than the NDT temperature plus 60°F to take into account the initial NDT of the vessel and any shift that might occur as a result of irradiation. With such control, brittle fracture was ruled out as a likely source of difficulty.

A study was then made to determine whether the initial cracks could grow to a size sufficient to cause failure (leakage) during the life of the vessel. The highest elastically calculated stress in the vessel (considered a reliable indicator of peak cyclic strain) occurred at the inside corner of the feed nozzle. This stress was a combined pressure and thermal stress. By comparing the Elk River vessel data with full-scale test results[36] (to be discussed later), it was concluded that fatigue failure was unlikely. Finally, although it had already been ruled out for the Elk River vessel, it was concluded that, in general, for a boiling-water reactor the possibility of failure by brittle fracture is considerably greater than by fatigue because of possible failure of operating personnel to adhere to prescribed procedures of operation and test.[55] It was stated that it is not possible to say, categorically, that crack propagation and failure are impossible, but it is reasonable to assume that the risk is small for this particular service. It is evident that the relative probabilities of the occurrence of fatigue and brittle fracture are still not certain. Langer[40] has stated that, "If a catastrophic failure ever occurs in a vessel in a nuclear plant, it will probably originate in an undetected defect which grows under cyclic action to the critical size necessary for brittle fracture." Langer therefore concludes that three areas of research are of prime importance: (1) detection of defects, (2) crack growth, and (3) brittle fracture.

In 1963, the present nuclear pressure vessel design code, Section III of the ASME Code, was issued, and a commentary on the Code[56] was published. This commentary contains a fairly complete explanation of the requirements for fatigue analysis. (Reference 56 is included as Appendix C in Ref. 57.) It should be noted that the derivation of Eq. (5) on page 16 of Ref. 56 is not available in the open literature.[58] Equation (5) is a semiempirical formula for the fatigue analysis of high-strength bolts. This formula has been found to be overconservative and is now being revised by the ASME Pressure Vessel Code Committee.[58] Code Case 1366 pertains to this formula.

6.2.2.2 Plasticity

The theory of plasticity has three main areas of application in stress evaluation of nuclear pressure vessels: (1) prevention of excessive plastic strains under steady load, (2) analysis of fatigue, and (3) analysis of brittle fracture. The first application is discussed here; the second has been discussed (see Sect. 6.2.2.1); and the third will be discussed later.

The definition of stress intensity is based directly on the maximum shear-stress criterion for yielding. To a close approximation, mild steel yields when the maximum shear stress reaches a critical value. The maximum shear stress equals one-half the difference between the largest and the smallest principal stresses. At yielding, this difference equals the yield stress in uniaxial tension. Hence the stress intensity is a direct measure of proximity to yielding. After yielding, the maximum principal stress difference stays constant until strain hardening sets in, but in mild steel this does not occur until a strain of about ten times the yield strain, and so should not occur in a pressure vessel.*

Pressure vessels are statically indeterminate structures and are analyzed according to the same philosophy as are indeterminate frames. Although some local yielding may occur, the distributions of shears and moments throughout the structure are determined by the theory of elasticity (see Sect. 6.1.5). The capacities of individual cross sections are then analyzed plastically according to Section III of the ASME Code.

While the stress limitations in Section III for combined axial load and bending are stated in terms of stresses, these are artificial elastic stresses computed by applying the familiar formula

$$\sigma = \frac{Mc}{I} + \frac{P}{A} ,$$

in which M is the actual moment producing a plastic hinge and P is the actual thrust; both are determined by plastic analysis. Plastic analysis consists of assuming a linear strain distribution over the cross section and assuming the same stress-strain relation in bending as in uniaxial tension. In the limit, elastic strains disappear at the neutral axis and

*The ASME Code, Section III, consistently assumes a "flat-top" stress-strain diagram (see Fig. 5 in Ref. 56).

the stress distribution becomes a pair of rectangles (see Sect. 6.2.2.3). However, with the safety factors chosen, no loading beyond initial yield is permitted under primary stresses. This aspect of stress evaluation is covered in detail in Ref. 56. It should be noted that the nominally fully plastic condition can only be attained if the material strain hardens beyond the yield plateau; otherwise the bending strains would become infinite. Therefore, strain hardening is an important characteristic of pressure vessel steels.

6.2.2.3 Derivation of the Stress Limits for Primary Stresses Based on Plastic Collapse

The cross section of a structural element of ideally plastic material is incapable of carrying any additional load once yielding has occurred over the entire cross section. In the case of a rectangular section carrying an axial force and a bending moment, the collapse load will cause stresses equal to plus or minus the yield stress over the entire cross section, as shown in Fig. 6.11. The neutral axis occurs at the point where the stress changes sign. The magnitude of the net axial force and the bending moment acting on the cross section can be obtained directly from Fig. 6.11.

The net axial force, per unit thickness, acting on the cross section is

$$F_m = S_y c \ . \tag{1}$$

Therefore, the average primary membrane stress is

$$P_m = \frac{S_y c}{h} \ . \tag{2}$$

Consequently,

$$\frac{c}{h} = \frac{P_m}{S_y} \ . \tag{3}$$

The moment acting on the cross section is given by

$$M = \frac{S_y(h^2 - c^2)}{4} \ . \tag{4}$$

ORNL-DWG 67-3792

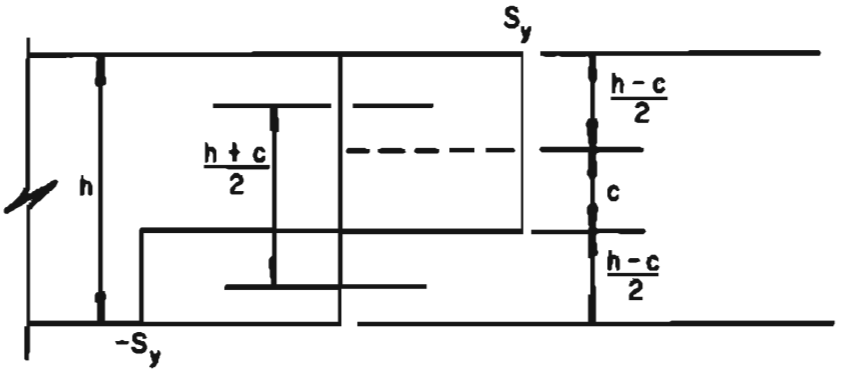

Fig. 6.11. Stress Distribution at Collapse Under Combined Axial Force and Bending for a Rectangular Section.

The elastically computed bending stress for the moment M is given by

$$P_b = \frac{M\frac{h}{2}}{\frac{h^3}{12}} = 1.5S_y\left[1 - \left(\frac{c}{h}\right)^2\right] . \tag{5}$$

Substituting Eq. (3) into Eq. (5) then gives

$$\frac{P_b}{S_y} = 1.5\left[1 - \left(\frac{P_m}{S_y}\right)^2\right] , \tag{6}$$

and adding P_m/S_y to both sides of Eq. (6) gives

$$\frac{P_b + P_m}{S_y} = 1.5\left[1 - \left(\frac{P_m}{S_y}\right)^2\right] + \frac{P_m}{S_y} . \tag{7}$$

Equation (7) is plotted in Fig. 6.12. Since P_m/S_y alone cannot exceed 1.0, Eq. (7) applies only up to $P_m/S_y = 1.0$. As can be seen from Fig. 6.12, the safety factors specified by Section III restrict actual maximum stresses to magnitudes equal to or less than the yield stress.

6.2.2.4 Fracture Mechanics and Plasticity

It has already been stated that a reliable quantitative understanding of the brittle fracture problem is necessary for the development of

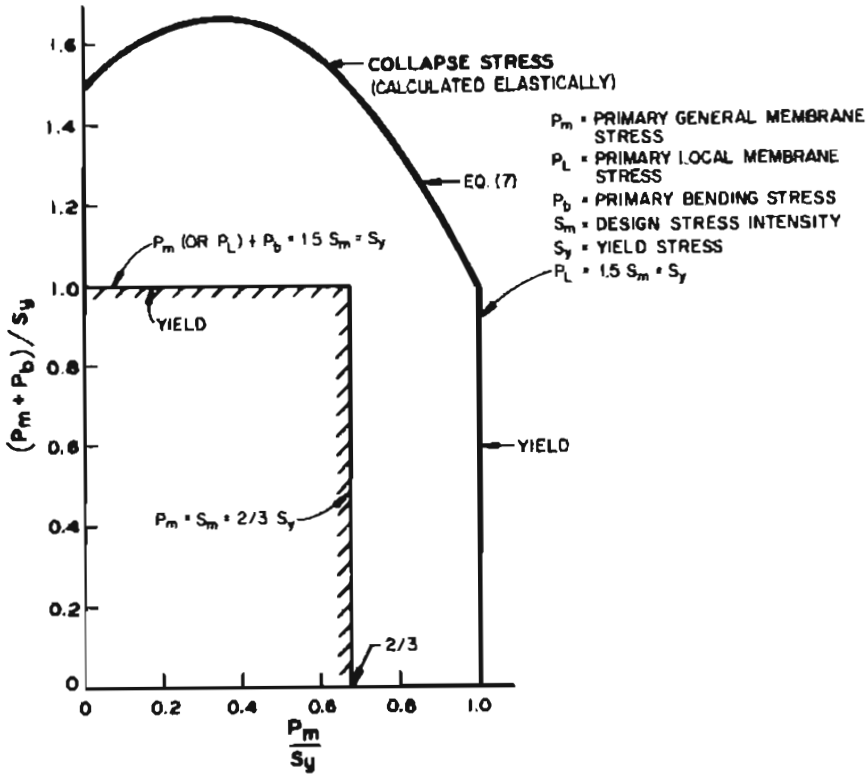

Fig. 6.12. Stress Conditions for Development of a Fully Plastic Rectangular Section Under Combined Bending and Normal Force and the Primary Stress Limitations to Guard Against Plastic Collapse. (From Ref. 56)

a completely adequate method of designing high-strength nuclear pressure vessels. Such a method, known as fracture mechanics, has been under development for the past several years. Fracture mechanics is an analytical method of predicting the load on a structure at which a crack of known location and dimensions will start to propagate. Historically, the prediction of the load at which a crack will start to propagate is based on the principle used to predict the load at which a column will buckle. This is the principle of conservation of energy. In the case of a column, buckling occurs when the rate of work done by the external load equals the rate of absorption of strain energy of the column in its buckled configuration. Three factors are involved: a rate of energy supply, a rate of energy absorption, and a change in shape. During crack propagation, the rate (with respect to crack area) at which the external loads do work plus the rate of release of elastically stored strain energy behind the crack tip equals the rate of energy supply. The rate of energy absorption

equals the rate at which plastic work is done ahead of the crack tip plus the rate of increase of kinetic energy of the system.[59] Changes in kinetic energy have in almost all cases been assumed to be zero. Also, it has generally been assumed that the work done by the external forces during fracture is negligible.[60,61] In fact, it has been argued that regardless of the external force variations during crack extension (fixed or constant load conditions), the rate of release of elastically stored strain energy with respect to crack area remains unchanged.[42] The resulting relationship then states that

$$\frac{dW_p}{da} = -\frac{dU}{da},$$

where W_p is plastic work ahead of the crack tip, U is the elastically stored strain energy, and a is crack area. The plastic work rate is usually assumed to be a material property and is denoted by G_c,[42,60] the value of which may be affected by environmental factors, such as temperature and neutron irradiation.

It should be noted that the equation above defines a state of neutral equilibrium in the same sense that the Euler formula for the critical buckling load on an elastic column defines a state of neutral equilibrium. It does not tell whether a crack will continue to propagate, and if so, how fast. Whether crack arrest or rapid crack propagation will ensue may well depend on the nature of the external load. As pointed out by Bueckner,[62] the rates of energy supply for crack extension under constant load and for fixed grips are equal only at the onset of fracture. During crack propagation the rate of energy supply for crack extension under constant load is larger than the rate of energy supply for fixed grips.[62] This fact has a very important bearing on interpretation of the crack-arrest test results to be discussed later. Needless to say, it is equally important in a design analysis. (Note that Corten[42] and Bueckner[62] do not agree on this point. This disagreement stems from the question of whether the external loads can supply energy to the fracture zone during crack propagation. Historically it was thought that they could, although a more recent view is that crack extension is controlled strictly by the stresses at the crack tips. Some uncertainty still seems to exist on this point.)

Brittle fracture is most likely to initiate from a sharp crack located in a section thick enough for yielding at the crack tip to be inhibited by tensile stresses parallel to the crack tip. For this case, the strain parallel to the crack tip is small, and in the limit, zero. This case is referred to as "plane strain" (zero strain normal to a specified plane*) as opposed to "plane stress" (zero stress normal to a specified plane). In the case of plane strain the plastic zone ahead of the crack tip tapers from a maximum size on the external surfaces to a minimum size at the midplane of the section.[63]

Because a plastic zone exists at the tip of a crack in metals that are not completely brittle, it is necessary to consider the effect of this plastic zone on the stress distribution in the surrounding elastic material. The general effect of the plastic zone is to cause a reduction in the stresses in the elastic zone. In order not to invalidate the elastic analysis of stresses near crack tips, the length of the crack is usually assumed to be increased by a small amount to account for the presence of the plastic zone.[42,60,64,65] The full effects of this approximation on the accuracy of fracture mechanics analysis have not been determined. It is known that one of the effects of crack tip yielding is to blunt the crack tip[60] and thus reduce peak stresses. The amount of displacement at the crack tip due to yielding has been considered as a fundamental parameter in fracture mechanics.[66]

One important element in the application of fracture mechanics is the assumption of a crack shape and size. In the examination of fracture failures, it is rare to find that the initial starting crack extends completely through the thickness. A partly through crack is more likely.[64] For instance, several high-strength-steel polaris-air-launch tanks failed during pressure testing because of metallurgical defects extending nearly (but not completely) through the wall thickness.[67] Therefore, most fracture analyses involve hypothetical partly through cracks.

---

*This is a mathematical definition of plane strain. In fracture mechanics, plane strain is often used to imply a condition of transverse restraint at the tip of a crack such that the transverse contraction tangential to the crack tip is no greater than in the surrounding elastic material.

The size of crack assumed for analysis is also important with respect to the feasibility of using high-strength steel.[53] Brittle fractures can initiate from smaller flaws in high-strength steel than in lower strength steel.[42] Furthermore, for large flaws, high-strength steels tend to be weaker than lower strength steels.[53] Therefore, if large flaws are assumed, or permitted to exist, the use of high-strength steel may not be feasible.[53] Obviously, high standards of fabrication and inspection are vital when using high-strength steel.[42,53,68] In fact, nondestructive testing may use up as much as one-fourth of the man hours required to construct a high-strength vessel.[53] Despite this care, some types of flaws, such as those associated with alloy segregation, are still not detectable with present-day techniques (see Sect. 9.5.3).[53] Therefore, further improvements in nondestructive testing are required in order to insure the reliability of high-strength vessels.[68]

Another difference between high- and low-strength steels is their "strain-rate sensitivity." Strain-rate-sensitive materials undergo a strong rise in yield point but a sharp decrease in ductility over a narrow range of temperature or strain rate as the temperature decreases or the strain rate increases. Ferritic structural steels are strain-rate sensitive, whereas high-strength steels* are not.[42] For temperature and strain-rate-sensitive materials, the stress necessary to sustain a running crack can be smaller than the stress required for initial crack extension.[42] This is true because a rapidly propagating crack produces a high strain rate, which causes a marked decrease in fracture toughness. Therefore it appears that although larger cracks may be required to initiate fracture in mild steel than in high-strength steel, once started a running crack may traverse a region of reduced stress in mild steel, whereas it might not do so in high-strength steel.

Residual stresses have already been identified as a primary cause of brittle fracture. For stress evaluation purposes, the sum of the residual, loading, and thermal stresses appears to be an appropriate stress to be

---

*This statement is controversial because there is no universally accepted definition of high-strength steels and because some steels referred to as high-strength steels have a moderate degree of strain-rate sensitivity.

limited for preventing brittle fracture.[42] However, it has been argued that residual stresses also decrease ductility and therefore that their effect is more than proportional to their magnitude.[42] Welding is a primary cause of residual stresses. It is apparent that further research is needed regarding the effects of these stresses.

The effects of residual stresses can be made beneficial. If a pressure vessel is loaded to a pressure below failure at an elevated temperature, plastic zones will form at the tips of any existing sharp cracks. Since these plastic zones are confined by elastic material, their unloading is governed by strain rather than stress, as explained in Fig. 3 of Ref. 56. Thus, upon unloading, there will be a residual compressive stress at the crack tip that is probably equal to the tensile yield stress value. Upon reloading, at a lower temperature, no further yielding at the crack tip will occur until the last previous load has been reached. Furthermore, the crack tip is no longer as sharp as it was originally because it has been blunted by yielding. Some experiments by Bevitt, Cowan, and Stott[69] have indicated that failure will not occur at the lower temperature until the maximum previous load at the higher temperature has been exceeded. This phenomenon is known as "warm prestressing"[42] or "mechanical stress relieving."[50] The reliability of warm prestressing has important implications with respect to safety during startup and shutdown and to the benefits of proof testing. It should be noted that although initial yielding may blunt a crack tip, fatigue has also been found to be an effective means of sharpening and extending a crack. Thus it is not obvious that a margin of safety provided by initial yielding will still be fully available after several thousand loading cycles. It is apparent that warm prestressing should be studied further and thoroughly explained.

Crack growth is not always rapid. Besides fatigue growth, slow crack extension at low stress caused either by a few cycles of stress or by moisture (water vapor) has recently been observed.[42,60] Crack growth has important design implications, since the fracture stress decreases as crack size increases during service.

If an energy balance view of crack propagation is assumed, it follows that the energy rate at fracture, presumably a material property, should

be obtainable by two different approaches. The first approach, which is the most common because it is based on the theory of elasticity, is to calculate the rate of release (with respect to crack area) of elastically stored strain energy near the crack tip. This can be done analytically or experimentally. The other approach is to calculate the rate of doing plastic work ahead of the crack as the crack propagates. Romualdi,[70] Johnson,[60] and Rizzo[61] have taken this approach. In 1960, a method of optically measuring the total strains in the plastic region near a crack tip was developed.[70] From these measured total strains, it was possible to compute the total plastic work done at a given point near the crack tip at the onset of crack propagation for plane stress conditions. Therefore the increase in plastic work could be determined at a given point that occurred prior to the propagation of a slightly longer crack. By summing these increases, the plastic work associated with the difference in crack length could be computed. The ratio of the plastic work increment to the crack area increment was the energy rate being sought, and it compared favorably with a value obtained with a conventional elastic calculation of fracture toughness.

In a recent thesis, Rizzo[61] formulated an approximate mathematical model for directly estimating the plastic work rate at the onset of fracture under plane-strain conditions. While the model gives an indication of the relationship between the inelastic stress-strain properties and the plastic work rate, some of its predictions vary from experimental evidence. This may be caused by the fact that it does not consider stress redistribution in the elastic region. This model is potentially useful for estimating the effects of irradiation on fracture toughness.

At present, fracture mechanics is considered applicable to brittle metals but not to high-strength* metals or soft annealed metals.[60] It is evident that the application of fracture mechanics to pressure vessel steels requires improvements in plastic analysis as well as in elastic analysis. In fact a more accurate description of the stresses and strains

---

*This statement is controversial both because the definition of high-strength steel is controversial and because plate thickness and temperature also influence the applicability of fracture mechanics.

in the crack-tip plastic zone may well provide the key to an understanding of fast fracture in pressure vessel steels.[42] Reference 42 mentions several elastic-plastic analyses of notched specimens. Elastic-plastic stress analyses of a notched tensile and an Izod impact specimen are reported by Hendrickson, Wood, and Clark.[71] They show that when "brittle fracture" occurs the true maximum principal tensile stress in the notched tensile specimens is constant. In contrast, Rizzo's[61] analysis was based on an ultimate plastic strain condition at the crack tip. If ductility is a fracture criterion, it may vary with stress state, as postulated by Lubahn.[72,73] The strain gradient may also be a significant parameter. The analysis of Hendrickson, Wood, and Clark was extended by Grubin and Likachev[74] to include strain hardening.

It has been shown by experiment that, in general, no unique relationships exist between stress and total plastic strain in material undergoing yielding. Rather, the relationships that are unique are between the stresses and the plastic strain increments. Theocaris[75-77] has developed a method of calculating the actual stresses in a plastic zone around a notch from the measured plastic strain increments. This approach should be ultimately quite useful in the further development of fracture mechanics. At present, Theocaris' analysis is limited to ideally-plastic material (strain hardening is neglected). Rizzo's approximate analysis[61] utilized the total plastic strains and was limited to linear strain hardening. An approximate method of computing actual stresses from total measured strains beyond yield, which utilizes any stress-strain curve, has been developed by Merkle at ORNL.[78]

There is great concern with regard to the magnitude of the "constant" G_{Ic}, which is the critical strain-energy release rate for the opening mode of crack surface displacement. (The subscript I indicates plane-strain conditions.) Considerable variability of the constant-temperature G_{Ic} may be expected for a single material; a range of at least two orders of magnitude can result from heat treatment of steel.[60] To the designer interested in stress (proportional to the square root of G_{Ic}), this means that a variation in critical stress of about a factor of 10 can be caused by heat treatment alone.[60]

6.2.2.5 Fracture Mechanics and Fatigue

A combined fracture mechanics and fatigue analysis has been developed for certain high-strength steels and titanium and aluminum alloys by Tiffany and his co-workers.[43,79] The existence of small surface or internal flaws is accepted as inevitable. For thin-walled low-pressure tanks, flaw growth that leads to complete penetration and leakage is likely. However, due to the high strength obtained by heat treating or low service temperatures, brittle fracture is possible. The analysis is based on the hypothesis that an invariant relationship exists between the initial fraction of critical stress intensity and the number of cycles to failure, independent of specimen geometry. Such a relationship was obtained from laboratory specimens and applied to the analysis of test vessels with good results. Test data were in the low-cycle fatigue range ($N < 10,000$ cycles).

The hydrotest is considered a vital element in design against fracture. A hydrotest at the lowest anticipated service temperature can be used to define the largest flaw that could exist and not cause failure.[79] To determine whether an initial overstress (i.e., the proof test) has any major influence on cyclic flaw growth at a lower stress, a number of round notched specimens were given a two-cycle 10% overstress prior to cycling to failure. There was no significant effect.

It was noted that causes of slow crack growth other than fatigue, such as hydrogen and stress-corrosion cracking and sustained stress effects, render such an analysis invalid. Prevention rather than prediction of these effects was recommended.[79]

6.2.2.6 The Fracture Analysis Diagram

Since cracks may propagate through strain-rate sensitive materials at lower nominal stresses than are required to initiate a crack, a test has been devised to measure the minimum propagation stress. This is known as the Crack Arrest Test, and its results are known as a CAT (Crack Arrest Temperature) curve.[42,47,69,80] The CAT curve is a plot of minimum propagation stress versus temperature, and it undergoes a transition in the same manner as impact energy. The minimum propagation stress is measured as

the largest stress at which an artificially initiated crack will not continue to propagate at a given temperature. It appears to be a common practice to interpret the crack arrest test in terms of the fracture mechanics assumption that energy release rates are the same for fixed grips as for fixed load,[42] because the loading system is a hydraulic (essentially fixed grip) loading system.[81] However, in veiw of Bueckner's conclusion that the energy release rates during propagation are not equal[62] and the results of large-scale tests, there is real doubt as to the validity of this assumption. To make matters worse, size effects have been observed in the crack arrest test; thus thick-section tests[42] are required, and constant-load tests are doubly difficult. Nevertheless, the CAT curve is a prime basis of the widely used fracture analysis diagram.

The fracture analysis diagram, shown in Fig. 6.13, is commonly presented as a semiempirical method of material selection and approximate analysis to prevent brittle fracture. Detailed explanations of the method can be found in Refs. 42 and 47. The dashed lines give the stress at which a crack of given size will start to propagate, as a function of

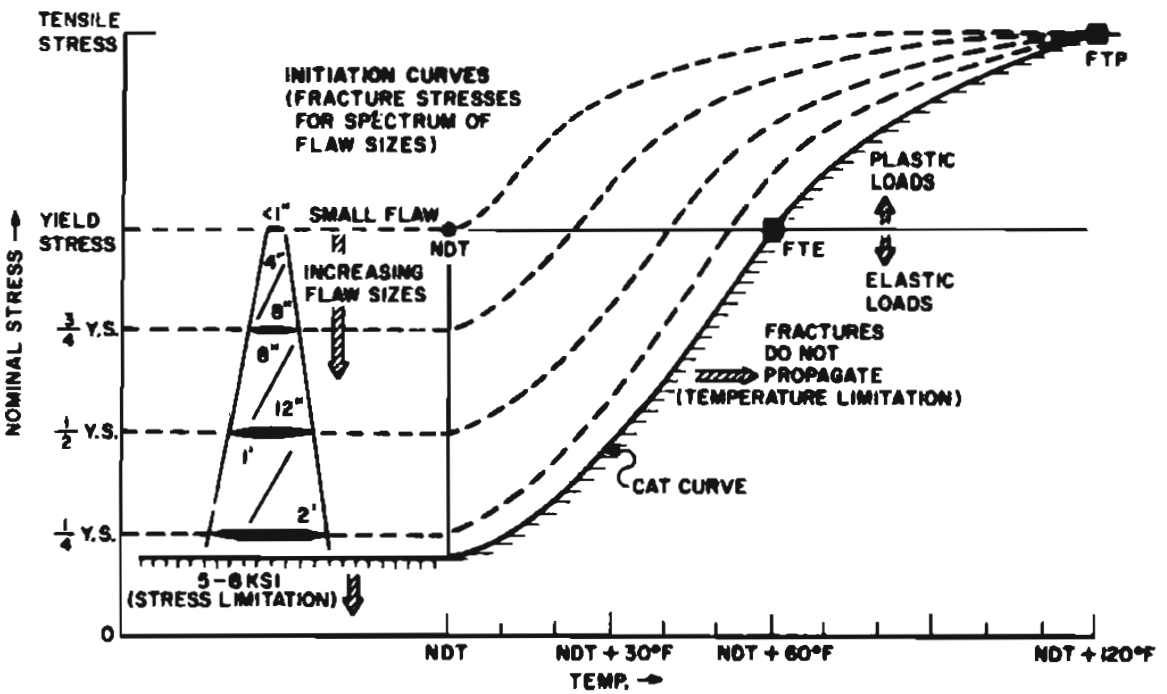

Fig. 6.13. Generalized Fracture Analysis Diagram as Referenced by the NDT Temperature.

temperature, referenced to the NDT temperature. The NDT temperature is determined directly from a drop-weight test and, indirectly, by correlation with the simpler Charpy impact test. The parametric crack size curves were determined partially by fracture mechanics and partially by plotting actual failure data. For most strain-rate sensitive steels,[46] the CAT curve crosses the yield stress curve at about the NDT temperature plus 60°F (the FTE: fracture transition elastic) and joins the ultimate strength curve at about the NDT temperature plus 120°F (the FTP: fracture transition plastic). For temperatures above the FTE temperature, cracks supposedly will not propagate through regions carrying a nominal stress below yield. Since primary stresses are limited to values below yield, full-load operation is generally permitted above the NDT temperature plus 60°F, with only reduced loads permitted below the NDT temperature plus 60°F so as to stay below the CAT curve.[82]

It should be remembered that the fracture analysis diagram is based on a nominal stress[42] defined as the stress computed without considering the presence of a crack. Residual stresses must be considered. The great advantage of the transition temperature approach, including the fracture analysis diagram, is its simplicity; no stress analysis beyond the traditional procedures required to prevent gross yielding is necessary. However, the method is mainly applicable to temperature and strain-rate sensitive materials, which exclude high-strength steels.[42] In addition to lacking strain-rate sensitivity, high-strength steels may have a yield-to-ultimate strength ratio as high as 0.9. For these materials, the FTP must occur at a stress level that is only slightly higher than the stress at which the NDT and FTE occur. Therefore, even if the fracture analysis diagram concept is valid for high-strength steels, a new set of curves will probably be required. Therefore a method of fracture prevention is available for brittle metals (fracture mechanics) and for low- and medium-strength steels (the fracture analysis diagram), but no proven method is presently available for high-strength steel.* Because of size effects,

---

*This statement is controversial. The development of a proven method of fracture prevention in high-strength steel is the subject of current research.

Ref. 42 concludes that the fracture analysis diagram can be used only as a means of comparing materials and not for analysis.

A recent Swedish report by Grounes[82] gives a good description of the transition temperature method and its application. The Swedish use the crack arrest temperature as a safety criterion. An estimate of this transition temperature at the end of the reactor's lifetime must take into account increases due to fabrication, welding, geometry, aging, and irradiation. The transition temperature versus stress curve (CAT curve) moves to the right during the reactor's lifetime. As long as this curve does not cross the reactor vessel's stress versus temperature curve, the vessel is considered safe. Thus the Swedish consider temperature to be the only real safeguard against brittle fracture.[82] Hence pressure vessel steel is selected with three requirements in mind: high strength, low initial transition temperature, and good corrosion resistance.

6.2.3 Stress Evaluation

One familiar feature of the present ASME Design Code for nuclear pressure vessels, Section III, is a method for classifying the stresses in the pressure vessel according to their potential effects. This method of classifying stresses is described by the "hopper diagram," which is shown in Table 6.1, and by the stress classification table reproduced here as Table 6.2. One aspect of this classifying system has already been discussed (the stress conditions required for plastic collapse, as shown in Fig. 6.12), but some further discussion is still warranted. Section III specifies that the limiting stress intensity,* S_m, should equal 2/3 S_y or 1/3 S_{ult}, whichever is least, where S_y is the uniaxial yield stress and S_{ult} is the uniaxial ultimate strength. For the purpose of this discussion, it will be assumed that S_y governs the value of S_m, which is generally the case at operating temperatures.

The "hopper diagram" in Table 6.1 embodies four basic design criteria:

1. The structure must be safe against plastic collapse under the loads that could cause plastic collapse.

---

*S, the stress intensity, equals twice the maximum shear stress.

Table 6.1. Stress Categories and Limits of Stress Intensity.
(Fig. N 414 of Section III of ASME Code)

Stress Category	Primary			Secondary Membrane plus Bending	Peak
	General Membrane	Local Membrane	Bending		
Description (For examples, see Table N-413)	Average primary stress across solid section. Excludes discontinuities and concentrations. Produced only by mechanical loads.	Average stress across any solid section. Considers discontinuities but not concentrations. Produced only by mechanical loads.	Component of primary stress proportional to distance from centroid of solid section. Excludes discontinuities and concentrations. Produced only by mechanical loads.	Self-equilibrating stress necessary to satisfy continuity of structure. Occurs at structural discontinuities. Can be caused by mechanical load or by differential thermal expansion. Excludes local stress concentrations.	(1) Increment added to primary or secondary stress by a concentration. (notch) (2) Certain thermal stresses which may cause fatigue but not distortion of vessel shape.
Symbol (Note 4)	P_m	P_L	P_b	Q	F
Combination of stress Components and Allowable Limits of Stress Intensities.	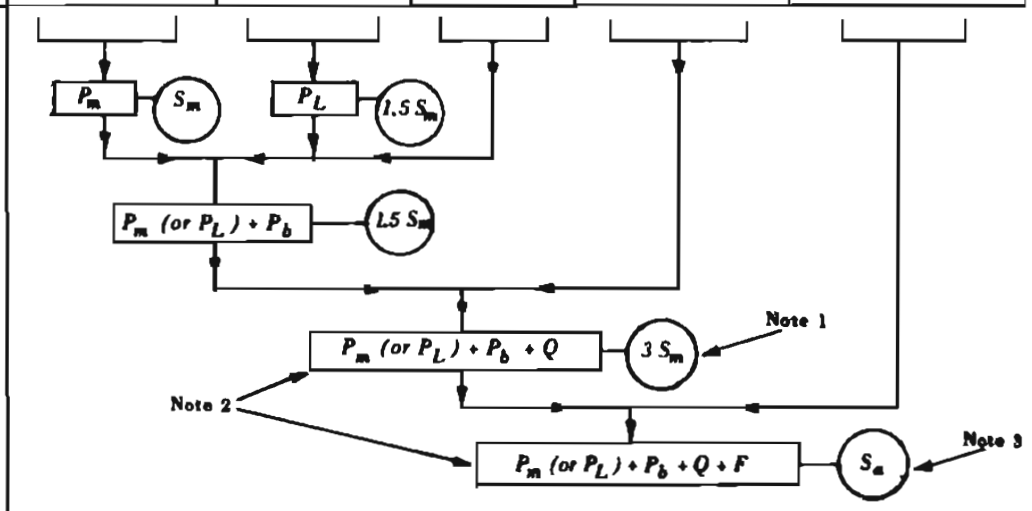				

NOTE 1 — When the secondary stress is due to a temperature excursion at the point at which the stresses are being analyzed, the value of S_m shall be taken as the average of the S_m values tabulated in Tables N-421, N-422, and N-423 for the highest and the lowest temperature of the metal during the transient. When part or all of the secondary stress is due to mechanical load, the value of S_m shall be taken as the S_m value for the highest temperature of the metal during the transient.

NOTE 2 — The stresses in Category Q are those parts of the total stress which are produced by thermal gradients, structural discontinuities, etc., and do not include primary stresses which may also exist at the same point. It should be noted, however, that a detailed stress analysis frequently gives the combination of primary and secondary stresses directly and, when appropriate, this calculated value represents the total of P_m (or P_L) + P_b + Q and not Q alone. Similarly, if the stress in Category F is produced by a stress concentration, the quantity F is the additional stress produced by the notch, over and above the nominal stress. For example, if a plate has a nominal stress intensity, S, and has a notch with a stress concentration factor, K, then $P_m = S$, $P_b = 0$, $Q = 0$, $F = P_m(K-1)$ and the peak stress intensity equals $P_m + P_m\ (K-1) = KP_m$.

NOTE 3 — S_a is obtained from the fatigue curves, Figs. N-415 *(a)* and *(b)*. The allowable stress intensity for the full range of fluctuation is $2\ S_a$.

NOTE 4 — The symbols P_m, P_L, P_b, Q, and F do not represent single quantities, but rather sets of six quantities representing the six stress components σ_t, σ_l, σ_r, τ_{tl}, τ_{lr}, and τ_{rt}.

Table 6.2. Classification of Stresses for Some Typical Cases. (Table N-413 of Section III of ASME Code)

Vessel Component	Location	Origin of Stress	Type of Stress	Classification
Cylindrical or spherical shell	Shell plate remote from discontinuities	Internal pressure	General membrane Gradient through plate thickness	P_m Q
		Axial thermal gradient	Membrane Bending	Q Q
	Junction with head or flange	Internal pressure	Membrane Bending	P_L Q
Any shell or head	Any section across entire vessel	External load or moment, or internal pressure	General membrane averaged across full section. Stress component perpendicular to cross section	P_m
		External load or moment	Bending across full section. Stress component perpendicular to cross section	P_m
	Near nozzle or other opening	External load moment, or internal pressure	Local membrane Bending Peak (fillet or corner)	P_L Q F
	Any location	Temp. diff. between shell and head	Membrane Bending	Q Q
Dished head or conical head	Crown	Internal pressure	Membrane Bending	P_m P_b
	Knuckle or junction to shell	Internal pressure	Membrane Bending	P_L* Q
Flat head	Center region	Internal pressure	Membrane Bending	P_m P_b
	Junction to shell	Internal pressure	Membrane Bending	P_L Q
Perforated head or shell	Typical ligament in a uniform pattern	Pressure	Membrane (Av. thru cross section) Bending (Av. thru width of lig., but gradient thru plate) Peak	P_m P_b F
	Isolated or atypical ligament	Pressure	Membrane Bending Peak	Q F F
Nozzle	Cross section perpendicular to nozzle axis	Internal pressure or external load or moment	General membrane av. across full section. Stress component perpendicular to section	P_m
		External load or moment	Bending across nozzle section	P_m
	Nozzle wall	Internal pressure	General membrane Local membrane Bending Peak	P_m P_L Q F
		Differential expansion	Membrane Bending Peak	Q Q F
Cladding	Any	Differential expansion	Membrane Bending	F F
Any	Any	Thermal gradient thru plate thickness	Bending	F**
Any	Any	Any	Stress Concentration (notch effect)	F

* Consideration must also be given to the possibility of wrinkling and excessive deformation in vessels with large diameter-to-thickness ratio.

** Consider possibility of thermal stress ratchet (see N-417.3).

2. The plastic strains produced by any single application of load must be limited.

3. There must be no cyclic plastic strains due to any stresses except those produced by local stress concentrations and local thermal effects.

4. At points where cyclic plastic strains do occur, a fatigue analysis must show that fatigue failure will not occur.

The two modes of failure not specifically considered by the hopper diagram are buckling and brittle fracture. Buckling must be designed against on an individual basis, as specified in article N-410(C) of Section III. At present, design against brittle fracture is assumed to be accomplished through the application of a transition temperature (NDT) criterion.

Design against plastic collapse begins with the assumption that only force (mechanical) loads can produce unrestricted plastic deformation (plastic collapse). Secondly, use is made of the Lower Bound Theorem in plasticity, which states that if any set of reactions and internal stresses can be found that will hold a structure in equilibrium under a given load without producing a failure mechanism, that load is less than the plastic collapse load. In practice, this theorem is modified so that its physical significance is more obvious. If a structure is statically indeterminate, it may be rendered statically determinate by introducing a sufficient number of hinges or cuts so that the internal stresses and reactions can be computed from the equations of statics (equilibrium) alone. This is standard practice in the plastic design of steel frames. It is also standard practice in the discontinuity type of elastic shell analysis. In any event, the effect of hinges or cuts on the real structure would be to lower its plastic collapse strength. Therefore, if the weakened statically determinate structure does not collapse, the unweakened real structure cannot collapse. In Section III the further restriction is added that in the weakened structure, primary stresses can only cause yielding if the zones of yielding will be local and will be elastically restrained. Consequently, the plastic strains under any single application of loading will remain small, and plastic collapse can certainly not occur. The stresses considered capable of causing plastic collapse

are called primary stresses. Primary stresses are of three types: primary general membrane, primary local membrane, and primary bending. If raised to the yield point, a primary general membrane stress would cause general yielding, while a primary local membrane stress would cause only local yielding. The definition of a bending stress is obvious. However, it should be noted that bending in a shell is a local phenomenon, and therefore yielding due to bending should also be a local phenomenon. Since in the case of a primary general membrane stress, yielding would be general rather than local, yielding is prohibited by the requirement that

$$P_m \leq \frac{2}{3} S_y , \tag{8}$$

where P_m is the primary general membrane stress intensity and S_y is the uniaxial yield stress. If

$$S_m = \frac{2}{3} S_y , \tag{9}$$

where S_m is the allowable stress intensity, then

$$P_m \leq S_m , \tag{10}$$

which is the limitation on primary general membrane stress shown in Fig. 6.12. In the case of a primary local membrane stress, which is a membrane stress that has been increased locally by a discontinuity, yielding is permitted because the plastic strains will be limited by compatibility with the surrounding elastic material. This requirement is expressed by the equation

$$P_L \leq 1.5 S_m , \tag{11}$$

where P_L is a primary local membrane stress. This requirement is shown graphically in Fig. 6.12. In the case of primary bending, with or without axial force, only the extreme fibers of the section are allowed to yield. Thus, the rest of the section remains elastic and no plastic strain can actually occur. This requirement is expressed by the equation

$$P_m \text{ (or } P_L) + P_b \leq 1.5 S_m , \tag{12}$$

where P_b is a primary bending stress. This condition is also shown graphically in Fig. 6.12. Thus the limits on primary stresses are based on a restricted Lower Bound Theorem, applied to a statically determinate analysis of each part of the structure, with a correction being made for the effects of local discontinuities and local loads on the local membrane stress.

Since some plastic strains have been permitted at discontinuities and thermal effects have not yet been considered, it is necessary to place additional limits on the plastic strains. These limits are listed as criteria (3) and (4) in the previous list. At the discontinuities, two additional types of stress can be active besides primary local membrane and primary bending. These are secondary stresses, which include thermal stresses and discontinuity-produced bending stresses and peak stresses due to stress concentrations. Considering the combination of all primary and secondary stresses, that is, all stresses except peak stresses, it is desired to prohibit cyclic plastic strains. This problem is approached as follows. With reference to Fig. 6.14, yielding first occurs when the maximum principal stress difference equals the uniaxial yield stress. From point O to point A, loading is elastic and all stresses remain proportional. For additional loading, the stresses at a point that has yielded can either remain at A or move along the yield locus. Using intuition based on the results of analytical studies, it is assumed that if the stress point does move along the yield locus, it moves toward the nearest corner and does not go beyond it. This is a necessary but not a proven condition for the following conclusions to be valid. The effects of removing the load are entirely elastic until yielding occurs again. Unloading will produce a state of stress that moves along a path parallel to OA but in the opposite direction. It can be seen that BC must be equal to twice OA for yielding to occur upon unloading if the Bauschinger effect is ignored. This conclusion applies for initial loading to any portion of the yield surface. Therefore, if the elastically calculated stresses, indicated by the point D in Fig. 6.14, are not greater than twice the stresses at point A, no cyclic yielding will occur. It is to be noted that movement of the stress point between A and B provides for stress redistribution due to plastic flow following initial yield. Thus

ORNL-DWG 67-3793

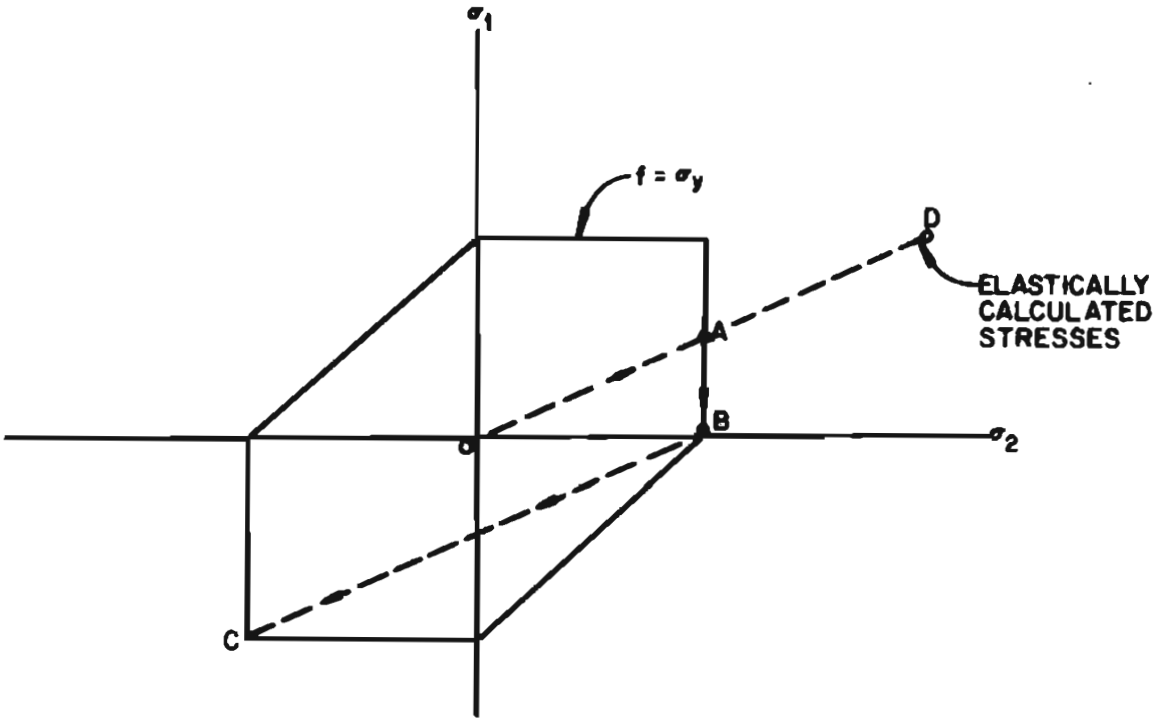

Fig. 6.14. Tresca Yield Criterion for Biaxial Loading.

the requirement placed on the sum of primary plus secondary stresses, as shown in Table 6.1, is that

$$P_m \text{ (or } P_L) + P_b + Q \leq 3S_m \,, \tag{13}$$

where Q is the secondary stress.

The final requirement regarding plastic strains is that peak stresses must not cause fatigue failure at points of stress concentration. This requirement, as shown in Table 6.1, is expressed by the equation

$$P_m \text{ (or } P_L) + P_b + Q + F \leq S_a \,, \tag{14}$$

where F is a peak stress and S_a is an allowable elastically calculated stress amplitude that specifies the cyclic total strain range. The assumption that the elastic analysis gives a good estimate of the cyclic total strain range at points of local yielding is an important assumption. For this assumption to be valid, a zone of local yielding must be small

and be highly constrained by the surrounding elastic material. One reason for requiring Eq. (13) to hold is that the foregoing assumption might not be sufficiently valid away from a stress concentration.

The hopper diagram shown in Table 6.1 has recently been modified* (see Table 6.3) to eliminate a minor inconsistency with paragraph N-441 of Section III. Paragraph N-441 defines the design pressure as the normal operating pressure plus an allowance for probable pressure surges up to the setting of the pressure-relief devices. It is the design pressure that is used for insuring compliance with the limitations on primary stresses, bolt design stresses, bearing stresses, pure shear stresses, and triaxial stresses. The actual operating pressure, which is by definition less than the design pressure, is used to insure compliance with the limitations regarding cyclic plastic strain. There is no limit placed directly on the secondary bending stresses due to the design pressure, but there is a limit placed on the secondary bending stresses due to the maximum operating pressure. If there is a difference between the design pressure and the maximum operating pressure, it is a margin of safety to which the limits on cyclic plastic strain need not apply. Even if the design pressure were to cause large plastic strains at the discontinuities, the vessel would not fail plastically because the limits on primary stresses have already been applied. However, the safety criteria regarding buckling and brittle fracture do need to be applied to the design pressure conditions. It will be noted that the alternative statements regarding P_m and P_L that appear in Table 6.1 and Eqs. (12), (13), and (14) have been eliminated in Table 6.3. This change is for clarity only and is not a change in definitions.

Section III of the Code allows an elastically calculated secondary moment equal to twice the yield moment, but an actual moment equal to 1.5 times the yield moment renders a rectangular section fully plastic and is the maximum moment that can be carried by the section without a normal force. Therefore, Section III allows a fully plastic section to develop at a discontinuity during initial loading. Actually, a section will never become fully plastic because the discontinuities in rotation

*See the Winter 1966 Addenda to Section III of the ASME Code.

Table 6.3. Revisions to the Hopper Diagram

Revise the central portion of Table 6.1 so as to appear as:

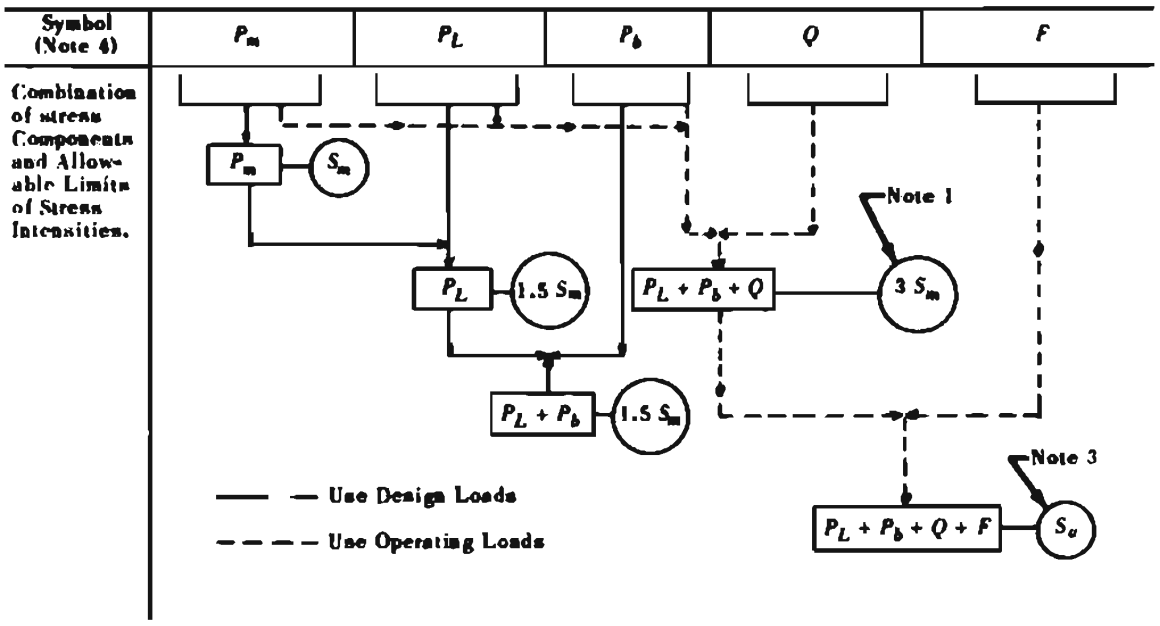

Note 2 *Revise the last sentence to read:*

For example, if a plate has a nominal stress intensity, $P_m = S$, $P_b = 0$, $Q = 0$ and a notch with a stress concentration K is introduced, then $F = P_m (K - 1)$ and the peak stress intensity equals $P_m + P_m (K - 1) = KP_m$.

Also revise: P_m (or P_L) + P_b + Q *to read:* $P_L + P_b + Q$.

Also add to this note the following: However, P_L is the total membrane stress which results from mechanical loads including discontinuity effects, rather than a stress increment. Therefore the P_L value always includes the P_m contribution.

N-414.3 *Revise* P_m (or P_L) *to read:* P_L.

N-414.4 *Revise* P_m (or P_L) *to read:* P_L.

N-414.5 *Revise* P_m (or P_L) *to read:* P_L.

and displacement for which is must provide are limited. Also, since the maximum allowable moment is beyond the capacity of the section, load redistribution within the elastic parts of the vessel is inevitable. Little information regarding the actual plastic strains and stresses developed at discontinuities and the accompanying load redistribution is available. However, it appears that such data are available as a byproduct of proof testing by the methods for plastically analyzing experimental strains,[77,78] as discussed previously. The effects of shear force on yielding have also been neglected.

It should be noted that residual stresses are not considered in the hopper diagram. These stresses are due to yielding under the thermal stresses produced by welding. They are, in fact, residual thermal stresses and are self-equilibrating. Residual stresses have no effect on the fully plastic strength of a cross section, nor should they affect the cyclic plastic strains in a pressure vessel. They can, however, cause the plastic strains that occur under initial pressurization to be larger than expected or to occur at unexpected locations. If a cross section is loaded to its fully plastic capacity, whatever residual stresses existed before that loading will be eliminated, but a new pattern of residual stresses will develop upon unloading. This is likely to be the case at points of high secondary moment, such as the head and nozzle junctions. On the other hand, the residual stresses that initially exist in the membrane regions, such as those associated with welds, are likely to remain in substantially their original pattern.

The discussion above makes one point fairly clear. In order to classify the stress intensity at a point, it is necessary to know not only the shape of the structure and the origin of the load but also to understand the behavior of the structure in response to the loads. Judgement may be necessary, especially if the stress analysis is not amenable to one of the strength of materials approaches — for example, shell theory or beam theory. In such cases, it may not be possible to separate the stress distributions into membrane and bending components, and therefore it may be difficult to assign the proper stress categories. There is apparently quite a bit of uncertainty when the stress classification problem is not one of those listed in Table N-413 of the code. The code

gives very little help in this respect in the way of examples. Even the appendices, where several stress analysis problems are worked, do not assign stress categories to the computed value. Experienced stress analysts and designers can usually assign stress categories properly. Nevertheless a valuable service would be performed if additional guidelines were available, either as worked examples or as a more complete reference table, such as N-413.

Reference 56 contains an extensive discussion of the fatigue criteria employed in the present code. The assumption that the effects of biaxiality have been taken into account is implicit in the prescribed method of analysis. Since the strain range at a point of peak stress can be estimated by an elastic analysis, the provision for biaxiality can be explained in terms of elastic analysis. The stress intensity $(\sigma_1 - \sigma_3)$ is a direct measure of maximum shear strain, according to the equation

$$\gamma_{max} = \frac{\sigma_1 - \sigma_3}{2G} ,$$

where γ_{max} is maximum shear strain and G is the shear modulus; G is related to the elastic modulus, E, and Poisson's ratio, ν, by the expression

$$G = \frac{E}{2(1 + \nu)} .$$

Therefore, the code criteria for fatigue relate the range of fluctuation of the maximum shear strain to the steady value about which the variation takes place. Studies of the effects of biaxiality have been made, and the most recent biaxial fatigue data are those of Ives, Kooistra, and Tucker[83] at the Babcock & Wilcox Company. These data were obtained especially to complement a series of large-scale pressure vessel tests (see Sect. 6.3.2). Three pressure vessel steels, A 201, A 302, and T-1 (the same as the materials being used in the large-scale pressure vessel tests), were tested in low-cycle equibiaxial fatigue. It was found that the data could best be correlated with the existing uniaxial data by plotting equivalent strain versus the number of cycles to failure, where equivalent strain was defined by the equation

$$\bar{\epsilon} = \frac{\sqrt{2}}{3}\left[(\epsilon_x - \epsilon_y)^2 + (\epsilon_y - \epsilon_z)^2 + (\epsilon_z - \epsilon_x)^2\right]^{1/2} .$$

The data plots and curves for each of the three steels tested[83] are shown in Figs. 6.15, 6.16, and 6.17, and a summary plot of the biaxial fatigue curves is shown in Fig. 6.18. Figure 6.18 does not show exactly the same variations in fatigue resistance with yield strength as are shown in Fig. 6.9. Contrary to Fig. 6.9, Fig. 6.18 shows that T-1 steel has slightly more fatigue resistance than A 302 for all low-cycle strain levels. In addition, the crossover points between A 201 steel and the higher strength steels are nearer to 1000 cycles than to 10,000 cycles. The trends shown in Fig. 6.18 are encouraging with respect to the use of higher strength steels in nuclear pressure vessels.

The use of elastic stress concentration factors to estimate fatigue-strength reduction may be conservative under most conditions. The stress gradient may also be an important parameter.[41]

Periodic shutdowns and load fluctuations during operation[84] may subject a reactor pressure vessel to low-cycle fatigue. Fatigue is most likely to occur at points of high stress concentration, such as discontinuities and nozzle attachments. Reinforcement of openings may reduce load stresses but it may increase thermal stresses. The requirements for minimizing force load stresses and thermal load stresses are sometimes in opposition, and it is their sum that must be minimized.

Despite the prominence given to fatigue analysis in Section III of the Code, this mode of failure may still not be as likely as brittle fracture.[85] However, it should be noted that the fatigue analysis of Section III does not consider the prior existence of flaws, except by virture of its conservatism. Most failures are due to a combination of causes rather than a single cause.[50] It has been argued that if a through crack of length equal to twice the plate thickness would not cause brittle fracture, the growth of an initial partly through crack would lead to leakage before brittle fracture.[66] This is the "leak-before-break" criterion proposed by Irwin (see Chap. 7).

The fracture analysis diagram was used as a basis for evaluating the safety of the EGCR pressure vessel.[86] Although the assumed flaw sizes were

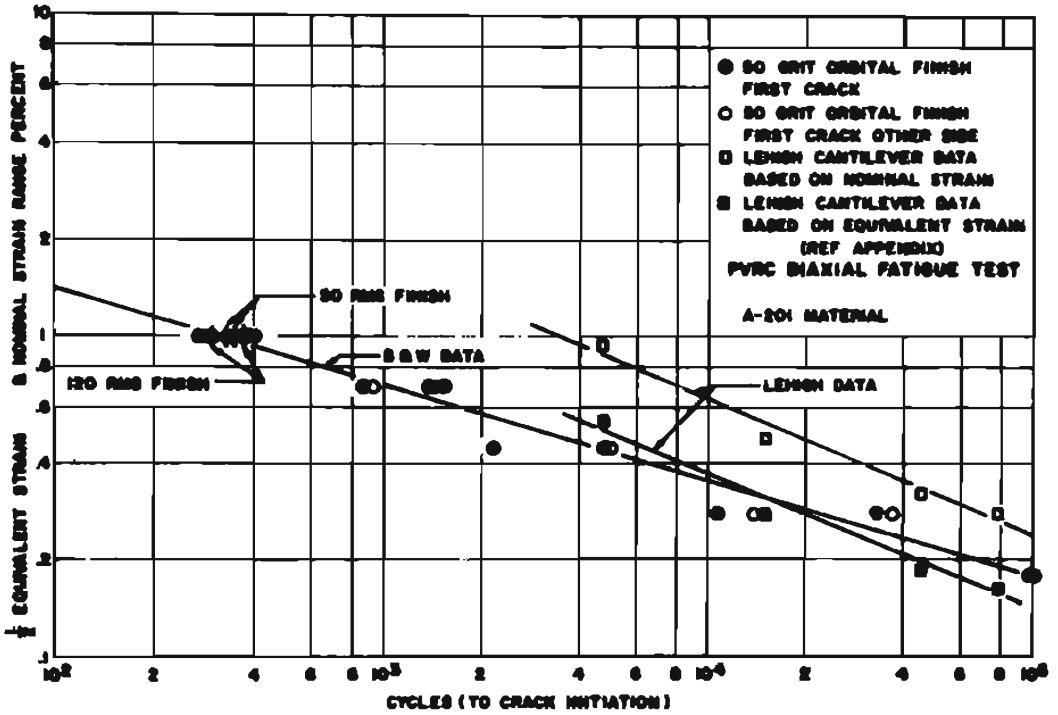

Fig. 6.15. Fatigue Test Results for A 201 Steel. (From Ref. 83)

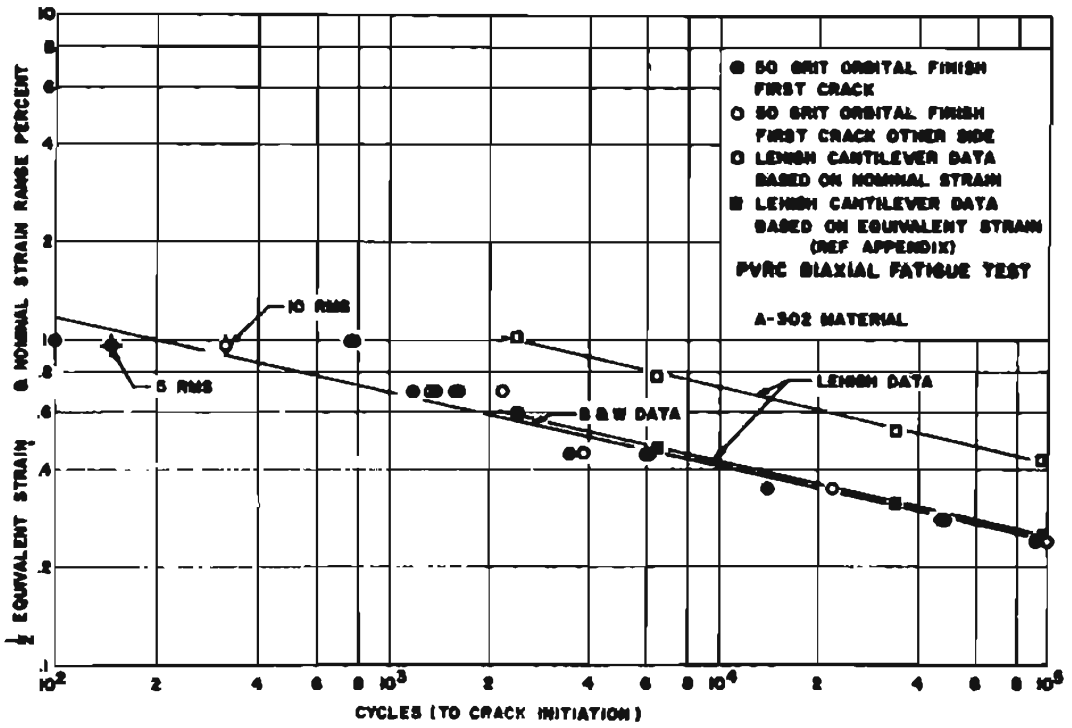

Fig. 6.16. Fatigue Test Results for A 302 Steel. (From Ref. 83)

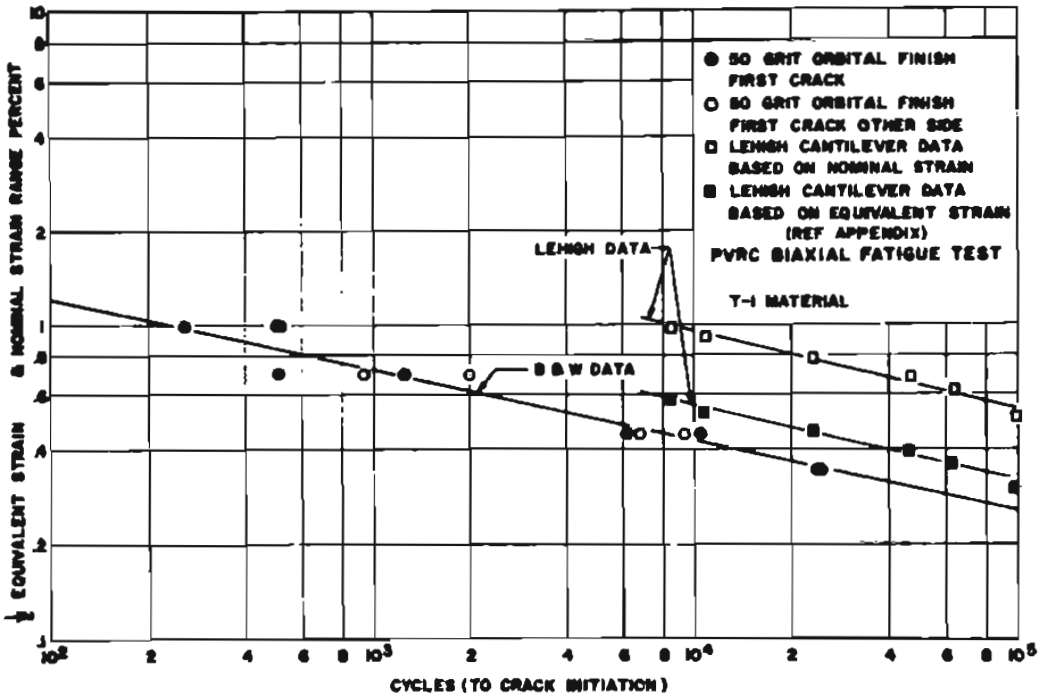

Fig. 6.17. Fatigue Test Results for T-1 Steel. (From Ref. 83)

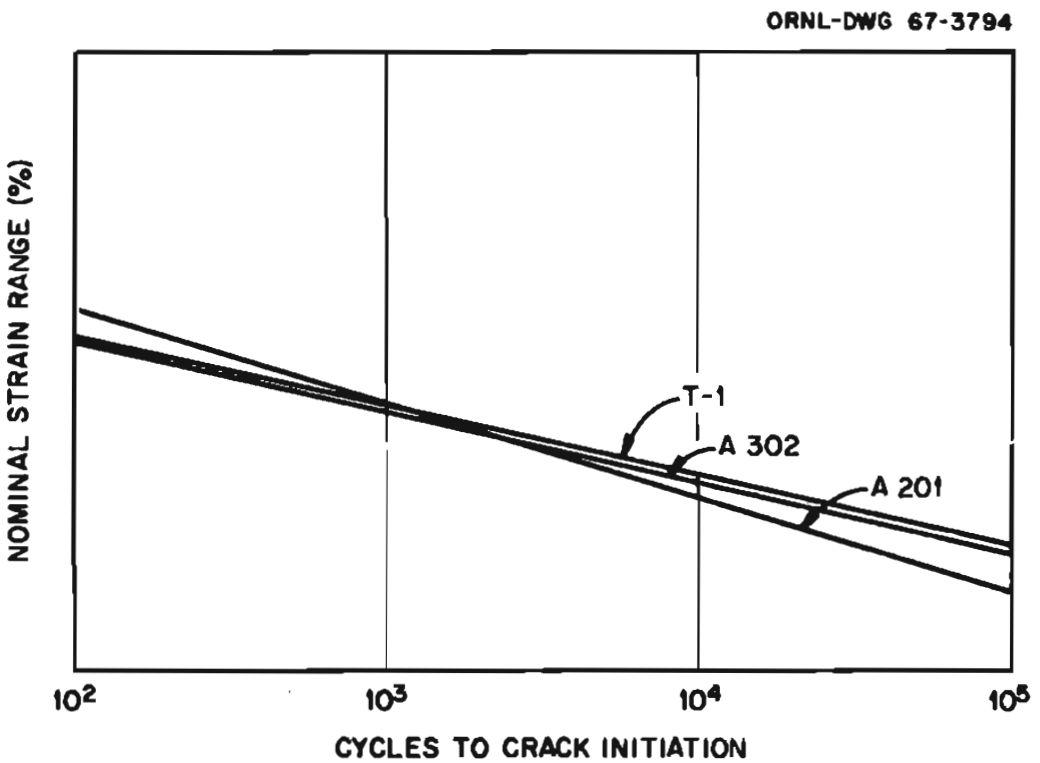

Fig. 6.18. Summary Plot of the B&W Biaxial Fatigue Curves.

increased by one size range to compensate for the effects of irradiation, the effects of size on transition temperature were not specifically mentioned.

6.2.4 Other Design Considerations

The process of engineering a nuclear pressure vessel consists of a series of steps that begin with the establishment of design criteria and end with planned inspection and maintenance during the service life of the vessel. Some additional comments on particular phases of the engineering process not previously discussed are given in this section.

6.2.4.1 Division of Responsibility

The reactor designer and the pressure vessel designer are usually not in the same organization. Therefore, it is important that the division of responsibility between their two organizations be made clear. Pressure vessel design is an engineering specialty. Pressure vessels are designed for a wide variety of industrial purposes, and it appears to be the established practice that the buyer of the vessel is responsible for anticipating the effects of service environment on the vessel, and the seller of the vessel is responsible for furnishing an initially sound vessel. This philosophy appears adequate in cases where the environmental effects are only chemical. However, it is not obvious that it is adequate in cases where the environmental effects may be structural as well as chemical. Specifically, when the environmental effect is a change in structural properties due to irradiation, it would appear prudent for the vessel designer to understand and anticipate these effects. As present, reliance could be placed on the fact that irradiation raises both the yield stress and the ultimate strength, and therefore ignoring both effects should lead to a safe design. However, this concept will break down in any case where ductility or fracture strength govern the design, since both quantities decrease due to irradiation. It is quite possible that a change in design philosophy will be necessary for the design of a high-strength steel vessel, since either ductility or fracture strength may govern the design. It has been argued that the reactor system designer

should be responsible for anticipating irradiation effects,[46] but no mention has been made of high-strength steel. Until generally reliable irradiation effects design criteria are developed or the problem is eliminated by the improvement of material, it will be necessary to modify the operating procedures for each reactor vessel according to the results of its own surveillance program.

It has been noted that the design lifetime of a nuclear pressure vessel may be as much as 40 years,[46] but the lifetimes of some existing vessels may be shortened by NDT considerations.[49] Since the existing vessels referred to are mild steel vessels and the stress limits of Section III do not consider the effects of irradiation, it follows that compliance with Section III cannot be used as the sole basis for arguing the incredibility of pressure vessel failure. Provisions for insuring vessel safety during operation are the responsibility of the owner and the enforcement authority.

6.2.4.2 Material Selection and Geometric Design

Present practice is to select pressure vessel steels with low initial NDT in order to provide the greatest margin for change.[48] Steels such as A 212 grade B and A 302 grade B, which have been used in U.S. reactor vessels, are specified to have an initial NDT temperature of −20 to +40°F. The addition of 2 to 3% nickel produces steels with improved toughness like those used in the Army's SM-1A and PM-2A vessels with NDT temperatures of −40 to −80°F. However, some of these steels are hypersensitive to irradiation. The best high-alloy quenched and tempered steels of the type used in submarine hulls have NDT temperatures of −120 to −160°F.[48] However, from previous discussions, it is obvious that a low initial NDT temperature does not guarantee a relatively greater fracture strength at higher temperatures. In fact, the NDT approach has been shown to be least applicable to nonstrain-rate-sensitive materials.[42] The specific purpose of the quench and temper operation is to improve fracture strength and lower the NDT, particularly of heavy (thick) sections.[46]

The neutron flux distribution in a vessel wall varies considerably in the vertical direction and reaches a maximum near the core midplane.[48,49] Therefore good design practice requires that discontinuities not be located

near the core midplane.[46] However, longitudinal welds may be required at the midplane because of the size of the vessel, and therefore they are of special interest.[49] The stresses at nozzles are important, of course, because they are high, even if they do not occur at the point of peak flux.[49]

6.2.4.3 Fabrication (see Chap. 8)

The effect of fabrication on vessel properties must be considered.[46] It has been estimated that stress relieving at temperatures low enough to preserve mechanical properties is only 80% effective. Therefore residual stresses may be as high as 20% of yield.[46] Stress relieving accordingly involves a compromise. If residual stresses are completely eliminated, mechanical properties may be affected.[85] If mechanical properties are preserved, some residual stresses will remain.[46] The British employ on-site stress-relieving techniques for their site-constructed vessels.[85] (On-site stress relieving is also planned by Chicago Bridge and Iron Company for their forthcoming site-constructed vessel.)

6.2.4.4 Hydrotesting and Operation (see Chap. 10)

Hydrotesting indicates the maximum possible flaw size, as well as strength.[85] When a reactor vessel has been exposed to neutron radiation and has experienced a shift in NDT, careful attention must be given to the advisability of additional hydrotests.[46] This is particularly true if the hydrotests are conducted at room temperature.

Present practice is to establish limits on operating loads for vessel temperatures below the FTE (NDT temperature plus 60°F). However, since the neutron flux varies with position, the FTE varies with position.[48] Thermal stresses as well as pressure stresses need to be considered in setting the operating limitations.[46,48] Operating limitations are usually stated in terms of reactor pressure versus reactor temperature, with a specified maximum rate of change of temperature to make transient thermal stresses a known function of reactor pressure.[48] For example, in 1962 two days were required to shut down the Army Package Power Reactor (APPR).[87] For some pressurized-water reactors, a lower bound to the pressure-temperature range may be set by the boiling point of water.[48] A lower limit on

pressure may also be established by the pressure necessary for main coolant pump operation.[46,49] A recent survey by the AEC indicated that the irradiation embrittlement problem has affected the operation of four reactors and may effect ten more.[46] It is conceivable that the upper- and lower-bound pressure versus temperature curves for a reactor vessel may meet. In this case, the NDT approach gives no safe operating mode. The possibility of such a situation provides a strong motivation for the development of a fracture mechanics analysis that will indicate whether or not a safe mode of operation actually exists.[46]

It has been argued that warm prestressing can be used to provide for safe operation at reduced temperatures. Cowan and Nichols[85] state,

> We think advantage of this test (an initial warm pressure test) can be taken only if service conditions are similar to the test conditions and especially there should be no risk of impact loading or of defects lengthening beyond their original yielded stability limits. We consider that there is insufficient experience of this approach to recommend operation of a reactor pressure vessel in the brittle range.

6.2.4.5 Surveillance, In-Service Inspection, and Maintenance (see Chaps. 9 and 10)

Since the estimates of irradiation dosage available during design are only approximate and the energy spectrum of an actual reactor may differ from that of the test reactor in which irradiation tests are performed, surveillance programs are conducted. This method of evaluating irradiation effects for a particular vessel has an advantage in that it reduces the reliance on dosimetry. Irradiation effects can then be assumed similar in the vessel and in the specimen without a precise knowledge of the dose.[48] To give an idea of the potential inaccuracies in flux estimates, actual fluxes within the SM-1, PM-2A, and Dresden-I vessels were 14, 57, and 200 to 300% greater than estimated.[48]

6.3 CURRENT RESEARCH ON THE DESIGN OF PRESSURE VESSELS

Design codes are based on research and experience. There are many areas of research that have led to the excellence in design and construction that currently exists in the nuclear pressure vessel industry. Foremost among these are the forming and forging procedures, quenching and

tempering techniques, material behavior investigations (thermal- and load-cycling fatigue, creep, relaxation, flaw formation, flaw growth, etc.), weld development programs, and experimental and theoretical stress analyses of the various design configurations that commonly occur in reactor pressure vessels.

Most of the areas of research are discussed in other sections of this chapter. In particular theoretical analyses of shells have been treated at some length, as has the more recent research in the fracture mechanics and transition-temperature approaches to pressure vessel design. This section is devoted to summarizing information on how the analytical techniques are used and reviewing the experimental work that provides data for both design use and for verifying the analytical work. Attention is also focused on a series of failure tests of large model and full-size pressure vessels, as well as a recent failure by brittle fracture of a pressure vessel during the proof test.

6.3.1 Theoretical and Experimental Research

The techniques for analyzing the more common axisymmetric shell configurations are quite well developed and have culminated in a series of computer analyses[88-106] and analytical parameter studies[107-116] (mostly for nozzles attached to spherical shells) for design application. Unsymmetric loads, such as moment or transverse shear loads on the nozzle, can be accounted for by some of the computer programs.[98-100,105]

The methods used in the computer programs range from finite difference applications through direct applications of the analytical solutions that exist. In some cases the shells must be quite thin, while in other cases relatively thick shell analysis may be performed. Kraus[32] discusses the Kalnin,[100] CEGB,[88] AVCO,[91] and Bettis[101] programs. Rodabaugh, Witt, and Cloud[111] discuss the CERL II (ORNL)[105] and Seal-Shell-2 (Bettis)[101] codes, as well as analyses by Waters[107] and Bijlaard.[112-115] A boundary-point collocation method is also discussed.[117] Comparisons with theory and experiment are discussed in Refs. 105, 110, 111, and 118.

In general the comparison of theory and experiment has been surprisingly good. Most often in such comparisons the analytical and

experimental models differ somewhat. Usually the small differences in results are attributed to this. Actually the assumptions for the analyses (for instance those listed in Sect. 6.1.2) are usually violated at the discontinuity regions where the highest stresses exist. Most nozzles that penetrate pressure vessels are relatively thick, and thin-shell analyses tend to overestimate the stresses in such configurations. Fillets generally tend to reduce the stresses but are not readily accounted for in the theoretical analyses. All in all, for radially attached thin nozzles in spherical shells with at least nominal fillets, the theoretical analyses are usually conservative.

Plastic (limit-load) types of analyses have also been examined in some detail.[119-123] These analyses in general assume the formation of a plastic hinge at the discontinuity and are applicable to ideally plastic materials such as mild steel (i.e., the material has a flat-top stress-strain diagram). Such analyses are potentially valuable when yielding occurs, such as is permitted by Section III of the ASME Code.

Nozzles attached normal to cylinders under pressure loading have been investigated.[124,125] A parameter study is presented in Ref. 125. Rodabaugh has shown these results to compare favorably with experimental results.* Eringen has also analyzed a nozzle normally attached to a cylinder under an out-of-plane moment loading on the nozzle. This analysis is being programmed for a computer at Oak Ridge National Laboratory.

General Electric Company is conducting a rather broad program for the analysis of reactor primary coolant systems, with particular interest on rupture.[126] Included in this program is a computer analysis for piping systems based on the finite-element method. This analysis may also be applied to the nozzle-to-cylinder problem that arises in the design of nuclear pressure vessels. Axisymmetric finite-element programs applicable to thicker and more complex pressure vessels have been developed.[127-129]

Nonradial nozzle attachments have also been examined theoretically.[130] Much more effort, however, has been placed on the analyses of cylinders

---

*Personal communication from E. C. Rodabaugh, Battelle Memorial Institute, Columbus, Ohio.

with oblique edges.[131-137] References 131–137 have application to nozzles in pressure vessels for only very specific cases.

Nozzles attached in clusters to spherical and cylindrical shells also have broad applications to pressure vessel design. The initial work leading up to a general analysis has been confined to specific arrays of holes in plates and spherical shells.[138,139] Currently, Applied Technology Associates, under subcontract to Oak Ridge National Laboratory, is extending work to the analysis of clusters of nozzles in spherical shells. The shallow-shell approach is being taken initially; that is, curvature terms are neglected. Later, curvature and obliqueness will be incorporated into the analysis.

The analytical treatments of shell problems become significant only when their validity and degree of approximation can be established experimentally. Thus, an active experimental program with both photoelastic and machined steel models exists for investigating the more pertinent problems in pressure vessel design. Mershon,[140] as of May 1962, described the results obtained from programs associated with the Pressure Vessel Research Committee. This report includes discussions of several cylindrical and spherical shells with attached nozzles and represents much of the basic experimental technology current at that time.

Since 1962 several experimental programs have been completed and others have been undertaken. The tests on the photoelastic models are described in Ref. 141. In this report results from over one hundred photoelastic models are described, and there are a summary and evaluations of the results.

Several steel models have also been tested recently (Refs. 111, 118, 123, 142–146). Most of them have been spherical heads with a radially attached nozzle. However, other configurations are discussed in Refs. 123, 143, 145, and 146. As previously noted, the results from both the steel and photoelastic models have been compared, where applicable, with the theoretical analyses in Ref. 111.

Cloud* and Lind† have performed tests on steel models in support of limit analysis theory. These test results are compared with theory in

*Westinghouse Electric Corporation, Bettis Plant, Pittsburgh.

†University of Waterloo, Waterloo, Ontario.

Ref. 120. Gill has also made theoretical investigations in the same field.[147]

Several experimental studies are currently in progress. Lind* of the University of Waterloo is investigating a steel cylinder with a nozzle attached at 45° to the perpendicular. The ratio of the diameters is 0.5. Leven,† under subcontract with the Bureau of Ships, is analyzing a perpendicular nozzle attached to a cylinder, with the ratio of diameters being 0.129. He is also investigating several spherical shells with nonradially attached nozzles. All of Leven's work is with photoelastic models. Maxwell,‡ University of Tennessee, is investigating a steel spherical shell with a single attached nozzle of various sizes.[144] Angles of attachment being investigated are 0°, 22.5°, and 45°. Protruding and flush nozzles are being investigated by both Leven and Maxwell. Swinson,§ Auburn University, is analyzing nozzles attached in clusters to steel spherical shells. Clusters of two to five parallel nozzles (standpipes) are being examined, as well as clusters of closely spaced radial nozzles. Mathews,‖ University of Tennessee, is examining clusters of nozzles in flat steel plates. The plate will be subjected to biaxial tension and the nozzles pressurized. Thus, small clusters of nozzles in a large head (either cylinders or spheres) are simulated.

In summary many of the more common design configurations that occur in reactor pressure vessels are being systematically investigated both theoretically and experimentally. Most of the theoretical analyses are based on the elastic behavior of the structures; however, the applications of the theory of plasticity to shell analyses are receiving considerable attention.

---

*Under contract with PVRC.

†Westinghouse Electric Corporation, Research and Development Center, Pittsburgh, Pennsylvania.

‡Under subcontract with Oak Ridge National Laboratory, Union Carbide Corporation, Nuclear Division, Contract No. 2203.

§Under subcontract with Oak Ridge National Laboratory, Union Carbide Corporation, Nuclear Division, Contract No. 2670.

‖Under subcontract to Oak Ridge National Laboratory, Union Carbide Corporation, Nuclear Division, Contract No. 2673.

Most of the theoretical analyses are for shell structures axisymmetric with regard to both geometry and load. The ability to perform a completely general shell analysis does not exist at present. The more important problems of nozzles in cylinders, nozzles nonradially attached, and nozzles in clusters are currently under analytical study.

Experimental programs are either under way or have been completed that provide the backup for the theoretical analyses. Most of these programs are also oriented to provide empirical design information.

Areas that have been investigated only in specific applications are those with a high degree of asymmetry, such as a nozzle attached near the junction of a torispherical head and a cylindrical shell. Systematic treatments of such problems have not been seriously undertaken, and they await the completion of the analyses of the somewhat more common design configurations. This being the case, experimental investigations of such asymmetric design must be made if the intent of Section III of the ASME Code is really to be met.

6.3.2 Large-Model and Full-Scale Strength Tests

It is quite apparent that full-scale tests are necessary to provide initial observations, as well as test hypotheses, concerning the strength and behavior of steel pressure vessels. Three series of full-scale tests are discussed here. The results of all three series have been extremely valuable, and therefore full-scale testing has more than justified its expense. The three series of tests to be discussed are the PVRC series, the British series, and the PM-2A tests.

6.3.2.1 The PVRC Series

The PVRC tests were a continuation of the laboratory and scale-model tests sponsored by PVRC to evaluate the feasibility of using higher strength steel in pressure vessels. The basic purpose of the tests was to evaluate fatigue strength, and the tests were designed as full-scale plastic-fatigue tests. Neither the fracture analysis diagram nor the analytical method of fracture mechanics had been developed to its present

status when these tests began. The PVRC test results provided essential data for the development of both analytical techniques.

The important variables involved in a full-scale test were listed by Kooistra and his co-workers[68] as material characteristics, shape, surface condition, manufacturing variables, imperfections in shape, plate thickness, welding, and size effects. Three pairs of vessels were tested. Vessels 1 and 2 were of A 201 grade B steel, vessels 3 and 4 were of A 302 grade B steel, and vessels 5 and 6 were of T-1 steel. It has already been mentioned that the stress-strain curves of high-strength steel and irradiated mild steel are very similar. Therefore, the concern over the reliability of high-strength steel vessels is understandable. However, it should be noted that it may be possible to design a nuclear pressure vessel so that no part of the pressure vessel receives an irradiation dose above the threshold limit (10^{18} neutrons/cm^2). In this case, the problem is solved by being eliminated rather than by being analyzed. It should also be noted that T-1 steel is not necessarily typical in all respects of the high-strength steels that are now being considered for use in nuclear pressure vessels. Therefore, the primary benefit of the T-1 vessel tests is that they provide experimental data with which to compare analytical or empirical failure theories. It does not follow that all high-strength nuclear pressure vessels will behave exactly as the two T-1 vessels tested.

Many high-strength steels have yield points as high as 90% of ultimate strength, whereas the commonly used low carbon steels have yield strengths nearer 50% of ultimate strength.[36] Therefore, to operate at a given fraction of yield strength, it is necessary to operate nearer to the ultimate strength of a high-strength steel. Since the elastic modulus does not change with yield strength, membrane and local strains are both greater for high-strength vessels, and fatigue is more likely. Since stresses are a greater fraction of ultimate strength, fracture may also be more likely. Such is the motivation for the PVRC full-scale tests.

The PVRC vessels were 36-in.-ID 7-ft-long cylinders with hemispherical heads and various blanked-off nozzle attachments.[36] Cylinder wall thickness was 2 in., which is the minimum thickness classified as thick

plate.[36] Loading was hydraulic,[148] and the vessels were tested at ambient temperature.

Prior to strength testing, vessel 1 was used for conducting an extensive experimental stress analysis; both brittle lacquer and strain gages were used. The peak strains were found to occur on the inside corners of nozzles, with relatively little variation in peak strain between nozzles.[36] Therefore, it appeared that the magnitude of the strain-concentration factor for a nozzle was not strongly influenced by shape. During strength testing, the fatigue cracks as a rule did start and propagate from points of peak strain predicted by the experimental stress analysis.

Initially one vessel of each pair was to be cycled at a pressure estimated to cause fatigue failure in 20,000 cycles, based on laboratory test data, and the other in 100,000 cycles. The corresponding pressures were calculated from uniaxial strain-controlled fatigue data by dividing the strain range for failure in a given number of cycles by the strain concentration factor, multiplying by Young's modulus, and then multiplying by the thickness-to-radius ratio.[36] These loading criteria were later modified as data were obtained.

During the first few cycles of full-pressure loading on the vessels, peak strains at points of strain concentration were very high, far higher than indicated by the elastic experimental stress analysis or would have been indicated by an elastic calculation. Some peak strains were as much as 10 to 12 times membrane strain.[36] However, these initial peak strains are not believed to have any significant effect on fatigue life, which depends on the stabilized cyclic strains. After about 10 cycles, the peak strains leveled off to a stable ratio very near the elastically calculated ratio. In fact, the peak strain range in vessel 1 tapered off to exactly the strain range estimated to cause failure in 20,000 cycles.[36]

During cycling, fatigue cracks were observed to form at or near various nozzles, as described in Ref. 36. It was generally observed that, except in the high-strength steel vessels, fatigue cracks propagated only from regions of prior plastic strain.[149] It was also observed that, in general, fatigue failures occurred earlier in the test vessels than

predicted according to laboratory test data. The reason for this difference was determined to be the existence of initial defects in the test vessels. For instance, as shown in Fig. 6.19, while a fatigue crack did start to grow from the inside corner of nozzle 6 in vessel 4, a more severe fatigue crack also grew from an initial flaw in another part of the nozzle. Thus, it appears that a fully adequate method of fatigue

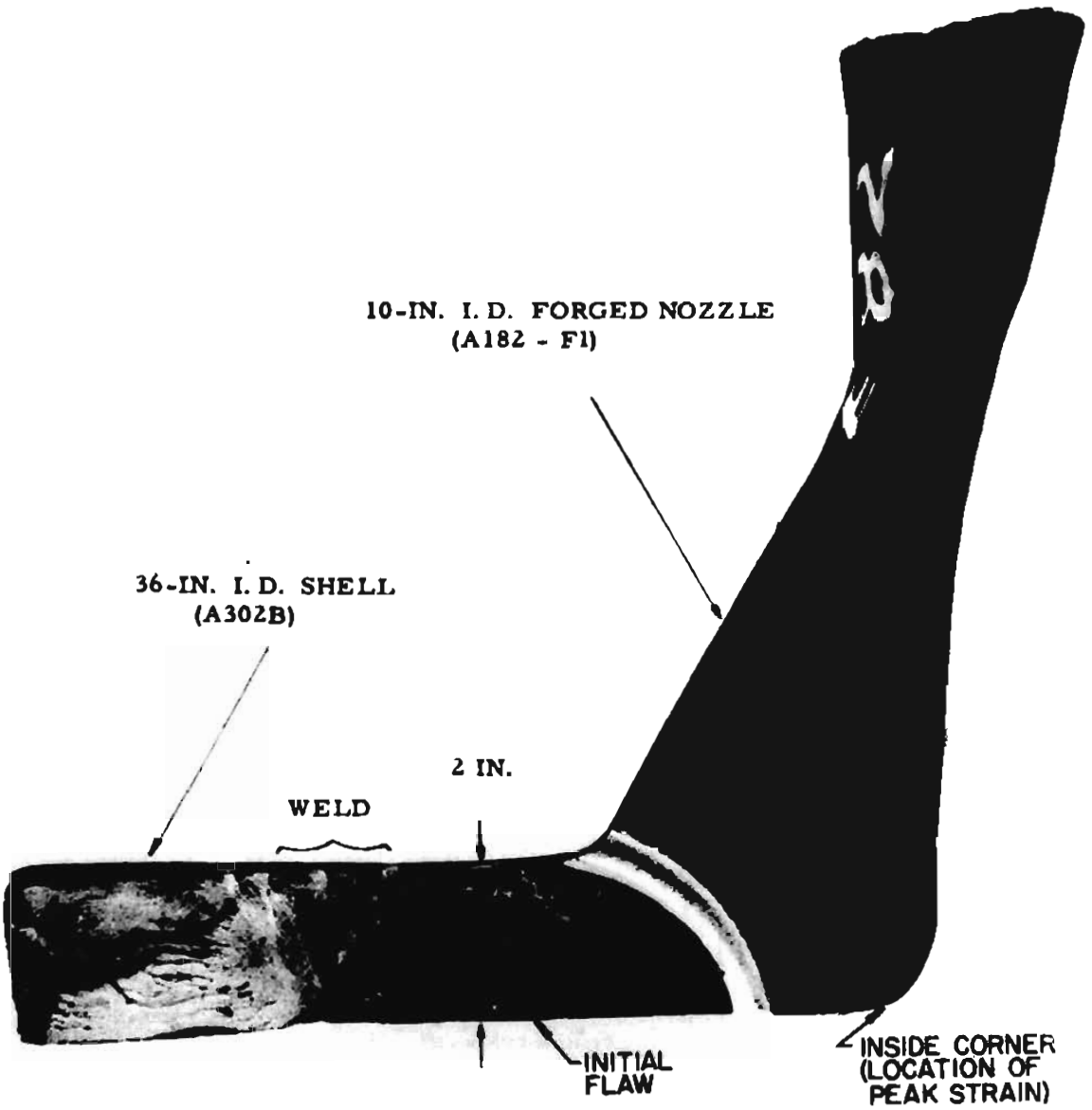

Fig. 6.19. Section of Nozzle 6 of PVRC Vessel 4 Showing Two Fatigue Cracks. Section was cooled to −30°F and broken by impact. (From Ref. 150. Southwest Research Institute photograph.)

analysis must consider both the possible existence of initial defects and the occurrence of cyclic plastic strains.[149] Since in the absence of initial defects, the most likely point of origin of a fatigue failure is the inside corner of a nozzle, at which stresses are uniaxial (ignoring surface pressure), the Southwest Research Institute investigators recommend the use of Stowell's method of predicting the cyclic plastic strains for a fatigue analysis.[150] They believe that strain-gage data might be inaccurate for this purpose because of fabrication imperfections. To demonstrate the accuracy of the proposed method of fatigue analysis, Fig. 6.20, taken from Ref. 150, shows that the PVRC-SWRI test-vessel data, with strain ranges calculated by Stowell's method with an elastic stress-concentration factor of 3, fall on a single fatigue-strength curve. The points in Fig. 6.20 are terminal failure (leakage or fracture) points.

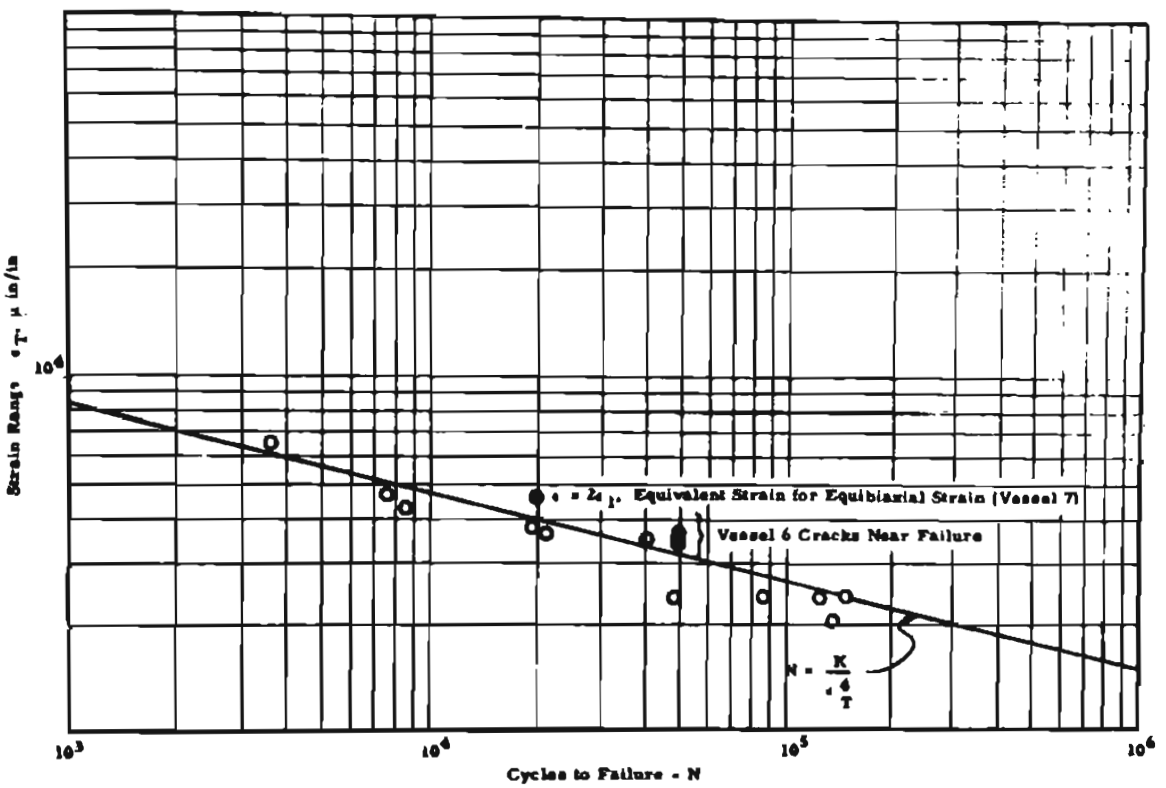

Fig. 6.20. Results of Full-Size Pressure Vessel Fatigue Tests Showing the Relationship Between Life Cycles and the Fourth Power of Total Strain Range. (From Ref. 150)

At the end of only 7516 cycles a major failure occurred in vessel 1, as shown in Fig. 6.21. The failure occurred as a fast running crack that originated at a 6-in. fatigue crack at the inside corner of a nozzle in the cylindrical part of the vessel and propagated in both directions.[150,151] This crack did not run through the longitudinal weld seam.[36] Vessel 2, operating at a lower stress, failed by leakage due to the growth of a fatigue crack at the end of 85,868 cycles. It was observed from these two tests that the fatigue performance of heavily reinforced insert-type nozzles does not seem to be as good as that of other more economical type nozzles. Therefore the advisability of 100% reinforcement was questioned.[36]

Both vessels 1 and 2 failed in less than the estimated number of cycles based on laboratory test data, and the cycles for vessel 1 were less by a considerable margin.[36] One possible cause for the early failure of vessel 1 was the fact that some yielding occurred in the body of the vessel, which was unexpected.

Pellini, Steele, and Hawthorne[80] analyzed the failures of vessels 1 and 2 in terms of the fracture analysis diagram. In the case of vessel 1, the shell stress-temperature conditions produced a point above the CAT curve, and brittle fracture occurred from a crack that grew to critical size by fatigue. In the case of vessel 2, which carried a lower pressure in order to lengthen the fatigue life, the stress-temperature point was below the CAT curve, and failure occurred by leakage without rapid crack propagation. Both modes of failure were to be expected according to the fracture analysis diagram.[69,80,152]

Testing procedures for vessels 3 and 4, constructed of A 302 grade B steel, were similar to those for vessels 1 and 2. Vessel 3 failed after 8500 cycles of load, and vessel 4 after 40,041 cycles.[68] Both vessels failed by leakage, as had been expected according to the fracture analysis diagram.[68,152] The terminal failure for vessel 4 was, nevertheless, a surprise because it was initiated at a position away from the region of maximum strain. This was due to an undetected defect that was largely subsurface. The PVRC test vessels were inspected during fabrication by radiography and by the magnetic-particle method.[148]

The test results for vessels 5 and 6, which were constructed of high-strength T-1 steel, provided important evidence of the differences

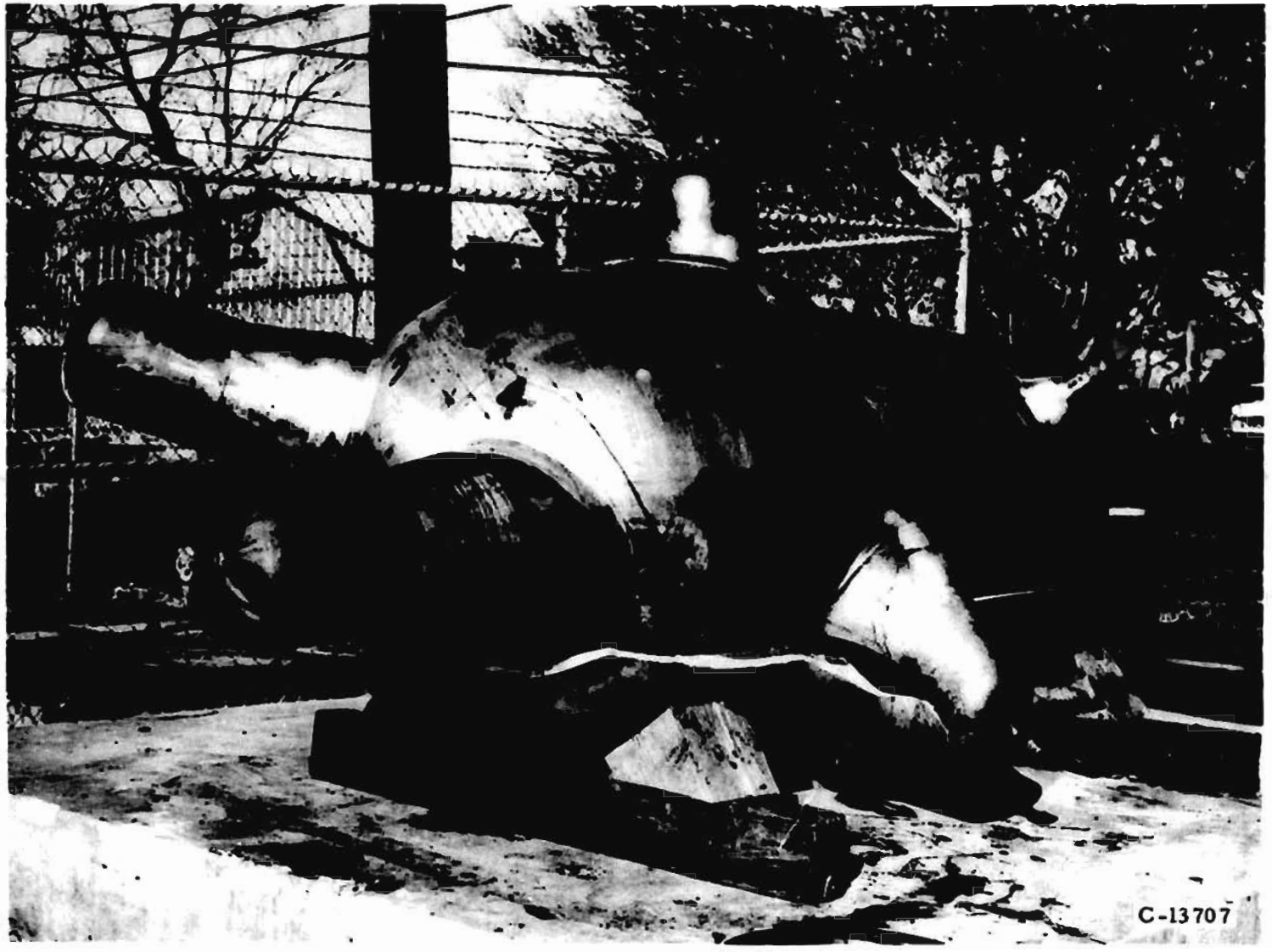

Fig. 6.21. Terminal Failure of Vessel 1. (From Ref. 151. Southwest Research Institute photograph.)

in behavior between high-strength steel vessels and vessels of lower strength materials. It was observed that as yield strength increases, strain redistribution decreases.[68] For the lower strength steel vessels, a considerable portion of the total strain remained in the plastic range after several cycles. For the high-strength steel vessels, plastic action reduced to practically zero, and the action became virtually elastic. Although the low-strength steel vessels operated with a plastic hysteresis and the high-strength steel vessels without apparent plastic action, the low-cycle strain range for a given number of cycles appeared to be the same for the three steels tested. This phenomenon is rather surprising in view of the somewhat general assumption that fatigue damage is caused mainly by plastic deformation. However, the observation is in agreement with previous PVRC test results, which showed little difference between the fatigue strengths of different steels in the low-cycle range.[39,68]

Vessel 5 failed by brittle fracture[148] after 3603 load cycles. Figure 6.22 shows a photograph of failed vessel 5. Vessel 6 failed, apparently by leakage, after 19,272 load cycles.[68] This vessel was subsequently made to fail by fracturing by lowering the temperature to 30°F and raising the pressure to 5250 psi. Despite the existence of other more obvious fatigue flaws, the fracture initiated from a 1/8-in.-deep fatigue flaw that apparently grew from an arc strike on the outside of the vessel.[149] The possible effects of warm prestressing on the fracture strength of vessel 6 were not discussed in Ref. 149.

The failure of vessel 5 was especially significant because it was unexpected;[148] that is, failure by a rapidly propagating fracture was unexpected. It had been assumed (presumably on the basis of the fracture analysis diagram) that the terminal failure would be by leakage through a fatigue crack initiated at the inside corner of a nozzle, where the highest surface strains had been measured. Instead, failure was by fast fracture, but the fracture initiation point was a flaw in the body of the vessel, near a nozzle, and near the longitudinal weld seam, as shown in Fig. 6.22. Some bulging did occur near the point of crack initiation. The fracture propagated to the heat-affected zone (HAZ) of the longitudinal weld and at that point initiated catastrophic failure. Perhaps of some importance in this case is the fact that initial surface strains in

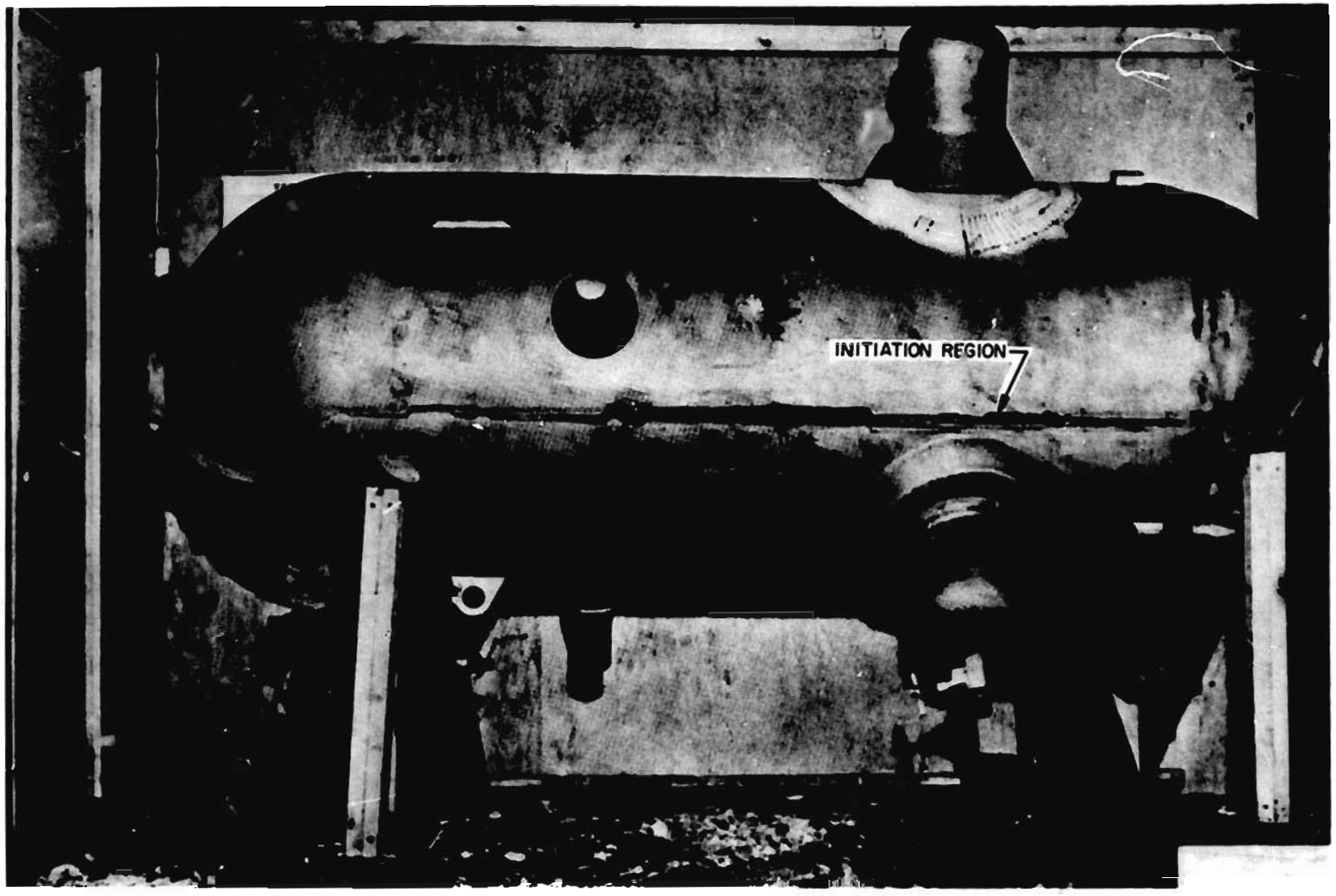

Fig. 6.22. Vessel 5 After Failure by Fracture. (From Ref. 148. Southwest Research Institute photograph.)

a quadrant of the shell that was 1/4 in. out of round were 50% higher than theoretical.[148] No hydrostatic test was performed on the vessel prior to these strain measurements.

At the present time, it is not obvious whether the failure of the fracture analysis diagram to predict the correct mode of failure is evidence of its inapplicability to high-strength steel in general or of a variation in properties between the heat-affected zone and the base metal in this particular case. With regard to the latter explanation, Pellini and Puzak[151] have commented on the failure of vessel 5 as follows:

> This behavior is not inherently characteristic of Q and T (quenched and tempered) steels as a family but derives from improper (specific to the steel) welding conditions and stress relief heat-treatments which degrade the HAZ fracture toughness. In this case the fracture surfaces do not involve cleavage but a form of low energy absorption tearing. This fracture mode (tear fracture of low energy absorption) does not involve a transition temperature and is therefore relatively independent of temperature.

A material with these characteristics would not be considered suitable for use in a nuclear pressure vessel.

The failure of the fracture analysis diagram to predict the correct mode of failure of vessel 5 has, of course, given the proponents of fracture mechanics an opportunity to point out the deficiencies of the transition-temperature approach. Accordingly, Johnson[60] mentioned that the transition-temperature approach is unquantitative and that failures of the type being considered can occur well above the transition temperature at stresses below yield.

Inspection of vessel 5 after failure revealed that the terminal fracture had originated at a crack 6 in. long that penetrated 35% of the shell plate.[148] It was surmised that this crack had grown by fatigue from a small toe crack at the edge of a nozzle fillet weld. This occurred despite the fact that the vessel had passed radiography and magnetic-particle tests, which should have disclosed any such defect.[33] That the nondetection of such a flaw was more than a chance occurrence was demonstrated in the postfailure inspection. Ultrasonic inspection indicated a 5-in.-long defect at the juncture between the intact longitudinal weld seam and the base metal. Radiography indicated no such flaw.[148] This is an example in which supposedly adequate inspection

methods were used without finding critical flaws. Ultrasonic inspection methods have greater sensitivity than radiography for the detection of cracks.

Since the dimensions of the initiating defect are known, it is possible to make a fracture mechanics calculation of the stress required to cause brittle fracture in vessel 5. The appropriate equation is that for a semielliptical partly through crack:[43]

$$K_{Ic} = 1.1 \sqrt{\pi}\, \sigma \left(\frac{a}{Q}\right)^{1/2} , \tag{15}$$

where K_{Ic} is plane strain fracture toughness, σ is nominal stress, a is the depth of the elliptical surface flaw in inches, and Q is a function of the eccentricity of the semielliptical flaw and the ratio (σ/σ_y), where σ_y is the yield stress; Q is available directly from curves in Ref. 43. Equation (15) can be rearranged to give the failure stress in terms of fracture toughness. Thus,

$$\sigma = \frac{K_{Ic}}{1.1 \sqrt{\pi} \left(\frac{a}{Q}\right)^{1/2}} . \tag{16}$$

From the given flaw dimensions, the eccentricity is computed as follows:

$$\frac{a}{2c} = \frac{0.7}{6.0} = 0.117 .$$

The membrane stress at failure was 60,800 psi.[148] The yield strength of the plate material was about 107,000 psi.[33] The ratio of nominal stress to yield stress is then

$$\frac{\sigma}{\sigma_y} = \frac{60,000}{107,000} \sim 0.6 .$$

From Fig. 1 in Ref. 43, $Q \sim 1.05$. The room temperature value of K_{Ic} for T-1 steel is about 130,000 psi·in.$^{1/2}$ (Ref. 153). However, since the fracture strength of the heat-affected zone is evidentally less than that of the base metal, a value of K_{Ic} = 90,000 psi·in.$^{1/2}$ will be used for

a trial calculation. Using Eq. (16), the computed value of nominal stress at fracture is 57,000 psi.

Of course this is, in a sense, a back calculation [Eq. (15) could have been used to get a value of K_{Ic} and would have given σ = 60,800 psi exactly]. However, the calculation does illustrate the relative simplicity of a fracture mechanics calculation and the probable weakness of the heat-affected zone in this case. An additional approximation inherent in this calculation is that the fracture of vessel 5 was not entirely, if at all, by cleavage. Nevertheless, the calculation provides a good illustration of the application of fracture mechanics. Normally, the ratio σ/σ_y would not be known in advance, and a series of successive approximations would be used. By plotting assumed versus calculated values of σ/σ_y, convergence can always be obtained in no more than four trials.

The T-1 vessel plates were cold formed and stress relieved in steps. Stress relieving was at 1100°F for 2 hr.[148] Soon after completion of the welding of the two longitudinal joints (one of which was the failure path), transverse weld-metal cracks were noted in the joints. These cracks were repaired. The welds were inspected by radiography after their first stress relief and by the magnetic-particle method following subsequent stress reliefs. Altogether the vessel plates were stress relieved six times and the longitudinal welds five times. Metallurgical analysis has indicated that microcracks existed in the heat-affected zone through which the fracture passed. These microcracks probably formed by stress (creep) rupture during the first stress-relieving operation following welding,[151] but they were not detected by one radiographic inspection and four magnetic-particle inspections. Pellini and Puzak[151] conclude that stress relief is actually detrimental to the fracture toughness of some quenched and tempered plates, welds, and heat-affected zones. Nonetheless, residual stresses are also a primary cause of brittle fracture. To abandon stress relieving completely might be to invite brittle fracture due to high residual stresses.* The basic problem, of course,

---

*The appropriateness of stress relieving for quenched and tempered steels is currently a problem. Code Case 1358 requires it, but a change is being considered.

is ductility. Stress relieving involves creep and relies on the strain capacity of the material. High-strength steels have less ductility than mild steels and evidently not enough to stand the welding and stress-relieving procedures previously developed. New welding and stress-relieving procedures that do not overstrain the material may be needed for high-strength steels. How much strain capacity is left in the material must also be determined. The concept of ductility exhaustion[42,68] is relevant to this problem.

Metallurgical examination showed that there was a noticeable variation in mechanical properties through the thickness of the plates in vessel 5. Fracture toughness, as indicated by the Charpy V-notch energy values, was 16% lower in the center than at the outer surface.[148] However, this phenomenon was not considered a contributing factor in the failure of vessel 5.

Postfailure examination also revealed corrosion pits and cracks associated with pits on the bottom surface of vessel 1. Although there was pitting at other locations, cracks only developed in the areas of plastic strain.[148]

An obvious conclusion from the test results on vessel 5 is that further research is needed concerning the properties of steels that have markedly reduced ductility and impact properties. Weld-metal and heat-affected-zone properties should be investigated along with those of the plate material.[68] In fact, for these steels, the heat-affected-zone properties present the most important questions because the heat-affected zone is the element of greatest potential variability.[151] Because of this potential variability, it cannot be overemphasized that the effective utilization of the new high-strength materials can only be achieved with refined design and superior fabrication and quality control procedures.[68] Refined design means greater attention to stress-concentration factors, out-of-roundness effects, and operating temperatures.[36] Superior fabrication and quality control procedures include welding and heat-treatment procedures appropriate to the material and more sensitive and reliable means of nondestructive inspection, such as ultrasonic inspection. The ability to achieve refined design depends on research. However, research

will be effective only if it is directly related to the results of large-scale tests.

In summing up the results of the PVRC tests, Kooistra, Lange, and Pickett[68] commented somewhat philosophically on the need for full-scale strength testing as follows:

> Full-size pressure-vessel testing should not be necessary. All of us, active in the development of pressure-vessel technology, are consciously or subconsciously trying to eliminate it because it has many drawbacks. The objections to full-size pressure-vessel testing are so simple and obvious that it is difficult to see why it should be done at all. To illustrate how simple and obvious the objections are, let us mention just two here. Full-size testing is expensive and produces very few data points per test that cannot be obtained from a model or an even smaller specimen. These are powerful reasons why it should not be done. The weight of the obvious argument is all on the side of the objector.
>
> Needless to say, that when full-size testing is decided upon, it is an action somewhat similar to getting married. It is entered into advisedly, soberly, and in the fear of God and the consci tious objector.
>
> Now, under pain of being accused of wasting a lot of time and money and getting small return on the research dollar, what are the valid considerations that lead to such a defiant decision?
>
> Why not follow an organized scientific and safe approach? Why not determine from accurately dimensioned specimens and closely controlled laboratory tests what the material can stand? Then, by theoretical analysis, compute precisely the stresses and strains of the critical regions in a pressure vessel and apply this knowledge to design the structure, so that the material's strength and endurance properties are not exceeded by a predetermined margin. Why is this not all there is to do?
>
> There are two reasons: (a) Because in the practical application, it does not give us the right answer; and (b) because we can't wait that long. There is nothing wrong with the principle of the organized scientific approach. In fact, it is the ideal most engineers and scientists are striving for. What, then, keeps us from attaining this ideal?
>
> It is the imperfections existing in all mundane things. For instance, the material is not isotropic; different heats of supposedly the same composition do not have the same properties; surface finish cannot be defined exactly; vessels are not perfect cylinders; theoretical computations of stress or strain in critical areas are complex and, at best, close approximations; our inspection methods do not pick up all the

flaws; welds and weld repairs introduce metallurgical discontinuities, and so on. Not only do our materials fall short of the mark, but so do our mental capabilities. When all these imperfections are imposed on one another, they can mount up to major uncertainties and broad scatter of results. A very gloomy outlook indeed!

It ought to be clear by this time that the engineer dealing with this mess cannot be an idealist — he must be an arbitrator. In order to predict performance, he must devise a strategy. To preserve his reputation he must err on the safe side, to keep his sanity he must evaluate the degree of imperfection that can be tolerated.

Lest the reader conclude that everything is in a complete state of uncertainty, Fig. 6.23, also taken from Ref. 68, shows that the fatigue strengths of all six vessels tested, as well as some others, lie above the design curve recommended. In addition, Fig. 6.24, taken from Ref. 56, shows that the present ASME design curve is conservative with respect to all test data. No crack initiation was detected at any stress level below the allowable stress, and no crack progressed through a vessel wall

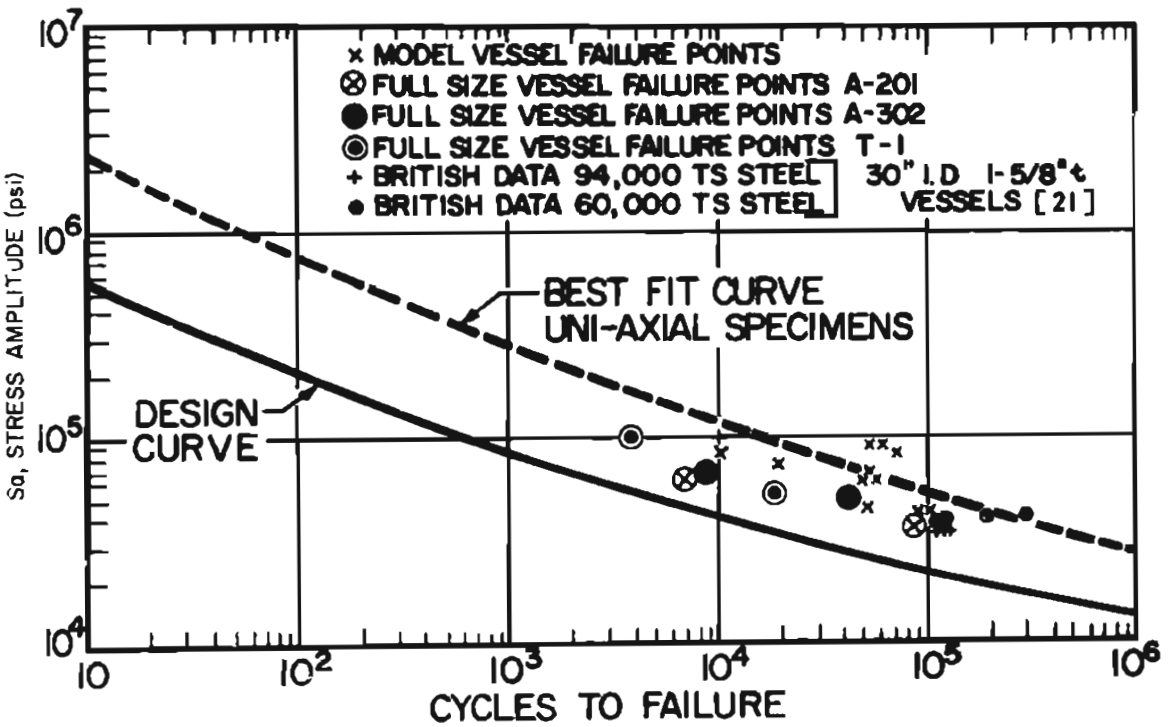

Fig. 6.23. Comparison of Results of Low-Cycle Fatigue Tests. Failure criterion is fatigue-crack propagation through plate thickness. (From Ref. 68)

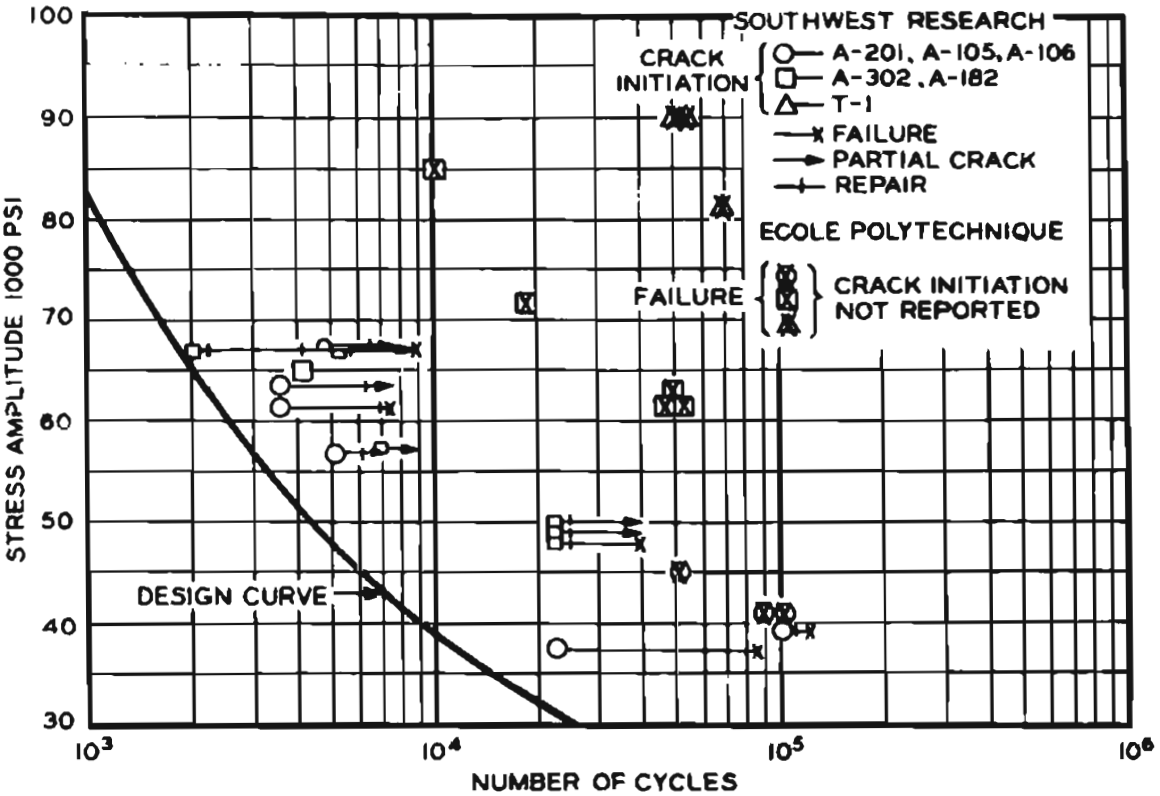

Fig. 6.24. Plot of ASME Design Curve and Fatigue Test Data from Model and Full Scale Vessels. (From Ref. 56)

in less than three times the allowable number of cycles.[56] The large scatter of the data does indicate that further research on specific materials and further studies of nozzle stresses could eventually lead to less restrictive rules for some materials and some nozzle designs.[56]

As an extension of the original PVRC test program, two additional vessel tests were performed.[150] In order to obtain additional data on the effects of cladding cracks and nozzle design, vessel 2, which had not previously failed by brittle fracture, was rebuilt and renumbered vessel 7. The desired information was obtained from vessel 7, with several planned leak-type fatigue failures being produced in the process. One of these fatigue failures was produced at a nozzle-to-shell intersection in an area of high equibiaxial strain. As shown in Fig. 6.25, the points representing fatigue crack initiation at 20,737 cycles and leakage failure at 23,908 cycles plot consistently with the B&W data,

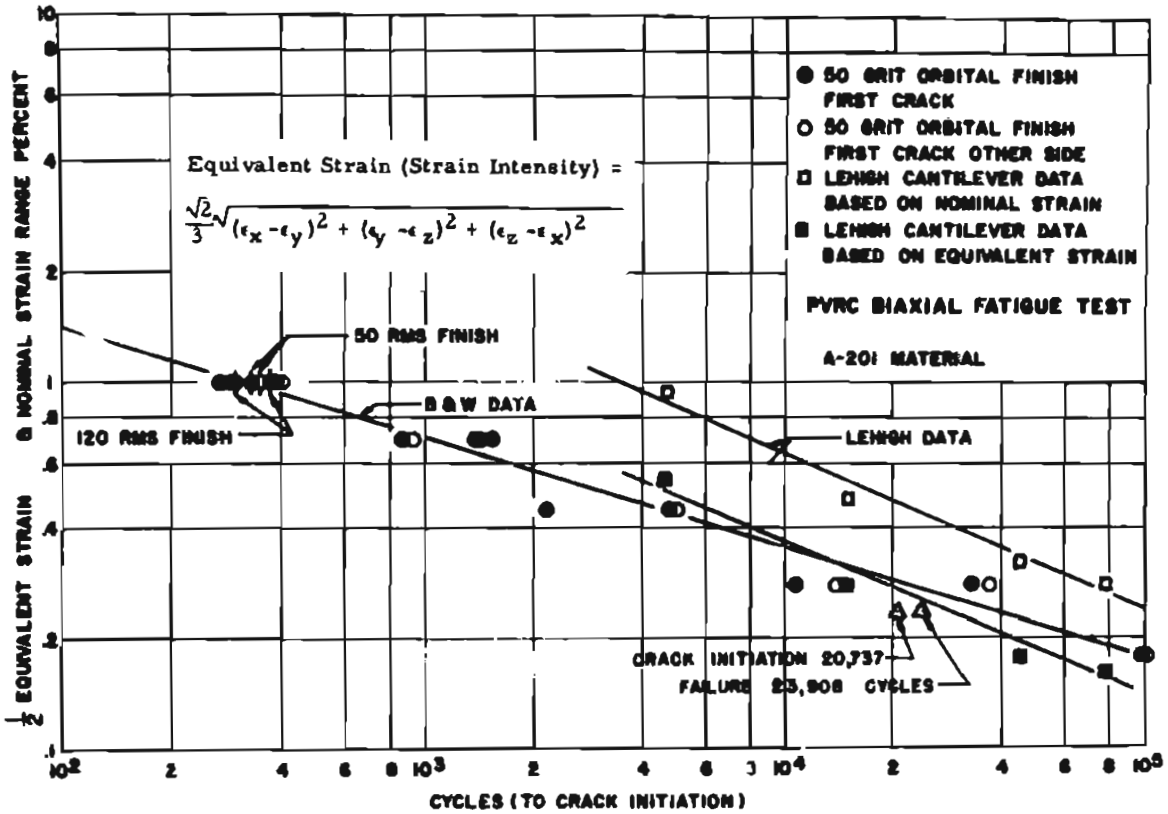

Fig. 6.25. PVRC Vessel 7 Failure Data Compared with Babcock & Wilcox Biaxial Fatigue Test Results for A 201 Material. (From Ref. 150)

as summarized in Fig. 6.15. (Figure 6.25 is Fig. 6.15 with the addition of the two additional data points from vessel 7.)

Following the fatigue tests on vessel 7, several attempts were made to produce a brittle fracture in the vessel. All were unsuccessful. The loading temperature was 90°F, and the maximum pressure employed was 4275 psi.

The last vessel tested was vessel 8, which was constructed of A 542 class 2 steel,[150] which has a specified minimum yield stress of 100,000 psi (see Table 4.4).* Two leak-type fatigue failures were produced at two different nozzles. Then, under high pressure, a brittle fracture was produced in a nozzle, as shown in Fig. 6.26. The test pressure at failure was 4800 psi and the vessel temperature was between 27 and 38°F.[150]

*Table 1 of Ref. 149 identifies this material as 2 1/4% Cr–1% Mo steel, with a 0.2% offset yield strength of 102,000 psi.

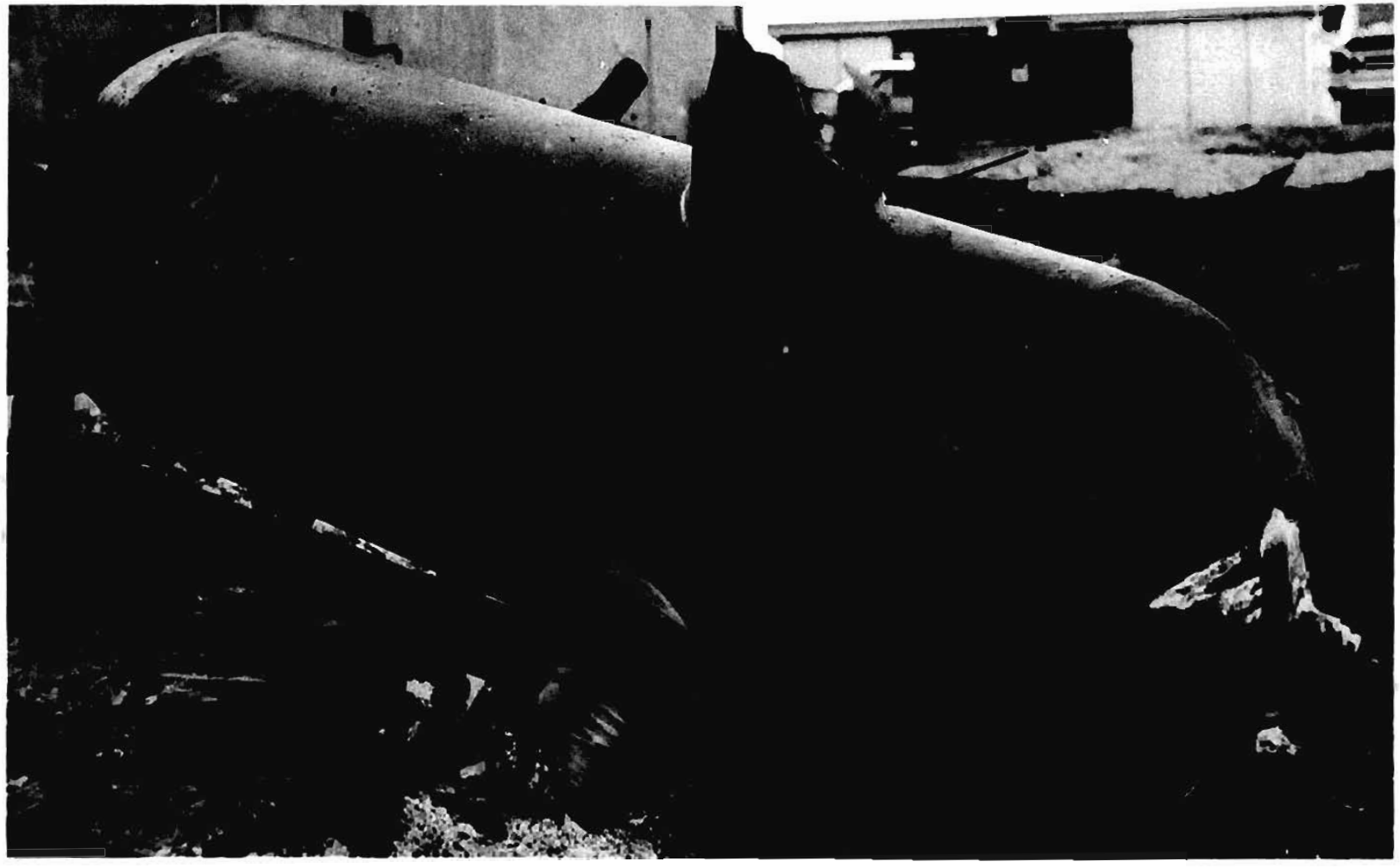

Fig. 6.26. Vessel 8 After Fast Fracture Test. (From Ref. 150. Southwest Research Institute photograph.)

The authors of Ref. 150 conclude that the fracture analysis diagram is adequate for predicting the strength of mild and intermediate-strength steel vessels (e.g., vessels 1, 2, 3, 4, and 7) but not of high-strength steel vessels (e.g., vessels 5, 6, and 8). They also conclude that fracture mechanics provides an estimate of crack size and stress level required to initiate fast fracture that is accurate enough for predicting the strength of a high-strength steel vessel.[150] Furthermore, they conclude that service life, in terms of low-cycle fatigue, can be assured for all classes of materials if initial defect sizes are adequately controlled. These controls include specifications, fabrication procedures, quality control and acceptance procedures, and surveillance procedures. The stress levels given by codes and standards (e.g., Section III) should not be exceeded when the transition temperature approach is the basis for fracture analysis.[150]

6.3.2.2 The British Series

In developing methods of insuring the reliability of large pressure vessels, the British have been guided by the following general philosophy as summarized by Irvine,[154]

> "... if initiation (the existence of cracks) is possible, then generally speaking, in small pressure vessels with diameters of the order of inches, all modes of fast failure will be incredible, in vessels where the areas of secondary stress are of the order of inches fast brittle failure will be credible, and in reactor vessels with areas of secondary stress of the order of tens of inches, quasi brittle (shear) and brittle (cleavage) fracture will be credible."

This reasoning was based on the diagram of Fig. 6.27, which indicates the size of defects believed capable of causing fractures at given stress and temperature levels. (Note that the possibility of ductile fractures at temperatures above the brittle range is not explained by the transition-temperature method. Whether these are "plane-strain" fractures or something else is not indicated.)

The British tests were performed on steel cylinders 5 ft in diameter, 14 ft long, and 1 in. thick.[69] These dimensions were chosen so as to avoid having large ratios of fault length to diameter or fault length

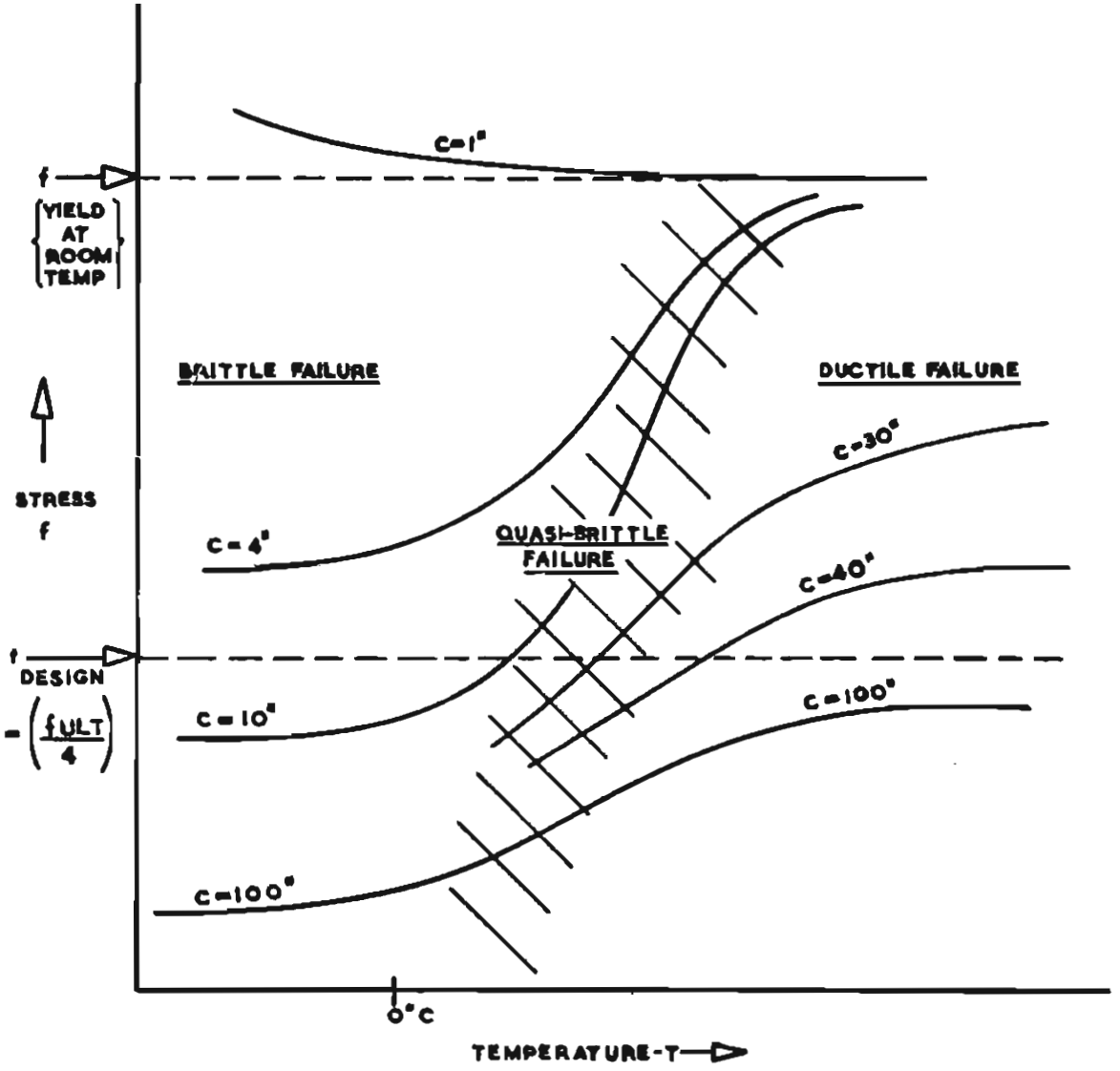

Fig. 6.27. Relationship Between Stress and Critical Crack Size for Mild Steel Plate.

(plus plastic-zone size) to length. Note that 1-in. plate is not considered thick plate. For most of the tests, thickness slits were cut in the vessel walls to simulate defects.[69] The major portion of the fault length was flame cut. This length was extended beyond the heat-affected areas by sawing. The final 1/16 in. of the fault was sawed with a 0.008-in.-wide hacksaw blade. The fault tips were not sharpened by any other means, such as fatigue. Backing seals were used to prevent leakage. For a few tests, partly through defects were employed, and there were

some interesting differences in test results. When through-thickness defects were used, the behavior of these vessels was indicative of the behavior of a vessel after a crack had penetrated the wall. The conditions required for a crack to grow completely through the wall must be determined from a fatigue analysis. Whether leakage or fracture occurs following penetration depends upon whether the pressure required to cause fracture is greater or less than the pressure at penetration. The objective of these tests was to determine this criterion.

The plate material used in the British tests was a high carbon (0.36%) steel that had a high normalizing temperature in order to give a transition temperature above ambient.[69] This eliminated the need for refrigeration[23] and was intended to simulate the effects of irradiation. The FTE temperature of the vessel was about 50°C (122°F). Tensile strengths were about 29 to 33 tsi (~70,000 psi) and yield strengths about 14 to 17 tsi (~35,000 psi)(1 long ton = 2240 lb). Fracture strain was about 30 to 40%.

The vessel temperature was controlled by passing hot water over the upper half of the vessel. Test temperatures ranged from 1°C (34°F) to 88°C (176°F). At the base of the vessel the temperature remained virtually at ambient in all the tests.[23] The effects of thermal stresses caused by unequal heating were not discussed. Therefore they must have been assumed or proven small.

Since relatively large plastic zones were expected to form at the crack tips prior to fracture, a photoelastic surface coating was applied to the crack tip region during two of the tests.[69] No strain gaging was attempted very close to the crack tip. The plastic-zone size, S, defined as the distance over which yielding occurred along the projected line of the crack, was found to increase markedly as the nominal stress approached the yield stress. Measured values of S ranged from 2 to 24 in., with the latter value being considerably greater than the fault length. According to Irvine, Quirk, and Bevitt,[63] when the plastic-zone size is much less than the plate thickness, fracture is flat (i.e., occurs under plane-strain conditions), and when the plastic-zone size is equal to or greater than the plate thickness the fracture will be of a shear type. In the region between these two types of behavior, mixed fracture may occur, the shear component often being termed the shear lip. Therefore, at least

some of the fractures observed in these tests were not plane-strain fractures.

In most of the tests water was used as the pressurizing medium, similar to the PVRC tests. However, because of ambiguity in failure conditions in some of the high-temperature hydraulic tests, some additional tests were made with partial pneumatic pressurization. Fragmentation was considered a definite risk in these tests, and protective measures had to be taken that consisted of using sandbags and remote operation. Fully hydraulic tests made below 50°C (the estimated FTE temperature) showed comparatively brittle fracture with comparatively little bulging at the center of the fault. At temperatures above 50°C, a series of discrete jumps (pop-ins) occurred under hydraulic loading. This behavior, representing initial instability followed by arrest, was the ambiguity that led to the partially pneumatic tests. The question to be answered was whether crack arrest was caused by the characteristics of the material or of the load. In the pneumatic-loading tests initial crack instability occurred at about the same nominal stress as for hydraulic loading,[155] but crack arrest did not occur. For example, in one test, the crack, which initiated as a shear fracture, changed abruptly to a brittle fracture, propagated axially for several feet, and then branched at both ends and curved back toward the center of the vessel; this severed a large fragment.[23] Other tests under partial pneumatic loading gave similar results.[23]

A plot of test results[63,69,155] on the same coordinates as those used for the fracture analysis diagram is shown in Fig. 6.28. It can be seen that for a particular crack length, the nominal stress at failure increases smoothly with temperature without an abrupt increase in what is supposedly the transition region[69] and that fast fracture occurred at stresses well below yield at temperatures definitely above the FTE temperature. These findings are in disagreement with the fracture analysis diagram (Fig. 6.13),[69,156] as were the results of the tests on vessels with partly through cracks. In addition, since fracture under plane-strain conditions supposedly occurs at lower nominal stresses than under mixed or plane-stress conditions,[42,60] these tests results may not even represent a lower limit. An explanation is certainly in order. The

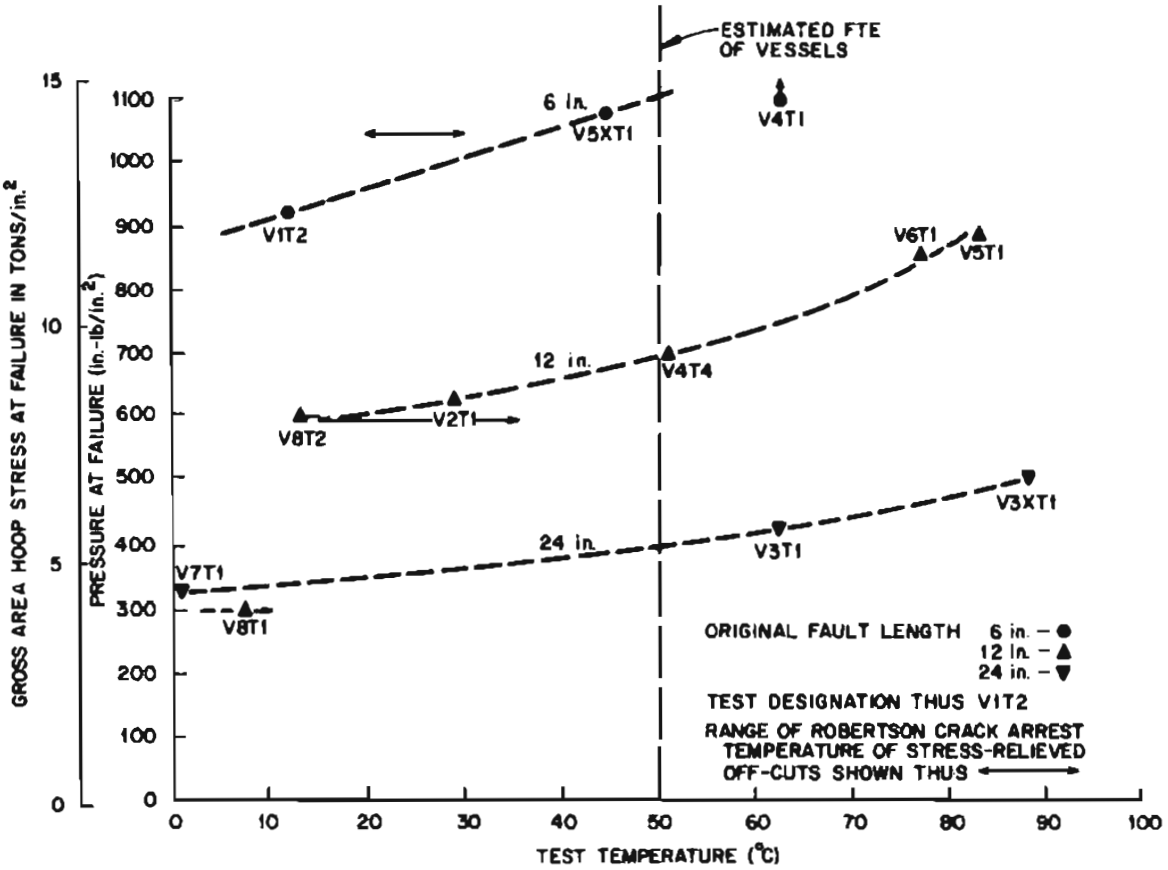

Fig. 6.28. Fault Length-Temperature-Failure Stress Diagram for Longitudinal Faults in 5-ft-diam Cylinders. (From Ref. 155)

hypothesis advanced by Bevitt, Cowan, and Stott[69] was that of Pellini and Puzak,[151,152] namely, that bulging at the crack tip, which had been observed, had led to plastic tensile instability. However, this explanation requires stresses to be estimated by considering the degree of bulging at the crack tip.[152] Thus, nominal stresses are inadequate for predicting this mode of failure by the fracture analysis diagram. There are two ways to examine the hypothesis that tensile instability caused by bulging is the cause of the observed failures below the CAT curve. The first is a plastic stress analysis, and the second is a flat-plate tensile test in which there would be no bulging. The latter course was followed, and the results are described later. Note, however, that tensile instability does not require bulging, so similar behavior in a flat-plate test may rule out the relevance of bulging but not of local plastic instability.

The occurrence of local plastic instability could be determined by the methods of plastically analyzing experimental strains discussed previously.

The nominal stresses shown in Fig. 6.28 do not include residual stresses.[69] The effects of residual stresses acting around the crack tip were inadvertently demonstrated when a vessel failed at approximately one-half the expected nominal stress due to a heat-affected zone at one end of the crack.[63] In this case, the crack tip had not been sawed beyond the heat-affected zone caused by the cutting of the major portion of the slit with a torch. It was recommended that the FTE temperature of a pressure vessel still be kept below the fabrication temperature in order to avoid failures during construction caused by high residual stresses prior to stress relieving.[63]

The deliberate development of a favorable pattern of residual stresses by warm prestressing has already been mentioned. The validity of this concept for the conditions considered was demonstrated in one of the British tests.[63,69] If warm prestressing works, the only way in which a brittle failure could be initiated during a shutdown would be by the application of a loading significantly different from the warm prestressing load.[155] The use of the proof test as a means of warm prestressing is suggested.[155] Since yield stress decreases as temperature increases, the plastic zone grows in size at constant stress as the temperature is raised and thereby effectively lengthens the crack. Therefore, it is conceivable that raising the temperature could cause a brittle fracture. Consequently, Nichols[155] argues that the proof test (i.e., the hydrotest) should be performed at the maximum operating temperature. This is in contrast to the previously cited argument of Tiffany and Lorenz,[43] who recommended the minimum operating temperature for the purpose of defining the maximum possible flaw size.

One obvious method of analysis of the failure data plotted in Fig. 6.28 is the method of fracture mechanics. According to fracture mechanics, for constant temperature and geometry, the nominal stress at failure should vary inversely as the square root of crack length [see Eq. (16)]. However, the data in Fig. 6.28 do not obey this relationship.[69] Instead, the nominal stress at failure for a given temperature seems to be inversely proportional to the two-thirds power of the crack length. This criterion

is usually stated as

$$f^3 l^2 = \text{constant} ,$$

where f is nominal stress and l is crack length.[63,155]

In analyzing the results of the foregoing tests, Irvine, Quirk, and Bevitt[63] concluded that the possibility of fast fracture is determined by the unloading path of the structure during crack propagation (constant load versus constant deflection) and physical size (because of bulging), as well as the fracture toughness of the material. The first two variables are not shown on the fracture analysis diagram, and the first is not commonly considered in fracture mechanics.

Approaching the crack propagation problem from a new viewpoint, Irvine, Quirk, and Stott[63] reasoned that three modes of crack propagation could be possible. Crack propagation could be controlled strictly by the nominal stress acting normal to the plane of crack extension or by the difference between this stress and either of the other two stresses. The first mode of failure would be cleavage, and the latter two would be shear modes. In seeking a semiempirical failure criterion, they plotted the parameter $f^3 l^2$ versus Charpy impact energy and detected a transition between the first two modes of failure, each being the lowest mode of failure over a certain range of Charpy value.[63,155] More recent (unpublished) research has indicated the existence of the second shear mode. This shear mode is governed by the difference between the nominal hoop stress and the applied pressure.[63]

Because of the possible size effects, Irvine, Quirk, and Stott[63] recommended a continuation of large-scale testing. They also noted that in structures where long welds offer possible paths for crack propagation, the properties of the weld material are relevant. By utilizing an assumed shape of the crack cross section and measured values of crack-opening displacement (COD), Hake[156] estimated the open-crack area as a function of nominal stress. This estimate is relevant to the analysis of a loss-of-coolant accident.

To test the hypothesis that plastic bulging of the cracked region influences the fracture strength of cylindrical vessels, artificially cracked flat plates were tested in tension.[80] The plate specimens were

either 7 or 5 ft wide by 4 ft high and 1 in. thick (the same as the model pressure vessels). These plates were, of course, free of any bulging effects. Three materials were tested. One material was the same as used in the 5-ft-diam vessel tests, and the other two were an aluminum-treated mild steel and a silicon-killed mild steel. These tests were conducted in a hydraulic testing machine that produced essentially constant deflection conditions during crack propagation. As in the hydraulic tests of pressure vessels, pop-ins were observed. The first pop-in always occurred at a nominal stress below yield and thus proved that fast fractures can propagate from long flaws at nominal stresses below yield without the prior occurrence of bulging. The variation of nominal (net section) stress at failure, as shown in Fig. 6.29, was even less than for the same steel in the 5-ft-diam pressure vessel. In general, the stress distributions at the ends of the plates were found to be nonuniform. However,

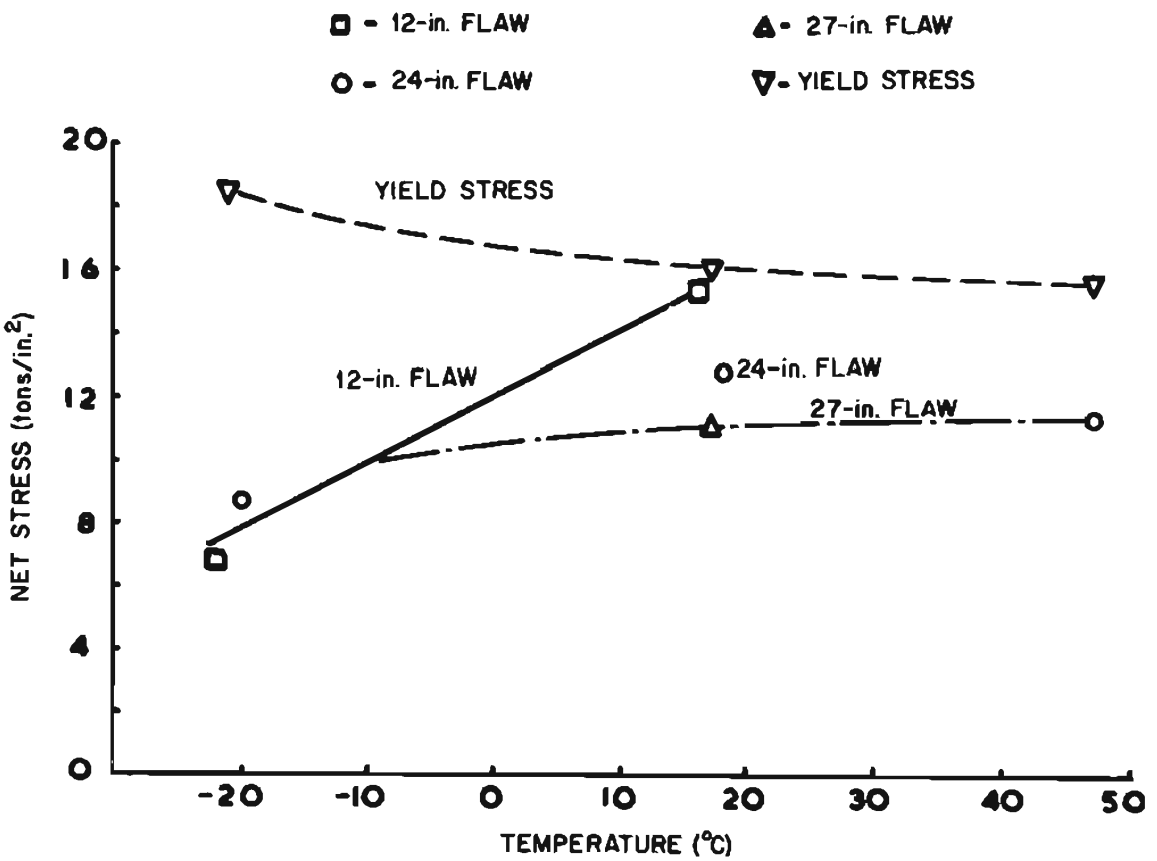

Fig. 6.29. Variation of Pop-In Stress with Temperature. (From Ref. 80)

for a 12-in. crack length, the stress at the ends was found to be uniformly distributed at failure and to be the same as the nominal stress at failure in a 5-ft-diam vessel. It was concluded that for cleavage fracture governed only by the nominal stress normal to the crack plane, there is little difference between the failure stresses for flat plates and 5-ft-diam vessels.[86] Therefore, the British believe that bulging does not influence cleavage fracture. This does not rule out local tensile instability at the crack tips, however, as was previously explained. Also, since a flat plate represents a cylinder of infinite radius, there should be no practical difference between a model vessel 5 ft in diameter and a full-scale vessel 60 ft in diameter. After supplementing the tests on 5-ft-diam vessels and flat plates with tests on 3- to 9-ft-diam vessels, it was finally concluded that neither bulging nor cylindrical geometry is the cause of the observed low-stress fast fractures above the CAT curve.[155] It was also concluded that a strength analysis that considers flaw size will be particularly necessary for high-strength steel vessels. Also, since the flaws required to cause fast fracture above the CAT curve are very large (of the order of feet rather than inches), the safety of present vessels is not in question,[155] even if the validity of the fracture analysis diagram CAT curve is.

Based on the foregoing information, the question of the credibility of failure of a nuclear pressure vessel was considered. Nonfailure was defined as a critical defect size larger than can possibly exist.[155] In other words, the question of the credibility of failure was converted into the question of the credibility of defect sizes. If an upper limit of defect size can be established, larger defect sizes are incredible. If fast fracture requires defects larger than the upper limit, fast fracture is incredible. Nondestructive inspection can reduce the probability of large defects to a very small level but not to zero. However, a proof test more severe than the most severe service conditions can establish the upper limit of defect size with certainty and with a margin of safety between test and design conditions. Then, in the opinion of the British, if all causes of crack growth and change of properties in service can be accounted for, the incredibility of failure can be guaranteed, at least for a specified length of time. Subsequent proof tests can be used to

extend the safe life. An accurate stress analysis and a proven theory of failure is required to relate the proof-test conditions to a critical defect size. Furthermore, a proven theory of crack growth must be available, as well as a highly reliable means of nondestructive inspection, in order to prove that no existing defect can become critical for a specified number of years after the proof test.

6.3.2.3 The PM-2A Tests

The objective of the PM-2A tests was to determine the fracture strength and mechanical properties of an actual nuclear pressure vessel after operation. The PM-2A steel pressure vessel was in service from February 1961 to July 1963 at the U.S. Army base at Camp Century, Greenland. The Camp Century reactor was a pressurized-water type. The vessel had an inside diameter of 37 1/2 in., a wall thickness of 2 3/8 in., and a height of 10 ft 3 in. The body was fabricated from ring forgings of SA 350 grade LF 3 steel with stainless steel cladding.[157] SA 350 steel is an intermediate-grade steel with a yield point of 59,600 psi and an ultimate strength of 80,500 psi.[49] The initial NDT temperature of the vessel material was −80°F.[48] The anticipated 20-year shift in the NDT temperature was 400 to 600°F, which is far greater than the average.[49] The maximum measured fast-neutron dose in the vessel wall was 1.4×10^{19} neutrons/cm^2 ($E > 1$ Mev).[157] The coolant inlet temperature was 500°F; the coolant outlet temperature was 518°F;[47] the design temperature was 600°F; and the design pressure was 2000 psi.[46] A surveillance program was specified[47] in which three tensile and 36 Charpy specimens were included.

The strength test consisted of machining a notch part way through the vessel wall from the outside in the region of maximum flux and pressurizing the vessel to failure at a temperature sufficiently low to produce brittle fracture. Using Eq. (16) and estimated materials properties, it was calculated that failure should occur at a pressure of 4000 psi ± 25% at −20°F.[157] Materials properties were estimated on the basis of irradiation tests on the parent materials but apparently without using data from the surveillance specimens. Among the assumptions used in the analysis were the assumptions of linear relationships between initial transition temperature and both the change in transition temperature and the change

in yield stress. Why the surveillance specimens were not used to determine these quantities is not explained. A lack of information on the effect of yielding on K_{Ic} was noted. Warm prestressing effects were believed to be small.[69] The plastic zone size at failure was estimated to be about 0.030 in., and thus full transverse restraint and the applicability of fracture mechanics were insured.

Of particular importance in this case is the admitted uncertainty in the initial strength estimate, which was made under conditions identical to or even more favorable than those existing during an actual design when the vessel has not been built. Reference 157 states that, "Detailed evaluation of the uncertainty ... is unwarranted in view of the multiplicity of approximations; the accuracy claimed can be no greater than ±25%."

Evidently the accuracy of the initial strength estimate was not as good as hoped for because the vessel did not fail at a pressure of 5000 psi and a temperature of −20°F. The most likely reason for the vessel not failing was judged to be the fact that the electrodischarge machined notch was not sufficiently sharp for K_c to be a minimum.[158] Therefore, after some experimentation, the notch was sharpened by stress corrosion with 1:1 HCl, with the vessel under a load of 5000 psi at 70°F. Following this procedure, the vessel was depressurized, the defect flushed with water, and the vessel cooled to −20°F.[158] Subsequent pressurization at −20°F resulted in a brittle fracture that originated at the artificial defect and occurred at a pressure of 4475 psi. The results of these tests are still being analyzed. It should be noted that the failure conditions of the PM-2A vessel were considerably more severe, both in terms of temperature and in terms of load, than its operating conditions. It should also be noted that failure occurred at a lower pressure than the maximum previous pressure at a higher temperature; this apparently contradicts the predictions of warm prestressing theory. However, the effects of stress corrosion on the notch sharpness are not considered in this apparent contradiction.

6.3.3 Brittle Fracture of a Pressure Vessel

Perhaps even more enlightening than the results of large-scale tests are the rare but sometimes spectacular results of actual failures, which serve to point out a fact that many engineers would like to forget: Failures can happen. Further, they serve to demonstrate possible modes of failure and consequences of failure that may have been overlooked or incompletely understood previously.

On December 22, 1965, the failure of a large thick-walled nonnuclear pressure vessel during proof testing in England[65] provided the most accurate and dramatic example yet of the catastrophic mode of failure that is to be prevented in nuclear power plants. The vessel was a long cylinder with end closures, one welded and the other bolted, and was intended for use in an ammonia plant. The cylindrical part of the vessel was 52 ft 8 1/2 in. long, 5 ft 7 in. in diameter, and had a wall thickness of 5 7/8 in. The vessel material was a low-alloy manganese-chromium-molybdenum-vanadium steel with a yield stress of about 60,000 psi and an ultimate strength of about 85,000 psi. This material is classified as a low-alloy intermediate-strength steel. The design pressure was 5100 psi at 250°F. Failure occurred by brittle fracture during a proof test at a temperature of 50°F and an internal pressure of 5000 psi. The intended proof-test pressure was 6950 psi. Pressure was applied hydraulically, with water as the pressurizing fluid. The vessel withstood the ultimate pressure for 30 sec before failing. A photograph of the failed vessel is shown in Fig. 6.30. Several heavy fragments separated completely from the vessel, including one which weighed 2 tons and was thrown a distance of 152 ft. This fragment is shown in Fig. 6.31. The projection of missiles from this vessel is particularly significant in view of the fact that the loading was hydraulic, which implies a rapidly decaying loading; however, the elastic stored energy was very substantial. The fracture was initially axial and appears to have been started by a 3/8- by 1/8-in. partly through crack in the heat-affected zone of the weld between the cylinder and the flange forging.*

*The flange forging is the forging to which the bolted flange is attached.

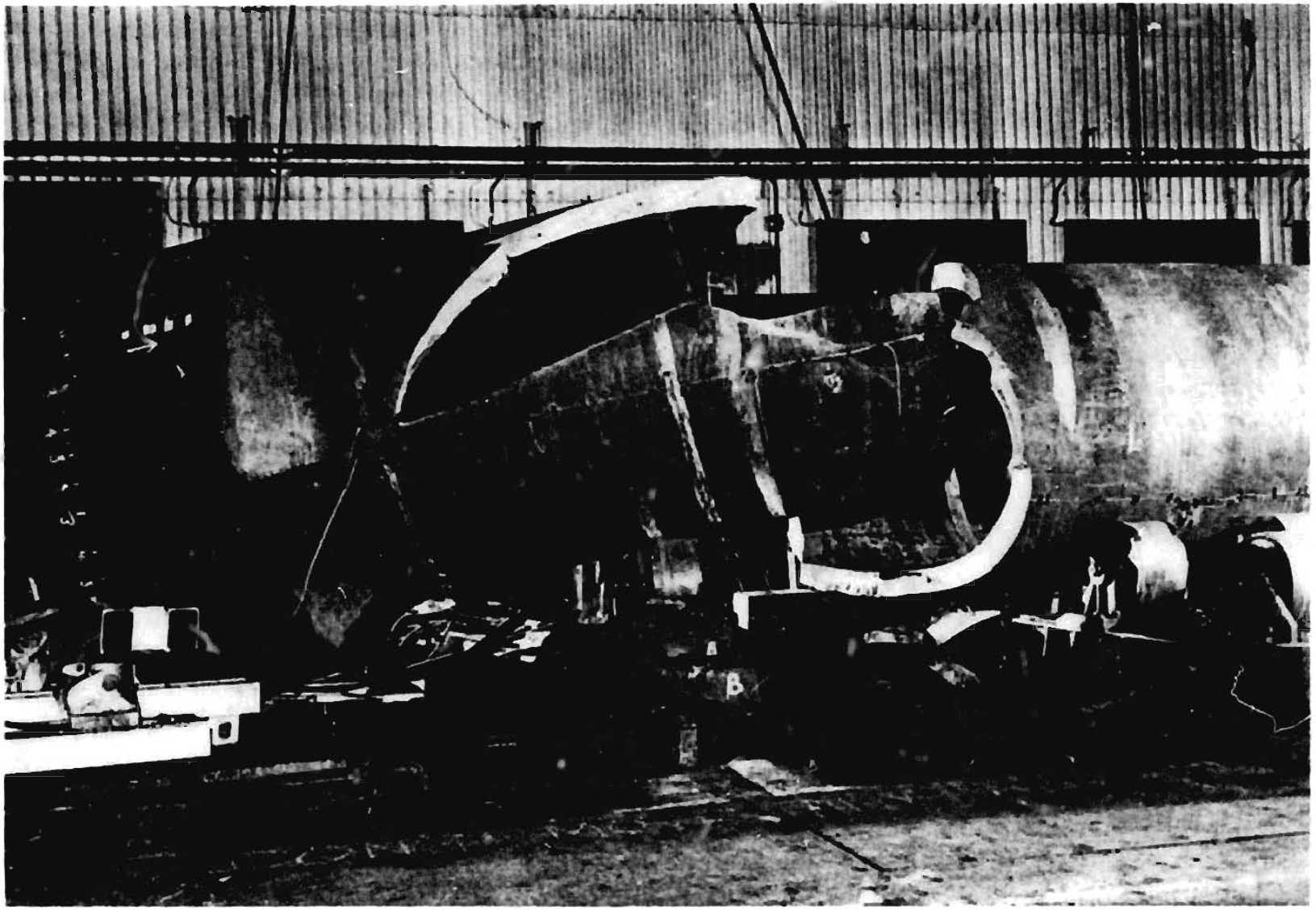

Fig. 6.30. General View of the British Ammonia Plant Pressure Vessel That Failed by Brittle Fracture at a 5000-psi Internal Pressure During Hydraulic Proof Testing. (From Ref. 65)

Fig. 6.31. Two-Ton Segment of Vessel That Was Thrown 152 ft on Failure. (From Ref. 65)

The inquiry following the failure revealed the following facts.[65]

1. Although the vessel was designed "generally in accordance with" Section VIII of the ASME Boiler and Pressure Vessel Code, the factor of safety applied to the ultimate strength of the material was 2.35. (Section VIII prescribes a factor of 4.0, and Section III prescribes a factor of 3.0.)

2. The transition section of the welded closure (not the location of failure) was expected to become almost fully plastic at full proof-test pressure.

3. Residual stresses probably existed at the location of failure (at the bottom flange-to-cylinder junction), but they were not specifically considered in design.

4. Metallurgical segregation had occurred at the location of crack initiation.

5. The weld heat-affected zones near the location of failure initiation were vulnerable to hydrogen cracking (which can occur in a matter of seconds).

6. The actual heat-treatment temperature at the location of crack initiation was lower than it should have been. The specified heat treatment for the vessel was "stress relief for 6 hr at 620°C/660°C." Although it was not possible to determine precisely the actual stress relief temperature, the results of postmortem reheat treatments can be interpreted to indicate that the actual heat-treatment temperature was approximately 550°C.

7. The Charpy impact-energy curves of the plate, forging, and weld metal showed that the weld metal was dangerously below strength (see Fig. 6.32).

8. The detrimental effects of fabrication on material properties were not anticipated in design.

9. The transition temperature (presumably the FTE temperature) of the base metal was estimated to be about 55°F, which was 5° above test temperature. Therefore, since stresses were expected to reach yield at the end closure transition, rapid crack propagation would have been possible at full proof-test pressure even without residual stresses.

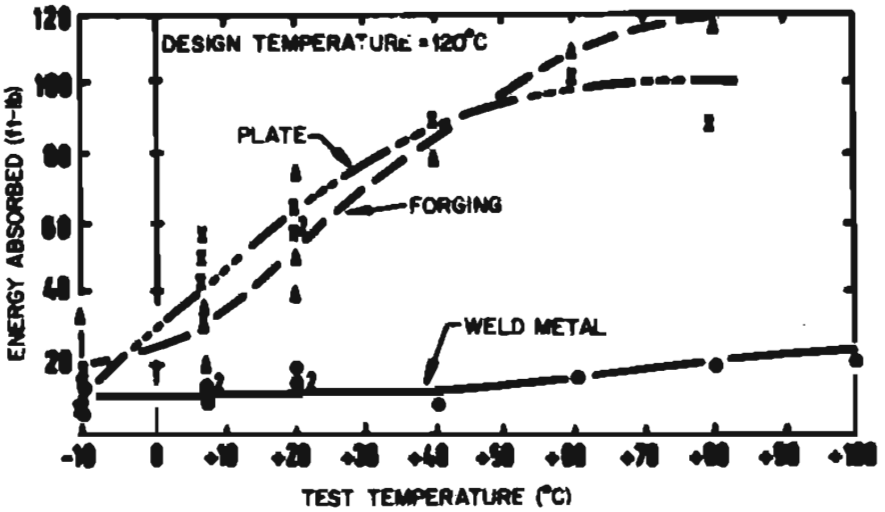

Fig. 6.32. Charpy V-Notch Impact Test Data on Plate, Forging, and Weld Material of Failed Vessel. (From Ref. 65)

10. Radiographic, ultrasonic, and magnetic-particle inspection were carried out on the circumferential weld seams prior to stress relieving. Therefore, any cracking that occurred during stress relieving went undetected.

It may be concluded that this failure had multiple causes, which is typical of actual failures. Furthermore, at least one factor of each major group of factors controlling brittle fracture, as previously outlined, was active. These factors are summarized as follows:

1. Environment
   a. Temperature
   b. Hydrogen embrittlement
2. Loading conditions – residual stresses
3. Design and construction features
   a. Flaws
   b. Low safety factor applied to ultimate strength
   c. Stresses near yield and loading temperature below the FTE temperature
   d. Detrimental effects of fabrication on material properties not anticipated in design

4. Metallurgy
   a. Segregation
   b. Improper heat treatment
   c. Low fracture toughness of the heat-affected zone
   d. Nondestructive inspection not carried out after heat treatment
   e. Susceptibility to hydrogen cracking

6.4 CURRENT DESIGN PRACTICE AND THE STRESS REPORT

6.4.1 Current Design Practice

There are at present five major industrial concerns involved in the design and fabrication of nuclear pressure vessels. These include two primary reactor vendors, General Electric Company (GE) and Westinghouse Electric Corporation (Westinghouse), and three fabricators, Babcock & Wilcox Company (B&W), Combustion Engineering, Inc. (Combustion), and Chicago Bridge and Iron, Inc. (CB&I). Both Combustion and B&W also provide primary vendor service.

Section III places the responsibility for the initial structural integrity of the pressure vessel on the manufacturer. As part of the design responsibility the code requires that the manufacturer or a design agent responsible to him make a complete set of stress analysis calculations which establish that the design conditions, as specified by the user in the Design Specifications, have been fully satisfied. This information is to be documented in a stress report (see Sect. 6.4.2 for a discussion of the stress report).

Discussions were held with each of the two vendors and three fabricators in order to ascertain as nearly as possible their current practice regarding Section III Class A pressure vessel design and stress analysis. Company personnel at these meetings numbered from 3 to 7 and represented the most expert and directly responsible individuals. The discussions centered on a series of eight categories of questions designed primarily to open areas of discussion concerning as much of the detailed operational methods as could be covered in conference. In this regard, the visits

were quite successful; free and open discussions were held with each group. It can be correctly reported that in every case a high degree of competence and responsibility was evident. The eight categories of questions for discussion were:

1. What is your design philosophy for boiling- and/or pressurized-water reactors?

2. In what manner do you treat the stress report as required by Section III of the ASME Code? To what degree is it reviewed? Are the reviews and recommendations timely?

3. To what degree do you cooperate with the fabricator or customer (as the case may be) in preparing the stress report?

4. In what areas do you feel that Section III of the ASME Code is deficient? Do you agree that design codes should be limited to the quality of new construction? If so, what is the best way to insure safety during operation? Is a separate code necessary for this purpose and if so who should write it?

5. What experimental stress analysis do you support and to what extent do you require new design features to be "proven" beyond that required by Section III?

6. What methods of theoretical stress analyses are employed in your work? What mathematical methods are used? How are stress analysis computer programs verified experimentally? Is a complete vessel analysis performed, including a thermal stress analysis?

7. What type of failure analysis is performed? What is your philosophy on failure of the vessel?

8. What research do you support relative to the above questions in order to extend the state of the art?

Particular interest was shown in obtaining copies of stress reports and design specifications that reflected the present practice relative to Class A nuclear vessels. When such material was documented it was made available, even when it contained privileged information and required a release from several interested parties. At the time of the discussions there were only two Class A Section III vessels far enough along to get specific documented design and stress report information. These documents were studied in detail and the state of the art as revealed is reflected

throughout this entire chapter. Two companies each are responsible for these vessels; Westinghouse and Combustion for the Zorita vessel, and General Electric and Babcock & Wilcox for the Dresden-2 vessel. At this time Chicago Bridge and Iron is working actively with General Electric on the design of the Monticello plant vessel, which will be field erected. It would be a mistake to indicate that nuclear pressure vessel technology is in its infancy; however, it is a pertinent fact that the industry does not have much experience in working with Section III of the code.

The relationship between the vessel fabricators and the system designers has worked especially well. Technically speaking, the system designers are fully responsible for writing complete specifications, whereas the fabricators are fully responsible for detailing the design, including the stress analysis and stress report. However, it has been necessary and will continue to be necessary for the process designer and the vessel designer to maintain very close contact. Process designers are still learning how to write complete and adequate specifications, and the fabricators are still learning how best to complete the mass of detailed stress analysis and documentation required by the customer and Section III. The stress analysis review by the process designer is thorough and complete. All groups feel that such second-party review is highly desirable and contributes significantly to the quality of the final product. The question of third-party review was also discussed. The general feeling was that such a review would not add quality to the product if an adequate and timely second-party review was performed as at present. No one was against a third-party review provided it would be performed by competent personnel and that proprietary interests of the major parties could be guaranteed. There would be certain advantages to the present five designers if persons not now in the business were required to pass third-party review. A complete and adequate stress analysis that meets not only the letter of Section III but also the intent, requires a significant expenditure of time and money, and it would be advantageous if the entire industry were required to compete according to the same set of ground rules. Third-party review would help in this respect.

All the companies have active membership on the ASME code committees, including Section III for nuclear vessels. In the main, it is felt that

Section III is a good code. Working to the requirements of Section III has increased the work load for some of the companies; however, most felt that the technology would have demanded the additional analytical work in any case. Section III essentially only requires that which was previously a matter of good practice. All parties expressed a desire for better analytical solutions backed up by experimental evidence. However, they questioned the advisability of including mathematical solution techniques into a code which will in all likelihood be written into the law in several states. It would be much more desirable if a separate document were available that contained acceptable analytical methods. Such a document would be easier to keep up-to-date with the technology without forcing the designer to use methods that might be less efficient because of peculiar circumstances.

It was the considered opinion that a code such as the ASME Pressure Vessel Code could only be written for new construction because of the problem of enforceability. A proper addition to the Code is that it could require that the design permit periodic inspection in the event that such technology becomes available. After the vessel leaves the dominion of the fabricators' influence, he has no control over the treatment the vessel will receive in operation (and does not want it). He can, however, and does write an operating and maintenance manual the new owner can use. There is very little or no direct feedback to the designer in the way of actual operating data, such as vessel temperature distributions and transients, pressure cycles, or unusual mechanical loads, not to mention actual stresses or strains. The designer, therefore, has no way of evaluating his design predictions, except in the event of structural difficulties.

All the companies have an experimental stress analysis program; the fabricators are much more active than the vendors since it is they who are ultimately responsible for the design. Their experimental work is primarily directed toward answering specific design questions. Problems of a general nature are taken under advisement by the Pressure Vessel Research Committee of the Welding Research Council. Industry supports a portion of the PVRC work. Dissemination of information is not the primary goal of the pressure vessel industry. However, much of the information in the open literature is a result of private industrial research programs.

Nobody is more interested in sound technical information than the designer who must bear the ultimate responsibility.

Up to the present time, failure analysis of a steel nuclear pressure vessel has not been considered as a valid design criterion. If the designer can meet the specifications written by the customer and the stress limit and other criteria established by the Code and uses his best judgement in the exercise of good design practice, including accurate analyses, it is his feeling that a failure analysis is not only unnecessary but could be seriously misleading. If overload conditions can be written into the specifications, they can be adequately covered in design. If they are not defined for purposes of design, design against their occurrence cannot be defended in a competitive environment. It was frequently stressed that the set of specifications is fully as important as the stress report in insuring that the final product is as good as present technology will allow. Careful consideration should therefore be given to establishing minimum standards for nuclear pressure vessel design specifications.

6.4.2 Stress Report

In order to assure that an adequate stress analysis of the vessel has been made, the Section III rules stipulate that a stress report be prepared, certified by a Professional Engineer, and filed with the proper authorities at the point of installation. The rules also provide that experimental stress analysis methods, either strain gage or photoelastic, may be used to verify specific design areas when theoretical solutions are unavailable or for determining fatigue-reduction factors for cyclic operation. The results of such tests are to be included in the design report.

The Code specifies only that a complete set of stress analysis calculations shall be made and reported. It does not specify that the calculational methods used must yield correct or conservative results as verified by experimental data or that such evidence shall be offered in support of the calculations. The Code does require that the stress report be certified by a registered Professional Engineer experienced in pressure vessel design. The Code does not specifically say that the Professional Engineer must be experienced or qualified in stress analysis. The Inspector who

affixes the Code Stamp is specifically not responsible for the completeness or correctness of the design calculations as set forth in the stress report.

Stress analysis by computer is fast becoming a necessity in the industry, both because of the enormous amount of labor that can be saved with the computer and because of the competitive advantage in being able, with a limited staff, to more thoroughly analyze a vessel. As remarked earlier, the investment in computing machinery and computer programs is high, and private industrial concerns quite naturally are interested in preserving their proprietary interest. Since the Code makes no mention of how to report the calculations in the stress report, it is conceivable that a stress analysis could be reported simply as a list of computer program "names" and a listing of the computer output. This would seem to be inadequate reporting if the purpose of the stress report is to justify the design as based on computation. However, if the purpose of the report is to certify that the computations have been made, it would be perfectly satisfactory.

No reputable manufacturer is unwilling to have his computations examined by an impartial investigator provided every other manufacturer is equally treated and his own investment is not jeopardized. During the visits discussed in the above section, each group interviewed expressed the opinion that his methods were as good as those of other groups and, in general, would welcome a stress report review. As remarked earlier it was not always possible to obtain complete stress report documentation because only one Section III Class A vessel stress report has been completed. The primary concern of industry is that persons not now in the business will later be able to capitalize on the information.

One of the specific questions to which this report is addressed is whether an independent third-party review of the stress analysis and stress report is advisable. This question is almost academic until a complete and adequate description of exactly what should be reported and how the report should be written is available. The following questions should be explored: (1) Are computer calculations acceptable? (2) Should the computer codes be part of the report, to what extent should the formulas and methods of evaluation be documented, and should the results be

computer output, tabular listing, or plotted curves? (3) What experimental justification for theoretical formulas is necessary and in what quantity? (4) Should the experimental investigations be part of the stress report or be reported separately?

Once these questions are fully explored and answered, the question regarding an independent stress evaluation can be answered. It may indeed be necessary in order to protect the interests of both the manufacturer and the public to establish an authority charged with the specific task of reviewing and establishing the adequacy of the stress report. Presently the qualifications for obtaining a Professional Engineer's license are not necessarily adequate to qualify a person as a pressure vessel stress analyst. Paragraph N-142 of Section III requires, however, that the engineer be experienced in pressure vessel design. It is our understanding that forthcoming revisions to Section III and ASME guidelines for the preparation of the stress report may satisfactorily answer many of the above questions.

6.5 SUMMARY AND RECOMMENDATIONS

The objective of this chapter on the design of nuclear pressure vessels has been to present the basic background material necessary to evaluate the current trends in pressure vessel technology, as related to design, and to make a judgement of the areas that need additional emphasis. Also, an attempt has been made to evaluate the impact that Section III of the ASME Code has had on the industry and the degree to which vessel fabricators and designers actually comply with the Section III requirements. The approach has been to answer the following questions: (1) How are stresses and strains calculated (see Stress Analysis of Pressure Vessels, Sect. 6.1)? (2) What do stresses mean when they are calculated (see Stress Evaluation for Nuclear Pressure Vessels, Sect. 6.2)? (3) What is being done to advance design technology (see Current Research on the Design of Pressure Vessels, Sect. 6.3)? (4) What is being done in actual practice (see Current Design Practice and the Stress Report, Sect. 6.4)? The answers to each of these questions are summarized below. Following

this is a list of specific recommendations based on the material presented in this chapter to pin-point the "soft" spots in design technology.

First, the linear theory of elasticity is discussed. This theory, which includes the theory of stress, the theory of strain, and Hooke's law, is the basis for all current methods of theoretical stress analysis. The theory of elasticity is complete in the sense that all the necessary theorems, including uniqueness, are available. However, the theory is mathematically complex, and relatively few complete and exact solutions have been found for structures of practical interest. The real utility of the theory, from an engineering point of view, is in the development of the approximate theories of shells and strength of materials. These approximate theories and the solution of specific design problems are based on certain assumptions about the gross behavior of a structure and therefore must be verified experimentally.

In general, the agreement between analytical solutions and experimental investigations on carefully constructed models has been quite good. However, there are still a number of weak points in the analytical stress analysis, and much of the experimental information reported in the literature is unfit for developing better solutions. These weak points include the immediate regions around those discontinuities, penetrations, support points, clustered nozzles, and other nozzle configurations that produce asymmetric stress distributions. Currently vigorous programs are under way in some areas to improve analytical methods and experimentally verify the results. Also these experimental programs are coordinated to provide explicit design information.

Methods and techniques for determining stresses experimentally have been developed to a high degree of reliability, except for thermal stresses. Recent developments, such as laser photoelasticity for three-dimensional work and computer techniques for data reduction, are continually improving the usefulness of experimental stress analysis. However, proper utilization of experimental methods requires very careful laboratory practice and an abundance of experience and training. Unfortunately this is seldom recognized.

It is important to realize that design details which can be analyzed should be the ones preferred in design practice. It follows then that the

designer should be involved in the conceptual stage of reactor design in order to avoid being "boxed" in by process requirements over which he has no control. Another problem not presently considered in most vessel designs is that of in-service inspection. The long service life of the many power reactors now being built would be accomplished with increased confidence if in-service inspections could be performed. Designs finalized with the possibility of such inspections give recognition to the rapid advances of nondestructive testing techniques.

A series of strength tests on flawed vessels is discussed in detail. From the results it is apparent that neither the transition-temperature approach nor the fracture-mechanics approach is entirely adequate for design against failure. Some of the large-scale tests have shown that cyclic crack growth is a significant problem and further research is needed in this area. The pitfalls in design and fabrication are emphasized by a short discussion of a dramatic catastrophic failure during hydrotest of a nonnuclear vessel at a pressure below the design pressure. Although the materials and fabrication practices in this case history are not representative of those of the reactor vessels being reviewed in this report, the importance of maintaining adequate control over the many variables involved is vividly illustrated.

For the first time, as far as ASME rules for pressure vessel construction are concerned, the acceptable stress limits are based on a theory of failure for combined stresses. The failure theory adopted is the maximum shear-stress theory (Tresca theory), which is the simplest and most conservative of the triaxial failure theories or yield criteria. The allowable stress intensity is a measure of the load required to cause the material to yield plastically. In order to compute the stress-intensity value at a point, it is necessary, in general, to determine all six of the stress components at the point. This requirement alone has made many of the solutions based on a strength-of-materials approach obsolete. Brittle fracture, although now considered a possible mode of failure, is not specifically mentioned as a possible mode of failure in Section III. However, the Code does specify Charpy V-notch impact energy values.

The rules of Section III and the allowable stresses permitted are based on the assumption that a complete and accurate elastic stress analysis of every nuclear pressure vessel can and will be made to insure that the stresses in the final structure will be within acceptable limits. In order to insure that the analysis has been done, the fabricator is responsible for the preparation of a stress report that includes a complete set of stress calculations and pressure vessel drawings. From examinations of stress reports and discussions with vessel fabricators, it is apparent that the Code requirement concerning the stress report may be inadequate if a document for third-party review is desirable. Each of the companies visited thus far expressed an interest in having a competent stress report review. However, they would require assurance that any such review would not jeopardize their own proprietary interests.

Visits have been made to the principal nuclear pressure vessel fabricators and system designers. In general, discussions were focused on (1) design philosophy, (2) writing and review of the stress report, (3) deficiencies and limitations of Section III of the ASME Code, (4) the place of experimental and theoretical stress analyses in the design of nuclear pressure vessels, and (5) the type of failure analysis performed on the vessel. The companies visited were most eager to discuss their competence and made available their key personnel in the areas for discussion. Their frankness and desire to make a meaningful contribution to subjects under discussion contributed much to the insight gained. It is interesting to note that while the persons visited were quick to discuss subjects brought up, they were reluctant in general to point out "soft" spots unless the item was fairly well identified in the discussion, as would be expected.

The requirement for a complete stress analysis places the manufacturer's analytical departments under increasing work loads, and these groups are being expanded. The cyclic analyses for fatigue evaluation and the determination of thermal stresses are both troublesome areas. In order to comply fully with the code requirements and handle an increased demand for nuclear pressure vessels, the manufacturers, in general, are expanding their analytical capabilities and upgrading their personnel. At least one company is installing new and bigger computers. Until they

are fully capable of performing their own stress analyses, at least a portion of the work will be subcontracted.

Irradiation is identified as one of the prime phenomena that may degrade a pressure vessel if the fluxes exceed 10^{18} neutrons/cm^2. The most significant effect is the loss of ductility. Irradiated mild steel has a stress-strain diagram similar to that of high-strength steel. This is very important in nuclear pressure vessel safety because the uncertainties regarding the behavior of high-strength steel vessels become applicable to irradiated mild steel vessels as well. However, Section III recommends and USAEC requires a comprehensive surveillance program to check for irradiation effects.

The analytical and experimental aspects of stress evaluation for nuclear vessels have been summarized. Special emphasis has been placed on the relationship of fracture mechanics to plasticity and fatigue. The transition-temperature approach is also discussed. The recent experiments on flawed test vessels have produced failures that have not been completely explained by present analytical methods. The two factors that appear to be the primary causes for these discrepancies between theory and experiment are (1) extensive yielding at the crack tips and (2) rate of change of applied load during crack propagation.

Several methods for design against fracture exist but none are infallible. The fracture analysis diagram does not account for the effects of stored energy in the load and is inapplicable to nonstrain-rate-sensitive materials. It is also subject to size effects and may not be accurate for some cases involving extensive crack-tip yielding prior to fracture. Basically, it is an empirical, not an analytical, method and therefore is subject to the usual shortcomings of empiricism. The effects of stored energy in the load are not considered in fracture mechanics either, although the onset of instability can be fairly well predicted if yielding is limited. No exact methods exist for correcting the elastic stress distribution near the crack for the presence of the crack-tip plastic zone in cases of extensive crack-tip yielding. The British empirical method implicitly considers extensive crack-tip yielding, but it lacks a proven analytical basis. Further research is needed to determine the effects on the fracture strength and mode of failure of the following: stored energy

in the load, yielding, residual stresses, stress gradients, size, and welding. An extension of the fracture mechanics approach appears most likely to be able to consider these factors. The effects of residual stresses are particularly important, since stress relieving at temperatures low enough to preserve mechanical properties may be only 80% effective.

Mild steel and high-strength steel have about the same fatigue strength in the plastic range. Therefore, since the "shakedown" fatigue strains are governed by the elastic modulus, which is about the same for both materials, fatigue must be prevented from governing the design if high-strength steel is to be used to advantage in nuclear pressure vessels. This requires refined analysis and improved geometric design and inspection in order to minimize strain-concentration factors.

Material selection, fabrication, surveillance, inspection, and maintenance all play a prominent roll in finalizing a pressure vessel design. These items are only mentioned here, since they are discussed in detail in other sections of this report.

It should perhaps be noted that while current vessels are being designed by Section III, those vessels designed under Sections I and VIII may not meet the requirements of Section III. Thus, such vessels now in operation could and perhaps should be reanalyzed and referenced to Section III. In some instances operating procedures may have to be amended in order to insure safe operation.

In considering this chapter, several areas stand out as ones that are in much controversy or are currently ill defined or, again, are little understood. Doubtlessly, much controversy could arise from just a listing of these areas. Nevertheless there is much work still to be done on the structural behavior of nuclear pressure vessels. The recommendations, as an outgrowth of this chapter, are the following:

1. The strong and vigorous program for theoretical analyses of pressure vessels should be continued. Areas such as nozzle-to-cylinder attachments and nozzles attached in clusters to vessels are currently of prime importance. However, other asymmetric configurations, such as a nozzle closely attached to a spherical head-to-cylinder junction, occur in almost every design. Such problems should also be covered in the general outline

of analytical work to be done. Unfortunately, these more complex problems must often await the successful analyses of those currently being analyzed.

2. The current experimental stress analysis efforts should be continued and expanded. Such efforts not only give data to support the theoretical analyses but also present interim information for design purposes. The experimental effort should be expanded to include the more common configurations for which theoretical analyses are not currently available. These configurations include closely spaced and grossly asymmetric configurations (e.g., a large nozzle near a major junction), brackets, and general support arrangements other than skirts.

3. Section III of the ASME Code should give more precise detail and direction with regard to (a) categorizing of stresses, (b) definition of loading conditions, (c) brittle fracture as a potential mode of failure, and (d) the stress report (this is discussed under the next item).

4. Section III should specify precisely what is acceptable as a stress report and what is not. Specifically, it is recommended that the stress report contain such details as would be necessary for a third-party review. Also, the fabricator should give evidence as to the accuracy of his analyses. For example, most boiling- and pressurized-water reactor pressure vessels have nozzles penetrating the cylindrical portion of the vessels. Only recently has a method become available for the analysis of such a design feature, and this method is not in common use. Short of an experimental analysis, it is difficult to say what would be acceptable for the stress report in this example.

5. To maintain a high quality of design and structural performance, it is recommended that a review of the stress report by a qualified engineer representing the system designer or owner be mandatory. Such a review should be timely so that recommendations by the reviewers can be incorporated into the design. In addition to this a third-party review board responsible to USAEC may be desirable. Such a board for a particular stress report could consist of a fabricator's representative, an owner's representative, and two qualified members at large who are not specifically associated with the industry. The board would be set up with very specific responsibilities so as not to conflict and seriously overlap with other review committees, such as the Advisory Committee on Reactor Safeguards.

6. The study of strength of pressure vessels below the transition temperature where brittle failure could perhaps occur should be continued. In the case of ductile fracture, an extension of the fracture mechanics approach probably has the best chance of providing a reliable estimate of strength.

7. The behavior of flaws in the presence of different geometries, residual stresses, stress gradients, yielding, and irradiation should be studied as a function of size. In particular, fracture mechanics should be extended to include these variables.

8. Section size and stored energy should be considered in the transition-temperature evaluation of pressure vessels.

9. The hydrotest and warm prestressing should be more carefully evaluated as means of preventing failure. In particular, the superposition of loadings on nozzles as a part of the hydrotest should be considered.

10. Studies on welds, heat-affected zones, out of roundness, biaxiality of stresses as related to fatigue, load-cycling rates, and slow growth of cracks by fatigue should be continued and implemented.

11. Additional emphasis should be given to design aspects that lend themselves to accurate analyses. Likewise, consideration should be given to designing the vessel to accommodate in-service inspection, even though current techniques of in-service inspection are not adequate.

12. Specifications play as important a part in the design of nuclear pressure vessels as the stress report. Thus, studies should be made that are aimed at establishing minimum standards for nuclear pressure vessel design specifications.

REFERENCES

1. Tentative Structural Design Basis for Reactor Pressure Vessels and Directly Associated Components, PB 151987, 1 December 1958 Revision, Department of Commerce, Office of Technical Services.

2. W. A. Shaw and F. S. Smith, Strength of Materials, McGraw-Hill, New York, 1967.

3. J. S. Sokolnikoff, Mathematical Theory of Elasticity, 2nd ed., McGraw-Hill, New York, 1956.

4. Ibid., p. 11.

5. Ibid., p. 21.

6. Ibid., p. 28.

7. Ibid., p. 41.

8. S. Timoshenko and J. N. Goodier, Theory of Elasticity, 2nd ed., p. 217, McGraw-Hill, New York, 1951.

9. R. S. Burington, Handbook of Mathematical Tables and Formulas, 5th ed., p. 7, Handbook Publishers, Inc., Sandusky, Ohio, 1955.

10. Op. cit., Ref. 8, p. 14.

11. B. A. Boley and J. H. Weiner, Theory of Thermal Stresses, Wiley, New York, 1962.

12. V. V. Novozhilov, Thin Shell Theory, second augmented and revised edition, P. Noordhoff Ltd., Groningen, The Netherlands, 1964.

13. Ibid., Chapt. 1.

14. S. A. Ambartsumyan, Theory of Anisotropic Shells, NASA Technical Translation NASA TTF-118, Washington, D.C., May 1964.

15. H. L. Langhaar, Foundations of Practical Shell Analysis, Department of Theoretical and Applied Mechanics, University of Illinois, 1962.

16. Op. cit., Ref. 12, p. 23.

17. S. Timoshenko and S. Woinowski-Krieger, Theory of Plates and Shells, 2nd ed., McGraw-Hill, New York, 1959.

18. F. A. Leckie and R. K. Penny, A Critical Study of the Solution for the Asymmetric Bending of Spherical Shells, Welding Research Council Bulletin No. 90, September 1963.

19. W. Flügge, Stresses in Shells, p. 371, second printing, Springer-Verlag, Berlin, 1962.

20. P. M. Naghdi and C. N. De Silva, Deformation of Elastic Ellipsoidal Shells of Revolution, pp. 333–343 in Proceedings of the Second U.S. National Congress of Applied Mechanics, 1954.

21. C. M. Friedrich, Seal-Shell 2 — A Computer Program for the Stress Analysis of a Thick Shell of Revolution With Axisymmetric Pressures, Temperatures, and Distributed Loads, USAEC Report WAPD-TM-398, Bettis Atomic Power Laboratory, December 1963.

22. Op. cit., Ref. 3, p. 93.

23. M. M. Lemcoe, Feasibility Studies of Stresses in Ligaments, Welding Research Council Bulletin No. 65, November 1960.

24. F. J. Witt and R. L. Maxwell, Stress Fit Applications to Experimental Shell Analysis, Experimental Mechanics, 7(1): 36–40 (January 1967).

25. B. F. Langer, PVRC Interpretive Report of Pressure Vessel Research, Section I — Design Considerations, Welding Research Council Bulletin No. 95, p. 38, April 1964.

26. E. A. Coddington and N. Levinson, Theory of Ordinary Differential Equations, Thm 2.1, p. 68, McGraw-Hill, New York, 1955.

27. Op. cit., Ref. 11, p. 78.

28. Y. R. Rashid, Finite Element Analysis of Axisymmetric Composite Structures, USAEC Report GA-6303, General Atomic, June 4, 1965.

29. J. A. Mirabal and D. G. Dight, SØR-II — A Program to Perform Stress Analysis of Shells of Revolution, USAEC Report KAPL-2292, Knolls Atomic Power Laboratory, Sept. 15, 1963.

30. R. W. Clough, The Finite Element Method in Structural Mechanics, pp. 85–119 in Stress Analysis, O. C. Zienkiewicz and G. S. Holister (Eds.), Wiley, New York, 1965.

31. D. Ngo and A. C. Scordelis, Finite Element Analysis of Reinforced Concrete Beams, J. Amer. Concrete Inst., 64(3): 152–163 (March 1967).

32. H. Kraus, A Review and Evaluation of Computer Programs for the Analysis of Stresses in Pressure Vessels, Welding Research Council Bulletin No. 108, September 1965.

33. P. G. Hodge, Plastic Analysis of Structures, McGraw-Hill, New York, 1959.

34. S. S. Manson, Thermal Stress Analysis and Low-Cycle Fatigue, p. 194, McGraw-Hill, New York, 1966.

35. W. D. Manly, letter to Dr. Seaborg, Nucleonics, 24(1): 17 (January 1966).

36. L. F. Kooistra and M. M. Lemcoe, Low Cycle Fatigue Research on Full-Size Pressure Vessels, Welding J., 41(7): 297S–306S (July 1962).

37. R. C. Gwaltney, Missile Generation and Protection, USAEC Report ORNL-NSIC-27, Oak Ridge National Laboratory (to be published).

38. J. G. Merkle, The Strength of Steel Containment Shells, Nucl. Safety, 7(2): 204–212 (Winter 1965–1966) and 7(3): 346–353 (Spring 1966).

39. L. F. Kooistra, Effect of Plastic Fatigue on Pressure-Vessel Materials and Design, Welding J., 36: 120S–130S (March 1957).

40. B. F. Langer, The Use of Materials Properties by the Reactor Vessel Designer, pp. 418–428 in Flow and Fracture of Metals and Alloys in Nuclear Environments, Publication ASTM-STP-380, American Society for Testing Materials, June 1965.

41. B. F. Langer, PVRC Interpretive Report of Pressure Vessel Research; Section 1 — Design Considerations, Welding Research Council Bulletin No. 95, April 1964.

42. H. Corten (Ed.), A Review of Engineering Approaches to Design Against Fracture, Publication ASME-I-60, American Society of Mechanical Engineers, November 1964.

43. C. F. Tiffany and P. M. Lorenz, An Investigation of Low-Cycle Fatigue Failures Using Applied Fracture Mechanics, Publication AF-ML-TDR-64-53 (AD-600375), Boeing Company, Aerospace Division, May 1964.

44. Effect of Radiation on Ductile-Brittle Transition of Steel, Power Reactor Technology, 3(4): 38–57 (September 1960).

45. G. D. Galletly, Torispherical Shells — A Caution to Designers, pp. 269–284 in Pressure Vessel and Piping Design, Collected Papers, 1927–1959, ASME, 1960. This paper was originally published in the J. Eng. Ind., 81: 51–66 (1959).

46. L. Porse, Reactor-Vessel Design Considering Radiation Effects, Trans. ASME, J. Basic Eng., Series B, 86: 743–749 (December 1964).

47. J. R. Hawthorne, H. B. Piper, and L. E. Steele, Brittle Fracture of Steel, Section 8.5 in U.S. Reactor Containment Technology, W. B. Cottrell and A. W. Savolainen (Eds.), USAEC Report ORNL-NSIC-5, Oak Ridge National Laboratory, August 1965.

48. D. W. McLaughlin, Neutrons Embrittle Reactor Vessels of Carbon Steel, Nucleonics, 21(2): 36–41 (February 1963).

49. J. J. DiNunno and A. B. Holt, Radiation Embrittlement of Reactor Vessels, Nucl. Safety, 4(2): 34–47 (December 1962).

50. E. C. Miller, The Integrity of Reactor Pressure Vessels, USAEC Report ORNL-NSIC-15, Oak Ridge National Laboratory, May 1966.

51. J. A. Gilligan, Higher-Strength Structural Steels, Civil Eng., November 1964.

52. Private communication from J. D. Lubahn, Colorado School of Mines, Dec. 7, 1966.

53. P. N. Randall and R. P. Felgar, Part-Through Crack Test — Relation to Solid-Propellant Rocket Cases, Trans. ASME, J. Basic Eng., 86(2): 685–692 (December 1964).

54. S. R. Vandenberg, Status of Pipe-Rupture Study at General Electric, Nucl. Safety, 8(2): 148–155 (Winter 1966–1967).

55. J. L. Mershon, Comments Concerning Structural Significance of Defects in Welds and Cladding of Elk River Reactor Vessel, USAEC Report ORNL-NSIC-F-1.23, Oak Ridge National Laboratory, April 1962.

56. Criteria of Section III of the ASME Boiler and Pressure Vessel Code for Nuclear Vessels, American Society of Mechanical Engineers, New York, 1963.

57. W. B. Cottrell and A. W. Savolainen (Eds.), U.S. Reactor Containment Technology — A Compilation of Current Practice in Analysis, Design, Construction, Test, and Operation, Vol. II, USAEC Report ORNL-NSIC-5, Oak Ridge National Laboratory, August 1965.

58. Personal communication from B. F. Langer, Westinghouse Research Laboratory.

59. G. R. Irwin and J. A. Kies, Critical Energy Rate Analysis of Fracture Strength, Welding J., 33: 193S–198S (April 1954).

60. R. E. Johnson, Fracture Mechanics: A Basis for Brittle Fracture Prevention, USAEC Report WAPD-TM-505, Westinghouse Electric Corporation, November 1965.

61. P. C. Rizzo, A Mechanical Model for Fracture Mechanics, Ph.D. thesis in Civil Engineering at Carnegie Institute of Technology, June 1966.

62. H. F. Bueckner, The Propagation of Cracks and the Energy of Elastic Deformation, Trans. of the ASME, 80: 1225–1230 (August 1958).

63. W. H. Irvine, A. Quirk, and E. Bevitt, Fast Fracture of Pressure Vessels: An Appraisal of Theoretical and Experimental Aspects and Application to Operational Safety, J. Brit. Nucl. Energy Soc., 3: 31–48 (January 1964).

64. G. R. Irwin, Crack-Extension Force for a Part-Through Crack in a Plate, Trans. ASME, J. Appl. Mech., Series E, 84(3): 651–654 (December 1962).

65. R. Weck, Brittle Fracture of a Thick Walled Pressure Vessel, Brit. Welding Res. Assoc. Bull., 7(6) (June 1966).

66. A. A. Wells, Application of Fracture Mechanics at and Beyond General Yielding, Brit. Welding J., 10: 563–570 (November 1963).

67. E. T. Wessel, Correlation of Laboratory Determinations of Fracture Toughness With the Performance of Large Steel Pressure Vessels, Welding J., 43: 415S–424S (September 1964).

68. L. F. Kooistra, E. A. Lange, and A. G. Pickett, Full-Size Pressure Vessel Testing and Its Application to Design, Trans. ASME, J. Eng. Power, 86(1): 419–428 (October 1964).

69. E. Bevitt, A. Cowan, and A. L. Stott, Failure Tests on Cylindrical Steel Vessels Containing Axial Faults, J. Brit. Nucl. Energy Soc., 3: 16–30 (January 1964).

70. J. P. Romualdi, The Effect of Loading Geometry on the Fracture Toughness of Biaxial Brittle Fracture Specimens, USAEC Report WAPD-TM-554, Carnegie Institute of Technology for Westinghouse Electric Corporation, April 1964.

71. J. A. Hendrickson, D. S. Wood, and D. S. Clark, Prediction of Transition Temperature in a Notched Bar Impact Test, Trans. ASM, 51: 629 (1959).

72. J. D. Lubahn, Correlation of Tests Using the Congruency Principle, Proc. ASTM, 58: 678 (1958).

73. J. D. Lubahn, A Review of Engineering Approaches to Brittle Fracture Design, Colorado School of Mines, 1961.

74. A. N. Grubin and U. I. Likachev, Analysis of Stresses Developing in the Stage of Large Plastic Deformations in Tension Tests of Cylindrical Specimens with Circular Notches, Zhurnal Technicheskay Fiziki, 25: 512 (1955).

75. P. S. Theocaris, Experimental Solution of Elastic-Plastic Plane-Stress Problems, Trans. ASME, J. Appl. Mech., Series E, 84(3): 735–743 (December 1962).

76. P. S. Theocaris and E. Marketos, Elastic-Plastic Strain and Stress Distribution in Notched Plates Under Plane Stress, J. Mech. Phys. Solids, II: 411–428 (1963).

77. P. S. Theocaris, The Effect of Plasticity on the Stress-Distribution of Thin Notched Plates in Tension, J. Franklin Institute, 279(1): 22–38 (January 1965).

78. J. G. Merkle, Calculation of Stresses From Total Measured Strains Beyond the Elastic Limit (to be published).

79. C. F. Tiffany and F. A. Pall, An Approach to the Prediction of Pressure Vessel Minimum Fatigue Life Based Upon Fracture Mechanics, Report D2-22437, The Boeing Company, March 1963.

80. W. S. Pellini, L. E. Steele, and J. R. Hawthorne, Analysis of Engineering and Basic Research Aspects of Neutron Embrittlement of Steels, Welding J., 41: 465S–467S (October 1962).

81. A. Quirk, T. C. Finnear, G. D. Fearnehough, and R. W. Nichols, An Experimental Study of the Failure Strength of Flawed Steel Plates, TRG Report 1086(C), December 1965 [see also Nuclear Engineering and Design, 4(1): 39–53 (May/June 1966)].

82. M. Grounes, Swedish Work on Brittle-Fracture Problems in Nuclear Reactor Pressure Vessels, Report AE-221, Aktiebolaget Atomenergi, Stockholm, Sweden, March 1966.

83. K. D. Ives, L. F. Kooistra, and J. T. Tucker, Equibiaxial Low-Cycle Fatigue Properties of Typical Pressure Vessel Steels, Trans. ASME, J. Basic Eng., Series D, 88(4): 745–754 (December 1966).

84. M. S. Wechsler and R. G. Berggren, Reactor Pressure-Vessel Materials, Nucl. Safety, 5(4): 342–345 (Summer 1964).

85. A. Cowan and R. W. Nichols, Assessment of Steels for Nuclear Reactor Pressure Vessels, Trans. ASME, J. Eng. Power, 86(1): 393–402 (October 1964).

86. R. G. Berggren, Fast Fracture Analysis of EGCR Pressure Vessel, USAEC Report ORNL-TM-1169, Oak Ridge National Laboratory, June 1965.

87. AEC Checks Reactor Vessels for Induced Brittleness, Nucleonics, 20(2): 70 (February 1962).

88. R. K. Penny, Symmetric Bending of the General Shell of Revolution by Finite Difference Methods, J. Mech. Eng. Sci., 3: 369–377 (1961).

89. R. E. Hubka, A Generalized Finite-Difference Solution of Axisymmetric Elastic Stress States in Thin Shells of Revolution, Report AFBMD-TN-61-43, Space Technology Laboratories, June 1961.

90. W. K. Sepetoski, C. E. Pearson, I. W. Dingwell, and A. W. Adkins, A Digital Computer Program for the General Axially Symmetric Thin Shell Problem, Trans. ASME, J. Appl. Mech., Series E, 84: 655–661 (1962).

91. P. P. Radkowski, R. M. Davis, and M. R. Bolduc, Numerical Analysis of Equations of Thin Shells of Revolution, ARS J., 32: 36–41 (1962).

92. J. A. Mirabal and D. G. Dight, SOR-II, A Program to Perform Stress Analysis of Shells of Revolution, USAEC Report KAPL-M-EC-19, Knolls Atomic Power Laboratory, June 1962.

93. P. E. Grafton and D. R. Strome, Analysis of Axisymmetrical Shells by the Direct Stiffness Method, AIAA J., 1: 2342–2347 (1963).

94. G. W. Smith, Analysis of Multiple Discontinuities in Shells of Revolution, General Dynamics/Astronautics Report 63-0044.

95. R. R. Meyer and M. B. Harmon, Conical Segment Method for Analyzing Open Crown Shells of Revolution for Edge Loading, AIAA J., 1: 886–891 (1963).

96. Z. Zudans, Computer Analysis of Axisymmetric Redundant Structures, The Franklin Institute, Philadelphia, Pennsylvania, April 1963.

97. P. E. Wilson and E. E. Spier, Numerical Analysis of Small Finite Axisymmetric Deformation of Thin Shells of Revolution, General Dynamics/Astronautics Report ERR-AN-153, June 1962.

98. B. Budiansky and P. P. Radkowski, Numerical Analysis of Unsymmetrical Bending of Shells of Revolution, AIAA J., 1: 1833–1842 (1963).

99. J. E. Goldberg and J. L. Bogdanoff, Static and Dynamic Analysis of Nonuniform Conical Shells Under Symmetrical and Unsymmetrical Conditions, pp. 219–238 in Proceedings of 6th Symposium on Ballistic Missile Technology, Academic Press, New York, 1961.

100. A. Kalnin, Analysis of Shells of Revolution Subjected to Symmetrical and Nonsymmetrical Loads, Trans. ASME, J. Appl. Mech., Series E, 86: 467–476 (1964).

101. C. M. Friedrich, Seal-Shell-2, A Computer Program for the Stress Analysis of a Thick Shell of Revolution With Axisymmetric Pressures, Temperatures, and Distributed Loads, USAEC Report WAPD-TM-398, Westinghouse Bettis Atomic Power Laboratory, August 1963.

102. D. A. Spera, Analysis of Elastic-Plastic Shells of Revolution Containing Discontinuities, AIAA J., 1: 2583–2589 (1963).

103. G. A. Thurston, A Numerical Solution of the Non-Linear Equations for Axisymmetric Bending of Shallow Spherical Shells, Trans. ASME, J. Appl. Mech., Series E, 86: 557–562 (1961).

104. P. E. Wilson and E. E. Spier, Numerical Analysis of Large Axisymmetric Deformations of Thin Spherical Shells, AIAA Preprint 61-440, AIAA Bull., 1: 271 (May 1964).

105. S. E. Moore and F. J. Witt, CERL-II — A Computer Program for Analyzing Hemisphere-Nozzle Shells of Revolution with Axisymmetric and Unsymmetric Loadings, USAEC Report ORNL-3817, Oak Ridge National Laboratory, October 1965.

106. F. J. Witt, R. C. Gwaltney, and S. E. Moore, pp. 184–185 in Gas-Cooled Reactor Program Semiannual Progress Report for Period Ending March 31, 1965, USAEC Report ORNL-3807, Oak Ridge National Laboratory, June 1965.

107. E. O. Waters, Stresses Near a Cylindrical Outlet in a Spherical Vessel, Welding Research Council Bulletin No. 96, May 1964.

108. H. Kraus, G. G. Bilodeau, and B. F. Langer, Stresses in Thin Walled Pressure Vessels With Ellipsoidal Heads, Trans. ASME, J. Eng. Ind., 83B: 29–42 (1961).

109. F. A. Leckie and R. K. Penny, (3) Stress Concentration Factors for the Stresses at Nozzle Intersections in Pressure Vessels, in A Critical Study of the Solution for the Asymmetric Bending of Spherical Shells, Welding Research Council Bulletin No. 90, January 1963.

110. F. J. Witt and B. L. Greenstreet, Analysis of Axisymmetrically Loaded Cylinder-to-Sphere Attachments, USAEC Report ORNL-3755, Oak Ridge National Laboratory, April 1965.

111. E. C. Rodabaugh, F. J. Witt, and R. L. Cloud, Phase Report No. 2 on Stresses at Nozzles in Spherical Shells Loaded With Pressure, Moment or Thrust (report to USAEC), July 15, 1966.

112. P. P. Bijlaard, Computation of the Stresses From Local Loads in Spherical Pressure Vessels or Pressure Vessel Heads, Welding Research Council Bulletin No. 34, March 1957.

113. P. P. Bijlaard, Local Stresses in Spherical Shells From Radial or Moment Loadings, Welding J., 36(5): 240S–243S (1957).

114. P. P. Bijlaard, Stresses in Spherical Vessels From Radial Loads Acting on a Pipe, Welding Research Council Bulletin No. 49, pp. 1–30, April 1959; Stresses in Spherical Vessels From External Moments Acting on a Pipe, Welding Research Council Bulletin No. 49, pp. 31–62, April 1959.

115. P. P. Bijlaard, Stresses in Spherical Vessels From Local Loads Transferred by a Pipe, Welding Research Council Bulletin No. 50, pp. 1–9, May 1959.

116. K. R. Wickman, J. L. Mershon, and A. G. Hopper, Local Stresses in Spherical and Cylindrical Shells Due to External Loadings, Welding Research Council Bulletin No. 107, August 1965.

117. D. R. Grieser et al., A Study of Rotary-Shaft-Sealing Concepts for Pressurized Water-Reactor Applications, Report BMI 1676, Battelle Memorial Institute, June 30, 1964.

118. F. J. Witt, R. C. Gwaltney, and B. L. Greenstreet, A Comparison of Theoretical and Experimental Stresses From Spherical Shells With a Single Radially Attached Nozzle, USAEC Report ORNL-TM-1634, Oak Ridge National Laboratory (to be published).

119. P. V. Marcal and C. E. Turner, Numerical Analysis of the Elastic-Plastic Behavior of Axisymmetrically Loaded Shells of Revolution, J. Mech. Eng. Sci., 5: 232–237 (1963).

120. R. L. Cloud and E. C. Rodabaugh, Proposed Reinforcement Design Procedure for Radial Nozzles in Spherical Shells With Internal Pressure. Phase 1. Report on Analysis of Data for Reinforced Openings to U.S. Atomic Energy Commission, Contract No. W-7405-eng-92, Battelle Memorial Institute, Columbus, Ohio.

121. R. L. Cloud, The Limit Pressure of Radial Nozzles in Spherical Shells, Nucl. Structural Eng., 1(4): 403–413 (1965).

122. F. Ellyin and A. N. Sherbourne, Limit Analysis of Axisymmetric Intersecting Shells of Revolution, Nucl. Structural Eng., 2(1): 86–91 (July 1965).

123. M. A. Salmon, Studies of Reactor Containment Structures, Report No. IITRI-578P22-11, IIT Research Institute, June 1966.

124. A. C. Eringen and E. S. Suhubi, Stress Distribution at Two Normally Intersecting Cylindrical Shells, Nucl. Structural Eng., 2(3): 253–270 (September 1965).

125. A. C. Eringen et al., Analysis of Stress and Deformation in Two Normally Intersecting Cylindrical Shells Subject to Internal Pressure, General Technology Corporation Technical Report No. 3-8, December 1965.

126. Reactor Primary Coolant System Rupture Study Quarterly Progress Report No. 6, July–September 1966, USAEC Report GEAP-5279, General Electric Company, November 1966.

127. Y. R. Rashid, Finite Element Analysis of Axisymmetric Composite Structures, USAEC Report GA-6303, General Atomic, June 4, 1965.

128. D. C. Cornell, SAFE-PCRS, A Computer Program for the Stress Analysis of Composite Bodies of Revolution, Input Instructions, USAEC Report GA-6588, General Atomic, Aug. 1, 1965.

129. D. C. Cornell, SAFE-AXISYM, A Computer Program for the Design of Composite Bodies of Revolution, Input Instructions, USAEC Report GA-6697, General Atomic, Oct. 15, 1967.

130. K. Foster, The Hillside Problem: Stresses in a Shallow Spherical Shell Due to External Loads on a Non-Radial Rigid Cylindrical Insert, Ph.D. thesis, Cornell University, September 1959.

131. A. Kornecki, The State of Stress and Strain in a Thin-Walled Tube Rigidly Fixed in an Oblique Cross Section (in Polish), Rozprawy Inżynierskie, 65: 117–134 (1957).

132. M. I. Estrin, Analysis of a Cylindrical Shell Clamped Along an Oblique Contour (in Russian), Izv. Akad. Nauk SSSR, Otd. Teckh. Nauk, 2: 151–155 (1959), Moscow.

133. A. van der Neut, Bending at the Oblique End Section of Cylindrical Shells, Proceedings of Symposium on the Theory of Thin Elastic Shells, edited by W. T. Koiter, pp. 247–269, North-Holland Publishing Co., Amsterdam, 1960.

134. A. E. Green and W. C. Emmerson, Stresses in a Pipe With a Discontinuous Bend, J. Mech. Phys. Solids, 9: 91–104 (1961).

135. M. V. V. Murthy, Stresses in a Mitred Pipe Joint Due to Internal Pressure or Pure Bending, Indian National Aeronautical Laboratory Technical Note No. TN-SA-4-63, Bangalore, 1963.

136. J. M. Corum, A Theoretical and Experimental Investigation of the Stresses in a Circular Cylindrical Shell With an Oblique Edge, Ph.D. thesis, Department of Theoretical and Applied Mechanics, University of Illinois, 1965.

137. J. M. Corum, A Theoretical and Experimental Investigation of the Stresses in a Circular Cylindrical Shell With an Oblique Edge, Nuc. Eng. Design, 3(2): 256–280 (February/March 1966).

138. J. B. Mahoney, V. L. Salerno, and M. A. Goldberg, Analysis of a Perforated Circular Plate Containing a Rectangular Array of Holes, Welding Research Council Bulletin No. 80, pp. 1–8, August 1962.

139. J. B. Mahoney and V. L. Salerno, Stress Analysis of a Circular Plate Containing a Rectangular Array of Holes; and Stress Distribution Around Periodically Spaced Holes in a Spherical Membrane Shell Under Uniform Internal Pressure, Welding Research Council Bulletin No. 106, July 1965.

140. J. L. Mershon, PVRC Research on Reinforcement of Openings in Pressure Vessels, Welding Research Council Bulletin No. 77, May 1962.

141. C. E. Taylor and N. C. Lind, Photoelastic Study of Stresses Near Openings in Pressure Vessels; M. M. Leven, Photoelastic Determination of the Stresses in Reinforced Openings in Pressure Vessels; J. L. Mershon, Preliminary Evaluation of PVRC Photoelastic Test Data on Reinforced Openings in Pressure Vessels, Welding Research Council Bulletin No. 113, April 1966.

142. J. W. Dally, An Experimental Investigation of the Stresses Produced in Spherical Vessels by External Loads Transferred by a Nozzle, Welding Research Council Bulletin No. 84, January 1963.

143. W. F. Riley, Experimental Determination of Stress Distributions in Thin-Walled Cylindrical and Spherical Pressure Vessels With Circular Nozzles, Welding Research Council Bulletin No. 108, pp. 1–11, September 1965.

144. R. L. Maxwell, R. W. Holland, and J. A. Cofer, Experimental Stress Analysis of the Attachment Region of Hemispherical Shells With Radially Attached Nozzles, Report ME-7-65-1, University of Tennessee Engineering Experiment Station, Knoxville, Tennessee, June 1965.

145. R. T. Rose et al., Stresses at Oblique Nozzles in Spherical Pressure Vessels, Parts I-V, Proceedings of Symposium on Pressure Vessel Research Towards Better Design, pp. 41–66, Institution of Mechanical Engineers, London, 1962.

146. R. Hiltscher and G. Florin, Die Spannungen an schiefen symmetrischen Rohrstutzen in kugelförmigen Druckkesseln, Konstruktion, 11: 444–449 (1963).

147. S. S. Gill, The Limit Pressure for a Flush Cylindrical Nozzle in a Spherical Pressure Vessel, Intern. J. Mech. Sci., 6: 105–115 (1964).

148. E. A. Lange, A. G. Pickett, and R. D. Wylie, Failure Analysis of PVRC Vessel No. 5; Part 1 — A Study of Materials Properties and Fracture Development, Welding Research Council Bulletin No. 98, August 1964.

149. A. G. Pickett and S. C. Grigory, Studies of the Fatigue Strength of Pressure Vessels: Technical Summary Report, Part I — Cyclic Pressure Tests of Full-Size Pressure Vessels, Report SWRI 1228-1-29, Southwest Research Institute, September 1966.

150. A. G. Pickett and S. C. Grigory, Studies of the Fatigue Strength of Pressure Vessels: Technical Summary Report, Part II — Predictions of the Low Cycle Fatigue Life and Terminal Failure Behavior of Pressure Vessels, Report SWRI 1228-1-36, Southwest Research Institute, February 1967.

151. W. S. Pellini and P. P. Puzak, Practical Considerations in Applying Laboratory Fracture Test Criteria to the Fracture-Safe Design of Pressure Vessels, Trans. ASME, J. Eng. Power, 86(1): 429–443 (October 1964).

152. W. S. Pellini and P. P. Puzak, Fracture Analysis Diagram Procedures for the Fracture-Safe Engineering Design of Steel Structures, Welding Research Council Bulletin No. 88, August 1963.

153. E. T. Wessel and L. E. Hays, Fracture Characteristics of Some High Strength, Weldable, Structural Steels, Welding J., 42: 512S–528S (November 1963).

154. W. H. Irvine, Fast Fracture in Reactor Pressure Vessels, British Report AHSB(S) R46, 1963.

155. R. W. Nichols, Prevention of Catastrophic Failure in Steel Pressure Circuit Components, Nucl. Eng., 11(120): 369–373 (May 1966).

156. G. Hake, A Note on the Fast Fracture of a Pressure Vessel, Canadian Report AECL-2432, May 1966.

157. J. M. Monahan and P. A. Halpine, PM-2A Reactor Vessel Test — Phase I, USAEC Report WAPD-TM-604, Westinghouse Electric Corporation, July 1966.

158. J. M. Monahan and T. J. Walker, PM-2A Reactor Vessel Test — Description of Testing and Failure Conditions, USAEC Report WAPD-TM-640, Westinghouse Electric Corporation, January 1967.

7. BASIC ASPECTS OF CRACK GROWTH AND FRACTURE*

7.1 DEFECTS AND FRACTURE CONTROL

Strength failures of load-bearing structures can be either of the yielding-dominant or of the fracture-dominant type. Defects are of importance in both types of failure, but those of primary importance to a fracture failure differ in an extreme way from those that influence resistance to plastic flow. For the latter, the significant defects (dislocation arrays, interstitial atoms, out-of-size substitutional atoms, grain-boundary spacings, bonded precipitate particles) are those that tend to warp and interrupt the crystalline lattice planes and thus interfere with easy glide of dislocations. The resistance to plastic deformation thus provided is essential to the strength of high-strength metals. Larger defects, such as inclusions, porosity, surface scratches, and small cracks, may influence the effective net section bearing the load but otherwise have no significant effect on resistance to plastic yielding.

In the case of failures of the fracture-dominant type (fracture prior to general yielding of the net section), the size scale of those defects of major significance depends on the toughness of the material. For the common structural steels, surface scratches, regardless of sharpness, do not lower the strength of a tensile specimen unless the testing temperature is far below the NDT temperature (small-flaw drop-weight nil-ductility transition temperature). The 1/4-in. brittle-weld-bead flaw used in NDT fracture testing and the notch depth used in Charpy V-notch fracture-appearance transition temperature (FATT) evaluations are indications of the major (directly significant) flaw size for steels in the NDT to FATT temperature range when a tensile stress equal to the dynamic yield stress is applied. Rapid crack propagation at smaller stresses or smaller loading speed would require cracks of larger size. The minor flaws that influence the fracturing process range downward toward smaller sizes. The

---

*This chapter was prepared by G. R. Irwin and J. M. Krafft of the Naval Research Laboratory, P. C. Paris of Lehigh University, and A. A. Wells of Queens University, Belfast, North Ireland.

minute flaws that control resistance to plastic flow are of interest to macroscopic fracture behavior primarily through the fact that resistance to plastic flow is related to crack toughness.

At temperatures near or above the NDT temperature, a structural component of interest for this report must contain at least one crack-like flaw of substantial size in order for fracture to occur prior to general yielding. The size necessary for crack propagation is a function of toughness and average tensile stress and can be estimated by the methods of fracture mechanics, as will be explained later in this chapter. Depending on the size and shape characteristics of a structural component and on its stress-environment history during service use, a critical condition for crack propagation may develop gradually in the following ways:

1. crack growth by fatigue,
2. crack growth by stress-corrosion (or hydrogen embrittlement),
3. reductions of crack toughness, for example by radiation damage.

It is unlikely that a crack large enough for propagation by a normal service load would be introduced during fabrication. In any case, the pressure vessels of interest will be pretested with pressures higher (by 25%, say) than the largest expected during service. Thus the attention of a fracture control plan can focus on achievement of a satisfactory time duration of fracture-safe operation relative to the three dangers stated above. These can occur in various combinations. The "safe life" depends on suitable limiting of these dangers in such ways as are possible.

Unfortunately, interest in studies of crack growth rate for fatigue and stress-corrosion conditions is comparatively recent, and data directly applicable to the materials and conditions of interest are quite limited. Some assurance can, however, be obtained if conservative estimates of stable growth added to the plausible initial crack sizes still leave situations well removed from rapid crack propagation. In addition the possibilities for stable cracks large enough to allow leakage through the vessel wall can be examined. In this way the principal elements of a fracture control plan can be illustrated and the kinds of information necessary for more accurate predictions can be understood.

Comments bearing on the anticipated kinds of initial defects and their possible sizes at the outset of service life of a vessel are presented next. The gross defects that can be identified both in hot-worked steels and in welded joints may be divided into geometrical forms that are one, two, and three dimensional. Examples of the first form are stringers of nonmetallic inclusions in rolled plate; the second form, laminar inclusions and cracks; and the third form, distributions of porosity. Planar defects and cracks are important because they may extend in area when the surrounding material is stressed in tension. Stringers and globular defects represent comparatively weaker stress concentrations. They are undesirable when present in clustered groups because these regions have a weakened resistance to the development and extension of a crack. A more serious consideration is the contribution of such segregations to weakness of solidification boundaries in a welded region. Defects of the volume type, that is, those in the nature of holes, do not represent a fracture-initiation hazard unless, in combination with other holes or inclusions, they assist the low-stress extension of a separation through a damaged region. Holes are readily detected by radiography if they present a nonmetallic path length exceeding 2% of metal thickness. Conversely, the detection of planar defects by radiography is difficult. A flat, open separation aligned with the radiation and giving a sharp linear indication on the radiographic film is rare. More often such defects are not flat and are not well-enough aligned with the radiation so that the film record permits recognition of the defect. Furthermore little confidence can be given to estimates of crack size from such radiographic indications as are seen. Chapter 9, Quality Assurance, discusses these matters in more detail and points out the increasing disadvantage to crack detection by radiography with increasing wall thickness.

Inspection methods that use ultrasonic waves are more sensitive than radiography in revealing cracks and have greater improvement potential for that purpose. It is recognized that present specifications for the pressure vessels of interest do not require advanced shear-wave-type ultrasonic inspections. However, the degree of fracture safety that will be required in future large-size boiling-water and pressurized-water reactor vessels suggests that development and systematic use of such methods

would be desirable. In the case of heavy rotating components for large steam turbine-generators, extensive ultrasonic inspection studies are conducted by the large producers. Thus ultrasonic inspection methods suitable for the specialized regions of most interest have been developed, are routinely used, and are essential to the fracture-control plan for large steam turbine-generators.[1,2]

Longitudinal-wave pulse-echo methods are currently used in the inspection of plates for lamination defects. However, the cracks such methods disclose are those that are nearly parallel to, rather than normal to, the largest expected tension in service. The seriousness of a crack left after inspection is roughly proportional to the short dimension of the crack area times the square of the tensile stress normal to the crack. A low-toughness condition of the region containing the crack contributes additionally to the chance of crack extension. Surface cracks are usually transverse and thus have a dangerous orientation relative to the expected tension. Magnetic-powder and dye-penetrant methods are used to find such cracks and are better for this purpose than radiography. However, a high degree of detection accuracy requires smooth surfaces devoid of the troughs and ridges commonly present on as-welded surfaces. In addition, only a crude indication of crack size, particularly of crack depth, is possible.

In simple concept it might be imagined that after all fabrication is complete and a successful hydrotest has been passed, meticulous direct inspection could be employed to guarantee absence of any significantly dangerous crack. The effect of the heating cycles and hydrotest would be to open any overlooked cracks and make them more easily seen in inspection. However, many parts of the vessel are much easier to inspect in detail at an intermediate stage of assembly and cladding (see Chap. 9, Quality Assurance). For this reason considerable reliance is placed on intermediate inspections. This means that the fabrication process must be trustworthy with regard to avoidance of cracking in already inspected parts.

A major contribution to the control of crack-like flaws in nuclear pressure vessels is obtained through the general practice of using clean vacuum-degassed steel for shell and forging stock. Thus hydrogen in the

steel is restricted to the transient concentrations that may result if some hydrogen is introduced during welding. The stirring action of the degassing treatment tends to restrict impurity segregation, and amounts of impurity are reduced by the reduced dependency on chemical action for deoxidation (see Chap. 4, Materials). At the same time the amounts of sulphur and phosphorus allowed in the final composition are relatively small. The advantages thus achieved in terms of freedom from hydrogen-induced slow crack extension and by reduced segregation at solidification boundaries during welding are an essential part of the program for minimizing the presence and danger of crack-like flaws in the final pressure vessel.

In view of the fabrication care and intermediate inspections pertaining to steel used for shell and nozzles (as discussed in Chaps. 4 and 9), the greatest chance for prior crack-like defects of transverse orientation and significant size is in the welded regions. Some concern must be reserved for regions away from the welds that are subjected to tension during straightening and for unexpected damage, such as arc-strikes from poor control of prods used for magnetic-particle inspection and cracks under handling tabs.

The welding methods anticipated are mainly electroslag welding and submerged-arc welding. From past experience both methods have produced crack-like defects. The causes are thermal stress, residual stress, coarse dendritic solidification, and impurities in various combinations. Cracks along the borders of a submerged-arc weld have sometimes occurred, particularly when the top surface of the weld bead was permitted to join the base metal with a relatively sharp angle. Cracks of this nature of substantial size can remain undetected unless the weld border is ground to a smooth contour. Since these cracks are open to the surface and are in a region of obvious suspicion, only very small cracks of this kind should escape notice. Cracks may be introduced during the process of overlaying the internal surface of the pressure vessel with a stainless steel coating. Since a residual tensile stress is probable in and near the solidified layer, some cracks might form through this layer after a time delay, with such crack formation being assisted by any hydrogen

introduced during the overlaying process or by stress-corrosion extension of small prior cracks.

Crack-like defects produced internally within a large solidifying segment of welding represent a special danger. Impurities such as sulphur and phosphorus tend to segregate on the solidification boundaries. In multiple-pass welding of the TIG (tungsten, inert-gas) type, the solidification structure is often on a relatively fine scale. This lessens the impurity segregation. Furthermore, some homogenization and grain refinement are introduced by the temperature cycle from subsequent adjacent weld beads. In the case of the submerged-arc welding process, fewer passes and larger masses of solidifying metal are customary, and hence there is greater danger that weak solidification boundaries may be formed. Such defects may not be pulled open until subjected to a tensile stress. Even when pulled open, they are difficult to recognize in radiographic inspection. When solidification defects of this kind present an opening to the surface, the defect size may be much larger than the size suggested by the irregular elements of separation visible at the surface.

In the case of electroslag welding the solidification pattern is gross; that is, it is much larger than for multiple-pass submerged-arc welding. A subsequent quench-and-temper treatment is used to refine the grain size and improve the properties. Despite the coarse-grained nature of the electroslag weldment, considerable success has been achieved with this method (see Chap. 8, Fabrication). Nevertheless undesirable amounts of center-line weakness, where impurity segregation is most serious, have sometimes occurred. It may be correct to assume that significant degrees of center-line weakness can be eliminated by careful control of the electroslag welding process and of the impurity level. However, the term "significant degree" is not yet clear, and studies of how to recognize intolerable amounts of this defective condition by inspection are needed.

When a welded region is subjected to a heat treatment after welding, experience has indicated that more defects are disclosed by nondestructive inspection after the heat treatment than before, and thus postheat-treatment inspection would be advantageous to establish final quality in the case of the pressure vessels of interest here. The inspection advantages provided by some opening of defects during heat treatment are additionally

enhanced by the stress applied during internal pressure testing prior to service. An increased detection sensitivity for flaws of the weak solidification-boundary type is needed. Repetition of certain inspections after hydrotesting, with the assistance of ultrasonic techniques, therefore deserves careful study.

The transverse crack-like defects previously discussed were primarily those oriented to favor crack extension parallel to the line of welding, either at the weld border or within the weld. Cracks may also be formed in the heat-affected zone normal to the direction of welding, particularly when the preheating and postheating are inadequate. Cracks of this type that have extended through the zone of residual stress and have been arrested are often observed where two stiff members of steel are joined by a line of tack welding. Cracks of this general class have caused fracture failures in numerous field-welded structures. The danger of such a crack is increased first by the fact that once instability by stable growth or stress elevation is achieved, the crack extends immediately through and beyond the region of residual tensile stress bordering the weld. A second enhancement of danger results from the moving nature of the crack, which means that crack arrest is resisted only by the minimum dynamic crack toughness of the steel.

Development of prior cracks of the type discussed above is essentially eliminated in thick-walled boiling-water and pressurized-water reactor pressure vessels because of the slow heating and cooling rates and the postwelding stress relief. However, the fabrication plan may require making a girth weld across a previously completed longitudinal seam weld. In this case small welding defects in the seam weld may be opened. The danger of such new cracks would be increased by any residual tensile stress parallel to the girth weld that remained after the girth welding operation.

A large number of fracture-failure examination records resulted from the hydrotest failures of high-strength-steel solid-propellant rocket chambers. Several comments based on these records may be of interest here.[3] Initially, attachment of small brackets needed to support test equipment or guidance mechanisms was attempted by tack welding. It was not feasible either to reliably detect cracks produced by the welding

beneath the bracket or to avoid making such cracks. Prior to adoption of different joining methods (brazing, for example), a significant fraction of the hydrotest fractures initiated beneath such small tack-welded attachments. Repair welding of the rocket chamber might seem an unrelated cause for fractures. However, in both cases, the tack welding of the attachment and the repair welding of the rocket chamber, a welding operation was contemplated on a component already fabricated to the desired size and shape. Apprehension over possible alteration of dimensions furnished an incentive toward preheating and postheating treatments subsequently proved to be inadequate. As a result many of the fractures that originated in a longitudinal seam weld started in a region of repair welding.

Full cooperation in the development of improved inspection for cracks in steel rocket chambers was initially difficult to obtain. Presumably, a "zero-defects" rating was wanted, and the fabricator preferred an inspection system that detected only the flaws of "significant" size. In the case of the Polaris and Minuteman rocket chambers, wall thicknesses were generally less than 0.2 in. Flush grinding of the seam and girth welds plus careful radiography sufficed to furnish the sensitivity needed so that cracks of insignificant size could often be observed in those regions and could be seen clearly enough to permit sensible decisions with regard to need for repair welding.

In the case of boiling-water and pressurized-water reactor pressure vessels, it is desirable not only to detect cracks of marginal size relative to significance, but also to "see" these cracks well enough, say with ultrasonic shear waves, to obtain estimates of their dimensions. Inspection procedures have not, so far, attempted to do this in a systematic way, and considerable additional study is certainly required. Meanwhile estimates of the sizes of unseen cracks allowed by present fabrication and inspection methods will be difficult to fix. The estimates depend on confidence in the fabrication controls, as well as on confidence in the direct inspections. For example, there is evidence that surface cracks about 0.5 in. long and 0.2 in. deep might be overlooked by present inspection methods, even with the advantage of smoothly ground surfaces (see Ref. 15 of Chap. 9). Whether or not cracks of 0.5-in. depth

are discovered with negligible error might be questionable. However, in regions where cladding is applied to shell or nozzle base metal, such a choice of maximum crack depth seems reasonable, simply because of the small thickness of the added metal and the considerable experience and machine control now available for cladding nuclear pressure vessels. A larger estimate of maximum prior crack size, say 3/4 in., might be best for surface regions of welds.

Transverse cracks of substantially larger sizes than those suggested above are less significant if located near the midpoint of wall thickness, for three reasons: (1) exposure of a crack to a free surface essentially doubles its effective size relative to stress elevation near the leading edge, (2) the midthickness crack does not feel stress elevations due to superimposed bending, and (3) stable extension of the midthickness crack cannot be assisted by contact with the water inside the vessel or with the water vapor outside.

The most reliable indicator of the kinds of defects likely to cause serious fracturing of thick-walled boiling-water and pressurized-water reactor pressure vessels would be extensive experience with internal pressure testing of vessels of similar wall thickness, geometry, materials, and fabrication methods. Such a test program would not, however, settle all doubts. For a number of reasons, such as differences of design, size, location, and construction date, each large nuclear reactor pressure vessel will possess certain fabrication problems individual to that particular vessel. Unquestionably continued accumulations of experience will be quite helpful, but a requirement for nearly absolute fracture safety suggests that experience should be assisted by a very conservative fracture control plan. Such a plan must assume that any crack-like defect that is plausible and which has not been proved absent by inspection may actually exist in the vessel. The plan must then establish methods of estimating fracture-safe life based on stable crack-growth data, service environment, and service stress cycles. An additional degree of confidence can be predicted if the toughness and stress level at the end of the safe life correspond to a leak-before-break condition.[4] A complete specification of such a fracture control plan requires a more detailed understanding of progressive fracturing than currently exists.

However, present fracture mechanics technology provides general features of the control plan and a number of answers that are of interest. Subsequent sections of this chapter discuss current knowledge of progressive crack extension, largely in terms of fracture mechanics, and illustrate application of this information to the planning of fracture control.

Throughout this chapter many formulas involving extended usage of symbols are presented to illustrate the development of fracture mechanics. The following nomenclature listing provides definitions for the symbols not otherwise presented in the text:

a	Defect size, generally half-length, in.
a_i	Initial crack size, in.
a_c	Final or critical crack size, in.
a_0	Crack length correction for double cantilever specimen, in.
$\dot{a}$	Crack speed, μin./sec
b	Crack semimajor axis, in.
b_0	Size of strip-yield plastic zone, in.
B	Plate thickness, in.
B_n	Specimen thickness at crack plane, in.
B_0	Specimen thickness, in.
C_0	Compliance, in./lb
C, C_1, C_2, C_3	Constant relating crack growth to stress-intensity range and crack size
C_4	Constant
C'	Constant relating crack growth to stress range and crack size
C''	Constant relating cyclic life for moderately high-cycle fatigue to stress range and initial and final stress intensity
C'''	Constant relating cyclic life for moderately low-cycle fatigue to stress range and initial and final stress intensity
c_2	Elastic shear-wave speed, ft/sec
da	Increment of crack extension
d_n	Net ligament size, in.
d_0	Original ligament depth, in.

d_T	Length factor, spacing of fine-scale elements of separation
$\frac{da}{dN}$	Rate of crack growth, μin. per loading cycle
E	Uniaxial tensile (Young's) modulus, psi
F	Force, lb
$\mathcal{G}$	Strain-energy release rate, in.-lb/in.^{2}
$\mathcal{G}_1$	Plasticity adjusted value of $\mathcal{G}$, in.-lb/in.^{2}
$\mathcal{G}_I$	Strain-energy release rate for opening mode of crack surface displacement, in.-lb/in.^{2}
$\mathcal{G}_c$	Critical strain-energy release rate, in.-lb/in.^{2}
$\mathcal{G}_{Ic}$	Critical strain-energy release rate for opening mode of crack surface displacement, in.-lb/in.^{2}
H_1	Function relating N_F to P, a_i, and a_c
H_2	Function relating N_F to P, K_i, and K_c
H_3	Function relating crack growth to stress intensity
h	Beam depth, in.
$i\gamma_{xz}$	Imaginary component of shearing strain expressed as complex number
K	Stress-intensity factor, ksi·in.$^{1/2}$
K_c	Final or critical stress-intensity factor, ksi·in.$^{1/2}$
K_i	Initial stress-intensity factor, ksi·in.$^{1/2}$
K_M	Stress-intensity factor for relative mean load P_M, ksi·in.$^{1/2}$
K_{th}	Theoretical geometry-dependent stress-concentration factor (function of P)
K_I	Stress-intensity factor for opening mode of crack surface displacement (tensile), ksi·in.$^{1/2}$
K_{II}	Stress-intensity factor for forward shear mode of crack surface displacement, ksi·in.$^{1/2}$
K_{III}	Stress-intensity factor for parallel shear mode of crack surface displacement, ksi·in.$^{1/2}$
K_{Ic}	Critical stress-intensity factor for opening mode of crack surface displacement, ksi·in.$^{1/2}$
K_{Id}	Stress-intensity factor corresponding to minimum fracture toughness for dynamic loading, ksi·in.$^{1/2}$
K_{ISCC}	Critical stress-intensity factor associated with stress-corrosion cracking, ksi·in.$^{1/2}$
$\dot{K}$	Stress-intensity rate, ksi·in.$^{1/2}$/sec
l	Total load displacement, in.

Mode I	Opening mode of crack surface displacement
Mode II	Forward shear mode of crack surface displacement
Mode III	Parallel shear mode of crack surface displacement
m	Flaw distribution exponent
N_F	Cyclic life, cycles to failure
n	Strain-hardening exponent
P	Applied load, lb
P_M	Relative mean load, lb
P_p	Proof load, lb
p	Internal pressure, psi
q	Constant
R	Radial position at the elastic-plastic boundary measured from the apparent crack leading edge, in.
R_0	Radial position at the elastic-plastic boundary measured from the apparent crack leading edge in the plane of the crack, in.
r	Radial position coordinate measured from the crack leading edge, in.
r_1	Radial position coordinate for plastic zone measured from the apparent crack leading edge, in.
r_Y	Plasticity adjustment factor
S	Limiting strength associated with a defect
S_{MIN}	Minimum limiting strength associated with worst defect
T	Temperature, °F
T'	Temperature following load rise time, °F
T_1	Temperature associated with allowable load criterion, °F
t	Time, sec
t_A	Time required for temperature equalization across a distance x, sec
U_W	Energy from weld residual stress field, in.-lb
U_L	Energy from superimposed stress, in.-lb
v	y-direction displacement, in.
W	Width of strip, in.
x	Coordinate direction
x_0	Dimensionless ratio; $x_0 = (a + a_0)/h$
x_1	x coordinate distance determined by θ_1 and r_1

x_2	Distance in x direction, in.
X	Service time, hr
X_L	Service time associated with S_{MIN}, hr
y	Coordinate direction
y_1	Dimensionless ratio σ/σ_{YS} or σ_{LB}/σ_{YD}
z	Coordinate direction
α_0	Plastic-zone size parameter
α	Thermal diffusion coefficient, in.^{2}/sec
β_c	Dimensionless ratio relating plastic zone size to plate thickness
β_{Ic}	The value of β_c computed by using K_{Ic} in place of K_c
γ	Shear strain, in./in.
$\vec{\gamma}$	Shear strain in vector form
γ_1	Dimensionless ratio stress-intensity factor
δ	Crack-opening displacement or dislocation, in.
δ_c	Critical opening dislocation, in.
$\Delta\epsilon$	Strain range, in./in.
ΔK	Stress-intensity factor range, ksi·in.$^{1/2}$
ΔP	Load range, lb
$\Delta\sigma$	Stress range, psi
ϵ_1	Critical average strain for plastic instability, in./in.
ϵ_{TS}	True strain, in./in.
$\bar{\epsilon}$	Mean strain, in./in.
$\dot{\epsilon}$	Strain rate, in./in.·sec
θ	Angular position coordinate measured from the crack leading edge, radians
θ_1	Angular position coordinate for plastic zone measured from the apparent crack leading edge, radians
μ	Shear modulus of elasticity, psi
ν	Poisson's ratio
ρ	Crack root radius, in.
σ	Nominal stress on the crack plane, psi
σ_N	Nominal stress on a given cross section, psi
σ_0	Stress constant in strain-hardening relationship

σ_x	Tensile stress component parallel to the plane of a crack in the x-coordinate direction, psi
σ_y	Tensile stress component normal to the plane of a crack in the y-coordinate direction, psi
σ_z	Tensile stress component parallel to the crack leading edge in the z-coordinate direction, psi
σ_Y	Critical yield-stress value, psi
σ_{LB}	Leak-before-break tension stress, psi
σ_{TS}	True stress, psi
σ_{Yd}	Dynamic yield stress, psi
σ_{YS}	Uniaxial tensile yield stress, psi
$\bar{\sigma}$	Standard deviation
τ	Shearing stress, psi
τ_{xy}	Shearing stress in the y direction on a plane perpendicular to x; equal to τ_{yx}, psi
τ_{yz}	Shearing stress in the z direction on a plane perpendicular to y; equal to τ_{zy}, psi
τ_Y	Shearing stress in y-coordinate direction
Φ_0	Elliptic integral function

7.2 LINEAR ELASTIC MODELING OF CRACKS

7.2.1 Progressive Crack Extension

The nature of the fracture behavior for which a suitable analysis is needed is termed progressive crack extension. A brief description of this is given below.

The distribution of a tensile load across a region containing a crack (normal to the tension) results in elevated tension adjacent to the perimeter or leading edge of the crack. The tension at the leading edge is somewhat relaxed by local plastic strains. This local change in the stress distribution eliminates the linear analysis stress infinity but causes very large strains adjacent to leading elements of the opened crack. The combination of local plastic strains, advance separations, elastic constraint, and tension near the leading edge may be sufficient or less than sufficient to cause sudden rapid spreading of the crack.

If less than sufficient, plastic strain reversals in the material near the leading edge may occur, with the aid of repeated changes of stress during service, and cause stable forward growth of the crack by fatigue. In addition, the environment, with or without fatigue assistance, may cause stable spreading of the crack by stress-corrosion cracking. Liquid water or water vapor suffices for this purpose in the case of many structural metals. Hydrogen in the steel also assists slow, stable extension of a crack subjected to tensile stress. When a structural member containing such a crack is in general tension, as for the wall of a vessel containing internal pressure, extension of the crack area results in larger stress elevation near the leading edge and hastens the pace of stable growth. The onset of rapid crack extension provides a relatively abrupt endpoint for the stable growth period. To appreciate how this can happen at a nominal tensile stress well below the yield strength it is best to focus attention on the leading-edge stress elevation associated with a crack, rather than on brittleness per se, because large local plastic strains occur as an essential part of progressive crack extension in the customary structural metals, even when their behavior is somewhat brittle.

Studies of running cracks have been conducted by using a variety of techniques to measure crack speed and the stresses near the crack. Such studies are more easily done with glass and brittle plastics. However, for a brittle crack traversing a plate of steel, Wells[5] observed the temperature rise parallel to the path of the crack. From these observations the separation region was found to be acting as a heat source with a strength increasing with crack length. Edge-notched plates were used, as in later work by Wells and Post[6] in which the rate of strain-energy release was calculated from photoelastic observations and was proportional to crack length. At the time of Wells' thermal observations the evolved thermal energy seemed somewhat higher than the stress-field energy release, but this was not regarded as significant in view of experimental uncertainties. Currently available stress analysis information applied to the experiment would increase the estimate of rate of strain-energy release and would reduce the moderate difference of this estimate from the observed rate of thermal energy production.

In terms of the old modified Griffith theory,[7,8] the condition critical for onset of rapid fracture was a point of stable balance between stress-field energy-release rate and rate of plastic work near the crack, which was to be followed by a regime of unstable rapid crack propagation. However, study of the implications from Wells' thermal measurements suggested, quite oppositely, that the point of onset of rapid fracture was an abrupt instability point followed by a stable regime in which work rate and loss of stress-field energy were balanced through a considerable range of crack speeds. Indeed the instability point could be preceded by a slow regime of crack extension in which the crack-extension process was also stable. From these facts it was not clear that writing an equality between rate of strain-energy release and plastic work rate would be helpful as a means for understanding sudden onset of fast crack extension.

The preceding conclusions have been verified by numerous subsequent observations of running-crack behavior. The latest results of this kind are discussed in a recent paper by Clark and Irwin.[9] During the mid 1950's, the effect was to shift the emphasis of fracture mechanics toward characterization of the onset of fast progressive fracturing as the primary task. In the modified Griffith theory, this characterization of onset of fast progressive fracturing was linked unnecessarily with an energy balance relationship that was uncertain both in terms of usefulness and validity at the measurement point. The dubious validity aspect is discussed by McClintock and Irwin,[10] who use calculations of a plasticity model for illustration.

Progressive crack-extension behavior ranges from several kinds of slow, stable extension through the fast, stable regime. At very high crack speeds a limiting velocity is observed that is followed by crack division tendencies when the tensile driving force is still further increased. A single service fracture failure may exhibit all these crack-extension behaviors. In order to understand and prevent such fractures, appropriate use of experimental data from laboratory testing is essential. The characterization plan should permit application of laboratory fracture-testing data to service components in the simplest adequate way. Linear-elastic-fracture mechanics provides an appropriate and simple

characterization method applicable to any component in which we have a reasonable idea of the stress distribution. With some care with regard to interpretation, the linear analysis method retains usefulness as the stress level approaches a general yielding condition. The method is not suitable for use at higher stresses.

7.2.2 Linear-Crack Stress-Field Analysis

For purposes of linear stress analysis, a crack is regarded as a flat separation bounded within the material by a leading edge that is approximated as a simple curve. For example, if a sharp groove of small length is cut into one face of a metal plate and subjected to fatigue stressing, a leading-edge contour resembling half an ellipse is produced. At a relatively small tensile stress across the cracked region, plastic strains are confined to a small zone, as shown schematically by the shaded area in Fig. 7.1. The plane of Fig. 7.1 is normal both to the crack and to its leading edge and represents only a small segment of the leading

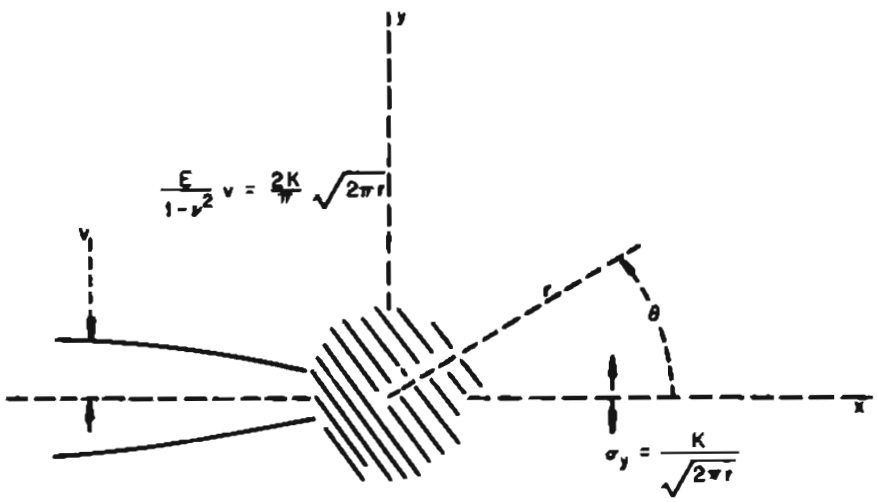

$\mathcal{G} = \left(\frac{1}{E}\right) K^2$, PLANE STRESS

$\mathcal{G} = \left(\frac{1-\nu^2}{E}\right) K^2$, PLANE STRAIN

Fig. 7.1. Schematic Diagram of the Leading Edge of a Crack.

edge. Following the practice customary for stress analysis near a crystalline dislocation line, the region containing plastic strains is regarded as a line-disturbance zone. The natural locus for the leading edge of the linear-analysis-model crack is a central position within the plastic zone rather than the left side of this zone where the leading separational elements are situated. This aspect is considered later. At this point of the discussion, since the plastic zone is assumed to be very small relative to crack size, the above difference of crack border location for analysis purposes is not important.

For the region of the tensile crack shown in Fig. 7.1 (close to the leading edge), the stress distribution is two-dimensional and, from linear analysis, the stresses are

$$\sigma_y = \frac{K}{\sqrt{2\pi r}} \cos\frac{\theta}{2}\left(1 + \sin\frac{\theta}{2}\sin\frac{3\theta}{2}\right),$$

$$\sigma_x = \frac{K}{\sqrt{2\pi r}} \cos\frac{\theta}{2}\left(1 - \sin\frac{\theta}{2}\sin\frac{3\theta}{2}\right), \qquad (1)$$

$$\tau_{xy} = \frac{K}{\sqrt{2\pi r}} \sin\frac{\theta}{2}\cos\frac{\theta}{2}\cos\frac{3\theta}{2},$$

and

$$\sigma_z = \nu(\sigma_y + \sigma_x)(\text{plane strain}), \qquad (2)$$

where the coordinates are as shown in Fig. 7.1 and ν is Poisson's ratio.

The y-direction displacements, v, at the crack plane, from which crack-opening size would be estimated, are given by

$$Ev = \frac{2K}{\pi}(1 - \nu^2)\sqrt{2\pi r}, \qquad (3)$$

where E is Young's modulus. From Eqs. (1) and (3), computation of the work done in an increment of crack closure shows that the Griffith-theory strain-energy release rate, $\mathcal{G}$, is proportional in a simple way to K^2.

The terms on the right sides of the above equations are the leading terms of the linear stress analysis solution, which would be completed by adding terms proportional to higher powers of the ratio r/a (where a

is a length factor indicative of crack size). In the limit of small enough values of r/a, the terms show dominate and form a leading-edge stress system that is characteristic of Mode I (tensile) cracks. The parameter K is proportional to the applied tensile load and is a function of the crack and specimen size and shape factors. The stress-intensity factor K, termed K_I for the opening (tensile) mode of crack surface displacements, provides a simple one-parameter characterization of the stresses tending to cause crack extension. Use of the $\mathcal{G}_I$ value corresponding to K_I, for characterization purposes, is optional and equivalent. A well-known example of characterization is the determination of the critical value, K_{Ic}, for onset of fast crack extension.

A general mathematical treatment would refer to Mode II (forward-shear) and Mode III (parallel-shear) stress equations in order to represent stresses developed by application of shears parallel to the crack plane. This complexity is unnecessary here, since the primary concern is with tensile cracking in which the stresses τ_{xy} and τ_{zy} on the plane of expected crack extension (ahead of the leading edge) are zero. An article by Paris and Sih[11] provides a comprehensive summary of linear-crack stress-field analysis.

The tensile-crack stress field near the leading edge of a crack is regarded as either of the plane-strain or of the plane-stress type. The plane-strain model is three dimensional in the sense that the stress conditions must be uniform in the z direction across a leading edge region that is large compared with the size of the zone containing plastic strains. The plastic zone is then held within a plane-strain stress system with its size somewhat reduced by elastic constraint. Of course, if the crack is what is termed a "through-crack," with leading edges right through the plate thickness, even if the plastic zone is small a plane-strain condition near the free surfaces is not possible. Customarily the linear analysis applied to crack problems of this kind is the one termed the generalized plane stress in which $\sigma_z = 0$ is assumed. In this case Eqs. (1) remain applicable with the stresses interpreted as averages through the plate thickness. Such a model is two-dimensional, since the z-direction dimension plays no role in the analysis. The effect of assuming $\sigma_z = 0$, instead of Eq. (2), is to eliminate the factor $(1 - \nu^2)$

from Eq. (3). The two-dimensional plane-stress situation permits larger shear stresses and thus a larger plastic zone size than would occur for plane-strain with the same stresses in the x,y plane. The relation of this to the brittle-ductile change in fracture toughness is discussed at a later point.

From Eqs. (1), K is the limiting value on $\theta = 0$ of the product $\sigma_y\sqrt{2\pi r}$ as r approaches zero. Given any valid stress analysis solution for σ_y, even though it is not expressed in the r/a power series form, the preceding limiting process may be used to obtain the value of K. In fact, if a small-flank angle notch of root radius ρ is subjected to the nominal stress σ_N, and if the stress-concentration factor K_{th} is available as a function of ρ,

$$K = \lim_{\rho \to 0} \frac{1}{2} \sigma_N K_{th} \sqrt{\pi\rho} \ . \tag{4}$$

In the calculation of K_{Ic} from tensile fractures of circumferentially notched round bars, Eq. (4), along with published stress-concentration factors pertaining to that geometrical shape, furnished the first approximate answers. This procedure is reviewed by Paris and Sih.[11]

The same basic analytical rules apply to determinations of K for a laboratory specimen with a crack of controlled size and shape inserted for testing as are used to determine K for a crack in a service component. However, for the most used types of laboratory specimens, the analytical accuracy has been improved by considerable numerical work. In the case of cracks in service components the estimates used are usually of the "engineering-approximation" type based on one or more of the crack stress-field results discussed next.

For an infinite plate subjected to an in-plane uniform stress σ perpendicular to a through-the-thickness crack of length 2a,

$$K = \sigma\sqrt{\pi a} \ . \tag{5}$$

Cutting this configuration in half results in a through-crack of length a into the edge of a semiinfinite plate with the stress, σ, parallel to

the edge, where

$$K = 1.13\ \sigma\sqrt{\pi a}\ . \tag{6}$$

The 1.13 factor may be regarded as the correction factor for increased crack opening due to the free surface.

For a strip of width W with a central crack of length 2a perpendicular to a longitudinally applied stress, σ, approximate values of K can be obtained from

$$K = \sigma\left(\pi a \sec\frac{\pi a}{W}\right)^{1/2}\ , \tag{7}$$

where a is 0.9W or less.

Returning to the idea of calculating K as a limit, the addition of any uniform tension or compression to a crack stress-field solution would not change the value of K, because this would not change the limit of the product $\sigma_y\sqrt{2\pi r}$ as r approaches zero. Thus if a uniform compressive stress numerically equal to σ is superimposed on the problem of Eq. (5), the K value is not changed. However, the stress σ at infinity is thereby cancelled, and a uniform pressure numerically equal to σ is placed on the crack surfaces. In this way it can be seen that Eq. (5), with σ replaced by p, provides the answer to the problem of a two-dimensional crack of length 2a opened by an internal pressure p. If both σ (at infinity) and p (on the crack surfaces) act at the same time, the K value is obtained by substituting $\sigma + p$ for σ in Eq. (5). Similar comments pertain to the influence of internal pressure, say from hydrogen, in connection with the three-dimensional problems discussed next.

For a circular (penny-shaped) crack of radius a imbedded in an infinite three-dimensional body with uniform stress σ applied perpendicular to the crack,

$$K = \frac{2}{\pi}\ \sigma\sqrt{\pi a}\ . \tag{8}$$

This is really a special case of a similarly oriented elliptical crack of semiminor axis a and semimajor axis b. At the semiminor axis, where

K is largest,

$$K = \frac{\sigma\sqrt{\pi a}}{\Phi_0} \tag{9}$$

and

$$\Phi_0 = \int_0^{\pi/2} \left(1 - \frac{b^2 - a^2}{b^2} \sin^2 \theta \, d\theta\right)^{1/2} ,$$

where Φ_0 is recognized as the complete elliptic integral function whose values are

a/b	Φ_0	a/b	Φ_0
0	1.0	0.6	1.277
0.1	1.016	0.7	1.345
0.2	1.051	0.8	1.418
0.3	1.097	0.9	1.493
0.4	1.151	1	$\pi/2$
0.5	1.211		

For the extreme values of a/b, Eq. (9) leads to Eq. (5) or to Eq. (8), as would be necessary. Thus Φ_0 can be regarded as a correction factor for the elliptical nature of the crack shape.

Influences on the K value of proximity to a free surface and changes of crack shape can often be approximated in a simple way with good enough accuracy for practical applications. Equation (6) is known to be the free-surface modification of Eq. (5) from numerical calculations. Equation (7) is simply an approximate empirical representation of the results from numerical calculations for a central two-dimensional crack in a finite-width plate. Comparisons to accurate numerical results, when these became available, showed Eq. (7) to be preferable to a tangent-function representation previously used.

Often the shape of a surface crack suggests representation of the crack as half of an ellipse, with the long principal dimension at the surface of the plate. The analysis problem is a difficult three-dimensional calculation, and exact numerical results are not available. However, from comparisons of test results, the controlling K value for this problem can be estimated with the equation

$$K = \frac{1.12\ \sigma\sqrt{\pi a}}{\Phi_0} . \tag{9a}$$

The factor 1.12 was guessed from comparison with the problems represented by Eqs. (5) and (6) at a time when the third figure of the coefficient in Eq. (6) was not well determined.[12] Careful measurements of K_{Ic} for semielliptical cracks and Eq. (9) have agreed well with K_{Ic} values from other methods so long as the value of a was not more than half the plate thickness.[13]

7.2.3 Experimental Fracture Mechanics Analysis

In view of the inherent difficulty of some three-dimensional-crack stress-field problems, experimental methods of determining K are briefly reviewed below. The first of these employs compliance measurements and leads directly to values of $\mathcal{G}$ rather than K. For tensile cracks the relationships connecting $\mathcal{G}$ and K are

$$\mathcal{G} = \frac{K^2}{E}(1 - \nu^2) \text{ (plane strain)} \tag{10}$$

and

$$\mathcal{G} = \frac{K^2}{E} \text{ (plane stress)} . \tag{11}$$

Figure 7.2 shows a single-edge-notched plate specimen sometimes used for crack-toughness measurements. This is a through-crack problem for which a generalized plane-stress analysis viewpoint is natural. The experiment consists in repeated measurements of specimen compliance with the crack-notch depth into the specimen fixed at a series of values, say from 0.1W to 0.7W, where W is the specimen width. If P is the applied load and l is the total load displacement (between the two loading points), the compliance, C_0, is given by

$$C_0 = \frac{l}{P} . \tag{12}$$

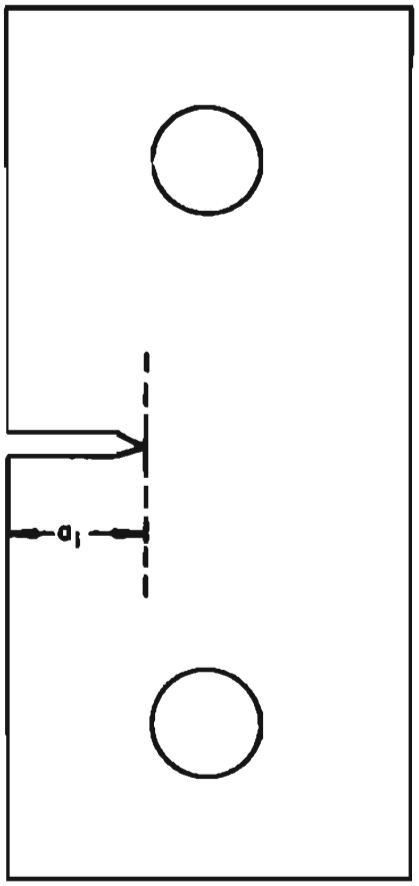

Fig. 7.2. Single-Edge-Notched Specimen.

In a graph of P as a function of l for a series of increasing crack depths a, each load-unload line would have a slope $1/C_0$, which would be a decreasing function of the depth a. Simple analysis of the strain energy lost from the specimen in a small increment da of crack extension shows that the energy loss per unit of plate thickness B is given by

$$\mathcal{G} = \frac{1}{2}\frac{P^2}{B}\frac{dC_0}{da} . \tag{13}$$

The expression for K^2 can be written in the form

$$K^2 = \frac{1}{2W}\frac{P^2}{B}\frac{d(EBC_0)}{d(a/W)} , \tag{14}$$

where the final derivative term is dimensionless and, for a long specimen, depends only on the relative crack depth a/W. As discussed by Srawley and Brown,[14] comparisons of K from compliance measurements with numerical collocation-analysis values of K can be done with sufficient accuracy to show agreement within about 3% for the specimen of Fig. 7.2, and equivalent agreement has been found using notched bend specimens. When this method is applied in a simple way to three-dimensional problems and K does not have a constant value along the entire leading edge of the crack, the method provides only the average value of K^2 across the leading edge.

Attempts to measure K based on determinations of stress near the leading edge of the crack, either with photoelasticity or with bonded strain-gage methods, have not been equally successful. Approximate answers can be achieved, but errors of 10 to 15% have been apparent in work of this nature so far. The reason is probably the dependency of the definition of K on a limiting process in which the distance r must approach zero. In the compliance technique an uncertainty as to the exact location of the leading edge contributes only a small error. However, the leading-edge location is of critical importance to the photoelastic and bonded strain-gage methods. Further study of the positioning of the leading edge of the crack for analysis purposes will be required to reduce the existing analysis uncertainties.

Other experimental methods are possible that may well be more accurate than those discussed above but which have received very little trial. Two such methods would proceed as follows:

1. Calibrate a test material for fatigue striation spacing as a function of K in tension-tension fatigue, and then use measurements of striation spacing to measure K values for crack geometries of interest.

2. Form a model of the component of interest from glass or another suitable transparent material. Move a crack into the model as desired and use a fixed low humidity to assist stable crack extension. Measure crack-opening displacement as a function of distance from the leading edge with the use of optical techniques and interference fringes. Use Eq. (3) to obtain K.

Except for reservations based on accuracy troubles, frozen-stress photoelasticity methods might seem well suited to the determination of

ratios of K to applied nominal stress for, say, deep cracks in the throat regions of nozzles. The results from frozen-stress methods would have improved value if these results could be checked with a different technique, such as one of those suggested above.

When artificially inserted increments of crack extension are used, along with the compliance technique, to determine K values for the specimen of Fig. 7.2, the extensions are straight across the plate, because this is the natural path for tensile-mode crack extension. In general the natural trajectory for a moving tensile crack may be a curved surface. Where this surface is not known in advance it can usually be determined by three-dimensional model studies with the use of fatigue or stress-corrosion to produce stable extension of the crack. The determination of K for a crack or slot that does not correspond to a natural tensile-mode crack surface is complicated by the fact that the leading-edge stress system will contain contributions from Mode II and Mode III stress fields. In the case of the single-edge-notched plate or a notched-bend-bar K_{Ic} test, available analysis methods provide only the average value of K^2 along the nearly straight leading edge of the crack. The actual value of K_I^2 in central regions should be larger than the average value of K^2, but the amount is uncertain. Some workers estimate the increase factor as the reciprocal of $(1 - \nu^2)$. Others report a value of K_{Ic} that may be conservative (possibly by as much as 5%) by taking the central region K_I^2 value as equal to the average K^2 across the specimen. The difference is of small practical importance, since replicate test results tend to vary by amounts in the range of 5 to 10%.

7.3 PLASTICITY ANALYSIS CONCEPTS FOR CRACKS

Studies of fracture suggest that a close relationship to plastic flow properties exists. It is impossible to explore interests of this kind in a quantitative manner without use of analytical models to define properties that can be computed as well as observed and discussed. Exact elastic-plastic solutions are not available for the tensile cracks of

interest. Furthermore the structural metals possess fine-scale inhomogeneities, and this limits the realistic accuracy of any continuum mechanics representation. Despite these difficulties, significant progress has been made with the aid of several relatively simple analytical methods. Three elementary and widely used plasticity analysis concepts for cracks are described below. A fourth section discusses fracture characterization problems in relation to plasticity analysis ideas.

7.3.1 The r_Y Plasticity Adjustment Factor

Critical values, $\mathcal{G}_c$, for onset of rapid fracture in high-strength aluminum-alloy sheets were among the first crack-toughness measurements attempted. Tensile sheets of various size with a central, sharp-ended slot to represent the initial crack were employed for these measurements. Results showed a trend for $\mathcal{G}_c$ to increase with the lateral dimensions of the specimen that was nearly eliminated by adding a plasticity adjustment, r_Y, to the crack size.[15]

No specific model of the plastic zone was attempted. The idea was simply to remove a leading-edge positioning error from the linear elastic analysis model. A central position inside the plastic zone, as shown in Fig. 7.1, was assumed to be a better location for the analytical model leading edge than the apparent tip of the crack at the left side of this zone. From the first of Eqs. (1), with $\theta = 0$,

$$\sigma_y = \frac{K}{\sqrt{2\pi r}} . \tag{15}$$

It was assumed that the distance r_Y from the central location to the elastic-plastic boundary could be estimated by inserting a critical yield-stress value, σ_Y, for σ_y in Eq. (15) and that this distance could also be taken as the separation of the analytical model leading edge from the apparent tip of the crack.[16] From these rules,

$$r_Y = \frac{1}{2\pi}\left(\frac{K}{\sigma_Y}\right)^2 . \tag{16}$$

In fracture-testing applications the value of σ_Y was taken to be the 0.2% offset uniaxial tensile yield strength, σ_{YS}, for situations of plane stress. The length factor, $2r_Y$, was used as an approximate estimate of the size of the plastic zone. The influence of plane-strain conditions in elevating the tensile stress necessary for yielding was assumed representable by taking $\sigma_Y \cong \sqrt{3}\ \sigma_{YS}$.

Crack-toughness testing of the plane stress kind is not yet carefully defined. Within the limited accuracy of available results for onset of rapid crack extension in high-strength metal sheets, use of the leading-edge positioning adjustment, r_Y, results in $\mathcal{G}_c$ values that are essentially constant with change of test sheet size as long as the net section stress is less than σ_{YS}.

Historically, the length factor, $2r_Y$, was used as an approximate estimate of the plastic zone size. Studies of the change in the ratio of $2r_Y$ to test-plate thickness across the brittle-ductile fracture-mode transition range showed clearly the dominating influence of elastic constraint and led to interpretation of this fracture transition as a plane-strain to plane-stress change in the leading-edge plastic zone.[17] Clark[18] investigated the apparent size of the plastic zone in silicon iron both for plane-stress and plane-strain conditions and at a stress level where the net section stress was well below σ_{YS}. He concluded that the size estimates provided by calculating $2r_Y$ for plane stress and plane strain were approximately correct both in magnitude and in terms of the three-to-one size ratio for the two conditions of elastic constraint.

Substitution of r_Y for r in Eq. (3) permits calculation of a crack-opening dimension that is of interest for various fracture analysis applications. Wells[19] has used terms such as crack-opening displacement and crack-opening dislocation for the crack-opening size $2v = \delta$ estimated in this way. He noted that the result $4\mathcal{G}/\pi\sigma_Y$ is obtained regardless of whether a plane-stress or plane-strain condition is assumed.

7.3.2 The Strip-Yield Zone Concept

Linear analysis of stresses near a crack can always be formally done by solving the stress problem, ignoring the crack, and then superimposing

a solution that contains forces at the crack plane just sufficient to restore free-surface conditions. The analysis can be adjusted so that, adjacent to the leading edge, the crack surfaces are not force free but are subject to crack-closure forces arising, say, from attraction between opposite crack surfaces. Barenblatt[20] assumed that such a system of crack-closure forces always exists near the leading edge. The closure tensions and their distribution were balanced to eliminate the linear-analysis stress infinity.

Dugdale[21] noted that this idea could be applied to representation of the plane-stress yield zone for a crack in a thin metallic sheet. In this application the force system became simply a constant tensile stress across the linear yield zone equal to the tensile yield strength. Since Dugdale's analysis ignores the sheet thickness, the analysis-model plastic zone is simply a line segment extending ahead of the apparent tip of the crack. Concentration of all the plastic strain into a line results in a representation that permits calculations of the opening-displacement discontinuity but does not permit calculations of plastic strains.

Interest in this type of representation also developed among dislocation scholars who saw that a strip-yield zone could be thought of in terms of a continuous distribution of dislocations. A criterion for onset of rapid crack extension based on a critical value of crack-opening displacement might, it seemed, provide a way to connect macroscopic fracturing directly with dislocation mechanics.[22] Modifications toward greater realism are possible by assuming various line patterns of concentrated yielding at the expense of greatly increased analytical complexity.

For those with less ambitious analytical objectives, there are other reasons for interest in the strip-yield plasticity analysis idea. For example, the analysis for a single line of yielding can be accomplished with only moderate computational difficulty for certain tensile-fracture specimens that might be used for crack-toughness evaluation. Wells' crack-opening displacement, δ, could be estimated for such tests from the strip-yield analysis model in terms of observations of applied load and crack size until the yield zone extends completely across the net section. Only theoretical studies of this kind have been done. These

resulted in δ values not significantly different from the value of $\mathcal{J}/\sigma_Y$ resulting from a linear analysis with the usual r_Y positioning adjustment.[23]

When the size, b_0, of the strip-yield plastic zone is small relative to crack size and net section size, the following relationships hold:

$$\mathcal{J} = \sigma_Y \delta \tag{17}$$

and

$$K = \frac{2\sigma_Y}{\pi} \sqrt{2\pi b_0} \ . \tag{18}$$

Examination of stress and opening-displacement equations for the strip-yield model in the small plastic-zone limit show that the "best fit" location for the leading edge of a linear-analysis-model crack is at the distance $b_0/3$ from the apparent leading edge of the crack. Comparison of

$$\frac{b_0}{3} = \frac{\pi}{24} \left(\frac{K}{\sigma_Y}\right)^2 \tag{19}$$

with Eq. (16) shows that $b_0/3$ is smaller than r_Y by only 18%.

Compression of all the yielding into a thin layer ahead of the crack might seem too unrealistic to be of value for thick-section tensile fracturing of metals. However, it is helpful to learn what concepts associated with various models of the plastic zone have magnitudes that are nearly independent of plastic-strain distribution. Comparison of Eqs. (19) and (17) with the r_Y and δ values from Section 7.3.1 suggests that the linear-analysis positioning adjustment r_Y and the crack-opening displacement δ are two concepts possessing a considerable degree of strain-distribution invariance.

7.3.3 The Mode III Elastic-Plastic Treatment

The system of deformations near the crack border termed Mode III is a distribution of shear strains such that all the particle displacements are parallel to the leading edge of the crack. Limitation of displacements

to a single coordinate direction reduces the mathematical difficulty for linear analysis (with yielding suppressed) and for strip-yield analysis (with yielding confined to a line segment). In fact, Mode III elastic-plastic solutions can be obtained without arbitrary restriction of the region of yielding and, for zero work hardening, with a degree of mathematical difficulty only moderately greater than that for the strip-yield analysis. The Mode III plasticity analysis idea introduced by McClintock and his associates[24-26] became of increasing interest as the inherent difficulty of the corresponding Mode I analysis became increasingly evident. The reason for this is the need for analytical representation of plastic strains very close to the leading separational elements of the crack.

If zero work hardening and either the Von Mises or Tresca criterion for yielding are assumed, Mode III plasticity analysis predicts a distribution of shear strains representable in the form

$$\vec{\gamma} = \gamma_{yz} + i\gamma_{xz} \ , \tag{20}$$

where

$$\gamma_{yz} = \gamma_Y \frac{R}{r_1} \cos \theta_1 \ , \tag{21}$$

$$\gamma_{xz} = -\gamma_Y \frac{R}{r_1} \sin \theta_1 \ , \tag{22}$$

and $\gamma_Y = \tau_Y/\mu$ is the shear strain at the elastic-plastic boundary.

The coordinates r_1, θ_1 are cylindrical coordinates about an axis coincident with the apparent leading edge. R is the value of r_1 if the latter is extended to the elastic-plastic boundary. The preceding result is not generally valid; however, it is valid for any series of equally spaced equal-length two-dimensional cracks on the x,z plane and for a uniform stress, $\tau_{yz} = \tau$, acting remote from this plane. This problem has been studied because it can be regarded as the Mode III analog for the centrally cracked and symmetrically edge-cracked finite-width tensile specimens used for crack-toughness evaluation.

Analytical considerations[10] show that as the plastic zone reduces in relative size, the elastic-plastic boundary approaches the shape of a circle (or cylinder) with the coordinate axis of θ_1 at the left extreme

of the x-direction diameter, as suggested by Fig. 7.1. The size R_0 of this diameter is

$$R_0 = \frac{1}{\pi}\left(\frac{K_{III}}{\tau_Y}\right)^2 . \tag{23}$$

For comparison, the leading-edge equations for the elastic strains predicted by linear analysis in Mode III are

$$\gamma_{yz} = \gamma_Y \frac{K_{III}}{\tau_Y} \frac{\cos\frac{\theta}{2}}{\sqrt{2\pi r}} \tag{24}$$

and

$$\gamma_{xz} = -\gamma_Y \frac{K_{III}}{\tau_Y} \frac{\sin\frac{\theta}{2}}{\sqrt{2\pi r}} . \tag{25}$$

If we locate the origin of the r,θ coordinates at the center of the plastic zone and put $r = R_0/2$, Eqs. (24) and (25) predict the same strain as do Eqs. (21) and (22). Thus the linear analysis value of r_Y for this problem is

$$r_Y = \frac{R_0}{2} = \frac{1}{2\pi}\left(\frac{K_{III}}{\tau_Y}\right)^2 . \tag{26}$$

Clearly, Eq. (16) is the tensile analog of Eq. (26).

If $R = R_0 \cos\theta_1$ is assumed, corresponding to the small plastic-zone situation, integration of the total strain γ around the elastic-plastic boundary provides

$$\delta = \frac{2}{\pi}\gamma_Y\left(\frac{K_{III}}{\tau_Y}\right)^2 . \tag{27}$$

By using $2\mu\mathcal{G}_{III} = K_{III}^2$, this equation becomes,

$$\delta = \frac{4\mathcal{G}}{\pi\tau_Y} . \tag{28}$$

Equation (28), with σ_Y in place of τ_Y, is the same as the value for δ in the case of the tensile mode when the linear analysis approach, supplemented by the leading-edge positioning adjustment r_Y, was used.

For the Mode III elastic-plastic problem of a finite-width plate, such as was indicated above, values of δ have been calculated by Rice[27] as a function of τ and crack size a for various levels of net section stress. From comparisons with these results it is found that the value of δ provided by Eq. (28) is still accurate to better than 5% when the net section stress is 0.95 τ_Y.

An additional result of interest from studies by Rice[28] pertains to the influence of strain hardening. By using a nonlinear stress-strain law in the plastic range of the type

$$\tau_Y = \tau_0 \gamma^n , \tag{29}$$

Rice was able to study the shape of the Mode III crack opening and the shift of the elastic-plastic boundary for the small plastic-zone situation with a work-hardening influence present. He found that the elastic-plastic boundary remained circular. The diameter was still given by Eq. (23), and the crack opening at the intersection of the elastic-plastic boundary with the crack differed negligibly from Eq. (28) for small values of n.

7.3.4 Fracture Characterization Problems in Relation to Plastic Analysis

As noted in previous sections, much has been learned about progressive crack extension through direct observation of the behavior trends as functions of K (or $\mathcal{G}$). The degree of success thus achieved resulted from giving primary analysis attention to the region close to the leading edge. Intuitively, a similar procedure should be followed in plasticity studies. Primary attention should be given to regions of the plastic zone close to the leading separational elements of the crack. The K or $\mathcal{G}$ value represents a controlling aspect of the elastic stress field. Presumably a controlling aspect associated with plastic strain would be appropriate in the case of plasticity studies. However, the

task of selecting a simple characterization plan based on plasticity analysis can only be done, at present, on a judgment basis. Essentially, the answer sought is needed in order to find this answer — a dilemma not uncommon in exploratory science.

Two judgment-type answers are the following:

1. Characterization in Terms of the Crack-Opening Displacement, δ. Intuitively, an average strain of some kind would seem most promising as a single-parameter characterization of critical "state of strain" for onset of rapid crack extension. One special kind of averaging, potentially suitable, would be that measured by the value of the crack-opening displacement, δ. Although, conceptually, values of δ might be obtained by direct observation, the feasibility of doing these measurements with useful accuracy is still not clear. Calculations of δ can be made that are based on a specific elastic-plastic model as the integral around the elastic-plastic boundary of the extensional strain normal to the crack. A simpler plan would be to compute δ as equal to ϕ/σ_Y. Both these methods become inapplicable after development of general yielding. Beyond general yielding, estimates of δ can be made with a rigid-plastic slip-field viewpoint. Obviously, somewhat different values of δ would be obtained with different methods, and use of δ as a characterization parameter in a consistent way would require arbitrary standardization of the calculation procedures.

2. Characterization in Terms of a Critical Average Strain, ϵ_1, for Plastic Instability. This procedure is based on Krafft's correlations between K_{Ic} and strain hardening, which suggest that local plastic instability is a significant controlling aspect for onset of rapid crack extension.[29] In the calculational plan used by Krafft, the critical average strain, ϵ_1, is assumed to be given by

$$\epsilon_1 = \frac{K_{Ic}}{E\sqrt{2\pi d_T}} . \tag{30}$$

The length factor d_T for a given test material was determined by Krafft[29] by assuming ϵ_1 equal to the strain-hardening exponent n for isothermal conditions of straining. Direct measurement comparisons of K_{Ic} and n

for similar conditions of strain rate and temperature then permitted finding a best-fit proportionality factor. More recently, following suggestions by Williams and Turner, Krafft assumed

$$\epsilon_1 = \frac{n}{2} + \frac{\sigma_Y}{E} , \tag{31}$$

where the terms on the right represent the influence of an assumed specific type of elastic constraint on the critical strain for plastic instability.[30]

It is possible to arrive at somewhat similar equations by defining an average strain close to the leading edge in terms of the Mode III elastic-plastic model, Eqs. (21) and (22), as follows. From the preceding equations, the maximum shear strain at a point r_1, θ_1 is given by

$$\gamma = \gamma_Y \frac{R}{r_1} . \tag{32}$$

By assuming

$$R = 2r_Y \cos \theta_1 ,$$

the average strain $\bar{\gamma}$, along a vertical line at $x = x_1$, where $x_1 \ll 2r_Y$, is given by

$$\bar{\gamma} = \gamma_Y \left[\frac{\pi}{2}\left(\frac{2r_Y}{x_1}\right)^{1/2} - 1\right] \tag{33}$$

$$= \frac{\pi}{2} \frac{K_{III}}{\mu\sqrt{\pi x_1}} - \frac{\tau_Y}{\mu} . \tag{34}$$

The tensile analog of Eq. (34) is

$$\epsilon_1 = \frac{\pi K_{Ic}}{2E\sqrt{\pi x_1}} - \frac{\sigma_Y}{E} . \tag{35}$$

In this calculational plan the elastic constraint might be assumed representable by $\epsilon_1 = n/2$ in order to derive a relationship between K_{Ic} and n similar to that provided by Eqs. (30) and (31).

At the present time, correlation studies between plastic flow properties and crack toughness need additional support from plasticity analysis. Equation (35) is of no special importance in itself, but the derivation has illustrative values. Plasticity investigations intended to assist extension of fracture mechanics toward basic factors at finer scale should provide help of that kind in terms of better plasticity models. Previous calculations of plastic strain fields near a tensile crack made with computer programs have not been planned so as to assist the characterization task either in terms of a crack-opening displacement concept or along the lines of the K_{Ic}-n correlation.

7.4 SLOW, STABLE CRACK GROWTH

7.4.1 Crack Growth Rates as Affected by Fatigue

In assessing the severity of flaws in a structure, the possibility of their growth to a dangerous size from the effects of repeated loading, including cyclic thermal stresses, and/or environment should be considered. Two related approaches have been adopted for making this assessment:

1. to give attention to analysis of the rates of growth of subcritical flaws[31,32] that can subsequently be used to estimate a "life" from an initial flaw size to the critical size,
2. to give attention to a direct analysis of the "life" of typical flaws.[13]

Of these two approaches, the first is the more detailed and fundamental and, as a consequence, leads to a better understanding of service behavior. On the other hand, the second approach is simpler and has been demonstrated to be adequate for certain analyses of the life of pressure vessels of very high-strength metal alloys, such as rocket-engine cases, etc.[13] For a full understanding of flaw growth considerations in the design and behavior of pressure vessels, both approaches should be employed.

In the initiation of subcritical growth of flaws due to fatigue, planar defects are most likely to develop into growing fatigue cracks. However, in a conservative assessment of the danger, all flaws and defects are potentially growing cracks with a slight amount of sharpening. As one might expect, the most severe flaws are normally those that are largest and in the most highly stressed regions of a structure, and such flaws are often associated with damage to the material during fabrication.

The analysis of growth rates of flaws from those too small to find in normal inspection to those of critical size for unstable running fracture proceeds on a similar basis as that for final failure itself. The increment of crack growth experienced in a cycle of loading depends on the corresponding excursion in the stresses surrounding the crack tip, as measured by K.

For a given material and environment, the rate of crack growth, da/dN, depends primarily on the stress-intensity-factor range, ΔK, and secondarily on the relative mean value, γ_1, of the stress-intensity factor, K_M, or relative mean load, P_M; that is,

$$\gamma_1 = \frac{K_M}{\Delta K} = \frac{P_M}{\Delta P} . \tag{36}$$

Also of secondary (but not negligible) importance are the frequency of loading, plate thickness effects, and processing of material, which should be assessed in a refined analysis.[33,34]

Since growth rates can be correlated by stress-intensity factors, the effects of the location of applying the loading and the solid body and crack configuration are known, provided the growth rates are known for some laboratory test configuration at the corresponding ΔK level; that is, plotting da/dN versus ΔK may be regarded as a basic way to represent a material's crack growth rate behavior, and the effect of secondary variables is to cause shifts in the curve so obtained.

Many such plots of da/dN versus ΔK (or K) for steels are available in the literature.[32,33-36] If the plots for steel are superimposed, a curious result is obtained. For zero-tension loading ($\gamma_1 = 0.5$), all the data for steels fall very close to each other; that is, within a

factor of 2 (or perhaps at most 3) in the growth rate for a given ΔK. For example, Brothers' data[35] on low-alloy medium-strength rotor steels are very close to Carman's data[36] on high-alloy very-high-strength rocket-engine pressure vessel steels. Moreover, the meager data (Fig. 7.3) available on low-strength steels for pressure vessels, such as A 302 grade B, indicate that they are no exception.[37]

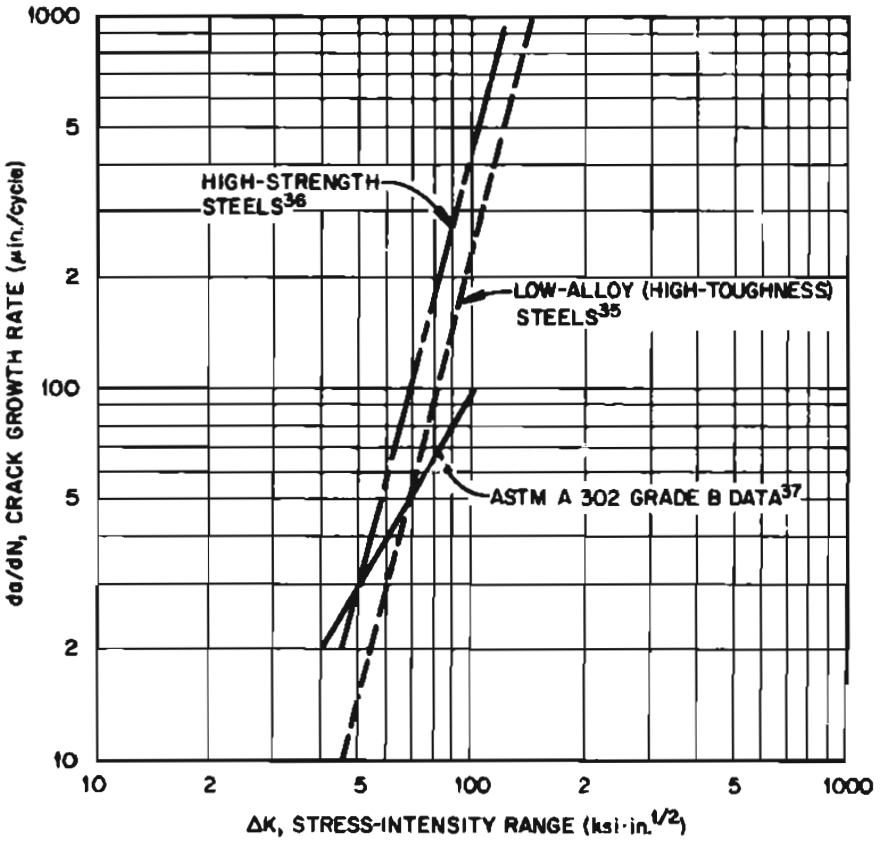

Fig. 7.3. Crack Growth Rate, da/dN, as a Function of Fatigue Cycle Range of the K Value, ΔK.

Consequently, from the steel data now available, a rather crude empirical relationship may be devised to describe the normal rates of growth of cracks in all steels in air at room temperature.[32,33,35-37] It is

$$\frac{da}{dN} = C(\Delta K)^4 , \qquad (37)$$

where, referring to Fig. 7.3,

$$C_1 = 2.0 \times 10^{-24}$$

for mean data on medium- and low-strength steel,

$$C_2 = 3.2 \times 10^{-24}$$

for mean data on all steel,

$$C_3 = 4.0 \times 10^{-24}$$

for conservative estimating of fastest rates on all steels; the units of da/dN are inches per cycle and ΔK is given in ksi·in.$^{1/2}$. Equation (37) gives a reasonable estimate for growth rates from 10^{-6} in./cycle up to final failure, provided the cyclic K stays below K_{Ic} for the material and the cyclic nominal stress is below the static yield point. These restrictions are normally no loss in general in describing flaw behavior in relatively thick pressure vessels of conservative design.

The crude relationship of Eq. (37) may at least be used to estimate whether fatigue-crack growth is a real problem for an anticipated flaw in a steel pressure vessel. For example, for a known or anticipated flaw, the stress range and subsequently the range of K (or ΔK) may be estimated, and an anticipated rate of growth may then be estimated by using Eq. (37). The relative severity of flaws of various sizes and locations may thus be estimated also. In this manner, Eq. (37) provides useful information on fatigue-crack growth rates expected in vessels.

However, Eq. (37) is not recommended for actual estimates of the fatigue life of vessels. By itself, it is too crude an empirical relationship for this purpose. It does not contain the effects of mean load, frequency, environment, or temperature, which surely play a role in the flaw-growth fatigue life of vessels. For estimating flaw-growth lives with some precision, it is necessary to revert to the fundamental concept of measuring fatigue-crack growth rates in laboratory tests that simulate the ΔK levels under conditions of mean load, environment, and temperature expected in a vessel. Under the expected conditions, the rate of crack growth, da/dN, versus the stress-intensity-factor range, ΔK, may be plotted to give the basic behavioral pattern of the material being tested.

Differences in materials may be readily observed by comparisons of such curves. Moreover, carefully obtained data, as represented on these curves, may be used to estimate the fatigue-crack growth life of a vessel. A numerical integration of crack growth rates from the initial flaw size to the critical size that precipitates failure is all that is required to make such estimates.[33,36]

Data on fatigue-crack growth rates under expected environmental conditions are not yet available for pressure vessel steels. Nevertheless, data that are available on aircraft materials[33,38] and some data taken on pressure vessel steels[39] with an unfortunate choice of specimen configuration (the K levels cannot be computed) allow some tentative conclusions to be drawn on the effect of environment on fatigue-crack growth rates. The presence of water (or high humidity) tends to accelerate fatigue-crack growth rates in pressure vessel steels, as well as others. For example, data[40] on A 302 grade B steel indicate that simulated boiler water increases the rates of fatigue-crack growth by a maximum factor of 2.5, whereas for salt water the factor is about 3 (Fig. 7.4). Data on

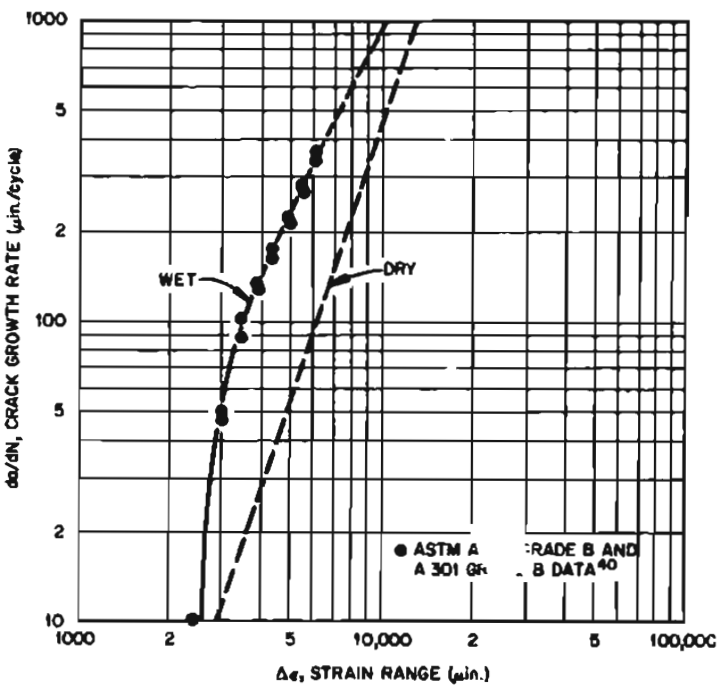

Fig. 7.4. Crack Growth Rate, da/dN, as a Function of Displacement Range in Low-Cycle Fatigue Testing. Data from Ref. 40.

A 201 grade B steel show virtually identical behavior, which leads to the conclusion that a factor of 3 is rather reasonable for A 302 grade B steel. These factors may be directly applied to the estimates for crack growth rates made with Eq. (37), as discussed earlier. Although this factor of 3 is an approximation, since it was obtained from a test for which stress-intensity factors cannot be computed, its precision is at least consistent with the precision of Eq. (37).

The more precise and fundamental approach of simply gathering and plotting data on a da/dN versus K basis is preferred. The relationship is implied that

$$da/dN = f(K) \ , \tag{38}$$

where f(K) is a function that depends on the material and environmental conditions. Equation (37) is representative of the gross features of the function f(K), which shows the main trend but not the details.

Similarly it may be recalled that the stress-intensity factor formula for any given solid body configuration depends linearly on the load, P, and also in some way on the crack size; that is,

$$K = P\ f(a) \ . \tag{39}$$

In general, Eq. (39) may be substituted into Eq. (38), which may be integrated to give the "life," N_F of a given configuration of a given material and environmental conditions. The life, N_F, can be written as a function of the load, P, and, alternatively, either the initial and final crack size or stress-intensity factor values; that is, the form is

$$N_F = H_1(P, a_i, a_c)$$

or (40)

$$N_F = H_2(P, K_i, K_c) \ ,$$

where H_1 and H_2 depend on material and environment and the effect of the configuration through the form of the variation in its stress-intensity factor with crack size.

From Section 7.2 and other references[11] on stress-intensity factor formulas, it may be casually noted that for flaws which are relatively

small compared with other body dimensions, the formulas take the form

$$K = C_4 \sigma \sqrt{a} \ , \tag{41}$$

where σ is the nominal stress on the crack plane and C_4 takes on values from $2/\sqrt{\pi}$ for an embedded circular crack of radius a to $1.12\sqrt{\pi}$ for a long surface crack of depth a or an edge crack in a sheet. For typical flaws that cause concern in pressure vessels, for example, surface flaws that are of fairly similar proportions, the coefficient C_4 is nearly always roughly the same value. It is therefore reasonable, as well as informative, to combine Eqs. (37) and (41) in order to observe the broad trends of variables in life calculations, as implied by Eqs. (40).

Making the substitution of Eq. (37) into Eq. (41) gives

$$\frac{da}{dN} = C'(\Delta\sigma)^4 a^2 \ .$$

Rearranging and integrating leads to

$$\int_{a_i}^{a_c} \frac{da}{a^2} = C'(\Delta\sigma)^4 \int_0^{N_F} dN$$

or

$$N_F = \frac{1}{C'(\Delta\sigma)^4}\left(\frac{1}{a_i} - \frac{1}{a_c}\right), \tag{42}$$

or again making use of Eq. (41),

$$N_F = \frac{1}{C''(\Delta\sigma)^2}\left(\frac{1}{K_i^2} - \frac{1}{K_c^2}\right). \tag{43}$$

Note that Eqs. (42) and (43) are rough approximations of the forms of Eqs. (40), where C' and C'' are constants that depend on the material and environment and to a lesser degree on the configuration of the flaw or crack.

Some important conclusions on flaw growth life may be extracted from Eqs. (42) and (43). First, if the initial flaw size, a_i (or K_i), is small compared with the critical size, a_c (or K_c), moderate changes in the critical fracture toughness, K_c (or a_c), have little effect on the flaw growth life. This is the case of moderately "high-cycle fatigue." It is only in the case where the initial flaw size is nearly of the order of magnitude of the critical size that the critical size, or K_c, becomes important. This case is relatively "low-cycle fatigue." Moreover, upon lumping the material constant K_c^2 into C'', Eq. (43) becomes

$$N_F = \frac{1}{C'''(\Delta\sigma)^2}\left(\frac{K_c^2}{K_i^2} - 1\right) . \tag{44}$$

Quite independently of the derivation of Eq. (44), Tiffany[13] and others have observed that data on the lives, N_F, of flawed laboratory test specimens and typical structures of a given material are correlated very well in terms of K_i/K_c, provided the stress ranges, $\Delta\sigma$, are roughly comparable. Moreover, Eq. (44) has a certain measure of appeal to those who follow the Coffin-Manson type of approach to low-cycle fatigue, where the relationship

$$(\Delta\epsilon)^2 N_F = \text{constant}$$

is observed to correlate data for many materials. Equation (44) implies agreement to this relationship but that life also depends strongly on initial flaw size, a_i, or stress-intensity level, K_i.

Equation (44) is only the result of crude approximations for the detailed behavior of flaws growing by fatigue loading, Eqs. (37) and (41), and though it would be inadvisable to apply it directly, using it to study the significant variables and to understand their relative roles is quite appropriate. It is perhaps used best as originally suggested by Tiffany[13] through plotting test data on K_i/K_c versus N_F in order to observe effects of flaw size, environment, etc., in a way that lends itself to selecting proper materials and assessing directly the severity of subcritical flaws. Again, some preliminary data[37] on flaw lives in A 302 grade B steel are shown in Fig. 7.5. These data indicate lives of thousands of cycles for

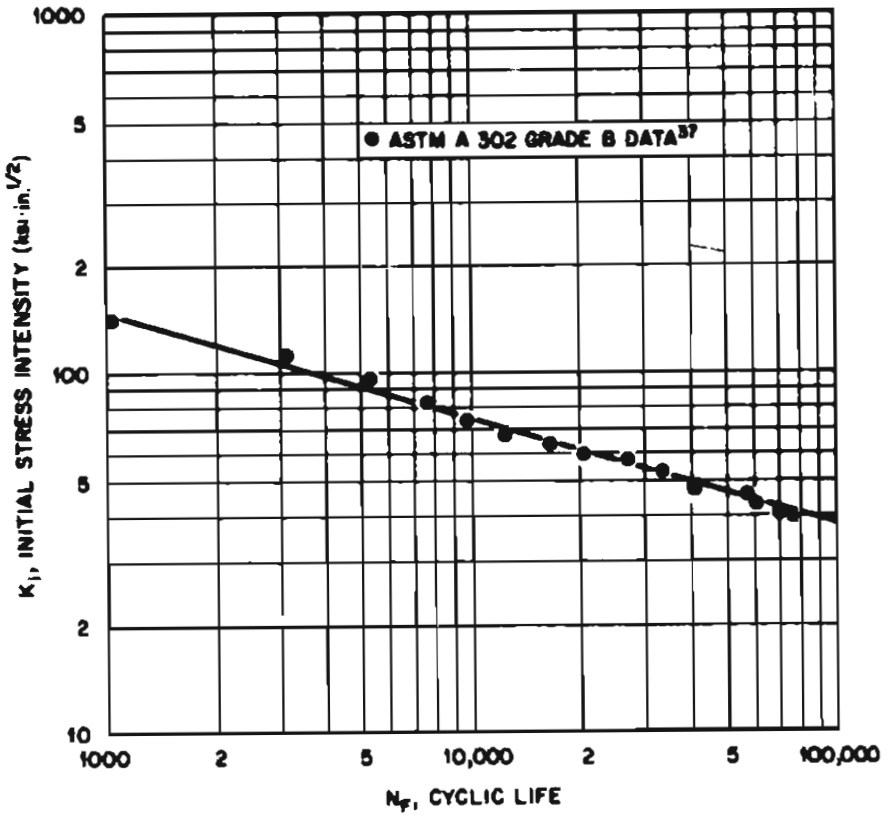

Fig. 7.5. Cycles to Failure as a Function of the Initial K Value, K_i. Data from Ref. 37.

flaws of about 4 in. or more depth and breadth in A 302 grade B base-metal plates tested dry at room temperature and cycled at half the yield strength. Similar tests should be performed on welded plates and with various typical environments for pressure vessels.

The method of plotting data on Fig. 7.5 also implies the value to overload pressure testing in assessing the remaining cyclic life.[13] Since K is proportional to load P if any flaw survives an overload, the overload K must be less than K_c; or, as a consequence, its initial K at operating load, K_i, must be less than K_c multiplied by the ratio of the operating load to the overpressure load, P/P_p; that is,

$$\frac{K_i}{K_c} < \frac{P}{P_p} . \tag{45}$$

Moreover, the overpressure load can be deliberately applied at a lower

temperature, where K_c (low temperature) is lower (see Sect. 7.6.5). If the K_c values are known at both temperatures,

$$\frac{K_i}{K_c} < \frac{P}{P_p} \frac{K_c \text{ (low temperature)}}{K_c} . \tag{46}$$

From a fracture-mechanics flaw-growth viewpoint, there are no known disadvantages of overload pressure testing. On the contrary, Eq. (46) combined with data in the form of Fig. 7.5 offer decided advantages by quantitatively guaranteeing a certain flaw-growth life independently of other inspection procedures.

7.4.2 Crack Growth Rates as Affected by Environment

The growth of cracks in a corrosive environment may be analyzed in much the same manner as fatigue-crack growth by using the stress-intensity factor, K, as the local stress variable for the "driving effect" of stress near the crack tip.

In stress-corrosion crack propagation, relatively weak environments, such as water, often have pronounced effects in materials where the same environment may have very small effects on pitting corrosion (i.e., crack initiation from a smooth surface under stress). Moreover, the crack-tip stress state, plane stress versus plane strain, has marked effects on the growth of stress-corrosion cracks; that is, where the plate thickness is large compared with the plastic-zone size and the plane strain, the conditions for environmental crack growth are much more severe than for relatively thin plates. Since most stress-corrosion tests have been performed on thin, smooth samples of materials, for the preceding reasons, most ordinary stress-corrosion data are of doubtful value for assessing the possibility of crack growth in the design of thick-walled pressure vessels with flaws.

In some work on high-strength steel alloys[31,38,41] it has been shown that environmental flaw-growth data can be correlated in terms of stress-intensity factors; this implies the form

$$\frac{da}{dt} = H_3(K) . \tag{47}$$

This equation is analogous to Eq. (38), but here statically applied loads and environment are present (or fatigue loading and environment) with a stress state of plane strain (thick plates). For the case of a statically applied load for each material and environment combination, there appears to be a threshold level, K_{ISCC}, below which crack growth does not occur. This is also evident in other recent works,[13,42,43] which in addition have shown that the K_{ISCC} value is substantially elevated under stress conditions tending toward plane stress (thin plates). On the other hand, under repeated fatigue loading (a few cycles per second), no threshold level seems to exist.[38] However, the normal case in reactor vessels is probably the former, where the occasional changes in load do not significantly alter the rate of progress of a stress-corrosion crack.

In low-strength high-toughness steel alloys, the K_{ISCC} stress-corrosion-cracking threshold level is not unlikely to be nearly as high as K_{Ic} itself.[43] Consequently, it appears that it may be possible to completely avoid static-load stress-corrosion cracking in reactor vessels simply by judicious choice of materials. The tests of the materials should be for the absence of any crack growth over long periods of time under environments and load variations (K-variations) anticipated in service. Currently in such tests fatigue-cracked notches are used as simulated flaws, and examination for absence of growth is by fractographic examination upon completion of the test. Other techniques such as sectioning of the crack-tip region to show blunting of the crack are perhaps even more convincing.

However, if K_{ISCC} is determined to be a significant amount below, K_{Ic}, several alternative considerations must be suggested. First, the time to failure (or rates of growth) for cracks with applied K levels above K_{ISCC} should be determined.[13,42,43] Normally, these times are relatively short; that is, a matter of minutes or a few hours from first load application. Consequently, a reator vessel with a flaw stressed above K_{ISCC} would fail in a short time unless it was protected from the environment or unless plane stress conditions prevailed for cracks through the wall. In some cases, protection is possible, but not in general. In

the cases where protection is not possible, the fatigue analysis of Section 7.4.1 should obviously be terminated at K_{ISCC} [i.e., replace K_c in Eqs. (40) through (46) with K_{ISCC} with a corresponding change in interpretation]. Above K_{ISCC}, either there is no significant life remaining or if plane stress conditions occur at K-levels between K_{ISCC} and K_{Ic}, there is some chance of arrest or inhibition of static stress-corrosion-crack growth, whereupon the fatigue-crack growth mechanism might again prevail. Again, this is an area where little work has been done, and there has been especially little on low-strength high-toughness materials.

In summary, for corrosion considerations, K_{ISCC}, or its equivalent, should be established for the materials considered in reactor vessels. Hopefully, K_{ISCC} will be very close to K_{Ic}, in which case no special provision for stress-corrosion cracking need be made in addition to that in the fatigue-crack growth analysis (with environment) in Section 7.4.1. However, if K_{ISCC} is appreciably below K_{Ic}, either K_{ISCC} should be used as the "failure level" in design or special procedures must be developed to assess the remaining life.

7.5 CRACK PROPAGATION AND FRACTURE TOUGHNESS

7.5.1 Measurements of K_c and K_{Ic} for Very-High-Strength Metals

Crack-toughness measurements based on linear-crack stress-field analysis lead to critical values of the stress-intensity factor K for either onset of rapid fracture or crack arrest. Measurements of crack-arrest K values are less common, mainly because such tests require larger amounts of material. Similarly, for reasons of convenience, the testing speed most often used has been slow. The loading time to fracture in slow testing is usually about 2 min. The primary interests supporting K_c and K_{Ic} test development pertained to very-high-strength metals for use in rocket or ordnance applications. Adequate reviews of this field of work have been made (Refs. 10, 11, 13, 14, 44, 45), and this discussion summarizes only selected major points.

Onsets of rapid fracture and crack arrest are naturally of interest for use as crack-toughness measurement points, in part because they tend to occur abruptly and in part because present knowledge suggests no alternative choices. In the slow, stable and fast, stable regimes of crack extension, the average crack speed changes continuously in response to changes in the value of K or $\mathcal{J}$. The in-between points, called onset of rapid fracture and crack arrest, under ideally brittle conditions appear to be true instability points at which there is an abrupt upward or downward jump in the crack speed. As toughness increases and the plastic zone grows in size, the crack length for onset of rapid fracture becomes more difficult to select unambiguously in a simple way. Even for plane-strain K_{Ic} testing, material properties leading to unexpected amounts of stable crack extension prior to onset of rapid fracture sometimes occur. After some years of study, the ASTM E-24 Committee recently approved for trial, as a tentative K_{Ic} testing standard, a method remindful of a percent-offset tensile-yield-strength testing practice.

In K_c and K_{Ic} testing, some stable crack growth prior to the measurement point is expected because the natural contour of the leading edge of the crack at the fracture load usually differs from the crack shape inserted, say, by low stress fatigue. When the specimen has a through crack, as in Fig. 7.4, plastic yielding near the plate surfaces results in added stress on central regions of the leading edge. The central region then advances. Whether this advance takes the form of an unstable plane-strain pop-in or appears gradual depends on the length of the leading-edge segment that becomes nearly unstable at the time of forward movement. From experience, a pop-in often occurs when the plate thickness B is more than four times the plane-stress value of $2r_Y$, and it nearly always occurs when B is more than $10(2r_Y)$. Also from testing experience, a substantial, stable forward motion of central regions of the crack can be assumed to be governed by a K_{Ic} level of K so long as environment effects that would cause continuing stable crack extension are absent.

In K_c testing of very-high-strength steel and aluminum alloys, the test method of Ref. 46 employed an ink-staining technique to mark the region of slow, stable extension prior to onset of rapid fracture. Study

of a large number of these results showed stable extensions were rarely less than r_Y and rarely more than $2r_Y$ (Ref. 10), where these length factors were computed on a plane-stress basis regardless of the degree of plane-strain influencing the test result. The presence of water in the ink no doubt assisted the observed stable extensions. However, "Elox" notches (about 0.002-in. root radius) were used for most of these tests, and this tended to reduce the stable growth. On general grounds a stable crack extension of about r_Y in size is expected as normal behavior and represents, primarily, readjustment of the leading-edge contour toward the shape most natural for the onset of a rapid fracture instability that severs the specimen.

Roughly speaking, the present K_{Ic} testing method favored by the ASTM E-24 Committee is based on the assumption that when the load-deflection curve indicates stable crack growth of more than r_Y, a load corresponding to the K_{Ic} value has been achieved. Other details of the test method tend to encourage use of large enough test specimens so that most tests will terminate with an abrupt onset of rapid fracture prior to visible indications of stable growth. No change in the average level of K_{Ic} test results from those using presently customary methods is expected.

During the past eight years, many thousands of K_c and K_{Ic} test results were reported from test methods suggested by the currently available technical literature. Results reported in Refs. 30 and 45 are typical. The scatter band for a group of results from similar specimens of the same plate material usually extends 5 to 10% above and below the mean value. Welded regions tend to have larger variations of microstructure and impurities, and the scatter range of test results is larger. K_{Ic} values reported by Kies and his associates[45] for various welds in ultra-high-strength maraging steel show ±15 to 25% scatter bands for central regions of the welds. The report states that these variations correlated with variations in quality of microstructure in the local region tested.

The difference in test result scatter between fracture-toughness tests and tensile-yield-strength tests corresponds in part to the contrasting influences of small defects on these properties, as discussed in the first section of this chapter. The larger defects, which tend

to be less uniform in distribution, influence the crack toughness but do not influence resistance to plastic deformation. An additional factor is related to the test volume size.

When the size of the fracture-toughness specimen is increased, the leading edge of the crack samples a larger volume of material. The result is a reduction in the absolute size of the test result scatter zone. A corresponding reduction of the average critical K value should occur, in accordance with a "worst flaw" statistical treatment of the problem. In the case of K_{Ic} evaluations of the through-crack type of specimens, one dimension of the test volume is the plate thickness diminished by regions comparable in size to $2r_Y$ (plane stress) adjacent to the test plate surfaces. The area that would be used in completing the test volume estimate would be the square of a small dimension intermediate in size between δ and r_Y (plane-strain) and might be guessed as simply the product of these length factors. Such a test volume is quite small. Yield-strength tests respond to the average critical stress through a test volume comparable in size to the cube of the test-bar diameter, a volume several orders of magnitude larger than can participate in determining a K_{Ic} test result.

The substantial scatter of test results inherent to crack-toughness measurements has a definite bearing on a fracture control plan, which assumes that certain levels of crack toughness, established by testing, will be present as a barrier to crack propagation. There are no conventional methods for selecting a worst K_{Ic} value for a particular application on a probability basis other than straight-forward statistical theory.

On the basis of statistical theory, suppose K_{Ic} tests, say of an electroslag seam weld, have been done in sufficient number to permit determination of the standard deviation $\bar{\sigma}$, then a Weibull theory flaw distribution exponent, m, can be estimated[46] from the equation

$$\frac{\bar{\sigma}}{(K_{Ic})_{av}} = \frac{1.2}{m} . \tag{48}$$

From the statistical theory, the average K_{Ic} for a large crack through the wall thickness B should be less than that for the small test cracks

in specimens of thickness B_0, in accordance with the equation

$$K_{Ic} = (K_{Ic})_{\substack{\text{average} \\ \text{from tests}}} \left(\frac{B_0}{B}\right)^{1/m} . \tag{49}$$

The value of $\bar{\sigma}$ applicable to the large cracks would be reduced in size by the same factor, $(B_0/B)^{1/m}$. Several times this reduced $\bar{\sigma}$ value would then be subtracted from the large crack K_{Ic} to determine a conservative estimate for the service vessel. The details of this would depend on judgment factors best settled at a later point in fracture control planning.

7.5.2 The Brittle-Ductile Fracture Transition

During fracture investigations associated with welded steel rocket chambers for the Polaris and Minuteman programs, K_c measurements were made on a variety of ultra-high-strength metals. It was noted that the percentage of oblique shear on the fracture surface showed a trend type of correlation with the dimensionless ratio

$$\beta_c = \frac{1}{B}\left(\frac{K_c}{\sigma_Y}\right)^2_{\text{plane stress}} . \tag{50}$$

Since

$$2r_Y = \frac{1}{\pi}\left(\frac{K_c}{\sigma_Y}\right)^2 \tag{51}$$

is regarded as a formal measure of plastic-zone size, the ratio of plastic-zone size to plate thickness was β_c/π. As was noted in Refs. 17 and 47, less than 50% oblique shear was usually present when β_c was less than π. Furthermore, the condition $\beta_c = \pi$ represented one in which the value of K_c, as a function of β_c, was increasing rapidly. Clearly $\beta_c = \pi$ represented a midrange condition for the change from a flat-tensile fracture with relatively small shear lips to an oblique-shear fracture with

substantially increased fracture toughness. The $\beta_c = \pi$ criterion for midrange behavior was the same regardless of whether the fracture transition was induced by changing testing temperature or by changing test plate thickness. In the case of high-strength aluminum, K_c did not change appreciable with temperature (excluding temperatures below −250°F) but did change with changes of test-plate thickness in the same manner as for steels.

At the time Ref. 17 was prepared, fracture-toughness data for several rotor steels at about 100-ksi yield strength were available. These showed the same behavior pattern relative to the brittle-ductile transition as did the high-strength metals. With regard to low-strength mild-steel plate material, only approximate estimates of fracture toughness based on crack-arrest tests were available. However, rough estimates of β_c based on elevated dynamic yield strength were made. The same correlation between β_c and fracture transition was again evidenced.

A clear mechanism exists for the control of the brittle-ductile transition in terms of the plastic-zone size. For a plate in tension that contains a round hole straight through the plate thickness, the thickness-direction stress close to the hole at midthickness of the plate shows a large amount of plane-stress relaxation unless the hole diameter is less than half the plate thickness.[48] From this it is expected that plane-strain confinement of the plastic zone will disappear as we increase the plastic-zone size factor, $2r_Y$, relative to the thickness of the fracture test specimen. If the open hole is allowed a moderate advantage over the crack-tip plastic zone in causing thickness-direction stress relaxation, the $\beta_c = \pi$ criterion for a midrange fracture transition condition is quite plausible.

The crack-opening displacement, δ, decreases with testing temperature for a steel and thus changes in size relative to the grain size and relative to Krafft's d_T. Alterations of this kind may have a bearing on appearance features of a flat tensile fracture; for example, on the fraction of the exposed fracture surface composed of cleavage facets. However, the role of fracture appearances in relation to macroscopic fracture toughness is still not very clear. Notched-bar fracture tests of steels conducted at a series of temperatures and with a series of specimen sizes

do not show one fracture transition associated with crystalline cleavage and a second transition associated with the relative size of the plastic zone. Only the transition associated with relative plastic-zone size is consistently observed.

Several tensile fracture tests were performed at the Naval Research Laboratory with 60-in.-wide 3/4-in.-thick 2024-T3 aluminum plates centrally notched. The toughness was so large that the average net section stress roughly equaled the yield strength at the load for crack propagation. However, the first test produced a flat tensile fracture normal to the plate surface extending nearly to the side boundaries of the specimen. In a second trial, the hacksaw extension of the central slot was tilted to 45° with the plate surfaces. This time the fracture was entirely oblique shear, but the load and net section stress did not differ significantly from that for the first test plate. According to J. G. Kaufman (Alcoa Research Laboratory, New Kingston, Pa.), similar observations have been made at his laboratory. Formal reports of this curious behavior do not seem to be available. The rapid room-temperature aging of 2024 aluminum after plastic straining is thought to be a factor.

Anomalous flat tensile fracturing also occurred with certain rotor-steel alloys tested in the form of centrally notched 4- and 6-in.-thick spin disks at the General Electric Company's Large Steam Turbine Division.[49] A thickness reduction at the root of the notch was observed that was indicative of large plastic strains, and the computed fracture toughness was high; however, the fracture showed shear lips that were almost negligible in size. In these tests an arrest line could usually be seen on the fracture surface that marked the zone in which an oblique-shear fracture, if present, would have provided normal behavior. The temperature range for these tests was room temperature to 450°F, and the anomalous flat-tensile fractures tended to occur in the upper half of this range. A report of recent fracture tests of beryllium plates states that large amounts of plane-stress yielding accompanied a flat tensile fracture appearance.[50]

The interest in K_{Ic} testing has led to use of brittle boundary coatings and face notching to assist establishment of plane-strain fracturing. The results show that shear lips can be eliminated in this way. However,

the results also show that a fracture transition, in terms of plastic-zone size and fracture toughness, occurs despite elimination of the shear lips. From such observations as these, it is concluded that the position of a fracture-toughness test relative to elevation of toughness by plane-stress yielding is best judged by direct measurements of thickness reduction or in terms of a parameter such as β_c, rather than solely from appearance aspects of the fracture surface.

7.5.3 Double-Cantilever and Face-Grooved Specimens

The single-edge-notched bend and tensile specimens most used for fracture-toughness evaluations are well described in Refs. 10, 11, 13, 14, 44, and 45. For investigations of rate-sensitive materials and for other special purposes, specimens sometimes referred to as "double-cantilever" and sometimes as "crack-line loaded" are of interest and will be discussed here. The testing advantage sought in this type of specimen is control of the K value. In remotely loaded tensile and bend specimens, the increase of K with crack length at onset of rapid crack extension is too fast, and continued crack extension is beyond control by the loading system.

A double-cantilever specimen of simple design is shown in Fig. 7.6. If the beam depth, h, is small compared with the crack length, a, an

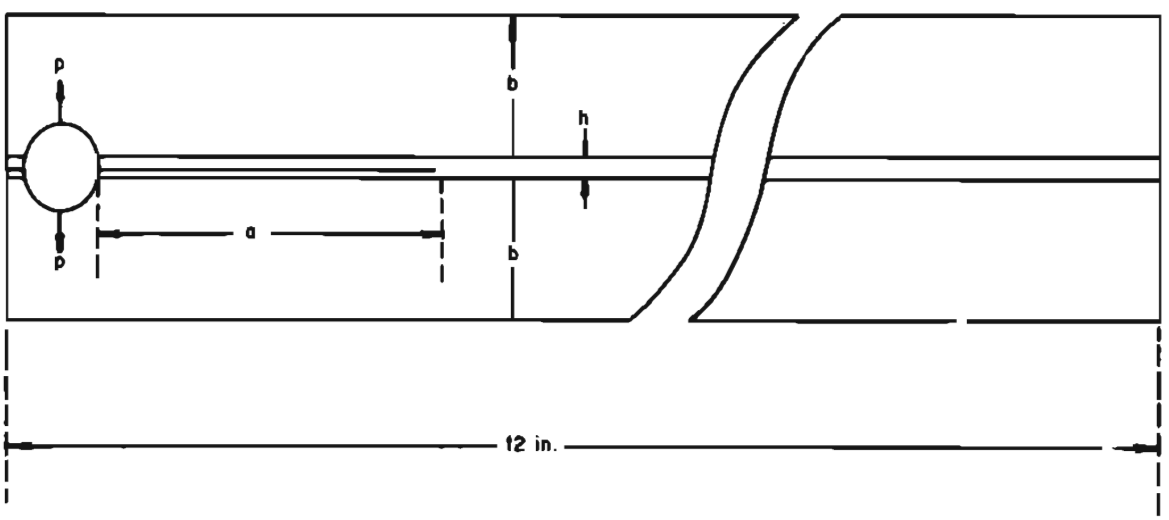

Fig. 7.6. Double-Cantilever Specimen.

adaptation of St. Venant's principle suggests an approximate but useful method of analysis. Since the section above the leading edge of the crack is remote from the applied force P, the load-displacement l can be estimated from a simple beam-theory stress distribution across the beam near the leading edge of the crack. So long as the assumed stress distribution possesses a bending moment equal to the applied moment, $P(a + a_0)$, the fact that the stress singularity is ignored causes only a relatively small error. By using the customary equations for beam deflections,[51]

$$l = C_0 P = \frac{8}{E} (x_0^3 + x_0) \frac{P}{B} , \tag{52}$$

where

$$x_0 = \frac{a + a_0}{h} \tag{53}$$

and a is the crack length as measured from a point close to the applied load. Then from Eq. (13),

$$\mathcal{G} = \frac{4P^2}{EhB^2} (3x_0^2 + 1) , \tag{54}$$

and using $K^2 = E\mathcal{G}$ provides the value of K. Adjustment of the small length correction a_0 with the aid of several direct observations of C_0 permits approximate representation of K across a substantial range of crack lengths. Because of the relatively large compliance of the specimen, a careful experimental calibration for improved accuracy is not difficult.

From study of the way beam-stiffness factors influence Eq. (54), it can be seen that the beam depth contributes only in terms of its value near the leading edge of the crack and that a tapered contour, with bear depth increasing in the direction of crack extension, can be devised such that the coefficient of P^2 in Eq. (54) is held at a constant value. Tapered specimen contours of this kind have been developed by Mostovoy and Ripling.[52] For these specimens, the $\mathcal{G}$ or K values depend only on the applied load and do not depend on the length of the crack.

Reference 51 discusses applications of specimens similar to that of Fig. 7.6 in studies of separational behavior of adhesive joints. For a layer of relatively low-modulus adhesive between two metal bars, x-direction strains in the direction of crack extension are suppressed. Thus the stress σ_y normal to the adhesive layer readily dominates in controlling orientation of the tensile crack. Unless the interface regions are weak, the crack moves straight ahead nearly at the midpoint of the layer thickness. Usually the load-displacement speed can be adjusted so that crack extension consists of a series of abrupt run-arrest sequences. As many as a dozen or so samplings of the K value for onset of rapid fracture and of the K value for crack arrest can sometimes be obtained with a single specimen.

A specimen that permits repeated observations of K for onset and arrest of rapid fracture is of natural interest for studies of crack extension in metals, particularly for the rate-sensitive metals. However, unless a very stiff specimen is used with the beam depth large relative to crack size, the desired path for the crack, straight-forward along the plane of the initial starting crack slot, is unstable. For specimens similar to that of Fig. 7.6, σ_x is so large compared with σ_y at a short distance from the crack that a slight turning of the crack from the line of symmetry is enough to start a cracking path that breaks off one arm of the specimen.

By machining the faces of the specimen along a strip containing the symmetry plane, a situation similar to that for the adhesive layer between metal bars can be restored. Essentially the σ_y/σ_x ratio can be increased sufficiently in this way so that the stress system controls and the crack plane lies in a region near the middle of the reduced-thickness strip.

Face grooves of moderate depth (10% of specimen thickness or less) and moderate sharpness (0.1-mm root radius or more) have seemed to improve the abruptness of onset of rapid fracture for K_{Ic} testing of single-edged notched tensile and bend specimens. For face-notched specimens of these types, the test result K value is simply the K computed without regard to the face grooves multiplied by the square root of B/B_n, where B_n is the specimen thickness at the crack plane.

Use of face grooves with double-cantilever specimens requires more careful study. In addition to reducing the size and influence of shear lips, the face groove is expected to control the direction of crack extension. These are two separate tasks and must be done in a cautious manner relative to the following points:

1. The compliance calibration (or two-dimensional analysis) furnishes the average of $\mathcal{G}$ across the specimen thickness at the leading edge of the crack. The total strain-energy release rate can be divided by the reduced-section thickness to obtain the $\mathcal{G}$ value applicable to the leading edge of the crack under observation with about the same accuracy as for situations with no face grooving as long as the crack front maintains a normal shape. A normal crack-front shape for plane strain would lead slightly at midthickness in a way corresponding to the anticlastic curvature of the crack surfaces. If the face groove is very sharp and produces a crack front leading at the side boundaries, there are several barriers to clear interpretation of results. One of these is the need for a three-dimensional analysis, which is currently not available.

2. Unless the reduced-section thickness B_n is greater than $\alpha_0(2r_Y)$ (plane-stress), a significant elevation of toughness from thickness reduction yielding may be present. The value of α_0 needs to be investigated. For deep notches, a probable result would be $\alpha_0 = 3$.

3. The effects of too much depth and sharpness of the face grooves and too little net-section thickness tend to offset one another in their contributions to the formally computed K value. Thus comparisons showing K_{Ic} from deeply face-grooved specimens equal to K_{Ic} from large test specimens (known to be of adequate size for plane-strain control of test results) do not prove that the face-grooved specimens are testing the material in the desired manner. Thickness-reduction yielding may have occurred far enough in advance of the crack so that test results are influenced by a nontypical distribution of plastic strains. In addition, the crack-front shape may require a different stress analysis than the one usually assumed, as suggested in item 1.

7.5.4 General Aspects of Dynamic-Crack Stress-Field Analysis

A stress distribution was published by Yoffe[53] for a two-dimensional crack of constant length 2a moving at a fixed crack speed in an infinite solid with the tension σ acting normal to the crack at infinity. The value of K for the leading edge of this crack was $\sigma\sqrt{\pi a}$, the same as for the similar static problem. Since Yoffe's analysis was based on crack-closure action proceeding at the same speed as the opening process, the usefulness of this solution was not at first clear. However, after some study it can be seen that the prediction from Yoffe's analysis that the limit to the speed of a crack fixed by inertia is the Rayleigh wave velocity is generally correct. A stable crack speed higher than this would not be possible because a fixed pattern of crack-opening displacements could not then advance as fast as the leading edge of the crack. Thus the limiting velocity of a brittle crack from purely inertial limitations is about $0.9c_2$, where c_2 is the elastic shear-wave speed. In addition, the pattern of stresses and strains very close to the leading edge of the Yoffe crack can be assumed to apply generally to a running brittle crack because this stress field is dominated by the leading-edge stress singularity local to the region under consideration. In the dynamic leading-edge stress pattern the principal change from the static pattern is a tendency for the maximum value of σ_y, at about $\theta = 60°$ from the crack plane, to become more pronounced with increase of crack speed. The change is gradual and no alterations worth attention occur when the crack velocity is below $0.4c_2$.

The highest crack velocities so far observed[9] were found in nearly pure silica glass and were about $0.6c_2$. More often the limiting velocity is about $0.5c_2$ and is far enough below $0.9c_2$ so that only a moderate dynamic influence can be found in the calculated stress pattern for cracks moving at maximum real crack speeds. For low-velocity cracks, less than 3000 ft/sec for steels, the elastic stress pattern around the plastic zone of the crack does not differ from that for a stationary crack in tension.

In concept, the stresses near a running crack in a structural component might be found in the following way. The leading-edge stress

pattern (dominated by the singularity terms) could be assumed to be given by the Yoffe solution. This pattern would have a one-parameter K value characterization. A small circle would be drawn around the crack tip to establish a boundary for the assumed crack-tip stress field, and then stress waves (in the y direction, primarily tensile unloading waves) from the crack-tip stress field and wave reflections would be constructed from the boundaries in sufficient detail to establish the K value for the crack. No accurate solution of a problem of this nature is known.

Such analytical study as has been given to practical dynamic-fracturing problems — for example, crack arrest studies in large welded test plates — has been of the static kind. There is some evidence from data consistency that errors from not using a dynamic treatment have been relatively small. These observations are discussed in Section 7.5.7.

For the running crack, the inertia of surrounding plate material delays interaction of the crack-tip stress field with the points of load application and specimen boundaries. The effect of this delay is a moderate reduction of the K value below the static estimate. Essentially the plate material inertia provides a short-specimen fixed-grip condition to a partial degree. Subsequent reflection of tensile unloading waves might add positive increments to K if free boundaries existed directly above and below the crack. However, such a situation is not expected for the tensile direction of loading.

After arrest of the crack, restoration of the original load results in a total stress-field energy in the structure larger than the original amount. Suppose the total energy consumed in crack extension is $U_W + U_L$, where U_W comes from the weld residual-stress field and U_L comes from the superimposed stresses due to loads on the structure. Roughly the increase of stress-field energy in the structure is U_L, and the loading forces have added twice U_L during a short period following crack arrest. During this time period the K value must change from a dynamic-arrest value, somewhat lowered by the inertial effects, to the static value. Occasionally several arrest markings are visible close to a position of final arrest; this suggests that added crack extension may occur during the transient time interval prior to the final static stress distribution.

In summary, static methods of analysis serve well enough for purposes of estimating the crack arrest possibilities in a structure. The error from not using a dynamic analysis method is probably small and probably conservative. Run-arrest segments of crack extension comparable in size to the wall thickness would not be expected in carefully fabricated boiling-water and pressurized-water reactor pressure vessels. This phenomenon requires a local region of large residual tensile stress, say from welding without stress relief, or a substantial local region where resistance to crack extension has been lost for some reason (for example, an extensive concentration of undesirable impurities). Both conditions should be eliminated by fabrication and inspection controls, as discussed in Section 7.1 of this chapter.

7.5.5 Fracture-Process Zone, Time-Rate Effects, and Minimum Fracture Toughness

The term "fracture process zone" is used here for the region at the leading edge of the crack within which small separational elements form and within which plastic-strain conditions critical for their rapid joining develop. The length factor δ seems a large enough estimate of the size of this zone. Krafft's d_T length factor is smaller and is thought of as the spacing of the fine-scale elements of separation.

A rough estimate can be made of a time, t_A, necessary for a substantial degree of temperature equalization across a distance, x_2, in a metal, with the equation

$$t_A = \frac{x_2^2}{\alpha}, \tag{55}$$

where the thermal diffusion coefficient α is the ratio of the thermal conductivity to the product of density times specific heat.

In order to obtain the value of t_A, an opening dislocation, δ, which would be typical for A 302 grade B steel at onset of rapid fracture (plane strain), is used for x_2, and rapid load application in a time of several milliseconds at room temperature is considered. For these conditions $K_{Ic} = 75$ ksi·in.$^{1/2}$ can be assumed. The yield strength is taken as

62 ksi plus 20 ksi for elevation by rapid loading. The sum of these times $\sqrt{3}$ for plane-strain constraint gives σ_Y = 142 ksi. Thus

$$\delta = \frac{K^2}{E\sigma_Y} = \frac{(75 \times 10^3)^2}{30 \times 10^6 \times 142 \times 10^3} = 1.3 \times 10^{-3} \text{ in.} \tag{56}$$

If we assume α = 0.16 cm^2/sec = 0.025 in.^{2}/sec, it is found that

$$t_A = \frac{(1.3 \times 10^{-3})^2}{0.025} = 68 \times 10^{-6} \text{ sec} . \tag{57}$$

The resulting value of t_A is so small in comparison with the loading time of several milliseconds that there is assurance that a fracture-process zone comparable in size to δ would be quenched by surrounding metal to an isothermal condition.

For a running plane-strain crack approaching an arrest point in the same metal, a K value of 70 ksi·in.$^{1/2}$ and a minimum crack speed of 50 ft/sec would be reasonable estimates. The estimate of loading time for a zone of size δ near the leading edge of the running crack will be approximated as δ divided by 600 in./sec. Because of the shortening of the loading time, σ_Y is estimated as $\sqrt{3}$ (62 + 40) = 178 ksi. Thus

$$\delta = \frac{(70 \times 10^3)^2}{30 \times 10^6 \times 178 \times 10^3} = 0.92 \times 10^{-3} \text{ in.} \tag{58}$$

and

$$t_A = 34 \times 10^{-6} \text{ sec} . \tag{59}$$

However, the loading time is only

$$\frac{0.92 \times 10^{-3} \text{ in.}}{600 \text{ in./sec}} = 1.5 \times 10^{-6} \text{ sec} . \tag{60}$$

This time is so short compared with t_A that there is assurance that thermal

gradients will be maintained corresponding to differences in local plastic work across dimensions in the metal substantially smaller than δ.

Use of d_T in place of δ in the preceding illustrations would not have changed the conclusions. For metals, quite generally, the most rapid loadings feasible with testing equipment (2 msec for fast hydraulic testers and 0.2 to 0.5 msec for drop-weight and Charpy impact testing) are not fast enough to prevent quenching of the fracture process zone of the stationary crack to an isothermal condition. In contrast, the smallest speeds that have been observed for cracks approaching an arrest in a rate-sensitive steel are equivalent to loading times so short that the fracture-process zone has an adiabatic thermal condition down to length factors as small as d_T.

The running crack approaching a crack-arrest point and a stationary crack approaching instability due to rising tensile load are clearly different in terms of thermal conditions. Nevertheless, a strain-rate comparison is of some interest. Section 7.3 of this chapter discussed the characterization of the fracture-process zone in terms of an average strain concept, ϵ_1. It will be assumed that attention can be restricted to the fracture process zone and that only the strain rate pertaining to ϵ_1 need be considered. For this purpose the relation suggested by Krafft serves well enough. Thus the critical strain, ϵ_1, for the fracture process zone is represented in the form

$$\epsilon_1 = \frac{K}{E\sqrt{2\pi d_T}} . \tag{61}$$

For a K_{Ic} test conducted with a linear increase of load with time up to the fracture point, the strain rate, $\dot{\epsilon}$, is given by

$$\dot{\epsilon} = \frac{\epsilon_1}{t} = \epsilon_1 \frac{\dot{K}}{K_{Ic}} . \tag{62}$$

As noted in Section 7.3, other representations of ϵ_1 are possible. An averaging procedure that would predict proportionality of ϵ_1 to K^2 could be shown. However, this would merely insert a factor of 2 in the

numerator of the last term of Eq. (62), and changes occur slowly enough with strain rate so that a factor of 2 error in $\dot{\epsilon}$ would not be serious in correlation studies.

The strain rate for a crack traveling at some relatively low constant speed, a, is considered next. As in the case of the thermal estimate, the time for elevation of the strain to ϵ_1 at a fixed point approached by the process zone will be taken to be $\delta/\dot{a}$. Thus the strain rate for the running crack becomes

$$\dot{\epsilon} = \frac{\dot{a}\epsilon_1}{\delta} . \tag{63}$$

A match between strain rates for the stationary and moving cracks, except for difference in values of ϵ_1, would occur for a loading time equal to $\delta/\dot{a}$. In the case of the 50-ft/sec crack in A 302 grade B steel employed for a thermal condition illustration, this time was found to be only 1.5 μsec, a factor of 300 smaller than the loading time estimate for a notched-bar impact-fracture test. Actually K value estimates from studies of crack arrest in strain-rate-sensitive steels do not seem to differ from K_{Ic} values derived from notched-bar impact tests, despite the difference in the corresponding estimates of strain rate.

Figure 7.7 provides a concise summary of plane-strain crack extension behavior in schematic form. A solid curve and a dash-dot curve show the fast, stable and slow, stable regimes in terms of log a as a function of log $\mathcal{G}$. The vertical line segment forming the lower left portion of the solid curve represents the tendency for crack arrest in rate-sensitive materials to occur abruptly from a certain minimum velocity. This vertical portion should be thought of as a stretched-out end point of the fast, stable regime. Crack extension is stable only where the slope of the line is positive and finite. In terms of a loading-speed scale at the right of the graph, log 1/t, the dashed line represents the tendency of $\mathcal{G}_{Ic}$, for onset of rapid fracture, to decrease with increase of strain rate. All the behaviors are for a fixed temperature. With increase of temperature the slow, stable curve would tend to shift upward, while the

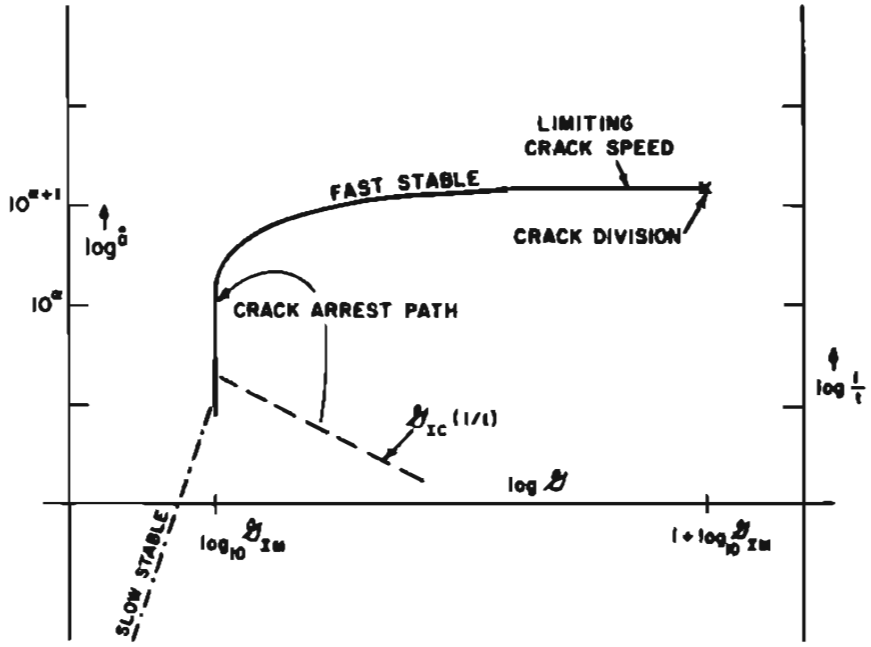

Fig. 7.7. Crack Extension Behavior as a Function of the Force, $\mathcal{G}$, at a Fixed Temperature.

fast, stable and $\mathcal{G}_{Ic}$ curves would shift to the right. For a rate-insensitive metal, such as 7075-T4 aluminum, the $\mathcal{G}_{Ic}$ curve would coincide with the left vertical portion of the solid curve, which would then not shift appreciably over the temperature range of rate insensitivity.

For tests of layers of epoxy adhesive between metal bars in the double-cantilever specimen form, the crack speed has been measured with vibration-induced ripples on the fracture surface,[52] and the observed behavior corresponds to the crack-arrest curve shown in Fig. 7.8. The load-time curves for these tests showed a saw-tooth appearance. Each run-arrest burst produced a vertical segment of load drop that was followed by an upward slanted reloading line to the next instability point. With increase of loading speed a record could be produced showing no load change discontinuities, while the fracture surface still exhibited arrest markings. This means that the values of $\mathcal{G}$ (or K) for onset and arrest of rapid fracture had become very nearly equal. In terms of Fig. 7.8 this means that the $\mathcal{G}_{Ic}$ line, extended to high enough loading speeds, was meeting the vertical end-point portion of the fast, stable behavior curve.

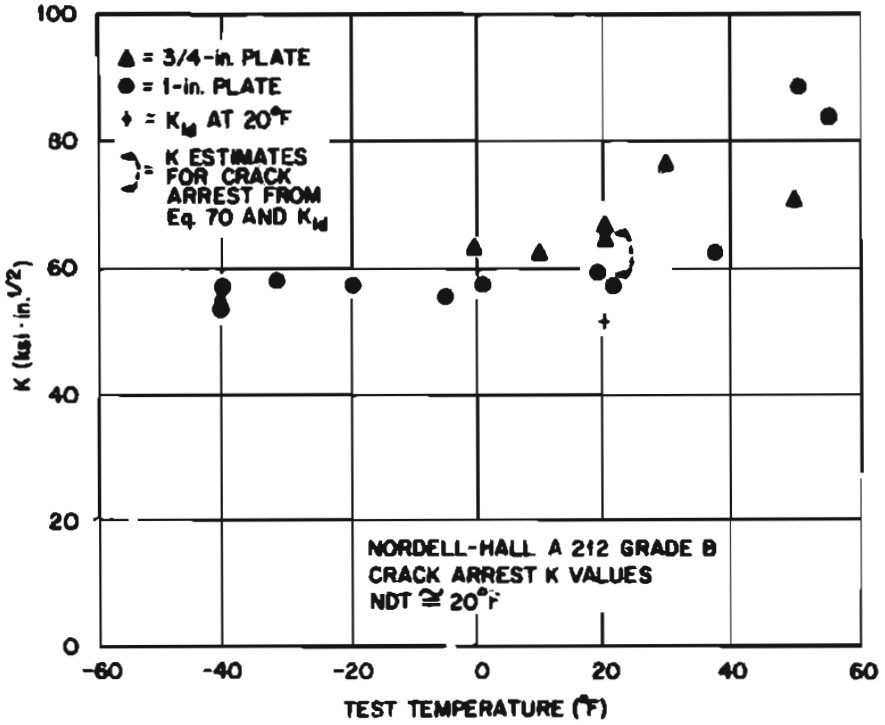

Fig. 7.8. Crack-Arrest K Values from Wide-Plate Tests.

It would be most reasonable to expect rate-sensitive steels to behave in a similar manner. Evidence for this will be discussed in a later section. For strain-rate sensitive steels, the evidence suggests that a loading time about equal to that for a notched-bar impact-fracture test is fast enough to reduce the fracture toughness to the minimum value.

7.5.6 Fracture Toughness in Relation to Plastic Flow Properties

The two plastic flow properties of primary interest in relation to fracture are yield strength and strain hardening. These may be measured and represented in various ways. The yield property wanted is that which would serve best in estimates of plastic zone size, such as $2r_Y$. For this use the 0.2% offset uniaxial tensile yield strength, which is most often available, has served satisfactorily.

With regard to strain hardening, the purpose is to assist prediction of fracture-process-zone strain, ϵ_1, as a critical strain for plastic instability. For this purpose it is a natural choice to define the measure

of strain hardening as the exponent n in the equation

$$\sigma_{TS} = \sigma_0 \left(\epsilon_{TS}\right)^n , \tag{64}$$

where σ_{TS} and ϵ_{TS} are the true stress and true strain, respectively. For a uniaxial tensile specimen, this equation predicts that plastic instability will occur when $\epsilon_{TS} = n$. Krafft measures n with small cylindrical compression specimens as a function of temperature and strain rate. To obtain isothermal n values, it is necessary either to avoid adiabatic temperature rise (by step loadings separated by time intervals) or to correct for the effect of the temperature increase.

To compare n values with K_{Ic} values for equal temperatures and strain rates, Krafft assumes

$$\frac{\dot{\epsilon}}{\epsilon_1} = \frac{\dot{K}}{K_{Ic}} = \frac{\dot{\epsilon}}{n} . \tag{65}$$

This amounts to assuming $\epsilon_1 = n$ as the condition for onset of rapid fracture. The justification for this assumption is found in the results. As illustrated in Ref. 29, a comparison on this basis over a wide range of strain rates and temperatures shows that a trend exists for K_{Ic} to vary in proportion to the isothermal n value. Successful trials have been made with a wide variety of steels and several titanium alloys.

Fracture toughness is expected to depend in a joint way on small defects and plastic flow properties. Krafft assumes that the influence of the defects which assist advance separations in the fracture-process zone can be represented by the K_{Ic}/n ratio, a factor assumed to be invariant with temperature and strain rate. This invariance and the simple K_{Ic}/n proportionality are, no doubt, oversimplifications that will receive some modification after closer study. Nevertheless, the large degree of success and the information resulting from this approach provide essential guidance for basic research and for certain practical applications as well.

When a series of σ_{TS} versus ϵ_{TS} curves are made for a ferritic steel at a series of decreasing temperatures, these show regular increases of

yield strength with lowered temperature, but the absolute slopes of these curves after yield are quite similar.[54] The same observation can be made for a series of increasing strain rates when an adiabatic temperature rise is avoided. This means that if the n value measure of strain hardening is known for one of these curves, approximate n values for the other temperatures and strain rates can be estimated on the basis of an inverse proportionality of n to yield strength. Combining this procedure with the idea of a direct proportionality between K_{Ic} and n means that given knowledge of a $K_{Ic}(T_0)$ measured at the temperature T_0, the value of $K_{Ic}(T)$ for the temperature T can be estimated from the relation

$$K_{Ic}(T) = \frac{\sigma_{YS}(T_0)}{\sigma_{YS}(T)} K_{Ic}(T_0) \ . \tag{66}$$

The values σ_{YS} are regarded as 0.2%-offset uniaxial tensile yield strengths for the strain rates pertaining to the K_{Ic} tests. Use of Eq. (66) over a very wide range of temperatures and strain rates would not serve well because Krafft's studies show a closer degree of proportionality of K_{Ic} to n than to $(\sigma_{YS})^{-1}$. Trials indicate that Eq. (66) estimates of the increase or decrease of K_{Ic} due to a ±60°F temperature change do not show appreciable error. When the range is extended to ±120°F the results tend to be moderately conservative.

Investigations of σ_{YS}, for a steel, as a function of temperature and strain rate in the range from very low temperatures to room temperature can be nearly represented by a single curve in terms of a speed-temperature equivalence. In fact, Bennett and Sinclair[55] show that data for a variety of metals with crystalline similarity can be fitted to this same curve by a uniform shift of each curve parallel to the σ_{YS} coordinate direction.

In later sections it will be desirable to estimate σ_{YS} for certain rapid strain rates and at various temperatures from the room-temperature static value of σ_{YS}. A recent report by Wessel, Clark, and Wilson[56] provided measurements of σ_{YS} for two large-thickness plates of A 302 grade B steel and a plate of rotor steel across the temperature range from −320°F to room temperature. From the basic idea in the Bennett-Sinclair paper,

a single curve representation of this data was made.[57] A convenient equation with a good fit to this curve was given by the expression

$$\sigma_{YS}\Big|_{T,t_0} = \sigma_{YS}\Big|_{-100°F,\ t_0} + \frac{14,500\ \text{ksi}}{T + 459} - 40.4\ \text{ksi}\ , \qquad (67)$$

where T is the temperature in degrees Farenheit, and t_0 is the load rise time for static (slow) testing and is assumed for later purposes to be 50 sec.

To estimate the σ_{YS} for a shorter load rise time, t, the temperature-rate equivalence idea leads to the relations

$$\sigma_{YS}\Big|_{T,t} = \sigma_{YS}\Big|_{T',t_0}\ , \qquad (68)$$

where

$$\frac{T' + 459}{T + 459} = \frac{\log\,(2.10^{10}\ t)}{\log\,(2.10^{10}\ t_0)}\ . \qquad (69)$$

The frequency constant in this equation is adapted from Ref. 55.

Equation (67) was written in terms of matching the σ_{YS}-temperature curves at −100°F. This is better than matching the curves at 70°F because it eliminates effects of strain aging. If the reference temperature is changed to 70°F, the negative term at the right of the equation becomes −13 ksi. Primarily, Eqs. (67), (68), and (69) are intended for use in estimating dynamic yield values at various temperatures in a simple way. It is not possible to include effects of strain aging without a large increase of complexity in the equations. Correspondingly the tendency of Eq. (67) to predict static σ_{YS} values above 0°F that are somewhat low was thought not to be harmful.

A recent paper by Corten and Shoemaker[58] suggests that correlation of K_{Ic} values over a range of temperatures and strain rates might be simplified by going directly to a rate-temperature parameter approach, such as that used by Bennett and Sinclair,[55] for correlation studies of yield strength. Reference 58 notes that an approximate proportionality

of K_{Ic} to n can be implicit in this method and that an n-value-independent relationship of K_{Ic} to σ_{YS} can, in this way, be included.

The most prominent influence of plastic flow properties on fracture toughness is the brittle-ductile transition introduced when the crack-tip plastic zone becomes comparable in size to the dimension of the part parallel to the leading edge of the crack. This was discussed previously. Because of material and testing-machine limitations, the critical K for onset of rapid fracture, which is measured and reported often, contains some elevation above K_{Ic} due to plane-stress yielding. If these results correspond to β_c less than π, approximate values of K_{Ic} can be obtained from the relationship,[17]

$$K_c^2 = K_{Ic}^2 \left(1 + 1.4\, \beta_{Ic}^2\right) , \tag{70}$$

where

$$\beta_{Ic} = \frac{1}{B}\left(\frac{K_{Ic}}{\sigma_{YS}}\right)^2 . \tag{71}$$

The use of Eq. (70) to predict K_c from a given value of K_{Ic} is subject to a larger uncertainty than its use in the opposite way. However, if conditions representable as $\beta_c < \pi$ or $\beta_{Ic} < 1$ are met, the error of a K_c value obtained in this manner should be of tolerable smallness in relation to other uncertainties.

A variety of estimation relationships have been reviewed in this section because their employment has proved to be useful in checking the general consistency and meaning of fracture-testing information of many kinds from a variety of sources. Readers should not infer that these relationships are preferable to possession of the accurate test information, absence of which motivates their use.

7.5.7 Dynamic Fracture-Toughness Measurements and Fracture Transition Temperature Tests

Figure 7.8 shows results of crack-arrest observations by Nordell and Hall[59] for 1- and 3/4-in.-thick plates of A 212 grade B steel. At

the NDT temperature of this material, 20°F, the plastic-zone size factor, $2r_y$ (plane stress), is about 1/3 in., which is small enough for the shear lip borders of the fracture to be small but large enough to allow some plane-stress elevation of the K value. The fact that the results show negligible temperature effect below 0°F may not be significant, because only a small range of temperatures was covered. The upward trend of the crack-arrest K values above 20°F is due to the approach to the midrange fracture transition conditions expected at about 85°F. These results may be compared with an estimate of a rapid load K_{Ic} from the small-flaw drop-weight impact tests used to find the NDT value for the plate material.

The critical section for the fracture produced in NDT temperature testing is shown in Fig. 7.9. The bar is broken in drop-weight impact bending with a notched brittle weld on the tensile side to serve as a representative small flaw. In original concept the NDT separated the temperature region in which a flat break occurred from the higher temperature region in which noticeable platic bending accompanied separation. In the course of test development and standardization, it was convenient to make use of the rapid increase in tendency for arrest of lateral cracking, with increase of temperature, through the region of the NDT. Thus stops were used under the bar that made these arrests positive, and the failure or success of arrest is critical to the test result. However, in the analytical interpretation it is best to return to the original idea.

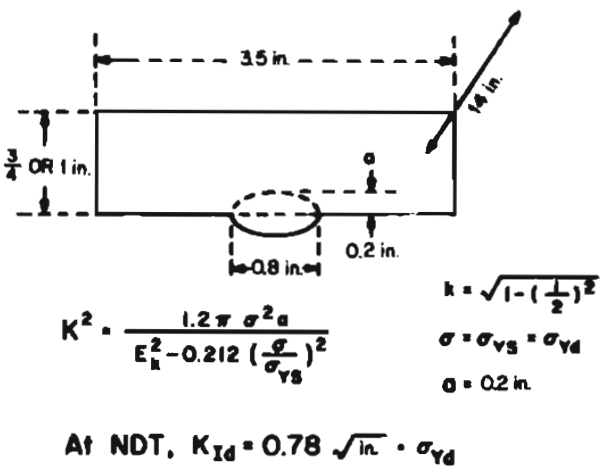

Fig. 7.9. Schematic Diagram of Fracture Section of NDT Test Specimen.

As the specimen bends, the notched brittle weld bead produces a small partly through starting crack. If propagation of this crack occurs prior to yielding at the tensile surface, the quick motion of the crack causes separation without noticeable plastic distortion. At temperatures 10 to 30°F above the NDT temperature, tests with the stops removed have shown that plastic bending does occur. At the NDT temperature, the stress level for crack propagation is very nearly the dynamic yield stress for the plate material, σ_{Yd}. By making a fixed arbitrary estimate of the size and shape of the small starting crack, use of the equation for a semi-elliptical surface crack, as indicated on Fig. 7.9, gives the result

$$K_{Id} = 0.78 \text{ in.}^{1/2} \sigma_{Yd} . \tag{72}$$

Examination of typical fractured NDT specimens (by G. Irwin and P. Puzak at Naval Research Laboratory) suggested that dimensions about as shown in Fig. 7.9 could be justified in terms of hesitation lines seen on the fracture surfaces. These dimensions might be adjusted moderately, but the magnitudes given lead to K values that are, so far, consistent with other experimental evidence. The result from Eq. (72) is a K_{Ic} value. However, it might be helpful to have a special designation for the dynamic crack arrest or rapid-loading K values, which are considered to represent minimum fracture toughness of the material at the testing temperature. The suggested designation is K_{Id}.

The room-temperature σ_{YS} for the material of Fig. 7.8 was reported as 36 ksi. Assuming a loading time of 0.5 msec for the NDT tests and a loading time of 50 sec for static (slow) measurement of σ_{YS}, use of Eqs. (67), (68), and (69) results in σ_{Yd} = 60.4 ksi at the NDT temperature, which was 20°F. Thus the prediction from Eq. (72) becomes

$$K_{Id} = 0.78 \times 60.4$$

$$= 47.1 \text{ ksi}\cdot\text{in.}^{1/2} . \tag{73}$$

The values of β_{Ic} for 0.75- and 1.0-in. plates were therefore 0.81 and 0.61, respectively. Using Eq. (70) to estimate the toughness elevation due to plane stress yielding results in K values of 65 ksi·in.$^{1/2}$ for

0.75-in. plates and 58 ksi·in.$^{1/2}$ for 1.0-in. plates. These values agree with the tests results in Fig. 7.8 somewhat better than might be expected, particularly since neither the Nordell-Hall calculations nor the estimates developed here for comparison have an accuracy likelihood greater than about 10% in the K value.

At the Materials Research Laboratory (Richton Park, Illinois), measurements by Ripling and Crosley are in progress with the objective of K_{Id} determinations from rapid hydraulic loading and a tapered double-cantilever specimen. The procedure employs a rapid loading surge superimposed on a moderate initial tension on the specimen. Figure 7.10 shows a set of results that was informally available in October 1966 for specimens of A 302 grade B steel. The estimate of K_{Id} from NDT was uncertain because results of direct NDT testing of the material were not available. From the yield strength and the fact that the material was from a large-thickness plate, an NDT temperature of 20°F was selected for comparison purposes. The estimate of K_{Id} for this choice of NDT is 70 ksi·in.$^{1/2}$. Assuming inverse proportionality of K_{Ic} to yield strength provided the

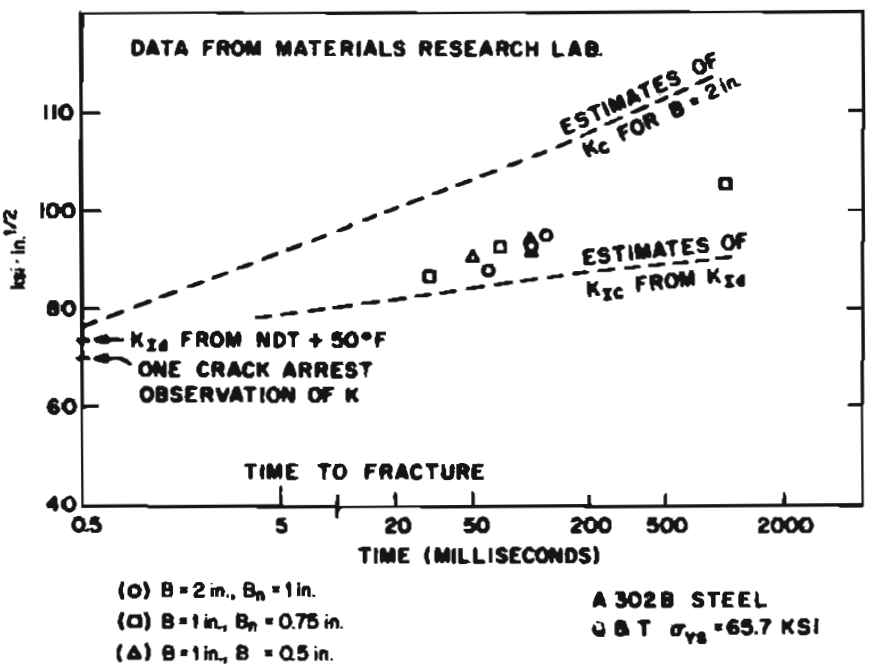

Fig. 7.10. Rapid Load K_{Ic} Values from Face-Notched Double-Cantilever Specimens (Ripling and Crosley).

lower dashed curve of Fig. 7.10. The measured results lie not far above this curve.

In order to consider whether the specimens were of adequate size, values of $2r_Y$ (plane stress) are needed. At a 0.5-msec load-rise time the value of σ_{Yd} is estimated as 85.5 ksi. With K_{Id} estimated as 74 ksi·in.$^{1/2}$ at 70°F, the value of K_c based upon B = 2 in. for 70°F is 81 ksi·in.$^{1/2}$. From this, the value of $2r_Y$ (plane stress) is 0.29 in. At a 50-msec load-rise time, $2r_Y$ (plane stress) has increased to 0.38 in. For a net section thickness three times $2r_Y$ for adequate constraint, the size of the 2-in.-thick test specimen used in the Ripling-Crosley tests was marginal. However, the specimen size is close to that desired, and the results correspond to expected behavior relative to loading time. Thus some confidence can be placed in estimating the 70°F value of K_{Id} to be about 74 ksi·in.$^{1/2}$.

Several crack-arrest events were noted during the tests discussed above. Only for one of these was the load for crack arrest indicated clearly enough to permit a calculation. The result of this single arrest trial provided a K_{Id} value of 70 ksi·in.$^{1/2}$.

Figure 7.11 shows K_{Id} values estimated for HY-80 steel at the NDT temperature (−150°F), at NDT temperature plus 60°F, and at NDT temperature plus 120°F. Fragments of comparison data were available from Lehigh University[60] and (informally) from Krafft. The experiments at Lehigh University were tests of a wide 1.75-in.-thick ship-steel plate. The test plate contained a rectangular welded insert of HY-80 steel in line with the crack starter slot for a trial at crack arrest. At 0°F, one trial gave a successful arrest. In a second trial, with the crack much longer at the arrest position, the HY-80 steel separated with a ductile fracture, and no arrest was observed. Rough estimates of the minimum K_c value for crack arrest in the first trial were possible. The conversion to K_{Ic} gave the value 135 ksi.in.$^{1/2}$ as a minimum estimate, and this is shown in Fig. 7.11.

Krafft's measurements of K_{Ic}, indicated by the symbol K in Fig. 7.11, were made with slow-speed loading at −320°F. An n coefficient estimate of the static K_{Ic} at −220°F was available and is shown as the point S in Fig. 7.11. The short vertical line to the right of S indicates the

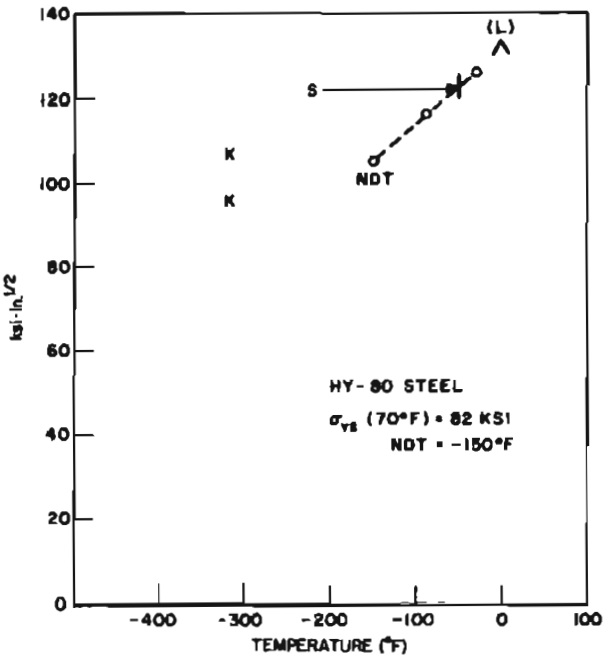

Fig. 7.11. Fracture Toughness Estimates for HY-80 Steel.

temperature at which σ_{Yd} for HY-80 would be expected to equal the static σ_{YS} at −220°F. Thus the estimate of K_{Id} from the point S is in close agreement with the estimates of K_{Id} from the NDT measurement. Results of a direct measurement of NDT for the material used in the Lehigh University tests were not available.

The toughness indicated by the crack-arrest trials discussed above is encouraging. A room-temperature fracture toughness above 140 ksi·in.$^{1/2}$ may be required for a fracture-safe 12-in.-wall nuclear reactor pressure vessel. This would seem to be obtainable with steels having a toughness quality similar to that of HY-80 steel.

A variety of crack-arrest tests have been employed for crack toughness evaluations led by work of this nature by Robertson at the Admiralty Construction and Repair Establishment. These are well summarized by Tipper.[61] Generally the procedure consists in rapid application of wedge-opening forces to a sharp notch in the specimen. The notched region is chilled to a low enough temperature for brittle fracturing. The balance of the specimen may be held at a fixed gradient of temperature rise. Alternatively, the temperature of test portions of the plate may be placed at a series of uniform temperatures in a sequence of tests. Variations

of superimposed tension permit finding a relationship between the machine tensile load and the temperature for successful arrest of the crack. Although, in concept, a fracture-mechanics analysis of these tests might be used to determine the K value for crack arrest, the testing plans do not provide for control and measurement of the applied forces to a degree adequate for such calculations. Crude estimates of the wedge-opening forces for certain SOD (Standard Oil Development) tests of 3/4-in. ship-steel plates were made by Wells,[62] and values of K (for crack arrest) were found that agree roughly with those of Fig. 7.8.

By standardization of lateral test dimensions and restriction of testing to a limited range of plate thicknesses, crack-arrest tests have served quite usefully for comparative assessments of crack toughness. The recommendations therefrom regarding safe range of operating temperature are generally similar to those from NDT testing.

The test most used for assessment of fracture toughness on a transition-temperature basis is the Charpy V-notch test. So much information has been collected in this form that an attempt at its use for K_{Id} estimates seems desirable, even though the foundations for such estimates are far from ideal.

The definition of Charpy V-notch transition temperature that seems best for analytical purposes is the FATT, the temperature at which the side border shear regions occupy half of the fracture surface. Use of a test result corresponding to greater brittleness, say, the 12 ft-lb temperature, seems undesirable because this is known to depend on notch sharpness and shifts to considerably higher temperatures when a fatigue crack is used at the notch root. The energy level in regions less sensitive to notch sharpness can be used in terms of an analysis suggested by Wells.[63] This provides a plausible K_c-type estimate but one which is too far from plane strain to permit use of Eq. (70) to derive a value of K_{Id}. The fracture appearance itself is not truly indicative of relative plastic-zone size because the run of the crack is too short relative to specimen thickness and does not permit the shear-lip development that would be found in a long crack traversing an equal thickness plate of the same material.

Two facts that do appear useful are the following:

1. The Charpy V-notch FATT corresponds generally to a 50% shear fracture appearance for a low-velocity crack in steel plates of 3/4- or 1-in. thickness. By assuming $\beta_c = \pi$ for each of these two thicknesses, the proportionality of K_{Id} to σ_{Yd} can be estimated from Eq. (70).

2. The Charpy V-notch FATT is often not far from the NDT temperature plus 60°F. From Eqs. (66) and (72),

$$\left(\frac{K_{Id}}{\sigma_{Yd}}\right)_{\text{at FATT}} = 0.78 \text{ in.} \left(\frac{\sigma_{Yd \text{ at NDT}}}{\sigma_{Yd \text{ at FATT}}}\right)^2 . \tag{74}$$

Trials of (1) and (2) above with data typical for A 212 grade B, A 302 grade B, and HY-80 steels suggested that an approximate estimate of K_{Id} at the FATT is given by

$$K_{Id} = 0.95 \text{ in.}^{1/2} \sigma_{Yd} . \tag{75}$$

Except for flaw statistical considerations, K_{Id} is a thickness-independent fracture-toughness property of the material which, for steels, increases in a regular way with temperature. Transition-temperature results from Charpy V-notch (or NDT) testing can be thought of as assessments of the temperature at which $\left(K_{Id}/\sigma_{Yd}\right)^2$ achieves a value within a certain size range. Use of transition temperature for judging fracture toughness in comparative terms is not, in general, misleading to the metallurgist in his efforts to improve the toughness of the material. Caution is required, however, in applications to design. As the yield strength increases, a design stress that is proportional to the static yield strength becomes a larger fraction of σ_{Yd}. Thus some flaw tolerance is lost, even if the transition temperature remains unchanged. Influences of thickness are discussed in Section 7.6 of this chapter.

Extension of K_{Ic} testing to very large bend tests and to rapid loading has been under discussion and has achieved various degrees of development at a number of laboratories. Progress has been steady but slow due to the expense of equipment and specimens. A paper giving initial exploratory results was published by Raden and Turner.[64] Their work was

at Charpy bar size, but it illustrated successful use of the striking tup as a dynamic weigh bar to furnish load-time records necessary for K value calculations. Similar work across a range of sizes is in progress at the Naval Research Laboratory.

More study has been given to K_{Ic} testing of very-high-strength steel, aluminum, and titanium alloys than to the rate-sensitive steels of interest for boiling-water and pressurized-water reactor pressure vessels. However, the testing deficiencies are not in the areas of concepts and analysis so much as in matters of equipment and technique. The vessels of interest will be designed sufficiently below the level for general yielding that the fracture prevention problem largely concerns plane-strain toughness properties and crack situations for which existing methods of fracture mechanics analysis are suitable.

The high values of $(K_{Ic}/\sigma_Y)^2$ of interest indicate that rather large specimen sizes will be required, precracking of the notches will be more difficult, and some testing problems no doubt will develop that are not at present foreseen. Within a given size limitation, K_{Ic} values can be measured across a range of loading speeds and up to higher temperatures for dynamic than for static loading. There are also interpretation difficulties in practical applications. For example, the relative usefulness of static and dynamic fracture toughness is in question with nuclear reactor vessels. However, the entire subject has advanced greatly since the 1955–1960 period. During that period three major fracture problems (de Haviland Comets, heavy-section rotating parts of large steam turbine-generators, solid propellant rocket chambers) assisted fracture-mechanics testing developments and at the same time benefited therefrom. Hopefully, the concern over the vessels of interest for this report will contribute and benefit in a similar way relative to rate-sensitive high-toughness metals.

7.5.8 Comments on Crack-Opening Dislocation Measurements

In previous comments, attention was drawn to the analytical usefulness of the small length factor, δ. This is perhaps better called "crack-opening dislocation" than "crack-opening displacement." The former term

has been used at times by Wells and avoids confusion with crack-opening measurements at other positions than the actual leading edge of the crack. If a sharp fatigue crack is used at the leading edge of the crack-representing notch in the specimen, some slow crack growth cannot be avoided, even under plane-strain conditions. Thus it is not clear how a direct measurement would cope with the gage-positioning problem. In addition there would be the normal irregularities of the fracture surface.

In trials of direct measurement of δ, attention was given primarily to rate-sensitive structural-grade steels. The leading portion of the notch was a jewlers hack saw cut with no fatigue-crack extension.[65] It can be argued that under conditions of moderate ductility the notch sharpness would not cause a significant difference in the fracture load. Static testing was used and the temperature range covered did not go far below the region of plane-stress to plane-strain fracture transition. At these lower temperatures the δ value, of the order of 10^{-3} in., became comparable to the limits of measurement precision. The strain-rate sensitivity and the notch sharpness tended to suppress slow crack growth, and the hack saw cut provided smooth surfaces for the gage. For these reasons the results of Ref. 64 are of special value from a model-testing viewpoint.

The results verified that the condition for onset of rapid fracturing could be characterized by a critical opening-dislocation value, δ_c, which was a function of temperature and degree of plane stress. Aside from considerations of elastic constraint, δ_c did not depend on dimensions of the crack and specimen. Comparison of wide-plate and bend test results permitted examination of the accuracy with which δ_c could be estimated from the plastic bend angles of bars that were too small to prevent general yielding prior to fracture.

The preceding work is summarized in Ref. 19. A more recent review, which also contains additional applications of the δ concept in fracture testing, is provided in a current paper by Wells.[63] In this paper Wells derives a method for estimating δ_c from the energy loss measurement of a Charpy impact test. Of special interest is Wells' comment regarding a relationship of δ to thickness reduction. He reports that Burdekin of the British Welding Research Association studied more than 78 measurements

of δ in comparison with thickness reduction (just beneath the notch) and found that they were equal to within a standard error of 20%.

If δ is assumed to be equal to the thickness reduction, the latter should be about 0.013 in. for a steel with a K of 200 ksi·in.$^{1/2}$ and a σ_Y of 100 ksi. In the temperature range 200 to 500°F, values of K_{Ic}/σ_Y of 2 in.$^{1/2}$ or more would be expected for a steel similar in toughness to HY-80 steel. The corresponding thickness reductions would be easily measurable with a precision greater than the fracture-toughness variations inherent in the material. After suitable testing experience, methods of correlation should be possible that would permit use of such measurement results to provide approximate values of fracture toughness in terms of K_{Ic}, as well as in terms of δ_c.

7.5.9 Comments on Load Toughening and Strain Aging

Various testing experiences have indicated that a steel pressure vessel preloaded to a given pressure at a warm temperature will not fracture appreciably below that pressure if subsequently tested at a cold temperature.[66,67] Trials of this nature with precracked tensile specimens by Brothers and Yukawa[68] and by Srawley of the Naval Research Laboratory gave a similar indication on an average basis. The scatter of these results might not encourage absolute confidence in warm preload strengthening relative to low-temperature service. Krafft of the Naval Research Laboratory has noted unexpectedly large values of K_{Ic} in rapid load K_{Ic} testing for occasional specimens that had been accidentally preloaded at a slow speed; this is presumably the same effect as the influence of warm preloading.

Since the nuclear reactor vessels of interest will be used at elevated temperature, it seems that the warm preload would primarily assist a successful proof test. However, if the preloading is done at a temperature well above the service temperature and if the strengthening by crack blunting is verified by a 70°F proof test, confidence in warm preload strengthening is merited. Furthermore a substantial advantage relative to fracture safety during service can be obtained. Sonic monitoring during the preloading might indicate locations of previously unseen flaws.

In addition, the cracks should be more visible to ultrasonic inspection after the preloading than before and a reinspection at that time would be advantageous.

Room-temperature notched-bend-test fractures of mild steel[7] were observed to show a segment of sudden brittle fracture if they were precracked and then left unloaded overnight. No such indication of local embrittlement was found when the specimens were broken within an hour or so of the precracking. Observations of this kind are not uncommon, and the embrittlement is considered to be from the influence of strain aging. In the tests discussed in Ref. 7, brittle fracture segments did not appear at lower loads than those used for precracking. However, in fracture trials directed toward K_{Ic} testing, Turner (at Imperial College, University of London) found that a specimen with a notch that had been compressed at room temperature broke at −40°F with a K_{Ic} value of about the magnitude observed for crack arrest in similar mild steels. In this case, the strain aging occurred after compression normal to the fracture plane, and some residual tensile stress was present.

Tests by Mylonas at Brown University and his "exhaustion-of-ducility" concept stimulated several British investigations of compresssive prestrain damage. Tipper[61] showed that a substantial portion of the compressive-strain-embrittlement effect is not due to residual stress by applying 10% compressive plastic strain to a large block of low-carbon structural steel from which Charpy specimens were later made and tested. When the fracture plane was normal to the direction of compression, the results showed a substantial increase of transition temperature. The original toughness was restored by stress-relief heat treatment. It seems significant that fracture planes parallel to the direction of compression showed only a relatively small increase of transition temperature.

Although steels differ in their strain-aging tendencies, a significant influence on fracture toughness would not be expected for plastic strains less than three times the yield strain regardless of material or fracture plane orientation. General yielding of this order, say at the throat section of a pressure vessel nozzle, would not be harmful unless a crack was already present. A substantial amount of strain aging would,

then, occur in the local regions close to the leading edge of the crack. During unloading the material closest to the leading edge receives some reverse plastic straining in compression. Thus, greater damage is expected if the strain aging occurs mainly after rather than before unloading.

A question of interest to thick-walled nuclear reactor pressure vessel safety concerns whether an abnormal fatigue or stress-corrosion crack growth should be expected due to strain-aging embrittlement. Answers to this question should be sought experimentally. The crack growth per cycle observed experimentally could be compared with the size of the crack border strip in which substantial amounts of reverse plastic straining are predicted by analysis.[27]

7.6 FRACTURE CONTROL PLANS

7.6.1 Elimination and Slow Growth of Defects

Among the cracks or sharp reentrant notches present in a large structure after initial inspections and repairs, a single remaining "worst flaw" would be difficult to select. Granted that all cracks could be clearly "seen," a substantial number might appear comparably dangerous because of judgment uncertainties that would require disproportionate time and new information for settlement. Real inequalities would doubtless exist. However, even if the real inequalities were small, stable crack growth during service would tend to develop large differences in crack size. Because of the high power of K controlling stable crack extension, small differences of size and growth rate are continually amplified so that, eventually, a comparatively few cracks emerge as obvious "worst" defects. From service fracture examinations it is clear that there is never more than one winner of this growth race because the fracture of the structure can always be traced back to a single origin.

Clearly, elevation of the initial fracture strength by the location, grinding out, and repairing of cracks has certain practical limits. Removal of the huge cracks found by inspection is obviously necessary and

helpful. In the smaller range of crack sizes, questions of necessity of repair arise that depend on a number of considerations. At some point the possible damage introduced by the repair practice itself becomes a limiting factor.

The reliability of the structure is greatly improved by improvements in the clarity with which cracks and localizations of impurities are seen by inspection techniques. This reduces the seriousness of the worst remaining overlooked defects and permits sensible decisions regarding repairs. However, even if all crack-like defects were clearly seen there would be a barrier to improvement of assured strength in terms of judgment uncertainties. In this regard consideration can be given to methods of using the amplifying effects of slow, stable crack growth to increase the efficiency of the overall inspection process. Inspections during and after proof testing would be of this nature.

If each defect were labeled with some value, S, of the limiting strength it would impose at the end of X_L hours of service use, the frequency of S would increase regularly with S. Inspection, repair, and trial loadings must give assurance that the value of $S_{MIN}(X_L)$ for the very worst defect is above the strength S_0 required in service. This means that $S_{MIN}(X)$, for X at the beginning of operational use, must be well above S_0, because the defects tend to move to smaller S values with increasing hours of service.

The level of $S_{MIN}(X_L)$ that can be regarded as assured by initial testing and inspection tends to reduce with increases of structural size. In part this is simply inherent in the probability aspects. In addition the size and variety of initial defects, prior to inspection, tend to increase with the size and complexity of the structure. Periodic structural inspections, as in the case of commercial aircraft, are very helpful to fracture control. In this practice, it is possible to use the amplifying effects of stable crack growth to assist identification of the most serious cracks. The periodic-inspection type of control is most reliable when stress-corrosion is not of serious importance. After a crack begins to extend with a corrosive type of assistance, the time to the failure point is likely to be less than the period between inspections. Because of uncertainties involved in crack growth-rate prediction,

extension of a fracture control plan to a larger structure is somewhat easier than extension of the plan to a larger value of X_L.

Service fractures due to stress-corrosion crack extension are sometimes observed in which a segment of fatigue cracking from the initial flaw preceded extension with corrosion assistance. Under steady loads with fresh- or salt-water environment, natural cracks produced by fatigue seem to possess a threshold K value below which the corrosive effect does not induce measurable crack extension. Crack-extension rates above this level are rarely studied. Most testing is in terms of total time for the crack to reach propagation size. However, the long times pertain to initial K values that do not exceed the critical K_{ISCC} by an amount that would be significant in reference to large nuclear reactor pressure vessels.

The situation need not be all one of disadvantage in regard to water-corrosion effects. The tough steel selected for use in very large nuclear reactor pressure vessels should be chosen to have a K_{ISCC} (for water environment) not far below the value of K_{Ic}. In this event, with initially much lower K values established by careful quality control, the leading edges of prior cracks might be static long enough for a corrosion-assisted blunting influence to assist continued resistance to crack growth.

7.6.2 Fracture Safety In Relation to Crack Arrest

Problems of crack propagation have received increased attention throughout the recent past in many diverse structures. Although these structures do not have characteristics necessarily similar to boiling-water and pressurized-water reactor vessels, it is of interest to review the measures employed to establish crack arrest in order to assess the applicability of such measures for the vessels of interest here.

The difficulty of arresting relatively large cracks in thin-walled pressure vessels was recognized and extensively studied in connection with the unfortunate fuselage explosions experienced by de Haviland commercial jet aircraft in 1954 (Ref. 69). The critical crack size for sheet material similar to the high-strength aluminum-alloy fuselage covering

was less than the size of a window opening at the stress level expected for 35,000 ft of altitude, even in a flat-sheet situation. Because of inadequate window reinforcements, a small fatigue crack could develop near a corner of a window and, with its effective size enhanced by the poorly stiffened window opening, could attain critical size for propagation before an inspection was likely to reveal its presence. In the investigations following the plane losses, a number of such small fatigue cracks were developed at windows during flight-simulating tests of additional Comet fuselages, and the bursting of these test fuselages occurred from such cracks in consistency with the above failure sequence.

The emphasis of the Comet-inspired investigations was turned from fatigue toward crack-arrest devices by information from United States studies of fracture mechanics,[70] coupled with the following facts. During the history of passenger aircraft aviation the discovery of small fatigue cracks during overhaul has never been uncommon. The de Haviland Comet fuselage sheet material was similar in toughness to the United States 7075-T4 aluminum alloy. Previous airplane material experience both in England and the United States was primarily with the much tougher 2024-type aluminum alloy. When 7075-type material is used in place of 2024-type material at the same percentage of the yield strength, the combined influence of higher working stress and less toughness is nearly a factor of 10 in terms of critical crack size for crack propagation. The fatigue-crack growth rate is increased roughly by a factor of 6 for equal size cracks. Clearly the safety of passenger planes prior to 1954 depended more on overhaul inspections and the long service life necessary to grow very large fatigue cracks to critical size than on elimination of fatigue cracking.

In the 1953–1957 period at the Naval Research Laboratory and the National Advisory Committee for Aeronautics the stresses for propagation of given size cracks in flat sheets of plastics and high-strength aluminum were compared with the critical hoop membrane stresses in cylindrical sections of these materials containing similar size axial cracks and subjected to internal pressure. The stress-elevating influence of outward bulging of the crack section (due to the internal pressure) was quickly recognized. The effect increased with crack length. By using a lubricated

(and strong) cylindrical cover over the cracked portion of the test cylinder, the nominal hoop stress for crack propagation in the cylinder could be made the same as the nominal stress on the flat-plate specimen in tension for the same size crack. No effort was made at detailed stress-analysis explanations of this special aspect of cracking behavior. However, the magnitude was so large (as much as a factor of 10 in effective critical size) that the outward bulging effect on propagation of long cracks in pressure vessels has been consistently emphasized in Naval Research Laboratory technical papers.[47,70,71] For the arrest of a long crack in a pressurized container by a riveted stiffener, an arrangement that would provide a local "flat-sheet" situation, as well as a stiffener-induced reduction of the stress field, was recommended.[70]

A number of United States investigations of bursting strength of containers damaged with various-length through-cracks have shown the long-crack bulging influence discussed above. Thus the results of UKAEA tests, as reported by Nichols,[72] were not unexpected. Of course, 6- to 12-in.-long cracks in a 1-in. wall thickness cannot be accepted as modeling 6- to 12-in.-long cracks in a substantially larger (3- to 12-in.) wall thickness. The increase of effective crack size due to local bulging would be much larger for the 1-in. wall thickness and would be expected to dominate the test results. In addition the modeling would be poor because of differences in elastic constraint of the crack.

A fail-safe crack-arresting fuselage is heavier than one that is not so designed. However, there is some saving in added weight because the customary design provides strong hoop-direction frames. Thus when skin attachments to hoop-direction stiffeners are used for the purpose of arresting longitudinal cracks, the frames customary to the design may be satisfactory for this purpose, except for spacing and the positioning of flanges adjacent to the skin.

In modern jet passenger aircraft, through use of tough (2024-type aluminum) skin material and suitable attachments to frames (or hoop straps), it is possible to arrest cracks with lengths that are several hundred times the thickness of the fuselage wall under service conditions of internal pressure. In the case of an accident starting such a crack, the crack would certainly bulge open, and maintenance of a low-altitude

pressure in the cabin might be impossible. However, the structure would be safe enough for operation of the airplane to a safe landing. This type of fail-safe crack-arrest design is peculiar to the nature of the aircraft fuselage structure.

A thick-walled steel pressure vessel built for internal liquid pressure containment has no natural reason for hoop-direction stiffeners. Furthermore, for the vessels of interest to this report, through-cracks could not be allowed to reach a length large enough for appreciable outward bulging, because this would permit very rapid escape of liquid and hot vapor. The addition of massive external rings at spacings of about two plate thicknesses would certainly improve the wall strength, particularly if these rings were installed so as to exert external pressure on the cylinder wall. Primarily the goal of a fail-safe scheme of this kind would be to suppress outward bulging of the cylinder wall along the region of any long through-crack (in a longitudinal seam weld, for example) and to provide enough strength to support the hoop tension load in event of such a crack. After some years in service the amount of remaining compression under the rings would be uncertain, and crack arrest under the ring would rest on too small a margin of stress difference to deserve any confidence.

The large-scale fracturing of welded ships was blamed in part on the continuity introduced by welding, which permitted a crack to run directly, without reinitiation at rivet holes, from one large plate into the adjacent plates. Separation of longitudinal rows of deck plates with an overlapping riveted connector has been employed with some success as a crack-arresting device. A "tough-strip" crack-arresting device for the same purpose has been proposed. In this plan the riveted connector is not used. Instead the deck plates are joined by welding to a connector of very-high-toughness material, such as HY-80 steel. In either case successful crack arrest depends on the stress-field force driving the crack, which increases with crack length. For a large enough stress-field force, no crack arrestor will be successful. The unsuccessful crack-arrest trial with an HY-80 steel crack-arrest strip, discussed above in Section 7.5.7, merely indicated that the K_{Ic} for HY-80 steel at 0°F was less than 200 ksi·in.$^{1/2}$.

If we regarded the pressure vessels of this report as welded regions connected by crack-arresting wall material, the most dangerous regions would be along segments of longitudinal welding and along welds joining the nozzles to the pressure vessel wall. A conservative crack-arrest plan would be to provide sufficient toughness so that cracks completely through the metal affected by welding would be stable at the expected service stress level. In addition, this crack length would need to be small enough so that the effect of outward bulging near the crack due to internal pressure would be small or negligible. Further study of this second requirement is needed. However, it can be assumed that a crack length as small as twice the plate thickness would be small enough for that purpose. To satisfy the first requirement the maximum lengths of such cracks would have to be in correspondence with the equation

$$K_c^2 = \frac{\pi\sigma^2 a}{1 - \frac{1}{2}\left(\frac{\sigma}{\sigma_{YS}}\right)^2} . \tag{76}$$

The crack length is 2a. For a conservative design (stresses well below yield) and $K_{Ic} = 170$ ksi·in.$^{1/2}$, a 2-ft-long crack in a 12-in.-thick vessel wall would be stable at stresses below 20 ksi.

Use of ring-rolled cylindrical sections to eliminate longitudinal seam welds was helpful to the fracture strength of steel chambers for solid propellant rockets. Continued consideration of this construction method in application to large boiling-water and pressurized-water nuclear reactor pressure vessels has merit where the approach is practical. However, when courses of a reactor vessel are made up from rolled and welded plates and the fabrication is of high quality, coupled with a thorough inspection, there is no reason to suspect that longitudinally welded regions could not be regarded as possessing the required crack-arrest toughness.

7.6.3 Relationship of Fracture Toughness to Pressure Vessel Design Load in Terms of a Leak-Before-Break Criterion

A criterion sometimes termed "leak-before-break" was proposed in connection with fracture problems of steel solid-propellant rocket chambers for Polaris.[72] Methods for K_c-type crack-toughness measurement had been accepted, and a statement of how much toughness was "enough" had been demanded by users of the K_c test. The proposal was then made that a crack of twice the wall thickness in length should be stable at a stress equal to the yield strength, or

$$\beta_c = \frac{1}{B}\left(\frac{K_c}{\sigma_{YS}}\right)^2 = 2\pi \ . \tag{77}$$

On the average, this proposal seemed to correspond to attainment of full shear fractures. The value 2π in Eq. (77) is obtained by putting $a = B$ and $\sigma = \sigma_{YS}$ in Eq. (76). By using Eqs. (70) and (71), this criterion can also be expressed as $\beta_{Ic} = 1.5$.

Observation of leakage prior to bursting was not actually of importance in the rocket-chamber application. The criterion was simply a reasonable guess that received a large amount of study and trial.[47] It was found that for steels meeting the $\beta_c = 2\pi$ criterion, the design, fabrication, and inspection could generally be done with sufficient care so that the completed chambers would withstand an average hoop stress in the cylindrical section nearly as large as the yield strength of the material without fracturing.[47] Such toughness as could be obtained in the weldments and in the thick-section reinforcements was helpful, but these parts rarely possessed a $\beta_c = 2\pi$ degree of toughness.

For pressure vessels tested and used at a hoop stress much less than the yield strength of the material, a smaller degree of toughness would be expected to meet with an equivalent degree of success. For such vessels the "leak-before-break" criterion was redefined in relation to K_{Ic} values by Irwin and Sullivan[73] in terms of Eqs. (70), (71), and (76). The requirement $a = B$ was retained, but σ was left undetermined. Thus the criterion could be met, for any toughness or wall thickness, by a sufficient reduction of σ. From the preceding three equations, it is

found that

$$\frac{\pi y_1^2}{1 - \frac{1}{2} y_1^2} = \beta_{Ic} \left(1 + 1.4\beta_{Ic}^2\right) , \tag{78}$$

where

$$y_1 = \frac{\sigma}{\sigma_{YS}} \tag{79}$$

and, repeating Eq. (71), β_{Ic} is given by

$$\beta_{Ic} = \frac{1}{B} \left(\frac{K_{Ic}}{\sigma_{YS}}\right)^2 .$$

A graph of y as a function of β_{Ic} from Eq. (78) permits determination of a leak-before-break hoop tension stress, σ_{LB}, from given values of K_{Ic}, σ_{YS}, and B. K_{Ic} and σ_{YS} pertain to the applicable temperature and loading speed throughout the computions. The estimates of K_{Ic} from the NDT and FATT kinds of testing are K_{Id} values. These approximate estimates of minimum fracture toughness are appropriate for applications where dynamic conditions can occur either from service loads or weld-zone residual stress effects. Values of σ_{LB} corresponding to these K_{Id} values for three steels are given in Tables 7.1, 7.2, and 7.3. The influence of wall thickness is shown at two temperatures, NDT temperature plus 60°F and NDT temperature plus 120°F. The general trend of results at each temperature is a decrease of σ_{LB} from the approximate value, σ_{YS} (static), by a factor of about 3 as the wall thickness increases from 1 to 5 in.

When a fracture-safe operating range is defined in terms of the NDT temperature plus 60°F or FATT, such a criterion should be regarded as a general experience-based rule. It tends to be conservative for wall thicknesses less than 1.5 in., but this conservatism would often be needed. With an increase of wall thickness, the designer should be more cautious. Stress relief of 5-in. wall vessels is a mandatory procedure. Estimates of allowable stress for dynamic crack instability conditions, as shown in the tables, can be formally developed from the fracture-

Table 7.1. Comparison of Leak-Before-Break Criterion for HY-80 Steel as a Function of Temperature and Wall Thickness with Static Yield Strength

σ_{YS} (70°F) = 82 ksi
NDT temperature = −150°F

B (in.)	β_{Ic}	σ_{LB}/σ_{Yd}	σ_{LB} (ksi)	Static σ_{YS} (ksi)	$\sigma_{YS}/3$ (ksi)
At −90°F, σ_{Yd} = 122 ksi, and K_{Id} = 116 ksi·in.$^{1/2}$					
1	0.902	0.686	83.7	94	31
2.5	0.361	0.357	43.5		
5	0.181	0.241	29.4		
At −30°F, σ_{Yd} = 113 ksi, and K_{Id} = 126 ksi·in.$^{1/2}$					
1	1.243	0.877	99.2	88	29
2.5	0.497	0.439	49.6		
5	0.249	0.287	32.4		

Table 7.2. Comparison of Leak-Before-Break Criterion for A 302 Grade B Steel as a Function of Temperature and Wall Thickness with Static Yield Strength

σ_{YS} = 62 ksi
NDT temperature = 0°F

B (in.)	β_{Ic}	σ_{LB}/σ_{Yd}	σ_{LB} (ksi)	Static σ_{YS} (ksi)	$\sigma_{YS}/3$ (ksi)
At 60°F, σ_{Yd} = 82.7 ksi, and K_{Id} = 74.4 ksi·in.$^{1/2}$					
1	0.808	0.629	52.0	63	21
2.5	0.323	0.334	27.6		
5	0.162	0.229	18.9		
At 120°F, σ_{Yd} = 77.8 ksi, and K_{Id} = 79.1 ksi·in.$^{1/2}$					
1	1.017	0.753	58.6	60	20
2.5	0.407	0.384	29.9		
5	0.203	0.258	20.0		
8	0.127	0.201	15.6		

Table 7.3. Comparison of Leak-Before-Break Criterion for A 212 Grade B Steel as a Function of Temperature and Wall Thickness with Static Yield Strength

σ_{YS} = 36 ksi
NDT temperature = 20°F

B (in.)	β_{Ic}	σ_{LB}/σ_{Yd}	σ_{LB} (ksi)	Static σ_{YS} (ksi)	$\sigma_{YS}/3$ (ksi)
At 80°F, σ_{Yd} = 55.9 ksi, and K_{Id} = 51.1 ksi·in.$^{1/2}$					
1	0.836	0.645	36.0	36	12
2.5	0.334	0.341	19.1		
5	0.167	0.232	12.9		
At 140°F, σ_{Yd} = 50.1 ksi, and K_{Id} = 57.0 ksi·in.$^{1/2}$					
1	1.294	0.904	45.3	33	11
2.5	0.518	0.452	22.6		
5	0.259	0.294	14.8		

mechanics-based equations without regard for experience. However, consideration of factors specific to the individual application is necessary in their use.

The leak-before-break criterion, in $\beta_c = 2\pi$ form, did not appear to be conservative in its application to ultra-high-strength steel rocket chambers, despite the fact that $\beta_c = 2\pi$ corresponds to a large degree of plane-stress toughening. Very careful design, fabrication, and inspection were required, even when the toughness criterion was satisfied. In that application, the problem of controlling slow crack extension due to stress-corrosion during hydrotesting was seriously underestimated. Very few fractures occurred below design stress in firing trials. Elimination of crack growth due to stress-corrosion during hydrotesting would have been most helpful.

The β_{Ic} values in Tables 7.1, 7.2, and 7.3 are well below the value necessary for tough plane-stress fracturing. Certainly, for vessels of more than 2.5 in. wall thickness, fracture safety in the past has depended much more on conservative design stress than on the toughening influence of a brittle-ductile fracture transition.

With reference to thick-walled nuclear reactor pressure vessels, the influence of temperature elevation in terms of the degree of plane-stress toughening is gradual and not very large. No support can be found on that basis for a step-function type of diagram of a limiting allowable load based on a critical temperature. The allowable load diagram suggested by this study would be one of gradual increase with temperature to the point where a decrease of yield strength with temperature was a limiting consideration. The computation might be made with Eq. (78). However, a simpler plan can be suggested, as follows. Available K_{Ic} data for steels over a wide temperature range can be fitted, to a fair approximation, for a simple direct proportionality between K_{Ic} and the absolute temperature. Thus, if a decision has been reached on the temperature T_1 at which operational pressure is allowable, a straight line on a load-temperature graph from that point to zero load at absolute zero temperature would provide a safe allowable load diagram for temperatures below T_1. Practices currently used would be applicable at temperatures above T_1.

A fracture of a glass rod or plate normally occurs from a small surface flaw, and a half-circle mirror region can be seen at the fracture origin. This outlines the shape of the crack front when the crack speed reaches the limiting velocity and efforts at crack division begin to roughen the fracture surface. Similar half-circle crack front shapes have been observed in other brittle solids, even when the crack depth was large and the stress on the section reflected some bending.

With regard to the leakage aspect of the leak-before-break analysis, a half-circle would be the expected shape for a crack deepening from one surface into the wall of a nuclear reactor pressure vessel in all regions where the stress is well below the static yield strength. As the surface length approaches 2B, the stress elevation in the net section beneath the crack would tend to cause relatively fast severing of that part. Thus the average length of the crack parallel to the wall after break-through and start of leakage should not exceed 2B.

In the nozzle throat section, the stress favors development of a longitudinal crack in a plane containing the axis of the nozzle and starting at an inside corner. The crack front would have an approximate

quarter-circle shape. It seems likely that a leak-before-break design stress would permit arrest, with completion of a through-crack on one side, but not if cracks formed simultaneously on both sides of a nozzle. This possibility could be explored with trials of small-scale models that had actual nozzle throat section configurations.

The toughness required by Eq. (78) for a 12-in. wall-thickness pressure vessel can be estimated along the following lines. It is assumed that the steel is such that σ_{YS} (static) is 100 ksi at 70°F and that an allowable load equal to the operating pressure is wanted at 200°F. By using estimation rules previously discussed, σ_{Yd} at 200°F is 110.5 ksi. If 31 ksi is selected as representing a design stress (interpreted here as equivalent to average hoop tension stress, σ), the value of y_1 at 200°F is 0.281. From Eq. (78), this corresponds to $\beta_{Ic} = 0.240$. The required K_{Id} at 200°F is then given by

$$K_{Id} = 110.5 \text{ ksi} \sqrt{0.240 \times 12 \text{ in.}}$$

$$= 187 \text{ ksi} \cdot \text{in.}^{1/2} \ . \qquad (80)$$

A value of K_I at 200°F of no less than 197 ksi·in.$^{1/2}$ would be expected for a steel with a toughness similar to that of HY-80 steel. Since problems related to heat treatment and welding would be restrictive, a suitable steel with sufficient toughness for the leak-before-break criterion is a reasonable hope, particularly if the yield stress and design stress can be lowered somewhat from the estimates assumed above.

7.6.4 NRL Fracture Analysis Diagram

A number of tests of the transition-temperature kind have received use as providing fracture-toughness information. The moderate differences of the order in which these tests rate the toughness of various steels are not of vital importance in use because the overall fracture control plan depends on design, fabrication procedures, and inspection, as well as on the toughness rating of the steel. For any selected method of fracture testing, experience with a given class of structures over a

period of time indicates the adjustments that are appropriate and necessary relative to the customarily used toughness evaluations.

In view of the complexities in the use of a transition-temperature toughness rating and with the aid of a collection of fracture-failure data, Pellini and his associates assembled guide lines for usage in terms of their NDT type of fracture testing.[71,74] The resulting fracture analysis diagram (see Fig. 6.9, Chap. 6) was intended to provide guidance for fracture-safe design as nearly as possible without reference to loading speed, elastic constraint, and crack location, and with only gross estimates of stress level. Uses of the fracture analysis diagram were illustrated, and cautions were provided for increase of plate thickness, low shear-tear strength, quality level of inspection, and opportunities for growth of large flaws under service operating conditions.[75]

Approximate methods applicable to low- and medium-strength steels can be followed to translate conditions such as the NDT temperature plus 60°F and the NDT temperature plus 120°F into the design stress level that would satisfy the leak-before-break criterion under dynamic loading, as previously discussed. The results vary with NDT and yield-stress level. On the average, for 3/4- and 1-in. thicknesses, the stress thus estimated reaches the static tensile yield strength between the NDT temperature plus 60°F and an NDT temperature plus 120°F, a result that is in fair correspondence with the fracture analysis diagram.

The large flaw sizes suggested for various fractions of the yield strength cannot be taken literally, and few would do so. Otherwise, the practice appears conservative in reference to low-strength steels of about 1-in. section thickness. The practice tends to become marginal for steels of that thickness with σ_{YS} above 100 ksi and for low-strength steels with section thicknesses greater than 2 in. However, most large welded structures are designed for stresses well below the yield stress and, often, the service loads are essentially static. Hence a large degree of success from use of the fracture analysis diagram would be expected and has been experienced.

Relative to the thick-walled pressure vessels of interest, there is a major handicap to use of the method because the NDT measurement points for the tough steels of principal interest lie too far below the range

of temperatures for service operations. A similar handicap would pertain to all the presently customary methods of toughness evaluation in terms of a transition temperature.

There is also a scarcity of K_{Ic} data for high-toughness steels, except at low temperatures. Although higher temperature large-specimen data of the K_{Ic} type should be available soon, fracture-toughness information from direct measurement for high-toughness steels, at temperatures above 200°F, will probably require completion of suitable testing plans based on one of the plasticity analysis viewpoints previously discussed.

7.6.5 Proof Test Estimates of Critical Crack Size in Relation to Fracture-Safe Life

The first question of interest concerns what can be deduced from the fact that a proof test with internal pressure is successfully completed. Estimates are made here on the basis of a semielliptical surface crack with a depth one-quarter of the surface length of the crack. The equation for K in relation to depth a, tension σ, and tensile yield strength σ_{YS} is

$$K^2 = \frac{3.77\ \sigma^2 a}{1.49 - 0.212\left(\frac{\sigma}{\sigma_{YS}}\right)^2} . \tag{81}$$

For A 302 grade B steel, σ_{YS} (static, 70°F) = 60 ksi and NDT temperature = 10°F, the estimates of σ_{Yd} and K_{Id} at 70°F are 79.8 ksi and 71.5 ksi·in.$^{1/2}$. If the design stress is 24 ksi and the proof test produces an average hoop tension in the wall of the cylindrical portion of 1.25 × 24 ksi = 30 ksi, use of these data in Eq. (81) shows that a crack size given by a = 2.2 in. would become unstable at a stress level of 30 ksi. This calculation is on a dynamic basis. On a static basis,

$$K_{Ic}\ (\text{static}) = \frac{79.8}{60} \times 71.5\ \text{ksi}\cdot\text{in.}^{1/2}$$

$$= 95\ \text{ksi}\cdot\text{in.}^{1/2} .$$

The new estimate of the crack size proved to be absent by proof testing inspection is given by a = 3.8 in. Cracks of about 40% greater depth and smaller surface length would be estimated for a semicircular crack shape. Larger cracks could be present if there had been a crack-blunting treatment by warm prestressing. The amount of the size increase would be uncertain and would depend on the degree of confidence in the crack-blunting effect of the warm prestressing.

With regard to regions of the nozzle where the stress is locally elevated, it will be assumed that an additional plastic strain equal to the yield strain occurs across the region containing the crack. When the stress level in this region first achieves 60-ksi tension across the crack, the dynamic basis estimate of the critical size is obtained from

$$(71.5)^2 = \frac{3.77\ (60)^2 a}{1.49 - 0.212\left(\frac{60}{80}\right)^2} \tag{82}$$

or

$$a = 0.45 \text{ in.}$$

It would, of course, be inconsistent to assume that continued straining occurs if such a crack is present and is resisted only by the dynamic fracture toughness. On the other hand to assume a smaller crack and add the influence of plastic strain to the opening dislocation, δ, amounts to crack blunting, and an onset of fast fracture instability cannot be certainly predicted. An increment of stable extension comparable to δ is more likely.

The critical crack-size estimates for base-metal cylindrical portions of the vessel were unreasonably large and can be viewed as incredible. However, if the locale of these calculations is shifted to a longitudinal weld, and if the fracture toughness in K-value terms is assumed to be less by 30%, the critical crack sizes are reduced by a factor of 2. The dynamic calculation estimate then becomes 1.1 in., which is small enough for a significant probability of existence. Furthermore a weld that joins a nozzle to a shell is subject to some superimposed bending

stress to a degree dependent upon the efficiency of the design. Increasing the tensile stress 30% would also halve the sizes of the cracks judged to be critical.

The preceding calculations are, of course, no more than illustrative. For good fracture control, each vessel should be studied in terms of the stress analysis, fabrication, and property data applicable to that vessel.

The critical crack sizes that would be required for failure under operating conditions are also considered. For simplicity it is assumed that the operating pressure is applied at 70°F. It is also assumed that the hoop tension developed is 0.8 × 24 ksi = 19.2 ksi. In order to keep the crack sizes within reason, the reduction by a factor of 2 suggested above is used. It is then found that the critical dynamic crack size has increased from 1.1 to 2.7 in., and the critical static crack size has increased from 2.6 to 4.7 in.

For these sizes, calculations based on the maximum fatigue crack growth rates, as discussed in Section 7.4 of this chapter, indicate that 10^5 or more cycles are needed for crack growth to unstable size by fatigue. If an allowance of an additional factor of 2 for 30% increase of stress is made, the critical crack sizes are reduced and the growth rate is greatly increased. However, the required number of cycles is still above 10^4.

In the nozzle regions where plastic straining occurred during the proof test, and where the stress may be about 60 ksi under operating conditions, an estimate of the above kind is not possible. A reasonable guess at the crack growth rate could be made; however, there is no clear way to fix the initial maximum crack size so that the number of growth increments can be estimated. It is quite possible that residual compressive stress from the proof test may provide adequate protection of such regions of highest strain.

The possibility for crack growth to critical size by means of stress-corrosion in any region of the vessel must be considered on a different basis. It is, in fact, not possible to guarantee safety relative to moisture-assisted slow growth of the maximum-size surface cracks unless

the material and the cracks are such that a "below K_{ISCC}" situation is always maintained.

Present information gives no positive indication that water plus steady tension causes slow crack growth in A 302 grade B vessels, except for conditions of fatigue. The water influence was already represented for fatigue by using the highest growth rate constant, C_3, from Section 7.4 of this chapter. Additional investigations of A 302 grade B steel and of candidate steels for future vessels are necessary relative to water-environment stress-corrosion crack growth. Evidence exists that K_{ISCC} can be increased by crack blunting. In the present application a substantial degree of crack blunting exists that is possibly enough so that this type of stable crack growth need not be a matter of concern.

In the case of the A 302 grade B steel vessel discussed in the preceding illustration the wall thickness was not specified. If the vessel is required to satisfy leak-before-break conditions in the terms of this chapter, the value of $y_1 = \sigma_{LB}/\sigma_{Yd}$ is given by

$$y_1 = \frac{24}{79.8} = 0.308 \ . \tag{83}$$

The corresponding value of β_{Ic} from Eq. (78) is 0.281. Thus

$$\beta_{Ic} = 0.281 = \frac{1}{B}\left(\frac{71.5}{79.8}\right)^2 \tag{84}$$

and

$$B = 2.86 \text{ in.}$$

The small value of B is in part due to stress level and, in part, to use of K_{Id} rather than a static K_{Ic}. If the stress level is reduced from 24 ksi (design) to 19.2 ksi (operating), B becomes 4.46 in. The thicknesses corresponding to these two stress levels if the static K_{Ic} is assumed are 8.14 and 13.9 in. For the dynamic-toughness estimate, K_{Id}, the 19.2-ksi wall stress would be below the calculated σ_{LB} for an 8-in. wall thickness of the assumed material at temperatures above some temperature in the neighborhood of 260°F.

This discussion cannot propose to settle such questions as whether the leak-before-break criterion should be used or, if so, whether on a dynamic or on a static basis. The primary purpose is to illustrate ways in which such questions can be discussed by utilizing macroscopic fracture analysis methods.

7.6.6 Radiation Effects Relative to Fracture Properties and σ_{LB}

Curves of true stress against true strain for HY-80 steel after various neutron exposures have been shown by Chow and McRickard.[76] These curves shift upward with increase in irradiation in much the same fashion as they would with a decrease of temperature or an increase of strain rate. In the case of similar curves for A 302 grade B steel,[77] the radiation hardening is accompanied by a decreasing trend in the slopes of the curves. Bearing in mind an approximate proportionality of K_{Ic} to the strain-hardening exponent n, these results suggest that a greater influence of irradiation embrittlement would occur for A 302 grade B steel than for HY-80 steel under the conditions of irradiation employed. The above authors estimated the irradiation temperature at 30°C. Measurements of the increase of the NDT temperature by Steele and Hawthorne[78] for irradiation temperatures below 450°F provide results in the direction indicated by the strain-hardening behavior.

In Section 7.1 of this chapter attention was directed to the fact that very small defects of the type that interfere with easy glide of dislocations, and thus have major importance to plastic flow properties, tend to influence fracture primarily in an indirect manner through their effect on the plastic-flow properties. The defects introduced by radiation are quite small, and it is probable that most of their influences on fracture toughness can be understood in terms of modification of plastic flow properties.

For irradiation below 5×10^{19} neutrons/cm^2 (E > 1 Mev), which is assumed here to be the region of major interest for the walls of large boiling-water and pressurized-water nuclear reactor pressure vessels, the stress-strain curves of irradiated steels seem to possess a normal

appearance; this indicates that K_{Id} estimates along the lines used previously in this chapter can be employed after irradiation to the same degree as before.

An interesting aspect of the effects of irradiation damage on vessel behavior at the NDT temperature can be hypothesized by using estimates of the changes in the significant materials properties.

The aspect of major interest is the tendency of an increase of σ_{YS} to accompany an increase of the NDT temperature and is best understood in terms of an illustration. As before, the steel is A 302. The data were collected by Steele and his associates[78,79] for material from a 6-in.-thick plate with neutron exposure at temperatures below 250°F. A graph was made of the NDT temperature as a function of σ_{YS} (static, 0.2% offset, 70°F) from measurements obtained after irradiation. The increase of σ_{YS} per 100°F elevation of the NDT temperature was 12 ksi up to 1×10^{19}-neutrons/cm^2 (E > 1 Mev) irradiation, where the NDT temperature had become 230°F. The overall slope corresponded to 15 ksi per 100°F change of the NDT temperature across the range to 8×10^{19}-neutrons/cm^2 irradiation.

The undamaged properties were an NDT temperature of 10°F and σ_{YS} (static, 70°F) = 67 ksi. Estimates of the dynamic yield elevation to obtain σ_{Yd} and estimates of K_{Id} as $0.78\sqrt{\text{in.}}\ \sigma_{Yd}$ gave the results shown in Table 7.4. The values in parentheses were formally obtainable from the estimation procedure, but the irradiation dosage might be high enough to require a different analytical treatment.

Table 7.4. Estimates of Dynamic Yield as a Function of NDT Temperature

NDT Temperature (°F)	σ_{YS} (ksi)	σ_{Yd} (ksi)	K_{Id} (ksi·in.$^{1/2}$)
10	67	92.5	72.1
230	100	108.7	84.8
425	134	(134.7)	(105)

Two estimates of the fracture-toughness radiation damage for an NDT temperature of 230°F were made in the following ways. First, the estimate of K_{Id} at 10°F for the undamaged material was used to estimate K_{Id} at 230°F (undamaged) with the idea of a direct proportionality of K_{Id} to absolute temperature. Second, estimates of K_{Id} (undamaged) at 230°F were made on the basis of inverse proportionality to dynamic yield strength. Method 2 would underestimate the damage effect because the temperature range is too large for this method. Method 1 gave

$$K_{Id} \text{ (undamaged, 230°F)} = 136 \text{ ksi}\cdot\text{in.}^{1/2} .$$

Thus the damage influence was a K value loss of 47%. Method 2 indicated a smaller amount, 30%. Thus a substantial damage to fracture toughness occurred. It is notable, however, that the elevation of the NDT temperature by irradiation is accompanied by an increase of K_{Id} at the NDT temperature.

This aspect was explored additionally by estimating σ_{LB} at the NDT temperature plus 60°F. Values of σ_{Yd} and K_{Id} were calculated for each of the three NDT temperature plus 60°F points. The results are shown in Table 7.5. Apparently the increase of σ_{Yd} that accompanies the increase of the NDT temperature is high enough so that a nuclear reactor pressure vessel that did not initially meet a leak-before-break operating-pressure criterion at the NDT temperature (or the NDT temperature plus 60°F) might reach such a condition after substantial radiation damage.

Table 7.5. Estimates of Dynamic Yield as a Function of the NDT Temperature Plus 60°F

σ_{YS} (static, 70°F) = 67 ksi

NDT Temperature Plus 60°F (°F)	σ_{YS} (ksi)	K_{Id} (ksi·in.$^{1/2}$)	σ_{LB} (ksi)
70	86.8	76.0	19.6
290	105.9	87.1	20.0
485	(133.7)	(106)	(24.4)

The estimates of σ_{LB} based on dynamic fracture toughness are normally more conservative than those based on static fracture toughness. However, the tensile stress-strain curves for A 302 grade B steel after various amounts of irradiation, given in Ref. 79, have an increasing abnormality toward "negative strain hardening" in the dosage range above 0.8×10^{19} neutrons/cm^2. This suggests that the static K_{Ic} would be seriously lowered by the increased tendency toward plastic instability. The "unhardening" behavior is expected to be time dependent and might be too slow to have a comparable influence on NDT and Charpy V-notch tests.

Static K_{Ic} measurements were made at Bettis Atomic Power Laboratory on A 302 grade B steel after various amounts of irradiation at levels above 10^{19} neutrons/cm^2; these were informally transmitted. Estimating back from K_{Id} values based on the NDT temperature after elevation to 230°F and to 425°F, the room temperature K_{Id} should be about 60 ksi·in.$^{1/2}$. However, the static measurements are much less than this at room temperature. In the approach of the test temperature to the NDT temperature, the static measurements tended to increase rapidly. The size of the test specimen did not permit great confidence in these higher values. A portion of this increase might be from plane-stress yielding. However, the fracture-toughness value approached at the NDT temperature would not have exceeded the K_{Id} estimate at NDT in any case.

Although more experience may be necessary with K_{Ic} measurements of radiation-damaged steels, it seems probable that beyond some dosage limit, a conservative calculation of fracture strength may depend more on the static K_{Ic} value than on the dynamic value. This aspect has only recently appeared and requires careful investigation.

7.7 RECOMMENDATIONS

Investigation of material crack paths and K values for cracks in high-stress regions at or near a nozzle should be performed. Such studies might employ a model constructed of a brittle transparent material with stable crack extension assisted by moisture or a model constructed of a low-toughness metal with stable crack extension produced by fatigue.

The residual compressive-stress type of protection that might be provided to such regions from the proof-testing method should be investigated.

Nondestructive inspection techniques should be developed for characterizing defects complementing the development of analytical techniques for predicting the strength and service life of the vessels.

The stable water-assisted crack-growth rate for steels of interest, based on pressures, temperatures, and radiation typical of service conditions, should be investigated, and the following steps should be taken:

1. determine da/dN versus K curves for fatigue of reactor vessel steels under plane strain,
2. explore effects of plane stress,
3. explore thermal and environmental effects under plane strain and plane stress,
4. determine K_{ISCC} (and K_I versus t curves) for reactor vessel steels
   a. under plane strain (thick plates),
   b. under the tendency toward plane stress (thinner plates),
5. do general studies of mixed conditions of flaw growth and fatigue; that is,
   a. fatigue versus corrosion,
   b. plane stress versus plane strain,
   c. K_{ISCC} versus K_{Ic} versus K_c.

If this stable growth rate is not negligible, a study of the possibility of suppression of crack growth by means of warm preloading crack blunting should be initiated.

In relation to the study of radiation hardening and embrittlement near and above a dosage of 10^{19} neutrons/cm^2 ($E > 1$ Mev), the influence of loading speed on K_{Ic} and on isothermal strain hardening should be investigated. A strong effect on both measurements is probably due to the unstable relaxation of hardening (from large amounts of radiation) in the presence of increasing plastic strain. Time-rate sensitivity in this hardening relaxation would be expected. The dynamic K_{Ic} (or K_{Id}) may be larger than the static K_{Ic}, and some revision of methods for assessing the degree of radiation damage may be necessary.

Sharp-notch tests should be performed on the materials developed for service, over the desired temperature range, at full section thickness.

The bend test is favored, in view of its reasonable static load requirement, suitability for impact loading, and convenient comparison with the drop-weight NDT test. However, fatigue notches would be preferred; to obtain clear conditions for fracture mechanics analysis, combinations of slow bend and impact tests would also be desirable. It is vital that these tests be both static and dynamic, and they should be fully instrumented for load, displacement, and either crack-opening displacement or transverse contraction at the notch root.

A materials evaluation program based on a large number of full-thickness specimens would be exorbitantly expensive. However, Charpy V-notch specimens may prove to be too small for adequate routine production control of toughness at the selected level. Consideration, therefore, should be given to an evaluation program based on half- or quarter-thickness tests with which a reasonable full-thickness correlation might be obtained by using crack-opening displacement mechanics methods. These tests should also be fully instrumented.

There is a possibility that certain microstructural combinations associated with welded joints that will give rise to low-toughness zones cannot be eliminated. Large in-situ tests of such joints, although desirable, may be prohibitive in terms of economics. However, in any case, there should be small-scale tests of the basic microstructures at the weld zone for low-toughness regions. This alternative is suggested, since it is considered that a small-scale test, such as the precracked Charpy test, should be further developed for the purpose. Instrumentation for recording of load and displacement would be advisable to permit extraction of relevant fracture mechanics data. The same procedure could be used to monitor the effects of irradiation.

If full-scale vessels representative of thick material are to be tested, it is recommended that the nozzle and shell configuration be employed in some tests, since the intersection region is considered to be the most critical in terms of presence of crack defects. The test should be performed under pulsating pressure in order to nucleate a natural crack defect at the most critical region, and it should be associated both with periodic applications of overpressure and measurements of slow growth of flaws in order to provide a basis for proof-test qualification in service.

It is recommended that the leak-before-break criterion of fracture be further examined in spite of increases in thickness and yield strength of reactor steels because of the extra conservatism that would occur from such an approach.

REFERENCES

1. A. W. Rankin and C. D. Moriarty, Acceptance Guides for Ultrasonic Inspection of Large Rotor Forgings, ASME paper 55-A-194, ASME Tran., 78: 1603–1622 (1955).
2. D. R. DeForest et al., Investigation of the Generator Rotor Burst at the Pittsburgh Station of Pacific Gas and Electric Co., ASME paper 57-PWR-12.
3. G. R. Irwin, Notes for March 24, 1959, meeting of ASTM Committee in New York.
4. G. R. Irwin, The Leading Edges of Fracture Mechanics, ASME Thurston Lecture 1966, ASME Trans. (in press).
5. A. A. Wells, The Mechanics of Notch Brittle Fracture, Brit. Welding Res., Vol. 7, April 1953.
6. A. A. Wells and D. Post, The Dynamic Stress Distribution Surrounding a Running Crack, A Photoelastic Analysis, Trans. Soc. Exp. Stress Analysis, 16(1): 69–93 (1959).
7. G. R. Irwin, Fracture Dynamics, in Fracturing of Metals, ASM, Cleveland, 1948.
8. E. Orowan, Fundamentals of Brittle Behavior of Metals, p. 139 in Symposium on Fatigue and Fracture of Metals, Wiley, New York, 1952.
9. A. B. J. Clark and G. R. Irwin, Crack Propagation Behavior, Exp. Mech., Vol 6, June 1966.
10. F. A. McClintock and G. R. Irwin, Plasticity Aspects of Fracture Mechanics, in Fracture Toughness Testing, ASTM Special Technical Publication 381, 1965.
11. P. C. Paris and G. C. Sih, Stress Analysis of Cracks, in Fracture Toughness Testing, ASTM Special Technical Publication 381, 1965.
12. G. R. Irwin, Crack Extension Force for a Part-through Crack in a Plate, Trans. ASME, J. Appl. Mech., Series E, 84: 651–654 (1962).
13. C. F. Tiffany and J. N. Masters, Applied Fracture Mechanics, in Fracture Toughness Testing, ASTM Special Technical Publication 381, 1965.
14. J. E. Srawley and W. F. Brown, Fracture Toughness Testing Methods, in Fracture Toughness Testing, ASTM Special Technical Publication 381, 1965.

15. G. R. Irwin, Relation of Crack Toughness Measurements to Practical Applications, Welding J., 41: 519S (1962).

16. G. R. Irwin, Plastic Zone Near a Crack and Fracture Toughness, 7th Sagamore Ordnance Materials Research Conference, August 1960, Proceedings published by Syracuse University, 1961.

17. G. R. Irwin, Fracture Mode Transition for a Crack Traversing a Plate, Trans. ASME, J. Basic Eng., Series D, 82: 417–425 (1960).

18. W. G. Clark, forthcoming Westinghouse Research Laboratory report of results reported at ASTM E-24 Subcommittee 1 meeting of June 1966.

19. A. A. Wells, Notched Bar Tests, Fracture Mechanics, and the Strength of Welded Structures, IIW Houdremont Lecture, Brit. Welding J., 12: 2–13 (January 1965).

20. G. I. Barenblatt, Advances in Applied Mechanics, Vol. VII, p. 55, 1962; there were previous papers by Barenblatt in Russian Journals.

21. D. S. Dugdale, Yielding of Steel Sheets Containing Slits, J. Mech. Phys. Solids, 8: 100–104 (1960).

22. B. A. Bilby, A. H. Cottrell, and K. H. Swinden, The Spread of Plastic Yield from a Notch, Proc. Roy. Soc. A, 272: 304–314 (1963).

23. G. R. Irwin, Fracture Mechanics Applied to Adhesive Systems, in Treatise on Adhesion and Adhesives, R. Patnick (Ed.), Vol. I, p. 254, Dekker, 1967.

24. F. A. McClintock and J. A. H. Hult, Proceedings of 9th International Congress on Applied Mechanics, Brussels, 1956, Vol. VIII, p. 51.

25. V. B. Walsh and A. C. MacKenzie, Elastic-Plastic Torsion of A Circumferentially Notched Bar, J. Mech. Phys. Solids, 7(4): 247–257 (1958–59).

26. M. F. Koskinen, Trans. ASME, J. Basic Eng., Series D, 85: 585–594 (1963).

27. J. R. Rice, The Mechanics of Crack Tip Deformation and Extension by Fatigue, Brown University, Division of Engineering Report, May 1966; also ASTM preprint No. 36, June 1966.

28. J. R. Rice, Stresses Due to a Sharp Notch in a Work Hardening Elastic-Plastic Material Loaded by Longitudinal Shear, Brown University, Division of Engineering Report, December 1965.

29. J. M. Krafft, Correlation of Plane Strain Crack Toughness With Strain Hardening Characteristics of A Low, A Medium, and A High Strength Steel, Appl. Mater. Res., 3(2): 88–101 (1964).

30. J. M. Krafft, paper for spring meeting of (British) Institute of Metals, 1967.

31. H. H. Johnson and A. M. Willner, Moisture and Stable Crack Growth in a High Strength Steel, Appl. Mater. Res., 4(1): 34 (January 1965).

32. P. C. Paris, The Fracture Mechanics Approach to Fatigue, p. 107 in Fatigue – An Interdisciplinary Approach, Syracuse University Press, 1965.

33. D. R. Donaldson and W. E. Anderson, Crack Propagation Behavior of Some Airframe Materials, Proceedings of the Crack Propagation Symposium, Cranfield, England, September 1961.

34. P. Paris and F. Erdogan, A Critical Analysis of Crack Propagation Laws, Trans. ASME, J. Basic Eng., Series D, 85(4): 528–534 (December 1963).

35. A. J. Brothers and S. Yukawa, Fatigue Crack Propagation in Low-Alloy Heat-Treated Steels, Trans. ASME, J. Basic Eng., Paper No. 66-MET-2 (to be published, 1966).

36. C. Carman and J. Katlin, Low Cycle Fatigue Characteristics of High Strength Steels, Trans. ASME, J. Basic Eng., Paper No. 66-MET-3 (to be published, 1966).

37. W. Clark and E. Wessel, Westinghouse Research Laboratories, private communication of data on A 302 grade B steel.

38. D. Piper, S. Smith, and R. Carter, Corrosion Fatigue and Stress Corrosion Cracking in Aqueous Environment, ASM National Metal Congress, Oct. 31, 1966.

39. T. Crooker, R. Morey, and E. Lange, Low Cycle Fatigue Crack Propagation in Quenched and Tempered Steels Under Corrosive Environments, Naval Radiation Laboratory Report 6196, September 1964, p. 3. (See also subsequent quarterly reports of Metallurgy Division of Naval Radiation Laboratory.)

40. T. Crooker and E. Lange, Naval Radiation Laboratory, private communication of data on A 302 grade B steel.

41. R. P. Wei, P. M. Taida, and C. Y. Li, Fatigue Crack Propagation in Some Ultra-High-Strength Steels, Proceedings of the ASTM Fatigue Crack Propagation Symposium, 1966 (in press).

42. B. F. Brown, A New Stress-Corrosion Cracking Test Procedure for High-Strength Alloys, Materials Research and Standards, ASTM, 1965. (See also subsequent Naval Radiation Laboratory reports by Brown et al.)

43. S. T. Rolfe, S. R. Novak, and J. H. Gross, Stress-Corrosion Testing of Ultraservice Steels Using Fatigue Cracked Specimens, paper presented at the Symposium on Stress Corrosion Testing, ASTM, Atlantic City, New Jersey, June 27–28, 1966.

44. J. M. Krafft and G. R. Irwin, Crack-Velocity Considerations, in Fracture Toughness Testing, ASTM Special Technical Publication 381, 1965.

45. J. A. Kies et al., Fracture Testing of Weldments, in Fracture Toughness Testing, ASTM Special Technical Publication 381, 1965.

46. ASTM Special Committee Reports, Fracture Testing of High-Strength Sheet Materials, ASTM Bulletin No. 243, pp. 29–40, January 1960, and Bulletin No. 244, pp. 18–28, February 1960.

47. G. R. Irwin, Structural Aspects of Brittle Fracture, Appl. Mater. Res., 3(2): 65–81 (April 1964).

48. E. Sternberg and M. A. Sadowski, Three Dimensional Solution for the Stress Concentration Amid a Circular Hole in a Plate of Arbitrary Thickness, J. Appl. Mech., 16: 27–38 (1949).

49. Informal communication from B. M. Wundt, General Electric Company.

50. Harris and Dunegan, Fracture Toughness of Beryllium, Trans. ASTM (in press).

51. E. J. Ripling, S. Mostovoy, and R. L. Patrick, Measuring Fracture Toughness of Adhesive Joints, Mater. Res. Standards, 4(3): 129–134 (March 1964).

52. S. Mostovoy and E. J. Ripling, Fracture Toughness of an Epoxy System, J. Appl. Polymer Sci., 10(9): 1351–1371 (1966).

53. E. H. Yoffe, The Moving Griffith Crack, Phil. Mag., 42: 739–750 (1951).

54. R. L. Smith, G. A. Moore, and R. M. Brick, Mechanical Properties of Metals at Low Temperature, Symposium of National Bureau of Standards, p. 153, 1951.

55. P. E. Bennett and G. M. Sinclair, Parameter Representation of Low Temperature Yield Behavior of Body Centered Cubic Transition Metals, ASTM paper 65-MET-11, 1965.

56. E. T. Wessel, W. G. Clark, and W. K. Wilson, Engineering Methods for the Design and Selection of Materials Against Fracture, Westinghouse Reserach Laboratory Report to Army Tank-Automotive Center, June 24, 1966.

57. G. R. Irwin, The Leading Edges of Fracture Mechanics, ASME 1966 Thurston Lecture, Trans. ASME (in press).

58. H. T. Corten and A. K. Shoemaker, Fracture Toughness of Structural Steels as a Function of the Rate Parameter, T log ($A/\dot{\varepsilon}$), ASME paper 66-WA/MET-8, 1966.

59. W. J. Nordell and W. J. Hall, Two Stage Fracturing of Welded Mild Steel Plates, University of Illinois Report, October 1963.

60. D. W. Gerridge and R. G. Slutter, The Brittle Behavior of High Strength Steel Weldments, Lehigh University, Report 200.61.364.8, April 1965.

61. C. F. Tipper, The Brittle Fracture Story, Cambridge University Press, 1962.

62. A. A. Wells, Strain Energy Release Rates for Fractures Caused by Wedge Action, Naval Radiation Laboratory Report 4705, March 1956.

63. A. A. Wells, Fracture Control of Thick Steels for Pressure Vessels, IIW Meeting, Düsseldorf, April 1967.

64. J. C. Raden and C. E. Turner, Note on the Relevance of Linear Fracture Mechanics to Mild Steel, J. Iron Steel Inst., 204(8): 842–845 (1966).

65. F. M. Burdekin and D. E. W. Stone, J. Strain Anal., 1: 145 (1966).

66. A. A. Wells, Welded Ferritic Steel Construction for Intermediate Low-Temperature Service, ASTM Special Technical Publication 302, p. 21, 1962.

67. W. H. Irvine, A. Quirk, and E. Bevitt, Fast Fracture of Pressure Vessels, J. Brit. Nucl. Energy Soc., 3: 31–48 (January 1964).

68. A. J. Brothers and S. Yukawa, Effect of Warm Pre-Stressing on Notch Fracture Strength, Trans. ASME, J. Basic Eng., 85: 97–104 (March 1963).

69. De Haviland official report on "Comet" Failures, 1955.

70. G. R. Irwin, J. A. Kies, and H. L. Smith, Fracture Strength Relative to Onset and Arrest of Crack Propagation, Proc. ASTM, 58: 640 (1958).

71. W. S. Pellini and P. P. Puzak, Practical Considerations in Applying Laboratory Fracture Test Criteria to the Fracture Safe Design of Pressure Vessels, Naval Research Laboratory Report 6030, November 1963.

72. R. W. Nichols, Fast and Brittle Fracture Studies Related to Steel Pressure Vessels, Proc. Roy. Soc., A285: 104–119 (1965).

73. G. R. Irwin and A. M. Sullivan, Proc. Roy. Soc., A285: 141 (1965).

74. P. P. Puzak and W. S. Pellini, Evaluation of the Significance of Charpy Tests for Quenched and Tempered Steels, Welding J., 35: 275S–277S (June 1956).

75. W. S. Pellini et al., Review of Concepts and Status of Procedures for Fracture Safe Design of Complex Welded Structures Involving Metals of Low to Ultra-High Strength Levels, Naval Research Laboratory Report 6300, June 1965.

76. J. G. Y. Chow and S. B. McRickard, Low-Temperature Embrittlement of Iron, Iron Alloys and Steels by Neutron Irradiations, p. 127 in Flow and Fracture of Metal and Alloys in Nuclear Environments, ASTM Special Technical Publication 380, 1965.

77. T. A. Trozera and P. W. Flynn, Effects of Irradiation on A-302B Steel Subjected to a Multiaxial Stress Distribution, pp. 337–349 in Flow and Fracture of Metal and Alloys in Nuclear Environments, ASTM Special Technical Publication 380, 1965.

78. L. E. Steele and J. R. Hawthorne, New Information on Neutron Embrittlement and Embrittlement Relief of Reactor Pressure Vessel Steels, pp. 283–311 in Flow and Fracture of Metal and Alloys in Nuclear Environments, ASTM Special Technical Publication 380, 1965.

79. L. E. Steele, J. R. Hawthorne, and C. Z. Serpan, Irradiation Effects on Reactor Structural Materials, May–July 1965, NRL Memo Report 1638, Naval Research Laboratory, Aug. 16, 1965.

8. FABRICATION*

A few years ago the technology of fabricating light-water nuclear power reactor vessels was applied to 75- to 300-Mw(e) development prototypes. Today emphasis is directed toward reactor vessels for second-generation or large demonstration nuclear power plants of 350- to 1050-Mw(e) capacity for central-station installation, and studies are being made to extend the technology to vessels for 1500-Mw(e) and larger reactors.[1] This chapter describes some of the facilities now used or planned for making the second-generation and larger vessels, typical sequences of fabrication operations, with allied inspection and examination steps, and some of the metallurgical factors related to the fabrication steps. Principal attention is given to current practice, but probable and possible modifications and advances to be expected in the next few years are also mentioned.

The early prototype reactor vessels have typical dimensions of about 9 ft ID and 30 ft overall height, with 5-in. walls for BWR's and 8-in. walls for PWR's. The larger second-generation vessels now being built range from 15 to 20 ft ID and from 50 to 70 ft high; they have walls up to 8 in. for BWR's and to 11 in. for PWR's and will weigh up to 800 tons or more. Projected studies of still larger reactors that take into account the capabilities of existing plants or plants under construction suggest that vessels can be shop fabricated with internal diameters from 20 to 30 ft, heights of 125 ft or more, 8- to 12-in. walls, and weights up to 1000 tons or more. However, continuing developments in core design, use of higher strength materials, and modified manufacturing practices may reduce some of these anticipated dimensions for the larger reactor vessels.

With increases in reactor vessel sizes and the complexity of the materials and fabrication problems, the number of potential fabricators has decreased. In the United States today, only two companies — Babcock & Wilcox Company (B&W) at its new plant in Mount Vernon, Indiana, and

---

*This Chapter was prepared by E. C. Miller of the Oak Ridge National Laboratory.

Combustion Engineering, Inc. (CE) in its new bays in Chattanooga, Tennessee — appear to have the combinations of design capability, facilities, experience, interest, and location of plants on navigable waterways required to design, manufacture, and transport shop-fabricated vessels for 350-Mw(e) and larger reactors. A few of the larger shipyards approach these capabilities but, to date, are not involved in large reactor vessel fabrication. Some overseas fabricators, mostly shipyards, in the Netherlands,[2] Japan, Germany, France, and possibly some Soviet bloc nations,[3] also can and do expect to fabricate vessels for light-water reactors for installation outside the United States. The shop-fabricated vessels now being built are too large for rail transportation, so water transportation combined with limited overland haulage from waterside to the site are used almost exclusively today. Most of the planned second-generation vessels will be sited near navigable water, although some vessels now under contract or planned will be sufficiently far from waterside that overland haulage of a completed vessel from the water to the final destination will not be feasible. Where shop-fabricated vessels cannot be transported as a unit to the site, it is planned to shop fabricate subassembly sections in as large sizes as can be handled by rail, boat, and overland transportation and then to assemble and erect the vessels at the site. There is a possibility that field fabrication may become competitive with shop fabrication in some cases where both are feasible.

The Chicago Bridge and Iron Company (CB&I), with a long history of field-erection capability and experience, proposes to field assemble partially assembled reactor vessel components. CE and B&W are also prepared to field fabricate, if circumstances require and warrant. Still other companies in the United States have field-fabrication experience and may well develop an active interest if the initial efforts at field fabrication appear successful.

The descriptions of current fabrication practices that follow represent methods now used or contemplated by the active U.S. participants in the light-water reactor vessel fabrication program. Some knowledge of related fabrication and welding practices in other shops in the U.S. and elsewhere, as well as other information from the extensive technical literature, is also included. Some details of fabrication are proprietary

and represent a considerable part of the experience and know-how that are a part of a manufacturer's competitive stock in trade. In fairness to these fabricators, such information is not described in extensive detail here if it does not appear essential to the objectives of the report.

8.1 FACILITIES[4]

Equipment used to manufacture large reactor vessels is generally similar to that found in most well-equipped boiler or pressure vessel fabricating shops, a principal difference being that some of the machines are simply bigger. These include such items as welding positioners and manipulators, forming presses or rolls, heat-treating and stress-relieving furnaces, horizontal and vertical boring mills and other machine tools, quench pits, hydrostatic test pads, cranes and other handling equipment, and suitable barge-loading dock facilities with ready access to a navigable waterway.

Several years ago, CE built bay 29 at its Chattanooga plant, mostly for nuclear work. Since that time many propulsion reactor and prototype power reactor vessels and other nuclear components have been built in this bay. As requirements for still larger vessels developed, CE added two new bays, 30 and 31. The older bay 29 has a 250-ton crane and continues to be used for smaller vessels and components. Bay 30 has a 100-ton crane and is used as an assembly shop to feed subassemblies into bay 31. It also has a clean room that can handle 100-ton components. Bay 31, with an 800-ton bridge crane capable of over 1000-ton lifts, is the principal production shop for the large second-generation reactor vessels. It contains machine tools, a hydrostatic test pad, and a 13/25-Mev 2400-r/min linear accelerator that give the shop a capability for making vessels for 1500-Mw(e) and even larger light-water reactors. A new loading dock adjacent to bay 31 on the TVA navigation system can load reactor vessels as large as 1000 tons into ocean-going barges.

There are several distinctive features of the new B&W (Mount Vernon) plant. These include a normalizing and stress-relieving furnace and an associated vertical cylindrical quench tank, and each is capable of

handling assemblies and subassemblies 30 ft in diameter. The shop contains specially designed and built rolls that can hot form plates as thick as 15 in. into cylindrical shell sections and can further cold size the shell courses to correct distortion from the forming and welding operations. Another feature of the new plant will be a tape-controlled machining center, now being installed, which will perform practically all the complicated machining operations on assembled vessel heads, bodies, and flanges concurrently or in closely coordinated sequence. There are additional more conventionally sized machine tools for use on nozzles, weld preparations, and smaller components before assembly. The machine tooling is modularized to minimize crowding of equipment and to provide a smooth flow of vessel components through the shop. Radiography will be done with a 12-Mev 600-r/min linear accelerator. The shop is served by two 500-ton cranes. One craneway runs the length of the assembly area from heat treatment through forming, weld assembly, and machining to the barge loading dock. The second crane serves the areas where the larger components are assembled and handled. The combined lifting capacity of both cranes is available to handle a completed vessel or large subassembly.

The Chicago Bridge and Iron Company has been active for many years in the field fabrication of large storage tanks, process vessels for the chemical and petroleum industries, and nuclear containment vessels and now plans to extend this experience to the combined shop and field fabrication of large reactor vessels concurrently with the outer containment shells. CB&I has shops in Chicago, Salt Lake City, Greenville, Pennsylvania (where some of the machining of reactor vessel parts will be done), and Birmingham, Alabama, where the shops will form, fit, and clad shell-course plates and form, preassemble, and clad the heads up to limiting dimensions convenient for rail and overland unloading and shipment, that is, about 13 ft across. For the first few reactor vessels, CB&I will purchase all plates from the mill in the quenched-and-tempered condition and cold form them in a series of repeated cold-bending and stress-relief operations planned so that the amount of cold deformation between successive stress-reliefs will not exceed 3% elongation in the outer fibers. By adopting this practice, no austenitizing heat treatment

will be required in the fabricator's shop or on-site — only a series of subcritical-temperature stress reliefs. Preliminary experimental test plates have been subjected to this sequence of repeated cold-forming and stress-relief operations to establish that the type of plate material to be used in CB&I's initial reactor vessel construction does not undergo any deleterious reduction in the mechanical and impact properties established in the original quench-and-temper treatment at the mill.

The shell courses will be fitted up and temporarily assembled in the shop to the extent necessary to establish the required dimensional tolerances, to insert nozzles in shell-course penetrations, and to clad the shell courses. These shell courses will then be separated into the individual plates (two per course) and shipped to an assembly shop at the site, where additional preassembly, particularly the welding and stress relieving of the longitudinal weld seams in the shell courses, will be done. This welding will be done under essentially shop-type conditions in an enclosure that will also serve as the stress-relief furnace as the shell courses are completed. The head sections will be partly preassembled in the shops and shipped to the site for erection. Final erection of subassemblies from the shops and the site-assembly yard will be done in a succession of seven major lifts, and the welding of the main circumferential joints and their stress relief will be performed inside the partially completed containment vessel, which will be erected concurrently with the reactor vessel, as mentioned further below.

CB&I uses most of the conventional welding methods but will place principal emphasis on the manual metal-arc covered-electrode process, which will be used almost exclusively in site assembly and erection and, to a considerable extent, in preference to the submerged-arc process in shop fabrication. In the shops, either gamma-radiography or a betatron unit will be used, as appropriate, for weld inspection. Gamma radiography will be used on the site. Where gamma radiography is used, it will always be done in conjunction with a "double" ultrasonic examination — the first on the completed weld before stress relief and the second after the stress-relief treatment is completed.

Weld-overlay cladding will be applied to completed or partly completed subassemblies in the shops. Field welds and adjacent areas will

have the overlay applied manually during the site assembly or as a part of the erection sequence.

A feature of the CB&I-proposed erection scheme involves coordinated erection of containment and reactor vessels by the same crews, equipment, and techniques. This should lessen delays, interference, and confusion from having different contracting organizations on site at the same time doing interdependent operations. Such a scheduling system permits the use of the partially completed containment vessel at convenient stages to control the environmental conditions and make them comparable to shop surroundings for critical welding, machining, stress relief, inspection, and testing of the reactor vessel. Special tools and techniques have been devised in the course of experience with large field-erected process vessels that will be used for finish machining of flange faces, double tongue-and-groove flange-seal closures, flange stud holes, head penetrations, control-rod housing and drive inserts, and miscellaneous attachments.

8.2 OPERATIONS AND MATERIALS[4]

The basic operations in fabricating reactor pressure vessels are similar for all fabricators, but there are differences in types of equipment and procedural details. There are also significant but more subtle features that characterize the work done by major fabricators of "quality" pressure vessels, both process and nuclear, when compared with the fabrication of presumably less critical nonnuclear, nonprocess, and "nonlethal" vessels. (This is a generalization and there are many exceptions. It does not imply that all nuclear equipment fabrication meets "quality" criteria nor that all "noncritical" component fabrication is substandard.) "Quality performance" features include developing detailed, workable written procedures for all phases of the operations; continuous monitoring of these operations by supervisory and technical groups to insure compliance with the established procedures; competence of craft, supervisory, and technical personnel; superior capability in design, metallurgy, cleaning technology, fabrication techniques, and nondestructive testing; availability and adequacy of equipment in efficiently designed shop layouts;

and the success of management in coordinating all these efforts responsibly and effectively. Of particular importance is the maintenance of complete records of all steps in the fabrication operation, including test reports, on both purchased material and in-plant testing, weld and examination procedure qualifications, authorized deviations and repairs, heat-treatment records, nondestructive testing inspection records, and the like. While some purchasers require that this material be combined into a "Vessel Fabrication Report," the practice and completeness are variable as actually applied. Such a requirement is not contained in the Code but might well be considered as a requirement to parallel the design and stress reports.

The steps described below include fabrication operations and quality control procedures, some of which are described further in Chapter 9. These descriptions are largely limited to components made of SA 302 grade B manganese-molybdenum steel modified with added nickel or A 533 steel or equivalent materials in thicknesses of 4 in. or more used for primary pressure containment for the large boiling- and pressurized-water reactor systems. Some consideration will be given to the prospective future use of higher strength quenched-and-tempered low-alloy steels in these vessels. These descriptions are a composite of operations typically performed by the principal fabricators; they do not describe in detail all the operations of any one individual shop.

The material product forms used are plates and forgings, bolting materials, bar stock, and welding materials. Castings, pipe, tubing, structural shapes, sheets, and strip are also used for appurtenances, attachments, supports, and core internals. These are discussed in more detail in Chapter 4. The principal vessel parts are a cylindrical shell, heads, flanges, nozzles, studs, nuts, supports, control rod sleeves, and other penetrations and attachments, as shown schematically in Fig. 8.1 for a typical reactor vessel.

8.3 SHELL FORMING[4]

The shell cylinder is made of several shell courses joined by circumferential butt welds. It is frequent practice to make a shell course

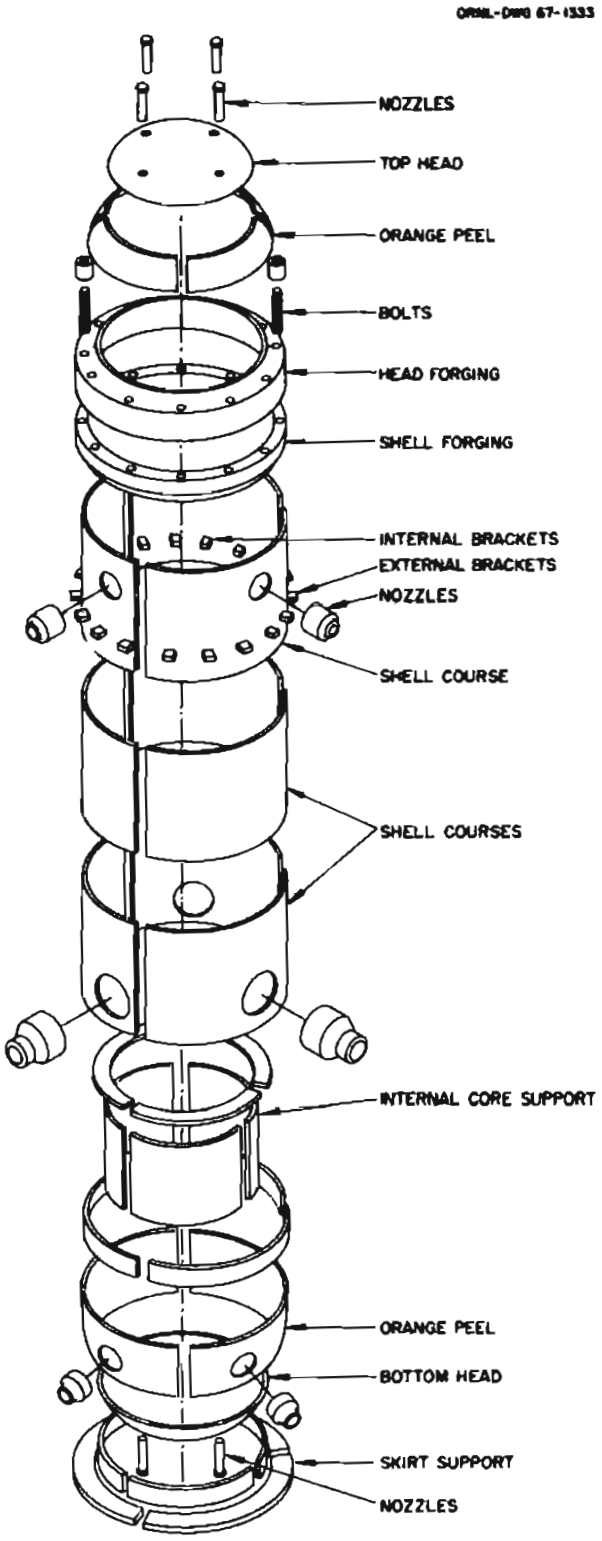

Fig. 8.1. Exploded Schematic View of a Typical Boiling-Water Reactor Pressure Vessel.

from three hot-formed plate sections joined with longitudinal welds, but the actual number of sections used is largely a matter of economy, design requirements, and convenience in handling and welding. Plate size is also set by such factors as ingot weight (about 100,000 lb maximum), wall thickness, and width of plate available. Large thick-walled vessels may require more than three shell plates per course, while a course for a smaller diameter vessel may be made from one or two plates. A course can also be made from a single-ring forging in sizes up to 140,000 lb, but this appears to be more expensive, although the shell of at least one European reactor vessel is being made this way. It has also been suggested that shell courses be made of several concentric thinner shells by one of the methods used for multilayer construction.[4,5] Plates and heads can also be forged to shape from ingots or forging billets, but costs and the equipment available in fabricators' plants generally result in hot forming (occasionally cold forming) of rolled plate. Flat plates for the shell courses are usually ordered from the materials manufacturer in the as-rolled or stress-relieved condition to specification requirements described in Section 4.3.1. Some inspections, such as ultrasonic inspection, are frequently performed after the plates are received in the fabricators' shop. Fabricators generally prefer to do any weld repair that is required on the plates, and by conducting the examination for plate defects in their own shops, they can control the repairs as a part of the manufacturing sequence.

Section III of the ASME Code requires ultrasonic examination of plates to N-321 or Code Case 1338 and Specification SA 435. These call for pulse-echo normal-beam examination by continuous scanning along grid lines at 9-in. intervals and rejection of laminations or other defects that produce indications that cannot be contained within a circle with a diameter greater than 3 in. or one-half the plate thickness. There are some permissible alternates to these requirements. The Code and ASTM committees are working to improve the procedures and acceptance standards. The principal fabricators and nuclear contractors work to somewhat closer requirements, such as added shear-wave examination, 100% coverage of the surface instead of the 9-in. grid, and smaller areas of acceptable indications, which may vary with the location in the vessel where the plate

will be used. If defects require repair by welding, the repair may be made after inspection or, if the defect is not expected to affect the plate in the forming operation, the fabricator may delay repair until after forming and heat treatment. He may also elect to make a temporary repair at this point with a more readily formable weld deposit and then replace this temporary repair with a weld deposit consistent with the chemical and mechanical requirements placed on the vessel materials after forming and heat treatment. The Code limits the depth of defects that may be repaired to not over one-fourth the nominal thickness; however, concurrence by the fabricator, purchaser, and authorized inspector is needed before any such repairs are made. Areas prepared for repair are examined by magnetic-particle or liquid-penetrant methods both before and after the repairs are made, and the weld repaired areas, unless they are very shallow, are examined by radiography as well.

Plates are trimmed before forming to sizes consistent with the design dimensions of the shell courses and vessel; this includes allowances for forming, trimming, weld-joint preparation, test plates, and specimens for surveillance and other mechanical property tests. The amount of material reserved for tests depends on the requirements of the fabricator, the customer, and the method of fabrication. A typical practice is to add 5 in. to the length of the plate from which the test specimens will be removed. In cases where plates are electroslag welded to form shell courses and the heat treatment is done on the shell-course subassembly, a 4-in. band may be left on each course for test specimens. The initial plate thickness also makes allowance for thinning in bending or rolling and for scaling in subsequent heat treatment. Trimming may be done by machining or by flame or arc cutting and grinding. This is followed by magnetic-particle or penetrant examination of the cut edges and repair of laminar or other exposed defects. Care is taken to preheat to a preestablished temperature before cutting or weld repair to lessen susceptibility to cracking due to residual stresses at plate edges and surfaces during heating and hot forming. Handling lugs may be welded to the plate to assist in the later subsequent forming and heat-treatment operations. Before forming, the plates (A 302 grade B, nickel-modified, A 533 type) are heated into an austenitizing temperature range, 1600 to 1750°F,

usually about 1700°F, and held at temperature for about 3/4 hr per inch of thickness, but not in excess of 4 to 6 hr. Toward the end of the holding period the plate surface temperature may be increased somewhat for a short time just before forming. The heating rates, metal temperature, and holding times established in the procedures are determined by the alloy composition, the plate size and thickness, the manufacturer's practices, the capabilities of the available equipment, and the estimated time required for forming. It is intended to complete almost all hot working when the plate has cooled to 1600°F, in the case of one fabricator, or 900°F for another. Heating for forming is generally done into the austenitic range. Heating rates, temperatures, and holding times are those required to obtain the desired metallurgical, structural, and mechanical properties in the formed plates. The plates are removed from the heating furnace and then hot formed in a brake press or rolls. A brake press forms the plate by a succession of applications of load to dies that bend a short length of the plate each time as the plate is moved forward in small increments; the operation consists of a series of closely spaced, parallel bends to the desired cylindrical contour and tolerances. While hot-press forming is the more common method for shaping thick-plate sections in most shops, the new B&W facility has rolls that can hot roll 15-in. plate (Fig. 8.2). A plate is usually formed to shape in one continuous operation without intermediate reheating, but if there are difficulties or delays, partly formed plates may be returned to the furnace and the heating and forming sequence continued.

After forming, the plates are cooled to room temperature and checked dimensionally. If the formed plates are to be arc-welded into shell courses, they are heat treated before welding; but if the longitudinal joints are electroslag welded, the heat treatment is done on the courses after welding to refine the coarse-grained structure of the weld and heat-affected zones and thus improve impact properties and permit more effective ultrasonic examination of the electroslag-weld zone. This austenitize, quench (or normalize), and temper sequence on thick sections of reactor vessel materials is intended to develop improved and uniform properties throughout the plate thickness, particularly, impact properties.

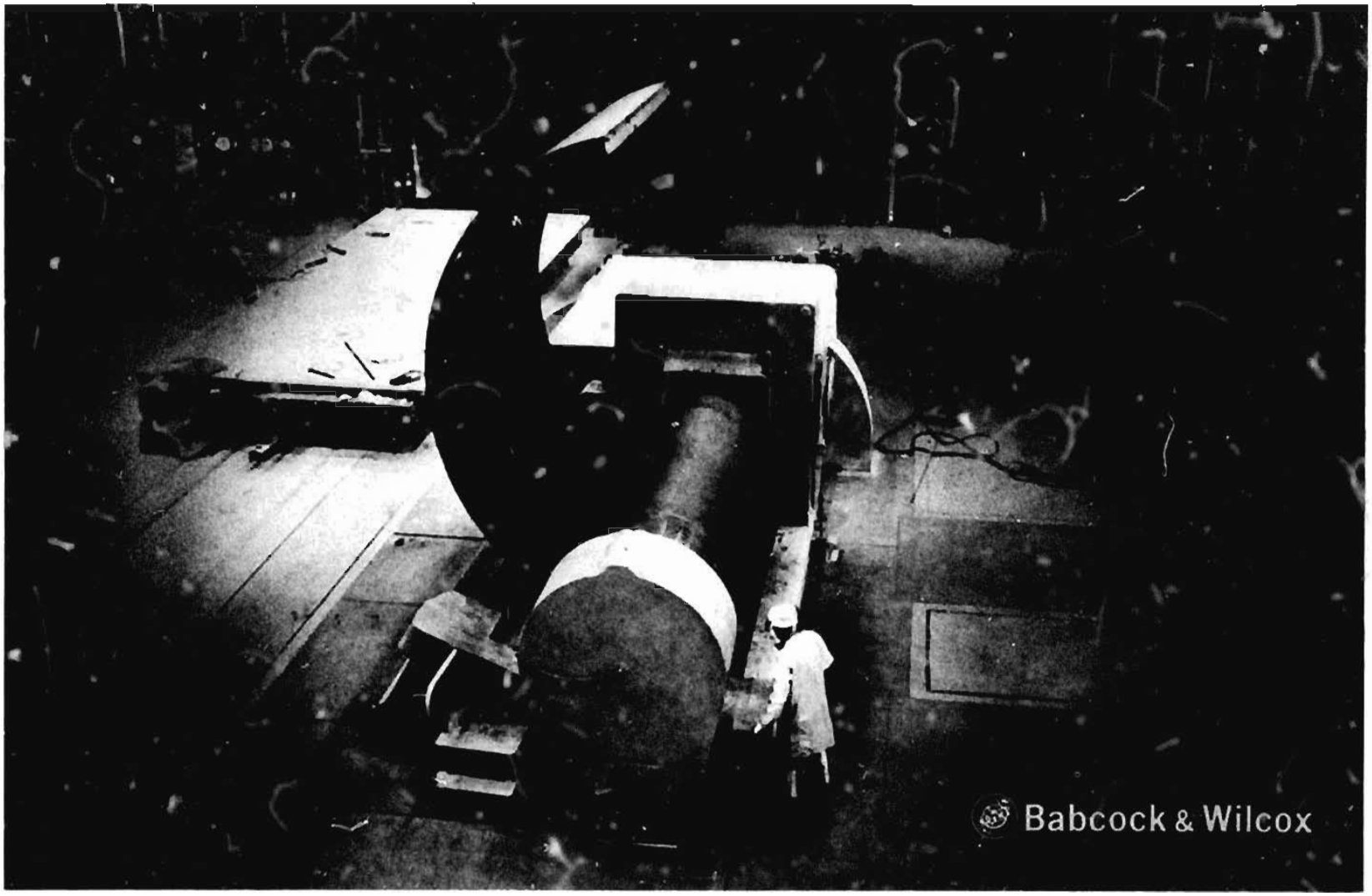

Fig. 8.2. Plate-Forming Rolls. (B&W photograph)

If hardenable higher strength and more highly alloyed steels, such as nickel-chromium-molybdenum or 2 1/4% Cr–1% Mo steel, are to be used in future larger size reactor vessels, this heat treatment sequence, modified to suit the specific materials, will have the important added function of achieving increased strength combined with acceptable ductility and toughness. Submerged-arc and manual metal-arc welding of previously quenched and tempered shapes or courses can generally be controlled to avoid the extremely coarse-grained heat-affected zones and coarse columnar weld deposits that often characterize electroslag welds. Therefore a postweld stress-relief heat treatment will generally be sufficient to restore adequate impact properties. In contrast, electroslag joints usually require a grain-refining heat treatment into the austenitic range.

8.4 HEAT TREATMENT OF FORMED SHELL PLATES[4]

Where longitudinal shell course-joints are to be arc-welded, the fabrication sequence after hot forming, air cooling, and cold sizing is approximately as follows; the sequence for electroslag-welded courses is described in a later paragraph. Formed plate thicker than 9 in. may be coated with a proprietary compound to help remove the scale that forms in heating and may lessen the effectiveness of the quench, but for thinner sections, the cooling rate in the quench will develop the desired properties, even with scale present. The formed plates are placed on a charging car, usually three at a time, charged into the furnace, brought to an austenitizing temperature of 1550 to 1650°F, and held for at least 3/4 hr per inch of thickness with a 1 hr minimum but not necessarily more than 4 hr for any thickness and in no case more than 10 hr total above 1550°F. The temperature is controlled by calibrated thermocouples located at the anticipated hottest and coldest areas of each plate. After the plate time-at-temperature requirements are satisfied, the charge car is withdrawn from the furnace. One plate from the multiple charge is removed and transferred to the quenching tank. The remaining plates are returned to the furnace, brought back to the austenitizing temperature, and removed later for quenching, without any extended holding time beyond that required to carry out the quenching of the previous plate and return the quench

medium to the proper temperature. The plates are quenched in water agitated by air, circulating pumps, impellers, or added cold water for times ranging from 9 min for 4-in.-thick plate to about 45 min for 10-in. plates to assure that plate surface temperatures after removal from the quench tank will not go higher than 400°F. This has been established experimentally as the procedure needed to assure the microstructure, mechanical properties, and specified impact values in each plate. The water temperature at the start of each quench is sufficiently low that it will not exceed about 100°F at the finish, although a maximum of 140°F is considered acceptable.

The maximum water temperature is intended to minimize steam formation and promote its removal; otherwise steam at the surface would unacceptably decrease the cooling rates. Air cooling or spray quenching may be used on thinner wall sections of some materials, but most heavy-vessel fabrication involves immersion quenching. After quenching, the plate is tempered at 1200 to 1250°F (for SA 302 grade B, modified) for from 1 to a maximum of 4 hr, depending on thickness. After tempering the plates are cooled to 600°F in the furnace and then air-cooled to room temperature. This is done to lengthen furnace-lining life rather than for any metallurgical reason. It is a procedure established at the option of the fabricator rather than as a specification requirement. After the quenching-and-tempering sequence, formed plates are cold sized to correct any out of roundness existing after heat treating. Cold forming or sizing is permitted if the elongation of the outer fibers will not exceed about 3.5%, which has been established as an acceptable limit to minimize the possibilities of cracking or deterioration of properties; but the strains from this cold-sizing operation seldom exceed a fraction of 1%. (Note the exception above for the CB&I sequence.) The plate is then inspected for contour and radius and layed out for removal of material test stock, test plate material, excess forming stock, and weld preparation. The test material and excess forming stock are removed by burning; this may be done by any of several methods, such as flame cutting, arc-air gouging, plasma-arc cutting, or other arc-cutting methods. The fused and immediately adjacent heat-affected metal is removed by machining or grinding to the extent necessary to remove oxides, irregular

surfaces, striations, or notches and make meaningful visual and magnetic particle examinations feasible. Part of the test material removed from plates for two shell courses at this point is used for making the surveillance specimens discussed in Section 10.2.1.

The material removed from individual plates for tests by the fabricator will typically measure 5 by 16 in. by full plate thickness. This test section is given a 40-hr stress relief at 1125 to 1175°F that is intended to simulate not less than 80% of the total time the plate will be subjected to later stress-relief treatments as it is fabricated into the vessel. The piece is air-cooled to room temperature after stress relief. Tensile, Charpy, and drop-weight specimens are taken from the 1/4 T (thickness) location on both sides of the plate. The specimens are tested to Code requirements and any additional contract specifications, which may vary with the customer and the vessel dimensions. Full-range Charpy curves are developed to get both upper and lower shelf values. Drop-weight specimens are broken at +10°F and at +40°F, if needed. If the 40°F test indicates a still higher NDT temperature, additional tests are run at higher temperatures to establish an NDT value. If failure occurs in the initial test, a 3T × 3T × T block is prepared for retest. If failure occurs in tests of this block, the entire course of which the plate is a part, together with sample test material sections, is given a second austenitizing and quenching treatment. This double-quench treatment has produced the required properties in every case to date (for one fabricator), so no plate or course has required rejection at this stage.

A 30-in. piece of steel is required for procedure and welder qualification tests. In the past, the Code has required a vessel test plate; however, this requirement has been modified recently in favor of a more effective welding-material and base-metal-properties control program, although the use of concurrently welded vessel test plates may be continued for a time.

8.5 ASSEMBLY OF FORMED SHELL PLATES INTO COURSES[4]

Details of weld-joint preparation are a part of the qualified procedures established by fabricators. A typical preparation for a

longitudinal submerged-arc weld joining the curved plate segments into courses involves a double U-groove joint with an off-center root face, usually 1/3 T or 3 in. maximum, and an included angle of 0 to 2°. Another type of weld-joint preparation has a single 6° V-groove with a backing strip that will be removed later (similar to nozzle insert joint design shown in Fig. 8.3). The weld-joint preparation is magnetic-particle examined to meet the requirements of paragraph N-513 of the Code, and defects are removed and repaired as necessary.

The required plate segments, usually three, are preassembled to form a course. Weld-positioning straps and strongbacks are manually welded, and end troughs and runnoff tabs are fitted to the shell course. The entire shell course is preheated to 200°F. The preheat equipment is then

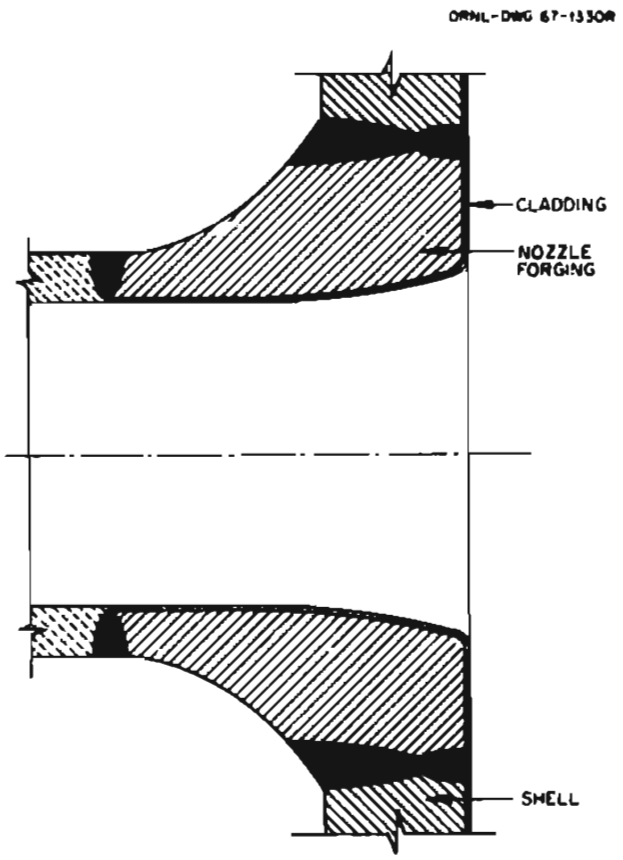

Fig. 8.3. Schematic Diagram of Typical Nozzle with Full-Penetration Welds.

removed, and the weld areas are locally preheated to a 250 or 300°F minimum, depending on customer requirements. The maximum interpass temperature is limited to 500°F. The submerged-arc welding procedure used in this instance has a larger number of smaller passes than generally used in welding other types of equipment. This serves to lessen any reduction in impact properties of weld metal and heat-affected zone material. It also tends to minimize the possibility of generating large interdendritic cracks and to facilitate their early detection and repair. The preheat temperature is maintained on each joint until the entire course is completed. The course is then given an intermediate stress relief by placing it in a furnace at below 600°F, heating to 1125 to 1175°F, holding for 15 min, furnace cooling to 600°F, and air cooling to room temperature. The subassembly is again locally preheated and the weld tabs and other attachments are removed by arc-air gouging.

8.6 ASSEMBLY AND HEAT TREATMENT OF ELECTROSLAG-WELDED SHELL COURSES BY ELECTROSLAG WELDING[4]

The use of the electroslag process for welding the longitudinal joints in shell courses involves some differences in fabrication procedures and sequence, in addition to the differences to be expected between different fabricating shops. The most obvious change is that the austenitize-quench-temper sequence is done after the three (more or less) longitudinal welds have been made to form the completed shell course.

After hot forming, cooling, cold sizing, and trimming of plates and examination and repair of edges, the formed plates are fitted together for electroslag welding (Figs. 8.4, 8.5, and 8.6). A square butt joint with a 1 1/2-in. gap is used, and about a 3 1/2-in.-wide weld-fusion zone is produced. Two electrodes are generally used for welds in 6- to 8-in. plate and four for 8- to 10-in. plate. The electrode filler metal is a six- to seven-strand braided wire selected and qualified to produce the desired weld-metal chemistry and properties. A 6-in. weld-starter pocket is used at the bottom of welds, and there is a runoff tab at the top. A 300°F minimum localized preheat is used to start the weld, but the heat of

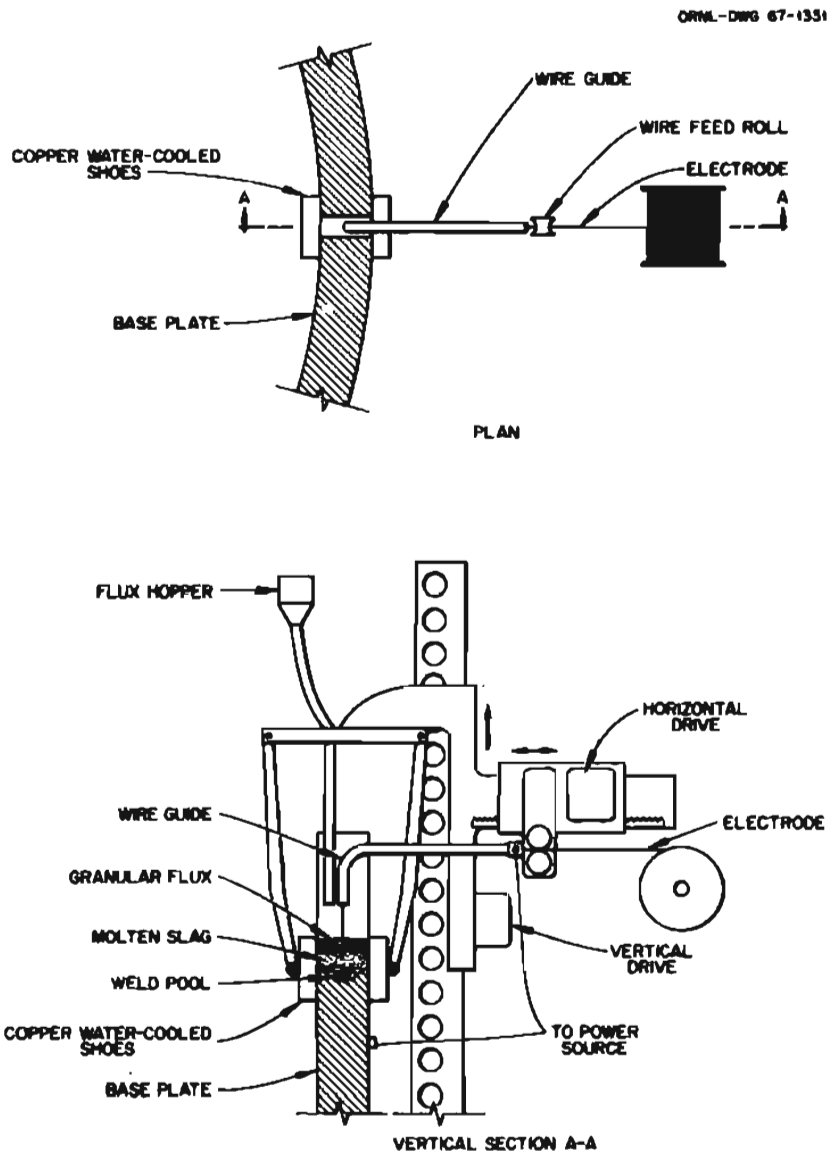

Fig. 8.4. Schematic Diagram of Vertical Electroslag Welding.

welding is sufficient to maintain the preheat temperature during the continuing operation. After all longitudinal welds (usually three) in a course are completed, the entire course is austenitized at 1675 to 1725°F for 1 hr per inch of thickness and then quenched in a circulating 10% brine solution at 150°F maximum at the start of the quench (Fig. 8.7). After the course has cooled to below 400°F it is removed, reheated to 1600 to 1650°F for 1 hr per inch of thickness, and again brine quenched. This double austenitizing treatment is used to obtain refinement of the coarse-grained

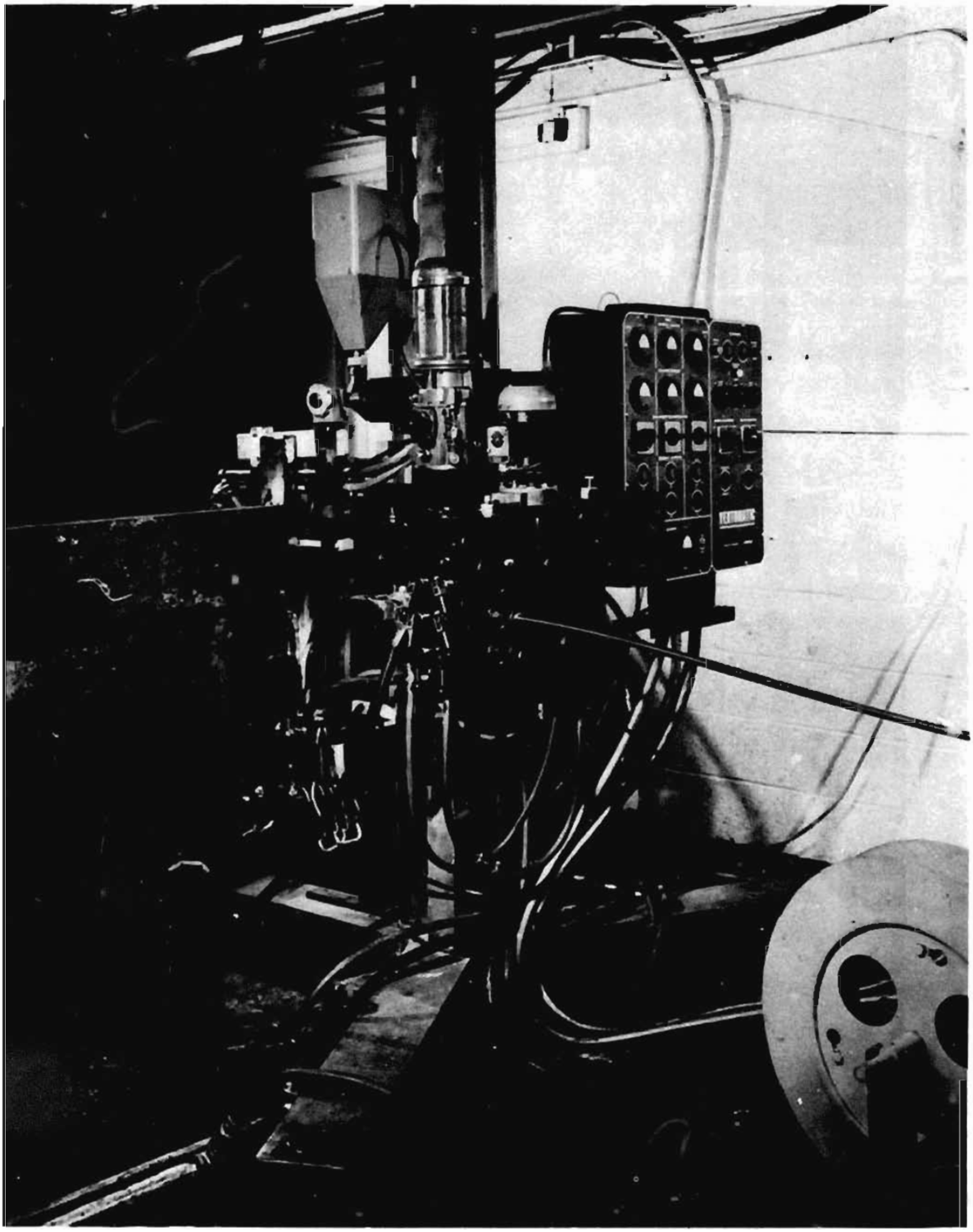

Fig. 8.5. Electroslag Welding Machine with Plate in Position for Welding. (Arcos Corporation photograph)

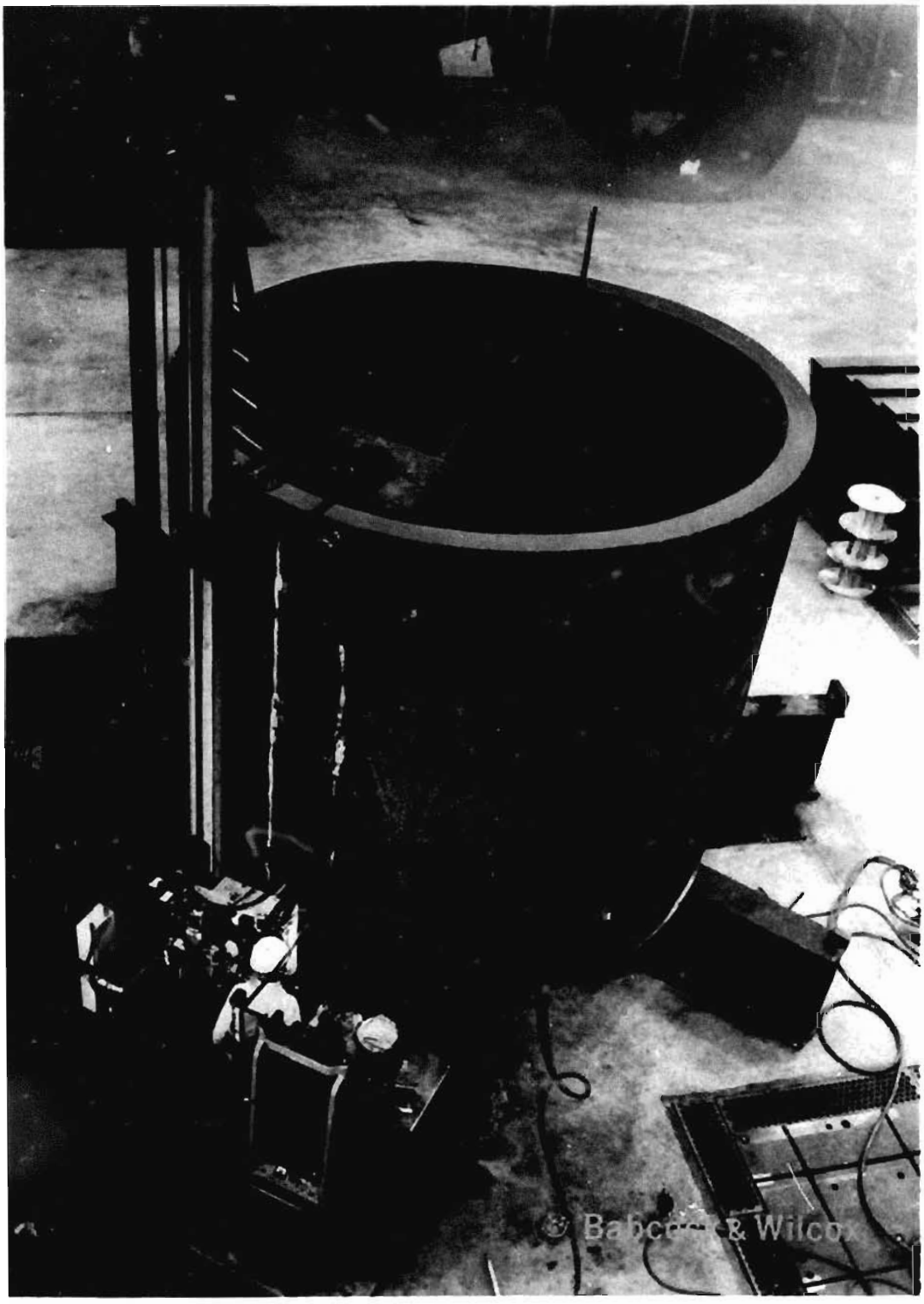

Fig. 8.6. Setup for Electroslag Welding of Longitudinal Seam in Shell Course. (B&W photograph)

Fig. 8.7. Shell Course Quenched in Vertical Cylindrical Tank. (B&W photograph)

structure of the electroslag weld and heat-affected zone. The course is then tempered at 1175 to 1225°F for 1 hr per inch of thickness and again brine quenched to get the required impact properties. Following this heat treatment, a 4-in. band of material is removed for tests. This width is acceptable because an insulator of the same type of steel is used during heat treatment to simulate the 1T thickness requirement. The 4-in. band is stress relieved for the total anticipated time that the material in the vessel will ultimately be in the course of fabrication. This ranges from about 20 to 45 hr, depending on the type and size of vessel. The required test specimens are removed from these bands, and base metal properties are determined for each plate that goes into the vessel. In addition, 12 drop-weight specimens are taken from each of the plates that make up the shell courses in the core region to establish the NDT temperatures. Additional material from these test rings is supplied to the buyer for surveillance and test programs.

Following the double quench-and-temper operation the electroslag welds are completely examined ultrasonically, as required by the Code.

Some problems have developed in maintaining dimensions in electroslag-welded courses after heat treatment, and it has been necessary at times to cut open a shell, reroll, and add one more longitudinal weld by submerged-arc welding to avoid repeating the austenitizing heat-treatment cycle. It is expected that this problem will be overcome in future fabrication.

8.7 JOINING SHELL COURSES INTO SHELL SUBASSEMBLIES[4]

The circumferential weld joints of the various subcomponents — shell courses, heads, and flanges — are made with essentially the same procedures, weld-joint preparation, and inspection as longitudinal submerged-arc welded seams, with the principal differences being the mechanical arrangement used to accomplish relative movement of the welding head and work-positioning equipment. The welds and inner surfaces of the subassemblies are examined by the magnetic-particle method, dimensionally checked, and repaired if required. The welds and any repairs in excess

of 3/8 in. are radiographed. Defects requiring repair are locally preheated and removed by arc-air gouging, and then approximately 1/16 in. of metal is ground out. The welds are repaired by manual metallic-arc welding. Repairs on inner surfaces are ground smooth and inspected by the magnetic-particle method.

8.8 FABRICATION OF VESSEL SUPPORTS[4]

Vessels may be supported, depending on the type of reactor vessel and on customer preference, by the addition of metal on the underside of the coolant nozzles (some PWR's) just below the vessel flange or by welding a skirt to the lower head (BWR's and some PWR's). The metal added to the coolant nozzle can be integrally forged with the nozzle, but it is generally added as a large weld-metal buildup that is thoroughly examined nondestructively. Where a cylindrical skirt is used, a weld-metal buidup is applied to the lower head that is frequently started as a weld inlay into the head. The built up weld metal is thoroughly inspected nondestructively and then machined to form one side of the weld preparation; the edge of the cylindrical skirt is machined to form the other weld preparation face. These weld buildups and joints are stress relieved and nondestructively examined.

8.9 NOZZLES AND DISSIMILAR METAL WELDS[4]

The methods of attaching nozzles and attachments of the types defined as Category D in N-461 of Section III of the ASME Code and further described in more detail in the text and illustrations of N-462.4, particularly those involving a transition from one type of material to another (e.g., a ferritic manganese-molybdenum steel, nickel modified, to an austenitic stainless steel or nickel-base alloy), represent perhaps the largest variety of practices to be found in nuclear reactor vessel fabrication. Practically all the types of weld detail illustrated in figures N-462.4(a), (b), (c), and (e) of the Code are used, with the

further complication of accomplishing the dissimilar-metal transition. The type of joint design and the welding procedure used are determined largely by the type of vessel, the service conditions to which the configuration will be exposed, and the fabrication practices used by the manufacturer, all within the requirements and restrictions imposed by the Code rules. Main coolant nozzles are generally made as integral forgings inserted through the vessel wall thickness and designed for full-penetration double-groove welds requiring 100% radiography, with requirements comparable to those for the main seams of the vessel. These welds are usually clad internally, as described in Section 8.10.

Where a dissimilar-metal transition is required, a "safe-end" or nozzle extension of corrosion-resistant material is generally added as an extension of the nozzle. This is added so that the dissimilar-metal joint may be stress relieved along with the vessel but will require no further stress relief when stainless or nickel-base attachments are made to the vessel safe ends in the field. Two general methods are used to make these transition joints. In one type the joint is a relatively conventional groove joint between the dissimilar metals made with a weld metal, generally an Inconel modification, that is compatible with both base metals (Fig. 8.3). In the other general type, the nozzle, usually a ferritic material, has an overlay or "buttered" extension of overlay deposit with a composition approximating or compatible with that of the safe end (e.g., type 308, 309, or higher ferrite-content weld metal for attachment to type 304). After the buttered weld deposit extension is inspected and nondestructively examined, it is machined for weld preparation for a conventional grooved-joint design and procedure.

When smaller diameter tubular attachments must be made, the thickness of the tubular insert is insufficient to justify full penetration through the vessel wall; in such cases, a weld buildup, partially inlaid and compatible with the vessel material, may be made to permit a full-penetration dissimilar-metal joint through the attachment thickness. Under certain limited conditions, partial penetration welds, as described and illustrated in N-462.4(d), may be made with a weld metal (e.g., Inconel type) compatible with the two base metals joined.

Partial-penetration nozzle welds in reactor vessels are limited largely to stub tubes for attachments involving substantially no piping reactions or thermal stresses greater than those expected in the vessel itself. These are used to attach control rod housings, flux monitor tubes, vents, and instrument attachments.

The practice follows the requirements of paragraphs N-457(c) and N-462.4(d) and generally uses the socket-weld type of joint design illustrated in Fig. N-462.4(d) (lower left corner) of Section III of the ASME Code, although the other designs illustrated in the figure may also be used. The Code requires that all compensation be integral with the part of the vessel penetrated, that the welds be of sufficient size to develop the full strength of the attachment, and that the nozzles have an interference fit or a minimum clearance fit, as stated in Fig. N-462.4(d). The welds are J-groove-plus-fillet joints with a minimum depth of 1 1/4 times the nominal thickness of the nozzle neck.

The nozzle tubes are generally stainless steel or Inconel. After cladding has been applied to the head or shell section, the weld joint preparation is machined with a sufficiently generous weld groove to permit the application of a thick buttered layer of weld metal — Inconel or stainless steel — over the base material exposed in the weld groove. The buttered layer is thick enough to permit subsequent welding to it without requiring that the full weld and housing (or other attachment) be subjected to any subsequent stress relief. The shell material with the overlay cladding is stress relieved, the weld groove in the overlay is further prepared, if necessary, and the weld is then made with Inconel or stainless steel filler metal, depending on the composition of the nozzle insert and the buttered overlay in the weld groove.

Welding is generally done by the manual metal-arc or automatic metal-arc processes. The root pass is checked by a liquid-penetrant method, and the remainder of the weld is checked progressively by a liquid-penetrant (or magnetic-particle) method. In some cases, the completed weld is also examined ultrasonically.

Flanges or safe ends are welded to the nozzle ends prior to shipment. The housings or other attachments are added in the field — typically, the

end of a control rod housing tube is inserted through the length of a stub-tube nozzle and welded to the free end of the nozzle, usually with a fillet or fillet-and-groove weld.

8.10 WELD-OVERLAY CLADDING[4]

Weld-overlay cladding is applied to courses individually or to multiple courses of a size that can be conveniently handled by the cladding equipment. For commercial power reactors, an austenitic stainless steel cladding is generally used for shells, heads, nozzles, and other openings. A nickel-base alloy overlay is sometimes used for flange faces or areas where bearing loads are expected or in places where crevices and high stresses prompt concern for possible stress-corrosion mechanisms. Such areas are largely determined by the designer and stated in the vessel specifications.

Preparation of shell sections preliminary to cladding will vary with the location of the course in the vessel with respect to the core, the type of reactor vessel, and the dimensional tolerances for those locations. Where dimensions are critical, the inside and outside of the shell courses are machined to a tolerance of, for example, ±0.005 in. for a 173-in.-diam vessel. The inner surfaces of courses that do not require these close tolerances are generally shot blasted rather than machined before cladding. In overlay cladding, the shell courses or subassemblies are usually rotated horizontally about the longitudinal axis on the mechanically driven rolls, with the welding head suspended from a beam extending the length of the vessel section and moved forward along the beam as welding proceeds. The entire shell section to be clad is preheated to 250 to 300°F for cladding. The overlay cladding is deposited as continuous spiral or concentric partly overlapping beads. The methods generally used in the stainless steel cladding of large reactor vessels are either a single oscillating arc or the series-submerged arc process, which uses a three-wire feed with the two outer wires being the electrodes connected to the power source and a cold center wire fed directly into the weld puddle. The wire compositions may be varied, for

example, between types 308 or 309, to get a balanced chemistry in the weld overlay, which is usually intended to approximate a nominal type 304 composition. The wires are fed into the bed of flux in such a way that arcs are struck in series between the electrode wires and the weld puddle.

A recently adopted practice is to apply cladding in a single layer of 1/8-in. minimum and 5/32-in. nominal thickness. Nickel-base alloy cladding is generally deposited by an automatic gas-shielded arc process. The various mechanical, electrical, and other welding parameters, such as speed of travel of the rotating cylindrical section, advance of the welding head, electrode-to-work distance, flux feed (or gas flow), weld feed, voltage, amperage, etc., are accurately controlled by automatic means and are continuously monitored and adjusted where needed by one or more operators. The details of weld overlay practice just described are typical of present-day practice, but the actual procedures vary from one fabricator to another and are determined in part by the requirements of the customer, the vessel type, and technical developments in weld overlay cladding equipment and processes. After cladding, observable defects are repaired by manual welding, usually with a type 308 covered electrode, with the work kept at the established preheat temperature. After this is done, the course is stress relieved at from 1125 to 1175°F for about 15 min. The internal surface is cleaned and prepared for penetrant examination. The repaired weld and base-plate areas that will require radiography are ground smooth, and the subassembly or assembly is examined as described below.

In early small reactor vessels, stainless steel or nickel-base alloy cladding or lining was applied by a variety of methods as an intermittent resistance spot-welded lining, a seam- and plug-welded lining, a vacuum-brazed cladding, a roll-bonded cladding, or an arc-welded overlay cladding.[6] Methods of arc welding that have been used for the cladding process, but not necessarily reactor vessels, include manual shielded metallic-arc, gas-shielded tungsten-arc, plasma-arc, and several variations of the submerged-arc process. Arc-welding processes have been further modified by the addition of cold filler wire or strip to the weld puddle,

the use of braided filler wire, the use of various types of automatic controls and programmed oscillation of the welding torch head, and the use of multiple arcs in series, tandem, or combination.

In the past, weld-overlay cladding has usually been deposited in two layers, with the first being moderately high-chromium stainless steel weld wire to balance the base-metal dilution and the second more nearly approaching the composition of the desired overlay surface. A recent development program has suggested the desirability of using type 309 stainless steel with added molybdenum for the first layer to permit a wider range of base-metal dilution without forming fissure-sensitive weld deposits.[7]

The first step in quality control of overlay cladding is the qualification of the procedure to the requirements of the Code and the satisfaction of the fabricator, the customer, and the inspector. While the Code provides for qualification of weld cladding procedures and operators, it does not contain detailed rules for the examination of the cladding, since it is not considered to contribute directly to the pressure-containing capability of the vessel. The acceptance standards for cladding inspection are jointly set by the fabricator and the customer.[4] Typical rejectable defects are a 1/16-in. maximum defect in the bond, any evidence of arc break, or more than ten small penetrant indications per square inch of cladding surface. No more than one of these can be in the range of 3/32 to 1/8 in., 1/16 to 3/32 in. for not over two, 1/32 to 1/16 in. for three, and 1/64 to 1/32 in. for four. However, the cladding seldom contains this number of indications.

8.11 HEAD SUBASSEMBLY[4]

Heads are made in much the same way as the cylindrical shell assemblies. For the larger vessels, the heads are made of hot-formed segments welded together. In smaller diameter vessels, one plate may sometimes be pressed to form an entire head. Some heads of relatively large diameter and less than 3 in. in thickness may be formed by hot spinning, but

this method is generally not applicable to heads for large reactor vessels. Plates for the large vessel heads are generally hot formed between closed dies to make each segment in a single application of load. The formed plates are then austenitized, quenched, and tempered; samples are removed and tested; the formed plates are inspected, cold sized, and machined to the desired dimensions; the edges are prepared for welding; the segments are preassembled with strongbacks and other supports; and the preassembled head is placed in a positioner that usually moves the weld joint under the torch (Fig. 8.8). The welds are generally full-penetration double-butt joints made by the submerged-arc process. Single-groove welds made with backing strips that are later removed are also used.

Other arc-welding methods can be used, however, subject to qualification and approval to the satisfaction of the fabricator, customer, and inspector. In U.S. reactor vessel manufacturing practice the electroslag process has been limited to straight longitudinal seam welds, although circumferential and other curved weld joints have been electroslag welded in Western Europe and the Soviet bloc countries[3] and to some extent in other types of equipment in the United States. Head-section dimensions are checked frequently. The adequacy of the metallurgical and mechanical properties is determined after simulated or concurrent heat treatments, and weld-overlay cladding is applied to the welded head assemblies (Fig. 8.9) in much the same way as for cylindrical shell sections. Because of the need to maintain accurate dimensions with reference to fixed reference planes and axes, machining for insertion of head penetrations, welding of these penetrations, and overlay cladding of the welds at the openings is generally delayed until most of the other operations on the heads, including attachment to the flange or cylindrical shell course, have been completed.

8.12. FLANGE AND NOZZLE FORGINGS[4]

Shell closure flanges and nozzles are generally made from forgings that have been heat treated, rough finish-machined to approximate surface

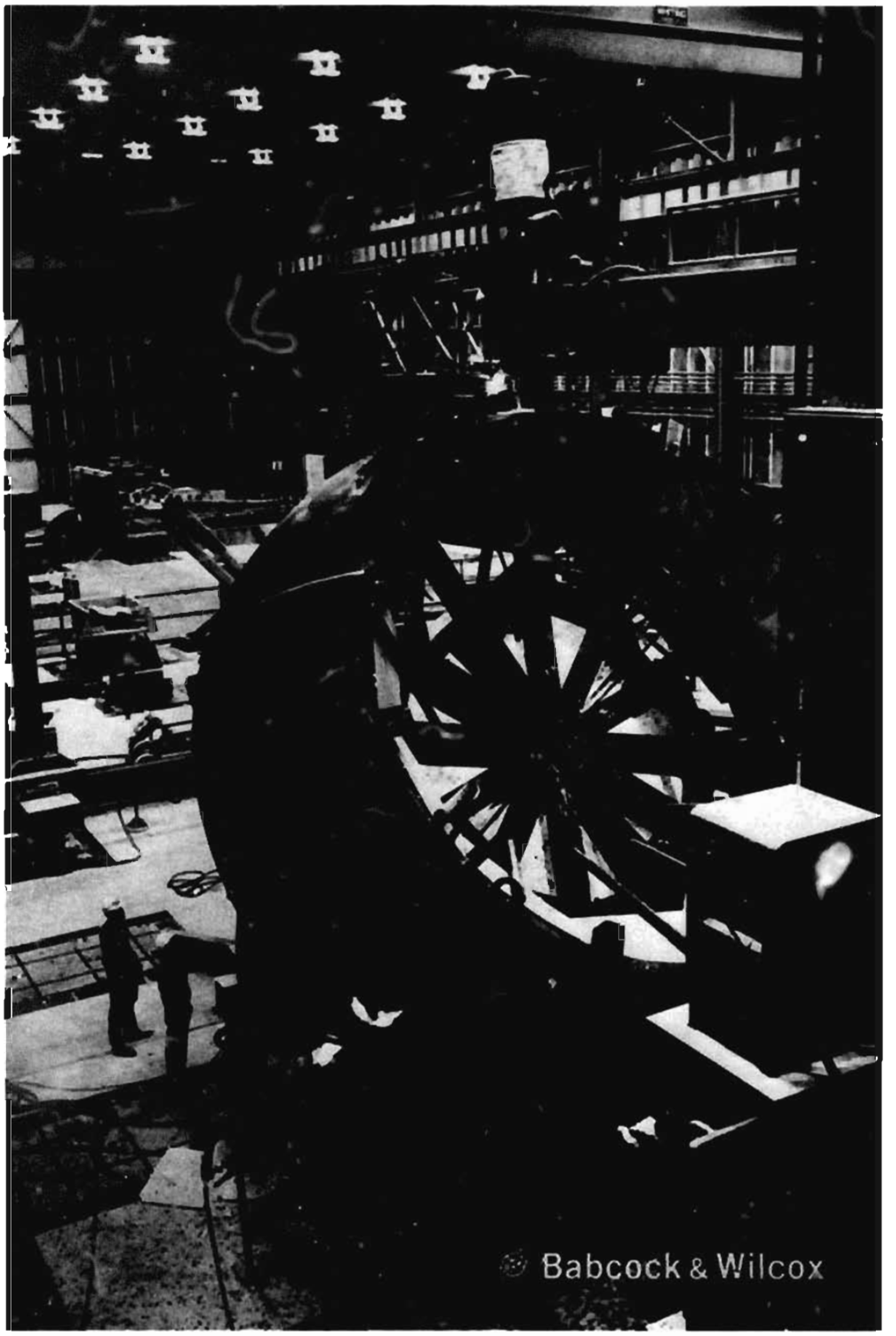

Fig. 8.8. Head Segments Assembled for Welding. (B&W photograph)

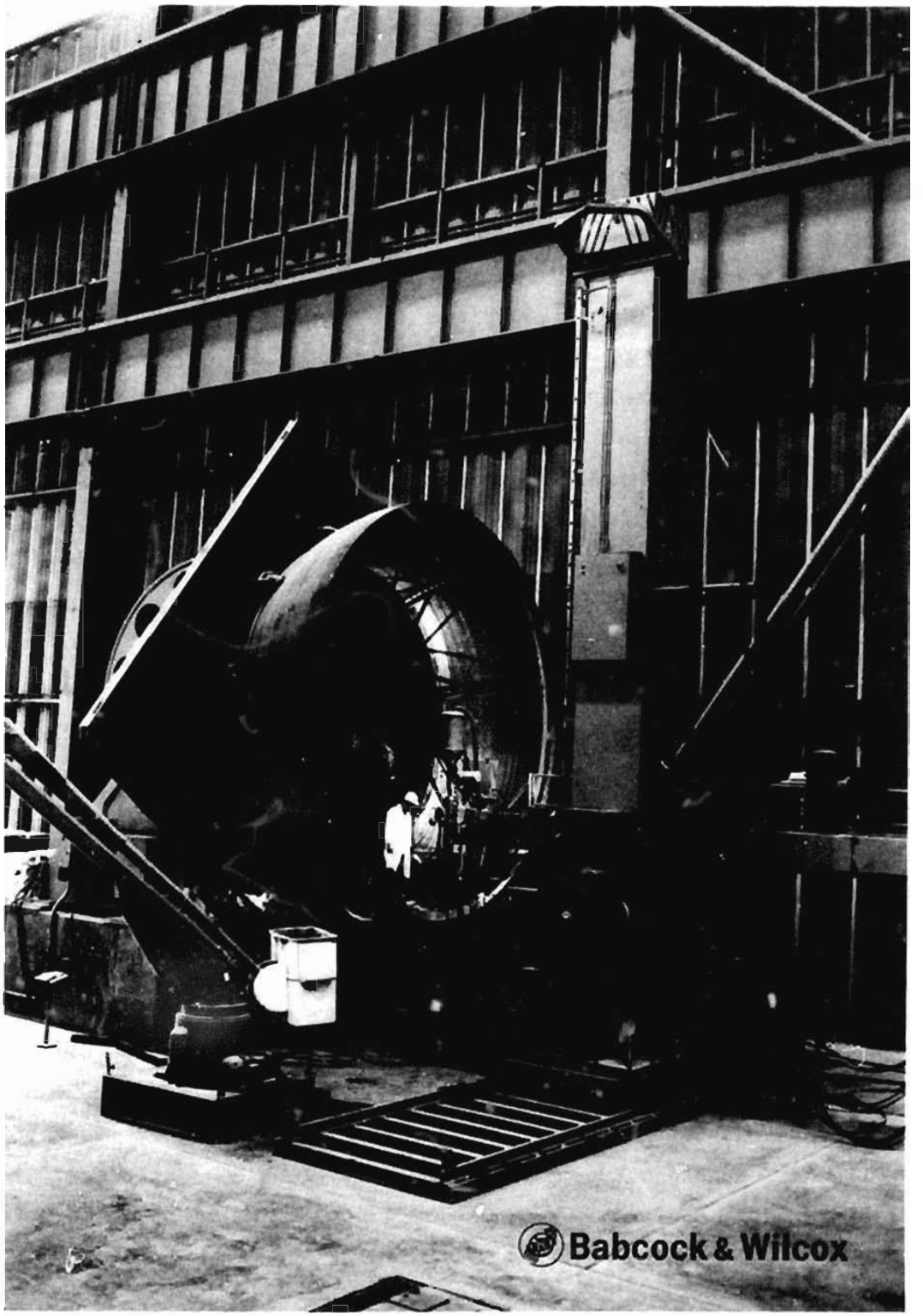

Fig. 8.9. Weld-Overlay Cladding of Segmented Head Section. (B&W photograph)

contours, tested, and inspected at the forge shop prior to shipment to the fabricator. The fabricator's operations then include preparation for weld-overlay cladding, together with the actual cladding, and weld preparation and welding of the forging to the vessel shell or head, followed by overlay cladding of these weld joints.

Weld-overlay cladding of flange faces may be done in much the same way as for the shell and head sections, although Inconel-type overlay, when used, is generally applied by the gas-shielded consumable-electrode process. The cladding of the inner surfaces of the flanges is generally done with stainless steel weld overlay in much the same way as the shell courses and often concurrently with them.

Nozzles and other pressure-boundary and pressure-containing attachments made of low-alloy steel forgings are clad by methods similar to those used for the shell, heads, and flange forgings, but some mechanical ingenuity is often needed to clad the inner bore of smaller diameter components. Other arc-welding methods, such as manual covered electrode or gas-shielded processes, may be used in cases where access is a problem. Nozzle and other penetration openings in head and shell sections are usually made after partial subassembly and cladding (Fig. 8.10). In preparing for placing full-penetration welded inserts into shell or heads, the cladding is generally removed for a few inches from the weld joint preparation to avoid overheating the previously deposited cladding and interface. Strength welds for nozzle penetrations may be made in several ways but are frequently made with covered electrodes by a manual process. Surfaces of strength welds in locations of complex geometry are frequently clad manually with covered or gas-shielded electrodes of either stainless steel or Inconel-type material. These joints may be locally stress relieved, but it is also desirable to stress relieve the entire assembled or subassembled components to remove residual stresses, minimize distortion, and permit early correction of dimensional discrepancies.

8.13 MACHINING[4,8]

When assembly, stress relief, and dimensional inspection are completed, the two major vessel sections (body and closure head) are finish

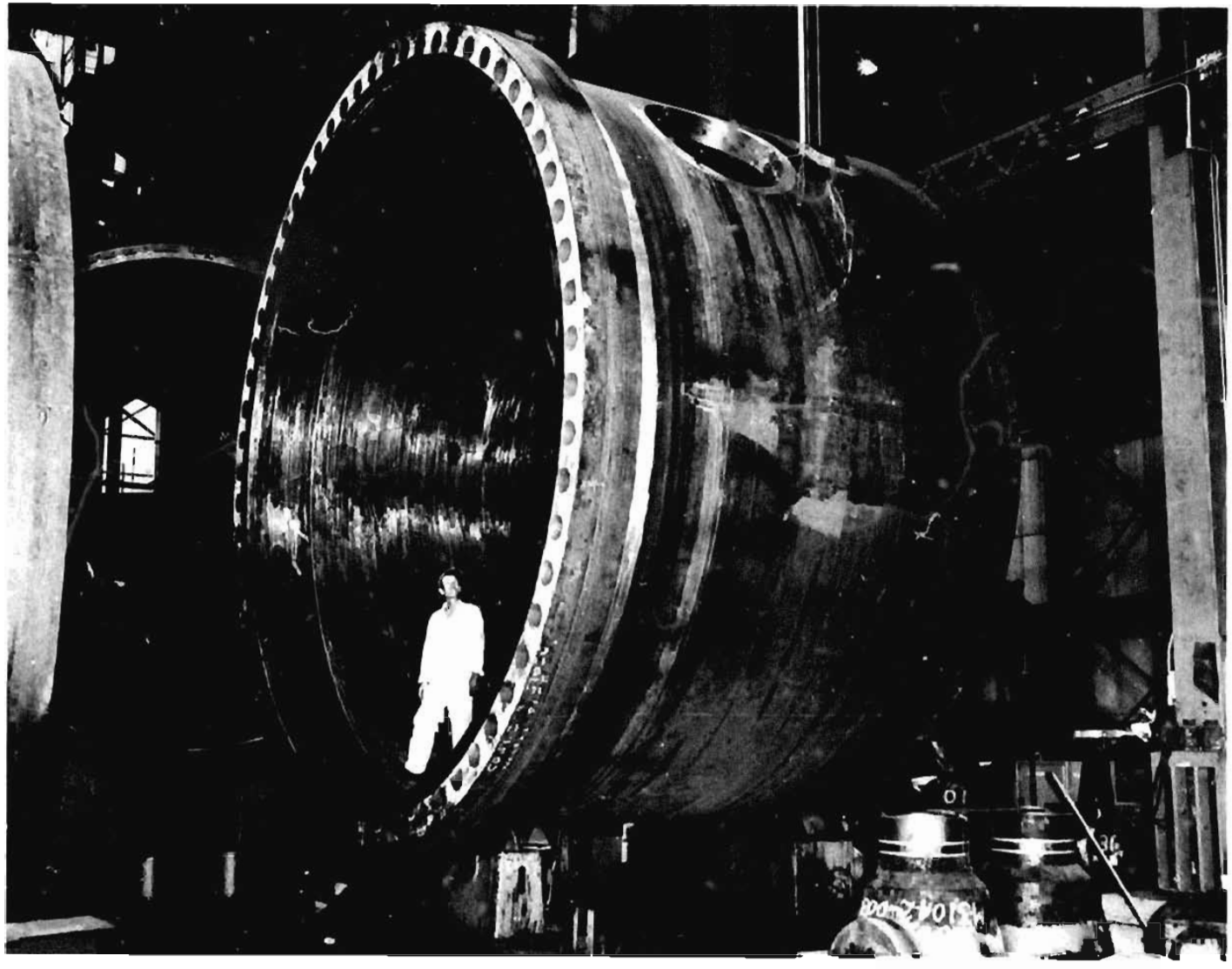

Fig. 8.10. Clad Flange and Shell Section Prepared for Nozzle Insert. (CE photograph)

machined. Machining requirements for reactor vessels are established by the sizes of the components and the dimensional tolerances required in certain critical areas. Large machine tools, particularly horizontal and vertical boring mills, capable of machining large-dimension vessels to very close tolerances and surface finishes may be needed. Accurate gaging, optical and calibration equipment for metrology for both setup and inspection, and good control of temperature, cleanliness, and atmospheric conditions are required where layout, inspection, and machining are done.

Out-of-roundness design tolerances permitted for the pressure container proper are 1% or less in the ASME Code, but the practices of the principal fabricators readily achieve 1/2% or less. Certain surface finishes are needed for some nondestructive test methods, but these are generally not too restrictive; they are discussed further in Chapter 9. The principal requirements for close tolerances are those that involve flange closures and core alignment. Machined surfaces of flange faces, grooves for gasket seals, bolt holes, and bolting materials, in addition to finish and flatness, etc., require verticalness and concentricity within a few thousandths of an inch that are generally established with optical equipment.

Additional information on these design requirements is contained in Chapter 6. Among the most exacting tolerances are those involving core alignment. They require precise alignment of weld penetrations, inserts, control rod sleeves, and core supports and are dictated by core physics, shielding, and the mechanical functioning of control rods. Typical tolerances and flatness requirements on flange faces are location to within 0.005 in. of the true position and flatness to within 0.005 in.; the surface finish requirement for gasket grooves is 32 rms. Alignment of the holes for closure studs is also a major problem and generally requires location to within 0.005 in. of the true position and parallelism between holes at 0.020 in. of full indicated runout.

8.14 TESTING[4]

When the vessel is substantially completed, it is subjected to appropriate leak and hydrostatic tests (Fig. 8.11), as discussed in Chapter 10.

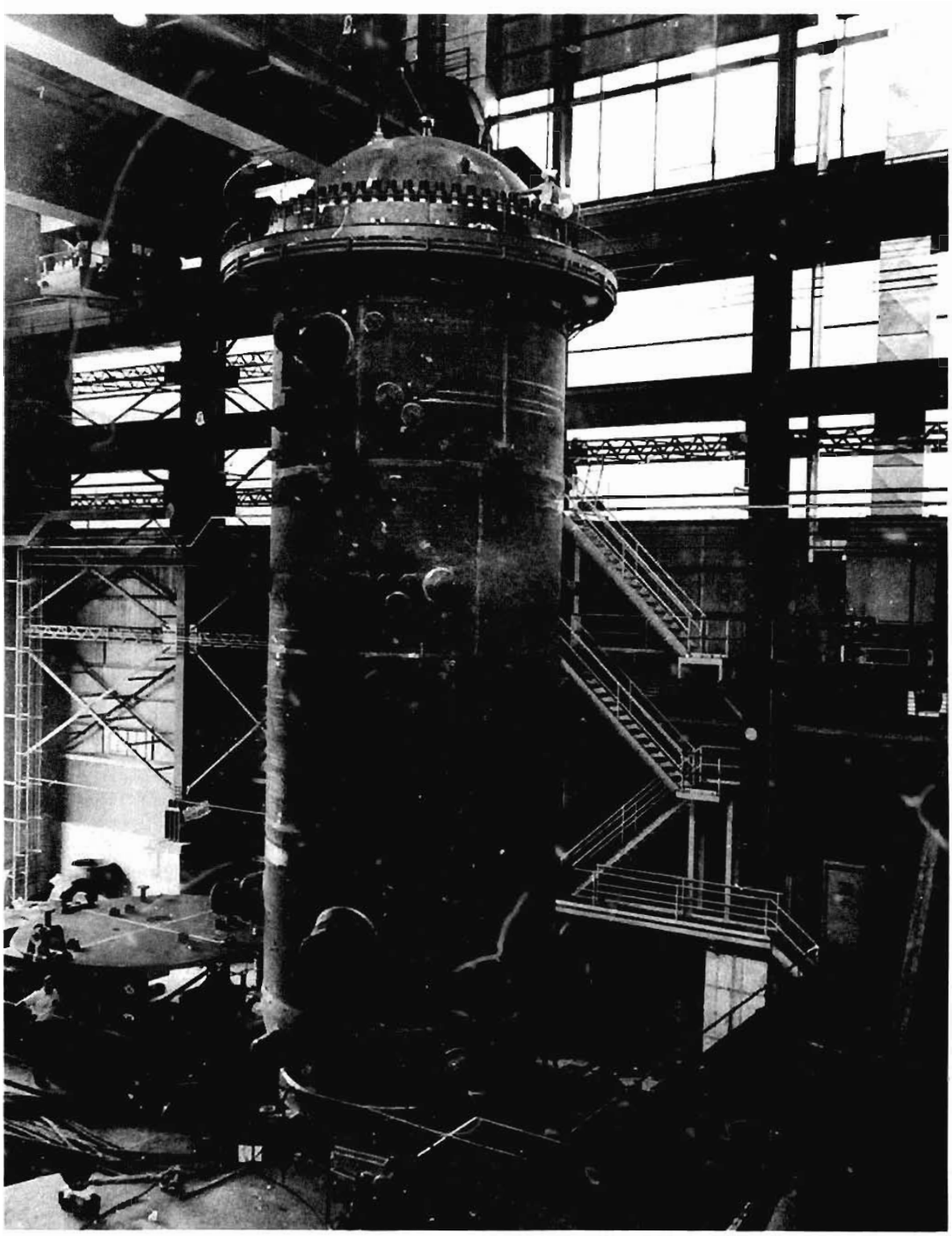

Fig. 8.11. Completed Reactor Vessel Prepared for the Hydrostatic Test. (CE photograph)

Since parts of the vessel may yield locally in the pressure test and produce some dimensional change, further dimensional inspection is conducted after the pressure test. Also all surfaces are examined visually after the hydrostatic test, and the external vessel surface is examined by the magnetic-particle method. These inspections are described in Chapter 9.

8.15 CLEANING

Details of cleaning practices for reactor vessels vary with the manufacturer's practices and customer requirements and are influenced in turn by the type of reactor system, the cleaning requirements to be imposed subsequently on the entire system prior to startup, and the environment to which the vessel will be exposed during transportation from shop to site. In addition to cleaning the vessel just prior to shipment (or after completion of field erection), some cleaning is generally required on as-received product forms and on subcomponents in various stages of manufacture. This latter involves principally the removal of any foreign material that might contaminate the base material or subcomponents if left on during welding or heat treatment. The cleaning which is a part of weld-joint preparation is essentially that required for most high-quality weld joints and is usually stated in detail as a part of the written-and-qualified welding procedure.

Cleaning requirements are intended to insure freedom from dirt and extraneous material visible to the naked eye, to remove grease and other potentially harmful chemical substances, and to prevent entrapment of foreign material in joints or crevices. Cleaning to remove foreign substances may include grinding, polishing, grit or shot blasting, water flushing, steam cleaning, degreasing, brushing or scrubbing, and a general wiping down. These steps may be taken at any stage of fabrication, particularly prior to welding or heat treatment, after machining operations and certain inspection steps, and as a final step after vessel completion. If crevices exist, protection from contamination is best provided at the time of crevice formation, with the protection then maintained throughout fabrication and shipment.

Upon its completion, a general cleaning of the entire vessel is usually performed. After freeing the vessel of chips and other solid material, it may be washed with acetone or other solvent. It is common practice to fill the vessel with city water for the hydrotest and as a part of the cleaning sequence. After draining and before any residue of city water can dry in place, the vessel is flushed by rinsing with distilled or demineralized water.

A final degreasing with ethyl alcohol or acetone may be carried out at this point, and steam cleaning may also be performed. When the desired condition of cleanliness has been achieved, temporary closures are applied to provide protection during shipment. Where the conditions to be encountered during transportation warrant, an inert gas, together with desiccants, may be sealed in the vessel in preparation for shipment.

There is no single generally accepted national standard for cleaning nuclear components, although a proposed "Standard Guide for Specifying Cleanliness of Nuclear Reactor System Components" has been prepared by the American Nuclear Society and is being considered by the Nuclear Standards Board of the USA Standards Institute. Existing standards to which commercial reactor vessel cleaning practices are most nearly related include MIL-C-19874 (SHIPS), Cleaning Requirements for Nuclear Primary Coolant Equipment Including Piping Systems, now superseded by MIL-STD-767A, Cleaning Requirements for Special Purpose Equipment Including Piping Systems (OUO); Federal Standard 209A, Clean Room and Work Station Requirements, Controlled Environment; and ASTM A-380, Descaling and Cleaning Stainless Steel Surfaces.

REFERENCES

1. Combustion, Babcock Tooling Up for 1500-Mwe Reactor Vessels, Nucleonics, 22(11): 24–27 (1964).
2. Based on visit of E. C. Miller of Oak Ridge National Laboratory to Rotterdam Dockyards, 1966.
3. Based on visits of E. C. Miller of Oak Ridge National Laboratory to USSR welding research facilities in 1962 and to Skoda Works in 1964.

4. Based on private communications in visits and discussion of ORNL representatives with personnel of Combustion Engineering Company (Chattanooga), Babcock & Wilcox Company (Mount Vernon and Barberton), and Chicago Bridge and Iron Company (Birmingham) during summer of 1966.

5. F. W. Davis (Ed.), Feasibility Study of Pressure Vessels for Nuclear Power Generating Reactors, USAEC Report AECU-3062, December 1955.

6. American Welding Society, Welding Handbook, Part 5, Chapter 87, Nuclear Power, 5th ed. (in press).

7. R. D. Wylie, J. McDonald, Jr., and A. L. Lowenberg, Weld Deposited Cladding of Pressure Vessels, Brit. Welding J., 12(8): 378–393, (August 1965).

8. R. D. Wylie and W. J. McGonnagle, Quality Control in Fabrication of Nuclear Pressure Vessels, American Society for Metals, 1964.

9. QUALITY ASSURANCE*

The term "quality assurance" implies verification of the composition, properties, soundness, and Code or specification compliance of materials; review and approval of vessel design and stress analysis; preparation of detailed procedures for fabrication operations; surveillance monitoring of the fabrication steps; resolution of deviations from specifications; and inspection and testing. Some quality assurance steps in nuclear vessel fabrication are requirements of the ASME Code, Section III, Nuclear Vessels, particularly those intended to establish safety of a fabricated vessel. Others are process control steps intended to minimize or prevent the generation of rejectable defects in the course of fabrication. Much of the examination and testing performed in intermediate steps of fabrication is intended to detect defects and accomplish their elimination early in the manufacturing sequence, rather than incur delays, additional costs, rejects, and extensive repairs by waiting until a later, or even final, Code-required inspection.

The principal concern of the Code is safety, and it requires examinations and tests intended to find and reject (or require repair of) defects at some stage of the construction and to verify the adequacy of the completed construction. It tries to avoid redundancy by minimizing Code-required intermediate examinations if their objective is primarily a matter of economy and convenience to the fabricator, who is then responsible for determining when and to what extent such intermediate examinations should be used. There is, of course, some contribution to safety from the earlier detection and elimination or repair of defects, and this consideration prompts some Code-required in-process examination. Still other specifications call for material samples and tests to develop a body of materials-properties data for guidance in design and specification of subsequent vessels; they serve incidentally in determining acceptability of the vessel actually being fabricated.

Most of the process control and inspection requirements cited here relate to actual Code requirements, which will not be repeated except

---

*This chapter was prepared by D. Canonico, R. W. McClung, E. C. Miller, S. E. Moore, and P. Patriarca, Oak Ridge National Laboratory.

where further clarification may be required. In the Code the term "inspection" is used to cover those tasks to be performed by the "qualified inspector" who holds certificates from a state jurisdiction and from the National Board of Boiler and Pressure Vessel Inspectors and is employed by a state, municipality, or insurance company; "examination" includes those operations, such as visual observation and nondestructive testing, that are done by someone other than an inspector, such as a nondestructive test operator employed in the quality control department of the supplier or fabricator. However, no particular effort is made to maintain this distinction in the discussion that follows.

Verification of materials properties includes the control, inspection, and tests necessary to establish that the material product form, as supplied by the materials manufacturer, meets the requirements of the Code, purchase specifications, and vessel design. Most of this work is performed by the materials manufacturer and certified to by him; however, in some cases, forming, heat-treatment operations, and subsequent tests may be done in the fabricator's shop, in which case the fabricator provides the certifications for these operations. The basic materials specification requirements are contained in the ASME Code, Section II, Materials Specifications, and correspond closely with similar ASTM specifications; however, Article 3 of Section III of the Code states a number of special requirements to be used in addition to, or in some cases, in lieu of, the materials specifications. Special requirements include N-313, which states details of preparation and testing of material test coupons to be given heat treatments simulating the approximate heat treatment to be given the materials in the course of vessel manufacture. Paragraph N-320 of Section III requires additional nondestructive testing of material product forms to verify specification requirements, and N-330 states special mechanical-property test requirements, mostly impact testing. The purchasers and fabricators of vessels generally add still more requirements for reasons of economy, improved fabricability, radiation effects surveillance, information, and to some extent, safety.

9.1 CHEMICAL AND MECHANICAL PROPERTIES

The materials channeled into a fabricator's shop during the construction of a nuclear pressure vessel comprise four primary categories: plate, forgings, bolting, and filler metal. Rod and bar are also used; however, their requirements are essentially those for plate. Castings have virtually not been used and will therefore not be discussed extensively. The first three general types of material are obtainable to ASTM specifications, which aid considerably in assuring that the products are acceptable. The fourth type, filler metal, except for shielded metal-arc electrodes, usually complies with proprietary company specifications based on experience with similar filler metals.

Assurance of quality in plates, forgings, and bolting material is achieved by requiring that the material be melted and processed by modern techniques proven to produce a high-quality product. The processing variables are detailed in the ASTM specification or in a purchaser's procurement specification. Article 3 of Section III of the ASME Code makes no reference to melting or pouring practices but, rather, sets definitive limits on the mechanical properties, particularly impact properties, of the materials and the location where they will be measured.

9.1.1 Chemical Analyses

The primary quality-assurance technique used is chemical analysis. The response of a material to a heat treatment is dependent on its chemical composition. The required mechanical properties cannot be obtained if the composition is not optimum for the properties desired. Hence, analyses are made during initial meltdown, periodically during melting and pouring, and finally as a check for certification.

The analysis made during melting and pouring allows the melter to make whatever compositional adjustments are necessary. The check analysis is run to ascertain that the expected chemical analysis has indeed been attained. Satisfying the requirements of the chemical analysis assures that the material will produce the correct mechanical properties, provided the heat-treatment parameters are correct. These parameters

include temperatures, holding times, and heating and cooling rates. Adherence to the correct heat-treating procedures is usually assurance that the required tensile and impact properties can be attained.

The methods used for making chemical analyses are usually left to the discretion of the supplier; however, ASTM E 30, Methods for Chemical Analysis of Steel, Cast Iron, Open Hearth Iron and Wrought Iron, is often used for referee purposes. Specification E 30 recommends that the analyst check his method and technique by means of a National Bureau of Standards sample that has a composition comparable to that of the material being analyzed. These standards assure that the resulting analysis is correct within tolerable limits. The procedure for sampling referred to in E 30 is detailed in ASTM E 59, Method of Sampling Steel, Cast Iron, Open Hearth Iron and Wrought Iron. For large sections, the 1/4 T (one-fourth thickness) location is recommended. This same location is normally used for obtaining specimens for the determination of mechanical properties. The minimum ASME code requirements for the frequency of check analyses is given in paragraph N-334.1 of Section III. It states that the number of check analyses shall not be less than the number of tensile tests. Often the analysis is run on the broken tensile specimens.

9.1.2 Mechanical Properties

Certain mechanical-property requirements, particularly the tensile and impact properties, must be satisfied for all materials used for fabricating pressure vessels. Additionally in the case of weldments, emphasis is placed on bend tests, both in the procedure and performance qualification tests. These weldment bend test requirements are listed in Tables Q-13 and Q-14 of Section IX of the ASME Code.

The tensile and impact testing is done in accordance with ASTM Specification A 370, Standard Methods and Definitions for Mechanical Testing of Steel Products. Specification A 370 recommends that the impact testing be done under the direction of ASTM E 23, Notched Bar Impact Testing of Metallic Materials. This document, E 23, requires that the accuracy of the tester's Charpy machine be calibrated against standards available

from the U.S. Army Materials Research Agency. The impact-property requirements are discussed under N-330, Special Mechanical Property Requirements and Tests, of Section III of the ASME Code. Paragraphs N-331 and N-332 are specifically concerned with the ductile-to-brittle transition. The locations from which the test specimens are to be taken are given in N-313.

In addition to the Charpy tests required by the Code, pressure vessel customers require that the actual nil-ductility transition (NDT) temperature be determined according to ASTM E 208. It is, however, General Electric Company practice to require such determinations for core-region plates only; the NDT temperature of other plates must be demonstrated to be below the required temperature.

9.1.2.1 Plate

Plate is purchased to a fabricator's procurement standard, which usually cites an ASTM specification but may redefine the limits imposed on the chemical composition. This procurement specification sets the chemical compositional limits and may also require or imply the desired mechanical properties. The plate material currently being used in the fabrication of nuclear pressure vessels, regardless of how it is procured, meets the requirements of ASTM A 533, Manganese-Molybdenum and Manganese-Molybdenum-Nickel Alloy Steel Plates Quenched and Tempered for Pressure Vessels.

The primary properties of interest are the tensile strength and the notch toughness of the heat-treated plate. The locations from which the specimens are taken are given in N-313 of Section III of the ASME Code. The required impact test values are given in Table N-332 of Section III. The temperature at which these minimum impact values are required is controlled by the temperature of the hydrostatic test. Paragraph N-332 of Section III requires that the minimum energy value (average 30 ft-lb) be achieved at a temperature of not more than 60°F below the hydrostatic test temperature. This is based on the assumption that for this ASTM A 533 (P3-type material) steel the Charpy V-notch fix for the drop-weight NDT test is 30 ft-lb. Hydrostatic testing is most easily done at room temperature (70°F), therefore +10°F has been set as the impact test

temperature. Specification ASTM A 533 does not require impact testing in the main text of the specification; however, it can be included as a supplementary requirement. Usually the customer knows the temperature at which he will conduct the hydrostatic test and sets the temperature at which the energy levels must be obtained. The energy values (average of 30 ft-lb for three specimens at a given temperature, with no energy value below 25 ft-lb) are set by Section III of the Code (paragraph N-332).

Plate materials are unique in that they are purchased in the hot-rolled condition and are subsequently formed and heat treated by the fabricator. Because of the manner in which it is handled, a supplier may or may not be required to guarantee the mechanical properties of his product. If mechanical-property guarantees are required the supplier will remove test blanks from the as-rolled plate. These are given simulated heat treatments, including at least 80% of the total time at the postweld heat-treatment temperature to which the material in the vessel will be subjected. This total treatment may be performed in one cycle, as described in N-313.1 of Section III of the ASME Code. These simulated heat treatments are a protective measure taken by the fabricator to assure himself that the heat-treated product will pass the final certification tests. The final certification tests are conducted by the fabricator as part of his fabrication procedure. If necessary, retest provisions are permitted by the ASTM specification.

The tensile properties required by ASTM A 533 are not difficult to achieve. Data are available[1] to show that the minimum tensile requirements can be achieved at the mid-thickness of heavy-section A 533 plate. Achieving the impact-property requirements is more difficult, but to date this has not been a problem. Tests conducted at the 1/4 T location have had energy values in excess of the minimum requirements.

Recently, in an effort to gather more data relative to the properties of the plate materials, the pressure vessel customers (General Electric Company and Westinghouse Electric Corporation) have been requesting mechanical-property tests in excess of those required as a minimum by Section III of the ASME Code. Some of these requirements should lead to more confidence in some of the assumptions currently made. A good example is the 30 ft-lb Charpy V-notch fix for the drop-weight NDT

test. It is currently felt that (1) the 30 ft-lb fix is conservative and (2) that it is too low and it should be 45 ft-lb. Present procurement specifications require that drop-weight testing be conducted on all base materials the Code requires to be Charpy V-notch tested. This is true for the welds and heat-affected zones, as well as the wrought material.

The choice of test location can also be open to criticism. The tests on the whole are taken from the 1/4 T at only two finite locations (top and bottom of the plates), and these may or may not be representative of the entire plate. Tensile tests, as well as impact tests, are being conducted at the outer surface and 1/2 T plate locations, as well as at the 1/4 T (only Code requirement) locations. The current studies will provide additional information regarding the uniformity of tensile properties throughout the thickness. (As has already been pointed out, data are available to show that significant differences are the exception, not the rule.)

In addition to the 0.505-in.-diam tensile specimens used in certifying a plate (in accordance with ASTM A 370), large (80% of plate thickness) tensile specimens are being tested. These specimens represent the material throughout the plate thickness and not at a finite and limited location. Preliminary information indicates that the results obtained from these large specimens are similar to those for the small 0.505-in.-diam tensile specimens. Furthermore, it is the practice of at least one fabricator to test specimens machined from nozzle cutouts. These tests further contribute to the information available regarding the uniformity of properties throughout the plate.

The investigations noted above are all in excess of the minimum requirements of the ASME Code, but they further assure the quality of the material that goes into the fabrication of a large reactor pressure vessel.

9.1.2.2 Forgings

Forgings are purchased by the fabricator in the quenched-and-tempered condition and, therefore, are certified by the supplier. Currently the forgings being used in nuclear pressure vessels satisfy the requirements of ASTM A 508, Quenched and Tempered Vacuum Treated Carbon and Alloy

Steel Forgings for Pressure Vessels. The steel that goes into a flange, shell course, or nozzle forging is of the highest grade; it is melted in an electric furnace and vacuum treated to reduce the hydrogen to levels in the range of 1 ppm. Moreover, aluminum is not used as a deoxidizing agent, and therefore the cleanliness of the product is further enhanced.

In the design of a forging, stock is provided that will receive the same working and heat treatment as the highly stressed region of the forging. After the final heat treatment, part of the test stock is removed from two locations 180° apart (in accordance with ASTM A 508). This material is given a simulated postweld heat treatment in accordance with N-313.2 of Section III of the ASME Code, and one tensile and three Charpy specimens are prepared for each location. These are tested to assure that the minimum requirements of the Code and/or customer have been achieved.

The tensile and impact requirements are given in the ASTM specification; however, the +40°F test temperature is usually lowered to +10°F. This is true for the main closure flanges; however, one customer requires that all ASTM A 533 and ASTM A 508 grade steels meet the +10°F criterion.

In the event the mechanical properties of the material fell below the minimum allowable values, retests conducted in accordance with the rules set forth in the ASTM specification would be permitted. Reheat treatment would also be permitted, but the supplier would be obligated to inform the fabricator of this procedure.

Currently, the forging suppliers are being asked to obtain complete Charpy V-notch transition curves and establish the upper and lower shelf energies. This is being done for information only and is not a criterion for rejection or qualification of a forging.

A requirement that has been imposed on some forging manufacturers has been that the forging meet the mechanical-property requirements at a depth of 2 in. below the nearest heat-treated surface. This requirement exceeds that imposed by N-313.2, which defines the location of the test specimens as a minimum of 3/4 in. below the surface. Moreover, shell courses manufactured by forging standards are being subjected to property requirements akin to those of plate materials. Specimens are being removed from essentially the 1/4-T location at least 1 T in from

a quenched end. These requirements also exceed the minimum of Section III of the Code and also those of ASTM A 508.

One customer requires that the Charpy specimens be taken from at least three locations (120° apart) around a forging. This requirement is in excess of the Code requirements. In addition to the mandatory Charpy data, the actual NDT temperature is being obtained by the drop-weight test (ASTM E 208). Currently, an effort is being made to include this requirement in the customer's procurement specification.

9.1.2.3 Bolting Materials

Bolting materials (bolts, studs, washers, and nuts) currently being used in nuclear pressure vessels satisfy the requirements of ASTM A 540, Alloy Steel Bolting Materials for Special Applications. The grades most commonly used are B 23 and B 24 of this specification. Because of the higher strength of these materials, the drop-weight NDT-Charpy V-notch fix has been set at 35 ft-lb. Consequently, the requirements are that the average value for three tests be 35 ft-lb, with the value for no one test below 30 ft-lb. As set by the specification, the test is conducted at +10°F.

The bolting materials are supplied to the fabricators in the heat-treated condition. The test specimens, in accordance with N-313.2 of Section III of the Code, are removed from a location at least 1 T from an end. The ASTM specification sets the depth of the test at 1/2 radius or 1 in. below the surface, whichever is the lesser. Specimen and notch orientation are also dictated. Meeting the mechanical-property requirements is not difficult for the bolting material; however, the nondestructive testing requirements are quite stringent, and hence a high-quality product is usually assured.

The reactor pressure vessels are fabricated by welding, and the fabricator has the responsibility of guaranteeing the quality of the weldments that he deposits. He satisfies these requirements by qualifying processes, welders, and materials in accordance with N-520, Welding Fabrication, and N-540, Addition Welding Qualifications, of Article 5, Fabrication, of Section III of the ASME Code. Other restrictions are also imposed by Section IX of the Code. These are concerned with the procedure

qualifications of the processes and materials (paragraphs Q-10 through Q-13) and the performance qualification of the welders and welding operators (paragraphs Q-20 through Q-26).

9.1.2.4 Filler Metal

The choice of filler metal is dependent on the welding process to be used. The metal-arc covered electrodes are purchased to ASTM A 316, Low Alloy Steel Covered Arc-Welding Electrodes. This material has tensile-strength as well as impact-property requirements imposed on it.

Filler metals for usage in the submerged-arc and electroslag processes are not nearly so well defined. These filler metals are usually tailored to produce a weld-metal chemical composition that will provide the required mechanical properties. The electroslag weld-metal properties are achieved after a complete austenitizing quenching and tempering heat treatment; therefore it is mandatory that this filler metal respond to the heat treatment. The filler metal must have a higher alloy content than that which would be used for a weld metal that did not have to respond to a heat treatment.

The quality of the filler metal is assured through chemical analysis of each lot prior to its use. Usually each coil is analyzed at its beginning and end, and a heat of the filler metal is randomly sampled and analyzed. Where the combination of filler metal and flux influences the chemistry of the weld deposit, the combinations are qualified as one, and stringent quality control assures that the combinations are used together.

9.1.2.5 Welding Procedures and Weld Tests

The rules for qualifying welding procedures are given in Q-11 of Section IX of the ASME Code. New procedure specifications must be qualified when changes such as those listed in V-1 through V-13 are made. These changes include welding process variables, as well as material changes. However, changes in heats of filler metals or fluxes, provided their compositions are within tolerable ranges, do not require requalification of the welding procedure. The tests that must be passed are listed in Tables Q-13.1 and Q-13.2 of Section IX.

In addition to the performance qualification tests, Article 7, Testing, of Section III of the ASME Code requires (paragraph N-713) that vessel test plates also be made and tested. These tests are conducted on a test plate of thickness equal to that of the thickest joint to be welded by the particular procedure. The test plate material may come from one or more heats of material used in the vessel or it may come from material of the same specification and heat treatment. These test plates, in addition to meeting the destructive test requirements of Tables Q-13.1 and Q-13.2 of Section IX, must also meet the impact requirements imposed by paragraph N-330 of Section III at the weldment zones (base metal, heat-affected zone, and weld metal) listed in N-712 of Section III. These requirements are to be met after the weldment has been subjected to its required postweld heat treatment.

The requirement of using one heat of material representing the steel that may or may not go into the construction of the vessel is satisfactory for a minimum base-metal dilution weld, such as a weld made by the submerged-arc process; however, it may not be completely satisfactory when the base metal constitutes over 50% of the weld metal, such as is the case in an electroslag weld. If, as is true of the plates and forging, each heat of metal used in the construction of the pressure vessel is qualified, it seems logical to impose a similar requirement on the individual electroslag welds (at least until sufficient data are gathered to assure that the dilution factor is insignificant). The submerged-arc weldments are not subjected to a reaustenitize and temper treatment; therefore their required properties must be achieved with only a subcritical postweld heat treatment. As has already been pointed out, Section IX of the Code does not impose any impact requirements on the weldments. However, Section III of the Code (paragraph N-712) requires that the base metal, heat-affected zone, and weld metal all meet the requirements of N-330. Paragraph N-713.4 states that the weld metal must be tested within 1/16 in. of the finished weld surface. This is a rather important requirement for a weld metal that will not be completely reaustenitized, quenched, and tempered after welding. The choice of welding parameters is important, and the mechanical properties of multipass

weldments are dependent on the fact that the subsequent passes reaustenitize and temper the previous passes. The passes exposed to the least amount of subsequent heating are those at the surface of the weld and, therefore, this location rather than the 1/4-T location is tested.

The location of the notch in the heat-affected zone of a weldment is usually left to the discretion and integrity of the tester. This zone, which encompasses the base metal from the unaffected base metal to the fusion line, contains a multitude of microstructures, each of which may possess completely different mechanical properties from those of its neighbor. Ideally, the notch should be situated in the region that possesses the poorest impact properties; however, geometric considerations do not always permit this. Hence the tester should pick a location that most nearly approximates this condition. As can be noted, the heat-affected zone is a nebulous area, and the notch of an impact specimen can be placed anywhere within this zone and still satisfy the Code requirements.

Recently, the pressure vessel customers have been requesting that drop-weight testing (ASTM E 208) be conducted on the weldments that are now subjected to Charpy testing. This program will establish the actual NDT temperature.

9.2 FLAW DETECTION

The minimum requirements for nondestructive examination of pressure vessel materials for the detection of flaws are incorporated in N-320, Nondestructive Examination and Repair of Materials, in Section III of the ASME Code. The materials discussed are plates, forgings, bars, castings, pipes, tubes, fittings, bolts, and bolting material. The inspection methods prescribed for various portions of the examination include ultrasonic, radiographic, liquid penetrant, magnetic particle, and eddy current or other electrical system. In many instances the current practice of the reactor prime contractor or the pressure vessel fabricator is to exceed the minimum requirements of the Code. This should increase assurance of the integrity of the materials over that provided by the Code. Of course, exceeding the requirements, although current

practice, is not necessary to gain the approval and acceptance of the vessel by the Code inspector and, under existing regulations, could be relaxed to the minimum requirements at the discretion of the pertinent management. As the individual materials and their respective examinations are discussed in the following, occasional mention is made of practices that exceed requirements. This is not intended to be an exhaustive survey of such conditions, but it serves to indicate general conditions.

9.2.1 Examination Procedures

Detailed examination procedures are provided in the Code for radiographic examination of welded joints, ultrasonic examination of welded joints, magnetic-particle examination, and liquid-penetrant examination. In addition, occasional reference is made to various ASTM documents for materials or performance of nondestructive examinations. In subsequent discussions, requirements for the nondestructive examinations are intended to be in accordance with the Code-included procedure unless otherwise stated.

The radiographic examination procedure (paragraph N-624) is specified for examination of repair welding and for tubular products to which it may be applicable. A primary requirement of this procedure is the designation of the appropriate penetrameter for thickness of material. The thickness of the penetrameter is 2% of the material thicknesses from 1/4 in. to 1 1/2 in. Between 1 1/2 and 6 in., the percentage thickness of the penetrameter decreases to 1%, and this value is maintained to the maximum designated thickness of 20 in. The penetrameter contains three holes and a slit. The holes, according to the Code, normally have diameters of 2, 3, and 4 times the penetrameter thickness. The minimum hole size is 1/16 in. For specimen thicknesses less than 1/2 in., the 1/4-in. × 0.010-in. slit is used to indicate the image quality. This is less demanding than the ASTM penetrameter prescribed in E 142, which sets a minimum hole size of 0.010 in. For thicknesses above 3 in. the ASME and ASTM 2T holes are comparable.

The approved magnetic-particle examination procedure is described in N-626 of the Code. The procedure allows the use of wet or dry particles,

direct or rectified magnetizing current, and prods, coils, or magnetic yokes to produce the magnetic field. The yoke method may be used if the sensitivity for surface cracks is equivalent to that of the prod method using a magnetizing current of 25 to 30 amp per inch of prod spacing. This is in contrast to the required 100 to 125 amp per inch of prod spacing for the prod method. All cracks and linear indications are considered unacceptable. Linear indications are those indications with a length more than three times the width. Nonlinear (rounded) indications with dimensions greater than 3/16 in. are unacceptable. Multiple rounded indications are unacceptable if they exceed a specified frequency of occurrence within a specified area.

The penetrant examination procedure is described in N-627. The procedure allows the use of both visible dye and fluorescent penetrants. In each case there are three acceptable types: (1) water washable penetrants, (2) postemulsifying penetrants, and (3) solvent-removable penetrants. Reference is made to ASTM E 165-65T, Methods for Liquid Penetrant Inspection, an educational document. These acceptable penetrant procedures differ considerably in their sensitivity. The described techniques allow considerable leeway, and some companies have found it necessary to be more restrictive in their written procedures. For instance, in surface preparation and cleaning, sand blasting is considered undesirable because it can close flaws with a peening action, although the Code allows abrasive blasting. More restriction is also being placed on allowable penetration and developing times. Limits of acceptance of discontinuities are similar to those for the magnetic-particle examination.

9.2.2 Plates

The only nondestructive examination required for unclad plates is the longitudinal-wave ultrasonic inspection for the detection of laminations. This is performed in accordance with a procedure that is essentially in accordance with ASTM A 435, Ultrasonic Testing and Inspection of Steel Plates of Firebox and Higher Quality. The plates are examined along 3-in.-wide paths on 12-in. centers. The reflection from the rear

surface of the plate is monitored. A loss of back reflection equal to that produced by a 1/2-in.-diam flat-bottom hole is considered unacceptable if it persists during a 2-in. movement of the transducer. With grid scanning there are unexamined areas approximately 9 in. square, which theoretically could contain laminar discontinuities up to that size. The opinion of many is that laminations are innocuous if they do not extend to cut edges or penetrate where welds are to be made. For the latter case, supplementary examination during fabrication is necessary, and repair is required if a detected lamination exceeds a length of 1 in. along the exposed edge.

If the plate is to be clad by the material manufacturer, the bond between the cladding and the base plate is to be included in this ultrasonic examination. Many of the vessels currently being fabricated have the cladding applied as a weld overlay in the formed vessel; requirements for examination are discussed in the section devoted to fabrication examination.

An interpretation of the ASME Boiler and Pressure Vessel Code, Case 1338-4, March 29, 1967, on Ultrasonic Examination of Plates, allows an examination in lieu of that noted in the Code. The principal differences include maximum 9-in. centers on the scanning grid lines (but no mention of the path width) and the use of reference specimens containing calibration holes. When indications of discontinuities reduce the amplitude of the back reflection equal to that of the calibration hole or the indication has an amplitude exceeding 50% of that from the calibration hole, the boundary of the discontinuity is established by complete scanning. The diameter of the calibration hole varies from 1/2 in. up to 1 1/4 in. as the plate thickness varies from less than 4 to more than 16 in. Unacceptable conditions include loss of back reflection greater than that produced by the calibration hole that cannot be contained in a circle with a diameter of 3 in. or one-half plate thickness, whichever is greater. In addition, rejection is based on a continuous flaw indication with an amplitude greater than that from the calibration hole and which cannot be contained in a circle with a diameter of 4 in. or the plate thickness, whichever is greater.

An alternate in Case 1338-4 is essentially that contained in the Code, except for changes in the acceptance limits. An unacceptable loss of back reflection is one that cannot be contained in a circle with a diameter of 3 in. or one-half the plate thickness, whichever is greater.

Case 1338-4 also provides an alternate examination for bonding of clad plate. A reference specimen containing a flat-bottom hole formed from the base-metal side to the plate-cladding interface is specified. The diameter of the hole is no greater than the diameter of the search unit. An indication of a flaw that persists through a 3-in. transducer movement in any direction is unacceptable.

The ultrasonic examination is performed by the plate fabricator although it has become the practice on the part of pressure vessel fabricators to reexamine the material upon receipt and prior to forming and welding into the vessel. The current trend in the reexamination of the plates is to use a 100% scan, rather than the 12-in. grid, to take cognizance of the amplitude of reflections from discontinuities and, on occasion, to use angle-beam examination in addition to detect transverse discontinuities. The procedures, reference standards, and acceptance limits for the supplementary ultrasonic examinations are established by the pressure vessel manufacturer or by the reactor contractor.

Detected defects may be repaired by the plate manufacturer if the repairs are approved by the vessel manufacturer and if other Code requirements are met. Some of the requirements include examination of the area after the defect is removed by the magnetic-particle or penetrant methods, examination of the weld repair by magnetic-particle or penetrant methods, and examination by radiography if the repair depth is greater than 3/8 in. or 10% of the nominal thickness. Although not specified in the Code, the good, current practice is to use the magnetic-particle method rather than penetrants on carbon steels because of the ability to find discontinuities that may be slightly subsurface. This pertains to both the area after defect removal and the weld repair.

Defects or unbonded areas in plate cladding may also be repaired by the material manufacturer with the vessel manufacturer's approval. The Code requirements are similar to those for repairs in plates. After the defective portion is removed, the area is examined by the magnetic-

particle or liquid-penetrant methods; after repair, the area is examined by liquid penetrants and the ultrasonic method used for the original examination.

9.2.3 Forgings and Bars

Forgings and bars for reactor vessels are examined by ultrasonic methods with the longitudinal-beam technique in accordance with ASTM A 388-59, Recommended Practice for Ultrasonic Testing and Inspection of Heavy Steel Forgings. This document references two other ASTM Practices that discuss longitudinal-wave testing with direct contact and ultrasonic testing by the resonance method. Details of the examination procedure are not specified and, although not stated, are dependent upon procedures established by the material or vessel manufacturer or the reactor contractor. The criteria for the reference specimen and acceptance standard established by the Code are the same as for the inspection of plate. Rings, flanges, and other hollow forgings are also examined with the shear-wave technique. The reference and acceptance standard for this technique is a groove 1 in. long with a depth 3% of the nominal forging thickness. Details of the shear-wave technique are not specified in the Code and are dependent upon the procedure established by the material or vessel manufacturer or the reactor contractor.

An interpretation of the ASME Code, Case 1359-1, March 14, 1966, on Ultrasonic Examination of Forgings, allows an examination in lieu of that noted in the Code. This Case provides additional procedural details. The entire volume is to be ultrasonically inspected. The longitudinal-wave test is to be applied from two directions approximately at right angles. Hollow forgings are tested from one circumferential surface and from one face, normal to the axis. Disk forgings are tested from one flat side and the circumferential surface. Rejection is based on any discontinuity that causes loss of back reflection. In addition, conditions are to be reported to the purchaser for approval if indications are detected that (1) exceed the amplitude of the back reflection, (2) are smaller but clustered, or (3) travel in time when the search unit is moved. The shear-wave test for hollow forgings is to be performed in

the circumferential direction, when practicable. Indications exceeding that from the calibration notch are unacceptable. In addition, conditions are to be reported to the purchaser for approval if indications are detected with amplitudes exceeding 50% of the calibration-notch amplitude or if clusters with smaller amplitudes are detected.

Discussions with personnel[2] at a forging company disclosed some of the current procedures that supplement or implement the Code and Case requirements. All the received stock that is to be eventually manufactured into components for nuclear service is examined by the ultrasonic method. The specific technique is dependent upon the size of the ingot. On the basis of past experience, a decision is made as to whether the item should proceed to the forging operation. For ring forgings the longitudinal-wave examination is performed with the ultrasound being introduced successively from the outer surface and both flat ends. One problem when performing the test from a flat end on ring forgings with a long axial dimension (e.g., 30 in.) is assuring calibration for discontinuities near the entry surface when comparing with flaws near the rear surface. The shear-wave examination is performed in the circumferential direction in accordance with Case 1359-1. Depending upon the individual specification, it may be made in only one or both of the circumferential directions.

Forgings of magnetic material are examined by a magnetic-particle method, and those of nonmagnetic material are examined by a liquid-penetrant method. Defects in forgings may be repaired in accordance with the requirements specified for the repair of plate.

9.2.4 Castings

The Code requires all portions of castings to be fully radiographed in accordance with requirements of the applicable documents — ASTM E71-64, Reference Radiographs for Steel Castings Up to 2 in. in Thickness; E186-65T, Tentative Reference Radiographs for Heavy-Walled (2- to 4 1/2-in.) Steel Castings; or E280-65T, Tentative Reference Radiographs for Heavy-Walled (4 1/2- to 12-in.) Steel Castings. These documents illustrate various types and degrees of discontinuities in steel castings of the

appropriate thicknesses. The castings examined must meet the requirements of severity level 2 of the documents. Only E71 contains any radiographic procedural details and these are limited to recommendations that the radiographs have a film density in the range 1.5 to 3.3 and a specified minimum sensitivity or quality level that is stated as "usually 2-2T." For all details necessary to the performance of adequate radiography, procedures or requirements are supplied by the material or vessel manufacturer or the reactor contractor.

Castings over 12 in. thick are to be examined by ultrasonic methods in accordance with ASTM E 114-55T, Recommended Practice for Ultrasonic Testing by the Reflection Method Using Pulsed Longitudinal Waves Induced by Direct Contact. This is now designated ASTM E 114-63. This document requires that agreement be reached between purchaser and manufacturer on many details pertinent to the performance of the test. Discontinuities are evaluated on the basis of the amplitude of their reflection as compared with that of the normal back reflection (a 20% value is unacceptable) and on the basis of a 30% loss in amplitude of the back reflection during a 2-in. movement of the transducer. The rejection criteria are qualified by allowing defect removal and casting repair and the use of other methods of nondestructive testing to demonstrate that the indications are acceptable. Caution must be exercised in the interpretation and implementation of this latter allowance, since the response of some discontinuities to other test methods will not be the same as to ultrasonic methods, and a misleading demonstration of acceptability could result.

Castings of magnetic material are to be examined by a magnetic-particle method in accordance with ASTM E 109-57T, Method for Dry Powder Magnetic Particle Inspection. This is now designated E 109-63 to show the date of adoption as a standard (from tentative status) without revision. The base document prescribes procedures, magnetizing current, etc., for the magnetic-particle method that uses dry powder and the prod technique. However, the document allows, by agreement between manufacturer and purchaser, other magnetic-particle methods, such as the wet method, overall magnetization, alternating current, etc., in which procedures and sensitivities can vary. Rejection levels are established

with the aid of ASTM E 125-56T, Reference Photographs for Magnetic Particle Indications on Ferrous Castings. This is now designated E 125-63 to show its adoption as standard without revision. In accordance with the Code, grounds for rejection include all linear discontinuities (hot tears and cracks), flaws (such as shrinkage, inclusions, internal chills, and unfused chaplets), and porosity that exceed the Degree I level (lowest order of discontinuity severity) of the E 125 photographs. Castings of nonmagnetic materials are examined by a liquid-penetrant method. Defects detected by ultrasonic, magnetic-particle, or liquid-penetrant examination may be repaired if appropriate requirements are met (similar to those established for plate).

9.2.5 Tubular Products

Tubular products that normally confine reactor coolant during operation are examined over their full length by either radiographic, ultrasonic, magnetic-particle, liquid-penetrant, or eddy-current methods of examination. "The method selected shall be applicable to the product to be examined." Vessel nozzles and nozzle attachments are examined ultrasonically over their entire surface and by at least one other method of examination. It is difficult to be specific about the optimum test for the many sizes and materials that could be encountered in tubular products. However, there are times in which a test may be applicable but inadequate or inappropriate to detect the discontinuities and provide assurance of product integrity. Therefore, additional clarification or supplementary requirements would be beneficial.

The ultrasonic examination is conducted to detect discontinuities that provide indications equal to or greater than the indications from reference grooves placed on the outside and inside surfaces of the product. The grooves are at least 1 in. long and have a depth that is the greater of 0.004 in. or 5% of the wall thickness. Although not stated, the grooves are probably oriented parallel to the product length and the sound is propagated circumferentially. Insufficient detail is provided to control the examination, so supplementary procedures are required from the material or pressure vessel manufacturer of the reactor contractor.

An ASTM procedure that could be used is E 213-63T, Ultrasonic Inspection of Metal Pipe and Tubing for Longitudinal Discontinuities.

The eddy-current examination specified has reference discontinuities similar to those for the ultrasonic examination. An additional requirement is the use of a 1/16-in.-diam radial hole. Supplementary procedural details would need to be supplied by the material or pressure vessel manufacturer or the reactor contractor. The magnetic-particle and liquid-penetrant examinations are performed in accordance with N-626 and N-627, respectively, of the Code. Discontinuities are unacceptable if they have a depth exceeding the greater of 0.004 in. or 5% of the wall thickness.

Radiographic examinations on products with wall thicknesses greater than 1/2 in. are conducted in accordance with N-624 of the Code with enough exposures to insure 100% coverage. The cited paragraph refers to radiographic examination of welded joints. There are no comments on limits of acceptability unless it is assumed that the acceptability standards for the welds are applicable. These specify, in N-624.8, that any type of crack and elongated inclusion with lengths greater than a value ranging from 1/4 to 3/4 in., depending upon the section thickness, are unacceptable. Other objectionable conditions are porosity and linearly arrayed inclusions. For tubular products with nominal wall thicknesses less than 1/2 in., a radiographic procedure must be qualified to show the capability of detecting discontinuities having depths exceeding 5% of the single wall thickness. Products having defects with an indicated depth exceeding the greater of 0.004 in. or 5% of the wall thickness are unacceptable.

In each case of examination of tubular products, defects may be removed by grinding if the remaining wall thickness is adequate, the ground area is blended smoothly into the surrounding surface, and the defect is eliminated or reduced to acceptable size. The product may be repaired by welding under certain restrictions, including the size of defect, assurance that the defect is removed by performance of a magnetic-particle or liquid-penetrant examination, and examination of the repaired area by radiography and a second "applicable" method of examination.

9.2.6 Bolts and Bolting Material

Bolts, bolting material, and nuts are to be examined after threading. The approved methods for magnetic material are either a wet magnetic particle or liquid penetrant. Axial linear defects with a depth greater than the thread depth and all nonaxial defects are cause for rejection.

A supplementary requirement of some companies that exceeds the Code is the use of ultrasonic testing of stud bolts with the same procedure as that used for bar and forgings. Any crack or sharply defined linear indication is rejectable.

9.2.7 Examination After Accelerated Cooling

If accelerated cooling is used to enhance the properties of carbon and low-alloy steel products, they are examined after the accelerated cooling. The Code allows a choice of a magnetic-particle method, a liquid-penetrant method, or the ultrasonic method described for the specimen configuration in earlier portions of the Code. This free choice seems questionable. The magnetic-particle and liquid-penetrant methods could give similar results on discontinuities opened to the surface by the accelerated cooling. However, the ultrasonic methods prescribed for the longitudinal-wave examination of plate, forgings, and castings would be sensitive to different types and orientation of discontinuities than the surface-examination methods. The shear-wave technique prescribed for hollow forgings and probably used for the examination of tubular products might be sensitive to the discontinuities detectable by magnetic-particle or liquid-penetrant examination. This would depend upon the direction in which the sound beam was transmitted, and the Code does not specify any direction for the performance of the shear-wave technique. Case 1359-1 specifies the circumferential direction. The choice of examination method must depend on the anticipated character, location, and orientation of the flaw that may be detected after accelerated cooling. If there is concern over objectionable flaws within the body of the material, an appropriate ultrasonic technique should be specified. If the suspected defects are on the surface, longitudinal-wave ultrasonics would

have questionable value; shear-wave techniques would depend upon sending the sound in the proper direction; and magnetic-particle or liquid-penetrant methods would probably be applicable.

9.2.8 Procedures and Personnel

As noted in comments on the various material items, the Code prescribes the method of examination that will be applied and specifies the acceptance criteria. A few procedural details are supplied, but frequently these are inadequate to control the process and must be supplemented. This is done in several ways. The reactor contractor or pressure vessel manufacturer may supply specifications containing the examination details he feels to be needed. In other instances the detailed procedures are supplied by the manufacturer of the material and reviewed for approval by the purchaser.

Whichever route is chosen for establishment of detailed examination procedures, it is important that the procedure be adequately controlled and specified to assure that the intended purpose is being served. Of course, the existence of ideal procedures would be of no avail if the equipment and personnel were inadequate to perform the prescribed procedures. For some examinations, such as radiography and ultrasonics, the calibration standards offer some demonstration that the equipment is functioning and may perform the examination adequately. For the magnetic-particle and liquid-penetrant examinations, no such calibration standard is required by the Code (nor is it as readily available). Some qualitative assurance of equipment or material performance may be gained by observation of background indications. In general, the company performing the inspection provides his own method for assuring proper performance of his equipment, although some evaluation of equipment may also be made by his customers. This is supplemented by various military specifications and requirements, since most of the suppliers of civilian power reactor vessels and components also have active military contracts, and the same examination equipment may be used.

Of equal or greater importance is the assurance that the operator is qualified to perform the test and/or make the proper interpretation.

The Code requires the manufacturer to certify that each operator has the proper vision and is competent in the techniques of the nondestructive examination method for which he is certified. There is no uniform method of testing or demonstrating competence prescribed by the Code. Here again, there are military requirements because of military contracts for personnel qualification and certification for many of the same manufacturers and operators who work on civilian reactor materials. Thus, as a fringe benefit at this time, there is some additional degree of assurance that several of the examination procedures are being performed and interpreted by operators who are certified in accordance with a uniform method. In addition to the military requirements, some companies who buy materials or components from subcontractors have their own methods of obtaining assurance that competent personnel are examining their material.

As a further supplement to Code Case and company requirements for examination procedures, equipment, and personnel, the reactor contractor and vessel manufacturer usually monitor their suppliers during contractual performance. This monitoring covers reviewing material and test reports and visits to the suppliers' facilities to witness and audit the calibration and performance of the various nondestructive examination procedures.

9.3 FABRICATION

The detailed ASME Code requirements for process control are contained in Articles 5 and 6 of Section III. Paragraphs N-511.1 and N-614.1 require that the vessel manufacturer certify compliance with all specified heat treatments, tests, and examinations and submit the certificates, together with other certificates of compliance with materials specifications and test results, to the inspector. Paragraph N-511.2 requires preparation of additional test coupons and tests representing material subjected to heat treatments beyond those anticipated when the test coupons were prepared by the materials manufacturer. Paragraphs N-512 and N-615 provide for the identification and marking of materials and verification of this by the inspector. Paragraph N-513.1 requires the

examination of exposed cut edges of material product forms during the course of fabrication by magnetic-particle or penetrant methods, supplemented at times with ultrasonic examination. It requires that all cracks and nonlaminar defects be removed, together with discontinuities, such as inclusions, that are parallel to the surface and exceed 1 in. in length. Paragraph N-514.1 provides for the welding or other repair of defects detected during the course of fabrication.

Paragraph N-513.3 requires dimensional checks of formed parts and makes provision for a limited amount of local undertolerance, but it requires that calculations establishing the acceptability of such deviations be included as addenda to the stress report of N-142 (see Sect. 9.4.2). Tolerance requirements for shells are given in N-516, and for formed heads, in N-517.

Paragraph N-530 contains heat-treatment requirements. The guides for preheating for welding in N-531 are quite general and place the principal obligation for establishing detailed preheating requirements on the fabricator in developing the welding procedure specification. Paragraphs N-532.1 and N-532.2 and Table N-532 cover postweld heat treatment (stress relief) in greater detail; N-532.3, N-532.4, and N-533 provide details of procedures for the postweld heat treatment; N-617 defines the responsibility of the inspector to satisfy himself that heat-treating operations have been correctly performed and that the temperatures and gradients conform to the requirements. Paragraphs N-532 and N-533 contain rather detailed requirements for postweld heat treatment. Paragraph N-333 permits but does not detail requirements for normalizing and tempering or austenitizing, accelerated cooling, and tempering of materials to improve their impact properties. The Code does not require the preparation of detailed heat-treatment procedures specifically tailored to the materials, product forms, and sizes and the fabricator's heat treatment and handling equipment, although the principal fabricators of reactor vessels, as a matter of good practice, establish such internal procedures and specifications in considerable detail for their own use. The requirement that detailed, written heat-treatment procedures (as well as other fabrication procedures) be prepared, demonstrated, and adhered to should be considered for inclusion in the Code.

Requirements for weld fabrication are given in N-520; N-522 requires that the vessel manufacturer establish welding procedures and conduct the mechanical, visual, and nondestructive tests required in Section IX and, in some cases, the special tests of N-540 to qualify welding procedures, welders, and welding operators. Separate welding procedures are qualified for each class of material, thickness range, and other listed "essential variables." The requirements for qualification are extensive and reference is made to the appropriate part of Section IX of the Code for the details. Paragraphs N-621 and N-622 require the inspector to assure himself that the procedures and welders have been properly qualified and to request requalification when there are reasons to question adequacy of the procedure or welder ability.

The Code contains a number of requirements that materials, welds, and components are expected to meet and which can be established by visual observation, but the fact that visual examination should be used is usually implicit, since the Code seldom states specifically that visual examination shall be performed. Some visual examination requirements are contained in N-526, N-527, and N-624, but the Code requirements in this area are generally considered insufficient. In the case of nuclear vessels, they are frequently augmented in the purchaser's specifications, but the more significant and effective supplementary visual requirements are those imposed by high-quality fabricators in their own process control procedures. Among the requirements frequently specified are (1) the visual examination of weld joint preparations to insure proper alignment, positioning, joint dimensions, soundness, and cleanliness of surfaces to be joined, (2) the use of qualified procedures and welders or welding operators, (3) adequate protection of the work from unfavorable weather conditions, (4) storage and moisture control of welding materials, (5) surveillance monitoring of the actual production application of the welding procedure, including control of voltage, current, arc length, travel speed, deposition rate, and observation of the arc and weld puddle, and (6) examination of finished welds for complete joint penetration, for freedom from undercut, overlap, abrupt ridges, or valleys, and for reasonably smooth weld surfaces that are either flush with the adjoining

base-metal surfaces or have a limited amount of weld reinforcement merging smoothly into the base-metal surface.

Nondestructive examination methods are given in N-624 (Radiography), N-625 (Ultrasonic Examination of Welded Joints), N-626 (Magnetic-Particle Examination), and N-627 (Liquid-Penetrant Examination). These procedures and acceptance standards apply both to materials, particularly those containing welds, in Article 3 of Section III of the Code, and to weld fabrication in Articles 5 and 6, as previously described in Section 9.2 of this chapter.

Paragraph N-623.2 requires that each nondestructive test operator be certified by the manufacturer to have adequate vision and competence in the technique of the method he is to use, including making the examination and interpreting and evaluating the results. The inspector designated in N-623 is required to assure himself that the nondestructive examination methods of N-624 through N-627 are followed and that the operators are properly certified by the manufacturer; he has the further right to require recertification of any operator. The actual technical competence of the nondestructive test operator is one of the most difficult things to put into Code or contract language or to enforce administratively; this is a matter that, together with other administrative problems, is being actively studied by technical and administrative groups in the Codes and enforcement agencies.

Paragraph N-612 of the Code states the requirements for qualification of the "authorized inspectors," who must be employed by a state, municipality, or an insurance company (not the manufacturer). Inspector qualifications are established by an examination prepared by the National Board of Boiler and Pressure Vessel Inspectors and administered under the rules of a state or municipality. The inspector meeting these qualifications may be certified by the examining jurisdiction or, reciprocally, by other jurisdictions, as qualified to inspect for adherence to any section of the Code. Since the Code had its inception as a Boiler Code, the examination is heavily weighted toward the requirements of Section I, Power Boilers, and secondarily to Section VIII, Unfired Pressure Vessels, with very little emphasis on Section III, Nuclear Vessels, other than that many of the requirements for materials, fabrication, welding, and

inspection in Section III are similar to – frequently identical with – those of Sections I and VIII. Unfortunately the present administrative procedures do not require that the inspector have sufficient understanding of the design requirements and some of the nondestructive test methods used more extensively in Section III than in other sections of the Code. The upgrading of the competence of authorized inspectors in those features particularly characteristic of Section III is a matter of considerable concern to the technical and administrative personnel involved in the development and enforcement of the Code. However, regardless of the background and abilities of the authorized inspector, his function is primarily that of an auditor of fabricator performance; he can accept or reject but he cannot usurp supervisory or management functions in the fabricator's shop, and he is not expected to perform the actual nondestructive tests or continuously witness and monitor all operations and tests performed in the course of fabrication. The primary responsibility for establishing and maintaining detailed and adequate procedures and continuous control over all details of fabrication and examination or inspection belongs to the fabricator, who has the further obligation of providing professionally or technically qualified supervisory quality control, welder, and operator personnel and coordination and control of their activities. The authorized inspection personnel then have the obligation to audit all these fabricator activities; this requires a level of competence, comprehension, and authority that will probably require professionally educated and experienced personnel in addition to the authorized inspectors qualified to N-612, even with additional "upgrading" training in Code requirements for nuclear vessels.

9.4 DESIGN

9.4.1 Stress Analysis and the Stress Report

Present ASME rules for the design and construction of class A nuclear pressure vessels, as given in Section III of the Code, are the result of a major change in philosophy with regard to stress analysis. Since it

is now possible to determine stresses in detail by either analytical or experimental means, the Code has placed the responsibility for determining and evaluating the stresses on the designer rather than on the Code writers, as was essentially the case under Section VIII and the applicable Code cases. The allowable stress limits were raised and three categories for stress evaluation were developed. In order to assure that an adequate stress analysis of the vessel has been made, Section III requires that a stress report be prepared, certified by a Professional Engineer, and filed with the proper authority at the point of installation.

The present Code is a considerable improvement over the previous rules, and industry has not yet fully adjusted, especially to the requirements for a complete stress analysis. The Code is, however, surprisingly weak with regard to the stress report. A clear and concise description of exactly what should be reported and how the report should be written is needed. The questions of whether or not computer output is acceptable, in what form results should be reported, and to what extent the formulas and methods of evaluation should be documented need detailed clarification. It should also be made clear whether and how much experimental justification for analytical formulas should be included in the stress report.

Third-party review of the stress report, once it is clear that the stress report fully documents the stress analysis, will probably be necessary in order to protect both the public interest and proprietary interests of private industry. The present Code provisions for inspecting and certifying the stress report can be rather easily complied with and yet not guarantee that an adequate stress analysis of the vessel has been made. It is recommended that the person who inspects the report be a fully qualified stress analyst, as well as a registered Professional Engineer.

9.4.2 Effects of Acceptable Deviations from Specifications

The design rules of Section III are intended to cover every conceivable situation, and since the new rules relate to the stresses in the vessel, this ideal is much easier to realize. Nevertheless an actual

pressure vessel will differ from both an analytical model and/or an experimental model in various respects. A discussion of these differences is the subject of error analysis, which includes (1) the differences between the mathematical model and the design and (2) the differences between the design and the completed hardware. The first item is the subject of the stress analysis section of Chapter 6 (Sect. 6.1). Review of the stress report and design specifications is the single most important step that can be taken to insure adequate and good-quality design. The second item should include fabrication, metallurgy, and inspection; however, these subjects are discussed at length in other sections of this report. Therefore, the following discussion is limited to geometric deviations that result from fabrication procedures.

Section III specifically discusses geometric deviations produced during fabrication, such as undertolerance on thickness (N-513.3), ovality detected by measuring the diameter on cylindrical, spherical, and conical-shell segments at different angular positions (N-516a), local out of roundness (N-516b), and fabrication misalignment (N-525). The first type of deviation, underthickness, produces a stress increase in the main vessel body that is classed as a local membrane stress provided the area of the underthickness is confined. The Code allows a value of 1.5 S_m, where S_m is the allowable design stress intensity, that is less than or equal to the yield stress and specifically requires that calculations be made and appended to the stress report that justify the resulting stresses.

The remaining allowable geometric deviations are limited by physical measurements. Ovality, local out of roundness, and fabrication misalignments influence the stresses by creating additional bending moments in the vessel. The Code does not attempt to identify or classify these stresses. However, it can be argued on the same bases that were used to establish the design limits that they should be classified as secondary bending stresses in order to insure shakedown. The primary criterion should be whether or not the deviation would be self-correcting by plastic action.

The consequences of geometric deviations have been of concern in this country and abroad since the mid-50's. This concern is reflected

in the rules of Section III, which require much tighter controls on fabrication tolerances than the rules of Section I and VIII. The allowable tolerances are apparently the results of careful deliberation and a compromise between what is ideally possible and what is reasonably attainable. However, the effects of even a permissible deviation are generally not appreciated in design. The experimental stress analyst, on the other hand, has eliminated the problem by using machined models. This, of course, is absolutely necessary in order to verify or develop theoretical treatment.

Since bending stresses are considered secondary, the primary concern of the designer is how much unaccounted-for bending occurs in regions that already contain large secondary or peak stresses. In order to evaluate the effects of geometric deviations on the stresses in these regions, more information is needed than is currently available. First, an adequate theoretical solution for geometrically perfect bodies is needed, and second, experimental data from models with known geometric deviations must be obtained. The absence of the first requirement has discouraged many investigators from seriously considering the second problem. There are, however, some recent experimental data on the stresses in boiler-drum penetrations[3] that indicate the degree to which geometric deviations in the main body of the vessel can affect the stresses in the penetration regions. Wellinger and Kragelah[3] report the results of strain-gage measurements on 16 commercial boiler drums that were experimentally stress analyzed as a result of finding fatigue cracks in several drums during normal service inspections. In all fairness to the nuclear pressure vessel industry and the present Code rules, it should be noted that boiler drums built in Germany are not constructed to ASME requirements for nuclear pressure vessels. For our purpose, these results can be used only to point out that potential problems may exist in nuclear vessels. The most serious problem would arise from a combination of high stresses due to dimensional variations and a partly through fatigue crack.

There is some experimental evidence of the effects of geometric deviations on the stresses in the main body of a vessel. Durelli, Dally, and Morse[4] reported in 1961 on experimental analyses of three large-

diameter thin-walled pressure vessels tested in support of the missile and space effort. In addition to ovality and local out of roundness, the test vessel wall thickness varied by as much as ±10%. Bending stresses of as much as 35% of the membrane stress were reported. Careful geometric measurements on the vessels were made, but unfortunately were not reported.

Maxwell, Holland, and Cofer[5] (see Sect. 6.4.1) tested a machined hemispherical shell 30 in. ID and 0.38 in. thick, with a 7-in.-diam centrally attached radial nozzle, under internal pressure. This model had an accidentally produced 1 1/2-in.-wide conically shaped flat region on the sphere that was centered at an angle of 26° from the axis of the nozzle. The maximum difference in diameter due to this defect was 6.24% of the vessel thickness. According to N-516 of Section III, this is an allowable deviation. Under internal pressure the surface meridional stresses were about 60 and 30% different from their calculated values. The meridional membrane stress agreed with the theoretical values for a geometrically perfect shell, as was expected.

PVRC vessel No. 5, a cylindrical vessel 36 in. ID, 7 ft long, and 2 in. thick tested at Southwest Research Institute, was reported to be 1/4 in. out of round,[6] with initial surface strains 50% higher than theoretical. This deviation is near the Section III, N-516, allowable limit.

Pickett and Gregory[7] have discussed determinations of out-of-roundness stresses in three PVRC cylindrical vessels, Nos. 5 and 6 and a 2 1/4% Cr—1% Mo vessel. A series of experiments for measuring out of roundness and its effects was performed as a part of the full-size pressure vessel test program. The out-of-roundness deviations were somewhat less than 1% of the internal diameter and produced bending stresses that effectively doubled the outer surface stresses in the center of the deviation (i.e., bending stresses equal to 100% of the membrane stress). In addition, the paper of Pickett and Gregory[7] gives several approximate formulas, gathered from foreign papers, for computing stresses for specific types of geometric deviations. The significance of out-of-roundness stresses is summarized as follows:

"a. The stress intensification for permitted deviations from circularity can be as great as for well-designed reinforced openings.

b. The resulting high stresses are not r stricted to specific and limited locations as are designed geometric discontinuities.

c. Even when the problem is self-correcting due to inelastic behavior, excessive strain hardening may result. The behavior of hardware made of materials with high ratios of yield to ultimate strength is little affected by loading history within permitted ranges.

d. The problem is most likely to be associated with longitudinal seam and reinforced opening weldments where residual stress, fabrication flaws, and materials properties are most likely to compound the problem so that fatigue and fast fracture can occur at such locations rather than, and prior to, damage at the nominally highest stress locations in a vessel. This poses problems not only in analysis but in quality control and in service inspection procedures."

In summary, general concern over stresses that arise as a result of geometrical deviations produced during fabrication has been recognized by the Code committee responsible for writing Section III. The action taken was to restrict allowable deviations in a somewhat more meaningful manner than in previous codes to values that can reasonably be obtained by careful fabrication methods. Experimental measurements to date indicate that further work needs to be done. However, none of the data have shown that the present nuclear code rules are inadequate.

9.5 INSPECTION METHODS — CAPABILITIES AND LIMITATIONS

The methods and acceptance standards for the nondestructive tests required by codes, specifications, and shop practice are covered in some detail in Sections 9.1 through 9.3. Consideration of the validity and utility of these methods is restricted here to their use in current heavy-wall reactor pressure vessel technology; these factors might be quite different in other applications. This section attempts to evaluate the abilities, probabilities, and limitations of the tests in locating significant flaws and in determining their type, size, shape, distribution, location, and orientation. It also discusses relevant but less readily

recognized contributions these methods make to early rejection of defective materials, to the production of relatively flaw-free weldments, and to minimizing the amount of weld repair required.

Objective evaluation of the tests is handicapped by the conflicting viewpoints from which the problems can be considered. Some observers ascribe something approaching infallibility to the tests without recognizing their limitations in flaw detection and the lack of precision with which size, type, and orientation of defect can be established. Those who expect exact numbers and positive assurance of detectability will be disappointed, for the effectiveness of nondestructive testing in reactor vessel technology is a matter of probability and approximation — not of certainty.

Certain features and limitations apply to practically all nondestructive test methods. Flaws are presented as signals or indications that seldom give exact, direct representation of the nature, geometry, and dimensions of the actual flaws. While reference acceptance standards of varying suitability may be established for these indications, most tests require considerable skill, experience, and judgment on the part of the operator to manipulate the equipment and interpret the significance of the signals in terms of size, shape, orientation, and type of defect. No one test can find all defects, and two or more complementary tests are frequently used to detect a broader range of material imperfections. On occasion, indications observed by one method are further explored and evaluated by a second technique. These are the two surest and quickest ways to improve the effectiveness and probability of defect determination — use of complementary nondestructive testing techniques, and use of a second method to further explore the indications from the method used initially.

9.5.1 Macroscopic or Visual Examination

Macroscopic, or visual, examination is the most widely used test for evaluating material soundness, surface condition, workmanship, and weld quality in general fabrication practice, where it is often the only examination method used; it is also important in reactor vessel fabrication,

but there it is generally used in conjunction with one or more of the other examination methods. It is rapid and relatively inexpensive. It may be used to evaluate smoothness and cleanliness; freedom from blisters, loose mill scale, sand, and dirt; edge preparation, bevel angle, alignment, and fitup for welding; and cracks, undercuts, surface irregularities, penetration, and dimensions of welds. A knowledgeable, experienced inspector or welder can infer much about the internal conditions and even defects inside welds from visual observation of such things as irregularity of weld-bead surface, excessive or insufficient weld buildup or penetration, cleanliness, surface oxidation, and overlap and undercut, but this is essentially an aid in process control and is not relied on as an actual basis for weld joint acceptance in nuclear vessel fabrication. Where the welding process is monitored during the course of welding (strictly speaking, process control, not just inspection), visual observation by a competent weld inspector, aided by indicating and recording equipment, is a particularly effective means of achieving quality welds, since the inspector can detect incorrect welding conditions and the production of defects in time to make corrections and prevent the formation of still more defects.

Visual examination is usually performed with the unaided eye, but various aids such as special lighting, mirrors, borescopes, magnifiers, telescopes, comparators, weld gages, and remote television may be used. An aid to visual inspection that is not used nearly enough in pressure equipment fabrication is the comparison sample, or "workmanship standard," described and illustrated in Figure 10.37 of the Welding Handbook.[8] This is useful in some phases of reactor vessel fabrication, particularly those involving manual welding processes. It is perhaps of more value in nonnuclear fabrication, but it is particularly effective in obtaining uniformity of interpretation in visual examination where there is not a previously established understanding between the fabricator's welders and quality control personnel or the inspectors and the customer's representatives, although such circumstances should not exist in nuclear work.

Penetrant and magnetic-particle techniques frequently serve as extensions of visual inspection, but since they involve specifically

detailed procedural control, acceptance standards, and special interpretation of indications, they are discussed separately later. Visual examination may also include mensuration, but since this involves compliance with dimensional tolerances, rather than examination for defects in materials and welds, it will not be further considered in this section.

As for limitations, visual inspection as a consistently useful acceptance method is generally limited to observation of relatively gross surface defects; imperfections such as fine hairline cracks may well be overlooked. Effectiveness of visual examination is largely dependent on the visual acuity, individual judgment, and experience of the inspector. Weld-surface finish is often specified in very general descriptive terms, such as that the surface "shall merge smoothly into the plate surface," or that the reinforcement may have a "reasonably uniform crown," or that joints shall be "free" from undercuts, overlaps, and "abrupt ridges or valleys." Such general descriptions can result in disagreement and differences in interpretation of what is or is not acceptable, particularly since different welding processes, procedures, and even welders can produce substantially different surface finishes that cannot be readily differentiated or evaluated on the basis of general descriptive statements.

9.5.2 Radiography

Radiography is a means of recording the internal homogeneity of materials and is used to detect cracks, voids, porosity, metallic and nonmetallic inclusions, incomplete fusion, undercut, incomplete or excessive penetration, and irregular surface contours. It depends on the ability of gamma radiation to penetrate the material being examined and on differential adsorption of the radiation, which depends on the relative thickness and density of the material. The emergent beam is recorded on a photographic film as a shadowgraph of the material shape and internal structure. Other means of presenting the differentially absorbed radiation include Xero-radiography, fluoroscopy, and television.

Penetrating radiation may be obtained from x-rays or radioactive isotopes. Radiation from an x-ray tube is produced when electrons from the cathode, accelerated to a high velocity in an evacuated tube, strike a

suitable target at the anode. Industrial x-ray units of various designs permit the use of accelerating voltages from 5 kv to 50 Mv. The most commonly used units in general radiography have a single-stage acceleration in the range of 50 to 400 kv, but for large reactor pressure vessels, multistage acceleration units, such as the linear accelerator or betatron, usually range from 1000 kv upward for the electron accelerating voltage. The most commonly used radioisotopes for reactor vessel tests are ^{60}Co and ^{192}Ir. The principal advantage of gamma-ray equipment is the small size of the source holder or tube, which permits it to be positioned in a space too small for an x-ray tube. A disadvantage is that gamma radiographs usually have a lower sensitivity than x-radiographs, and, since gamma sources emit penetrating radiation at all times, they must be kept in shielded carriers to permit safe handling and storage.

The ability of radiation to penetrate a material with sufficient intensity to make radiography practical is principally dependent on the thickness and density of the material and the energy (voltage) and intensity of the radiation source. Ability to detect discontinuities and interpret the film depends principally on the radiographic sensitivity.

Factors affecting radiographic sensitivity are

1. Radiographic contrast
   - (a) Object contrast, as affected by
     - (1) thickness and density differences in object,
     - (2) radiation energy (kilovolts),
     - (3) scattered radiation (controlled by the use of filters, masks, and screens).
   - (b) Film contrast, as affected by
     - (1) type of film (fine or coarse grained),
     - (2) film processing,
     - (3) film density.
2. Image definition (sharpness)
   - (a) Geometric factors
     - (1) focal spot or source size,
     - (2) source-film distance,
     - (3) object-film distance,
     - (4) screen-film contact,

(5) sharpness and orientation of flaws,

(6) motion.

(b) Graininess factors, as affected by

(1) type of film,

(2) type of screens,

(3) radiation energy,

(4) film processing.

The operator must use judgment in utilizing and balancing the variables to produce high-quality radiographs containing maximum information, and he must have suitable viewing equipment. Radiographs will have greatest sensitivity when contrast is high, density is adequate, and detail is sharp. The adjustment of variables in the direction that produces greater film sensitivity generally increases the exposure time.

The Code requires that the adequacy of radiographic sensitivity be verified by demonstrating the ability of the technique to show a plaque-type penetrameter. This penetrameter should have about the same radiographic density as the object, a stated thickness relative to the weld thickness (1 to about 1.5% for thicknesses greater than 3 in), and three holes, the smallest of which will have a diameter twice the penetrameter thickness. Penetrameter sizes vary with weld thickness, particularly as the weld thickness decreases below 1 1/2 in. The Code states the conditions requiring radiography of welds, the type and sizes of penetrameters to be used, and the types, dimensions, and quantities of discontinuities that constitute rejectable defects. A penetrameter with a thickness of 2% of the object thickness and a minimum hole diameter is described as a 2-2T penetrameter; and the radiograph that just shows it is said to have an "equivalent sensitivity" of 2%. If the penetrameter thickness is 1% of that of the object and the hole size is twice the penetrameter thickness, it is described as a 1-2T penetrameter, and the equivalent sensitivity, as 1%. One percent sensitivity can be readily achieved in good radiographic practice on through-thickness welds in reactor vessels; in fact, it is probable that most radiography (with accelerators) on the heavier thickness reactor vessels has a sensitivity nearer 0.5% or even better. Nondestructive test specialists emphasize that penetrameters are image quality indicators (IQI) intended to establish the adequacy and

sensitivity of radiographs and not to simulate defects. Even so, it is reasonable to assume that the smallest visible penetrameter hole is a rough approximation of the detectable size of three-dimensional spheroidal or elongated porosity or voids, and, to some extent, inclusions, depending on their radiographic densities. Then, assuming 0.5% equivalent sensitivity, reasonably good radiography of a 6-in. weld can be expected to show voids about 3/64 in. in diameter. The inclusion of these numbers is not intended to state exact limits on radiographic capability or to imply that radiography can consistently reveal all discontinuities of these and larger sizes. The numbers are simply intended to show approximate levels of detectability that characterize good, current commercial practice in reactor vessel fabrication. Several variables can modify these numbers, particularly in the direction of lesser capability; these are the shape and relative density of discontinuities, location in the weld, weld surface uniformity, general quality of the weld, and the competence of the radiographic procedures, operators, and viewers. However, even these approximations lose significance when discontinuities such as cracks, laminar inclusions, incomplete penetration, lack of fusion, and underbead, hydrogen, or hard-zone cracking approach being two dimensional.

Several investigations have attempted to establish the detectability of cracklike discontinuities, including those in welds of various thicknesses, and several have used artificial cracks in the form of machined slits to study the parameters involved. Criscuolo[9] used tapered slits aligned with the beam, a 2000-kvp x-ray beam, and fine-grained film to detect 0.02-in.-deep slits with a width of 0.01 in. that were nearly elongated voids in 3 in. of steel. For 0.001-in.-wide slits, which more nearly resembled cracks, the detectable slit depth (extrapolated) was 0.1 in. Slit or crack detection is sensitive to such factors as image contrast, slit dimension, unsharpness, and inclination of the slit plane to the direction of the beam of radiation.

Halmshaw[10] reviewed several studies made with good radiographic techniques and fine-grained film for determining the detectability of artificial cracks, that is, machined slits of uniform width and depth, deliberately set at different angles to the radiation beam. For a 4-in. thickness of steel and cracks 0.001 in. wide in line with the beam, a

crack 1/4 in. deep was detected by using 18-Mv x-rays, and a crack 1/2 in. deep was detected by using ^{60}Co. When inclined to a 5-Mv x-ray beam, a crack 0.001 in. wide and 0.44 in. deep was just detected at a 2 1/2° angle; a 0.01-in.-wide, 0.5-in.-deep crack was detected at a 27° angle. Halmshaw also reviewed investigations of actual weld cracks, but he stated that the variations in results reported by different observers were so great that no meaningful quantitative results could be assigned or assumed.

Ishi[11] made a study of 1/4-in.-deep, 0.002-in.-wide artificial (stress-corrosion) cracks in 1-in.-thick welds. These were radiographed at beam angles in 2° increments from 0 to 10°. Cracks inclined at beam angles of less than 5° showed on the radiographs; those at angles greater than 5° did not.

The British Engine Boiler and Electrical Insurance Company, Ltd.,[12] has reported an investigation intended to study the principal factors governing the radiographic detectability of defects and the dimensions of those that might not be detected. Tests were run by several research laboratories and contractors on specimens consisting of assemblies of artificial cracks (spaced optical flats) with material thicknesses ranging up to 4 1/2 in. of steel and a variety of radiographic techniques including gamma radiography, 250- to 400-kvp x-rays, a betatron, and a linear accelerator. The tests produced some significant results that are only directly and quantitatively applicable within the range of thickness covered by the work, that is, up to 4 1/2 in. Some of the findings of these studies are cited below:

1. For a specimen thickness of only 1 in., a crack with depth equal to one-tenth this thickness will not be detected radiographically if its width is about 0.00025 in. or less, and detection is doubtful if the width approaches 0.0005 in. or slightly more. This minimum width of crack that can be detected becomes larger as the thickness increases.

2. For a crack depth of 0.1 in., the effect of beam obliquity is insignificant up to about 5 1/2°. This will vary with a number of factors, but it is intended to be representative of simulated defects resembling those likely to be found in the welds under consideration in the British study.

3. There is a lower limit to the cross-sectional area of a crack-like defect that can be detected in a given material thickness; for example, the minimum detectable crack volume per unit length (or width times depth) is

$$w \cdot d \text{ for 1-in. thickness} = 5 \times 10^{-5} \text{ in.}^3/\text{in. } (0.00005)$$
$$w \cdot d \text{ for 2-in. thickness} = 15 \times 10^{-5} \text{ in.}^3/\text{in. } (0.00015)$$
$$w \cdot d \text{ for 3-in. thickness} = 30 \times 10^{-5} \text{ in.}^3/\text{in. } (0.0003)$$
$$w \cdot d \text{ for 4-in. thickness} = 50 \times 10^{-5} \text{ in.}^3/\text{in. } (0.0005)$$

Thus, for a 4-in. thickness, a detectable 2-in.-deep crack would be 0.00025 in. wide; a 1-in. crack, 0.0005 in. wide; a 0.5-in. crack, 0.001 in. wide (extrapolated); and a 0.1-in. crack, 0.005 in. wide (also extrapolated). The report emphasizes that these values are based on good commercial techniques, that they apply only to artificial cracks, and that consideration in any other context should assume a lesser borderline detectability.

Pollitt and Durant[13] have proposed a theory to determine penetrameter sensitivities and to extend this to predict crack dimensions calculated from penetrameter data for known conditions. For high-voltage, fine-grained-film techniques they present the minimum detectable crack cross-section area in the equation:

$$wd = 0.65 U_t S_x ,$$

where

w = crack width,

d = crack depth,

U_t = total unsharpness (a factor in the assessment of penetrameter sensitivities),

S_x = minimum detectable penetrameter step height.

Based on this relation and selecting conditions consistent with the British data,[11] the calculated detectable crack cross-sectional areas were within a factor of 2 to 3 less than the British observed results for a 4-in. thickness.

An investigation of a recent hydrotest failure of a 260-in.-diam motor case prompted a study of the relative effectiveness of radiography

and ultrasonics in identifying and describing crack-like defects in welds in 250,000-psi nominal yield strength, 0.7-in.-thick, 18% Ni-Co-Mo-Ti "maraging" steel.[14] While the materials and thicknesses involved in the investigation were not directly comparable to those used in reactors, the investigation of the limits to the relative capabilities of nondestructive test methods to detect defects is of considerable significance. Five relatively small flaws exposed by the actual fracture or by detailed postmortem examination, but not by the original nondestructive tests, were cracks in heat-affected zones or in welds (submerged-arc) underneath manual tungsten inert-gas (TIG) weld repairs. (This suggests the need for an incidental concern for the effects of high heat input rate welding processes in generating or extending weld cracks in materials that are sensitive to such cracking.) The defect that caused the failure was about 1.4 in. long by 0.1 in. deep.

Subsequent to the failure, additional test welds were made in test plates, and fatigue cracks of the order of 1/2 in. long by 1/10 in. deep were deliberately introduced into the welds; they were then examined by radiography and ultrasound with both commerical and laboratory techniques. Radiography was generally unsuccessful in locating these tight fatigue cracks; ultrasound was somewhat better but did not give very accurate estimates of actual defect sizes.

A second set of eight test plates[15] was prepared; some had semi-elliptical surface fatigue cracks, and some had cracks generated at the bottom of machined depressions that were subsequently filled by manual TIG welding. Radiography located the submerged cracks and thus indicated that the simulated weld repairs probably widened the gaps, but it had difficulty in finding the very tight cracks. Ultrasound found the cracks but had difficulty estimating their size and configuration, probably because of interfering reflections from the weld structure. Similar and even larger defects would be more difficult to detect in still thicker sections. It should be recognized that these small defects in high-strength materials are far more critical from the fracture-potential standpoint than they would be in relatively low-strength ductile steels used in reactor vessels. This test and the dimensions of cracks involved are discussed further in Section 9.5.3, Ultrasonic Testing.

A general review of the referenced experimental studies conducted with good radiographic techniques indicates limiting crack-detectability depths ranging from 0.1 to 0.5 in. in a 3- to 4-in. thickness for artificial cracks in line with the radiation beam. However, very tight cracks and cracks inclined more than about 5° to the beam are difficult, if not impossible, to detect. Since some cracks will follow twisting or curved paths, only a portion of them will be suitably oriented with respect to the radiation beam, so some cracks substantially deeper than the suggested detectability limits may not be observed on the radiographs. These limitations to the probability of detecting crack-like defects of various dimensions, configurations, and orientations obviously raise doubts regarding the basis for the confidence traditionally placed in radiography as assurance of the integrity of welds. It would be difficult, in fact impossible, to contend that even the best radiographic practice can provide complete assurance that a weld contains no rejectable defects, but there are factors, discussed below, that permit at least some confidence in weld integrity beyond the strict limitations of the ability of radiography to detect cracks.

The fact that the detectability of planar defects is restricted to those within perhaps 5° of the radiation beam is disturbing, particularly if completely random distribution of the defects is assumed. However, the more common crack-like discontinuities in relatively conventional single- or double-groove multipass full-penetration arc butt welds include incomplete penetration, lack of fusion, center-line cracks, interdendritic cracks or segregation, and underbead, hydrogen, or hard-zone cracks in the heat-affected zone. Since these welds are usually radiographed from a direction normal to the surface of the finished weld, most of these types of defect are favorably situated for detection by radiography. Incomplete penetration and center-line cracking are normally in line with the radiation beam, and cracks near the interface between the weld metal and the base metal, such as lack of fusion and heat-affected zone cracking, approach this orientation, since the joint-preparation angle is generally quite small for 6- to 12-in.-thick welds, and the cracks that roughly parallel the fusion line tend to follow a sinuous

path, at least a portion of which is likely to be suitably oriented. A type of cracking (or segregation) less likely to coincide with the direction of the radiation beam is that which parallels the elongated dendrites in the weld itself. These may be very small microfissures, which are present in a far larger percentage of welds than is generally suspected and are seldom detected by customary nondestructive test methods; their detection usually requires sectioning and microscopic or penetrant examination of cut sections. Longer interdendritic cracks, sometimes called "angle cracks," are large enough to be of real concern but are also difficult to detect, although ultrasonic examination of the completed weld appears to have more potential than radiography for locating them. This cracking is best controlled by making the weld in a multiplicity of small passes with limited heat input and metal deposition per pass and with frequent magnetic-particle examination as each layer (or several layers) is completed. Where the cracking is still more extensive, there is a limited possibility that the ends of the cracks paralleling the dendrites will eventually assume a direction more nearly normal to the finished weld surface as they extend toward the center of the weld and thus will be amenable, for a part of their length and to a limited extent, to radiography. The principal solution to this type of weld cracking is preventive, through procedure qualification and process control.

Among the important factors contributing to confidence in the adequacy of welds are the combination of integrity and competence of the fabricator and his personnel and the use of a welding procedure qualified to establish the limiting parameters within which sound, reasonably defect-free welds can be anticipated.

Another important factor is that the expectation that a weld is to be radiographed is one of the surest ways of improving weld quality, since it will need to be capable of meeting the radiographic requirements. Knowledgeable people who are quite conscious of the technical limitations of radiography are equally aware of this very real and effective psychological contribution that radiography makes to weld integrity. This influence is not limited to welders; it extends to essentially all personnel involved in achieving weld quality. This is most obvious in shops that do a variety of work, some radiographed and some not; nevertheless,

the fact of radiography makes a subtle but substantial contribution to weld quality beyond just detecting weld defects, even in shops where all welds are radiographed.

Another major factor that contributes to weld soundness is a quality assurance program, as discussed above. While effective methods of after-the-fact inspection are essential to the location and repair of defects and to more positive assurance of confidence in the welds, techniques that minimize the probability that defects will get into the welds in the first place are even more important — an initially defect-free weld is far better than a weld that contains a substantial number of repairs. The necessity for repairs introduces distortion and residual stresses, and it reduces confidence that the repaired weld does not still contain undetected defects.

9.5.3 Ultrasonic Testing

Ultrasonic testing can be used to examine welds, castings, most wrought product forms, and partial and completed assemblies and to locate and delineate cracks, laminations, lack of bonding, incomplete fusion, incomplete penetration, porosity, and slag inclusions, depending on what is being examined. It may also be used to determine thickness and sometimes to identify certain metallurgical conditions, such as incorrect heat treatments or excessive grain size.

Ultrasonic examination is based on the directional properties of beams of high-frequency (well above the audible range) sonic waves. The pulse-echo method is generally used for detecting defects. It involves the generation of an electrical pulse in a pulse generator, transmission of this pulse to a piezo-electric crystal or transducer that changes the electrical energy to mechanical energy in the form of a sonic wave, introduction of the sonic wave or vibrations into the material being tested, reflection of the sonic beam from the free surfaces and discontinuities in the materials, reception of the reflected sonic beam and reconversion to electrical energy in a transducer or search unit, and, ultimately, the presentation of a signal representing this reflected beam

in a device such as an oscilloscope. Ultrasonic methods other than pulse echo may be used for measuring thickness.

Straight-beam waves, which enter the material normal to its surface, are widely used for materials inspection. Shear waves introduced by angle transducers are particularly effective in weld inspection but are also used to inspect material product forms. Surface waves, Lamb or Rayleigh, are sometimes used in locating surface cracks and imperfections. A resonance method involving variation of the frequency of the sonic wave is used to gage thickness of materials; it may also be used to detect other defects, including the location of unbonded areas in cladding.

Like most other methods of nondestructive testing, ultrasonic examination requires experience and skill on the part of the operator to interpret the nature, shape, location, orientation, and size of defects. Under properly controlled and automated operating conditions, with well-designed circuitry, ultrasonic testing gives results that are consistent, accurate, and reasonably independent of human variability and error. It produces signals that can, in some cases, be used to estimate the approximate relative magnitude of the defects. The technique can be adapted to continuous inspection lines and automatic marking of defects; it is used in this manner in at least one pressure vessel fabricating plant in Great Britain. Three-dimensional representation of some defects can be achieved at times, and, subject to varying degrees of difficulty, a permanent record of test indications can be made and retained if desired.

Limitations of ultrasonic testing include a considerable variability in sensitivity and discriminatory capability between different types of ultrasonic instruments. Surface irregularities and internal metallurgical variables may cause spurious indications. Welding procedures and joint designs may be selected to insure compatibility with ultrasonic inspection, and others may be avoided because they are not amenable to meaningful ultrasonic examination. Defects such as porosity and more-or-less spherical slag and other inclusions are generally difficult to locate and measure as effectively as with radiography. Coarse-grained structures, such as austenitic stainless steel castings or weldments, in particular those that cannot be grain-refined by normalizing or heating

through a grain-refining transformation, may be difficult, if not impossible, to examine ultrasonically; some limited improvement can sometimes be made by lowering the frequency and otherwise modifying the techniques. This is generally not a problem in large power reactor vessels but does limit applicability to associated stainless steel components, such as pump casings. The usual ultrasonic methods are less effective when searching for defects very near the edge, end, or surface of a part. Special surface preparation may be necessary to insure proper introduction of the ultrasonic beam. When the longitudinal-wave technique is being used, defects near the surface may not be resolved due to inability to differentiate from a large front-surface indication.

Under ideal conditions the ultrasonic technique is sensitive to discontinuities approaching microscopic dimensions; but in practical applications, particularly in weld inspection, the sensitivity is limited by such things as weld and base-plate surface irregularities, coarse or nonuniform grains, inhomogeneities, and elongated dendritic weld structures, which can cause excessive scattering and mask the flaw reflections. The reflection from a flaw is portrayed as a trace on an oscilloscope screen; this trace can seldom be directly identified with the nature of the defect, although the reflection may give some indication of the size of the defect. To evaluate weld defects, the detection system is generally calibrated with a reference weld and a reference defect; the persistence of the trace with longitudinal and transverse movement of the probe then permits estimation of the nature, orientation, and size of the defect. The separation of the indications from interfering factors to permit weld-flaw evaluation is largely a matter of operator skill and his knowledge of ultrasonics and the nature of weld defects. As in the case of radiography, the probability of identifying defects and the estimation of their dimensions and location can vary several fold with these factors.

In the NASA investigations[14] discussed under radiography above, the use of good commercial ultrasonic techniques located cracks 0.3 in. long and 0.1 in. deep in 0.7-in.-thick welds; more sensitive laboratory techniques found cracks 0.1 in. long and 0.03 to 0.04 in. deep. In the NASA Second Cooperative Investigation,[15] cracks of the order of 1/2 in. long

and 0.1 to 0.2 in. deep were located, but the estimates of dimensions varied substantially between inspection organizations. It is important to realize that the size of a borderline ultrasonically detectable crack does not increase with section thickness to the extent it does with radiography; this is one of the major features of ultrasonic examination in thick sections.

9.5.4 Magnetic-Particle Examination

Magnetic-particle examination is used to detect discontinuities, particularly linear types, such as cracks, lack of fusion, and slag at or near the surfaces and edges of ferromagnetic materials. When a magnetic field is established in such a material, discontinuities in the path of the magnetic flux set up poles at the discontinuities that have a strong attraction for loose magnetic-powder particles applied to the surface of the material in the magnetic field. The parts to be inspected may be magnetized by the direct introduction of a high-amperage current through "prod" contacts or by an external magnetizing coil or "yoke." The areas to be inspected are covered with finely divided magnetic particles, sometimes colored or fluorescence coated, that concentrate in the vicinity of a discontinuity to form a pattern or indication on the surface that somewhat resembles the shape of the discontinuity.

Magnetic particles may be applied as either a dry powder or a wet slurry. The wet method is generally used on stationary equipment or smooth surfaces of production-type items. The dry powder is used quite successfully on moderately rough surfaces such as castings, on parts or structures in field operations where the wet method is not readily adaptable, and on welds, particularly in examining partially completed welds. Slag must be cleaned from the surface of the weld bead, but the dry-powder method can be used for moderately rough surfaces, although surface roughness does decrease sensitivity. The magnetic-particle method is primarily a surface inspection technique and to that extent is an aid to visual inspection. However, with the proper choice of technique, defects located as much as 1/4 in. below the surface can also be detected. Care must be used to avoid arcing and damage to the base metal or weld

surface at prod contacts. There is some variation in revealing power that results from a nonuniform magnetic field, prod location, and effectiveness of prod contact. The size of a defect is only approximated. Undercut, surface roughness, and some false indications are difficult to differentiate from more serious defects.

Acceptance and rejection are dependent largely on interpretation and judgment of the inspector, but some efforts have been made to develop standardized procedures and acceptance criteria, as described in Section 9.2.

9.5.5 Liquid-Penetrant Examination

Liquid-penetrant examination, like magnetic particle, is sometimes considered an adjunct to macroscopic or visual inspection. It may be used on either magnetic or nonmagnetic materials. Two types of penetrants, visible dye and fluorescent material, are used. The process involves the application of the penetrant to the dry surface of the part to be inspected; the penetrant enters relatively narrow exposed surface openings by capillary attraction. The excess penetrant is removed and, in the case of the visible dye penetrant, a developer is applied. Indications of discontinuities appear as a colored dye pattern on the chalky white developer in the case of the dye penetrant or as a brilliant fluorescent indication when the part is viewed in black (ultraviolet) light in a darkened area if the fluorescent penetrant technique has been used. Details of application are described in ASTM E 165, Methods for Liquid Penetrant Inspection, and in N-627 of Section III of the ASME Code.

The method is limited to examination for discontinuities that open to the surface, such as cracks and porosity; however, it can be effective in locating tight or shallow surface cracks where radiography may fail. Sensitivity and reproducibility are strongly affected by production practices, surface preparation, and control of time, temperature, materials, and techniques. Parts to be inspected must be thoroughly cleaned and dried. Welds cannot be examined at usual preheat or interpass temperatures. The penetrant method should be used with caution if there is a

possibility that the penetrant materials cannot be satisfactorily removed by subsequent cleaning, as in the crevices of a tube-to-tube sheet joint or in a lamination exposed at the surface at a weld-joint preparation not requiring complete removal of the lamination to permit subsequent welding. Difficulties are encountered in determining the dimensions, particularly depth, of a penetrant-detected discontinuity. Because of the sensitivity of the method, it may be difficult to differentiate between spurious indications due to surface roughness or variations in techniques of application and actual defects; defects may sometimes be masked by grinding or the peening effect of shotblasting. Interpretation in the presence of unusual conditions is often dependent on the judgment and skill of the operator. Defects that have substantial depth may have to be further evaluated by other nondestructive means or by actually removing sufficient metal to eliminate the discontinuity. Various types of "comparators" have been proposed for qualification of penetrant procedures, principally under nonstandard conditions; one is described in N-627.6.

9.5.6 Electromagnetic Methods

Electromagnetic methods use electromagnetic energy to detect discontinuities and metallurgical variations, and are of two types: (1) those that rely primarily on an eddy current flow due to variations in conductivity and (2) those that depend upon variations in magnetic properties. The use of the method in reactor vessel fabrication is relatively limited; its principal application is in the examination of tubular products and the surfaces of bar stock.

One or more coils energized by an alternating current with a frequency varying from 50 cycles to 1 megacycle are used. The alternating current produces an alternating magnetic field through the coil that extends to some shallow depth within the material being tested and induces eddy currents. Changes in material conductivity or permeability affect the magnitude of the eddy currents, and these, in turn, affect the coil impedance. Changes in coil impedance are sensed and exhibited on meters, recorders, or oscilloscopes. Discontinuities in the material are detected

primarily as local changes in conductivity. In most methods, encircling coils are used for the inspection of right-circular objects, but probe-type coils are also used for special applications, such as measuring cladding thickness.

Electromagnetic methods are used on both magnetic and nonmagnetic materials to detect surface and subsurface discontinuities and metallurgical variables. Sensitivity to defects decreases with depth. The process is fast and relatively inexpensive; it is well adapted to production-line inspection with automatic marking of defects and permanent recording of test indications. As in the case of ultrasonic examination, properly controlled conditions and properly designed and operated circuitry can produce consistent and accurate results, with signals more-or-less proportional to the size of defects. The method is frequently used in tube mills for quality control in intermediate production stages without necessarily being specified as an acceptance test.

The test is generally limited to surface and relatively shallow subsurface defects. It is extremely sensitive to metallurgical variations, but this sensitivity varies significantly with the circuit selected. Some types of material may contain localized changes in permeability that affect the coil impedance to a greater extent than unacceptable discontinuities.

Most systems are also extremely sensitive to the "lift-off" of the coil from the material and require a properly designed material drive mechanism.

REFERENCES

1. R. H. Sterne, Jr., Heavy Gage Plate Steels for Nuclear Service, Lukens Steel Company, Coatesville, Pa., June 1966.

2. H. Johnson and R. Mierzwa, Ladish Forge Company, personal communication to R. W. McClung, Oak Ridge National Laboratory, September 1966.

3. K. Wellinger and E. Kragelah, Stresses in Boiler Drums, Welding Research Abroad, 12(8): 63–85 (October 1966).

4. A. J. Durelli, J. W. Dally, and S. Morse, Experimental Study of Large-Diameter Thin-Wall Pressure Vessels, Exp. Mech., 1: 33–42 (February 1961).

5. R. L. Maxwell, R. W. Holland, and J. A. Cofer, Experimental Stress Analysis of the Attachment Region of Hemispherical Shells With Radially Attached Nozzles, Report ME-7-65-1, University of Tennessee Engineering Experiment Station, Knoxville, Tennessee, June 1965.

6. E. A. Lange, A. G. Pickett, and R. D. Wylie, Failure Analysis of PVRC Vessel No. 5; Part 1 – A Study of Materials Properties and Fracture Development, Welding Research Council Bulletin No. 98, August 1964.

7. A. G. Pickett and S. C. Gregory, Studies of Fatigue Strength of Pressure Vessels, Technical Summary Report, Part 1. Cyclic Pressure Tests of Full-Size Pressure Vessels, Report SWRI 1228 1-29, Southwest Research Institute, September 1966.

8. Welding Handbook, 5th ed., Sect. 1, 1962, American Welding Society, New York.

9. E. L. Criscuolo, Slit Detection by Radiography, Materials Evaluation, 24(IV): 201 (April 1966).

10. R. Halmshaw, The Detectability of Fine Cracks by Radiography, International Institute of Welding, Document V-288-65, 1965.

11. Unpublished report by Ishi, Japanese Committee to Review ASME Code Section III, November 1966.

12. British Engine Boiler and Electrical Insurance Company, Ltd., Limitations of Radiography in Detecting Crack-Like Defects in Thick Sections, British Journal of Nondestructive Testing, 4(4): 103–119 (December 1962).

13. C. G. Pollitt and R. L. Durant, Radiographic Sensitivity, Memorandum Report 19/61, Armament Research and Development Establishment, May 1961.

14. J. E. Srawley and J. B. Esgar, Investigation of Hydrotest Failure of Thiokol Chemical Corporation 260 Inch Diameter SL-1 Motor Case, Report NASA-1194, National Aeronautics and Space Administration, Oct. 19, 1965.

15. National Aeronautics and Space Administration, Results of Second Cooperative Program on Nondestructive Inspection for Cracks, Lewis Research Center internal memorandum, May 25, 1966.

10. TESTING AND SERVICE PERFORMANCE SURVEILLANCE*

Periodic reinspection of nuclear components is usually a complex operation because of the intense background irradiation, which may limit or entirely prohibit direct human access to the components. If maximum advantage of nondestructive testing methods that are currently available is to be obtained, accessibility must be considered in the design of the structures to facilitate remote or semiremote techniques for inspection and testing.

Surveillance programs designed to monitor the effects of irradiation on materials are currently specified to provide information on any increase in the brittle-fracture transition temperature. Plant operating limitations based on the transition temperature approach are specified for the primary purpose of limiting the stresses in the vessel to low values in the subtransition and transition temperature regions, and any upward shift in the transition temperature would be factored into these procedures.[1]

Overpressure testing after the initial hydrotesting is not specified nor have any such tests been performed as a regular inspection procedure for nuclear vessels. Periodic reinspection by overpressuring is frequently performed on nonnuclear vessels, and the requirement for inclusion of such testing on nuclear vessels is being given increased attention. Also a hydrostatic test of some sort, not necessarily at overpressure, is generally performed following maintenance operations on the pressure barrier of the vessel.

10.1 HYDROSTATIC TEST

The hydrostatic test has been a part of ASME Boiler and Pressure Vessel Code requirements since the Code was first issued some 50 years ago.[2] For many years the Code also required a hammer test as an integral

---

*This chapter was prepared by R. G. Berggren, R. W. McClung, and E. C. Miller of the Oak Ridge National Laboratory.

part of the hydrostatic test; however, the hammer test was eliminated some years ago, and it has never been a part of Section III, Nuclear Vessels. It is still used optionally in some shop and field nonnuclear fabrication and maintenance inspections.

Section III of the Code requires that completed vessels be subjected to a hydrostatic test at a pressure not less than

$$1.25 \times \text{design pressure} \times \frac{S_m \text{ (for test temperature)}}{S_m \text{ (for design temperature)}},$$

where S_m is the allowable design stress-intensity value. It places certain limitations, described in paragraph N-714.2, on the upper limit of test pressure, based on analyses of loadings that will exist during the test, to establish that the calculated primary membrane stress intensity will not exceed 90% of the yield stress at the test temperature. Following the application of the test pressure, paragraph N-714.3 requires examination for leakage at all joints, connections, and regions of high stress at a pressure reduced to the greater of the design pressure or three-fourths of the test pressure. The vessel and pressurizing medium are to be at about the same temperature during test, which is suggested as not less than the NDT temperature plus 60°F to minimize the possibility of brittle fracture. The estimate of the NDT temperature is determined from either drop-weight tests or from Charpy V-notch impact test requirements established by correlation with drop-weight tests (N-332). Some vessel purchase specifications require that the NDT temperature selected meet both Charpy and drop-weight test criteria. The Code (N-715) also permits the use of a pneumatic test in place of the hydrostatic test under conditions that are not applicable to the light-water reactor vessels covered by this survey.

The hydrostatic test is generally considered a leak test and, in some cases, a strength verification test. Also it has been credited at times as being a way to detect improper design, gross flaws, and faulty materials and also as a test for evaluating susceptibility of a structure to brittle fracture. It has also been contended that the test may actually modify a vessel to lessen or eliminate the possibility of rupture in

service by mechanisms variously described as plastic reshaping, mechanical stress relief, stress redistribution, notch nullification or crack blunting, and localized strain hardening, among others.

The satisfactory longtime performance of thousands of pressure vessels, many containing sizeable flaws and operating frequently at temperatures below the brittle-fracture transition range, is sometimes credited to the effects — separate or in combination — of thermal stress relief (postweld heat treatment), mechanical stress relief, or other influence of the hydrostatic or overpressure test.[3,4] However, some concern has also been expressed for possible detrimental effects of hydrostatic testing, such as excessive deformation of a vessel beyond permissible dimensional limitations, mechanical or metallurgical damage to the materials or structure resulting from overstressing, for example, embrittlement due to strain hardening or strain aging, and possibly failure during a high overpressure test of a vessel that might have operated satisfactorily if it had only been stressed within design limits.

The hydrostatic test requirements in present Codes have resulted from gradual modification of practices that antedate the ASME Code. It has proved a practical and useful test, although its development has been based largely on experience rather than on knowledge of present-day concepts of brittle fracture, fracture analysis, or fracture mechanics.

Some details of the history of the application of the hydrostatic test to welded vessels in the ASME Boiler and Pressure Vessel Code may help in evaluating its significance.[2] From 1919 to about 1930, Code coverage was limited to riveted vessels. When welded pressure vessels were first included in the Code, about 1930, common practice was to use a test pressure sufficiently high to produce observable plastic deformation in the vessel shell. The Code reduced this requirement to two times the working pressure adjusted to the test temperature, although this did not necessarily eliminate some localized plastic deformation. At that time, most Code design stresses were based on 20% of the tensile strength of the material, so the test pressure represented about 40% of the specified tensile strength or about 80% of the yield strength if it is assumed (admittedly an approximation) that the yield strength of carbon

steel, the principal structural material used at that time, is about one-half its tensile strength. In 1950 the design stress basis for most materials in the ASME Code, Section VIII, Unfired Pressure Vessels, was changed to 25% of the specified tensile strength and the hydrostatic test to 1.5 times the design or working pressure; as a result the hydrostatic pressure test then represented, in most cases, about 37.5% of the specified tensile strength or 75% of the yield strength. These numbers, based on minimum specification values, are somewhat conservative when considering actual properties. However, geometric discontinuities and materials imperfections produce localized stress concentrations in areas that may be subjected to stresses well above yield, so some localized deformation can be expected. The test pressure specified in Section III has been reduced to 1.25 times the design pressure to reduce (in some cases) dimensional distortion in relatively thin-walled vessels, to maintain essentially the same stress level in relation to yield strength as given in Section VIII for a hydrostatic test of 1.5 times design pressure, or to lessen the hazards resulting from the release of the greater amount of stored energy contained in a compressed gas, such as air, as compared with that in water, which is of limited compressibility, in a hydrostatic test. The pneumatic tests can still be expected to stress the vessel to about 62.5% of the minimum specified yield strength, which can still cause plastic yielding in some regions of high stress concentration.

Section III, Nuclear Vessels, follows the same general reasoning as that on which the overpressure tests for other Code sections are based but has a few added refinements and further restrictions. Since Section III design is based for the most part on one-third the minimum tensile strength of the material, the test pressure at 1.25 times the design pressure represents about 40% of the minimum tensile strength and slightly more than 80% of the yield strength, again based on the assumption that the yield strength is about one-half the tensile strength. Section III contains an additional requirement that limits primary membrane stress intensities during hydrostatic testing to not more than 90% of the yield strength of the material.

Another test of some significance, although it is not used in Section III, is the "proof test" in UG 101 of Section VIII, which is

intended to establish the maximum allowable working pressure for vessels whose design does not permit satisfactory computation of the allowable working pressure with the usual Code formulas. This proof test consists of first incrementally pressurizing the vessel and determining the pressure at which local yielding first occurs by using a brittle coating, strain gage measurement, or displacement measurement. Then a maximum allowable working pressure of not more than two-thirds the maximum pressure to which the vessel was subjected in the proof test is established after making appropriate adjustments for temperature and other factors.

Hydrostatic tests have also been studied and standardized for components other than those covered by the ASME Code. The Compressed Gas Association[5] has set up several standard procedures for testing and retesting compressed gas cylinders that have been accepted under Interstate Commerce Commission regulations. They include four methods: (1) water-jacket volumetric expansion, (2) direct expansion, (3) pressure recession, and (4) proof pressure. The Dow Chemical Company[6] offers a commercial service, MELOGRAF, which it calls "dynamic pressure testing." This provides automatic instrumented plotting of pressure against volume to test a vessel or pipe section to an indication of plastic (permanent) deformation. This method is widely used in the testing of cross-country fluid transmission pipelines, as well as other pressure-containing components.

From time to time the significance and validity of the hydrostatic test (and of the hammer test, which is not of concern here) have been questioned. Such concern prompted an extensive survey and examination of these tests some years ago, as reported[7] by the Pressure Vessel Research Committee (PVRC) in 1952; a summary[8] of the report was published in 1953. This PVRC document[7] reviews the history of the test requirements and reasons for their adoption and contains critical analyses of factors involved in the tests. The tabulation of test experience is particularly interesting. Of some 160,000 pressure vessel tests reported, noticeable defects were found by hydrostatic testing in slightly more than 4000, and about 30 failures were found by hammer testing. Of the 4000 or so defective vessels, only 21 were classed as "serious," the others principally involved only pinhole leaks. The 21 serious cases

were reported to be caused by faulty materials, a laminated head plate, and dissimilar metal welds joining materials of different thicknesses; eight involved cracks in welds or adjoining base metal. Shank[9] and others have reported a few brittle failures that occurred upon hydrostatic or pneumatic testing, some of which were probably included in the PVRC survey.[7] The summary of the PVRC report[8] indicates that enough leaks and fabrication difficulties were uncovered during hydrostatic testing to warrant its continuation as an inspection method.

The PVRC report, while considering the hydrostatic test primarily as an inspection method, recognized its possible beneficial effect as a means of peak-stress relief. Some of the contributors to the report described the improvements in probable vessel performance with remarkable clarity when it is considered that they did not have access to much of the fracture literature available today.

Several other publications have described actual studies of mechanical stress relief and the use of overpressure tests to improve and verify vessel properties, performance, and safety. A paper by Cecil[10] concerns the "reshaping" of the vessels at nozzles, openings, attachments, and other discontinuities and the resultant stress relief and improvement in fatigue behavior. A 1957 patent granted to McCutcheon[11] relates to one type of mechanical stress relief. A 1947 patent granted to Kennedy[12] covers a type of low-temperature selectively applied thermal stress relief, and Greene and Holzbauer[13] extended the work on the Kennedy concept in a 1946 paper on controlled low-temperature stress relief. Significant information is also contained in articles originating in Japan,[14,15] Sweden,[16] Great Britain,[17] and the United States.[18,19] Unpublished reports and correspondence within competent committees indicate a recognition of the importance of the hydrostatic test conducted above the ductile-to-brittle transition temperature and at a significant stress level in accomplishing mechanical relief of residual stresses by causing plastic yielding at the tips of small cracks or flaws.

Wallin of the Swedish Power Board reviewed the available literature in 1951 and offered the following summary:[16]

> Thermal and mechanical stress relieving appear to be equally effective in reducing residual stresses, to judge from experimental results, and that conclusion is also supported by theoretical considerations. Code rules, however, prescribe both thermal stress relieving and hydrostatic proof testing for first class pressure vessels, and both operations have other benefits besides residual stress relieving. Thermal stress relieving restores ductility after fabrication and aging, and proof testing causes local yielding thereby reducing stress peaks at notches, cracks or other initiating defects. Some test results further suggest brittle fracture initiation to become more difficult after yielding in the crack root during preloading. After mechanical stress relieving by hydrostatic proof testing the applied load appears to have to exceed the proof stress in order to initiate a brittle fracture. Consequently there would be no risk for brittle fracture initiation in proof tested pressure vessels as long as the design pressure is not exceeded and new stress systems are not introduced. As a matter of fact, the hydrostatic proof testing is the most hazardous event for the pressure vessel from the brittle fracture point of view, which is also supported by service records. Hydrostatic proof testing should then preferably be done at a temperature above the brittle-to-ductile transition temperature.

Contributions in these areas are also made by Pellini and Puzak in the following quotation:[18]

> It has been proposed that safe performance to temperature below the NDT may be assured in the absence of thermal stress relief by the application of "hot" pretests, that is, by loading at temperature near or above the CAT curve. Depending on the transition temperature of the steel this "hot" pretest could be cold by atmospheric temperature standards. The intent of "hot" pretests is to cause the small flaws to yield at the flaw tip, thereby resulting in a local relief of residual stresses and blunting of the crack tips. This procedure effectively places the residual stress level acting on the flaws to some low level which requires the presence of relatively large flaws for fracture initiation. The method has been shown to be effective experimentally. It is particularly applicable to pressure vessels because of the invariant direction of loading. It is not applicable to structures which might involve a spectrum of service load directions which cannot be reproduced in "hot" pretests.

As previously discussed in Section 6.3.2.2, investigators in the UKAEA have issued several publications in the past few years in which they suggest a hot (at or above anticipated operating temperature) overpressure test as a means of precluding rupture of a vessel at lower temperatures and pressures. These suggestions have evolved partly from an

extensive series of tests to rupture of deliberately flawed vessels, most of which were 5 ft in diameter by 15 ft long, with 1-in.-thick walls. The tests were conducted hydrostatically and by hydrostatic plus partially pneumatic pressurization. Details of the tests are contained in a number of UKAEA reports and articles in journals in Great Britain[20] and the United States. Based on analyses of the results of these and other tests, Nichols[21,22] and Irvine[23] have suggested several potential applications of the basic concept that hot overstressing gives additional protection against subsequent failure, even under conditions where failure would otherwise be expected. These investigators and their associates state[24] "that once a structure containing a notchlike defect has withstood a certain stress level at a given temperature, then fracture will not occur on stressing at a lower temperature unless the initial stress level is exceeded." According to their proposals if f_{op} and f_t represent the operational and test stresses, l_{op} and l_t are the critical crack lengths at the two stress levels, and the material properties are constant,

$$f_{op}^3 l_{op}^2 = f_t^3 l_t^2 .$$

It follows that if a vessel withstands an overpressure test to stress level f_t, where f_t is greater than f_{op}, the vessel contains no defect longer than l_t, which is something less than l_{op}. This hot prestressing technique was tried in the initial testing of the Dragon vessel at 400 psia and 340°C (294 psia and 350°C design) and the Windscale AGR vessel at 286 psig and 265°C (300 psig and 340°C design). It is not clear that these test conditions met all the requirements for "hot prestressing," perhaps because of difficulties in attaining the desired pressures and temperatures under nonoperating conditions. The UKAEA authors recommend that the test be made at operating temperature to eliminate influence of variations in material properties, but they state that it can be done at lower temperatures if suitable compensation is made for the changes in material properties.[25,26] The suggested overpressure is of the order of safety-valve settings. The possible application of the hot overpressure testing to the periodic retesting of reactor vessels and certain

possibly limiting considerations are discussed further in Section 10.2.2 below.

A comprehensive review and survey of overstressing techniques was recently prepared by Nichols of the United Kingdom Atomic Energy Authority for the 1967 meeting of the International Institute of Welding.[27]

10.2 POSTOPERATION TESTING

10.2.1 Material Surveillance

Sections II, Material Specifications, and III, Nuclear Vessels, of the ASME Code specify basic material requirements for nuclear pressure vessels. The purchasers and fabricators of vessels generally specify additional requirements for reasons of economy, radiation effects surveillance, information and, to some extent, safety. While the Code does not cover "deterioration which may occur in service as a result of radiation effects..." (Section III, paragraph N-110), it does state that "these effects shall be taken into account with a view to obtaining the design or the specified life of the vessel." To supplement current available data on irradiated properties the Code further states, in N-110,

> It is recommended that the increase in the brittle fracture transition temperature due to neutron irradiation be checked periodically by means of surveillance specimens of the same material which receive approximately the same neutron flux as the vessel wall at about the same temperature and neutron energy spectrum. The combined effects of fabrication, stress, and integrated neutron flux should be considered.

Recommendations for such surveillance tests are contained in the ASTM E 185, Recommended Practice for Surveillance Tests on Structural Materials in Nuclear Reactors. This recommended practice is "for the purpose of monitoring and evaluating, at periodic intervals, the radiation-induced changes occurring in the mechanical properties of the pressure vessel and internal structural components of nuclear power reactors." A secondary purpose is the gathering of data that may assist in the accurate prediction of radiation effects and, hopefully, may make possible the elimination of surveillance programs for most nuclear

reactors. This secondary purpose is expressed in paragraph 2b of ASTM E 185, which states:

> Surveillance tests can aid in the interpretation of radiation effects research programs. Suggestions, therefore, are presented for reference specimens and temperature and radiation monitoring which should be included in such programs where practical. Surveillance programs could provide an excellent opportunity to compare the effect of flux spectrum on engineering materials.

The primary purpose of the ASTM recommended practice and the intent of the Code, Section III, paragraph N-110, are served when test specimens typical of the fabricated component (pressure vessel) are irradiated in the reactor under conditions that closely duplicate the irradiation conditions experienced by the component being monitored. Test specimens are considered "typical" if they are taken from a portion of the material used in the fabrication of the vessel and receive the same thermal history (heat treatments and stress-relieving treatments) as the material in the component. Duplication of irradiation conditions (neutron flux, neutron spectrum, and temperature history) for pressure vessel surveillance is usually achieved by placing the test specimens, in a protective container, between the thermal-neutron shield and the inner wall of the pressure vessel in the region of highest neutron flux incident on the pressure vessel.

The test specimens recommended in ASTM E 185 are tension and Charpy-V-notch impact specimens. Almost all surveillance programs utilize both types of specimen. One very early program used subsize Izod impact specimens; however, the reactor was not a commercial power reactor, and Charpy-V-notch specimens were installed at a later date. Specimens for several recently established programs include, in addition to tensile and Charpy V-notch impact specimens, fracture mechanics specimens of the wedge-opening loading (WOL) type, and fatigue specimens are being irradiated in two reactors.

The secondary purpose of surveillance programs is served in many reactors by the inclusion of transmutation-type flux monitors and "correlation monitors" (mechanical test specimens from a standard reference steel), as specified in ASTM E 184-62, Recommended Practice for Effects

of High-Energy Radiation on the Mechanical Properties of Metallic Materials. The neutron spectrum is calculated or experimentally determined, and irradiation temperatures are recorded.

A summary of pressure vessel surveillance programs for commercial power reactors is given in Table 10.1. A number of the reactors listed were either in operation or under construction before ASTM E 185 and Section III of the Code were adopted, and surveillance programs for some of these reactors are not as complete as for later reactors. Most of the programs meet the majority of the suggestions of E 185. In fact, individuals associated with these reactor surveillance programs were active in the writing of the ASTM recommended practice. The experience gained in implementing the first surveillance programs helped in the planning and execution of such programs in the later reactors. No surveillance specimens were included in Indian Point I, specimens were installed in Yankee-Rowe after Core I, and a surveillance program was included in Elk River after construction was under way. Several of the surveillance capsules in Yankee-Rowe broke away from their attachments due to the turbulent coolant flow but were later recovered. In the program for Elk River none of the original pressure vessel material was available, and specimens were prepared from steel of the same chemical composition. Several heat treatments were used to bracket the heat treatment of the pressure vessel. In the Elk River design the pressure vessel wall was not accessible for the mounting of surveillance specimens, and all capsules were of necessity located nearer the reactor core.

Present pressure vessel surveillance practice is typified by the Westinghouse Atomic Power Division and General Electric Atomic Power Equipment Division programs. Contract specifications for fabrication of the pressure vessels provide for the removal of material from plates or forgings used for the portion of the vessel at the core midplane or from plate from the same heat. The heat treatment of the surveillance material duplicates the heat treatment of the pressure vessel material, including the postweld heat-treatment cycles of that region. The surveillance material may be heat treated as a portion of the pressure vessel plate or may be heat treated separately. In either case, surveillance specimens are taken at least one plate thickness away from a

Table 10.1. Summary of Pressure Vessel Materials Surveillance Programs in Light-Water-Moderated Reactors

Reactor Name	Pressure Vessel Material	Integrated Flux (E > 1 Mev) Over Reactor Life at Belt Line (neutrons/cm^2)	Origin of Surveillance Material[a]	Near-Core Region Specimens		Specimens at Pressure Vessel Wall		Thermal Control Specimens		Remarks
				Tensile	Charpy	Tensile	Charpy	Tensile	Charpy	
Shippingport	A 302 grade B	6×10^{19}	(b)	(b)	(b)	(b)	(b)	(b)	(b)	
Dresden I	A 302 grade B	9.2×10^{18}	V, W, HAZ (1 heat),[c] and GE Ref.	26	246	42	234	18	116	Additional structural materials are being irradiated
Yankee-Rowe	A 302 grade B	7.6×10^{18}	V (1 heat) and Ref.	16	56 and 24[d]	4	36 and 8[d]			Surveillance specimens installed after operation of Core I
Saxton	A 212 grade B[e]	9.5×10^{18}	V (1 heat) and Ref.			40	192[f]			
Indian Point I	A 212 grade B	7.6×10^{18}	No surveillance program							
Big Rock Point	A 302 grade B		V, W, HAZ (3 plates) and GE Ref.	22 and 2[d]	96 and 12[d]	30 and 4[d]	135 and 21[d]	47 and 4[d]	195 and 21[d]	
Elk River	A 302 grade B	2.3×10^{19}	(g) and Ref.	132	280					156 fatigue specimens included
Humboldt Bay	A 302 grade B	$<1 \times 10^{19}$	V, W, HAZ (3 plates) and Ref.	22 and 2[d]	96 and 12[d]	30 and 4[d]	135 and 21[d]	47 and 4[d]	195 and 21[d]	
BONUS	A 212 grade B	1.65×10^{18}	V, W, HAZ				60			Fatigue specimens included
Pathfinder	A 212 grade B	2.0×10^{18}	V and Ref.	28	80	14	40			
LaCrosse	A 302 grade B	9.6×10^{18}	V and Ref.	120	440 and 120[d]					
San Onofre	A 302 grade B		V (3 plates), W, HAZ (1 plate) and Ref.			40	192			48 WOL fracture mechanics specimens included
Connecticut Yankee	A 302 grade B		V (3 plates), W, HAZ (1 plate) and Ref.			40	192			48 WOL fracture mechanics specimens included
Oyster Creek I	A 302 grade B	$<1 \times 10^{19}$	(h)			(h)	(h)			
Nine-Mile Point	A 302 grade B	3×10^{18}	(h)			(h)	(h)			
Dresden 2	A 302 grade B	1×10^{17}	(h)			(h)	(h)			
Millstone Point	A 302 grade B	4×10^{17}	(h)			(h)	(h)			
Brookwood	A 302 grade B		V (2 forgings), W, HAZ (1 forging) and Ref.			54	288			54 WOL fracture mechanics specimens included
Indian Point 2	A 533 grade B		V (3 plates), W, HAZ (1 plate) and Ref.			27	256			42 WOL fracture mechanics specimens included
Palisades I	A 302 grade B, modified[j]	$<1.5 \times 10^{19}$	V, W, HAZ	(i)	(i)	(i)	(i)	(i)	(i)	
Turkey Point 3	A 508II[k]		V (2 forgings, W, HAZ (1 forging) and Ref.			27	256			42 WOL fracture mechanics specimens included
Brown's Ferry I and II	A 302 grade B, modified	$<5 \times 10^{17}$	(h)			(h)	(h)			
Dresden 3		1×10^{17}	(h)			(h)	(h)			
Boston Edison			(h)			(h)	(h)			
Quad-Cities I and II		2.5×10^{17}	(h)			(h)	(h)			
Monticello NGP			(h)			(h)	(h)			
Turkey Point 4	A 508II[k]		V (2 forgings), W, HAZ (1 forging) and Ref.			27	256			42 WOL fracture mechanics specimens included
Hartsville	A 533 grade B		(i)			(i)	(i)			
Point Beach	A 533 grade B		V (2 plates), W, HAZ (1 plate) and Ref.			54	288			54 WOL fracture mechanics specimens included
Duke Power Company I and II	A 302 grade B, modified	3×10^{19}	(b)	(b)	(b)	(b)	(b)	(b)	(b)	

[a] V = pressure vessel base plate; W = weld pressure vessel plate; HAZ = heat-affected zone in weldment; Ref. = ASTM reference plate specimen; GE Ref. = GE-APED standard material from Humboldt Bay material.

[b] Information not available.

[c] Weld and HAZ specimens were added in late 1962.

[d] Number of reference steel specimens in parentheses.

[e] Multilayer pressure vessel.

[f] Subsize specimens from multilayer vessel material.

[g] Steel of composition similar to that of pressure vessel.

[h] Anticipated program may be as described in text.

[i] Program not firm or no present decision.

[j] Nickel content of 0.4 to 0.7% (same as A 533 grade B).

[k] Forgings.

quenched and tempered edge. Weld metal and heat-affected-zone samples are obtained from a test weld representing a vessel welded joint fabricated from vessel base material. This test weldment is heat treated to duplicate the heat treatment of the vessel weldment. Tensile and Charpy V-notch impact test specimens are prepared from these materials and encapsulated to prevent corrosion of the specimens in the reactor. The location and orientation of the specimens in the plate, forging, or weldment are completely specified. Base-metal specimens are taken from the quarter thickness location.

In Westinghouse reactors either two or three core-region plates are represented in each reactor surveillance program, depending on the size of the reactor vessel. For vessels larger than 142 in. ID, eight capsules are placed at the pressure vessel wall at the core midplane. Five of these capsules contain eight Charpy, one tensile, and two WOL specimens of base metal from the three plates and eight Charpy specimens of ASTM reference steel. Three capsules contain eight Charpy, two tensile, and two WOL specimens from base metal of one of the core-region plates and weld metal and eight Charpy specimens from weld-heat-affected zone metal and ASTM reference steel. When two forgings are used a larger number of each specimen type for each forging is contained within the capsules. Each capsule for the vessel represented by three core-region plates also contains temperature monitors (melting-point alloys) and thermal- and fast-neutron monitors (iron, copper, and cobalt with and without cadmium shields). In addition, three of the capsules contain neutron monitors of nickel, ^{238}U, and ^{237}Np. One capsule is removed after each of several periods of reactor operation. The schedule calls for removal of capsules after 1 1/2, 3, 5, 10, and 20 years of operation, and three capsules are reserved for removal as determined by the need for the data.

For vessels less than 142 in. ID, six capsules are placed at the pressure vessel wall at the core midplane. Three of these capsules contain ten Charpy, three tensile, and three WOL specimens of base metal from the two plates or forgings and weld metal and ten and eight Charpy specimens from weld-heat-affected zone metal and ASTM reference steel, respectively. The other three capsules contain twelve Charpy, three tensile, and three WOL specimens of base metal from the two plates

or forgings and weld metal and twelve Charpy specimens from weld-heat-affected zone metal. Each capsule for the two core-region plates or forging vessel also contains temperature monitors and thermal- and fast-neutron monitors. One capsule is removed after each of several periods of reactor operation. The schedule calls for removal of capsules after 2, 5, 10, and 20 years of operation, and two capsules are reserved for removal as determined by the need for the data.

In the case of Yankee-Rowe, in addition to surveillance specimens outside the thermal shield, capsules were located near the core region. The results from these accelerated dose positions gave preliminary data about the effects of lifetime exposure.

In General Electric programs two or three core-region plates are represented in each reactor surveillance program. Twenty-three capsules are placed at the pressure vessel wall at the core midplane. Each of nine of these capsules contains 12 Charpy specimens of base, weld, or heat-affected-zone metal from a pressure vessel heat and one capsule contains 12 Charpy specimens of GE-APED standard steel (for comparison of data from several reactors). Thirteen of the capsules contain two tensile specimens of the same materials. Temperature and neutron monitors are included in each capsule. In reactors with predicted pressure vessel integrated neutron fluxes approaching 1×10^{19} neutrons/cm^2 in 40 years, groups of capsules are scheduled for removal after 2, 8, and 32 years of reactor operation. If the predicted integrated neutron flux is about 4×10^{17} neutrons/cm^2 in 40 years, capsules are removed when the need arises. The Dresden 1, Humboldt Bay, and Big Rock Point plants also had capsules located near the core for obtaining early information on the irradiation behavior of the vessel material. These capsules were removed after about one year of full-power operation.

Testing of all surveillance specimens is carefully supervised, and all possible information is obtained, since the number of specimens is limited. Each specimen represents an investment of many hours and dollars, and the results may greatly influence the future operation of the reactor.

The data developed in pressure vessel surveillance programs are used to judge changes in operating techniques for the reactor or to provide assurance the vessel material condition is satisfactory. Such judgments

are presently based on the "transition temperature concept" as presented in the fracture analysis diagram discussed in Section 6.2.2.7 of this report.

10.2.2 Hydrostatic Retest

Periodic reinspection is performed on nonnuclear components such as boilers, pressure vessels, compressed gas cylinders, and pressure piping as may be required by operating procedures, insurance companies, or regulations of states, municipalities, or other government regulatory agencies.[28] In some (not all) cases, these may include a requirement for a hydrostatic (or pneumatic) overpressure test, particularly if the vessel contains a suspected flaw or has been subjected to extensive repairs. The retest, when performed, is often the same as that originally required by the Code to which the component was initially built.

To date nuclear reactor vessels have not required such repeated pressure tests on shutdown after a period of service. UKAEA workers[21,23,26] have, however, suggested the possibility of using a periodic hot overpressure test, similar to that described in Section 10.1 above, as a routine requirement to establish (1) the maximum size defect the vessel can contain and (2) the prescribed conditions for continued safe operation. While the referenced UKAEA authors suggest the periodic repeated use of the hot overpressure test, there is no indication that this has yet been actually incorporated into the operating schedule for any reactor vessel. Before establishing the repeated postoperational overpressure test as an actual requirement, it appears that the British workers plan an expanded experimental program to resolve a considerable number of uncertainties. Some of the problems include (1) determining the preferred testing temperatures, with the NDT temperature and possible reduction in strength of the vessel material at higher temperatures taken into account, (2) changes in brittle-fracture characteristics with prolonged irradiation, (3) fatigue-induced crack growth, (4) other metallurgical changes that may develop from long-time exposure to an operating environment, and (5) the ability to establish desired test conditions in a system not actually operating.

The current British program[26] is designed to develop ways to estimate quantitatively the length to which cracks can propagate between proof tests, since, if the operating conditions will not cause defects shorter than l_t (see Sect. 10.1.2) to grow to l_{op}, the proponents contend they will have a completely safe situation between tests and that any risk of failure will then be transferred from the operational period to the proof test. They appear prepared to accept this risk on the basis that more effective precautions can be taken against the consequences of failure during the test than during operation, but this unpleasant possibility can hardly be considered a comforting alternative. They also propose[26] that the emphasis in neutron radiation effects studies be directed toward tensile properties and Charpy V-notch energy absorption at temperatures appropriate to reactor operation, in preference to the presently emphasized efforts to determine shifts in transition temperatures.

Periodic hot overpressure testing of U.S. water-cooled reactors has interesting possibilities as a means of lessening the existing uncertainties in determining or estimating the maximum size of the actual defects in highly stressed areas of vessels that have operated for a period of time. However, the pressures and stored energy of the pressurizing media in light-water reactors will be several-fold greater than in gas-cooled reactors of the type considered by the British. If serious consideration is to be given to this type of testing, it will be well to investigate the possibilities of using a higher boiling-point liquid or filling most of the vessel volume with a solid during testing to reduce the volume of compressible fluid required, even though such could increase the complexity, cost, and practicality of making the test.

Pellini[29] has sounded a note of caution in the matter of accepting hot proof stressing as assurance of structural adequacy and safety against failure in continuing service. He calls attention to some British tests in which a 3-in. notched steel bar was loaded to develop a plastic zone at the notch root and then aged at 400 to 500°F. The result was that the nil deformation temperature was raised by some 50 to 60°F.

He also mentions the failure of a large thick-walled (about 6 in.) pressure vessel on a third (preservice) hydrotest at a pressure well

below that of the first two hydrotests. He emphasizes that aging the plastically deformed region at the notch border zone may embrittle it and that service at elevated temperatures may still further accentuate aging embrittlement of the material just ahead of the notch root. This may not occur with all materials under all conditions, but he points out that it is a function of the strain developed, the type of steel, and the aging temperature and time and that there is no practical way of assessing the degree of local damage or defining the specific properties of the crack border material after such changes in a proof-stressed vessel. He suggests that tests conducted on a specific material in advance of use might indicate whether such sensitivity is involved and the relative degree; that is, it might determine whether the steel is a problem steel or not. If it thus developed that it was a problem steel, it would be difficult to assess the degree of local damage in practice.

He suggests that these factors indicate that the proof tests should be conducted at a minimum of overload compared with the service loads. He notes that the danger exists for subsequent service at temperatures below that of the dynamic-fracture-toughness transition. Since the NDT temperature is the temperature of rapid increase in dynamic-fracture toughness for the conditions expressed in the Pellini-Puzak fracture analysis diagram,[19] the situation remains safe if the service temperature is restricted to the NDT temperature plus 60°F or higher, which builds in the reserve protection required to offset the crack-lip damage condition.

Operators of large U.S. water-cooled reactors are understandably reluctant to adopt the hot overpressure test as a method for periodic retesting of vessels. Nevertheless, the method offers enough potential promise (as well as potential shortcomings, as noted above) to warrant a thorough study of the possibilities of the method and of its as yet incompletely resolved problems.

10.2.3 Nondestructive Examination

It is common practice to nondestructively examine nonnuclear thick-walled pressure vessels at intervals during shutdown for maintenance.

These examinations have been primarily visual, with possible enhancement with such aids as penetrants or optical systems. With an increasing number of nuclear pressure vessels being constructed and used, much of the nonnuclear pressure vessel examination philosophy has been carried over, and there is heavy dependence at the present on visual examination. However, because of inherent difference between the two types of vessel, a reevaluation of the philosophy has begun by many who are associated with the nuclear reactor industry. The differences include the reduced opportunity for examination. This is due to several factors: (1) infrequent intervals at which examination can be made, usually only at time of core change for region around the core, although such areas as the flange and certain nozzles may be inspected during any shutdown period (this may be compared with nonnuclear shutdowns for maintenance and repairs), (2) presence of insulation, thermal shields, and other components that cover large portions of the vessel wall and prevent visual examination of critical areas, and (3) presence of intense background radiation, which limits human access and restricts the visual techniques that can be applied. Other points of concern that are different for nonnuclear vessels (as discussed in more detail in other sections of this report) are the degradation of the mechanical properties of the pressure vessel steels due to prolonged exposure to the neutron flux and the consequences of a rapid failure of the pressure vessel with the associated release of radioactive materials. As discussed in Chapter 8, the pressure vessels are examined by nondestructive means during fabrication to assure that harmful discontinuities are not present in the vessel. However, because of limitations in method capabilities or because of imposed limits in sensitivity on the defined rejection level, discontinuities will be present in the vessel as operated. Consideration is being given to the possibility that the discontinuity may grow or propagate to a hazardous size when coupled with the reduced ductility of the irradiated material.

Discussions are presented in the following sections on current practice in the evaluation of operating nuclear reactor pressure vessels, nondestructive testing operations that have been performed on nonoperating pressure vessels or similar configurations and are amenable to remote operation, and methods being considered by some for potential application.

Remotely performed examinations offer the best possibility for application during operation and for use as monitoring systems.

10.2.3.1 Present Practice

Several reactor operators were contacted to determine current practice for the nondestructive examination of nuclear pressure vessels. Although the survey was not exhaustive, the similarity of response indicated that essentially the same available methods are considered by all to be applicable and necessary. In all cases the emphasis is on visual inspection. In limited cases dye-penetrant inspection of a portion of the cladding within the vessel has been performed. In most cases some optical aid, such as replication, borescopes, periscopes, or television cameras, is employed where direct viewing is not possible.

As a specific case, at each refueling of the Yankee reactor vessel,[30] there has been visual inspection of the vessel head and dye-penetrant inspection of areas of cladding under the vessel head. No defects have been found. Because of radioactivity, it has been necessary to flood the vessel with water up to the flange area. This has restricted examination of the flooded region to visual methods. Examination by borescope has detected the presence of small worn areas in the cladding on the bottom head, and replication with silicone rubber has shown the depth of wear to be 0.115 in.[31] Photography with a stereoscopic camera and use of a periscope have found application for gross examination of limited areas of the vessel wall. Indirectly related examinations have also been made on the pressurizer. The cladding on the inner surface was applied in similar fashion to that in the pressure vessel. Dye-penetrant examination has detected cracks in the stitch cladding, and repeated examinations are planned to determine possible changes. The cracks could not be seen with the naked eye or with a borescope.

A similar evaluation was made of the Indian Point reactor of Consolidated Edison.[32] With the reactor vessel empty except for the lower grid plate and core shroud, the water level was lowered to 15 in. below the closure flange. All the exposed cladding was visually examined. In addition, two areas of exposed cladding were selected at random, and a dye-penetrant examination was performed. Also, with the aid of a borescope,

a portion of the cladding below the lower grid plate was examined. No defects were revealed by any of these examinations. In addition to these examinations on the pressure vessel, two inspections of the core shroud were performed with binoculars and closed-circuit television cameras. Both spot welded and weld-overlay cladding were inspected by both visual and dye-penetrant methods with no defects being detected. Boat samples were removed and grinding was performed. No crack in the cladding was found to have propagated into the base metal.

The Dresden reactor likewise was examined during refueling outages.[33] A number of items, including the pressure vessel, were examined visually. The reactor vessel head was visually inspected on top and under sides and at bolt holes, penetrations, and flange surfaces, with no harmful defects being discovered. The reactor vessel flange, grooves, and bolt holes appeared to be free of defects, but the studs on the nine instrument flanges were suspected of being defective. Nineteen studs from the reactor vessel were ultrasonically tested and accepted. Many of the welds in piping and accessory equipment were visually examined after removing insulation. Concrete shield blocks were removed to provide access to the reactor inlet nozzle.

Although not currently an operating reactor, the results of post-operation examination of the Experimental Boiling Water Reactor (EBWR) are pertinent to this discussion.[34] The upper half of the interior of the vessel was accessible for visual and dye-penetrant examinations. Cracks were detected in the cladding, and some of these completely penetrated the cladding, as confirmed by a gas-leak test. Investigations indicated that the cracks originated with the cladding process and had existed throughout the operation of the reactor. To further explore the cladding cracks, portions of the cladding were ground away and boat samples were removed from the reactor vessel. No evidence was found of crack propagation from the cladding into the A 212 grade B carbon steel, although some microcracks up to 0.008 in. deep were found in the carbon steel. These were shown to have existed prior to cladding application. The most severe cracking of the cladding was found in the steam zone, with progressively less cracking below the water line. Although portions of the cladding were removed during the investigation, operation of the

vessel is to continue without cladding repair. After the vessel is reactivated, it will be reexamined at six-month intervals to monitor changes in cracking and corrosion. In addition to the visual and penetrant inspection of the cladding, other examinations included ultrasonic examination of the conical ring forging and ultrasonic and magnetic-particle examination of the closure bolt studs and the vessel cover plate.

From these case histories, it is obvious that visual inspection, enhanced by optical aids and dye penetrants within the accessible areas of the vessel interior, constitute the major portion of current practice in pressure vessel examination after operation. Since these tests are sensitive only to discontinuities open to the accessible surface, if it is considered plausible for the generation and/or propagation of harmful defects to occur in other areas of the pressure vessel, consideration should be given to the possibility and practicality of supplementary examination methods to detect such undesirable conditions. Several utilities are currently considering use of some additional methods of recurring examination. To this end feasibility studies are being conducted to determine the optimum approach.

10.2.3.2 Possible Postoperation Examination Methods

There are a number of possible approaches for pressure vessel examination that have been suggested or proposed by various proponents and advocates of testing technology. Many of these have, in some form, been applied to large vessels or similar configurations. Others are still in various stages of development. These candidate examinations may be restricted to application during shutdown periods or, in some instances, may be applicable during actual operation of the reactor and would thus allow continuous or intermittent monitoring of deleterious conditions. Undoubtedly visual examination will continue to play a major role in assuring the integrity of vessels. During design and fabrication stages, provision should be made for access for visual inspection of areas, such as nozzle penetrations, where higher stress concentrations could lead to defect growth. Most of the suggested supplementary methods involve some form of acoustic phenomenon (either sonic or ultrasonic), although radiography and other methods have been considered.

It may be that certain limited portions of the vessel, such as the flange region or nozzle weldments, are sufficiently remote from the reactor core that low-background radiation would allow conventional manual ultrasonic examination. As noted for visual inspection, this would require design to permit the necessary access from the exterior of the vessel. However, if supplementary examinations are deemed necessary, the manual ultrasonic inspection, even if possible, would not cover all areas of concern. Therefore, additional systems must be considered. For convenience in discussion the acoustic systems have been divided into two major categories: (1) those in which mechanical scanning of the acoustic probes is performed and (2) those in which the probes are fixed on the pressure vessel.

Ultrasonic Scanning Systems. There are several examples of past experience with ultrasonic scanning systems applied to reactor systems or other similar configurations that should serve to demonstrate the plausibility of such an approach. However, these cited examples are not intended to convey the thought that all problems are essentially solved. In the following, discussions of several cases that demonstrate past history are followed by brief discussions of some of the problems that must be resolved before an ultrasonic scanning system can be considered truly successful.

The pressure vessel from the PM-2A nuclear power plant operated in Greenland was removed and shipped to the Nuclear Reactor Testing Station (NRTS) in Idaho, where it was nondestructively tested to provide data for a detailed stress analysis associated with brittle-fracture studies.[35] At NRTS the closure head was stripped of insulation and extensively decontaminated. This allowed direct access of personnel to the head. A fluorescent-penetrant examination was performed, and no indications greater than established standards were detected. On the flange, one linear defect and several indications similar to weld porosity were located. An ultrasonic examination was also performed with contact shear-wave techniques. The reactor vessel was also examined by both liquid-penetrant inspection and ultrasonics. The penetrant inspection was performed remotely with the examiner located near the vessel opening behind

a personnel shield containing a viewing window. No surface discontinuities greater than the established standards were detected.

An ultrasonic scanning unit was designed and fabricated to allow immersed examination from the interior of the vessel. The unit rotated about a central shaft that swept the ultrasonic transducers 360° in a plane perpendicular to the vessel axis. Longitudinal positioning of the transducers parallel to the vessel axis was in 1/4-in. increments, and an adjustable transducer holder allowed radial movement to change the distance between the transducer and the vessel wall. Scanning could be accomplished on the cylindrical portions of the vessel, the flange, and the bottom head. An additional fixture was built to examine the primary nozzles. Both longitudinal- and angle-beam techniques were used, depending on the configuration of the section being examined. No discontinuity with an equivalent reflecting area greater than that from a 1/8-in.-diam flat-bottomed hole (FBH) was detected in the wrought metal or deposited cladding. For the heavy weld-metal deposit, the reference standard was relaxed to a 1/4-in.-diam FBH because of higher noise levels. No equivalent indications were detected. Test results and interpretations were based primarily on direct observation of the cathode-ray tube of the ultrasonic instrument.

These devices were somewhat similar in principle, although with different application, to the many devices developed for the remote maintenance and inspection of the Homogeneous Reactor Test core vessel and accessory items.[36-39] One of the devices was designed and fabricated to allow ultrasonic measurement of the wall thickness of the core vessel,[40] and such measurements were made several times at shutdowns for maintenance or other reasons.

One phase of the work performed by Southwest Research Institute (SWRI) to evaluate the serviceability of the Elk River Reactor pressure vessel[41] was directed toward the development of remote nondestructive testing equipment and techniques for detecting and monitoring gross defects in critical areas. Emphasis was placed on the 8-, 10-, and 16-in. nozzles. Ultrasonic techniques were selected as the most promising,[42] although other techniques were considered. During an "on-site" test with the reactor shut down, a demonstration[43] was made that the ultrasonic

energy could be propagated through the overlay cladding surfaces on both the pressure vessel and its closure head. Prototype mechanisms[44] were fabricated that contained several transducers for introducing the ultrasound into the zones of the nozzle weldments at different angles. The mechanism was designed to fit snugly and concentrically in the nozzle to maintain proper alignment of the sound beam, but when the system was tested it was found that the nozzle examined was not perfectly circular, so complete inspection could not be performed.[45]

Each of these case histories shows some of the capabilities and the potential of the ultrasonic method as a scanning system for the evaluation of pressure vessels. Considerable development effort would be required before an operating system could be applied in a standard test for postoperation examination. Some of the problems that must be overcome are listed below.

1. Quantitative determination is needed of the effect on ultrasonic penetration and propagation of the austenitic stainless steel weld overlay cladding. This includes the effects of the attenuation of the cladding, the acoustic mismatch at the carbon steel—cladding interface, and the irregular surface of the weld-deposited cladding. The extent of surface preparation required must be fixed and may vary from one cladding technique to another.

2. A method of assuring consistent angles of incidence of the introduced sound beams is required.

3. Complex scanning requirements around nozzles due to joint configurations must be accommodated. This is especially important because of higher stress levels in these areas.

4. Will it be necessary to remove some of the internal components to allow scanning of the areas of most concern? This question is based on the supposition that the optimum scanning will be from the interior of the vessel. The possibility should not be overlooked that the optimum scanning could be from the outside of the vessel. This would require the capability of temporarily removing external insulation and shielding.

5. A method for establishing bench marks for orientation and reproducing scans at successive inspections is needed.

6. A method of producing continuous records that can be maintained and compared with previous inspection records is required. This method would be coordinated closely with the method referred to in item 5 and both methods would be most useful with an automated system and with less dependence on operator interpretation and recording.

7. Assurance is needed that ultrasonic techniques are adequate and sufficiently sensitive to detect and properly interpret flaws of concern at all suspected orientations in the thick pressure vessel sections being used or planned.

Fixed-Probe Sonic Systems. An alternative to the use of ultrasonic scanning systems is the use of probes that are fixed at key positions at which they can monitor areas of concern. The probes can be of the active or passive variety. By active it is meant that the probe or probes initiate the sonic energy, as well as detect it, after it has undergone a change from being transmitted into and through the specimen. On the other hand, a passive system does not generate the sonic energy but detects that which may be caused by other conditions. Neither type has been used on a nuclear reactor vessel, but each has been applied to other test problems and in this way has shown a possibility for nuclear pressure vessel examination.

Active systems have been used in several instances in which ultrasonic transducers have been applied directly to fatigue specimens, intermittently or continuously, to detect and measure crack growth by the increased intensity of the reflected ultrasonic energy. One such examination[46] was conducted on longitudinal weld seam sections taken from 18-in. pipe that contained various known defects. Ultrasonic examination of the specimens during tests to failure showed an increase in flaw indication upon cycling at high stresses. Large changes generally occurred within the last 10 to 20% of specimen life. At lower stresses the signal growth was discontinuous. The ultrasound was introduced by 45° shear-wave transducers by using the contact method at intervals during the fatigue testing. In instances "where the point of impending failure could be identified," ultrasonic monitoring was continuous.[46]

Similar work has been reported by personnel at SWRI on pressure vessels which were being subjected at their laboratory to low-cycle plastic

fatigue conditions.[47] Experiences with ultrasonics and other test methods applied to a variety of pressure vessels being tested on various research contracts are discussed in the referenced report.[47] In general the application of the ultrasonic transducers was similar for all the tests. Prior to the cycling tests the welds and zones of high stress were examined by conventional ultrasonic pulse-echo techniques and radiography to disclose the presence of possible discontinuities. These examinations were repeated at intervals after a number of cycles. When there was crack initiation or defect propagation, as evidenced by increased test indication, ultrasonic transducers were affixed to the pressure vessel surface to allow monitoring of the crack growth by pulse-echo techniques during subsequent cycling. This frequently allowed continuous monitoring of the crack growth until it produced failure. However, in some instances failure did not occur at the area being monitored.

Another test system that has been suggested as having potential application in the use of fixed ultrasonic probes is one that has had limited application to the inspection of large pipe.[48,49] More recently a system was assembled for the evaluation of welds in rocket-motor cases. Since some of the principles of operation differ from the more common ultrasonic techniques, a few of the details will be noted here. This system uses multiple transducers or "wave directors" attached directly to the test specimen. The wave directors are designed to allow continuous motorized adjustment of the angle with which the sound beam is introduced into the specimen. Coupling can be accomplished through soft metallic shims, such as lead. The thickness of the specimen has an effect on the frequency that can be best transmitted because of wave-guide action, and the use of frequency analysis techniques optimizes the transmitter-receiver efficiency. If the sound beam (or beams) being transmitted into the specimen encounters a reflecting discontinuity, a portion of the energy may be reflected to one or more of the receivers. By proper analysis of the time-of-flight, signal intensity, and other factors, information may be deduced about the size and nature of the discontinuity. With the capability to adjust the angle of both transmitter and receiver wave directors, scanning of the specimen can be accomplished

with beam-intersection techniques, despite the fixed position of the probes.

For both these fixed-probe systems, further development would be required before an operating system could be applied as a standard test. Many of the problems that must be resolved are common to the scanning systems discussed previously. The problems that seem to be pertinent are listed below:

1. The effects on ultrasonic propagation of the weld-overlay cladding and the interface between cladding and carbon steel must be determined. The probes would probably be affixed to the outer surface of the vessel.

2. Methods of establishing bench marks for orientation and reproducing scans at successive inspections are needed. This would be particularly important in the Dickinson system in which sound-beam angles can be adjusted.

3. A method of producing continuous records that can be maintained and compared with those from previous inspections is required. As mentioned earlier, this would be coordinated closely with the previous method (item 2) and both methods would be most useful with an automated system and with less dependence on operator interpretation and recording.

4. Assurance is needed that the ultrasonic techniques are adequate and sufficiently sensitive to detect and properly interpret flaws of concern at all suspected orientations in the thick pressure vessel sections being used or planned.

5. Assurance is needed that the number, spacing, or position of the fixed probes is adequate to detect flaws of concern. This is particularly important around changes of section thickness and various penetrations, such as nozzles.

6. The effect of radiation and other environmental effects on the electrical or mechanical functioning of all components and constituents of the probes must be determined. If service life of the probes is significantly affected, means must be devised for removing the probes during reactor operation and reestablishing the probe position, orientation, coupling, calibration, etc., or the system will not be usable.

7. The effect of radiation damage on the ultrasonic properties of the vessel materials must be determined, since it may influence the propagation of ultrasonic energy.

A considerable effort is being expended on passive systems in various areas, including the phenomenon of acoustic emission, and suggestions have been made that acoustic emission be considered as a potential method for pressure vessel examination. The principle of operation is that metal deformation or crack propagation is accompanied by release of an acoustic stress wave. Since the stress wave propagates through the specimen, detectors may be placed at some distance from the source of the stress wave to detect the energy. Work on this technology has ranged from studies of deformation in single crystals, to crack propagation studies in small specimens, and to monitoring of large components. Some of the early work was accomplished by Schofield of Lessells and Associates, Inc., and some of his reports are referenced.[50-52] The early work was devoted to the study of single crystals and similar materials during deformation without crack formation. The various generated signals detected were attributed to phenomena such as dislocation pinning during slip deformation and the formation of stacking faults and mechanical twins. It is evident from the last reference[52] that Schofield's attention is now being directed toward pressure vessels.

The technique has been applied to the detection of crack propagation in small specimens by several experimentalists both for materials studies and for test method development. The detectors have varied from microphones,[53] to phonograph pickups,[54] and to accelerometers or other piezoelectric devices.[55] Experimental programs are currently in progress at Aerojet General Corporation, Sacramento, California, for various Navy, Air Force, and NASA departments to investigate the acoustic emission phenomenon from several aspects.[55] These include the various mechanisms of crack formation and growth in such materials as HY-80 steel, maraging steels, and titanium. Some of the variables that will be considered include sample heat treatment, loading conditions, effects of specimen surface finish, geometry, etc., and the sample environment. Work is in progress at Battelle Memorial Institute on detection of metal overstress by acoustic emission for pressure-pipe crack monitoring. Much of the

work to date has been directed toward evaluation of type 304-L stainless steel as cracks are formed and propagated along a groove in a double cantilever beam specimen.[56] Emphasis is being placed on development of a system for monitoring and detecting crack initiation and/or growth. Toward this end studies are being made to optimize the sensitivity, frequency response, and directivity of the detector probes.

By having knowledge of the velocity of the acoustic wave and by using multiple detectors, it is possible to use resection or triangulation techniques and to relocate the source of the acoustic energy. This has been investigated with promising results. One of the better-documented experiments was performed during a hydrostatic test of a 260-in.-diam SL-1 solid-rocket motor case.[57] Twenty-four accelerometers were dispersed over the case, which was over 50 ft long. During the hydrotest the accelerometer system indicated eight stress waves, including the wave that occurred at failure at a pressurization that was about 56% of the planned proof pressure. Several of the early waves were believed to be due to mechanical movement at bolt holes and not to deformation or failure processes. At that stage of development, immediate evaluation of the data was not possible. However, when the recordings were analyzed with the aid of a computer, the origin of the stress waves was determined. The accuracy with which the stress origin could be pinpointed was limited by the frequency response of the instrumentation and the accuracy in determining the wave-propagation velocity. The "circle of confusion" was approximately 20 in. in diameter. Failure analysis of the fracture patterns from the ruptured metal determined that the origin of failure was 12 in. from the center of the 20-in.-diam circle that represented the origin of the stress wave received coincident with failure. Two other stress waves (from the latter four of the eight waves), which occurred at lower pressurization levels, were received from the general vicinity of the origin of failure. The tabulated data indicated that these waves originated approximately 10 and 22 in. from the failure origin. Although the amplitude of the signal received at failure is not given in the report, the values of the other signals from the vicinity of the failure were considerably less than those received earlier in the hydrotest.

Additional work on large rocket-motor cases of maraging steel has been conducted to determine the possibility of detecting potential failure by the acoustic emission process and, by recognition of critical conditions, initiating remedial action to prevent destruction.[58] Hydrotests of several motor cases were run to determine the nature and timing of received signals. In some instances intentional discontinuities were introduced to induce failure. When using tensile specimens of the same material, it was demonstrated that unloading the stress just prior to failure (and thus preventing failure) could be accomplished on the basis of interpretation of the acoustic signals received. On a full-size pressure vessel the time to unload the stress might be too long to prevent failure after receipt of a "critical indication."

As with previously discussed systems, further development effort would be required before an acoustic emission system could be considered as standard for postoperation examination of nuclear system pressure vessels. Some of the problems, although common to the other approaches, are listed below:

1. It is necessary to introduce stress to generate deformation or defect propagation which, in turn, may be detected by the passive probe system. For postoperation examination this could be accomplished during hydrostatic testing, which is discussed in some detail in Section 10.2.2.

2. The effect of nozzle and other penetrations on the propagation of the acoustic wave must be determined.

3. Knowledge of the proper number, position, and spacing of probes to assure detection of any stress-wave origin within the vessel is needed.

4. A method of producing continuous records that can be maintained and compared with those of previous inspections is required.

5. The effect of radiation and other environmental effects on the functioning of all components and constituents of the probes must be determined.

6. If service life of the probes is significantly affected, means must be devised for removing the probes during reactor operation and reestablishing the probe position, orientation, coupling, calibration, etc.

7. The effect of radiation damage on the sonic propagation properties of the vessel material at the frequencies of interest must be determined.

8. It is necessary to determine whether all anticipated failure mechanisms in the pressure vessel materials will produce a detectable stress wave; for example, how will stress-corrosion cracking differ from the failure modes and what will be the effect of hydrogen or radiation embrittlement on the generated stress wave?

9. Data processing systems that can provide prompt display and interpretation of data are needed.

10. Improved resolution for locating the origin of signals is needed. Both improved instrumentation and probes, as well as better knowledge of propagation velocities, will be required.

11. Assurance is needed that the system can be applied to large thicknesses without difficulty.

12. It must be demonstrated that adequate discrimination can be made between signals due to defects and those due to noises in or around the vessel.

13. Means are needed for quantitatively relating the signal to the increment of crack growth so that record summation can be used to determine total crack size. If this latter requirement cannot be satisfied, a supplementary means of examination will be needed to investigate areas of significant acoustic emission to determine the total crack size.

Other Flaw-Detection Methods. Although the most promising methods for supplementary examinations seem to be those involving a form of sonic energy, thought should be given to other approaches. For instance, radiography is a standard technique for inspection of the pressure vessel during fabrication and has possibilities for postoperation examination. It has been used successfully to detect fatigue cracks at high strain locations, such as vessel-to-nozzle junctions.[59] The center line of the radiation beam must be aligned within a few degrees of the plane of the crack. Therefore, such a technique would require several radiographs in each critical area to assure coverage. An obvious problem for radiography would be the background radiation, which would expose the film and reduce the possibility of achieving a useful radiograph. However,

some work[59] has been done to determine radiation tolerance levels and to develop techniques for salvaging film that has been severely overexposed by background radiation. A radiograph of a 5-curie ^{60}Co capsule was taken as a demonstration of the capability of radiography. Development of adequate techniques and equipment would include ways to minimize film exposure except to the primary image-forming beam, determination of optimum exposure conditions for such formidable conditions, and development of remote-handling techniques for markers, penetrameters, film holder, etc. Since field erection of pressure vessels is being planned and radiographic equipment would be a necessary part of the fabrication inspection, it is anticipated that similar radiation-generation equipment could be utilized if postoperation radiography were found to be possible and necessary. Of course, this would require that the equipment be compatible with entry into the pressure vessel and that access be provided for film placement on the exterior of the vessel.

Although more difficult to visualize or be specific about at this stage, it is conceivable that advances in other nondestructive testing techniques may generate new and better examination methods. For this reason, continued awareness, coupled with feasibility studies, should be fostered to provide assurance that the best possible test methods will be available for use where needed.

10.2.3.3 Nondestructive Detection of Radiation Damage

The previous sections on postoperation examination have been concerned primarily with detection of flaws and measurement or monitoring of growth. However, as discussed in other sections of this report, a point of concern is the change of the mechanical properties caused by neutron irradiation of the materials of the pressure vessel. At present indirect information is obtained on reactor materials in extensive testing programs to establish tendencies or trends for degradation under irradiation. Also surveillance specimens are placed in the reactor and periodically tested. For the mild steels, which are common for current pressure vessels, these tests have served to determine the change in the value of the nil-ductility transition or ductile-to-brittle transition temperature. At times, however, difficulty has arisen because of loss

of specimens from desired locations.[60] It would be desirable therefore to be able to make in situ measurements on the components to determine the onset and degree of radiation damage. However, at this time there are no methods available for the nondestructive detection of such damage. A limited amount of work has been conducted in this area, but the problems are not yet resolved. One of the earlier programs was directed toward measuring the shift in the NDT temperature in reactor-grade steels by using methods such as electrical resistivity, the magnetoabsorption Barkhausen effect, through-transmission ultrasonics, and thermal conductivity.[62] Attention was directed toward simulating the shift in NDT temperature by cold rolling rather than radiation effects. More recently a study is being made of the effect of radiation damage on surface reflection of ultrasonic boundary waves.[63] The use of ultrasonic attenuation and Barkhausen noise to detect a shift in NDT or other effects of radiation is also being investigated.[64] Such efforts should be increased, not only because of the need to have a prompt indication of material degradation as it affects reactor operating parameters, but also because of the necessary feedback into calibration of the various proposed flaw-detection procedures that may be affected by radiation-induced changes in the vessel material.

10.3 IN-SERVICE EXAMINATION

Section 10.2.3 has dealt with current or potential examination methods that may be applicable to the examination of reactor pressure vessels at interim periods during refueling or some other time between operations. The approaches discussed could be quite valuable in determining the extent of degradation that might have occurred since the last examination and in assisting to establish guidelines for continual operation. If, however, there were concern about shorter term changes and the possibility of the onset and occurrence of vessel failure between examinations, it would be necessary to perform more frequent examinations or perhaps do continuous monitoring while the reactor was operating. The methods that seem to have the most potential have already been discussed

because of their possible application to postoperation examination. To avoid needless repetition, only the details pertinent to in-service examination are discussed here.

The fact that the reactor will be operating during these examinations will restrict access to only the outer surface of the pressure vessel. This, in turn, depending upon the test method, could require design changes to provide access within or through the insulation and shielding.

10.3.1 Ultrasonic Scanning Systems

Some form of mechanically scanned ultrasonic system might be applicable. The system would not continuously monitor the entire vessel, but there would be intermittent inspection, with the interval between examinations being at least as long as the time required to scan all areas of the vessel for which the mechanism is designed. With the examination system being in operation immediately adjacent to the exterior of the pressure vessel during reactor operation, the components of the system would have to be able to tolerate the environmental temperature, radiation, etc. The system would have to operate automatically because there would be little opportunity for direct operator control, and it would have to be arranged to not interfere with the normal functioning of the reactor. Since it is unlikely that any mechanical or ultrasonic system would continue in operating condition throughout the life of the reactor, it would be necessary to be able to repair or replace malfunctioning parts. In addition, most of the requirements discussed for mechanical scanning systems for postoperation examination (see Sect. 10.2.3) would be pertinent.

10.3.2 Fixed-Probe Systems

Both active and passive fixed-probe systems are discussed above (Sect. 10.2.3) in connection with postoperation examinations. As for mechanical scanning systems, most of the requirements mentioned also pertain here. Since these mechanisms would normally be applied to the vessel

exterior, little additional design change would be required to achieve capability for interim examination.

The active fixed-probe system in which no movement of the ultrasonic beam is required could be used for either continuous or intermittent monitoring that would depend only on the operating schedule for the ultrasonic instrumentation, which will be at the operator level. The probe is sensitive only to reflecting discontinuities that are close enough to the transducer, lie along a line in front of the transducer, and are nearly perpendicular to the sound beam. Therefore, there would be a practical limitation of the examination to only those areas in which discontinuities were known to exist or zones of critical stress in which crack formation and propagation would be likely.

The active fixed-probe system in which wave directors permit changing the angle or direction of the sound beam also could be used for intermittent monitoring during operation. Since there is a quasi-scanning action of the sound beams, the interval between scanning of given areas must be at least as long as the time required to perform a complete scan.

For both active fixed-probe systems, as well as for the mechanical scanning system, there must be a tolerance for the environment, ability to operate automatically without interference with the reactor, and capability of performing maintenance on the examination system. In addition, all the requirements discussed for postoperation examination with fixed probes pertain for this case.

The passive systems that utilize the phenomenon of acoustic emission (discussed in Sect. 10.2.3) also should be considered for in-operation surveillance. Since this system depends on the generation of the stress wave by the material deformation or crack propagation, it would be necessary to operate continuously to assure detection of all detrimental events. As discussed for the other in-operation monitoring systems, the components affixed to the vessel must have a tolerance for the environment, be readily repaired or exchanged, and, with an around-the-clock operation requirement, should operate automatically without interference with reactor operation. All the problems and requirements discussed for this type of system for postoperation examination are pertinent for this application. Emphasis should be placed on the requirement of ability to

discriminate between those signals due to defects and those due to noises in or around the vessel, since an operating reactor will undoubtedly be considerably noisier than a reactor that has been shut down.

10.3.3 Other Monitoring Systems

The only other monitoring systems currently envisioned that are applicable are those which could detect the presence of a leak through the vessel. These would include systems that could detect the presence of excessive moisture, radioactive fission products, or any other constituent that might be emitted during a noncatastrophic rupture. Such systems are common enough to make discussion unnecessary; however, the leak-before-break philosophy is a basic requirement for such an approach.

With the rapidly advancing state of nondestructive testing technology, new schemes may become available that will be applicable to continuous in-operation monitoring. A continuous awareness of the requirements, coupled with knowledge of new advances, should be maintained to assure that the optimum examination procedure is being applied.

REFERENCES

1. L. Porse, Reactor-Vessel Design Considering Radiation Effects, ASME Publication 63-WA-100, American Society of Mechanical Engineers, New York.
2. A. M. Greene, History of the ASME Boiler Code, American Society of Mechanical Engineers, New York, 1955.
3. Unpublished progress report of Subgroup on Notch Sensitivity, ASME Boiler and Pressure Vessel Code, February 1964.
4. J. S. Clarke and M. S. Northup, Design of Vessels for Petroleum Refining and Petrochemicals Services, ASME Publication 63-WA-195, American Society of Mechanical Engineers, New York.
5. Compressed Gas Association, Methods for Hydrostatic Testing of Compressed Gas Cylinders, Pamphlet C-1, 1959.
6. Dow Chemical Company, Theory and Practice of Melograf Dynamic Pressure Testing Service, 1966.
7. Pressure Vessel Research Committee of Welding Research Council, The Hydrostatic and Hammer Tests as Applied to Pressure Vessels — Are They Good, Bad or Indifferent? unpublished report, November 1952.

8. The Hydrostatic and Hammer Tests Applied to Pressure Vessels, abstract of Ref. 6, Welding J., 32: 303S–304S (June 1953).

9. M. E. Shank, A Critical Survey of Brittle Failure in Carbon Plate Steel Structures Other Than Ships, Welding Research Council Bulletin No. 17, January 1954.

10. R. E. Cecil, Pressure Vessel Design – Effects of Pressurizing, Supplement to 37th Annual Report, Compressed Gas Association, New York, 1949.

11. E. M. McCutcheon, Jr., Method for Preventing Rupture of Metal Structures, U.S. Patent 2,813,049, Nov. 12, 1957.

12. H. E. Kennedy, Method of Stress Relief of Welded Structures, U.S. Patent 2,429,320, Oct. 21, 1947.

13. T. W. Greene and A. A. Holzbauer, Controlled Low Temperature Stress Relieving, Welding J., 25: 171S–185S (March 1946).

14. H. Kihara et al., Effect of Stress Relieving on Brittle Fracture Strength of Welded Steel Plate, International Institute of Welding, Document X-218-59, republished in Welding Research Abroad, December 1959.

15. H. Kihara, K. Masubuchi, and H. Ishii, Brittle Fracture Strength of Welded Spherical Containers, Welding J., 38: 451S–456S (November 1959).

16. L. Wallin, Brittle Fracture in Pressure Vessels, Swedish State Power Board, Reprinted in Welding Research Abroad, February 1964.

17. R. Kennedy, The Influence of Stress Relieving on the Initiation of Brittle Fracture in Welded Plate Specimens, British Welding J., 4(11): 529–534 (November 1957).

18. W. S. Pellini and P. P. Puzak, Practical Considerations in Applying Laboratory Fracture Test Criteria to the Fracture-Safe Design of Pressure Vessels, NRL Report 6030, Naval Research Laboratory, Nov. 5, 1963.

19. W. S. Pellini and P. P. Puzak, Fracture Analysis Diagram Procedures for the Fracture-Safe Engineering Design of Steel Structures, Welding Research Council Bulletin 88, May 1963.

20. E. Bevitt, A. Cowan, and A. L. Scott, Failure Tests on Cylindrical Steel Vessels Containing Axial Faults, J. British Nucl. Eng. Soc., 3(1): 16–30 (January 1964).

21. R. W. Nichols, Prevention of Catastrophic Failure in Steel Pressure Circuit Components, Nucl. Eng., 11(120): 369–373 (May 1966).

22. R. W. Nichols, Overstressing As a Means of Reducing the Risk of Brittle Fracture, International Institute of Welding, Document X-394-66, June 1966.

23. W. H. Irvine, The Significance of Recent Developments in Fracture Mechanics in Great Britain in Relation to the Safety of Reactor Pressure Vessels, British Report AHSB(S) R81, United Kingdom Atomic Energy Authority, 1965.

24. R. W. Nichols et al., A Limit Approach to the Prevention of Pressure Vessel Failure, British Report TRG 1004(C), United Kingdom Atomic Energy Authority, 1965.

25. W. H. Irvine, A. Quirk, and E. Bevitt, Fast Fracture of Pressure Vessels — An Appraisal of Theoretical and Experimental Aspects and Application to Operational Safety, J. British Nucl. Eng. Soc., 3(1): 31–48 (January 1964).

26. W. H. Irvine, E. Bevitt, and A. Quirk, The Safety of Pressure Vessels Against Fast Fracture, British Report AHSB(S) R107, United Kingdom Atomic Energy Authority, 1966.

27. R. W. Nichols, The Use of Overstressing Techniques to Reduce the Risk of Subsequent Brittle Fracture, International Institute of Welding, X-409-67E, IX-530-67E, XI-167-67F, 1967.

28. National Board of Boiler and Pressure Vessel Inspectors, National Board Inspection Code, Chapter II, Model Uniform Boiler and Pressure Vessel Bill, Sections 10(a) and (d), and Chapter IV, Inspection of Existing Boilers or Unfired Pressure Vessels, Section EBI-26, Hydrostatic Test.

29. W. S. Pellini, Naval Research Laboratory, private communication.

30. W. J. Miller, letter dated July 21, 1966 to Robert Wylie, Southwest Research Institute.

31. Westinghouse Electric Corporation, Atomic Power Division, Evaluation of Yankee Vessel Cladding Penetrations, USAEC Report WCAP 2855 Oct. 15, 1965.

32. J. A. Prestele, Letter of February 11, 1966, to W. J. Cahill, Jr., Consolidated Edison Company of New York.

33. F. S. Palmer, State and Insurance Inspections at Dresden Station, April 8 and 28 and May 4, 1965.

34. N. Balai et al., Inspection, Evaluation, and Operation of the EBWR Reactor Vessel, USAEC Report ANL-7117, Argonne National Laboratory, November 1965.

35. J. M. Monahan and P. A. Halpine, PM-2A Reactor Vessel Test — Phase I, USAEC Report WAPD-TM 604, Westinghouse Electric Corporation, July 1966.

36. J. S. Culver, Viewing Equipment for Use in the HRT Core and Blanket Vessels, USAEC Report ORNL-2886, Oak Ridge National Laboratory, Mar. 1, 1960.

37. B. D. Draper and E. C. Hise, Remote Maintenance Procedure Report, USAEC Report ORNL CF-59-11-128, Oak Ridge National Laboratory, Nov. 26, 1959.

38. P. P. Holz, Some Miscellaneous Maintenance Tools Used to Manipulate Loose Objects in the HRT Core, USAEC Report ORNL CF-59-11-123, Oak Ridge National Laboratory, Nov. 17, 1959.

39. P. P. Holz, Additional Miscellaneous Maintenance Tools Used in the HRT Core, USAEC Report ORNL CF-60-9-103, Oak Ridge National Laboratory, Sept. 26, 1960.

40. R. W. McClung and K. V. Cook, Development of Ultrasonic Techniques for the Remote Measurement of the HRT Core Vessel Wall Thickness, USAEC Report ORNL-TM-103, Oak Ridge National Laboratory, Mar. 15, 1962.

41. U.S. Atomic Energy Commission Contract No. AT(11-1)-1228 with Southwest Research Institute, Task D, June 1, 1963.

42. Progress Report No. 3 on USAEC Contract No. AT(11-1)-1228, Southwest Research Institute, Mar. 31, 1964.

43. Progress Report No. 10 on USAEC Contract No. AT(11-1)-1228, Southwest Research Institute, Mar. 15, 1965.

44. Progress Report No. 12 on USAEC Contract No. AT(11-1)-1228, Southwest Research Institute, Sept. 29, 1965, and Progress Report for Period October 1, 1965 through December 31, 1965.

45. C. E. Lautzenheiser, Southwest Research Institute, personal communication, August 1966.

46. W. J. Love, Fatigue Test of "N" Reactor Primary Pipe Longitudinal Seam Welds Containing Production Weld Flaws, USAEC Report HW-76246, Hanford Atomic Products Operation, Aug. 2, 1963.

47. C. E. Lautzenheiser and A. R. Whiting, Nondestructive Testing of Plastic Fatigue Vessels, USAEC Report SWRI 1228-3-3, Southwest Research Institute, Nov. 5, 1965.

48. B. W. O. Dickinson, III, Method and Apparatus for Generating and Receiving Ultrasonic Helical Waves, U.S. Patent 3,186,216, Jan. 1, 1965.

49. B. W. O. Dickinson, III, Method and Apparatus for Flaw Detection by Ultrasonic Means, British Patent 1,001,857, Aug. 18, 1965.

50. B. H. Schofield, R. A. Bareiss, and A. A. Kyrala, Acoustic Emission Under Applied Stress, Report WADC-TR-58-194, Wright Air Development Center, Apr. 30, 1965.

51. B. H. Schofield, Acoustic Emission Under Applied Stress, Parts I and II, Report ASD-TDR-509, Lessells and Associates, Inc., April 1963 and May 1964.

52. B. H. Schofield, A Study of the Applicability of Acoustic Emission to Pressure Vessel Testing, Report AFML-TR-66-92, Lessells and Associates, Inc., April 1966.

53. H. E. Romine, Determination of the Driving Force for Crack Initiation from Acoustic Records of G_c Tests on High Strength Materials for Rocket Motor Cases, NWL Report 1779, Naval Weapons Laboratory, Oct. 4, 1961.

54. M. H. Jones and W. F. Brown, Jr., Acoustic Detection of Crack Initiation in Sharply Notched Specimens, Mater. Res. Std., 4(3): 120–129 (1964).

55. E. Hartbower and P. Crimmins, Aerojet General Corporation, personal communication, August 1966.

56. P. H. Hutton, Progress Report, March, April, May, June 1966, 04 Nuclear Safety, Pressure Piping Crack Monitoring, Detection of Metal Overstress by Acoustic Emission, USAEC Report BNWL-CC-762, Battelle Memorial Institute, Aug. 2, 1966.

57. J. E. Srawley and J. B. Esgar, Investigation of Hydrotest Failure of Thiokol Chemical Corporation 260-Inch-Diameter SL-1 Motor Case, Report NASA TMX-1194, National Aeronautics and Space Administration, Oct. 19, 1965.

58. R. K. Steele et al., Feasibility Study of Acoustic Depressurization System, Report NASA CR-55472, National Aeronautics and Space Administration, March 1966.

59. Southwest Research Institute, Evaluation of the Serviceability of the Elk River Reactor Pressure Vessel, Progress Report No. 4, Report SWRI 1228-19, Mar. 31, 1964.

60. R. W. McClung, Radiography in the Presence of Background Radiation, Materials Evaluation, XXIII(1): 41–45 (January 1965).

61. C. Z. Serpan, Jr., L. E. Steele, and J. R. Hawthorne, Radiation Damage Surveillance of Power Reactor Pressure Vessels, NRL Report 6349, Naval Research Laboratory, Jan. 31, 1966.

62. W. J. McGonnagle, J. R. Barton, and R. D. Wylie, Development of Nondestructive Testing Instrumentation for Reactor Pressure Vessels, Progress Reports on United States-EURATOM Joint Research and Development Program under USAEC Contract AT(11-1)-1243, February 1, 1963–July 10, 1964.

63. J. C. Spanner, Pacific Northwest Laboratory Monthly Activities Report, March 1966, p. 38 and subsequent monthly reports of the same series, USAEC Report BNWL-246 (Official Use Only), Battelle Memorial Institute.

64. R. W. McClung, Oak Ridge National Laboratory, unpublished work.

INDEX*

Acoustic emission; see Ultrasonic testing
Activation analysis
  activant cross-section curve conversion to idealized threshold-energy step function, 71-72, Fig. 3.4
  cross sections for $^{32}S(n,p)^{32}P$ reaction, 71, Fig. 3.3
  problems with specific activants, 72-74
  technique for neutron-flux measurement, 68, 70
Aging; see Strain aging
Aircraft, fuselage crack-arrest studies, 512-515
AISI 4340 steel; see also Steels
  tensile properties, 141, Figs. 4.11-4.13
Allotropic transformation; see Microstructure
Aluminum (2219), fracture mechanics and fatigue analysis, 347
American Society of Mechanical Engineers (ASME)
  Pressure Vessel Code, hydrostatic test requirements, 629-637
  Pressure Vessel Code, postoperation test recommendations, 637-661
  Pressure Vessel Code, quality assurance requirements, 577-628
  Pressure Vessel Code, stress report requirements, 410-412
American Society for Testing Materials (ASTM)
  neutron-flux measurement standard, 78-79
  steel designations cross index, 90, Table 4.3
Annealing; see Heat treatment
Arc welding; see Welding
ASTM A 201 Grade B
  biaxial fatigue tests, 362-363, Figs. 6.15, 6.18
  fatigue strength evaluation in full-scale test, 372-390
  strain effects on crack growth rates, 469, Fig. 7.4
ASTM A 212 Grade B
  fracture toughness, leak-before-break criterion, 520, Table 7.3
  mechanical property changes, effect of irradiation temperature, 250, Fig. 5.18
  radiation effects on fatigue strength, 234, 236-237, Figs. 5.13-5.15
  radiation effects on SM-1 reactor specimens, 255, Fig. 5.21
  reembrittlement during postirradiation annealing, 263, Fig. 5.27
  stress-strain behavior, effect of postirradiation annealing, 261, Fig. 5.23
  stress-strain behavior of irradiated, 223, Fig. 5.4
  tensile properties, effect of postirradiation annealing, 261-262, Figs. 5.24-5.25
  yield stress of irradiated, annealing time for 50% recovery, 264, Fig. 5.29
ASTM A 285 Grade A, radiation effects on notch-impact strength, 227, Fig. 5.7
ASTM A 285 Grade C, stress-strain behavior, 331, Fig. 6.7
ASTM A 301 Grade B, strain effects on crack growth rates, 469, Fig. 7.4
ASTM A 302 Grade B
  annealing during irradiation, effect on nil ductility transition temperature, 265, Fig. 5.30
  biaxial fatigue tests, 362-363, Figs. 6.16, 6.18
  fatigue strength evaluation in full-scale tests, 372-374
  fracture toughness, leak-before-break criterion, 519, Table 7.2
  fracture toughness, stress-intensity factor, 501, Fig. 7.10
  nil ductility transition temperatures of irradiated, 266, Fig. 5.31
  radiation effects on fatigue strength, 233-234, Figs. 5.11-5.12
  radiation effects on fracture toughness, 231, Fig. 5.10
  radiation effects on various heats, 252, Fig. 5.19
  radiation effects on Yankee Reactor specimens, 257, Fig. 5.22
  stress effects on crack growth rates, 467, Fig. 7.3
  stress effects on cyclic life, 473, Fig. 7.5
ASTM A 350 Grade LF-3
  nil ductility transition temperatures of irradiated, 266, Fig. 5.31
  notch-impact behavior, effect of postirradiation annealing time, 262, Fig. 5.26
ASTM A 508 Class II, fabrication processes, 132-140
ASTM A 533 Grade B, fabrication processes, 123-132
ASTM A 540, fabrication processes, 140-142
Austenite; see Microstructure

Babcock & Wilcox Company
  fabrication facilities, 541-542
  steel procurement standards, 125, 133
Bainite; see Microstructure
Bars, ultrasonic testing methods, 593-594
Basic steelmaking, electric furnace process, 126-132
Big Rock Point Reactor, materials surveillance tests, 256
Boiling-water reactors; see also specific reactors
  coolant conditions, 64-65, Table 3.2
  typical vessel proportions, 5, Fig. 1.1
  water chemistry control, flow diagram, 64, Fig. 3.2
Bolting materials
  fabrication processes, 140-142
  quality assurance requirements, 585-586
Bolts, nondestructive testing methods, 598
Brittle fracture; see also Fracture
  analytical methods, 339-350

Carbon
  effect on notch toughness of steel, 99, Fig. 4.4
  effect on pearlite and martensite formation in steels, 95, Fig. 4.2
  effect on tensile strength of steel, 94, Fig. 4.1
  effect on weldability of steel, 115-116, Fig. 4.7
  C-Fe, binary equilibrium phase diagram, 96, Fig. 4.3
Carbon steel; see also Steels
  blistering, 213-214
  corrosion behavior, 152-178
  decarburization, 214
  delayed failure, 214-215
  ductility, reduction in postyield, 215-217
  examination after accelerated cooling, 598-599
  failure, British tests on full-size vessels, 390-399
  fatigue-crack growth rates, effect of temperature, 335, Fig. 6.10
  hydrogen embrittlement, 212-217
  radiation effects on notch-impact strength, 227, Fig. 5.7
  stress variation at failure of flawed plates, 397, Fig. 6.29

*This Index was prepared by H. D. Raleigh, AEC Division of Technical Information Extension, Oak Ridge, Tennessee.

temperature effects on ductile-to-brittle transition, 328–329, Fig. 6.6
yield stress of irradiated, annealing time for 50% recovery, 264, Fig. 5.29
yield stress of irradiated, isothermal annealing curves for, 263, Fig. 5.28
C-Mn, underbead cracking, 116, Fig. 4.7
Castings, nondestructive testing methods, 594–596
Cementite; see Microstructure
Charpy impact test; see also Notch toughness
description, 504–506
Chemical properties, materials analysis methods, 579–580
Chicago Bridge and Iron Company, fabrication facilities, 542–544
Chromium steel; see also Steels
Cr-Mo, effect of temperature on fatigue-crack growth rates, 335, Fig. 6.10
Cladding; see Fracture
radiation effects on stainless steel, 266–267
weld-overlay, flanges and nozzles, 567–570
weld-overlay, head subassemblies, 569, Fig. 8.9
weld-overlay, materials and methods, 564–566
Coated-electrode welding; see Welding
Cold work; see Working processes
Cooling rates; see Microstructure
Copper-63, properties as activant for neutron-flux monitoring, 74
Corrosion
austenitic stainless steel, 178–195
carbon and low-alloy steels, 152–178
crevice-corrosion mechanisms, 171–174, 187–190
effect of additives, 183–184
effect of dissolved salts in water, 169
effect of heat treatment, 182–183
effect of hydrogen, 168, 181
effect of irradiation, 186–187
effect of oxygen, 162–168, 180
effect of temperature, 158–159, 181
effect of time, 159–161, 182, Figs. 5.1–5.3
effect of water pH, 156–158, 181
effect of water velocity, 161–162, 181–182
effect of wet oxygenated steam, 184–185
effects on crack growth rates, 474–476
galvanic attack mechanisms, 174–175, 190–192
pitting effects, 169–171
stress-corrosion cracking, 175–178, 192–195
Combustion Engineering, Inc.
fabrication facilities, 541
steel procurement standards, 124, 133
Computers, use in vessel design analyses, 368–372
Crack-arrest test, description, 347–350
Cracks
arrest, stress-intensity values, 494, Fig. 7.8
arrest estimates for HY-80 steel, 503, Fig. 7.11
arrest studies, 512–516
critical size estimates from proof tests, 524–528
critical stress-intensity factor for A 302 grade B steel, 501, Fig. 7.10
dynamic stress-field analysis, 487–489
elimination and slow growth, 510–512
extension behavior, effects of strain-energy release rate, 493, Fig. 7.7
fracture process zone analysis, 489–494
growth, basic aspects, 430–534
growth, effects of environment, 474–476
growth, effects of fatigue, 465–474
growth, testing recommendations, 531–534
growth rate analysis, 339–350, 465–476
linear elastic modeling, 443–455
linear stress-field analysis, 446–452
minimum fracture toughness, 489–494
Mode III elastic-plastic analysis, 459–462
opening dislocation measurements, 506–508
plastic analysis, fracture characterization problems, 462–465
plasticity analysis concept, 455–465
progressive extension behavior, 443–446
propagation, detection by passive acoustic detection systems, 656–660
propagation analysis, 476–510
radiographic detection, 612–621
schematic diagram of leading edge, 446, Fig. 7.1
schematic diagram of test specimen section, 499, Fig. 7.9
strain-rate effects on moving, 489–494
strip-yield zone analysis concept, 457–459
toughness measurements, 332, 476–480, Fig. 6.8
ultrasonic detection, 621–624
Creep, radiation effects on steels, 235–238
Cross section; see Neutron cross sections
Crud, effects on primary coolant system, 186

Defects; see also Cracks and Flaws
detection and control, 430–443
Deformation; see Stress
Deoxidization; see Basic steelmaking
Design
ASME Code requirements, 604–609
current industrial practice, 406–419
current research, 367–406
geometric deviations from specifications, 605–609
strength and fracture aspects, 331–350
stress analysis and failure modes, 282–418
summary for present commercial reactor vessels, 61, Table 3.1
Discontinuity stresses, definition, 315
Dosimetry, methods of neutron, 66–69, 70–72
Dresden-1 Reactor, materials surveillance tests, 257–258
Dresden-2 Reactor, pressure vessel dimensions, 3, Table 1.1
Ductility; see Steels and Tensile properties

E7016; see Weld metals
Economics, reactor design life, 12, 79
Elasticity, theory and application in stress analysis, 287–300
Elastic limit; see Fracture
Electric furnace; see Basic steelmaking
Electromagnetic inspection, capabilities and limitations, 626–627
Electroslag welding; see Welding
Elk River Reactor, pressure vessel examination, 206–207, 334, 336, 651–652
Embrittlement; see Steels and Tensile properties
Equilibrium diagrams; see Phase diagrams
Experimental Boiling-Water Reactor (EBWR), pressure vessel examination, 198–202, 648–649

Fabrication
ASME Code requirement, 600–604
bolting material, 140–142
current practice, 539–575
design considerations, 365–366
facilities, 541–544
flange forgings, 567–570
forgings, 132–140
geometric deviations from design specifications, 605–609
head subassemblies, 566–567
heat treatment of formed shell plates, 551–553
heat treatment of shell courses, 555–560
machining of major vessel sections, 570–572
materials, 544–555
nozzle forgings, 567–570
operations, 544–545

plate steels, 124–132
shell course assembly by electroslag welding, 555–560
shell course joining into subassemblies, 560–564
shell forming, 545–551
shell plate assembly into courses, 553–555
vessel supports, 561
Failure; see also Fracture
British tests on full-size vessels, 390–399
brittle fracture of a nonnuclear vessel, 401–406
design methods to prevent structural, 324–331
full-scale vessel tests, 372–399
notch toughness testing of failed vessel metal, 405, Fig. 6.32
photographs of a nonnuclear vessel, 402–403, Figs. 6.30–6.31
PM-2A vessel testing, 399–400
stress diagram for carbon steel vessels, 394, Fig. 6.28
stress relationship to critical crack size, 391, Fig. 6.27
stress variation in flawed plates, 397, Fig. 6.29
Fatigue
analysis for high-strength steel and aluminum vessels, 347
biaxial analysis, 350–364
effect on crack growth rates, 465–474
effect on pressure vessel integrity, 331–336
evaluation in full-scale vessel tests, 372–390
life cycle relationship to strain range, 376, Fig. 6.20
radiation effects on steels, 232–235
strength tests on full-scale vessels, 386–388, Figs. 6.23–6.25
transient effects on, 80–82, Table 3.6
Ferrite; see Microstructure
Firebox quality steel plate; see Plates
Flanges, fabrication methods, 567–570
Flaws; see also Cracks and Defects
detection requirements, 588–600
Fluid-penetrant inspection, capabilities and limitations, 625–626
Fluxes; see Welding
Forces, analysis in elasticity theory, 294–297
Forgings
fabrication processes, 106–107, 132–140
mechanical properties requirements, 583–585
Forming
process description for thick steel, 107–108
shell cylinders, 545–551
Fracture; see also Failure
analysis diagram, 347–350, 522–524
aspects in vessel design, 331–350
basic aspects, 430–534
brittle-ductile transition measurements, 480–483
characterization problems in plastic analysis, 462–465
control methods, 430–443, 510–531
crack-opening dislocation measurements, 506–508
critical crack size estimates from proof tests, 524–528
double-cantilever test specimens, 483–486, Fig. 7.6
face-grooved test specimens, 483–486
mechanics, description and application, 339–346
mechanics, experimental analysis methods, 452–455
mechanics, nomenclature, 439–443
mechanics, testing recommendations, 531–534
photographs of failed vessels, 375–390, Figs. 6.19, 6.21, 6.22, 6.26
toughness, dynamic measurements, 498–506
toughness, effects of preloading, 508–510
toughness, effects of strain aging, 508–510
toughness, leak-before-break criterion, 517–522
toughness, radiation effects on, 230–232, 528–531
toughness, relation to plastic flow properties, 494–498
toughness analysis, 476–510
transition temperature tests, 498–506
Fusion joining; see Welding

Gamma iron; see Iron
Geometry
design considerations, 365–366
experimental studies, 368–372
Grain size; see Microstructure
Griffith theory of fracture, progressive crack-extension behavior, 445

Hardenability, definition and measurement, 109–111
Hardness; see Steels and Mechanical properties
Heads, fabrication methods, 566–567
Heat-affected zone; see Welding
Heat treatment
effect on postirradiation embrittlement relief, 259–266
effect on stainless steel corrosion, 182–183
effect on tensile properties, 141–143, Figs. 4.11–4.13
electroslag-welded shell courses, 555–560
formed shell plates, 551–553
Heavy-Water Components Test Reactor (HWCTR), pressure vessel examination, 203–206
High-strength low-alloy steels; see Steels
Hooke's law, application in stress analysis, 288
Hot cracking, definition, 101
Hot shortness, definition, 101
Hot work; see Working processes
HY-80 steel; see also Steels
fracture toughness, 503, Fig. 7.11
fracture toughness, leak-before-break criterion, 519, Table 7.1
Hydrogen
effect on properties of steel, 101–102
effect on steel corrosion, 168, 181
embrittlement mechanisms in steels, 209–220
Hydrogen ion concentration; see pH
Hydrostatic testing; see also Testing
ASME Code requirements, 629–637
design considerations, 366–367
retest suggestions, 643–645

Impact testing; see notch toughness
Indian Point Reactor, nondestructive examination of vessel, 647–648
Ingots, steel; see Basic steelmaking
Inspection; see also specific methods, such as Electromagnetic inspection
design considerations, 367
Iron
yield stress of irradiated, annealing time for 50% recovery, 264, Fig. 5.29
C-Fe, binary equilibrium phase diagram, 96, Fig. 4.3
Iron-54
cross section for $^{54}Fe(n,p)^{54}Mn$ reaction, 76, Table 3.5
properties as activant for neutron-flux monitoring, 73–74
Irradiation effects; see Neutrons and Radiation
Isothermal transformation diagrams; see Transformation diagrams

Joining; see Welding
Jominy end quench test, description, 110–111

Killed steel; see Basic steelmaking

Lamellar pearlite; see Microstructure
Linear elastic modeling; see Cracks
Lukens Steel Company, steel plate manufacturing processes, 124-132

Machining, requirements for major vessel sections, 570-572
Macroscopic inspection, capabilities and limitations, 610-612
Magnetic-particle inspection, capabilities and limitations, 624-625
Maintenance, design considerations, 367
Manganese
  effect on notch toughness of steel, 101
  effect on tensile strength of steels, 94, Fig. 4.1
Manganese steel; see also Steels
  weldability, underbead cracking, 116, Fig. 4.7
Martensite; see Microstructure
Mechanical loading, considerations in vessel design, 82
Mechanical properties
  materials requirements, 91-92, 111-113, 580-588, Table 4.4
  radiation effects on steels, 221-267
Metallurgy, processes for vessel steels, 90-123
Microstructure
  effects of alloying elements on steel, 93-103
  effects of cooling rate on steel, 109-111
MIG welding; see Welding
Molybdenum steel; see also Steels
  Cr-Mo, effect of temperature on fatigue-crack growth rates, 335, Fig. 6.10
Multipass welding; see Welding

Naval Research Laboratory, steel fracture analysis diagram, 335, 522-524, Fig. 6.9
Neutron cross sections
  determination for neutron-flux-monitor activants, 70-72
  differential, for $^{54}Fe(n,p)^{54}Mn$ reaction, 76, Table 3.5
  differential, for $^{58}Ni(n,p)^{58}Co$ reaction, 75, Table 3.4
Neutrons; see also Radiation
  damage models, 69-70
  dose effects on mechanical properties of steels, 238-240
  effects on mechanical properties of steels, 221-267
  effects on vessel embrittlement, 66-67, Table 3.3
  effects on vessels, surveillance testing, 637-643, Table 10.1
  flux effects on mechanical properties of steels, 240-242
  flux measurement, ASTM standards, 78-79
  flux measurement methods, 67, 70-72
  flux spectral and spatial behavior calculations, 76-77
  spectrum effects on mechanical properties of steels, 242-248, Fig. 5.16, Table 5.1
Nickel, effects on notch toughness of steel, 101
Nickel-58
  cross section for $^{58}Ni(n,p)^{58}Co$ reaction, 75, Table 3.4
  properties as activant for neutron-flux monitoring, 73
Nitrogen, effects on properties of steels, 102
Nondestructive testing; see Testing
Notch toughness
  definition, 99
  effect of carbon content on steel, 99, Fig. 4.4
  effect of alloying elements on steel, 100, Fig. 4.5
  radiation effects on steels, 225-229
  requirements for forgings, 583-585
  requirements for plate, 581-583
  requirements for steels, 112
Nozzles
  attachment methods, 561-564
  fabrication methods, 567-570
  nondestructive testing methods, 596-597
  stress analyses for, theoretical and experimental, 368-372
  weld-joint design, 554, Fig. 8.3

Operating conditions
  design considerations, 366-367
  summary for present commercial reactor vessels, 61, Table 3.1
Organic Moderated Reactor Experiment (OMRE), radiation effects on grid plate, 259
Oxidation; see Corrosion
Oxygen
  effect on properties of steel, 102
  effect on steel corrosion, 162-168, 180

Palisades Reactor, pressure vessel dimensions, 3, Table 1.1
Pearlite; see Microstructure
pH, effect on steel corrosion, 156-158, 181
Phase diagrams, binary iron-carbon, 96, Fig. 4.3
Phosphorus, effect on notch toughness of steel, 101
Photoelasticity; see Stress
Pipes, nondestructive testing methods, 596-597
Piqua Reactor, materials surveillance tests, 256
Pitting-type corrosion; see Corrosion
Plastic flow, relation to fracture toughness, 494-498
Plasticity
  adjustment factor in crack analysis model, 456-457
  analysis concepts for cracks, 455-465
  crack analysis, fracture characterization problems, 462-465
  crack analysis, Mode III, 459-462
  strip-yield zone analysis, 457-459
  theory, application in stress analysis, 337-350
Plates
  fabrication processes, 124-132
  forming procedures, 545-551
  heat treatment of formed shell, 551-553
  mechanical properties requirements, 581-583
  shell assembly into courses, 553-555
  ultrasonic examination procedures, 590-593
PM-2A reactor
  fracture strength testing of pressure vessel, 399-401
  radiation effects on pressure vessel, 259
  ultrasonic examination of vessel, 650-651
Poisson ratio; see Stress
Pressure, operating bases for vessels, 60
Pressure testing; see Hydrostatic testing
Pressure vessel research committee, large-model and full-scale strength tests, 372-390
Pressurized water reactors; see also specific reactors
  coolant conditions, 64-65, Table 3.2
  typical vessel proportions, 6, Fig. 1.2
  water chemistry control, flow diagram, 63, Fig. 3.1
Proof testing; see Testing

Quality assurance
  chemical properties, 579-580
  inspection methods, 577-627
  mechanical properties, 580-588

Radiation; see also Neutrons
effects on corrosion of stainless steel, 186–187
effects on fracture properties, 528–531
effects on leak-before-break tension stress, 528–531
effects on mechanical properties of steels, 221–267
effects on steel properties at nil ductility transition temperature, 529–531
effects on vessel embrittlement, 67, Table 3.3
effects on vessel materials, nondestructive detection efforts, 660–661
effects on vessels, surveillance testing, 637–643, Table 10.1
Radiographic inspection
capabilities and limitations, 612–621
use in postoperation examination, 659–660
Range of stress; see Stress
Rate of strain; see Strain
Reactors; see specific reactors by name, such as Elk River Reactor
Rockets, solid-propellant chamber fracture toughness, 517–520
Rolling, process description for thick steel plates, 106
Rolls, plate-forming, 550, Fig. 8.2

Scaling of steel; see Basic steelmaking
Shear fracture; see Fracture
Shells
assembly by electroslag welding, 555–560
design analysis techniques, 368–372
fabrication procedures, 545–551
general theory summary, 300–307
heat treatment of electroslag-welded, 556, 560
heat treatment of formed plates, 551–553
joining courses into subassemblies, 560–561
plate assembly into courses, 553–555
Ships, crack-arrest studies on welded plates, 515
SL-1 reactor, radiation effects on pressure vessel, 259
SM-1 reactor, materials surveillance tests, 255, Fig. 5.21
SM-1A reactor, materials surveillance tests, 255, Fig. 5.21
Stainless steel; see also Steels
corrosion of austenitic, 178–195
crevice corrosion mechanisms, 187–190
galvanic corrosion mechanisms, 190–192
hydrogen embrittlement, 217–219
radiation effects on tensile properties, 266–267
stress-corrosion cracking, 192–195
Steam, corrosive effects on stainless steel, 184–185
Steels; see also AISI 4340 steel, Carbon steel, chromium steel, HY-80 steel, Manganese steel, molybdenum steel, stainless steel, T-1 steel, and steels by ASTM designation, such as ASTM A 201 Grade B
alloying element effects on properties, 93–103
ASTM designations, cross index, 90, Table 4.3
carbon effects on pearlite and martensite formation, 95, Fig. 4.2
chemical composition of vessel, 88–89, Table 4.2
corrosion behavior, 152–209
crack toughness of high-strength, 332, Fig. 6.8
critical stress-intensity factor measurements, 476–480
examination after accelerated cooling, 598–599
fabrication procedures, 123–146
fatigue resistances, 335, Figs. 6.9–6.10
fracture energy variation with transition temperature, 229, Fig. 5.9
fracture mechanics and fatigue analysis, 347
hydrogen embrittlement, 209–220
heat treatment effects on postirradiation embrittlement relief, 259–266
irradiation behavior, effect of composition, structure, and heat treatment, 251–254
joining processes, 117–121
mechanical properties, effect of irradiation temperature, 249–251, Figs. 5.17–5.18
mechanical properties, neutron-dose effects, 238–240
mechanical properties, neutron-flux effects, 240–242
mechanical properties, neutron-spectra effects, 242–248, Fig. 5.16, Table 5.1
mechanical properties requirements, 91–92, 111–113, 580–588, Table 4.4
melting process for large-ingot production, 103–104
microstructure, effect of cooling rate, 109–111
notch toughness, effect of alloying elements, 100, Fig. 4.5
notch toughness, effect of carbon, 99, Fig. 4.4
plate thickness effects on properties, 113–114
radiation effects on creep properties, 235–238
radiation effects on ductile-to-brittle transition temperature, 228, Fig. 5.8
radiation effects on fatigue strength, 232–235
radiation effects on mechanical properties, 221–267
radiation effects on nil ductility transition temperature, 253, Fig. 5.20
radiation effects on stress-strain behavior, 223–225
radiation effects on yield stress, 225, Fig. 5.6
radiation effects surveillance programs, 254–258, 637–643, Table 10.1
selection for vessels, 85–87, 365, Table 4.1
strain-cycling behavior, 335, Fig. 6.9
stress-corrosion cracking, 175–178, 474–476
stress effects on crack growth rates, 467, Fig. 7.3
stress relationship to critical crack size for failure, 391, Fig. 6.27
temperature effects on properties, 150–152
tensile strength, effect of carbon and manganese, 94, Fig. 4.1
vacuum treatment, effects on properties, 104–105, Fig. 4.6
weldability, 114–117
working processes; 105–108
Strain
effects on crack growth rates, 469, Fig. 7.4
energy release rate effects on crack extension, 493, Fig. 7.7
Mode III crack analysis, 459–462
theory of small deformations, 289–294
Strain aging, effects on fracture toughness, 508–510
Strain hardening, relation to fracture toughness, 494–498
Strength
aspects in vessel design, 331–350
large-model and full-scale tests, 372–400
theory applications, 307–309
Stress; see also Yield stress
ASME Code analysis requirements, 410–412, 604–605
analysis in elasticity theory, 294–297
analysis methods, 285–323
comparison of elastically and plastically calculated, for strains beyond the yield point, 351, Table 6.1
crack-arrest test description, 347–350
critical-intensity factor measurements for very-high-strength metals, 476–480

distribution at plastic collapse, 338-339, Fig. 6.11
dynamic-crack stress-field analysis, 487-489
dynamic yield, variation with nil ductility transition temperature, 529, Table 7.4
dynamic yield, variation with nil ductility transition temperature plus 60°F, 530, Table 7.5
effects of design specifications deviations on, 605-609
effects on crack growth rates, 467, Fig. 7.3
effects on cyclic life of steel, 373, Fig. 7.5
evaluation for nuclear pressure vessels, 323-367
evaluation of primary and secondary, 350-364
experimental measurement methods, 452-455
experimental analysis, 309-312
failure diagram for carbon steel vessels, 394, Fig. 6.28
fatigue analysis, 321-323
intensity definition, 298
intensity factors for A 302 B steel, 501, Fig. 7.10
intensity values for crack arrest, 494, Fig. 7.8
leak-before-break, radiation effects on, 528-531
linear analysis of crack propagation, 446-452
maximum conditions for plastic sections, 340, Fig. 6.12
relationship to critical crack size, 391, Fig. 6.27
relief, effect of hydrostatic testing, 634-637
residual, effect on brittle fracture, 343-344
steady state analysis, 313-321
strip-yield plasticity analysis, 457-459
theory of small displacements, 287-300
thermal, theory formulation for, 299-300
variation at failure of flawed plates, 397, Fig. 6.29
Stress-corrosion cracking, analysis, 474-476
Stress-strain relations, mathematical formulation, 297
Submerged arc welding; see Welding
Sulfur, effects on properties of steel, 101
Sulfur-32
cross section for (n,p) reaction, 71, Fig. 3.3
properties as activant for neutron-flux monitoring, 73
Surveillance programs; see also Inspection and Testing
materials tests results, 254-258

T-1 steel; see also Steels
biaxial fatigue tests, 363, Figs. 6.17-6.18
fatigue strength evaluation in full-scale tests, 367-390
stress-strain behavior, 331, Fig. 6.7
Temperature
effect on ductile-to-brittle transition, 328-329, Fig. 6.6
effect on fatigue-crack growth rates, 335, Fig. 6.10
effect on radiation damage in steels, 249-251, Figs. 5.17-5.18
effect on steel corrosion, 158-159, 181
effect on steel properties, 141, 150-152
operating bases for vessels, 60
Tempering, temperature effects on tensile properties, 141-143, Figs. 4.11-4.13
Tensile properties
effects of postirradiation annealing, 259-266
effects of tempering temperature, 141-143, Figs. 4.11-4.13
requirements for forgings, 583-585
requirements for plate, 581-583
requirements for steels, 111-112
Testing; see also Crack-arrest test, Hydrostatic testing, Jominy end quench test, and Ultrasonic testing
British series on full-size vessel failure, 390-399
hot overstressing effects, 635-637
in-service examination possibilities, 661-664
large-model and full-scale results, 372-401
nondestructive, current practice for operating vessels, 647-649
nondestructive, flaw detection procedures, 589-590
nondestructive, methods capabilities and limitations, 609-627
nondestructive, postoperation methods, 649-660
nondestructive, procedures and personnel requirements, 599-600
PM-2A vessel results, 399-401
postoperation, ASTM recommended practice, 637-660
preoperation procedures, 629-637
proof, estimates of critical crack size, 524-528
quality assurance requirements, 577-627
Thermal stress; see Stress
TIG welding; see Welding
Time, effect on steel corrosion, 159-161, 182, Figs. 5.1-5.3
Titanium-46, properties as activant for neutron-flux monitoring, 73
Toughness; see Notch toughness
Transformation diagrams, effects of carbon on pearlite and martensite formation, 95, Fig. 4.2
Transients, analysis for vessel design, 80-82, Table 3.6
Tresca yield criterion, diagram for biaxial loading, 356, Fig. 6.14
Tubes, nondestructive testing methods, 596-597

Ultrasonic testing; see also Testing
capabilities and limitations, 621-624
fixed-probe systems applications, 653-659, 662-664
in-service vessel examination, 662-664
postoperational vessel examination, 650-659
scanning systems applications, 650-653, 662

Vacuum treatment, effect on properties of steels, 104-105, Fig. 4.6
Visual inspection, capabilities and limitations, 610-612

Water
chemistry control methods, 62-65
coolant chemistry conditions, 65, Table 3.2
effect of dissolved salts on steel corrosion, 169
velocity effects on steel corrosion, 161-162, 181-182
Weld metals, E 7016, stress-strain behavior of irradiated, 224, Fig. 5.5
Welding
dissimilar-metals joining, 561-562
electroslag, process description, 118-121, 555-560, Figs. 4.9-4.10, 8.4-8.6
electroslag, shell course assembly by, 555-560
filler metal compositions, 144-145, 589
head subassemblies, 566-569, Figs. 8.8-8.9
hot cracking in steels, 115-117
joining processes for steels, 117-121
metallurgical problems in steels, 114-117
nozzle insert joint design, 554, Fig. 8.3
overlay cladding of vessel components, 122-123, 564-566
procedure specifications, 586-588
processes description, 142-146

submerged-arc process, 117-118, Fig. 4.9
underbead cracking in steels, 115-116, Fig. 4.7
Welds, test requirements, 586-588
Working processes, description, 105-108

X-ray inspection; see Radiographic inspection

Yankee Reactor
materials surveillance tests, 257, Fig. 5.22
pressure vessel examination, 196-197, 649
Yield stress; see also Stress
annealing time for 50% recovery in irradiated iron and steel, 264, Fig. 5.29
increases in irradiated steels, 225, Fig. 5.6
isothermal annealing curves for irradiated carbon steel, 263, Fig. 5.28
relation to fracture toughness, 494-498
Young's modulus; see Stress